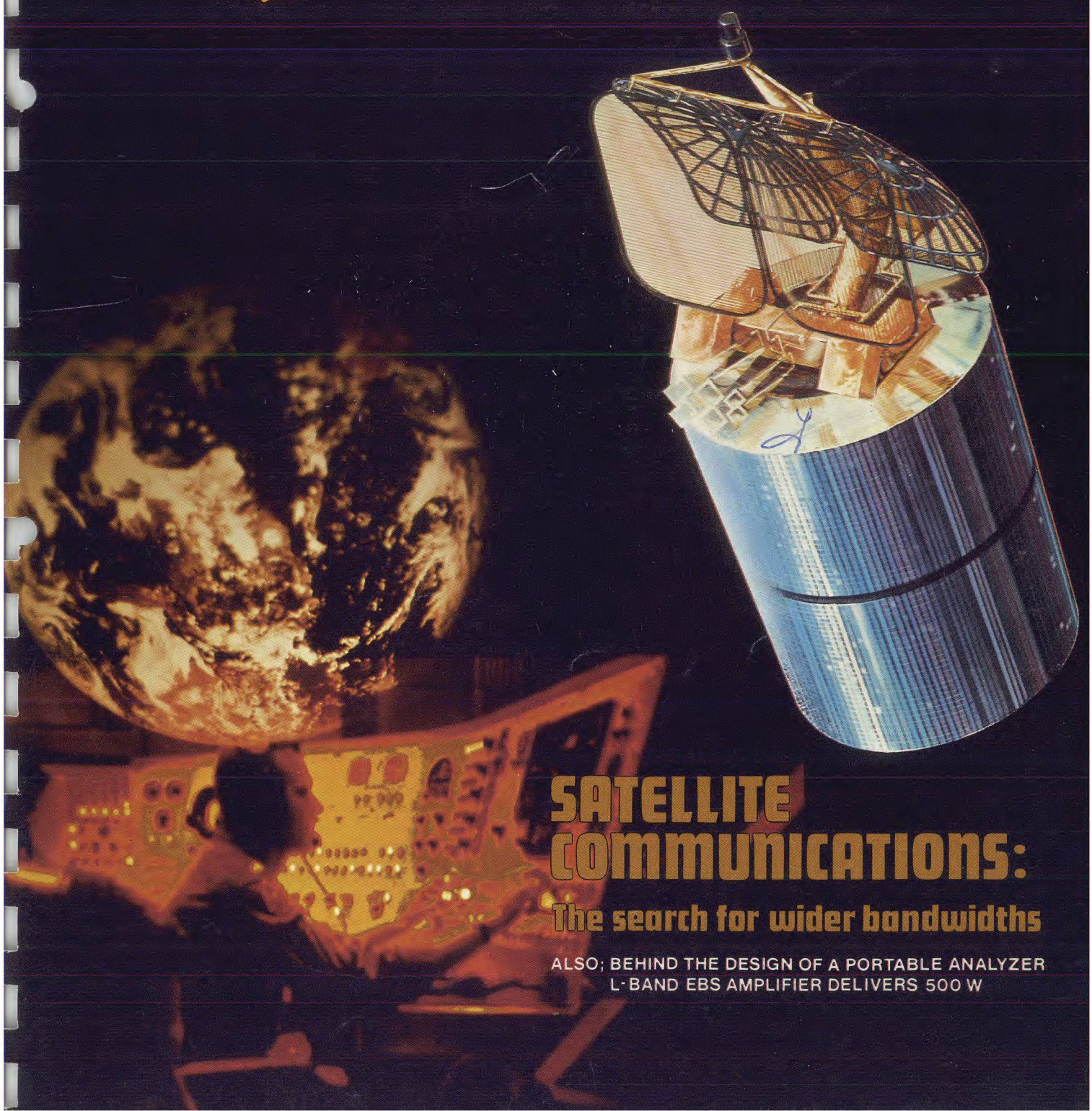
BEFORE YOU READ THIS ISSUE...
Renew your 1975 Subscription
Turn to card inside front cover

JANUARY
1975

MICROWAVES

laser technology



SATELLITE COMMUNICATIONS:
The search for wider bandwidths

ALSO; BEHIND THE DESIGN OF A PORTABLE ANALYZER
L-BAND EBS AMPLIFIER DELIVERS 500 W

MICROWAVES

January 1975
Vol. 14, No. 1

news

9 L-Band EBS Amplifier Belts Out 500 W
10 NY Crime Fighters Now Using Laser Beams For Fingerprint Identification
14 Satellite Communication: The Search For More Bandwidth
21 Washington
24 R & D
26 International
28 Industry
32 Meetings
34 For Your Personal Interest . . .

editorial

30 Someone's Shouting In The Ears Of The Silent Minority

technical section

Communications

52 **Wideband Phase Modulator Works Directly On Carrier.** R. R. Rippy of Goddard Space Flight Center describes a diode phase modulator that offers ±100° linear modulation with only ±0.5° incidental am enhancement, even when operating at 2.1 to 2.3 GHz.

62 **Transistor Mixer Boosts Upconverter Gain.** Klaus Breitkopf of RIAS-Berlin compares similar transistor and varactor upconverters. Designed for uhf broadcast operations, both circuits are built inside a 'rat race' hybrid.

68 **Transplexing SAW Filters For ECM, Part II.** Raymond Jones, James Schellenberg, Dr. William Tanski and Dr. Robert Moore of Westinghouse continue their examination of SAW filters and their application in multiplexed filterbanks. This second installment focuses on the role of miniature amplifiers in active transplexing.

77 Application Notes

TEST & INSTRUMENTATION

technical section

36 **Behind The Design Of A Portable Analyzer.** Bob Hoss and Frank Reisch of Collins Radio review the problems encountered in the design of a 2 to 25 GHz YIG-tuned spectrum analyzer.

41 Application Notes
43 **Product Feature:** Cost-Conscious Counter Provides 1Hz Resolution to 4.5 GHz.
47 New Products
46 New Literature

products and departments

74 New Products
79 Advertisers' Index
78 New Literature
80 Product Index

About the cover: Comsat General's domestic satellite for 1976, designed and built by Hughes Aircraft, is squeezing out additional channel capacity at the 4 and 6 GHz bands by using polarization diversity. It will also be evaluating the millimeter bands for possible future use. Photo composition by Robert Meehan.

coming next month: Semiconductors

HYBRID COUPLED AMPS: CAN THEY WEATHER A MISMATCH? Richard LaRosa of Hazeltine in Greenlawn, NY, examines the effects of an output mismatch on a pair of hybrid-coupled power transistors. The analysis reveals that one transistor is in jeopardy, even with a relatively minor mismatch. Surprisingly, this problem cannot be detected by monitoring the terminated hybrid output port.

MODELING TRANSISTORS FOR IMPROVED PERFORMANCE. Jim Curtis of PHI describes a practical method of modeling power transistors. The lumped-equivalent circuits derived are based on transistor loading. Large signal conditions apply.

Also: The 1974 Annual Index

Publisher/Editor
Howard Bierman

Managing Editor
Richard T. Davis

Associate Editor
Stacy V. Bearse

Contributing Editor
Harvey J. Hindin

Washington Editor
Paul Harris
Snyder Associates
1050 Potomac St., NW
Washington, DC 20007
(202) 965-3700

Editorial Assistant
Gail Murphy

Production Editor
Sherry Lynne Bogen

Art
Robert Meehan, Dir.

Production
Dollie S. Viebig, Mgr.
Dan Coakley

Circulation
Trish Edelmann, Mgr.
Peggy Long, Reader Service

Promotion Manager
Walter Salm

Editorial Office
50 Essex St.,
Rochelle Park, N.J. 07662
Phone (201) 843-0550
TWX 710-990-5071

A Hayden Publication
James S. Mulholland, Jr., President

MICROWAVES is sent free to individuals actively engaged in microwave work at companies located in the U.S. Canada and Western Europe. Subscription price for non-qualified copies is $10.00 for U.S., $15.00 a year elsewhere. Additional single copies $1.50 ea. (U.S.); $2.00 ea. (foreign); except additional Product Data Directory reference issue, $10.00 ea. (U.S.); $18.00 (foreign).

Hayden Publishing Co. Inc., James S. Mulholland, President, printed at Brown Printing Co., Inc., Waseca, MN.

Copyright © 1974 Hayden Publishing Co., Inc., all rights reserved.

L-Band EBS amplifier belts out 500 W

Stacy V. Bearse
Associate Editor

Specialists in vacuum tube and solid-state technologies have teamed up to push a high-power electron bombarded semiconductor amplifier into the gigahertz region. With potential TACAN and IFF applications in mind, researchers at Watkins-Johnson in Palo Alto, CA have designed a developmental EBS amp that produces more than 500 watts in L-band.

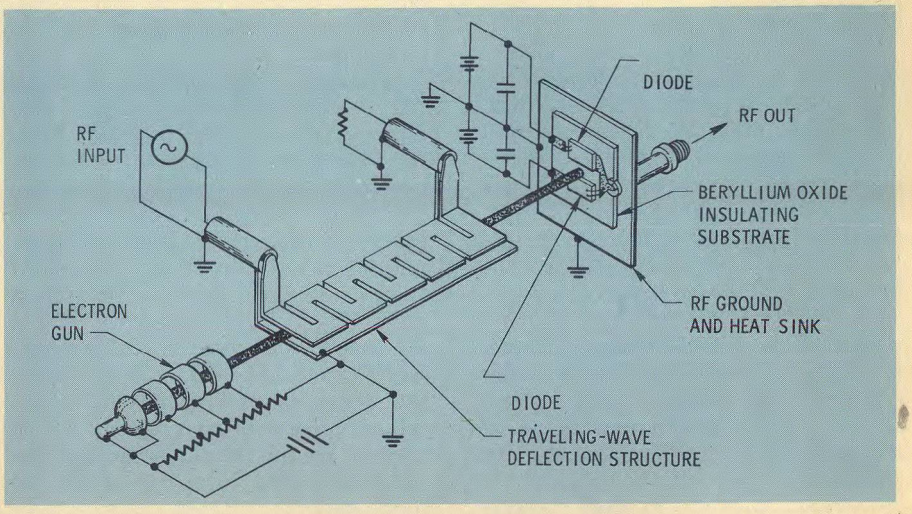
"The maximum output power obtained at 1.5 GHz is 520 W at 0.1% duty and 250 W at 1% duty. At the 500 W level, the saturated gain is 23 dB and the small signal gain is 29 dB. The 3 dB bandwidth is 106 MHz or about 6.8%," details James A. Long., a member of the technical staff of W-J's power tube department.

EBS amplifiers are hybrid devices that combine an electron-gun assembly, traveling-wave structure, semiconductor targets and an output coupling network within a single vacuum envelope (Fig. 1). "We're developing them because they offer significant advantages over triodes and solid-state devices in terms of power-bandwidth product and gain linearity," the W-J researcher notes.

W-J's EBS device, announced at the 1974 International Electron Devices Meeting, amplifies the current flowing though a pair of silicon diodes by belting them with a 20 kV electron beam. Before striking the semiconductor targets, the electron beam is modulated by passing it through a broadband meander-line structure. Here, an rf input deflects the beam and produces linear modulation.

Four years ago, a 400 W, 100 MHz EBS amplifier drew a lot of attention ("Hybrid tube-semiconductor device developed as high power amp", MicroWaves, February, 1971). The ability to get better performance at more than 10 times the frequency is largely due to the development of an improved output tuning circuit, Long indicates.

"The new amplifier uses a novel diode interconnection circuit which connects two diodes in rf series while they are biased in dc parallel (Fig. 2). Operation of the diodes in rf series is an advantage since the reactance level of a typical high-power diode is only a few ohms at microwave frequencies. By connecting two or more in series, it is possible to increase the load impedance into which the circuit will operate efficiently," he says.



1. EBS devices use a traveling-wave structure to modulate an electron beam. Bombarding the semiconductors with the modulated beam causes a current multiplication of approximately 2000:1.

Both diodes are isolated from ground and from each other by quarter-wave chokes, while two-radial line resonators and a coupling capacitor provide an impedance match to the 50-ohm output line.

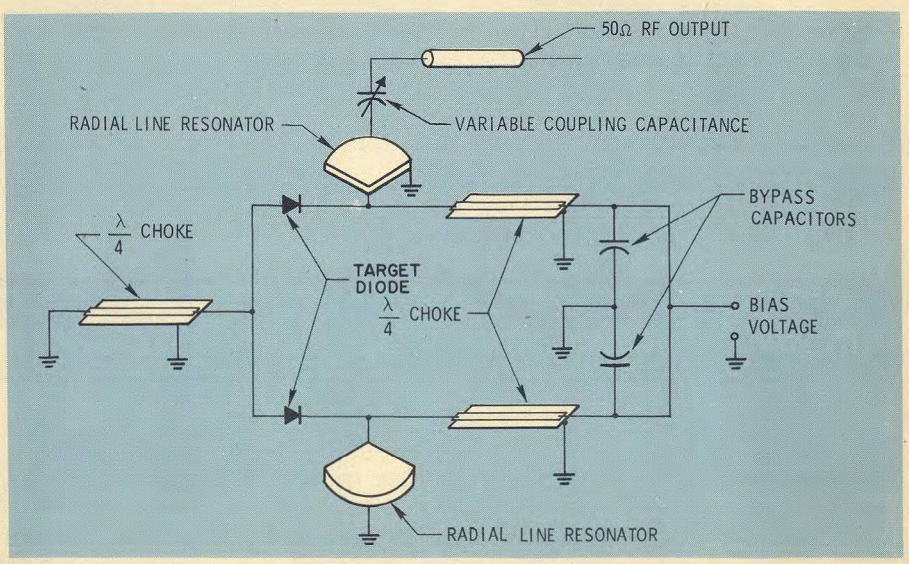
"The sectorial, radial resonators were designed by a combination of computer-aided and empirical procedures. The outer radius and coupling capacitance were determined by trial and error in a computer program to achieve the center frequency of 1.5 GHz, and the center frequency resistance of 10 to 15 ohms," Long explains.

Laboratory tests showed an unloaded resonator Q of 800.

Production problems cited

What remains to be done before this developmental design can be translated into practical hardware?

(continued on p. 12)



2. The development of an effective target tuning circuit was the key to high-power, gigahertz performance.

news

NY crime fighters now using laser beams for fingerprint identification

Howard Bierman
Editor/Publisher

Latent fingerprints left at the scene of a crime in New York City will now be rapidly scanned, coded and matched by a semi-automated system involving a laser beam technique. New York Police Commissioner, Michael J. Codd, recently announced this latent fingerprint system, designed by the McDonnell Douglas Electronics Co., that combines microfilmed suspect prints with a laser beam arrangement to provide data processing of keypunch input with optical scanning of fingerprint images at a speed of four comparisons per second.

"Prior to this system, single fingerprints had to be manually scanned, coded and matched against N. Y. City's Police Department's active file of over 130,000 major crime offenders," explained Dr. Marvin Berkowitz, Director of Applied Technology for the Police Department.

Matched filter correlation key to system

Matched filter correlation, using coherent optical processing techniques, is the heart of the latent fingerprint identification system. The optics approach offers several advantages over an all-electronic system: (1) there is no need to examine each fingerprint and describe the video wave-form prior to processing, (2) the optical approach permits simultaneous comparison of multiple fingerprints in a library file with the latent fingerprint and (3) a complex mathematical process can be implemented with a relatively simple set of equipment.

Basically, the optical matched filter correlation technique produces a measurable physical quality (light intensity) which is proportional to the similarity of the fingerprints being compared. In other words, if a latent fingerprint were to match a fingerprint in the library file, a maximum amount of light intensity would be produced when both prints were super-imposed. A non-matching fingerprint, compared to the latent fingerprint taken at a crime, would block some of the light and less intensity would be measured.

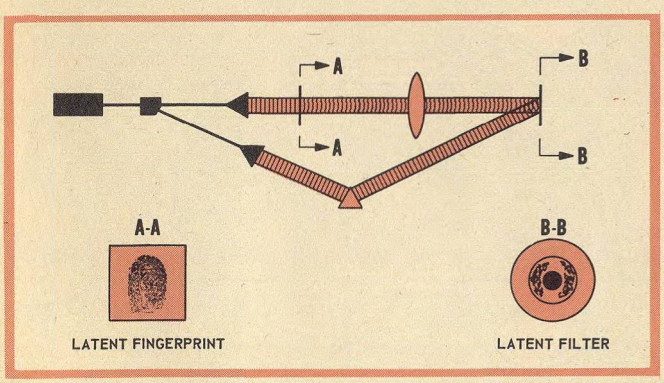
The Fourier transforming property of lenses forms the basis of the design of the electro-optical system. If a photographer transparency of a two-dimensional pattern (such as a fingerprint) is placed in the front focal plane of a lens and illuminated by a collimated right beam (laser), the light pattern which appears at the back focal plane of the lens is a Fourier transform of the input pattern. The inverse Fourier transform of the product of the two Fourier transforms (one from the latent fingerprint at the crime, the second from the library file), is a direct measure of the similarity and is the correlation function. By this technique, the electro-optic system can sort out of a library file those fingerprints that are most similar to the one being checked.

Microfilm transparencies of latent and library fingerprints are used to introduce them into the system for comparison. In the comparison process, the inverse Fourier transform of the product of the Fourier transforms of the fingerprints being compared is measured and probable matches are determined. This is accomplished by:

- Recording an interferogram of the Fourier transform of the latent print on photographic film, which provides a latent filter.
- Illuminating this filter with the Fourier transform of the library fingerprints.
- Focusing the light emerging from the filter.
- Measuring the peak intensity of the focused light to determine the correlation or degree of match between the fingerprints.
- Repeating the comparison process with each suspect contained in the library subfile and selecting those which exhibit the highest correlation as the most probable matches.

The Fourier transform of a fingerprint transparency is produced by an interferometric technique. A beam of light from a laser is split into two beams which are then separately filtered and collimated, Fig. 1. The lower beam (reference) is redirected by a prism to intersect the top beam (signal) at plane B-B. A Fourier lens is positioned in the top beam

(continued on p. 12)



1. An interferometric technique is used to develop a Fourier transform at the back focal plane (B-B) from a fingerprint transparency placed at the front focal plane of the lens (A-A).



2. The McDonnell Douglas latent fingerprint system costs N. Y.'s Police Dept. $300,000 largely covered by a federal grant from the Law Enforcement Assistance Administration.

NY crime fighters now using laser beams for fingerprint identification (cont.)

(continued from p. 10)

so that its back focus corresponds to the beam intersection (B-B). A microfilm of the latent fingerprint is placed in the top beam at the front focal plane (A-A) of the lens, causing its Fourier transform to appear at the back focal plane. Unexposed film is placed at B-B, and the interferogram is recorded. The bottom (or reference) beam is required to enable both phase and amplitude of the signal beam to be captured on film.

In the comparator section, a beam of light from a laser is expanded and passed through a microfilm aperture card containing the library suspect fingerprint to be compared with the latent fingerprint. The library aperture cards are sequentially placed in the front focal plane of a simple lens at a rate four per second by a card handler. The latent filter of the unknown fingerprint is placed at the back focal plane of the lens and resultant output of the filter is the product of the library and latent fingerprint Fourier transforms. The intensity of the resultant point of light is the desired correlation value of the fingerprint.

During the evaluation of each library aperture card, the average diffraction efficiency of the entire card is measured. This information is used by the video processing electronics and decision logic to evaluate that card for probably match. Also, the latent fingerprint filter is rotated during the evaluation process to compensate for the angular orientation difference between the library and latent fingerprints. The correlation light energy is a function of proper orientation between the fingerprints being compared. ••

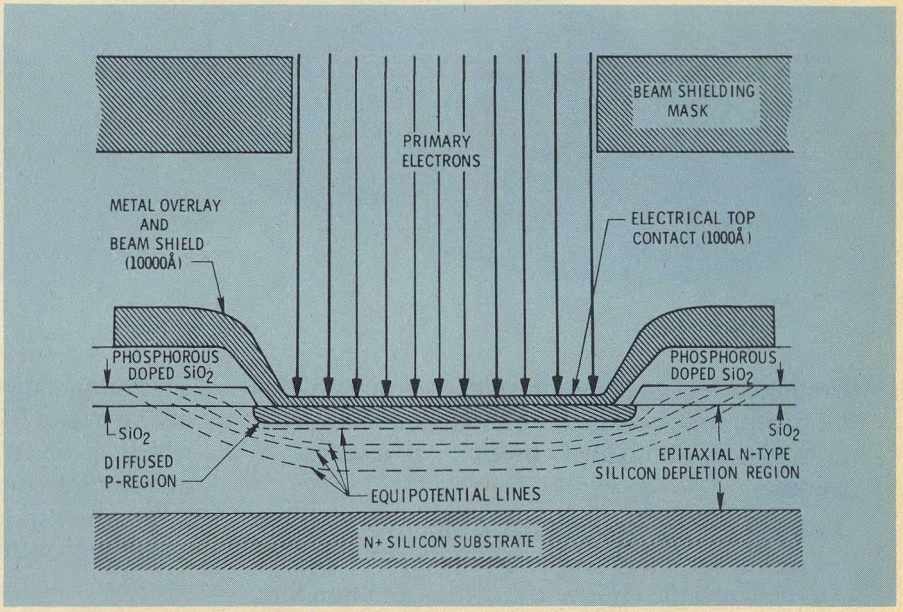
L-Band EBS amplifier belts out 500 W (cont.)

(continued from p. 9)

"We have some simplification that has to be done in the mechanical design, but I think that the principal thing that we have to do is develop a reliable target diode," Long comments.

The semiconductor targets have an epitaxial, n-type, silicon depletion region on top of an n+ silicon substrate (Fig. 3). A diffused P-region is covered by a thin aluminum top contact and is surrounded by a thick aluminum overlay which serves as a beam shield and an electrical contact. The metal overlay is separated from the depletion region by a layer of thermally-grown silicon dioxide and a layer of deposited phosphorous-doped glass to provide passivation and increase the reverse voltage breakdown. The depletion region is approximately 17 microns thick and has a resistivity of 10 ohm-centimeters.

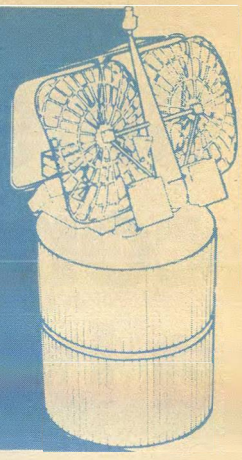
In operation, a copper beam-shield is placed in front of the diodes allowing electrons to strike the active area without bombarding the peripheral silicon and metal overlay.



3. The semiconductor targets have an active area of 2.5 x 1.0 mm. A beam shielding mask protects the peripheral silicon and metal overlays.

Although the diode targets for the developmental tube were fabricated by the Signetics Corporation, Long says that W-J is currently developing an in-house production facility. ••

Even if you filled out a card recently, YOU MUST RENEW NOW for a 1975 MicroWaves subscription. See card inside front cover.



Satellite communication: The search for more bandwidth

Richard T. Davis
Managing Editor

How to get more channel capacity for the dollar appears to be the major thrust for the next group of domestic satellites planned for launch in 1976. Typical of this thinking are the vehicles being developed by Comsat General for AT&T and by RCA Globecom. Both satellites will be using polarization diversity to effectively double their channel capacity while still only using the 500 MHz bandwidths available at the 4 and 6 GHz satellite bands. By using orthogonal linear polarization to achieve frequency reuse, the satellites will be able to carry 24 transponders, each providing 1200 voice grade circuits or twice the capacity of Western Union's Westar and the Canadians' service via Anik.

Polarization diversity isn't new to communications—at least terrestrial communications. "It's long been used on AT&T's TD and TH microwave radio links but without spectrum overlap," says Lance Froome, Member Technical Staff, Satellite Systems Engineering Department, Bell Labs, Holmdel, NJ. "But for satellite communications, using overlapping channels, the design is unprecendented. It will be essential that the antennas at both the ground terminals and in the satellites be capable of generating nearly perfect orthogonal polarizations. The design problems to accomplish this differ considerably, however, depending on whether it's the antenna on the satellite or at the ground station. For the ground station antenna, it's essential to maintain the polarization purity only at the peak of the narrow pencil beam and over the tracking beamwidth. The real problem at the earth station is compensating for Faraday rotation resulting from the magnetic fields that encompass the earth. The orientation of polarized signals passing through the ionosphere is affected by these slowly varying magnetic fields which must be tracked and compensated for.

On the other hand, the spacecraft must maintain polarization purity over the entire shaped beam—about a 3 degree x 7 degree contour. To do this polarization, selective reflecting or transmitting surfaces consisting usually of either parallel grids of wire or grating strips are used. Because wideband feed designs are involved to provide the desired earth coverage, gain and coverage contours are not optimized for each individual frequency band."

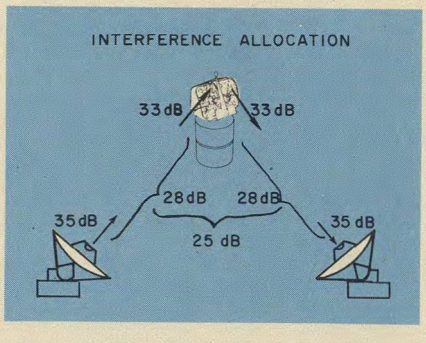
AT&T, who probably has the greatest interest to develop additional bandwidth capacity, is also looking into using higher frequencies for satellite communications. But the question remains whether these bands are practical in view of the high signal attenuation that occurs in heavy rain. To improve upon the sketchy statistics available on rain depolarization and attenuation, the Comsat General domestic satellite for AT&T services will incorporate a centimeter wave beacon experiment. With this advanced all solid-state package, AT&T hopes to be able to determine more precisely the outages at an earth station from heavy rain; and what design margins are needed to overcome losses.

Maintaining isolation between overlapping channels

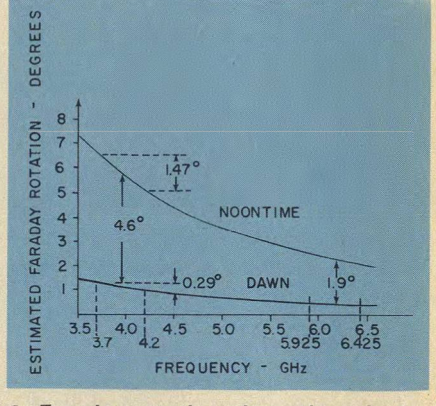
In selecting polarization diversity, both the RCA and Comsat/AT&T satellite systems need to provide an overall system polarization isolation of about 25 dB to maintain the required isolation between channels.

The budget for the AT&T system, Fig. 1 requires 35 dB polarization isolation at the earth stations and 33 dB at the satellite, resulting in 28 dB for each up and downlink and 25 dB overall. "This calls for a very sophisticated feed-design and a considerable hardware effect," explains Froome. "Independent rotation of transmitted and received polarizations requires a rather complicated waveguide system, while the polarization correction networks ($\Delta\phi$, ΔR) are based on recent theoretical work at BTL. As a result of the interference allocation, we're shooting for a 40 dB polarization isolation spec as a goal for the 30-meter antennas at

(continued on p. 16)



1. **To double capacity through frequency reuse,** an overall system polarization isolation of 25 dB is required. The interference from the three main sources are shown. Interference mechanisms in the antennas result from non-symmetries. In contrast, an Intelsat satellite only requires 14 dB of polarization isolation.



2. **Faraday rotation alters the orientation of linearly polarized signals** as they pass through the ionosphere. Maximum daily rotation is maximum during the day. It then subsides at cooler temperatures just before dawn. This graph does not include the effects of solar flares.

the ground terminal. We'll also have to be tracking the Faraday rotation." Since it is difficult to tell what rotation has taken place in the uplink, it was found necessary to monitor the misalignment in the downlink and intentionally transmit the signal to the satellite "crooked". The polarizations of the two signals must be received correctly because there is no way to compensate for the uplink Faraday rotation in the satellite.

Another problem in handling Faraday rotation arises from the fact that it is frequency sensitive, Fig. 2. "Our best theoretical estimates are that in the middle of the 4 GHz band, the orthogonal polarization can shift 4.6 degrees every day while at 6 GHz, the daily change is about 1.9 degrees," says Froome.

"If these effects were not compensated for, the results would be intolerable and would totally destroy the cross-polarization isolation." For example, interference due to angular misalignment is 20 log sin Θ. For a misalignment of only one degree, isolation drops to 36 dB and if the orthogonal signals are off by 4.6 degrees, only 22 dB of isolation is theoretically available. "It's, therefore, necessary that we track this misalignment to within 0.1 degree, by detecting and nulling the unwanted polarization."

To correct for polarization misalignment, Bell Labs has, therefore, developed a feed which incorporates a half-wave plate on a rotary joint controlled by a Faraday tracking system, Fig. 3. The Faraday tracking system is based on cross-correlation techniques. As the incoming vectors change, the half-wave plates shift to keep the signal aligned with the feed's output.

However, this is only part of the problem. "To obtain the 40 dB isolation, we need to tune the antenna," continues Froome. The vertical and horizontal signals as received are both eliptical and non-orthogonal. To clean them up, differential phase and attenuation elements ($\Delta\phi$ and ΔR) are used. Effectively they serve as conjugate

U.S. domestic satellites: what's up—what's going up?

Presently, there are two domestic satellite systems in orbit, Western Union's Westar and Telsat Canada's Anik. Each has two operational satellites in orbit. Both were built by Hughes Aircraft and are similar in design carrying 12 transponders with an average capacity of 7,000 two-way voice channels. RCA Globecom presently is leasing a transponder on Anik II and American Satellite Corporation is leasing two transponders on Westar I.

Both RCA Globecom and the AT&T/Comsat General domestic satellites, once they become operational, will provide double the channel capacity over their predecessors. These new entries in the U.S. domsat race are planned for launch in early 1976 and should begin service by late 1976. By using polarization diversity, 24 transponders are available, the equivalent of 14,400 voice channels.

The RCA Satcom System will consist of three 24 rf channel satellites in synchronous orbit and a series of earth stations to serve the U.S., Hawaii and Alaska. The RCA satellite Fig. A, being built by RCA's Astro Electronics Division, Hightstown, NJ, will use a three axis attitude-control system rather than the more common (and proven) spin stabilized system to keep the antenna pointing at the earth.

AT&T and GTE Satellite Corporation have petitioned the FCC to combine their satellite operations. Present plans include eight earth stations and three synchronous satellites providing coverage to the continental U.S., Alaska, Puerto Rico and Hawaii (Fig. B). The three satellites, being built by Hughes Aircraft will be placed in synchronous orbit by Comsat General, a subsidiary of Comsat, who then will lease the satellites to AT&T, and as proposed to General Telephone and Electronics Satellite Corporation (GSAT).

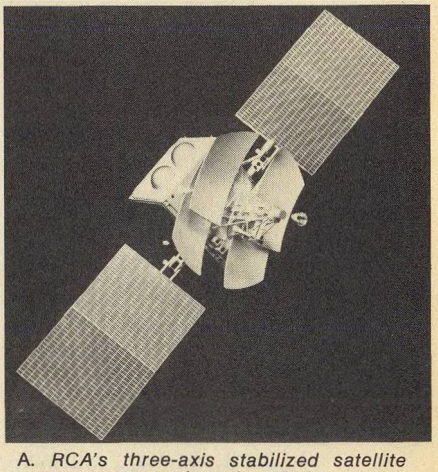
Th remaining entry in the U.S. domestic satellite plan is a proposed merger of Comsat General with IBM Corporation who wants to buy into the CML Saellite Corporation; now the property of Comsat, MCI Communications Corporation and Lockheed Aircraft. This merger is presently under scrunity by the Justice Department and the FCC. Western Union, among others, is contesting the venture on grounds that "the combination of Comsat General and IBM could form an impenetrable barrier to competition."

Comsat AT&T satellite design

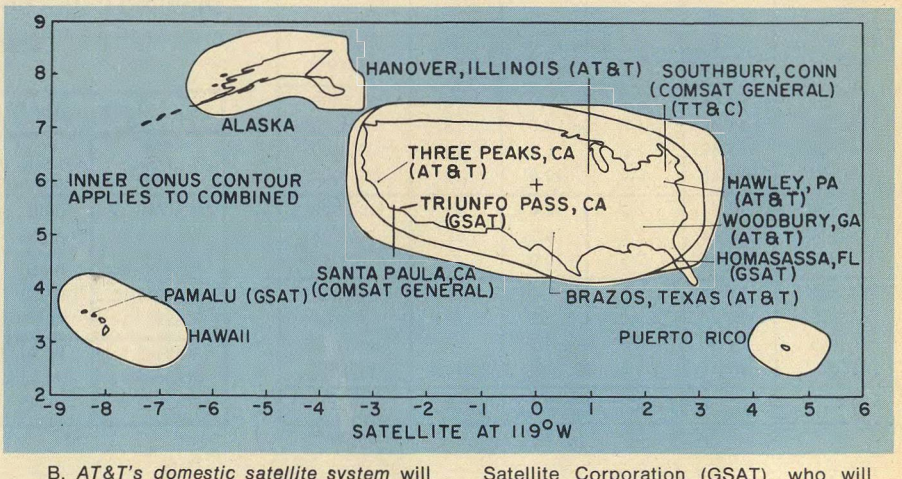
Like RCA's satellite, the AT&T/Comsat General domestic satellite consists of 24 transponders each operating in the 6/4 GHz band. When the system is fully loaded, 14,400 two-way telephone circuits will be available from each satellite. The diversity technique consists of transmitting vertical and horizontally polarized orthogonal signals to and from the satellite. All the vertical repeater channels receive from the combined Alaska and CONUS areas, while all the horizontal channels receive from the combined CONUS, Hawaii and Puerto Rico areas. Received signals are translated in frequency by 2225 MHz and retransmitted with the same polarization orienation. As shown in Fig. C, signals from the odd horizontal channels can be switched into either the CONUS or Hawaii spot beams. Similarly, the even horizontal channels can transmit to either CONUS or Puerto Rico. The even vertical channels can be switched in one of three ways: All power to CONUS, all power to Alaska or power divided between them. All power from the odd vertical channels is transmitted through the CONUS spot beam.

Two orthogonal (perpendicular) polarized offset parabolic reflector antennas are used measuring about 1.3 m x 1.8 m. Each has a multi-horn feed array to achieve the needed beam shapes for earth coverage and a polarization grating as shown on this months cover. The transmit gains (in dB) when added to the TWT power, yield a minimum EIRP of 33 dBW for spot beam coverage and 31 dBW for the combined service to Alaska and CONUS.

The vertically-polarized feed assembly consists of five offset feed horns and separate feed networks for transmit and receive. The feeds are mounted below to avoid blockage. Two feed horns are used to form the Alaska beam and three are used to form the CONUS beam. "The design of the vertically-polarized antenna was a bit more difficult than the horizontally-polarized antenna," explains Roger Rusch of Hughes Space and Com-



A. *RCA's three-axis stabilized satellite* measures approximately 5.3 ft x 4.1 ft x 4.1 ft and its orbiting weight is about 1,000 lbs. A telemetry horn antenna appears at right.



B. *AT&T's domestic satellite system* will consist of three stationary satellites (two operating and one for backup or for sun transit). The five AT&T earth stations are located at Hawley, PA; Woodbury, GA; Hanover, IL; De Luz, CA and the San Francisco area. GTE Satellite Corporation (GSAT), who will use some of the communications capacity, will have terminals in Hawaii, Florida and near Los Angeles. The telemetry tracking and command (TT&C) ground stations on the East and West Coasts are run by Comsat General.

matches to the imperfections inherent in either the satellite or earth station antennas.

The feed system, Fig. 3, being built by Ranatec Corporation, Calabassas, CA, does introduce a slightly increased insertion loss of about 0.2 dB—over systems without polarization diversity. For example, an Intelsat ground terminal feed without polarization equipment has about a 0.2 dB insertion loss operating into a 17-degree K low noise receiving system. This results in an overall station temperature of approximately 60°K. "The additional 0.2 dB will increase the overall station temperature to 79 degrees K (at a 20 degree elevation angle)," says Froome. This results in a slight degradation in G/T, "but we elected to take the loss in exchange for the cross-pole. We think the price is right when you consider we've doubled channel capacity."

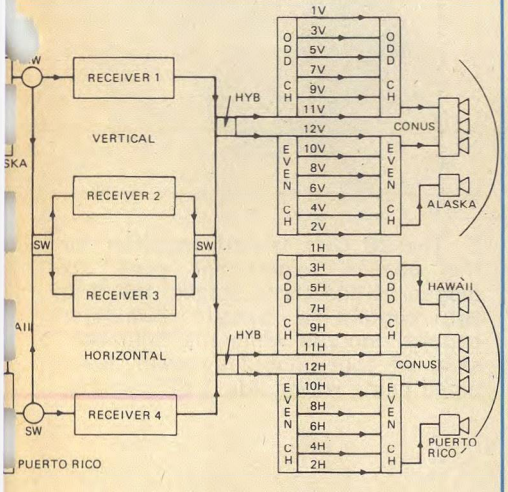
Bell Labs has tested the feed at Hughes Aircraft's cassegrain antenna facility in Glenwood, AR, and it has obtained some fairly encouraging results. The on-axis cross polarization is better than 40 dB, well within specifications. The cross-pole lobe structure allows a tracking error of more than ±0.016 degrees for the earth station's narrow pencil beam (3 dB beamwidth is 0.16 degrees at 4 GHz). This is important in case the earth station's 30 m antenna is moved off axis; for example by strong winds.

Interleaved channels important

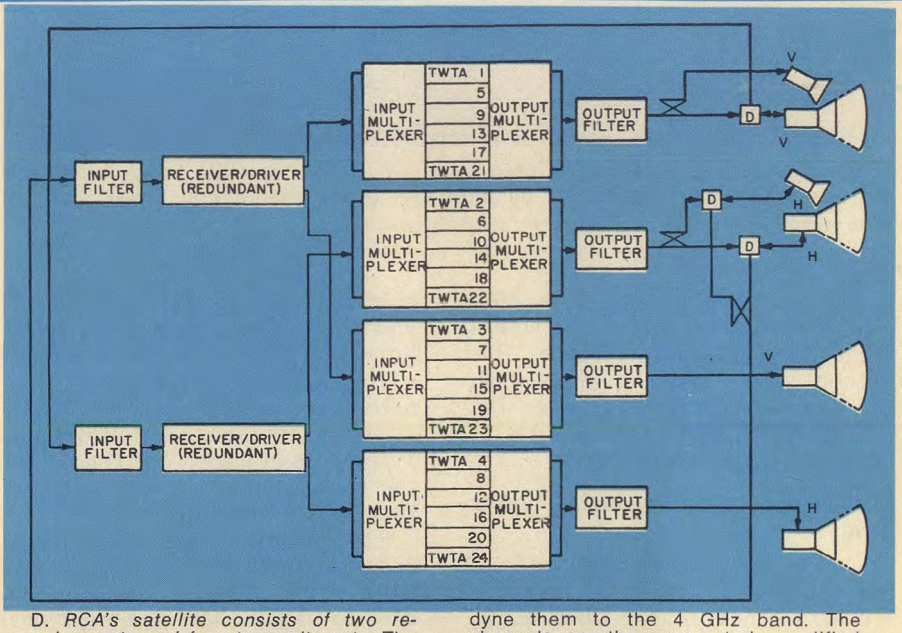
Another factor on why it's possible to achieve this polarization isolation between signals is the manner in which the channels are interleaved. According to Roger Rush of Hughes' System Engineering Department, El Segundo, CA, the spectrum is separated into 24 channels, 12 vertically polarized and 12 horizontally polarized, Fig. 4. Each 36 MHz channel is spaced 40 MHz apart resulting in 6 MHz guard bands.

"The guard band compliments the polarization isolation inherent in the antenna design," says Rusch. "For example, an overall noise budg-

(continued on next page)



C. *In the Hughes' satellite for Comsat/AT&T,* any two of four TDA receivers may be used (receivers 1, 2 or 3 with horizontal channels and receivers 4, 3 or 2 with vertical channels). Twelve 5 W TWTAs are used for the horizontal repeater and twelve 5.5 W TWTs for the vertical repeater (because of the lower gain from the vertical antenna).



D. *RCA's satellite consists of two receive ports and four transmit ports.* The receive ports, one for each polarization, amplify the two groups of odd and even-numbered channels and heterodyne them to the 4 GHz band. The channels are then separated, amplified in TWTs, and then collected into four groups of six channels by output multiplexers.

munications Group, El Segundo, CA. Essentially its a matter of not being able to place them in an optimum position in front of the reflectors because of lack of space. For example, the CONUS beam requires three feed horns but unfortunately, the optimal positions for the feeds overlap due to their physical size. "As a result, we get suboptimal performance on the vertical antenna. Because the CONUS horn array illuminates the reflector with less efficiency, transmit gain for the vertically-polarized antenna is 26.5 dB at 4 GHz vs 27 dB for the horizontally-polarized antenna. To handle this problem, Hughes' engineers have used 5.5 W TWTAs in the vertical channels vs. 5 W tubes in the horizontal channels. For receive, the vertical antenna has a gain of 24.5 dB because it has more area to cover.

The horizontally-polarized feed assembly consists of six feed horns and separate feed networks for transmit and receive. These feed horns are arranged to form beams for CONUS, Hawaii and Puerto Rico.

The polarization grids, which consist of conductive strips on a dielectric in front of the reflectors, can, in practice, reduce the polarization interference level to −33 dB. The strips are one inch wide and 0.5 inch apart. They are mounted to a rigid frame which is bent to form a 50 inches by 70 inches inside diameter.

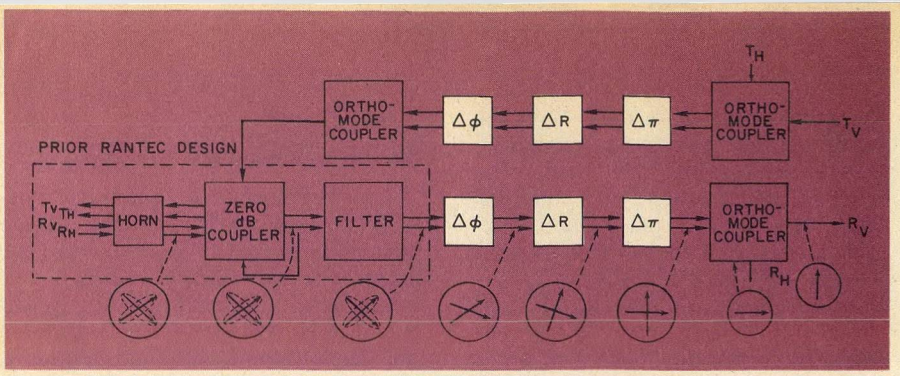
RCA's design

The antenna compliment on the RCA satellite, Fig. D, consists of four separate grated reflectors with offset horns mounted on the earth-facing platform. Two of the antennas generate vertically-polarized beams covering Alaska and the continental U.S., the other two produce identical horizontally-polarized beams. According to Robert Miller of RCA's Commercial Sat Com Group/Astro-Electronics Div., Hightstown, NJ, one of each pair operates at 4 GHz only while the other uses a duplexer for transmit operation at 4 GHz and receive at 6 GHz. In addition, feed horns placed off axis on the two western antennas produce beams toward Hawaii.

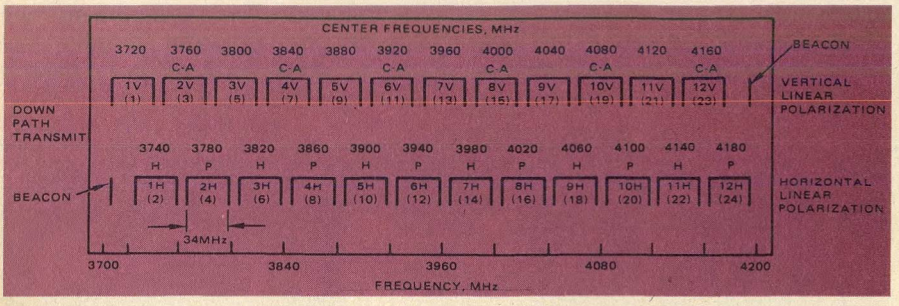
Unlike the Hughes design in which polarization grids are in front of the reflectors, the RCA reflectors are paraboloids of revolution whose surfaces comprise parallel wires embedded in fiberglass. The reflected waves are thus polarized along the wire direction. In addition to the gratings being virtually transparent to the orthogonally-polarized wave, the displacement of the feeds are both lateral and axial, providing the high polarization isolation required. The common parallel axes of all four reflectors are elevated approximately six degrees from the equatorial and the major axes of the reflectors are rotated by 20 degrees in a clockwise direction (looking toward the earth).

Lightweight graphite fiber epoxy components are used for the RCA transponders. "This gives a tremendous weight advantage," claims Miller. "An invar filter weighs about 2.1 lbs vs 0.5 lbs for one using graphite yet their performance is comparable. Also, because a three-axis attitude control is used, the solar arrays rather than being cylindrical consist of two rectangular panels each 7.15 sq. ft continously oriented toward the sun. "This means that only one-third the usual number of the silicon solar cells are required to power the 24 transponders," says Miller. As a result, a lower cost launch vehicle is planned.

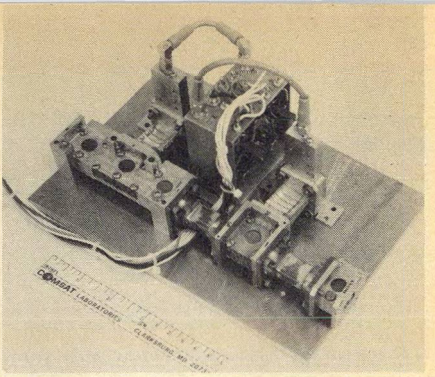
In the contiguous U.S., RCA has located earth stations near New York, San Francisco and Los Angeles. Additional stations are planned near Dallas, Atlanta, Seattle, Denver, Chicago, Washington, DC and Hawaii. Because of Alaska's topographic features, 16 earth stations are planned there. RCA is also preparing to construct and operate receive-only stations primarily for television or other broadband services. □



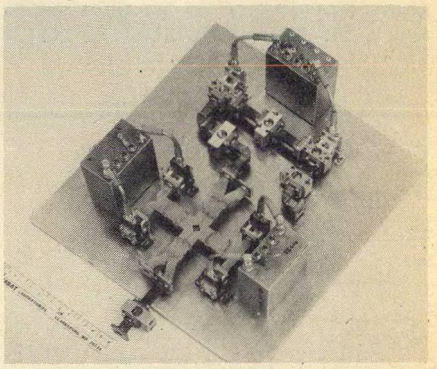
3. **The dual-polarized feed system of the AT&T ground station** uses a λ/2 plate to align the incoming vectors (misaligned from Faraday rotation). To correct antenna assymetrics, differential Δφ and ΔR elements are used to clean up the ellipticity and non-orthogonality of the signals received, resulting in an isolation of 40 dB.



4. **Frequency and polarization plan** for the 6/4 GHz satellite band shows how frequency spectrum is reused by interleaving and orthogonal linear polarization.



5. **Two-stage 19 GHz amplifier** uses Impatt diodes imbedded in circuit modules and coupled to reduced height waveguide to optimize dc-rf efficiency. Each module is coupled to its circulator via a seven section stepped impedance transformer.



6. **The 28 GHz Impatt amplifier** for the beacon experiment uses six diodes. It has three stages; the first two contain a single circulator coupled module while the final consists of four modules power combined using waveguide 3 dB hybrids.

et for the entire systems is 4800 pW. Fortunately, only 1/2% comes from cross-pole interference. But without the 6 MHz guard bands, the cross-pole contribution to the overall noise budget would be at least several hundred pW."

Beacon experiment evaluates higher bands

To test out the feasibility of using the higher bands for satellite service Comsat Labs, Clarksburg, MD, has designed and built two beacons that transmit at 19 and 28.6 GHz.

Their carrier frequencies are derived from a stable-master oscillator at 132.2 MHz and then multiplied up. Specifically, the signal is amplified, frequency doubled and fed to two cascaded transistor triplers, which multiply the frequency to 2.38 GHz. A transistor amplifier boosts the level to +27 dBm (two such oscillator chains are included for redundancy). A hybrid permits either oscillator chain to drive both the 19 and 28 GHz transmitter chain, but only one oscillator operates at a time. In the 19 GHz chain, a two-stage Impatt amplifier (Fig. 5) is used amplify the signal to +29 dBm. In the 28 GHz chain, a three-stage Impatt amplifier (Fig. 6) is used the level from 8.5 to 29.5 dBm.

The two solid-state transmitters are designed to operate for at least two years using excess power available during the early spacecraft operation. The beacon that transmits the 19.04 GHz uses a diode switch to transfer the signal alternately to vertical and horizontal polarized antennas. An ultra-stable 1 kHz oscillator controls the the switching speed. The EIRP of this beacon is 21 dBW.

The other beacon transmits at 28.56 GHz also with 21 dBW EIRP. This carrier is phase modulated to produce two first-order sidebands, 7 dB down at ±264.4 MHz (for the first two satellites) and ±528 MHz (for the third satellite once it is launched).

Two sets of linearly-polarized antennas are used on the satellite. One set is linearly polaried at 28 GHz. The other antenna set is capable of dual orthogonal polarization at 19 GHz. This dual polarized single aperture antenna is essential for phase-coherence measurements planned by Bell Labs. Each set is an array of two linearly-polarized pyramdial horns that are tilted to rotate the polarization angle. A magic tee divides the input power equally to the horns and a grating in the aperture of each horn insures polariaztion purity.

At the ground station located at Bell Lab's Crawford Hill Facility in NJ, the received power will be −98 dBm. The stable master oscillator allows these faint signals to be measured by the receiver because the bandwidth is only 100 Hz at 19 GHz and 150 Hz at 28.6 GHz. Short-term stability is such that 90% of the carrier power is contained in these bands. Long-term drift is less than 1 ppm.

According to Don Cox of Bell Labs Satellite Systems Research Department, Holmdel, NJ, the seven-meter dish being used to recover these signals has a surface tolerance that makes it suitable for frequencies over 100 GHz. This feature allows the antenna to be used for radio telescope purpose as well.

When the beacons are in operation, data will be gathered to determine earth station outage on a statistical basis. Heavy rain, 100 mm/hour or more has been found to introduce 50 dB total attenuation at millimeter frequency, more than enough to knock out any ground terminal. Besides attenuation, depolarization, bandwidth coherency and diversity, effects will also be studied. AT&T is encouraging institutions, universities, etc., to participate in this experiment to provide a good statistical base over diverse climatic regions. ••

r&d roundup

Harvey J. Hindin, Contributing Editor

Smith does it again

One would think that new uses for the Smith Chart, which has been around since 1939, would have been exhausted by now. It's been the subject of countless articles including a comprehensive book by Smith himself. Nonetheless, there are still things that the chart can do—and they are not obscure, trivial or of little interest particularly for transmission line analysis.

The latest use of the Smith Chart developed by R. M. Arnold of Bell Labs is discussed in "Transmission Line Impedance Matching Using The Smith Chart" (*IEEE Trans. on MTT*, Vol. 22, No. 11, pp. 977-978, November, 1974).

Arnold's detailed analysis and illustrative example finds the characteristic impedance and electrical length of a transforming section which converts a complex load impedance to match a real source impedance. Since we do not know the matching characteristic impedance, we cannot plot the load impedance on the chart by the usual methods. The graphical search procedure is a clever way around the problem.

A barrel full of microwaves

Permittivity measurements on dielectric rods at microwave frequencies when done in the classical manner, suffer from having to accurately machine the sample to fit snugly in the closed resonator. Otherwise, air gaps distort the measured resonant frequency. One solution to this problem is to use an open structure, Fig. 1. The spherical-mirror device (a) is ideal for flat sheet samples while for rod shaped specimens the barrel configuration (b) is appropriate.

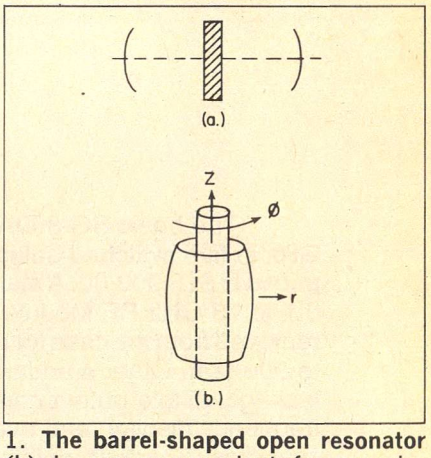
A complete analysis of the resonant frequencies and the cylindrical sample dielectric permittivity has been performed by P. Nagnethiram and A. L. Cullen of University College in London and presented in "A Microwave Barrel Resonator for Permittivity Measurements on Dielectric Rods" (*Proc. IEEE*, Vol. 62, No. 11, pp. 1613-1614, November, 1974).

The authors derive expressions for the desired resonant frequencies for the empty barrel in both E and H modes by two separate methods. In the first technique, the Hermite function form of the axial field variation is obtained from circular waveguide modes using a Fourier integral. The second method uses an approximate solution to the wave equation in prolate spheroidal coordinates, which is then used in a variation method to derive a resonance formula. Unfortunately, neither method is detailed.

The estimated accuracy of both methods is about 0.15%. Twenty-four E modes and 19 H modes are experimentally examined in X-band to verify the predictions. Comparison between theory and experiment is excellent. Equations for the dielectric-loaded barrel are then derived by matching field components across the air dielectric interface. Again, only the results are given.

These transcendental equations are then used to predict rod permittivity from known physical dimensions of the barrel system and the measured resonant frequency with the dielectric in place. Typically, for a dielectric with permittivity of 2.52 at 10 GHz, measured values for different diameter rods differed by about 0.01. The E_{050} mode is used.

Nagenthiram and Cullen close their paper with an error analysis and a discussion of the experimental techniques used to take their data. They also note that the same method may be used to make loss tangent measurements.



1. **The barrel-shaped open resonator** (b) is more convenient for examining cylindrical samples than the spherical mirror structure (a). Both structures have high Q values such that modes off resonance are highly attenuated.

The above mentioned references are available from IEEE, Single Sales Publication, 345 East 47 Street, New York, NY 10017.

◀ READER SERVICE NUMBER 24

MICROWAVES

HIGHLIGHTS OF THIS SECTION:

What's behind the design of a portable spectrum analyzer?...p.36

JANUARY 1975

TEST & INSTRUMENTATION SECTION



Low cost counter offers 1 Hz resolution...p.43

Behind The Design Of A Portable Analyzer

Here is a review of some of the important design problems encountered in building a 2 to 25 GHz Yig-tuned spectrum analyzer and how they were handled.

IMPROVEMENTS in Yig-tuned filters and MIC rf devices have made possible compact wideband spectrum analyzers that rival the performance of units which are considerably greater in size and weight. A case in point is the spectrum analyzer shown in Fig. 1. The unit measures only 5x9x13 inches and weighs 22 pounds, yet provides features such as preselected frequency coverage from 2-25 GHz, 70 dB dynamic ranges, video filtering or pulse stretching for signal enhancement, in addition to the customary sweep and tuning controls normally found on much larger analyzers.

The analyzer was developed for applications where broad frequency coverage, portability and preselection were of prime importance, such as for spectrum surveillance, emi/rfi measurements, and field installation and testing of microwave links or radar transmitters. By choosing the receiver tuning range from 2 to 25 GHz, the majority of radar, satellite communication and terrestrial microwave frequencies in use today or planned future are covered.

This article is not intended to be a tutorial on spectrum analyzer design. It does provide some insight into one solution to several key problems associated with the design of a portable, broad frequency coverage, preselected microwave analyzer/receiver.

Bob Hoss, Project Manager and **Frank Reisch,** Manager, Applied Research Department, Telecommunication Systems Division, Collins Radio Group, Rockwell International, Dallas, Texas 75207.

Features of the receiver

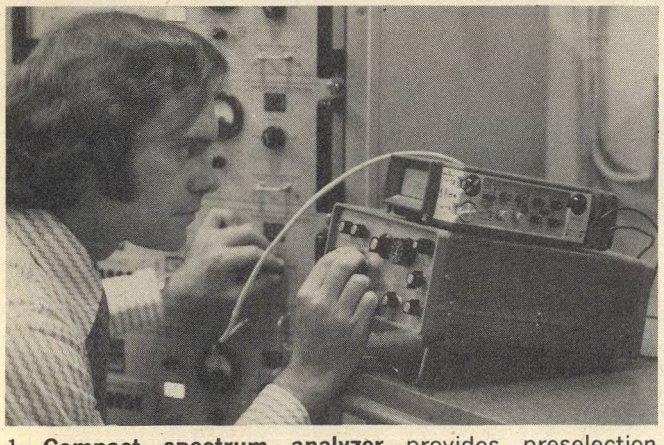
Table 1 summarizes the characteristics of the analyzer. The unit can be either manually tuned or swept over the 2-25 GHz frequency range in 1 GHz increments. The reasoning behind this choice of tuning increments and other features will be apparent later. As shown in Fig. 2, the preselector output is mixed with either the fundamental (in the range from 2-8 GHz) or third harmonic (in the range from 8-25 GHz) of the local oscillator chain output, to produce the first i-f of 425 MHz. A second conversion to 21.4 MHz permits the use of commonly available crystal filters to achieve bandwidths as narrow as 5 kHz. (However, a 50 kHz bandwidth provides adequate sensitivity for the intended applications).

Both am and fm detectors are provided for carrier demodulation. This feature can be useful for many purposes, as for example, to positively identify a signal source when conducting an rfi survey. An operational mode is also included which permits phase locking the receiver local oscillator to an internally-generated reference signal to improve short term stability and reduce the incidental fm inherent in yig-tuned oscillators. Achieving good performance up to 25 GHz requires special attention to problems in three areas—Yig preselector design, the mixing scheme, and tracking of the preselector with the local oscillator.

Preselector design

A Yig-tuned preselector permits a spurious free

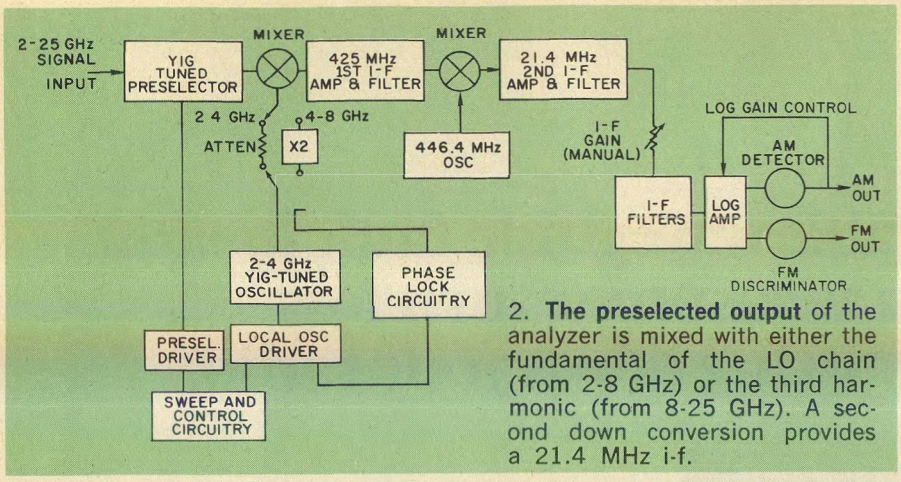
(continued on p. 38)



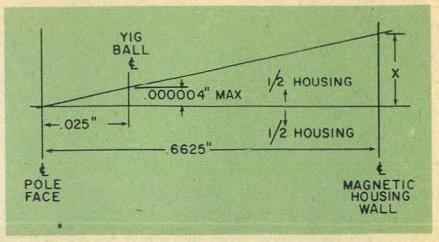
1. **Compact spectrum analyzer** provides preselection over a 2 to 25 GHz band yet measures only 5 in. x 9 in. x 13 in. and weighs 22 lbs.

Table 1. Performance Characteristics

Tuning range	2-25 GHz in 1 GHz Bands
Resolution	50 KHz, 500 KHz, 5 MHz
Log IF range	≃ 60 dB
Dynamic range	70 dB
Image and spurious rejection	≃ 60 dB
Video processing	UNFILTERED 2.5 MHz FILTERED 10 KHz STRETCHED 100 μSEC
Dispersion	FIXED 1 GHz OR VARIABLE 0-250 MHz
Sensitivity (Typical)	−100 DBM 2 GHz TO 8 GHz −95 DBM 8 GHz to 25 GHz
Power required	115 OR 220V (+10-20%) 47-420 Hz 60W NOM
Size	5" x 9" x 13"
Weight	22 LBS



2. **The preselected output** of the analyzer is mixed with either the fundamental of the LO chain (from 2-8 GHz) or the third harmonic (from 8-25 GHz). A second down conversion provides a 21.4 MHz i-f.



3. **The Yig-filter poles** can be ground flat to within $\pm 0.4 \times 10^{-5}$ inch by establishing a grinding plane to within 0.001 inch as shown.

display that simplifies signal identification. Using a Yig-preselector, however, does present some difficulties particularly in good linearity, low hysteresis and the tracking of the Yig resonators over the full 2-25 GHz frequency range.

For uniaxial ferrite Yig spheres oriented with their > 111 > axis aligned with the externally-applied magnetic field, the frequency of resonance is given by:

$$f_{res} = \gamma\ (H_o + H_A) \qquad (1)$$

where γ = The material gyromagnetic ratio
H_o = The extremely applied field strength
H_A = The crystal internal anisotrophy field.

Yig material has a negligible anisotropy field ($\simeq$ 45 gauss), therefore to tune to 25 GHz requires approximately 9000 gauss external field. The first step is then to achieve a magnet design that permits the attainment of that field strength with good linearity and low hysteresis.

For this analyzer design, the best magnet housing material that could be found was an alloy consisting of 47% nickel and 53% iron. This material has a saturation flux level (B_{max}) of 15,000 gauss and a coercive force (H_c) of less than 0.03 oersteds. Initially, there was some concern that adequate linearity could be achieved with a pole gap width that would permit a reasonable size rf structure, since large gaps result in undesired saturation effects with a subsequent loss of tuning linearity. After some experimentation, it was concluded that a linearity of better than ±0.1% overall (2-25 GHz) could be achieved with a pole gap of 0.030 in.—a spacing just sufficient for the rf structure.

If a larger pole gap had been necessary, a magnet housing material having a higher B_{max} would be required. Unfortunately, the materials having a higher B_{max} also have greater hysteresis. For example, a compound consisting of 2% vanadium, 49% cobalt and 49% iron offers a B_{max} of 23,000 gauss, but has an H_c which varies from 0.18 to over 1 oersted depending on how it is annealed. This is unacceptable for filter applications.

While even ±0.1% is still rather large, by tuning the receiver in 1 GHz steps, the tracking errors due to nonlinearities and hysteresis are greatly reduced, and were found to be ±3 MHz for linearity and 8 MHz maximum for hysteresis, over any 1 GHz segment.

The second area of concern deals with resonator mistracking. The ability of the two resonators to track each other over the full tuning range of the filter is related to the parallelism of the pole faces (i.e., the uniformness of the magnetic field). Calculations show that the pole faces must be parallel to within 0.000008 inches in order to keep mistuning to less than 10 MHz over the 2-25 GHz frequency range! This may be determined as follows: For a magnet with a large air gap:

$$H = \frac{0.4\pi NI}{l_g} \qquad (2)$$

where H = the magnetic field strength (gauss)
l_g = pole gap (cm)
N = number of turns on magnet coil
I = tuning current (amps)

Also, the frequency at which the yig sphere resonates is approximately

$$f_o = 2.8H \qquad (3)$$

where f_o = the resonant frequency in MHz

Substituting Eq. (2) into (3) yields

$$f_o = \frac{3.519NI}{l_g^2}\ (\text{MHz}) \qquad (4)$$

To determine the sensitivity to change in pole gap, the derivative of Eq. (4) is obtained with respect to l_g;

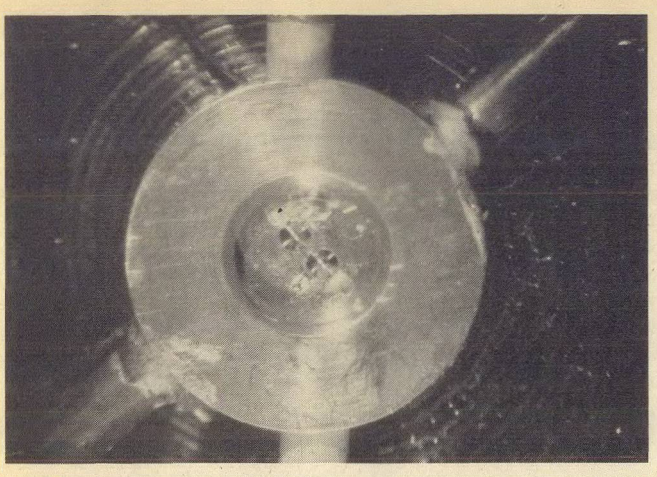
$$\frac{df_o}{dl_g} = \frac{-3.519NI}{l_g^2} \qquad (5)$$

Measuring a variation of 0.000008 in. is difficult unless interferrometer techniques are used. To avoid this, an indirect method is possible. By turning the filter housing about a centerline through the poles, and indexing off the walls of the housing, a grinding plane can be established to better than 0.001 in., which is the accuracy required to assure that each pole face is that to within 0.000004 in. As shown in Fig 3, this can be accomplished by using similar triangles:

$$\frac{X}{0.6625} = \frac{0.000004}{0.025}\ ;\ X = 0.00106\ \text{in.} \qquad (6)$$

This 0.001 dimension is easily measured.

The rf portion of the filter is shown in Fig 4. Based on an overall receiver maximum bandwidth requirement of 5 MHz, and considering all sources of preselector /LO mistracking, a minimum preselector bandwidth of 25 MHz was found necessary. The design procedure of Ref 1 was followed to establish the necessary coupling loop sizes for a 30 MHz minimum design bandwidth. Insertion loss of the final filter typically measured 3-4 dB and its bandwidth varied from 30 MHz at 2 GHz to 40 MHz at 25 GHz. Figure 5 shows typical filter passband shapes at 2 and 26 GHz. The key to obtaining satisfactory rf performance to 25 GHz is in keeping



4. **RF portion of the Yig filter** shows minute Yig spheres and the rf input band output ports.

circuit physical size to an absolute minimum.

A trade-off among size, weight, and power consumption was made with the result that the final filter design tunes to 25 GHz with less than 500 mA, dissipates less than 1.5 W at 25 GHz, weighs 1 lb, and is approximately 2.4 in. long by 1.5 in. diameter.

Mixer /LO design

Since the initial design objective for the receiver was small size and light weight, the trade-off between using fundamental mixing over the entire frequency range, and harmonic mixing over the higher bands, weighed heavily in favor of harmonic mixing. To use fundamental mixing only would have required a multiplicity of Yig oscillators and switches, which was avoided with the harmonic approach.

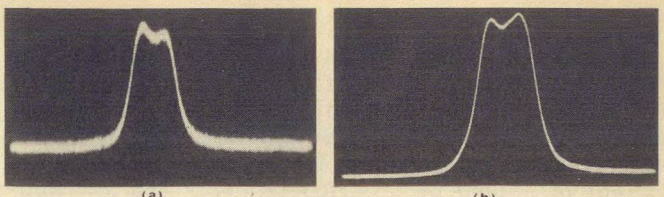
The next step was to obtain a suitable broadband mixer. Neuf[3] describes a double-balanced mixer, having broadband balun transformers on both the RF and LO ports, which permits the achievement of low conversion loss ($\simeq$8dB) over the full 2-25 GHz frequency range. Since a balanced mixer cannot be used as an even harmonic mixer, a times two frequency multiplier, Fig. 6, is needed in the LO chain to provide a 4 to 8 GHz output from the 2 to 4 GHz Yig oscillator. The resulting mixer /LO configuration shown in Fig 2 provides fundamental mixer operation from 2-8 GHz and third harmonic operation from 8-25 GHz.

The final receiver front end design yields a tangential sensitivity (using 50 KHz IF bandwidth) of -100dBm, typically, from 2 to 8 GHz, and -95dBm from 8 to 25 GHz. The maximum signal level into the receiver before saturation is -30dBm, yielding a 70dB dynamic range. A 70dB range i-f attenuator is provided, as well as an i-f long range of 60 dB.

Preselector and Local Oscillator Tracking

Besides the design of the 2-25 GHz preselector and mixer/LO chain, the third major consideration in this design is to minimize the mistracking between the preselector and local oscillator. If appreciable mistracking occurs, a loss of sensitivity results.

Magnetically tuned devices inherently have, depending on material and tuning range, some nonlinearity, hysteresis and retentivity, and a relatively slow response time due to magnet coils inductance. There is also a problem of drift with temperature due to both self heating and changes in ambient temperature. It is desired that this analyzer operate over a range of



5. (a) **Noisy filter passband** at 2 GHz results from lower signal generator level used to avoid limiting in filter. The 3 dB bandwidth is 30 MHz. (b) The 3 dB passband at 25 GHz is 40 MHz.

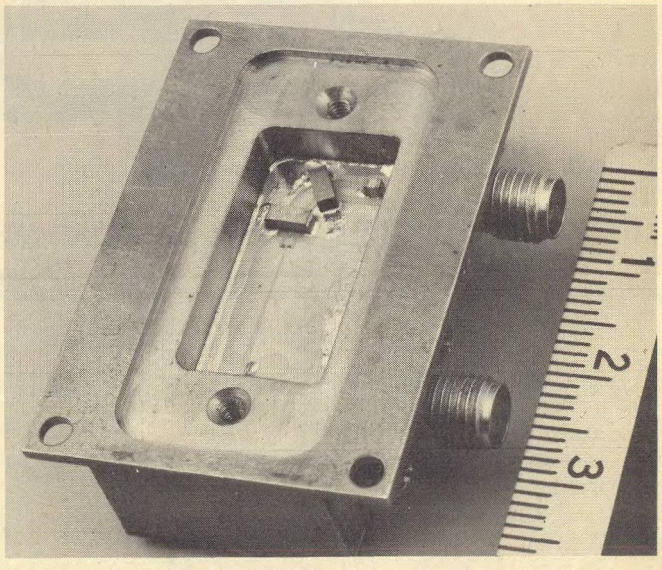
$-20°$C to $+55°$C, creating a need for stiff controls on frequency drift with temperature. The drift mechanisms are numerous. The Yig devices drift with temperature due to variations in magnet coil resistance, pole gap, and the Yig material itself. Voltage references, component values and semiconductor devices in the driver circuitry also vary with temperature and must be carefully considered in the design of the driving circuitry.

Aside from minimizing preselector and local oscillator linearity, hysteresis problems by proper magnet design and temperature drift by employing heaters if the temperature range is extreme, there are a number of circuit design approaches that may be taken to alleviate the tracking problem over frequency and temperature. In summary, they are:

- Limit the maximum frequency tuning range per band.
- Use low or zero temperature coefficient voltage references.
- Use of large amounts of current or voltage feedback.
- Sense ambient temperature changes and provide compensation.
- Provide dynamic hysteresis compensation.
- Limit power dissipation and provide ample heat sinking.

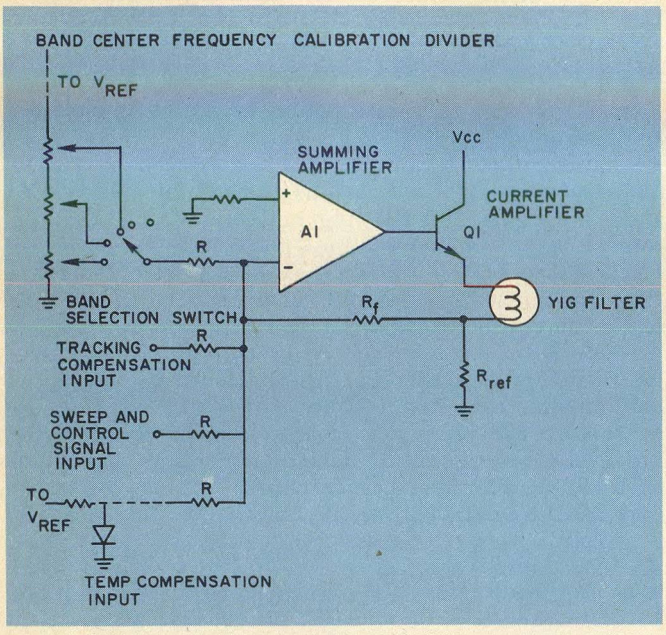
By tuning the receiver in 1 GHz steps, the linearity and hysteresis errors are considerably reduced. A precision, low temperature coefficient resistive divider chain establishes the center frequency of each band, thus piecewise approximating the YIG devices tuning curves.

Currents through the Yig devices are sensed by precision low temperature coefficient resistors in series with each device, and feedback to the driver



6. **Slotline/coplanar doubler** has a conversion loss of only 3.5 dB to 4.9 dB over the 2-4 GHz band.

op-amp minimizes drift due to magnet coil resistance changes. All active devices have been chosen for their low drift characteristics and large amounts of feedback have been used to stabilize the operating point. All critical summing and reference resistors and voltage references have a temperature coefficient of 1 ppm or less. All trimpots are low temperature coefficient cermets.



7. **Yig-driver circuitry is designed to minimize drift.** The summing and reference resistors and voltage references have a temperature coefficient of 1ppm or less.

Ambient temperature compensation is provided by a temperature controlled voltage source which uses a silicon diode as the temperature sensing element. A diode offers a relatively linear change in forward voltage with temperature. The sensor is mounted in the rf module with the Yig preselector.

Power dissipation has been limited to 3-5 watts per module. All major power dissipation devices, such as the Yig device driver transistors and voltage regulators, are attached to the receiver main frame whenever possible, rather than being included within a module. To compensate for dynamic hysteresis, a dual section potentiometer is used for the sweep rate control, with the second section supplying a correction voltage to the preselector which varies as a function of sweep rate.

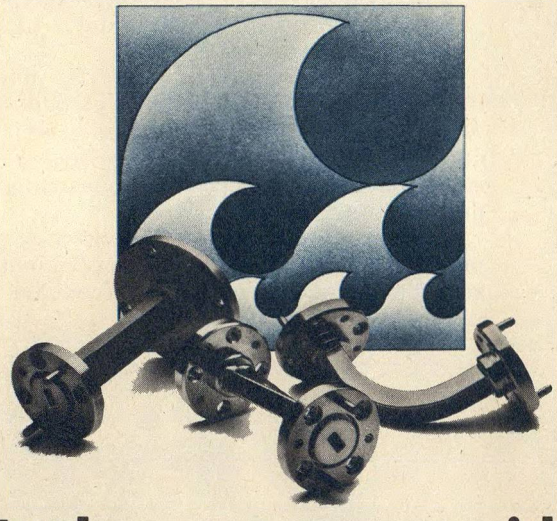
Figure 7 is a simplified schematic of the YIG driver circuitry which incorporates these features. By the application of all these techniques, the mistracking over a $-20°$ to $+55°C$ temperature range is reduced to the order of ± 10 MHz. ••

References

1) W. Venator, "Charting a Simpler Course to the Design of YIG Filters," Electronics, pp. 118-126, (Mar. 3, 1969).
2) J. K. Hunton and J. S. Takeuchi, "Recent Developments in Microwave Slot Line Mixers and Frequency Multipliers," 1970 Int'l Microwave Symposium Digest, pp. 196-199.
3) D. Neuf, D. Brown, and B. Jaracz, "Multi-Octave Double-Balanced Mixer," Microwave Journal, (January, 1973).

Test your retention

1. Why must mistracking between preselector and local oscillator be kept to a minimum?
2. What are the sources of tracking error?
3. Why is a doubler used in the LO chain?



Hughes mm waveguides cut insertion loss to a trickle.

Hughes announces three new series of millimeter waveguide components. E and H-plane bends, tapered transitions, and 45 and 90° twists are precision manufactured to assure minimum insertion loss and VSWR for lab and system applications. All three are available in six standard waveguide sizes in the 26.5 to 110 GHz range.

Call or write: Hughes Electron Dynamics Division, 3100 W. Lomita Blvd., Torrance, CA 90509. (213) 534-2121, Extension 215.

Making waves in millimeter-wave technology.

HUGHES
HUGHES AIRCRAFT COMPANY
ELECTRON DYNAMICS DIVISION

READER SERVICE NUMBER 40

EDITOR—FREELANCE
European Microwave Technology

MicroWaves is seeking a resourceful individual, who can keep abreast of advances in microwave technology in Europe. As a contributing editor, you'll be required to submit edited copy of up to 150 lines per month and meet copy deadlines. Must be capable of grasping the significance of developments as well as an insight for details.

Send resume to: **Richard T. Davis,** *Managing Editor.* **HAYDEN PUBLISHING/MICROWAVES, 50 ESSEX STREET, ROCHELLE PARK, N.J. 07662, U. S. A.**

APPLICATION NOTES

Hall effect helps magnetic measurements

Gaussmeters provide a convenient way to measure the flux density of magnetron assemblies, TWTs or other devices where a permanent or alternating magnetic field is encountered. The heart of these complex instruments is a tiny semiconductor chip acting as a Hall-effect generator.

The basic premise of a Hall generator is simple. When a magnetic field is applied to a semiconductor that is carrying a current, a voltage is developed at right angles to the current flow. Several semiconductor materials are suitable for Hall generation, but Indium Arsenide seems to have outstanding properties, including an extremely low temperature coefficient (approximately 0.04% per degree centigrade).

When using a gaussmeter, it's vital to select the proper probe. Hall-effect generators are packaged in several basic probe styles: flat, transverse, tangential and axial, for example. Two independent probes may be combined to form a differential probe, which is used for simultaneously measuring gradients in a field at two different points.

"Wide Range Guassmeters," a seven-page publication from RFL Industries, Inc., provides some interesting tips about selecting and using these little-discussed instruments. Although heavily laden with products, the brochure gives some insight to the principles and practice of flux-density measurements. **RFL Industries, Inc., Instrumentation Division, Boonton, NJ 07005.**

CIRCLE NO. 204

Are your standards up to snuff?

How often should your laboratory standards be calibrated? Knowing the required measurement accuracy and oscillator drift rate or stability, you could probably find a high-order equation to determine the proper calibration period. Or, you can simply use a nomograph. A handy three-column design-aid is available free, from: **True Time Instrument Co., 429 Olive Street, Santa Rosa, CA 95401 (707) 528-1230.**

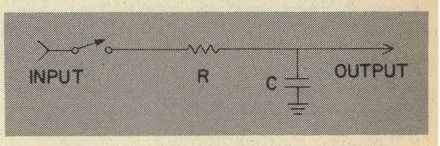
CIRCLE NO. 205

APPLICATION NOTES

Signal buried in noise? Try a boxcar integrator!

It is often necessary to reconstruct an entire waveshape of a repetitive signal buried in noise, or to measure the average value of a small segment of a repetitive signal. There are many sophisticated ways to make these measurements, but one of the most efficient and economical means is by a method called "boxcar signal integration."

A boxcar integrator is essentially a signal processor which uses a narrow filter to reduce the noise with little or no effect on the signal bandwidth. A simple integrator (see Fig.) consists of a gated switch and a low-pass filter. During the time when the gate is closed, the repetitive input signal is applied to the low-pass filter which acts as an integrator. After several pulses have been gated into the low-pass filter, the circuit's output is the average of the signal plus noise when the gate was closed. Since most noise has an average value of zero, the signal-to-noise ratio is improved.



The boxcar integrator is essentially a switched low-pass filter.

In its most fundamental practical form, the boxcar integrator is made up of a sampling oscilloscope, a few capacitors and a voltage-recording instrument. The sampling scope can be used with or without a display, and the voltage recorder can be either an X-Y recorder, an oscilloscope with camera or a storage oscilloscope. The basic principle is the process of controlled sampling and filtering of a repetitive waveform. By setting the rate at which the waveform is scanned and selecting the filter constants, the amount of signal integration can be carefully controlled.

The concept of boxcar integration can be used on almost any repetive signal to reduce or eliminate noise. An application note on the subject, No. 44L1.0 is available from: **Tektronix, Inc., P. O. Box 500, Beaverton, OR 97005 (503) 644-0161.**

CIRCLE NO. 203

Cost-conscious counter provides 1 Hz resolution to 4.5 GHz

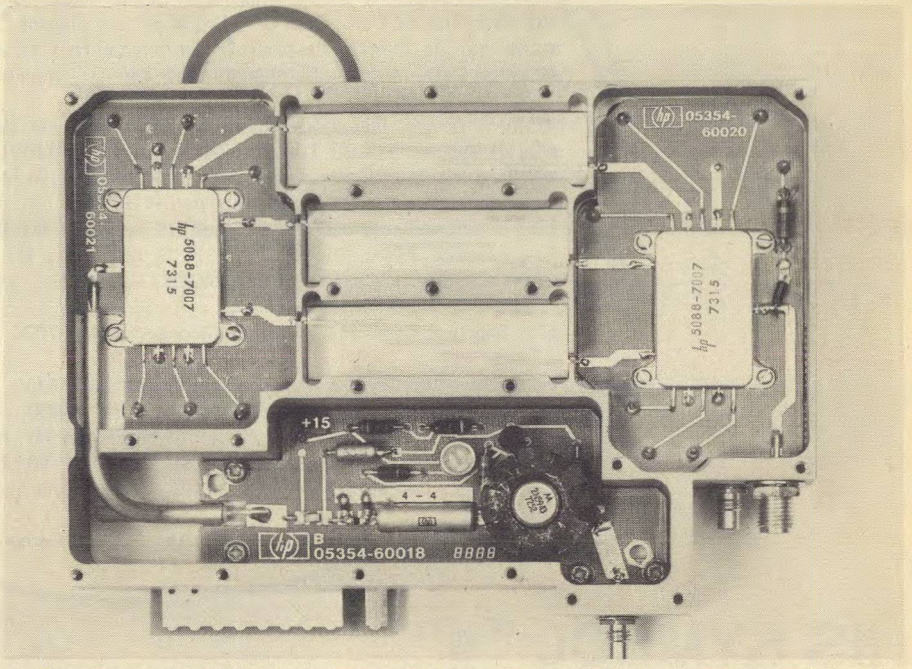
Hewlett-Packard's new 5341A automatic frequency counter offers several original ideas designed to provide a high level of performance at a modest cost. For example:

- Thin-film switchable filters are used to select comb lines for heterodyne mixing. Since the cost of this new technique is proportional to the number of filter sections, the 4.5 GHz counter sells for about $3,600, while a 1.5 GHz model (option 003) sells for about $1,000 less.
- Diagnostic aids allow the user to pinpoint the sources of internal malfunctions directly from the front panel.
- A choice of automatic or manual modes provides an option of searching the entire frequency range for the lowest frequency signal or restricting the search to one of ten relatively narrow frequency bands.
- Compatibility with ASCII codes means that no ancillary equipment is required to tie in with the HP Interface Bus System.

The 5341A's design is a departure from the rest of HP's automatic counter line since it is based on a heterodyne principle instead of a transfer oscillator technique. Midband tolerances specifications of ±250 MHz (max deviation; 0 to 500 MHz, 1.0 to 4.5 GHz) and +125 MHz (500 MHz to 1.0 GHz) are largely due to the counters 500 MHz direct counting ability (Fig. 1). At the band edges, fm tolerance is 30 MHz in the worst case. Even with this high degree of tolerance, sensitivity remains −15 dBm in the automatic mode and −20 dBm in the manual mode.

In the automatic mode of operation, the new counter will measure and display the lowest frequency cw signal within its sensitivity range. But in the manual mode, the operator can elect to search within any of ten frequency bands that cover the counter's full range. This is especially advantageous when attempting to find and measure several signals in a complicated spectrum or for applications where extremely low acquisition times are necessary. Acquisition time is slashed from 600 μs to 100 μs when measuring in the manual mode.

A diagnostic flow chart supplied with the counter guides the user through a self-check procedure that pinpoints failures to a modular level. Troubleshooting simply becomes a matter of observing the binary (zero or one) state of the three display digits that are activated when the internal test switch is thrown. The counter measures 500 MHz in its check mode (in contrast to the usual 10 MHz) in order to test the counting circuitry in a more demanding region.



1. Thin-film switchable filters select the proper comb line for heterodyne mixing. The modular design permits a low cost 1.5 GHz option.

Ten LED digits provide 1 Hz resolution throughout the full range of the counter (Fig. 2). Input frequencies from 50 MHz to 4.5 GHz are channeled in through a 50-ohm type N connector, while inputs ranging from 10 Hz to 80 MHz meet an impedance of 1 MΩ shunted by 50 pF through a BNC port. Sensitivity of the low frequency input is 10 mV and the max input is 5 V peak-to-peak.

The crystal oscillator time base operates at a frequency of 10 MHz. Standard aging rate is less than 1×10^{-7} per month, but an optional time base (option 001) ages less than 5×10^{-10} per day after a 24 hour warm-up. Temperature stability is normally $\pm 1 \times 10^{-6}$ from 0 to 50°C, but option 001 improves this to 7 parts in 10^9.

Other features include an accuracy of ±1 count ± time base error; a front panel variable resolution control, calibrated at 1MHz, 100 kHz, 10 kHz, 1 kHz, 100 Hz, 10 Hz and 1 Hz; and a sample rate that is continuously adjustable from 40 ms to 10 sec and HOLD. Operating temperature range is 0 to 50°C. The counter weighs 10.5 kg (23 lb) and measures approximately 425 × 467 × 88.2 mm (16.75 × 13.25 × 3.5 in.). P&A: model 5341A (4.5 GHz): $3,600: high stability time base (option 001): $500; rear panel inputs (option 002): $105; 1.5 GHz top range (option 003): less $1,000; remote programming-digital output (option 001): $390. **Hewlett-Packard, 1501 Page Mill Road, Palo Alto, CA 94304 (415) 493-1501.**

CIRCLE NO. 104



2. Ten LED digits can provide 1 Hz resolution for 4.5 GHz measurements.

Wideband Phase Modulator Works Directly On Carrier

Subharmonic modulators have many advantages, but suffer from excessive incidental am enhancement. This detrimental effect can be slashed in half if the output frequency is modulated directly.

MICROWAVE carrier frequencies are often phase modulated at a subharmonic level, then multiplied in a varactor multiplier to obtain the desired output. The advantages of doing this, when a large modulation index (±90 degrees) is needed, are quite clear. If the multiplication factor (n) is large, the modulation index required at the subharmonic is small and easy to obtain. Linearity is likely to be good, since only 1/n of the output phase deviation is actually needed in the modulator.

This approach has one serious disadvantage, however, and that is the undesirable effect that the varactor multiplier may have on the modulation spectrum. High-order multipliers are usually narrow-band devices with a variety of potential instability problems[1,2,3]. Incidental am enhancement, pm-to-am conversion and distortion of the modulator's baseband frequency response are often the results. These problems are particularly noticeable if the modulating frequency is several megahertz or higher.

The modulator circuit shown in Fig. 1 eliminates these multiplier induced problems, since it operates directly at the desired output frequency.

When properly compensated, it is linear to within less than ±4% deviation from the best straight line over a 190-degree phase excursion. Incidental am is less than 10%. A sub-harmonic modulator might be just as linear, but incidental am could be at least two or three times as great due to pm-to-am conversion and negative resistance effects in the multiplier. Also, transmitting high frequency modulation through the multiplier can trigger relaxation oscillations that render the data useless.

R. R. Rippy, National Aeronautics and Space Administration, Rf Technology Branch, (Code 724), Goddard Space Flight Center, Greenbelt, MD 20771.

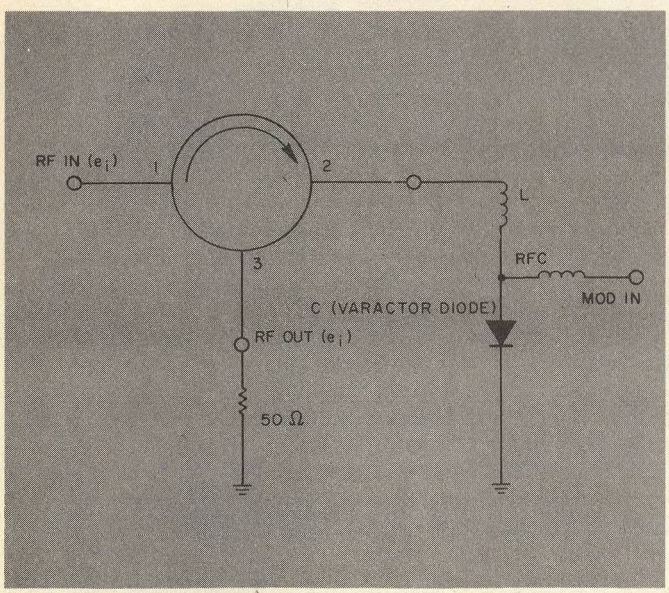
Here's how it works

The rf signal (e_i) enters port one of the circulator and travels to port two, which is terminated in a varactor-tuned series LC circuit. Assuming a purely reactive termination, all incident power is reflected to port three. Phase modulation is possible since the angle of the reflected voltage (e_r) varies with tuning of the diode. The relationship between e_r and e_i is given by the equation for reflection coefficient:

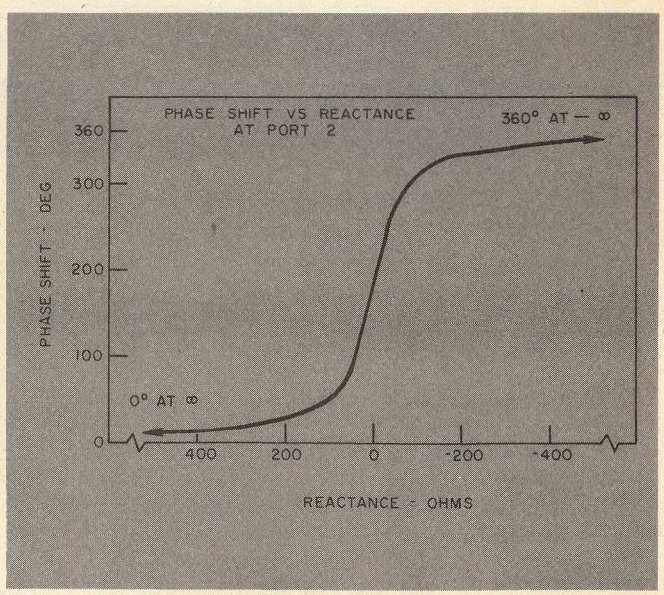
$$\frac{e_r}{e_i} = \frac{Z - Z_o}{Z + Z_o} \qquad (1)$$

Where: e_i is the incident voltage at port one,
e_r is the reflected voltage at port three,

(continued on p. 54)



1. **By directly modulating** the output frequency, this circuit circumvents many multiplier-induced problems.



2. **The theoretical phase relationship** of incident and reflected signals shows a linear portion of about ±100°.

Z_0 is the characteristic impedance of the circulator and
Z is the impedance at port two.

If, as in the case under consideration, Z is purely reactive and Z_0 is purely resistive, Eqn. (1) can be manipulated to give:

$$\frac{e_r}{e_i} = \frac{\sqrt{Z^2 + Z_0^2} \angle \tan^{-1}\left(-\frac{Z}{Z_0}\right)}{\sqrt{Z^2 + Z_0^2} \angle \tan^{-1}\left(\frac{Z}{Z_0}\right)} \quad (2)$$

which simplifies to:

$$\frac{e_r}{e_i} = 1 \angle -2 \tan^{-1}\left(\frac{Z}{Z_0}\right) \quad (3)$$

Equation (3) indicates that the circuit in Fig. 1 can produce up to 360 degrees of phase modulation.

A parameter of prime interest in a phase modulator is linearity. Figure 2 is a plot of the calculated phase relationship between e_r and e_i as the reactance at port two varies from $+j\infty$ to $-j\infty$. Note that there is approximately a ± 100-degree region in which a linear change in reactance at port two causes a linear change in phase at port three.

Unfortunately, varactor diodes do not have a linear characteristic. More commonly, their reactance varies as the square root of the applied voltage. But adding a simple inductor (L_1) linking port two with ground (Fig. 3) provides reasonably good compensation.

Two diodes are used to simplify biasing (the top diode prevents L_1 from shorting the dc bias voltage to ground) and to obtain a push-pull effect that tends to prevent large rf signals from detuning the circuit.

L_2 and C series resonate when the modulation input voltage is -3 V. In this low-voltage region, the reactance of the diode changes quickly with voltage ($X_c \propto \sqrt{V}$); but as the voltage goes more negative, the reactance changes more slowly which causes a flat region in the phase versus voltage curve. When L_1 is introduced to the circuit and the varactor voltage is less than -3 V, the L_2C branch looks like a capacitor that begins to parallel resonate with L_1. The approach of parallel resonance forces the rate of change in reactance to increase which tends to cancel the effect of the more slowly changing varactor reactance.

The equation for the reactance at port 2 is

$$Z = \frac{(jX_2 - JX_c)\, jX_1}{jX_2 - jX_c + jX_1} \quad (4)$$

where:
X_1 = reactance of L_1
X_2 = reactance of L_2
X_c = reactance of C

In order to show X_c as a function of voltage and to reduce the labor involved in calculations, Eqn. (4) can be written as:

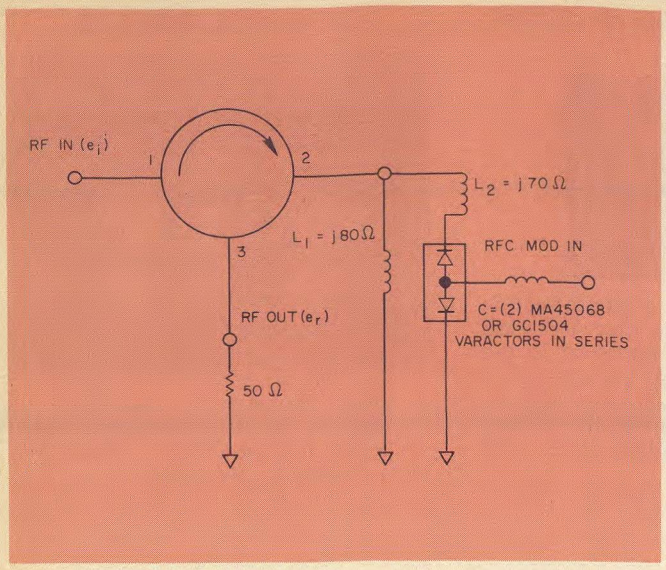
$$Z = \frac{\left(jX_2 - jX_2\sqrt{\frac{V}{K}}\right) jmX_2}{jX_2 - jX_2\sqrt{\frac{V}{K}} + jmX_2} \quad (5)$$

where
V = modulation voltage and
K = modulation voltage at which $jX_2 = -jX_c$
$m = X_1/X_2$

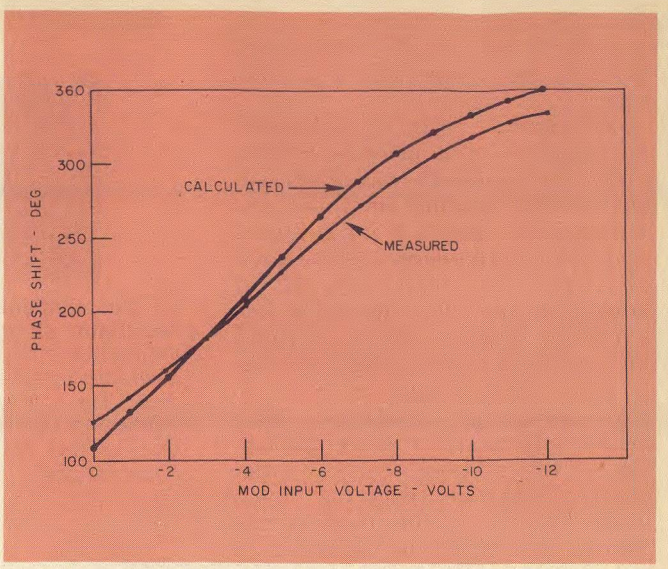
This reduces to:

$$Z = \frac{jX_2\left(1 - \sqrt{\frac{V}{K}}\right) m}{1 - \sqrt{\frac{V}{K}} + m} \quad (6)$$

The transfer function for the modulator is now obtained by substituting (6) into (3):



3. **L_1 is necessary** to compensate for the non-linear response of the varactor diode.



4. **A measured phase characteristic** shows that more than ±90 degrees of linear deviation is available.

$$\frac{e_r}{e_i} = -2 \tan^{-1} \frac{\left[\left(\frac{X_2}{Z_0}\right)\left(1 - \sqrt{\frac{V}{K}}\right) m\right]}{1 - \sqrt{\frac{V}{K}} + m} \quad (7)$$

Experimentally it has been found that good linearity is obtained with the following circuit parameters:

$$X_2 = -j70$$
$$m = 1.143$$
$$\frac{X_2}{Z_0} = 1.40$$
$$K = 3$$

A plot of the calculated and measured performance obtained with these values is shown in Fig. 4.

High-Q components necessary

Earlier, it was assumed that the tuned LC circuit is purely reactive. In reality, of course, this is not the case. A small resistive component absorbs a portion of the incident power which results in in-

(continued on next page)

cidental amplitude modulation. The amount of am can be kept small, however, by using high-Q components.

For example, Fig. 5 illustrates the response of a modulator with a 450 Hz sawtooth waveform applied to the modulation input. As can be seen, a ±5.0 V input signal produces a ±100-degree phase deviation with less than ±0.5 dB of incidental am. The insertion loss is 1.5 dB. From −30° to +70°C, the modulation index remains within ±1 dB of the value at 23°C.

A single-stage modulator may not be sufficient for every application. Two sections can be cascaded to obtain twice as much phase deviation (the total deviation is the sum of the deviation in each section). Or, better linearity can be obtained by operating each section at, say, one-half as much deviation to avoid the most nonlinear region in the phase versus voltage curve.

A two-section modulator is shown in Fig. 6. The specifications (Table 1) for this design show the potential of a multi-stage approach. The maximum specified power level (20 mW) is based on stability rather than burnout considerations. At high-drive levels, the modulator may behave like a parametric amplifier and break into oscillation. Under the ideal conditions, satisfactory performance has been obtained at up to a 100 mW input, but this much drive is not recommended.

Linear frequency deviation possible

In addition to providing linear phase deviation, the modulator can also produce linear frequency deviation when used in the oscillator design depicted in Fig. 7. The circuit shown oscillates at approximately the center frequency of the bandpass filter, and exactly at the frequency at which the loop phase shift is an integral multiple of 2π radians.

All components in the oscillator should be wideband, with the exception of the filter, which should have a flat group delay versus frequency characteristic in the bandpass region. If this criteria is met, the oscillator's stability is determined primarily by the filter, and its deviation linearity primarily by the phase modulator. This is illustrated in the following analysis which is analagous to Kirchhoff's voltage law with phase corresponding to voltage, frequency to current and group delay to resistance.

Let Θ be the phase shift through each element in the loop. Since the total phase shift around the loop in an oscillator must be integral multiple of 2π radians[4] or 0, we may write:

$$\Theta_a + \Theta_c + \Theta_m + \Theta_f = 2\pi\, n \quad (8)$$

where:

Θ_a = the phase shift in the amplifier
Θ_c = the phase shift in the coupler.
Θ_m = the phase shift in the modulator
Θ_f = the phase shift in the filter
n = an integer

Taking the derivative of Eqn. (8) with respect to frequency (ω) gives:

$$\frac{d\Theta_a}{d\omega} + \frac{d\Theta_c}{d\omega} + \frac{d\Theta_m}{d\omega} + \frac{d\Theta_f}{d\omega} = 0 \quad (9)$$

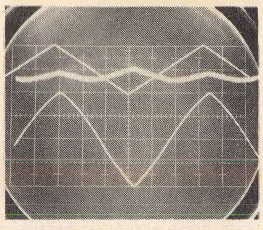
Each of these terms is the group delay (τ) of one element in the oscillator. Hence, we may write:

$$\tau_a + \tau_c + \tau_m + \tau_f = 0 \quad (10)$$

The delay in the modulator is

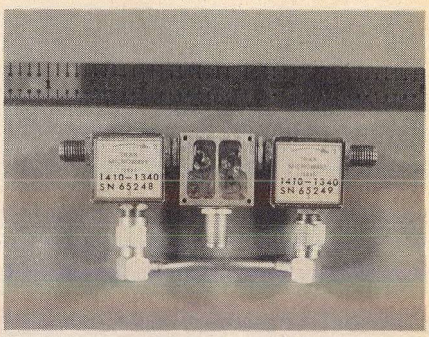
(continued on p. 58)

MODULATOR PERFORMANCE (ONE SECTION)



5. **This response of a single-section modulator** shows less than ±0.5 dB incidental am. The top trace is the sawtooth modulating voltage (5V/div). The center trace shows incidental am (1 dB/div) and the bottom one is the actual phase shift (50 degrees/div).

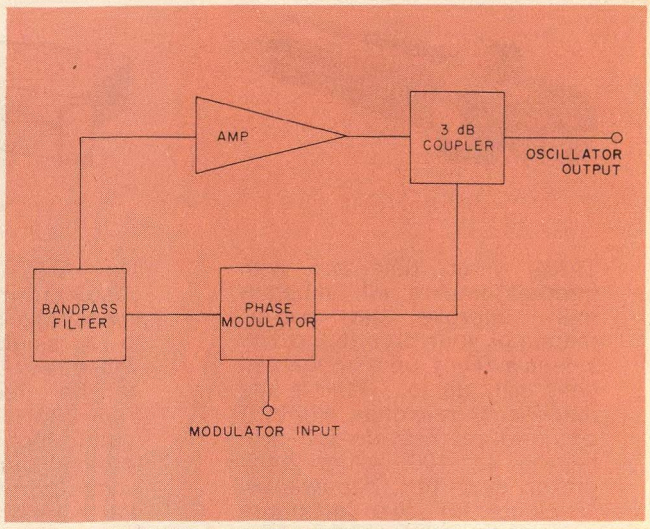
TWO SECTION MODULATOR



6. **This two-section modulator** is capable of ±180-degree modulation or ±90 degrees at less than 3% total harmonic distortion.

Table 1: Two Section Modular Specifications

Frequency	2.1-2.3 GHz
Modulation capability	±180° (typical)
Linearity	<3% harmonic distortion at ±90°
Modulation frequency response	dc to 55 MHz (upper 3 dB frequency)
Modulation input impedance	>1 MΩ shunted by 10 pF
Insertion loss	≤3 dB
Incidental am	± 0.5 dB at ± 90°
Modulation sensitivity	± 3V/100° (typical)
Input/output impedance	50 ohms
Maximum rf input	20 mW
Size	6.5 x 2.0 x 1.2 cm
Weight	71 grams



7. **Linear frequency deviation** is taken advantage of in this oscillator application.

Going up or down?
MITEQ
Upconverters and Downconverters take you there

- Single or double conversion
- Output frequency from 10 MHz
- Input frequency to 15 GHz
- Remote fault indicators
- Multi-channel phase and gain tracking
- Optional remote frequency selection
- Optional low noise preamplifiers

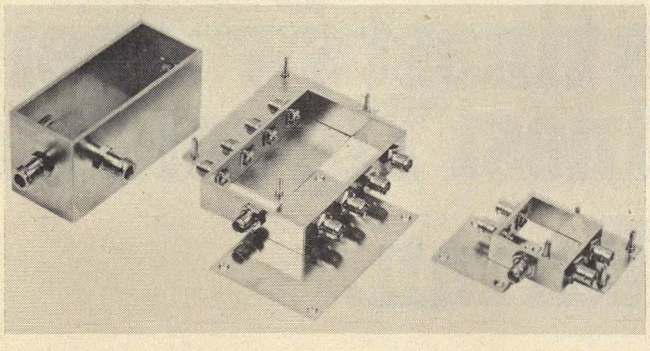




- Single or double conversion
- Output frequency to 15 GHz
- Input frequency from 10 MHz
- Optional remote frequency selection
- Hy-dynamic range

MITEQ INC. 100 RICEFIELD LANE, HAUPPAUGE, N.Y. 11787, (516) 543-8873

READER SERVICE NUMBER 58



Now you can get to it !

In our shielded packages, you can reach either side of your rf printed circuit board easily. Covers seal with only four screws countersunk so that your name plate or schematic can be attached to top cover. Pre-punched nickel-plated aluminum with choice of four rf connectors; TNC, BNC, type N, SMA. From $9.75, in 11 standard off-the-shelf packages within 24 hours or custom configurations in two weeks. Call or write for complete data package.

MODPAK
31A Green Street
Waltham, MA 02154
(617) 891-7048

READER SERVICE NUMBER 56

assumed to be negligibly small and constant in the frequency region of interest. The latter condition permits us to write:[5]

$$\tau_m = -\frac{\Delta\Theta_m}{\Delta\omega} \qquad (11)$$

Substituting Eqn (11) into Eqn (10) and solving for $\Delta\omega$ results in:

$$\Delta\omega = \frac{\Delta\ \Theta_m}{\tau_a + \tau_c + \tau_f}$$

This equation illustrates that if a phase change $\Delta\Theta_m$ is forced into the loop by the modulator, the oscillator frequency must change by $\Delta\omega$ in order to generate an equal and opposite phase change. Equation 12 holds true when the time interval for $\Delta\Theta_m$ is large compared to $(\tau_a + \tau_c + \tau_f)$.

If the group delay in each loop is constant, the linearity of the frequency deviation will be equal to the linearity of phase deviation. In some cases where the loop group delay is not constant, it may be possible to modify the modulator phase characteristic to compensate for phase nonlinearities in the loop.

The oscillator in Fig. 7 offers several practical features. Since each circuit element has a 50-ohm input-output impedance, each may be treated as a separate module and interconnected with 50-ohm cable. This is advantageous since it simplifies open loop measurements on a network analyzer.

An apparent disadvantage is that the output signal can abruptly jump to a frequency above or below the desired frequency by $\frac{2\pi n}{\tau}$, where n is an integer and τ is the total loop group delay. This problem can be avoided, however, if the bandwidth of the loop filter is narrow enough that the loop gain at the unwanted frequency is less than one. ••

Acknowledgement

The author would like to thank Dave Hepler for computer programs and interesting discussions regarding the modulator.

References

1. D.B. Leeson, "Instabilities in Varactor Multipliers," G-MTT International Microwave Symposium, p. 30-34, (1966).
2. James C. McDade, "Negative Resistance in Junction Diodes." Procedings of the IRE, Vol. 49, No. 5, p. 957-958.
3. H. Endler et al, "Relaxation Phenomena in Diode Parametric Amplifiers," Proceedings of the IRE, Vol. 47, No. 8, p. 1375.
4. Jacob Millman, "Vacuum-Tube and Semiconductor Electronics, McGraw-Hill Book Co., New York, p. 474, (1958).
5. W. Hetterschied, "Transistor Bandpass Amplifiers," Phillips Technical Library, p. 65.

Test your retention

1. What simple component can be put in parallel with a varactor-inductor series circuit to compensate for the varactor's non-linear response?
2. How would a modulator be used in an oscillator circuit?

Transistor Mixer Boosts Upconversion Gain

A transistor-based design for a uhf broadcast upconverter can provide five times more gain than a similar diode design. Here's a comparison of both circuits, each built inside a rat race hybrid.

RF power transistors operated in the so-called harmonic mode can be the basis for some interesting high-power upconverters. An overlay transistor operating in this mode generates harmonics or acts as a parametric upconverter due to a non-linear collector-base junction capacitance—an effect that is very similar to the action of a varactor diode. In addition, the transistor provides power gain at the fundamental input frequency giving the effect of an amplifier in parallel with a varactor circuit.

The advantages of using transistors instead of varactors can best be demonstrated by comparing similar circuits designed with each device. A good design example is a family of parametric upconverters designed primarily to upconvert a 38.9 MHz video i-f to a vhf, uhf or X-band broadcast frequency. The circuits to be compared are push-pull designs built inside a 6/4-wavelength "rat race" hybrid ring. Both microstrip designs are fabricated on copper-clad Rexolene 1422.

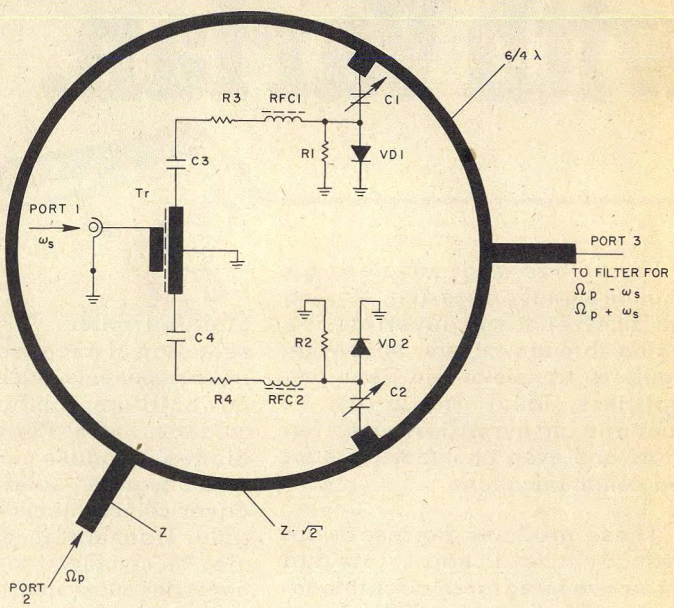
The basic parametric upconverter circuit using varactor diodes is shown in Fig. 1. An input signal (ω_s) enters through port one, where a small transformer (Fig. 2) wound on a Siemens' two-hole ferrite-core (Type 80 K 1) matches the 50-ohm impedance to the impedance of each varactor circuit, which can essentially be represented by R3 and R4 (each 15 ohms). The two diodes are push-pull driven through the input transformer, as well as by the pump power (Ω_p), which is introduced through port two on the hybrid ring. Trimmer capacitors (C1 and C2) match the diodes to the hybrid ring.

Upper ($\Omega_p + \omega_s$) and lower ($\Omega_p - \omega_s$) sideband signals are available at port three. One of these can be selected by an appropriate filter. For example, a three-section coaxial bandpass filter can provide more than 60 dB suppression to unwanted frequencies. With a 0.5-watt input, this varactor circuit produces about 1.5 watts in the lower sideband between 470 and 960 MHz. Pump power is in the range of six to seven watts.

Instead of specifying efficiency, it's more useful to deal with the conversion gain of an upconverter. This gain is defined as the ratio of upconverted signal power to the input signal power. Therefore, this

(continued on p. 66)

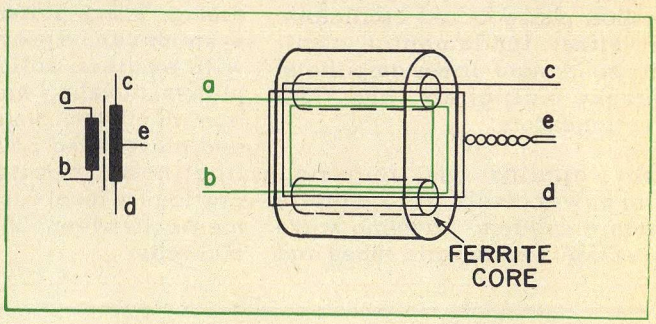
Klaus Breitkopf, Chief Engineer of RIAS-Berlin, Technische Direktion/Sendertechnik, 1 Berlin 62, Kufsteiner Str. 69, Germany.



Component Values

C 4.7: nF bypass capacitor.
C 1, C 2: 1 to 10 pF miniature air-dielectric trimmer capacitor (Tronser or equivalent type).
C 3, C 4: 10 nF, 30 Vdc, miniature disc ceramic capacitor (Siemens or equivalent type).
C 5, C 7, L 1 and C 6, C 8, L 2: Low-pass filter (π-section), values depending on input signal frequency range; input/output impedance approximately 15 ohms.
R 1: 1 kΩ, 0.5 watt, carbon resistor.
R 2: 500-ohm, 1 watt, linear

1. A simple 6/4 wavelength hybrid ring surrounds this varactor upconverter. An upconversion gain of 3 is possible at uhf.



2. This double-hole ferrite-core transformer matches the 50-ohm input impedance to the 15-ohm varactor circuits.

varactor circuit has a conversion gain of:

$$g_v = \frac{1.5}{0.5} = 3$$

C-B junction acts like a varactor

A comparison of varactor and transistor performance (Fig. 3) reveals that the nonlinear capacitance (C_{bc}) characteristic of a transistor's collector-base junction is very similar to the variation of a varactor diode's capacitance with changes in reverse voltage. A common-base transistor circuit (Fig. 4) corresponds to the varactor circuit described above, since the collector-base capacitance of the transistor is connected in shunt with the signal and pump inputs as well as paralleling the output circuit.

Using the transistors in a common-base configuration also provides excellent stability, good isolation and a high cutoff frequency. In practice, operation is limited by two distinct cutoff frequencies. One is the common-base current gain cutoff, $f_{\alpha b}$, which is the frequency at which h_{fb} has decreased to a value of 3 dB below h_{fbo}. This is normally much higher than $f_{\alpha e}$, the common emitter current gain cutoff, for any given transistor. The second cutoff factor, the cutoff frequency of the collector-base junction, is limited only by the collector series resistance. With the RCA 2N4012 transistors used in this design, substantial gain can be realized for input frequencies up to 450 MHz.

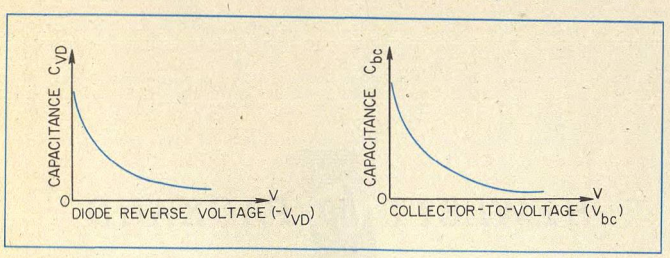
An added bonus is accrued when using the transistors in a common-base configuration. The grounded base acts like a shield between input and output circuits effectively preventing any part of the pump power or upconverted signal power from feeding back to the input circuit.

Many of the components used in the varactor upconverter can also be used in the transistor version. Input signals, introduced at port one, pass through a similar ferrite-core transformer, since the actual transistor input impedance is negligible compared to R3 and R4. A π-section low-pass filter supplements the input circuit of this design for improved impedance matching. With the cascaded transformer-filter arrangement, the transistor circuit has an input bandwidth of 30 to 70 MHz. The collector circuits are capacitively coupled to the hybrid ring.

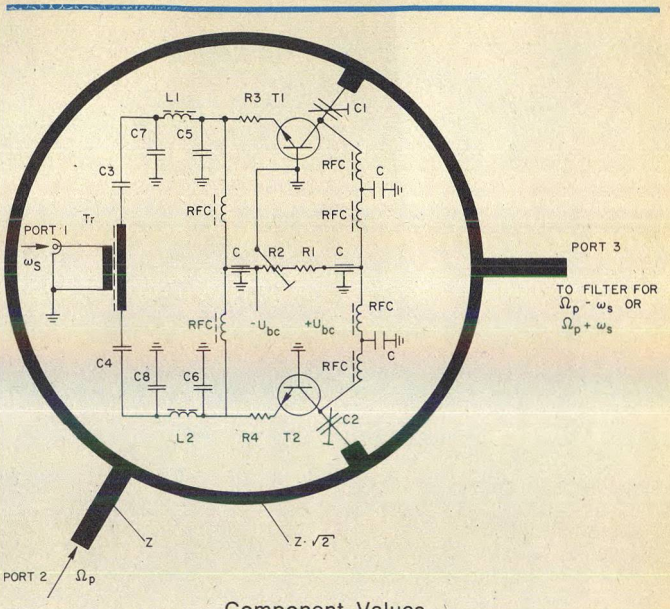
5:1 improvement in gain

With six or seven watts of pump power applied to port two, a 100 mW input signal results in an output power of greater than 1.5 W in the lower sideband for uhf television channels in the frequency range of 470 to 960 MHz. Under comparable conditions, the transistor circuit's upconvertion gain is 15—five times that of the varactor design. This indicates that the transistor circuit needs far less input power.

Both of these designs have been used in Germany as television broadcast upconverters. They are very simple to build. The microstrip "rat race" ring is not very critical with respect to its wavelength, and is made with a 10% tolerance. Strip width (ring impedance) can be calculated or taken directly from design curves. The substrate is fastened to a sheet of metal, which holds the transistors and acts as a simple heat sink. Flanged TNC or BNC connectors are used on ports one, two and three. The finished unit may simply be mounted in a metal box for complete shielding. ••



3. The collector-base capacitance of an overlay transistor is similar to the capacitance of a varactor diode. This feature allows frequency translation with added power gain.



Component Values

C 1, C 2: 1 to 10 pF air-dielectric miniature trimmer capacitor (Tronser or equivalent type).
C 3, C 4: 10 nF, 30 Vdc, miniature disc ceramic capacitor (Siemens or equivalent type).
R 1, R 2: 50 K 0.25-watt, bias resistor; carbon type with axial lead wires.
R 3, R 4: 15-ohm, 0.5-watt, input matching resistor; carbon type with axial lead wires.
RFC 1, RFC 2: Rf choke, consisting of a piece of 0.4 mm diam. wire, one-quarter of a wavelength (of the pump frequency) long, turned to a simple coil of 6 to 8 mm inner diameter.
VD 1, VD 2: Varactor diodes. Microwave Associates MA 4060B or equivalent.
Tr: Push-pull transformer (Fig. 2).
Ports 1, 2 and 3: TNC or BNC flange-type connections.
trimmer resistor or potentiometer (Dralowid or equivalent type) for base-bias voltage setting.
R 3, R 4: 15 ohm, 0.5 watt, emitter input matching resistor; carbon resistor with axial lead wires.
RFC: Rf choke, 6μH vhf choke with ferrite core and shrunk sleeve (Siemens or equivalent type).
T 1, T 2: Overlay transistor, RCA 2N4012, 2N5016 or equivalent.
Tr: Push-pull transformer (Fig. 2).
Ports 1, 2 and 3: TNC and BNC flange type connectors.

4. Transistor upconverters feature a high upconversion gain. A common-base circuit is used to take advantage of a varactor-like collector-base capacitance.

Test your Retention

1. Define conversion gain.
2. How long is a rat-race?
3. How should an overlay transistor be mounted to obtain a varactor-like response?

You may have just renewed, but . . . "Calendar Year Renewal" means YOU MUST RENEW NOW. See card inside front cover.

Transplexing SAW Filters For ECM, *Part II*

Miniature amplifiers can be effectively combined with SAW filters to form filterbanks with contiguous passbands. Advantages include insertion gain and a dynamic range of 45 dB.

This is the second of a two-part article on surface-acoustic wave filters and their use in multiplexed filterbanks. Part I appeared last month.

THE performance of a filter array with contiguous passbands is citically dependent on the manner in which the individual filter elements are interconnected. Usually it is not possible to simply parallel the filter elements and achieve the response of the isolated filters. The effects of channel interaction and source loading must be considered.

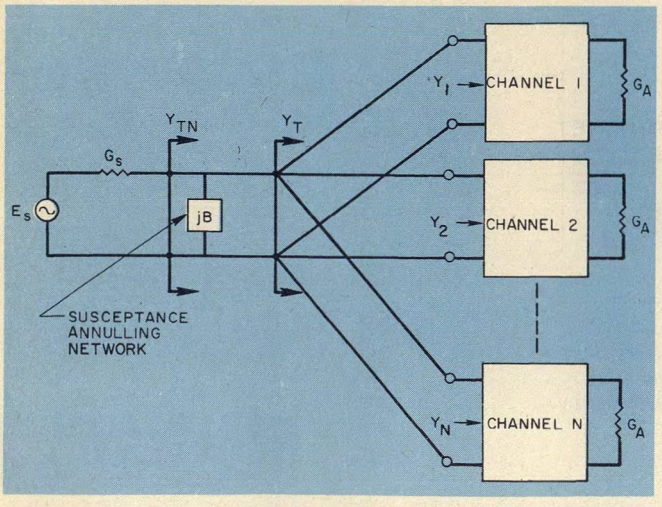
One common method of interconnecting filter elements[14] is shown in Fig. 1. The individual filter elements must be designed from a singly-terminated prototype since the input admittance of adjacent channels combines to form an equivalent voltage source at the terminals of a given filter. Also, the first element of each channel must have the characteristics of a series resonant circuit in order that its input conductance be zero for out-of-band frequencies and increase to a value equal to the source conductance for in-band frequencies. Since the power delivered to a given channel is proportional to the input conductance, the transmission characteristics of that channel are also proportional to the conductance. Thus when the specially-designed filters comprising the the multiplexer are paralleled, the real part of the total input admittance, Y_T, is relatively constant across the multiplexer bandwidth with a value equal to G_s. The imaginary part, B_T, is approximately zero.

There are many available techniques for multiplexing including the use of circulators to reduce adjacent channel interaction. However, all these techniques require that the input reflection coefficient of a filter element be zero across its passband. With surface wave acoustic filters, this is generally not the case due to the parasitic transducer capacitance.

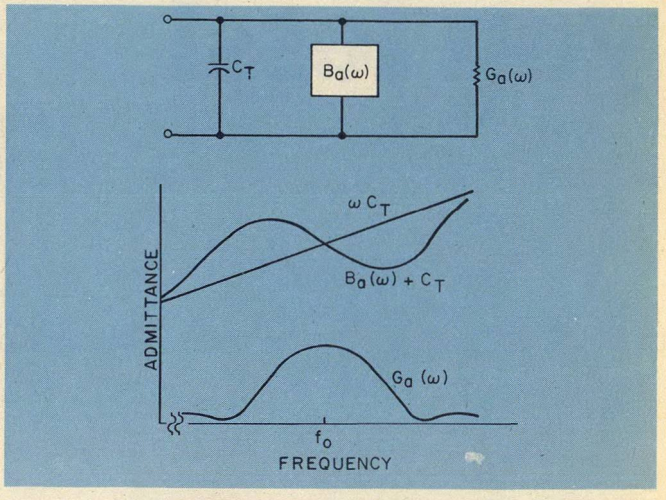
Active "transplexing"

Using the "crossed-field" model, Fig. 2, the input admittance of the interdigital transducer may be characterized by a circuit consisting of the total electrode capacitance in parallel with a radiation admittance which represents acoustic-wave excitation. The input power must be efficiently delivered to the real part of this radiation admittance. Note that $B_a(\omega)$ is zero and G_a is a maximum at band center, f_o, and that if C_T were zero, the input admittance would be similar in form to the multiplexer in Fig. 1. However, for transducers on a substrate with a low electromechanical coupling constant k such as quartz, the ratio of $\omega_o C_T$ to G_a ω_o, which is defined as the radiation Q, may be as high as 100. Fortunately for narrow-bandwidth filters, Q_r decreases due to the increase in the number N of interdigital periods required by,

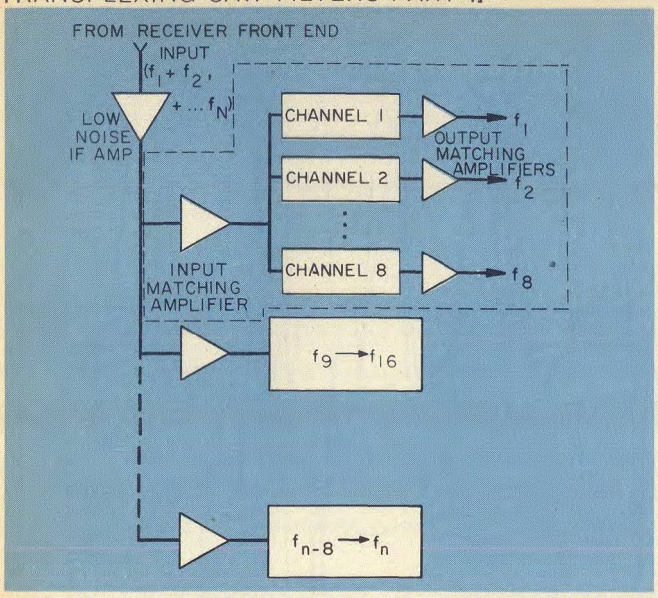
Raymond R. Jones, Fellow Engineer, Solid-State Microwaves, Electromagnetic Technology Laboratory, **James Schellenberg,** Senior Engineer, **Dr. William J. Tanski,** Senior Engineer and **Dr. Robert A. Moore,** Manager, Westinghouse Electric Corporation, Advanced Technology Laboratories, Box 1521, Baltimore, MD 21203.



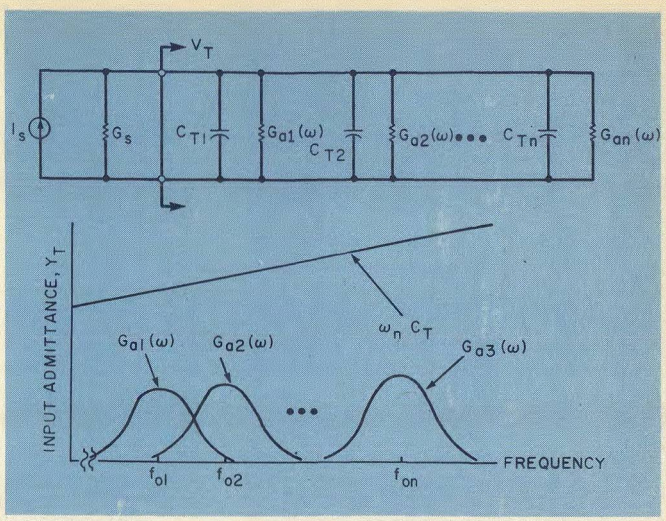
1. **For interconnecting filter elements,** the first element of each channel must present a series resonant circuit to reject out-of-band frequencies.



2. **Cross-field model of an interdigital transducer.** Input power must be efficiently delivered to the real part of the radiation admittance, Ga.



3. **In this n-channel filter array** active transplexing makes use of input/output matching amplifiers to drive up to eight SAW filters.



4. **Equivalent circuit of an n-channel filterbank** when driven by a single matching amplifier.

$$Q_r = \frac{\pi}{4} \frac{1}{k^2 N} \qquad (2)$$

However, Q_r may still be as large as 10-20 for filters with a bandwidth as small as 1%. Therefore, due to the presence of C_T, active impedance transforming, as opposed to passive networks, becomes an attractive method for interfacing contiguous acoustic filters to form a multiplexer. In active "transplexing," (transducing-multiplexing) a single matching amplifier drives a set of filters. This forms a broadband magnitude match with the total input capacitance C_T. Typically, eight filters are driven (as shown within the dotted lines of Fig. 3) but the number of channels is dependent on the maximum input Q which the amplifier can efficiently drive. A simplified input equivalent circuit for n channels in parallel driven by a single matching amplifier is given in Fig. 4. The radiation susceptance, B_a, is neglected since it is much smaller that ωC_T. One advantage of high-transducer susceptance is that it effectively masks the radiation admittance and thus minimizes interchannel interaction. Assuming that the filters have equal transducer capacitance and radiation Q, the total input Q is approximately n times that of a single channel. If the source conductance is adjusted equally to the load susceptance, the power delivered to the radiation conductance of a given channel is down by a factor of n from a channel driven by a separate matching amplifier.

An output matching amplifier at each channel also serves as an active admittance transformer, matching the output transducer to the 50-ohm load. It also provides gain to compensate for any remaining losses. The gain of the output-matching amplifier can easily be made variable, and, therefore, provides a convenient means of equalizing the signal output level of the filter array.

Figure 3 is an n channel filter array consisting of n acoustic filters and output matching amplifiers. An input matching amplifier is required for each set of eight filters. The input admittance of the individual input-matching amplifiers is designed to form a broadband power divider over the multiplexer bandwidth. Additional channels can be added to the multiplexer in sets of eight by simply adding another subsection in parallel. Due to the reverse isolation of the input matching amplifiers and their broadband input admittance, channel-to-channel interaction is minimized.

Selectivity determines dynamic range

One possible limitation to active "transplexing" is due to the nonlinear nature of active devices at high-power levels. This establishes the upper-power level which can be applied to the filterbank. However, if the matching amplifiers are properly designed, this power limit does not restrict the system's dynamic range. The available dynamic range of a SAW filterbank with matching amplifiers is typically 90 dB—bounded by the amplifier one dB compression point at the upper end and noise level at the lower end. However, due to the finite selectivity of acoustic filters (typically 56-60 dB), the practical limitation is the filter selectivity and not non-linear effects.

The level of intermodulation products is a convenient measure of linearity. It is also an important consideration in its own right with a frequency multiplexer. If two signals mix in the input-matching amplifier thereby generating a third, this spurious signal could be interpreted as a "real" signal and result in a false alarm.

The third order $(f_1 \pm 2f_2)$ intermodulation product is usually the largest spurious response, can be expressed as:

$$P_{IM} = P_1 + 2P_2 - 2P_{sat} - 18 \qquad (3)$$

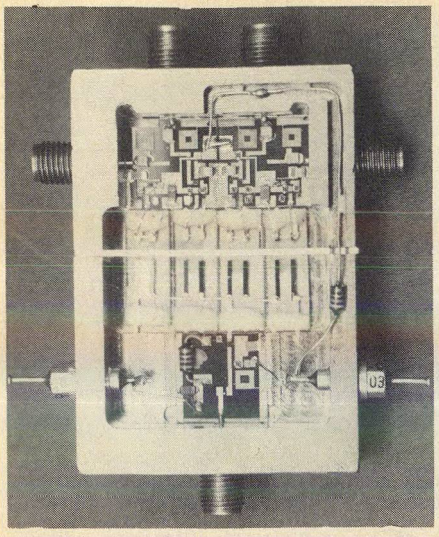
where

P_1 = power level (dBm) at f_1
P_2 = power level (dBm) at f_2
P_{sat} = power level (dBm) for which the gain is reduced 1 dB

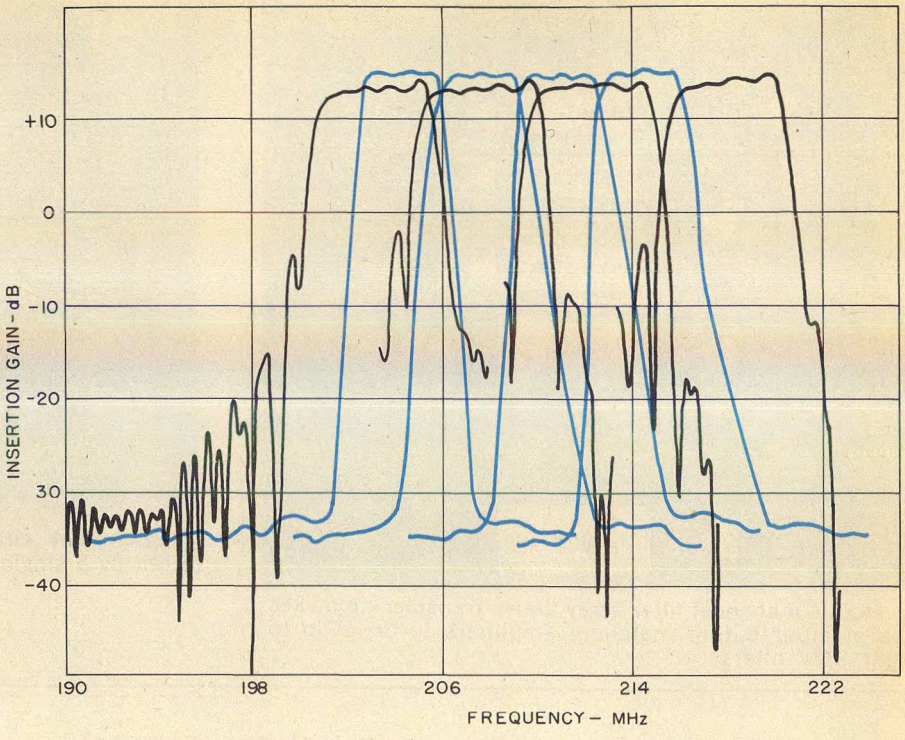
Actively "transplexed" filterbank

An example of a four-channel filterbank using one input and four output amplifiers is shown in Fig. 5. It uses frequency contiguous quartz filters with 5 MHz bandwidths at 200 MHz. The frequency response of the filterbank, Fig. 6, shows the nominal insertion gain for each of the four channels to be 13 dB. The relative gain distribution in each input channel is 4 dB from matching and 21 dB from the input amplifier. On the output, 26 dB is achieved with the output amplifiers and 6 dB from matching. Thus, a total of 10 dB reduc-

(continued on next page)



5. **Four-channel filterbank** is only 2.2 in. × 1.5 in. × 0.5 in. It uses SAW filters with 5-MHz bandwidth at 200 MHz.



6. **Frequency response of filterbank** (Fig. 5) shows a total insertion gain of 10 dB from the matching input/output amplifiers. "Electrically apodized" filters increase dynamic range as shown in color tint.

tion in insertion loss for each channel is achieved due to magnitude matching alone. The wideband (100-600 MHz) frequency response of channel one of the filterbank is plotted in Fig. 7. Dynamic range is near 30 dB. By employing new filter synthesis techniques which suppress diffraction effects and thereby reduces sidelobe levels, a dynamic range of greater than 50 dB with shape factor of 2:1 (45 dB to 3 dB frequency ratio) are possible up to and above 800 MHz. The predicted frequency performance of a multiplexer using the "electrically apodized" filter is shown in Fig. 6 (color tint). Triple transit leakage on this design is in excess of 60 dB. For most filter bank applications, a −40 dB intermodulation level is sufficient. However, if it is desired to reduce intermodulation products or raise the upper power limit, the input-matching amplifier can be modified to do this. One of the critical design tradeoffs is the amount of gain provided before the acoustic filters as opposed to after the filters. For minimum noise figure, it is desirable to put as much gain as possible before the filters. On the other hand, for minimum distortion, the gain should be placed after the filters. With the four-channel multiplexer, Fig. 5, the gain was proportioned equally between the input and output matching amplifiers. However, in most applications, sufficient system gain is provided before the filterbank to establish the system noise figure and, consequently, the filterbank has little effect on the system noise figure. Typical specifications for an n-channel filterband module are given in Table 1.

Cross-channel interference

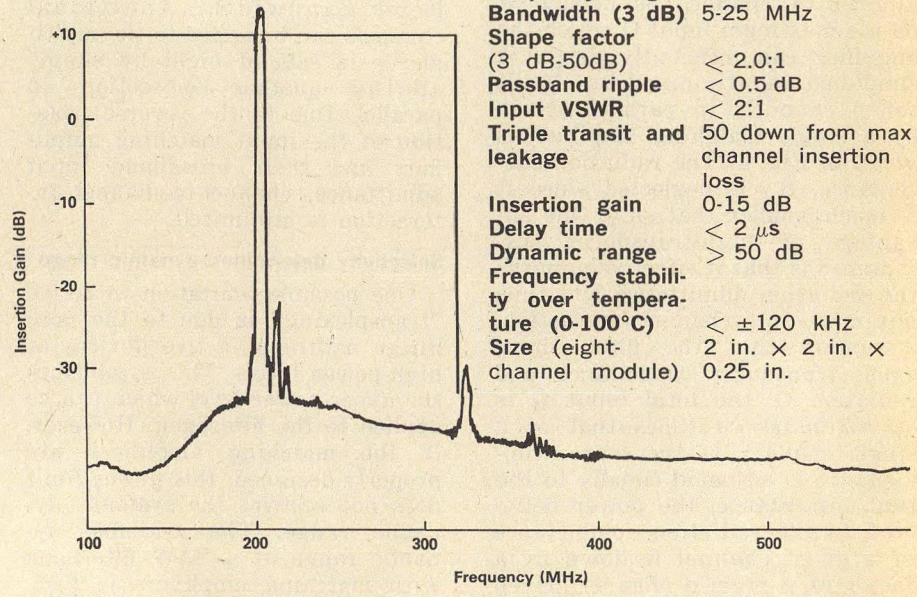
An important consideration in the design of channelized filters is the effect of cross-channel interference on the dynamic range. Due to the finite slope of the filter skirts, a practical limit is imposed on the input dynamic range. In fact, the filter skirts are the single most important parameter for determining the dynamic range.

A "threshold" power level must be set for the purpose of deciding on the presence or absence of a signal. It must be set such that with minimum input power, P_{min} is at least 3 dB above the threshold. Then in the case of maximum

(continued on p. 72)

Table 1 Filterbank characteristics

Frequency range	100-500 MHz
Bandwidth (3 dB)	5-25 MHz
Shape factor (3 dB-50dB)	< 2.0:1
Passband ripple	< 0.5 dB
Input VSWR	< 2:1
Triple transit and leakage	50 down from max channel insertion loss
Insertion gain	0-15 dB
Delay time	< 2 μs
Dynamic range	> 50 dB
Frequency stability over temperature (0-100°C)	< ±120 kHz
Size (eight-channel module)	2 in. × 2 in. × 0.25 in.



7. **Wideband frequency response** of a single channel of the filterbank (Fig. 5) shows dynamic range of over 30 dB.

input power, the threshold will be exceeded in more than one channel, over a frequency band in the region of crossover. The frequency range in which two channels are triggered is given by

$$\Delta f_{max} = \Delta f \frac{\eta - 1}{\Delta \alpha} \Delta P_{in} \qquad (4)$$

Δf = crossover bandwidth of the filters = 3 dB bandwidth

η = filter shape factor (defined as a bandwidth ratio between two attenuation points)

$\Delta \alpha$ = the difference in dB between the two attenuation points used to define η

ΔP_{in} = input dynamic range = $P_{max} - P_{min}$

For example, with $\eta = 1.6$ between the 54 dB and 3B points and $\Delta P_{in} = 40$ dB.

$$\frac{\Delta f_{max}}{\Delta f} = 57\%$$

Therefore, in this example, two adjacent channels will be simultaneously triggered by a signal level P_{max} over a 57% baindwidth in the region of crossover.

In order to eliminate any such ambiguities, a double-detection scheme[1] could be used. This increases the effective filter selectivity, without exhibiting "ringing" for narrow pulses which would occur for the equivalent highly selective filter. The major drawback to this technique is additional complexity (therefore cost) incurred by using extra detectors and compartor circuits for each channel.

Quasi-monolithic filter bank

Significant cost reductions can be realized by using monolithic amplifiers in the actively "transplexed" filter bank. The monolithic amplifier, Fig. 8, is a (0.100 in. × 0.100 in.) chip fabricated by various epitaxial diffusions in N-type silicon. These chips are so designed to permit thermal compression wirebonding combinations of resistors, transistors, etc., into any configuration. Once the design is firm, a final overlay metallization may be added, and the amplifier design becomes monolithic. The f_T of the transistors used in the hybrid amplifiers is approximately 2 GHz; whereas, values of f_T near 650 MHz have been measured for the monolithic-bipolar transistors. Monolithic amplifier chips with transistor f_T as high as 2 GHz are under development. These amplifiers would be mounted on the quartz substrates and only the interconnects between filters and amplifiers would be thermal-compression wirebonds. Holding costs to a minimum dictate the use of a flat-pack with the output connectors replaced by hermetic tabs.

The ultimate in cost-effective designs would be the fabrication of filters and amplifiers on one silicon substrate. Since silicon is not piezoelectric, ZnO transducers would be required to launch surface waves. However, the design would truly be monolithic since metallizations for filters and amplifiers would be deposited simultaneously. One serious problem with this approach is maintaining input to output electromagnetic isolation on silicon. Measurements indicate greater than 50 dB at this time.

Next: SAW filters as noise jammers

The use of surface-acoustic filters to synthesize stable discrete frequencies in the uhf frequency range was recently described by the Air Force Cambridge Research Labs[15]. The synthesizer is composed of a clock-controlled pulse generator which drives in parallel 21 frequency-contiguous SAW filters. The clock-pulse frequency and the filter design are configured in order to produce 21 continuously available cw output frequencies in the 500 MHz range separated by approximately 5 MHz.

The SAW noise jammer described in this article makes use of the same actively-transplexed filters for transmit and receive. Thus, the filters are deployed as frequency multiplexers during receive and during transmit the filters become noise generators. (In conventional noise jammer applications, the same filters are used for transmit and receive; however, during transmit a broadband noise source is inputed to the filters).

To understand this concept, it is helpful to review the operation of SAW oscillators. A basic SAW oscillator, Fig. 9, consists of an amplifier with a SAW filter (delay line) and a feedback element[16]. The advantages of a SAW oscillator are:

- Frequency is determined by the filter-tranducer pattern, not quartz crystal dimensions.
- Fundamental oscillators are possible at frequencies over 3 GHz (crystal oscillators have a 200-MHz maximum) using electron-beam fabrication.
- Fm capability exceeds 1%.
- Its excellent short-term frequency and temperature stability is close to that of AT-cut quartz cystals.
- It's low cost, simple and rugged.

Providing there is net-loop gain, oscillation will take place at a frequency given by:

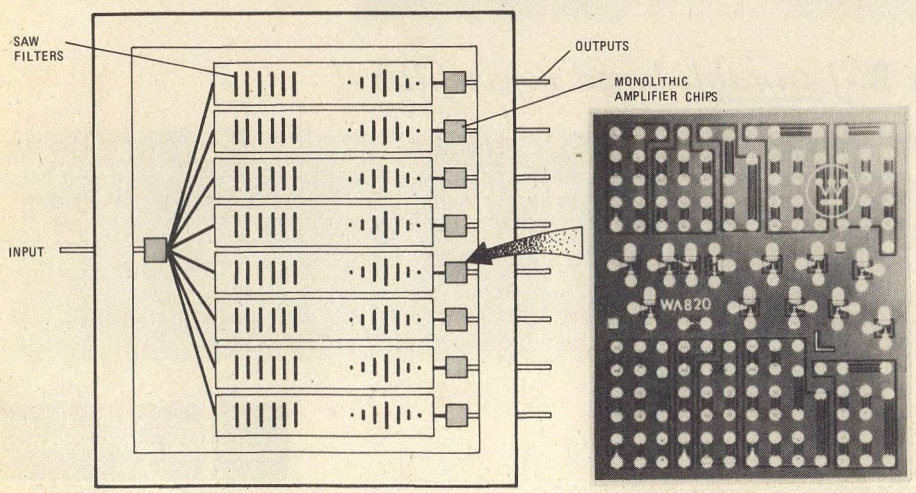
$$\frac{2\pi f \ell}{V_s} + \phi_L = 2n\pi \qquad (5)$$

ℓ = center-to-center separation between input and output transducers

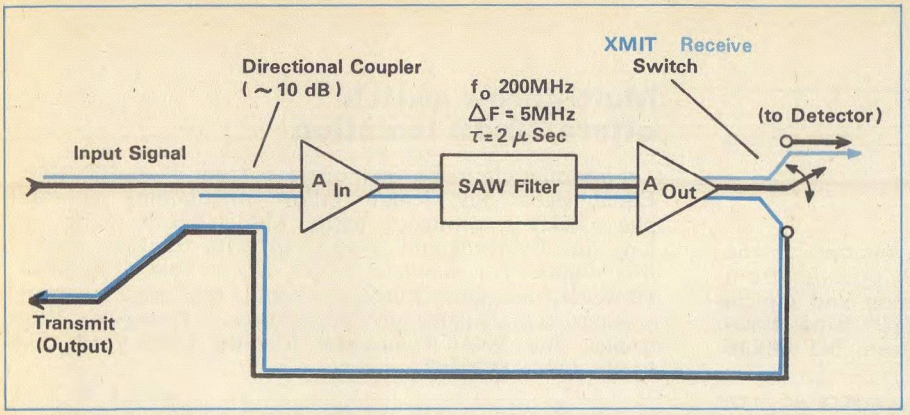
V_s = acoustic velocity

ϕ_L = loop phase shift

In an acoustic filterbank, by switching in a return line, each channel can be converted into an oscillator upon command via a PIN diode SPST switch. The frequencies of oscillation are determined by the center frequency, bandwidth and time delay of the acoustic filter. For example, a filter at 200 MHz with 5 MHz bandwidth and 2 μsec delay will oscillate at approximately 10 frequencies separated by 500 kHz. If the transmit-receive switch is opened and closed (during transmit cycle) at some random rate of three or four times the loop delay, all the frequencies within that filter passband are transmitted with an am modula-



8. **This monolithic amplifier** measures 0.1 × 0.1 in. sq. and is fabricated by epitaxial diffusions in N-type silicon.



9. **SAW oscillator** consists of an amplifier and SAW filter (delay line) with a feedback loop.

tion component. The SAW filter bandpass is designed for maximally flat response in order to achieve equal amplitude signals. Since the fm modulation rate is limited by the acoustic transmit time of the filter (2 μs which implies 500 kHz rate), the fm is accomplished by frequency modulating the upconverter LO. The combination of the am and fm modulation is used to simulate a noise transmission.

The filterbank could also be used as an "fm noise jammer" by switching in a return line (as opposed to cycling transmit-receive switch). After several circulations (depending on loop gain and filter design), only one frequency will remain, i.e., the loop gain for the other spectral lines will be less than unity. For this application, the acoustic bandpass filter must be designed to have lowest insertion loss at desired frequency of oscillation. As before, the modulation will be accomplished by frequency modulating the upconverter LO.

A n-channel actively "transplexed" transmit-receiver filterbank, Fig. 10, would sum all transmit signals by a resistive combiner and input to an upconverter. ••

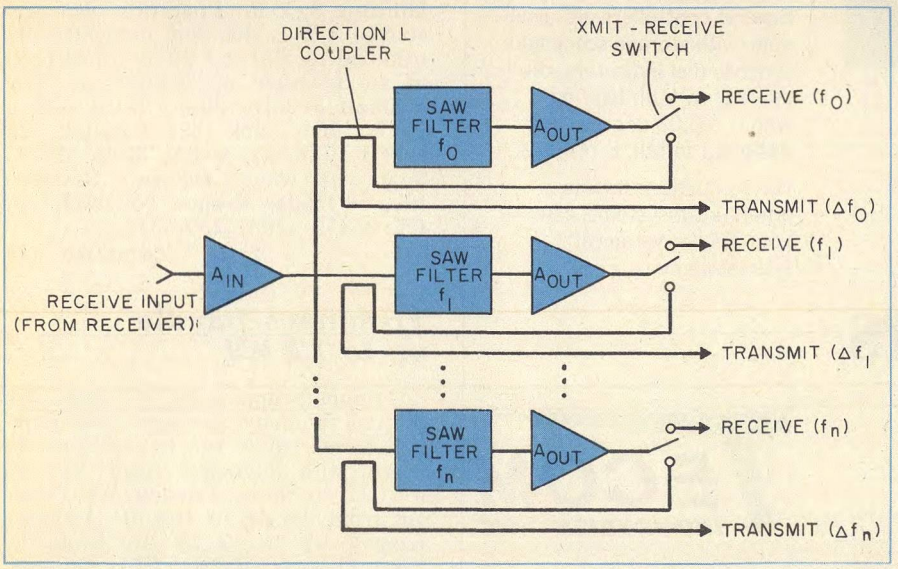
References

(continued from last month)

15. G. L. Matthaei, L. Young, E. M. T. Jones, *Microwave Filters Impedance, Matching Networks and Coupling Structures*, L. McGraw-Hill, New York (1964).
16. A. J. Budreau, Dr. P. H. Carr and Dr. K. R. Laker, "Frequency Synthesizer Using Acoustic Surface Wave Filters," *Microwave Journal*, pp. 65-68, (March, 1974).
17. M. F. Lewis, "Surface Acoustic Oscillators," *Microwave Systems News*, pp. 29-31, (December-January, 1974).

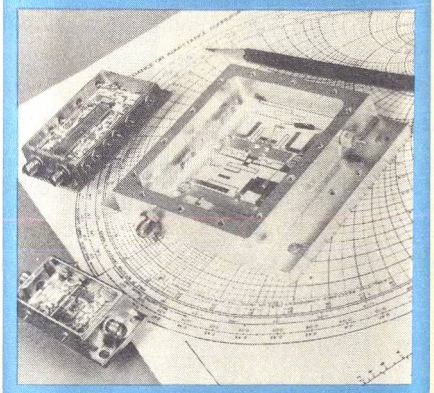
Test your retention

1. What are the three main functions of active "transplexing?"
2. What restricts the dynamic range of an actively transplexed filterbank?
3. For which other application is active transplexing uniquely suited?



10. **Proposed fm noise jammer** using SAW filterbank could automatically detect threat frequencies and transmit am and fm modulated noise signals back to the threat source.

Need sources of supply for LOG AMPLIFIERS?



The more available sources of supply you can locate, the better your chances for lowest price, fastest delivery and quickest application assistance.

Here are the facts on the two directories serving the microwaves market in 1974:

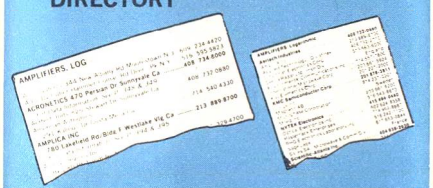
Total pages: Microwaves Products Directory . . . **592 pgs.** Microwave Journal . . . **252 pgs.**

Editorial pages: Microwaves Product Directory . . . **184 pgs.** Microwave Journal . . . **47.3 pgs.**

No. of companies included: Microwaves Product Directory . . . **3,370 pgs.** Microwave Journal . . . **341 pgs.**

Why gamble on your next search? Use Microwaves Product Data Directory when immediate action is demanded.

NUMBER OF COMPANIES LISTED
MICROWAVES PRODUCT DATA DIRECTORY — MICROWAVE JOURNAL



39 24

MICROWAVES
PRODUCT DATA DIRECTORY

new products

SWITCHES

Switch/driver costs $55

Rf/i-f diode switch/driver combination operates in the 3-300 MHz range. The SPDT unit which operates from a +24 V supply offers 60 dB min isolation and typical insertion loss of 0.75 dB. P&A: $55; stock. **Vitek Electronics, Ins., 200 Wood Avenue, Middlesex, NJ 08846 (201) 469-9400.**

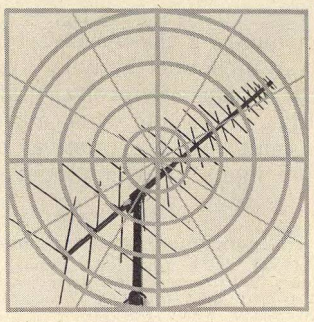
CIRCLE NO. 117

Multi-throw switch offers 70 dB isolation

Fifty-ohm circular switch operates from dc to 700 MHz. Equal signal line lengths allow maintaining constant phase delay transmission paths. Model CSAZ-IX8B uses long life dry reeds and is equipped with transient protection diodes. The standard switch is one-pole-eight-throw. However, one-pole four-throw and one-pole six-throw versions are available on special order. **Trompeter Electronics, Inc., 8936 Comanche Avenue, Chatsworth, CA 91311 (213) 882-1020.**

CIRCLE NO. 116





Turn on... Tecom Rotators

Now, Tecom Industries manufactures its own family of rotators and controllers to offer you a complete subsystem capability from one reliable source. Light, medium and heavy rotators bear up to 12,000 lbs. limited or continuous rotation, with speed variable from 0 to 2 RPM. Essentially backlash-free with readout accuracy better than 1 degree. All units are thermostatically heated for instant service in bad weather.

Several controllers are available, with storage scope and synchro dial indicators, displaying azimuth bearing within ±0.03 degrees and designed to MIL-E-16400.

For complete rotatable antenna subsystems, call your Tecom technical representative.

TECOM INDUSTRIES INC.

9000 Owensmouth Ave.
Canoga Park, Ca. 91304
(213) 341-4010

READER SERVICE NUMBER 74

PASSIVE COMPONENTS

Tiny circulator covers 7-17 GHz



Circulator/isolator, model T7S83T, covers 7-17 GHz and offers 16 dB isolation with an 83% bandwidth. VSWR is 1.45:1 while insertion loss is 0.75 dB. Temperature range is −54°C to +125°C and size is 0.78 × 0.63 × 0.56 in. **Teledyne Microwave, 1290 Terra Bella Avenue, Mountain View, CA 94040 (415) 968-2211.**

CIRCLE NO. 137

Calibration delay line trimmed to 500 ±3 ns

Model 83500 is a 500 ns calibration delay line for oscilloscopes, altimeters, radar and similar equipment. Utilizing 1/2 in. Foamflex dielectric coaxial cable, the unit is electrically trimmed to 500 ±3 ns and measured to an accuracy of ±0.020 ns. The calibration delay line is fitted with a 19 in. relay rack that measures 8.5 x 21 x 19 in. and weighs 80 lbs. P&A: $450; 6-8 wks. **Cablewave Systems, Inc., 60 Dodge Avenue, North Haven, CT 06473 (203) 239-3311.**

CIRCLE NO. 138

Trimmers handle up to 12 KV

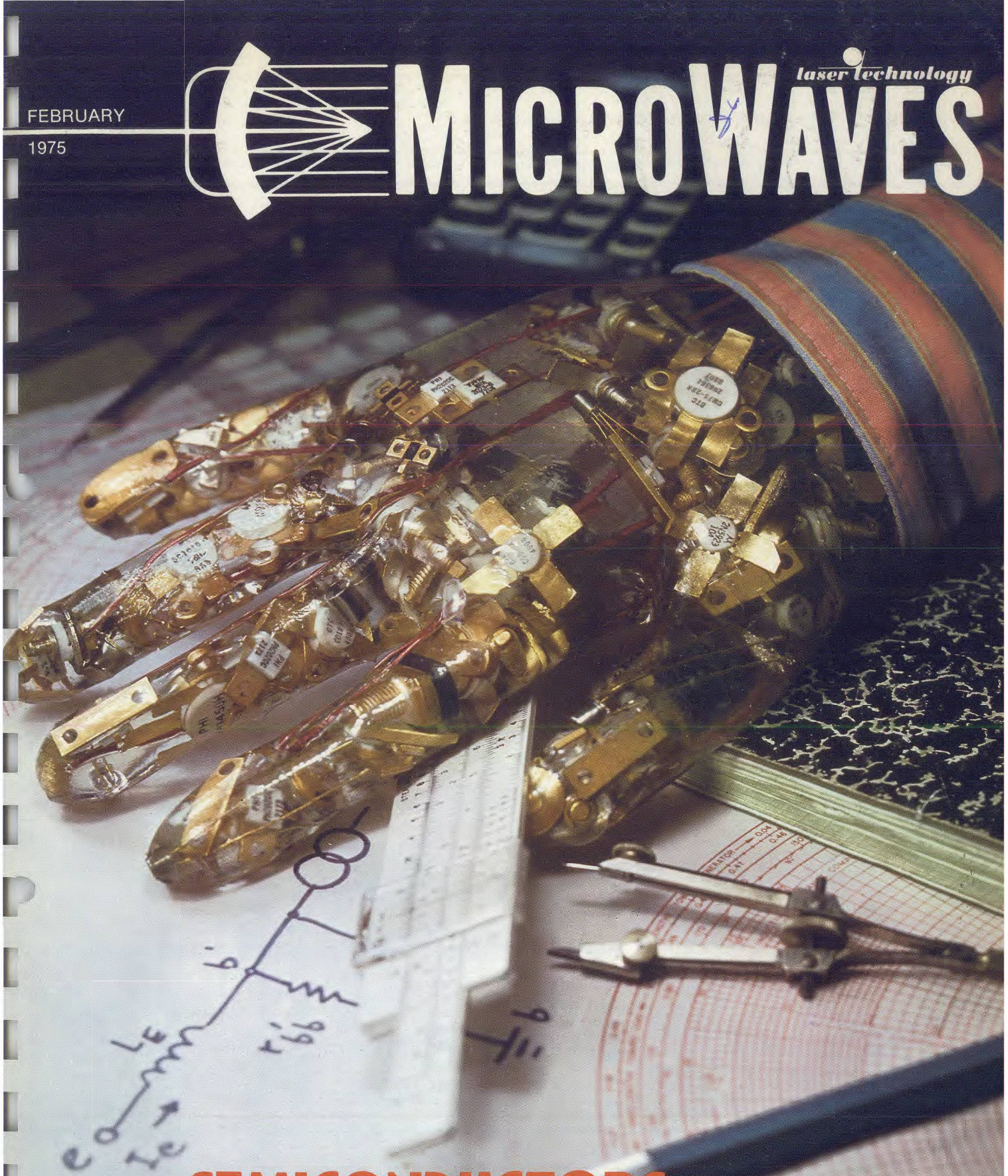
Trimmer capacitors, VC series, are offered in many standard sizes ranging from 1.625 in. to 4.25 in. in length with diameters from 0.25 in. to 1.12 in. max. Capacitance values are from 0.6 pF to 100 pF. Voltages from 1 kV to 12 kV are available. P&A: in qtys of 100, $30; 4-6 wks. **Polyflon Corporation, 35 River Street, New Rochelle, NY 10801 (914) 636-7222.**

CIRCLE NO. 139

FEBRUARY
1975

MICROWAVES

laser technology



SEMICONDUCTORS:

Modeling transistors for improved performance

Hybrid Coupled Amps: Can They Weather A Mismatch?

Semiconductor R&D shifts into high gear

Also: What's new in microwave frequency counters?

MICROWAVES

February 1975
Vol. 14, No. 2

news

9 Semiconductor R & D Shifts Into High Gear
10 Miniature SAW Filters Developed, Offer Low Insertion Loss
14 AWACS Flies Through First Trials
Artificial Radio Aurora Extends HF Communications
16 Industry
19 Washington
22 International
24 R & D
31 Meetings
30 For Your Personal Interest . . .

editorial

26 Don't Say It's Half Empty When It's Half Full

technical section

Semiconductors

33 **Modeling Transistors For Improved Performance.** Jim Curtis of Power Hybrids uses a transistor loading analysis to derive equivalent circuits for popular power transistors. Impedances are predicted for a wide range of operating conditions.

44 **Hybrid-Coupled Amps: Can They Weather A Mismatch?** Dr. Richard LaRosa of the Hazeltine Corp. examines the behavior of transistors combined by a quadrature coupler. Under mismatch conditions, one device may absorb rf power from the other.

72 Application Notes

TEST & INSTRUMENTATION

technical section

52 **What's New In Microwave Frequency Counters?** Duncan Mac Vicar and David Martin of Hewlett-Packard evaluate several approaches to counter design. Transfer oscillator, heterodyne converter and reciprocal frequency counters are described.

63 Application Notes
70 Measurement Notebook
58 Product Feature: Measure Insertion Loss Accurately, 50 MHz-18 GHz.
60 Product Feature: Signal Generator Adds 1300 to 2600 MHz Band, Offers Push-Button Frequency Control.
60 New Products
62 New Literature

products and departments

66 New Products
74 New Literature
64 1974 Annual Index
75 Advertisers' Index
76 Product Index

About the cover: An accurate power transistor model can be like a third hand for harried circuit designers. Jim Curtis of PHI helps you get a better grip on the subject, beginning on page 33. Construction and photo by Robert Meehan.

coming next month: Test and Measurements

A NEW WAY TO MEASURE NOISE. Algie Lance, et al, of TRW Systems presents a unique and very exact noise figure test procedure that requires only a known cold or known hot reference temperature. This single Y-factor method eliminates the error associated with small Y-factors (as encountered in the three Y-factor method).

MIXER NOISE MEASUREMENTS. Dan Cheadle of Watkins-Johnson describes a simple way to measure mixer noise using hot and cold resistor noise sources and an ordinary power meter. While similar to the familiar Y-factor method, this new technique does not require a precision, calibrated attenuator, which makes it ideal for production-line testing. Accuracy is ±0.2 dB.

CALCULATE TRANSISTOR EFFICIENCY AUTOMATICALLY. Ray Gutierrez of MSC describes how to build a direct reading calculator for measuring the efficiency of transistors and transistor amplifiers. It's inexpensive, saves time and is ideal for optimizing collector efficiency in newly designed transistor circuits.

Publisher/Editor
Howard Bierman

Managing Editor
Richard T. Davis

Associate Editor
Stacy V. Bearse

Contributing Editor
Harvey J. Hindin

Washington Editor
Paul Harris
Snyder Associates
1050 Potomac St., NW
Washington, DC 20007
(202) 965-3700

Editorial Assistant
Gail Murphy

Production Editor
Sherry Lynne Bogen

Art
Robert Meehan, Dir.

Production
Dollie S. Viebig, Mgr.
Dan Coakley

Circulation
Trish Edelmann, Mgr.
Peggy Long, Reader Service

Promotion Manager
Walter Salm
Albert B. Stempel (Reprints)

Editorial Office
50 Essex St.,
Rochelle Park, N.J. 07662
Phone (201) 843-0550
TWX 710-990-5071

A Hayden Publication
James S. Mulholland, Jr., President

MICROWAVES is sent free to individuals actively engaged in microwave work at companies located in the U.S., Canada and Western Europe. Subscription price for non-qualified copies is $10.00 for U.S., $15.00 a year elsewhere. Additional single copies $1.50 ea. (U.S.); $2.00 ea. (foreign); except additional Product Data Directory reference issue, $10.00 ea. (U.S.); $18.00 (foreign).

Hayden Publishing Co. Inc., James S. Mulholland, President, printed at Brown Printing Co., Inc., Waseca, MN.

Copyright © 1974 Hayden Publishing Co., Inc., all rights reserved.

Semiconductor R&D shifts into high gear

Stacy V. Bearse
Associate Editor

In spite of the stagnant picture painted for the semiconductor market, on-going R&D programs continue to grind out solid-state innovations.

Microwave researchers, in particular, are advancing semiconductor technology on several fronts —bipolar transistors, FETs and diodes. New materials and improved fabrication techniques have given rise to a new class of trapatt diode, high-power X-band FETs and high-speed differential amplifiers, complete with current sources, that fit on a one square-millimeter chip.

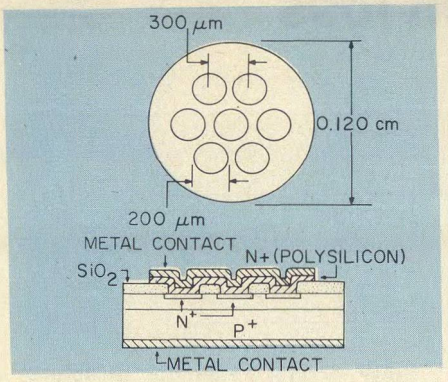
Of course, at this stage, most of these devices are laboratory prototypes and it's anyone's guess if or when they will find themselves in operational systems or on your distributor's shelf. But wasn't this the status of the transistor just 25 years ago?

Trapatt diodes have traditionally been mesa structures, but it appears that a planar design may offer significant advantages. Researchers at RCA Laboratories in Princeton, NJ, have successfully fabricated both p and n-type planar trapatt diodes, singly and in multiple diode arrays. One experimental seven-diode array reportedly produces 500 W of pulsed power at 1.4 GHz, with an efficiency of 30%.

Reliability looks promising

The major advantage over mesa devices is reliability, according to Dr. Shing-Gong Liu, a member of the technical staff at RCA. "Planar diode chips have sustained thermal tests at 500°C for over 800 hours without any change in their i-v characteristics. Similar mesa trapatts were also tested, but deteriorated at a lower temperature in less time," the researcher told conferees at the 1974 International Electron Devices Meeting in Washington, DC.

RCA's planar trapatts are fabricated on p/p^+ or n/n^+ silicon epitaxial wafers (Fig. 1). Diode areas are defined by growing silicon dioxide patterns on the p surface of the wafer. A polysilicon layer that interconnects multiple



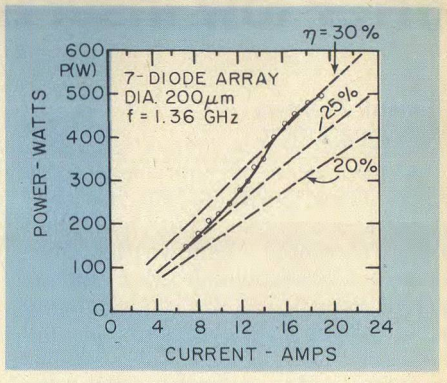
1. Top and cross-sectional views illustrate the size and construction of a p-type ($n^+ pp^+$) seven-diode planar trapatt array. The polysilicon layer enhances thermal reliability and provides a large shunt capacitance. If failure mechanisms are assumed to be strictly thermal in origin, a lifetime of 10^7 hours at 200°C is predicted.

diodes and acts as a diffusion source is then grown epitaxially over the entire surface. "Epitaxially grown arsenic-doped polysilicon is used for an n^+ diffusion source in the p-type diode, and boron-doped polysilicon is used for a p^+ diffusion source in the n-type diodes. By controlling the thermal growth times of the SiO_2 and subsequent n^+ or p^+ diffusion time, the depletion region is reduced to approximately 4 μm, which is suitable for trapatt oscillation in the upper L-band frequency range," Liu reports.

The top of the polysilicon layer as well as the bottom of the wafer are metalized for electrical contact and heat sinking.

"The shallow (≈1 μm) diffusion junction is isolated from the metal contact by the polysilicon layer which helps to increase the reliability of the device," Liu explains.

The polysilicon cap and the SiO_2 layer act to form a large shunt capacitance across the diode array. Liu says that this capacity is important to sustain the high current states necessary for trapatt oscillation at high bias current levels. The seven-diode array cited earlier, for instance, has a shunt capacitance of about 9 pF. RCA's data indicates that at a pulsed output level of 500 W, the array operates at a current level of 19 amperes (Fig. 2) or a bias current density of approximately 9000 A/cm².



2. Operating current is approximately 19 A at 500 W for the seven-diode array.

All tests were conducted in a microstrip circuit at the fundamental trapatt frequency. The planar diode chip is soldered, epitaxial-layer-side down, on a gold plated copper stud. Typical applied pulsewidths ranged from 0.5 to 1.0 μs.

1.6 W FET features f_{max} of 23 GHz

New fabrication concepts continue to expand the scope of future applications for field-effect transistors. Once eyed only as replacements for bipolar transistors in small signal, low-noise applications, FETs are beginning to look attractive for X-band power and switching applications.

At Fujitsu Laboratories in Kawasaki, Japan, a double-mesa interdigitated construction technique has led to the design of an 8 GHz FET that belts out 1.6 W of saturated output power with about 45% drain efficiency. This particular design is actually a parallel combination of two FET cells, each featuring interdigitated source and drain electrodes and a novel overlaid gate structure which parallels 52 gates to form an overall gate length of 2600 μm per cell. Individually, each cell is capable of providing a 0.7 W saturated output at 8 GHz.

Fujitsu's FET is based on a semi-insulating GaAs substrate on which an S-doped, n-type epitaxial layer has been grown (Fig. 3). The epitaxial layer is removed outside the active area by two-step mesa etching. Thin films of Au-Ge and gold are deposited on the wafer and the interdigitated source and drain fingers are de-

(continued on p. 12)

Miniature SAW filters developed, offer low insertion loss

Richard T. Davis
Managing Editor

A new type of surface-acoustic wave filter, suitable for narrow-band applications (i.e., less than 1% fractional bandwidth), has been developed which offers an order-of-magnitude size reduction and much lower loss over conventional surface-wave filters. The device called a surface-acoustic wave resonator uses a series of distributed reflectors which fold a wave back onto itself many times, as in a conventional microwave cavity. Because the reflection coefficient is 98% or better, very little energy is lost and Q's of 10,000 at 400 MHz have been obtained. Typically, a conventional SAW filter has an insertion loss of anywhere from 5 to 55 dB when unmatched.

According to Edward Staples, senior staff engineer at Piezo Technology, Inc., Orlando, FL, there are several main advantages to the SAW resonator:

- Fundamental frequency operation extends throughout the uhf frequency range.
- The Q is insensitive to substrate mounting or crystal thickness.
- Trimming can be acomplished during dielectric passivation.
- Batch processing is possible using photolithography.

This last advantage presents the possibility of LSI techniques being implemented for these miniature filters.

The SAW resonator could be used as a frequency stable cavity in oscillators and thus could compete with crystal-controlled oscillators. It's also suitable for a wide range of i-f filter applications such as in radar and communications systems.

A SAW resonator, Fig. 1, consists of two surface-wave grating reflectors which form a cavity. In between is an interdigital transducer (IDT) that provides the electrical input/output coupling to the resonator.

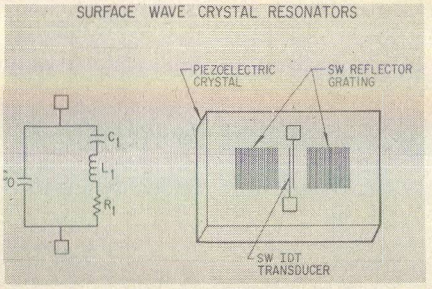
"When an rf voltage is applied to the pads of the IDT, surface-acoustic waves are generated and propagate away from the transducer in both directions. As the waves propagate into the grating reflectors, coherent multiple reflections occur and a large standing wave is set up within the cavity," says Staples. The spacing of the reflectors determines the resonant or anti-resonant behavior of the cavity in much the same way of a Fabry-Perot interferometer. If the separation is an integral number of half-wavelengths, then the cavity will resonate and a standing wave will exist between the reflectors. If the separation is an integral number of half-wavelengths plus a quarter wavelength, then the cavity will be anti-resonant and the surface waves within the cavity will not be reinforced.

Staples maintains that because surface waves are a complex mixture of shear and longitudinal motion (held together by the presence of a stress-free boundary condition), the use of distributed discontinuities is essential. "The coherent addition of many small reflections gives rise to almost total reflection. Any abrupt discontinuity, on the other hand, such as used in bulk-acoustic wave devices, would cause the SAW wave to break down into individual shear and longitudinal bulk waves propagating away from the discontinuity."

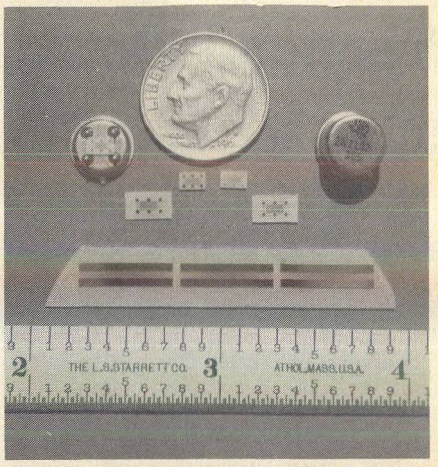
Because the SAW propagation folds over upon itself, the size of a SAW resonator is inversely proportional to its center frequency. As such, it is considerably smaller than conventional surface acoustic wave filters whose bandwidth is determined by the crystal length and is independent of frequency, Fig. 2.

At Texas Instruments, Dallas, TX, where much of the work on surface wave resonators originated (based on theory originally proposed by Dr. Eric Ash, then of IBM Research Labs, now at University College, London), several devices have been constructed on various substrates. According to Dr. Jeff Schoenwald, MTS, at TI's Advanced Technology Laboratory, the resonant behavior of a YZ cut $LiNbO_3$ device was observed at 650 MHz with a Q of 3,000 and at 140 MHz a Q of 10,000 was obtained using ST-quartz. "Another model is also being tested at 860 MHz using $LiNbO_3$ but fabrication resolution is yet a problem," says Schoenwald.

Equivalent circuits based on the electrical and elastic properties of the substrate and thin films have been found to be similar to those of bulk resonators. However, the similarity between the devices ends here. For example, the surface-wave resonator has spurious responses that are over 30 dB down. In bulk devices, the spurious are much higher. "This is because a SAW resonator does not have the inherent reflecting surface of a bulk device since each series of fingers only reflects over a very narrow band," explains Schoenwald. ••



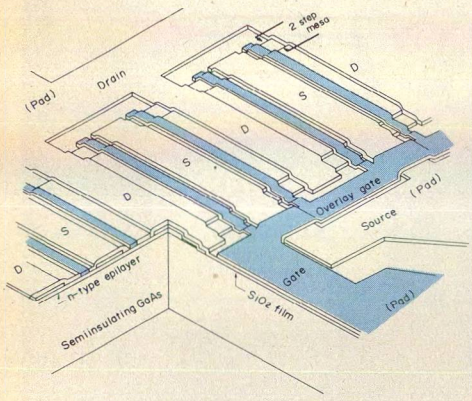
1. **SAW crystal resonator structure** has an interdigital transducer placed inside the cavity formed by two surface-wave reflectors. The overlap of the IDT electrodes is made large compared to an acoustic wavelength to minimize diffraction. The resonator equivalent circuit is identical to a conventional bulk-wave resonator.



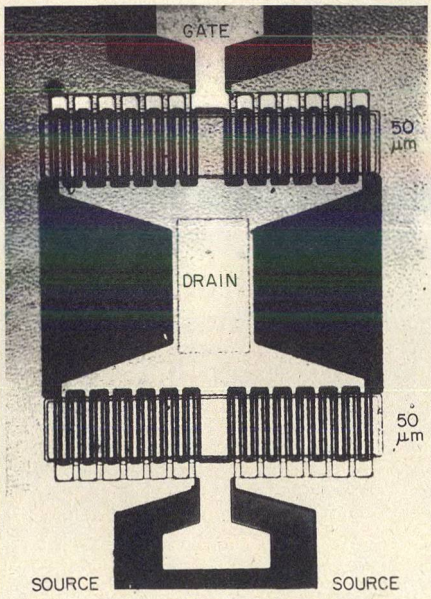
2. **Size comparison of SAW resonators** with a conventional SAW filter (bottom) of comparable bandwidth (200 kHz) shows at least an order-of-magnitude size reduction. SAW resonators are small enough to fit onto a transistor header and could lend themselves to LSI techniques.

Semiconductor R&D shifts into high gear

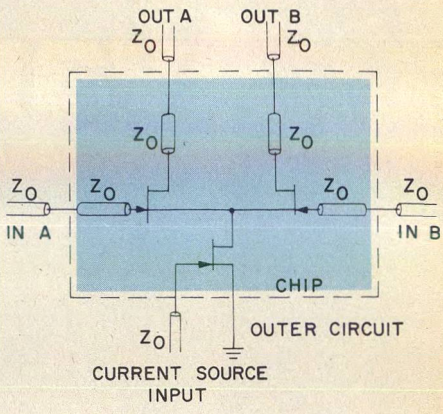
(continued from pg. 9)



3. Interdigitated construction and an overlay gate structure contribute to 0.7 W, 8 GHz performance and an f_{max} of 23 GHz. The gate structure measures 2 x 2600 μm. Separation between source and gate is 1 μm, while the drain to gate gap measures 2 μm.



4. Two of these 'FET cells' have been combined to produce 1.6 W at 8 GHz. The sheet-grounding technique used to combine source fingers minimizes source lead inductance.



5. Three FETs are combined on a single chip to form a differential amplifier with an integral current source. A gain bandwidth product of 8.5 GHz is reported.

fined using standard photoresist techniques. "These contacts are alloyed at 450°C for 120 seconds in N_2 gas. A rapid temperature rise of the wafer (10 seconds from room temperature to 450°C) is the key to getting uniform Au-Ge and GaAs alloying and a low-omic contact," remarks Masumi Fukuta, senior scientist at Fujitsu and a speaker at the 1974 IEDM.

After the source and drain fingers have been defined, the substrate is coated with a 0.4 μm thick SiO_2 film, which is carefully etched to expose gate windows. A 0.5 μm thick aluminum layer is deposited on top of the SiO_2 and selectively etched to form 52 parallel Schottky gate fingers.

Finally, source and drain bonding windows are opened by again etching the SiO_2 film. The FET chip is thinned to 80 μm to reduce its thermal resistance and mounted on a gold-plated copper carrier. The whole surface of the chip, except for the active area, is metalized by a gold-tin solder, (Fig. 4) and electrically connected to the source electrode in order to reduce the common source lead inductance.

Eight GHz performance, the Fujitsu researcher reports, includes a MAG of 9.3 dB, (extrapolating at 6 dB per octave, this indicates an f_{max} of 23 GHz) a unilateral gain of 12.7 GHz and a maximum stable gain of 13.7 dB.

5 to 10 W predicted in the future

Dr. Fukuta says that future work will be directed toward minimizing common source lead inductance. "If the common source lead inductance is lowered to one-fifth of the present value, it is expected the MAG at 8 GHz would increase about 2.5 dB," he speculates.

Dr. Fukuta, inventor of the web mesh FET structure, told the assembled engineers that he expects to see X-band FETs producing five to ten watts in the near future.

55 ps switching times realized

Researchers at Germany's Institute of Semiconductor Electronics have been investigating potential high-speed switching applications for field-effect transistors. One of their most interesting devices to date is a high-speed differential amplifier that incorporates three FETs on a single semi-insulating GaAs substrate (Fig. 5).

"To achieve a voltage gain with a 50-ohm load, the two differential MESFETs are laid out with five gate stripes (measuring 1.5 x 750 μm) resulting in a transconductance of 40 mmhos per FET. A current source, realized by means of a third FET, is integrated on the chip and directly coupled to the source contacts of the differential pair," outlines Erhardt Kohn of the Semiconductor Institute.

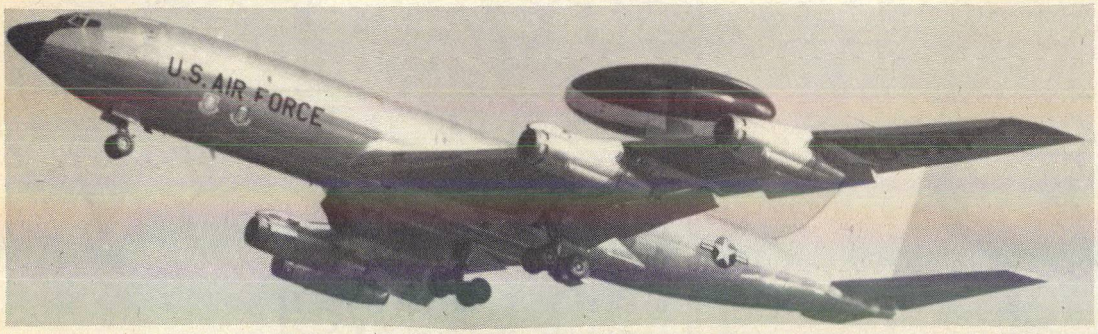
Performance is impressive. An output risetime of about 55 ps, common mode rejection ratio of 26 dB and switching power of 185 mW are reported.

Although most new devices reported at the 1974 IEDM are based on Si or GaAs substrates, work performed at Cornell University indicates that indium phosphide (InP) may be a superior material under certain conditions.

Basic FET theory assumes that carriers in the channel instantly respond to an electric field by acquiring a velocity given by the equilibrium velocity curve for a particular field. But a time-dependent, statistical Monte Carlo analysis of non-equilibrium electron transport in InP and GaAs short channel FETs shows that electrons can acquire velocities considerably greater than the velocity curve predicts.

"This velocity overshoot is more pronounced in GaAs than InP, and thus, given the proper conditions, submicron channel GaAs FETs can be expected to cut off at a higher frequency that InP FETs, owing to a faster transit time," Cornell's Timothy Maloney explains. "But for channels from one to ten microns long, the high peak-velocity and threshold field of InP may lead to devices superior to those of GaAs," he adds. ••

AWACS flies through first trials



The U.S. Air Force Airborne Warning and Control System (AWACS), a flying command post for control of air warfare, has completed a month-long demonstration of its capabilities in a series of complex air engagements. This initial operational test and evaluation phase of the AWACS development program involved some 45 airborne hours during eight flights throughout the United States.

Using a modified Boeing 707-320B airframe topped by a 30-foot rotating array, AWACS is based on a Westinghouse high-prf, pulse doppler radar designed to detect and track aircraft flying at high and low altitudes (see Rush Is On to Complete First AWACS Radars, MicroWaves, September, 1973).

During a two-day exercise on the East Coast, Air Force Test and Evaluation Center crews operated the Airborne Warning and Control System in control of interdiction, close-air support, aerial combat and search and rescue missions. During this operation, a test was conducted with the U.S. Navy to show the compatibility of AWACS data with the Navy Tactical Data System (NTDS). Data on low-altitude penetrating aircraft obtained by AWACS was fed to the NTDS for use in Navy control of their interceptors.

In a separate test with the U.S. Army, it was shown that AWACS could provide precise tracking information of attackers at long range directly to Hawk missile batteries, claims Brig. General Lawrence Skantze, AWACS program director at the Electronic Systems Division.

An Aerospace Defense Command (ADC) exercise called Felix AWACS was conducted over the Pacific Northwest. This involved multi-aircraft penetrations that included electronic countermeasures aircraft and fighter bombers playing the enemy role.

In the exercise, which simulated a major air defense engagement, AWACS scrambled interceptors from their bases and directed interceptors from their combat air patrol positions. Aircraft of the Canadian Armed Forces also participated.

A special survivability exercise carried out in the southwestern U.S. was designed to test AWACS' ability to protect itself from attackers. The attacking force whose mission was to incapacitate AWACS was composed of F-15s, F-106s, F-5s and F-4s working in conjunction with ground based and airborne jammers. The protective force under the direction of AWACS was made up of F-15s and F-4s.

"All of the attackers were neutralized at ranges in excess of their air-to-air weapon capability. In addition, successful simulated attacks against ground-based jammers were completed by AWACS-directed close-air support, aircraft," General Skantze reports.

Next major event for the AWACS testbed, now in the planning stage, is a demonstration of ship detection and tracking. Indications are that this demonstration in conjunction with NATO requirements may take place in Europe in the spring of 1975, according to General Skantze. An additional modification will be made to the testbed to improve the maritime capability for the European demonstration. •• *S.V.B.*

Artificial radio aurora extends HF communications

In trying to develop an interference technique for disrupting ionospheric scatter communications, The Defense Department's Advanced Research Projects Agency, Washington, DC, fell upon a way to extend and improve their own HF communications.

Normally, the ionosphere reflects signals from 3 MHz to 30 MHz back to earth for distances of about 100 miles. However by creating an artificial radio aurora, using large ground-based hf transmitters that put out approximately 2 mega-watts, signals have been found to be reflected over a 1,000 mile range and over frequencies extending to 450 MHz increasing both range and usable spectrum by an order-of-magnitude.

The power transmitters or "heater" installations use high-gain antennas to produce an EIRP of from 20 million to 30 million watts. This, in turn, raises the temperature of electrons in the ionosphere creating scattering irregularities aligned with the geomagnetic field. The result is a reflector 100 miles in diameter and 10 miles thick. This enormous cloud can't be seen by the eye, but it can be photographed with an infrared camera. When the transmitters are turned off, the artificial cloud dissolves instantly.

One of the group based HF transmitters that does the heating is located near Platteville, CO, and is operated by the Institute for Telecommunications Sciences. Another transmitter is the 1,000-ft dish at Arecibo, PR, managed by Cornell University. A third is at Gorki in the Soviet Union about 400 km east of Moscow. Stanford Research Institute, Menlo Park, CA, is studying the feasibility of the system as a communications technique. •• *R.T.D.*

Modeling Transistors For Improved Performance

Power transistor modeling is useful for predicting input/output impedances over a wide range of conditions. The equivalent circuits derived are based on loading and are useful for CAD.

THE optimum performance of a microwave power transistor depends largely on obtaining an input and output impedance match. Unfortunately, any change in operating parameters, be it a change in frequency, power, drive, voltage or mode, will cause a shift in impedance.

Transistor models or equivalent circuits are quite helpful in handling the situation, since they can predict the change in impedance that results from a change in transistor operation. Based on the usually available transistor data, it's possible to predict or extrapolate a transistor's expected impedance and then design a "first-cut" circuit that allows complete characterization. From this, a more detailed model can be developed which gives a good understanding of microwave transistor operation and, therefore, a good basis for analyzing the validity of measured performance parameters.

Unlike small-signal transistors, which can be characterized by s-parameters or the wave reflection and transmission parameters of the device, the large signal operation of a power transistor requires characterization in terms of loading. Since maximum power output is not usually obtained by a conjugate match of the transistor's internal impedance, external loads are transformed by package and transistor die parasitics to an intrinsic load that yields maximum power. By starting with an intrinsic die characterization, in terms of maximum power and gain, and then proceeding to the source and load by adding estimated package parasitics, a fairly accurate model can be developed.

These models are quite helpful in computer-aided design work, particularly those analytic programs offering an optimization routine.

Jim Curtis, Engineering Manager, Power Hybrids, Inc., 1742 Crenshaw Blvd., Torrance, CA 90501.

Operating region: cut-off to saturation

The majority of power transistors are operated either Class C (cw) or Class C (pulsed) with a constant power output. They are usually loaded for maximum power output and maximum gain (at that output) and as such, their operation falls into three areas: cutoff, saturation and a relatively linear region between these extremes.

By operating at or near saturation, (i.e., to within 1 dB) transistor conversion efficiency and bandwidth are maximized. It is also most cost effective in terms of power per dollar. Saturation—defined as the operating point where an increase in drive yields no increase in output—is caused by either current crowding in the base region (which reduces effective emitter current injection) or by the advent of secondary breakdown in which the collector-base junction begins to avalanche. As a result it clips the output voltage peaks before maximum current is achieved. Current saturation occurs first at lower voltages and secondary breakdown generally limits output power at higher voltages. Secondary breakdown can also occur simultaneously with catastrophic failure at higher voltages depending on transistor and circuit ballasting.

Saturation is both load and temperature dependent. The load dependence causes a transistor to deliver less than maximum output power at a given voltage, drive and frequency. Temperature dependence of saturation causes the maximum output power to be reduced with increasing junction temperature.

The relatively linear region in which a power transistor operates does have a point-by-point non-linear transfer function caused by current gain changes as a function of the absolute current. As such, this non-linear active region must be represented as input and output harmonic responses of impedance and gain in the frequency domain. The total effect thus produces impedance and transfer characteristics having harmonic components.

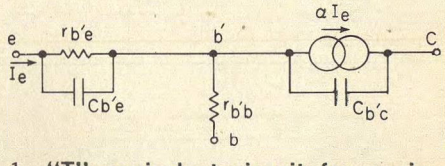
Since it is only the fundamental frequency that is of interest, these harmonics can be ignored and in practice, filtered by impedance matching and external filter structures. The characterization and modeling described in this article are only concerned with fundamental frequency matching.

Common base model

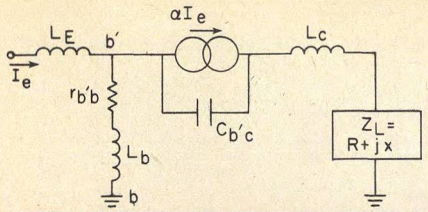
Since almost all microwave power transistors operate common base (it offers the highest gain), a good starting point to develop a model is to use the standard "T" equivalent circuit for the common base transistor, Fig. 1.

For microwave power transistors, $C_{b'e}$ in parallel with $r_{b'e}$ forms a low impedance compared with the base spreading resistance, $r_{b'b}$. Therefore, $C_{b'e}$ and $r_{b'e}$ can be ignored. When the transistor is packaged, bond inductances and package parasitics modify the simplified "T" equivalent circuit into the circuit of Fig. 2. This

(continued on next page)



1. **"T" equivalent circuit for an intrinsic common base transistor** is a good starting point for transistor modeling. $r_{b'e} = 1/q_m$; $r_{b'b}$ = base spreading resistance; α = current gain = $\alpha_o/(1 + j\omega/\omega\alpha)$; $C_{b'e}$ = base charging capacitance $\cong q_m/\omega_t - C_{b'c}$; $C_{b'c}$ = collector base depletion capacitance $\cong C_{ob}$.



2. **Simplified "T" equivalent model** can be developed by assuming certain elements to be negligible. The model includes package parasitics and load.

circuit results because power transistor impedances are low and package parasitics usually add distributed inductance to the normal bond inductances. Exceptions can occur for smaller (up to a few watts) transistors at high (S and C band) microwave frequencies.

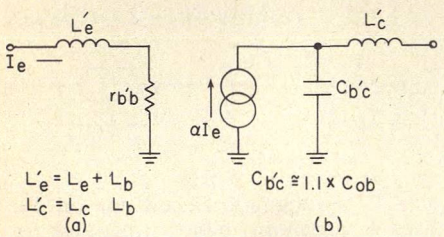
Figure 2 also shows the packaged microwave power transistor with a load Z_L. A further simplification, shown in Fig. 3, involves separation of the model to yield a unilateral equivalent circuit. It is based on assuming the sum of the collector reactances, (L_b, C_{ob}, L_c and I_m [Z_L]) is zero (conjugate collector match), and generally R_e [Z_L] >> $r_{b'b}$ (derivation is given in Appendix A). Both assumptions are almost always valid for microwave power transistors.

From Fig. 3, the input impedance can be found to be:

$$Z_{in} = r_{b'b} + j\omega (L_e + L_b) \quad (1)$$

The collector circuit (Fig. 3(b)) is represented by a parallel current generator and capacitor equal to $C_{b'c}$ and series inductance equal to $L_b + L_c$.

This model covers the transistor during the active part of the rf cycle. If all three regions of device operation are considered, however, it's important to note that the parameters $r_{b'b}$, $C_{b'c}$ and α are varying in the time domain. This time domain variation corresponds to a Fourier series expansion of voltages and currents in the frequency domain. A good approximation can be made by modifying the values of $r_{b'b}$, $C_{b'c}$ and α and considering the fundamental response only.



3. **Unilateral equivalent circuit** is a further simplification of the "T" equivalent circuit and is based on $R_e(Z_L)$ >> $r_{b'b}$ and a conjugate collector match. $L'_e = L_e + L_b$; $L'_c = L_c + L_b$; $C_{b'c} = 1.1 \times C_{ob}$.

If a good input/output isolation exists in a transistor, then the unilateral model in Fig. 3 can be derived and successfully used as a model. Another way of looking at the input characteristic of a microwave power transistor, however, is to consider it as a P/N diode in series with an inductor. The impedance characteristics of this diode-inductor series circuit can be approximated as an inductor, resistor and ideal diode all in series. The fundamental impedance is then a scaling factor times the diode dynamic resistance in series with the inductor. One way of evaluating the input "diode" characteristics of a microwave transistor is to bias the transistor "on" Class A and measure S_{11}, the input reflection coefficient. A good correlation exists between S_{11} (at V_{ce} = 5 V and I_c = quiescent collector current under normal operation) with measured large signal input impedance. In fact, the base-emitter junction may simply be biased at half the nominal collector current with the collector open to yield a good estimate of the input reflection coefficient. Either of these techniques will give values for $r_{b'b}$ and L'_e in the unilateral equivalent Model, Fig. 3.

To assign a value to the collector-base capacitance, $C_{b'c}$ of Fig. 3, it's important to understand what comprises collector-to-base parasitic capacitance. There are basically three components:

- Package or header capacitance
- Die MOS (metalization) capacitance
- Junction depletion capacitance.

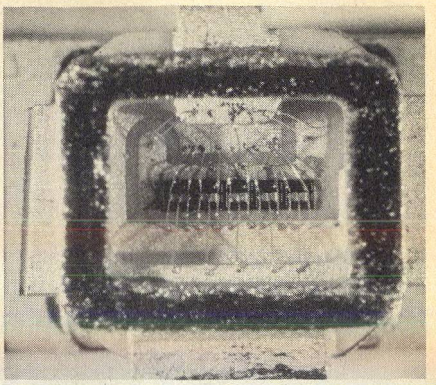
Of the three, package and die MOS capacitance are fixed. Junction capacitance is dependent on collector base voltage

$$C = \frac{K}{(V_{CB} + V_B)\,[1/n]} \quad (1)$$

where

K = constant based on junction area
V_{CB} = collector-base voltage
V_B = junction barrier voltage
n = exponential factor based on junction profile

Of the three components of collector-base capacitance, the static components typically make up one-third of the total at 28 Vdc bias. The effect of the voltage dependent junction capacitance is to yield a higher effective capacitance under Class C operation than the value at nominal collector voltage. Emperically, the value of collector base capacitance at nominal voltage is multiplied by a factor of 1.1. Remember that often manufacturers specify C_{ob} at a collector-base voltage of 28 Vdc. If a circuit is to be operated 22 Vdc, the C_{ob} value at 22 V must be measured on a capacitance bridge before multiplying the value by 1.1.



4. **Internal packaging and bonding geometry** of the Power Hybrid PH3006 shows bonding wires from the base bonding pads to the package ground plane.

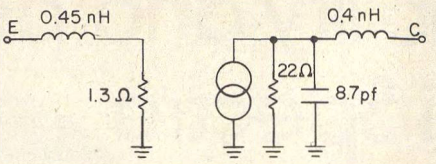
The final element to be determined in the collector equivalent circuit is the series inductance, L'_c. As previously explained, L'_c is composed of the effects of L_b, the base bond inductance, plus L_c, the collector lead inductance. Both are highly dependent on transistor packaging. The component L_b consists of effective bond wire inductance from the base bonding pads to the package ground plane. The value depends on the number of base bond wires and the geometry of the bonding. Current technology microwave power transistors use a cellular geometry similar to that shown in Fig. 4. Individual base cells are diffused into a common epitaxial collector. The metalized cells are paralleled by bonding individual cells to common "terminals" on metalization areas within the package. Lower power devices within a transistor family are made by using fewer cells of a common die geometry, and, therefore, have fewer bonds and a higher effective L_b.

Bonding geometry is a function of package design. The package in Fig. 4 has an electrically-isolated collector mounting pad surrounded by a ground plane. This particular geometry allows each base bonding pad to be bonded to ground with parallel wires, thereby further reducing the parasitic base bond inductance, L_b. The value of base bond inductance found for various geometries and power levels may vary from less than 0.1 nH to about 0.5 nH.

(continued on p. 36)

The second component of collector inductance is the collector lead inductance, L_c. Again, it varies from device to device and is highly dependent on package design. Packages having isolated collector pads use bond wires to connect the pad to the collector lead metalization. Therefore, the lead inductance is composed of bond wire inductance in series with, effectively, a microstrip transmission line (collector lead metalization). The transmission line acts as a distributed inductor because of the low collector impedance. It's equivalent inductance depends on the impedance it transforms, but generally will be in the area of 0.2 to 0.4 nH. That, plus a typical collector bond inductance of 0.2 to 0.3 nH gives a total collector lead inductance (L_c) of about 0.4 to 0.7 nH. Adding in the base lead inductance, the equivalent collector inductance (L'_c) will vary from 0.5 to 1.2 nH. Higher power devices (over 10 W) with more base bonds (therefore, lower base lead inductance) and lower equivalent package transmission line inductance are close to 0.5 nH. Using the reverse arguments, lower power transistors ($\approx$ 1 W) are closer to 1.2 nH. These are good "first cut" values for a transistor's L'_c. The value can be refined as actual measured data is taken.

The above description covers the equivalent electrical elements of a microwave transistor. For Class C power amplifier applications, it is necessary to match the input impedance of the transistor (conjugate match), and the load of the collector so as to extract a given amount of rf power (usually close to the saturated power of the device). The collector loading forms an integral part of the model, and it must be added in order to predict the collector load impedance. Under rf operation, the voltage waveform at the intrinsic collector (across the current generator), is a sinusoid having an average value of V_{cc}, and a peak rf value of $V_{cc} - V_{ce}$ (sat). The transistor parasitics, $C_{b'c}$ and L'_c, transform the external collector load impedance to some value $R_L + jX_L$ across this intrinsic collector-base voltage. Maximum power is generated when the loading is nonreactive (or conjugate matched); therefore, for maximum power, $jX_L = 0$. From Ohm's law, the resulting power delivered to the transformed load is:



5. Final model of a PH3006 power transistor is characterized for V_{cc} = 20 Vdc and P_o = 7 W. This model is used to predict the impedances shown in the table.

$$P_o = \frac{(V_{cc} - V_{ce(sat)})^2}{2}\left[\frac{1}{R_L}\right] \quad (3)$$

Solving for R_L

$$R_L = \frac{(V_{cc} - V_{ce(sat)})^2}{2P_o} \quad (4)$$

By including a virtual resistance, R_L, or a load parameter transformed to the intrinsic collector (rather than actually inside the transistor) placed across the current generator, the collector load impedance can be predicted. To solve Eqn. (3), it is necessary to know the value of $V_{ce(sat)}$. Under rf operation, the effective saturation voltage of a microwave power transistor is about 2 to 3 volts depending upon the degree of saturation and the geometry of the device being modeled. Usually, the saturation voltage can be estimated as 10% of the power supply voltage, V_{cc}.

Modeling example

Consider an amplifier that operates from 2.1 to 2.3 GHz with a 7 watt output power and a collector voltage of 20 Vdc. A Power Hybrids, model PH3006 transistor, will meet the power requirements and a 24 V impedance characterization is given in the data sheet. A measurement of the collector-base capacitance, C_{ob} at 20 Vdc gives typically 7.9 pF. From Eqn. (2)

$$R_L = \frac{(20 - 25)^2}{2 \times 7} = 22 \text{ ohms}$$

If further information on the transistor's impedance isn't available, assume that the collector lead inductance, L'_c, is about 0.5 nH. (The PH3006 is a relatively high-power device with lower parasitics due to its many bond wires). Since the data sheet gives characterization at 24 Vdc, it is important to derive a model for the collector at 24 V to check this estimate of L'_c. Without going into detail, it is possible following the procedure previously at 20 Vdc and using C_{ob} at 24 Vdc to modify L'_c to a closer approximation of 0.4 nH. The model for the collector circuit of the PH-3006 at V_{cc} = 20 Vdc and P_o = 7 W is then complete as shown in Fig. 5. Because the input impedance is relatively independent of collector voltage, the equivalent input circuit can be taken directly from the data sheet's impedance plot. At 2.3 GHz, the data sheet indicates:

$Z_{in} = 1.3 + j6.5$

The table below lists the theoretical impedance of the PH3006 derived from the model. A check of a PH3006 has indicated a good correlation with the model. Note that the model predicts collector impedance, and that the data listed in the table is the collector load impedance or the conjugate to conform with industry standards.

Table 1: Theoretical Impedance of PH3006

Frequency (GHz)	Z_{in}(ohms)	Z_{cl}(ohms)
2.1	1.3+j5.9	3+j2.3
2.2	1.3+j6.2	2.7+j1.7
2.3	1.3+j6.5	2.5+j2.3

Characterizing the transistor

So far, a model for a microwave power transistor has been developed, based on a few simple calculations, a capacitance measurement and an estimate of parasitic inductance which is determined by package geometries and power levels. If a manufacturer's data sheet contains some characterization information, these rough estimates can be refined. This usually ties down such things as the parasitic inductances and the input impedance model.

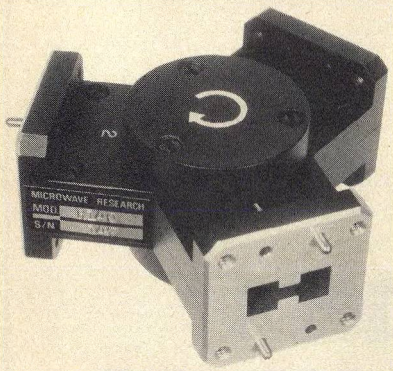
There are two uses of a model as shown in Fig. 5. First, with very little rf information, it will give a first cut estimation of the transistor's impedances. And second, if impedance characterization exists at one voltage, frequency and power level, a very good estimate can be made of the impedance at a different voltage power and/or frequency by an analysis of the model. For more accurate impedance information, a point-by-point impedance characterization is necessary, however.

Characterizing a microwave power transistor to a large part is subjective, and the accuracy of the characterization is somewhat dependent upon guessing the answer before making the measurement. Essentially, a power transistor is characterized by optimally tuning it in a circuit for maximum output power and minimum reflected power. When these conditions are met, the impedance presented by

(continued on p. 38)



WISE EYES ARE ON MRC's NEW HIGH POWER CIRCULATOR



We're Hooting about our Model R140 FERRITE CIRCULATOR in WRD-750-D24 Double-Ridge waveguide. It fulfills the need for HIGH POWER operation over an Octave band in the frequency range 8.0 - 18.0 GHz.

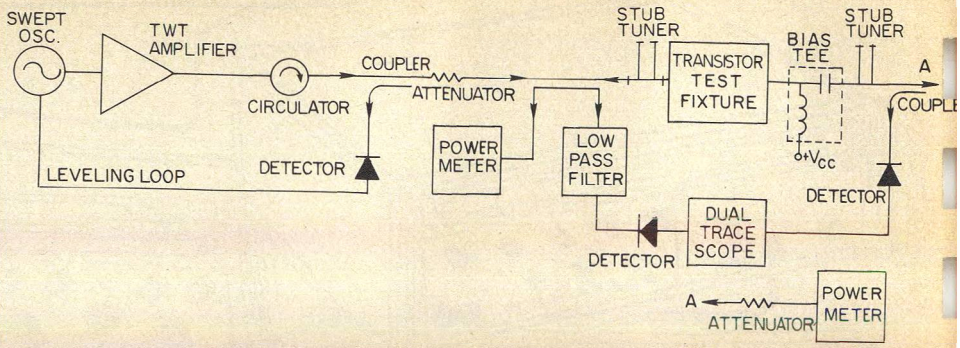
ISOLATION	15dB Min
INS. LOSS	0.5dB Max
VSWR	1.50 Max
POWER	200 W av
	5 KW pk

Let us fill you in on the details. For further information, contact:

mrc

MICROWAVE RESEARCH CORPORATION
1429 Osgood Street
North Andover, Mass. 01845
Tel. (617) 685-2776
TWX. 710-342-1249

READER SERVICE NUMBER 38



6. **Test setup for characterizing power transistors** uses a test fixture with low loss matching circuits. A frequency counter is also needed.

the circuit at the test frequency is measured using a network analyzer or slotted line. This gives the conjugate input impedance and the collector load impedance.

In order to optimize the transistor performance, the test circuit used must have low losses and be capable of presenting impedance variation at and around the optimum. Tuning adjustments should converge on the optimum impedances with low and constant loss (less than 0.2 dB) so that the exact impedance point may be determined. A circuit with varying losses will give more than one peak in performance and must be avoided.

Figure 6 shows a typical characterization setup for high power microwave transistors. Not shown is a frequency counter for both accurate frequency calibration during measurement and so the frequency can be monitored and held constant. This is important when using the swept oscillator to drive the network analyzer to measure the circuit impedance. The transistor test fixture serves to mechanically hold, thermally sink and to electrically interface the transistor. To satisfy the last requirement, the test fixture should contain low loss matching circuits that transform the low input and output impedance of the transistor to an intermediate level. These can finally be matched to 50 ohms using stub tuners or some other variable impedance matching elements. In order to keep the fixture short electrically, two short series transmission lines of different impedance are used for matching by transforming over a reasonable bandwidth. Low-loss microtrip circuits made on 0.015 in. thick duroid serve well for this purpose. The fixture should have sufficient thermal mass to keep the temperature fairly constant while tuning up a transistor.

A transistor-under-test is placed in the fixture and driven from the rf source at the nominal drive level. First, with the power supply set at 0 volts, the input tuner is adjusted for minimum reflected power as indicated by the minimum detected voltage at the input reflection port.

A low-pass filter is used to reject harmonics generated by the nonlinear characteristics of the transistor's input. Without the low-pass filter it is impossible to obtain good return loss because the tuning will tend to compromise matching the fundamental frequency and reflected harmonics. The power supply current peaks as the input power is matched to the transistor. With proper input match and with zero power supply voltage, the transistor draws one-third to one-half the current expected under full voltage. If the transistor does not draw current when driven at a nominal level and with the input tuned for minimum reflected power, there is something wrong with the setup.

The output is tuned by raising the supply voltage to about one-third the final V_{cc} and adjusting the output stub tuner for maximum output power. Because of some interaction, the input tuner will have to be slightly adjusted to keep the reflected power nulled. As the performance is optimized at a particular voltage, the supply is increased and the tuning reoptimized. As higher voltages are approached, make the power supply increments smaller (one to two volts) to avoid severe load mismatch. Remember that changing the supply voltage changes the optimum impedance. When the tuning is finally optimized for the frequency, voltage and power desired, lock the tuners.

Impedance measurement can be made in several ways. One way is to use a "break-apart" fixture that can be separated to allow mounting a connector in place of the transistor. A network analyzer is refer-

(continued on p. 40)

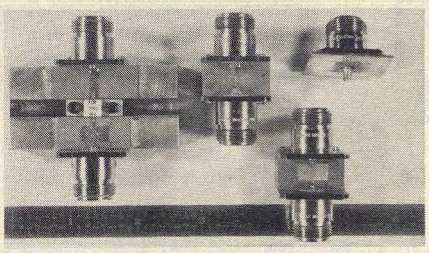
enced to the point where the transistor leads contact the test fixture, and the source and load impedances are measured. However, a preferred method is to build substitution circuits, as shown in Fig. 7, that duplicate the input and output microstrip fixture circuits. They avoid the necessity of breaking the test fixture apart and attaching connectors for each measurement. The input and output tuners are connected to their respective substitution blocks (output tuner plus bias tee), and the source and load impedances are measured with the network analyzer referenced to the transistor lead contact point.

Characterization is point by point for power transistors rather than swept as with small signal S-parameter measurements. If the point-by-point characterization doesn't show consistent performance and reasonable impedances, there may be a fixture or setup problem. As the tuners are adjusted, current and power should respond smoothly if the fixture properly matches the device. There should be no power or current discontinuities.

Designing the test fixture

The microstrip test fixture shown in Fig. 7 is specifically designed for the 20 V, 7 W operation of the PH3006. The fixture should be broad enough to cover the frequency range from 2.1 to 2.3 GHz so the 2.2 GHz predicted impedance data can be used in developing the model. To standardize on the required machining, the input and output circuits are constrained to lengths of one-half inch each. Within this one-half inch space, the circuits will be approximately 0.14 λ long at 2.2 GHz.

For the input matching, the transistor's input impedance is inductive, so a low-impedance (capacitive) transmission line should match fairly well. A simple 10-ohm line, 0.14 λ long (the full 0.5 inch length) will transform the transistors input impedance to 1.3+j6.2 ohms to 36+j50 ohms at 2.2 GHz. Also, this 10-ohm line will provide a reasonable match over a fairly broad frequency range.



7. Text fixtures for power transistors should also include reference short substitution circuits that duplicate the input and output microstrip fixture circuits.

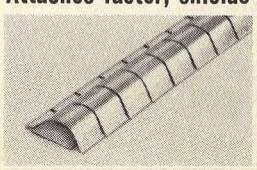
To match the collector, a distributed "L" network should yield a reasonable match. For the series inductor, a 50-ohm line will work. The distributed capacitance line should be as low an impedance as possible and six ohms is appropriate. From a Smith Chart plot, a 0.125 inch long 50-ohm line (0.033 λ) cascaded with a 0.25 inch long, six ohm line (0.070 λ) transforms the predicted impedance of 2.7+j1.7 ohms to 23+j21 ohms at 2.2 GHz. Again, this circuit is sufficiently broadband. The remaining 0.125 inch of the circuit board can be made with a 50-ohm impedance.

Modeling internally-matched transistors

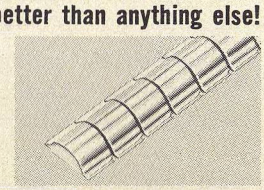
The modeling procedure described is also applicable to matched transistors[2]. Internally-matched transistors offer improved bandwidth capability and efficiency over conventional microwave transistors by means of LC matching sections at the input and output of the chip. The matching structure can be as simple as a single "L" section or

When RFI problems get sticky,
try sticky fingers®

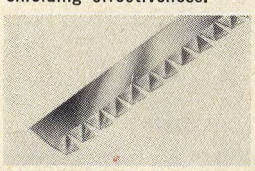
Attaches faster, shields better than anything else!



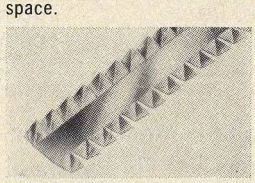
SERIES 97-500 The original Sticky Fingers with superior shielding effectiveness.



SERIES 97-520 A smaller size strip; highly effective in less space.



SERIES 97-555 New Single-Twist Series for use when space is at a premium. Measures a scant ⅜" wide.



SERIES 97-560 New ½" wide Double-Twist Series, ideal for panel divider bar cabinets.

Now you can specify the exact type beryllium copper gasket that solves just about every RFI/EMI problem. Perfect for quick, simple installation; ideal for retro-fitting. Self-adhesive eliminates need for special tools or fasteners. Write for free samples and catalog.



INSTRUMENT SPECIALTIES COMPANY, Dept. MW-57
Little Falls, N.J. 07424
Phone—201-256-3500 • TWX—710-988-5732

READER SERVICE NUMBER 40

EDITOR—FREELANCE
European Microwave Technology

MicroWaves is seeking a resourceful individual, who can keep abreast of advances in microwave technology in Europe. As a contributing editor, you'll be required to submit edited copy of up to 150 lines per month and meet copy deadlines. Must be capable of grasping the significance of developments as well as an insight for details.

Send resume to: **Richard T. Davis,** *Managing Editor.* **HAYDEN PUBLISHING/MICROWAVES, 50 ESSEX STREET, ROCHELLE PARK, N.J. 07662, U. S. A.**

READER SERVICE NUMBER 41

NOW PLAYING

THE 40 GHz CONNECTION

STARRING

MPC2

IN AN UNLIMITED ENGAGEMENT

the new MMC Coaxial Connector which takes you all the way to ***40 GHz*** *featuring*

- **LOW VSWR**
- **LOW INSERTION LOSS**
- **MODE FREE OPERATION**

and its supporting cast!

★ **CONNECTORS** .086, .070, .047 SEMIRIGID, PANEL MOUNT, ETC.

★ **ADAPTERS** MPC2 TO SMA, N, APC7 ETC. MPC2 TO WR90 THRU WR28. WRD750 & WRD180.

★ **MICROSTRIP LAUNCHERS**

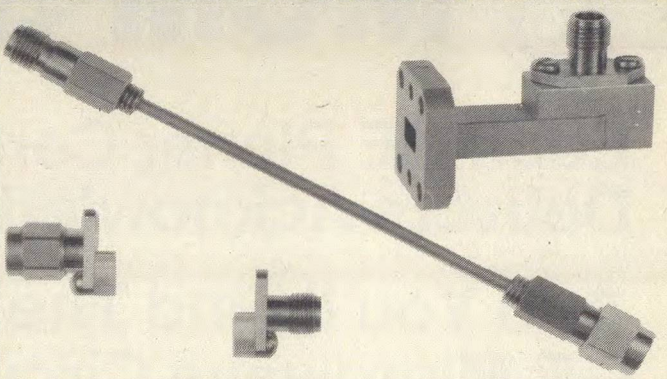
★ **TERMINATIONS** FIXED & SLIDING

★ **CABLE ASSEMBLIES**

★ **DIRECTIONAL COUPLERS**

★ *and many others* **TUNERS, SHORTS, ETC.**

Produced & Directed by **MMC** *Rated* **G** *(for Great!)*



The MPC2 connector now makes it possible to produce improved devices and systems operating to 40GHz. MMC offers a comprehensive line of MPC2 connectors for numerous applications as well as necessary components and measurement instruments so that you may achieve full utilization of this new connector in your system or laboratory. The MPC2 connector is intended for use in broadband communication, survailance, EMC, EW, etc. systems and devices which require superior performance to 40GHz. Consult us for applications assistance.

GO ALL THE WAY *– – – – – – to 40 GHz and make your State-Of-The-Art connection today – – – – – – – – – – – with* ***MPC2!***

MAURY MICROWAVE CORPORATION
8610 HELMS AVENUE • CUCAMONGA, CALIFORNIA 91730, U.S.A.

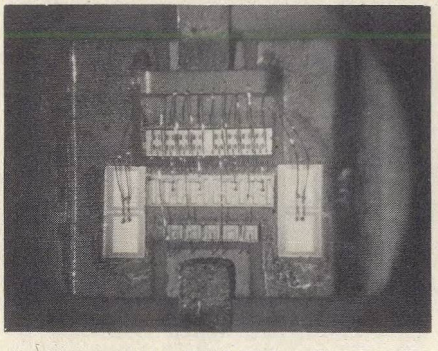
CALL 714-987-4715 OR WRITE FOR FULL DETAILS .... *Today!*

READER SERVICE NUMBER 42

as complicated as a multisection Chebyshev impedance matching transformer at the input. The output matching structure is usually a shunt inductance.

The object of internal input matching is to obtain optimum impedance transformation from the die resistance ($r_{b'b}$ in Fig. 3) to the source impedance (usually 50 ohms) over a given bandwidth. For high-power microwave transistors with low input resistance, the transformation ratio is high, and to obtain reasonable bandwidth, the first series inductance of a low-pass impedance transformer must be low (0.1 to 0.3 nH is typical). From the modeling discussed earlier, this magnitude of inductance is impossible to obtain in a discrete transistor. Therefore, one or more sections of the transformer are incorporated within the package, as necessary, to obtain optimum performance. The matching elements consist of series inductors and shunt capacitors that are realized using bond wire inductance and monolithic (MOS) capacitances as shown in Fig. 8.

The output matching consists of a shunt inductance from the collector pad to ground. In the model of Fig. 3, this inductance appears directly across $C_{b'c}$ and, therefore,



8. **Uncapped PH2310** shows internal matching capacitors and bonding geometry.

cancels a portion of the parasitic die capacitance. This yields a higher theoretical bandwidth and a higher collector load impedance[3]. With the collector terminal at a higher impedance point, circulating load current is lower, and, therefore, package and circuit losses related to metalization resistance are lower. This leads to higher efficiency and greater power output.

Characterizing matched microwave transistors follows the same procedures as for discretes. Test fixtures are constructed that partially transform the device impedances, and measurements are made at discrete frequencies using the test setup shown in Fig. 6. Usually, manufacturers will supply characterization at one power level that will give impedance points to begin the test fixture design.

Modeling matched transistors is more complicated than it is for discretes. Unless the internal component values are known, it may be impossible to model the device with sufficient accuracy to be useful. If internal components are known, they can be added directly to the basic model of Fig. 3 to arrive at a model for the input. A number of matched transistors have input matching only. For them at least, the collector model of Fig. 3 as discussed above is valid. If no input impedance information is known, the input reflection coefficient, S_{11}, can be measured. Figure 9 shows a Smith Chart plot of S_{11} for a PH2310 along with a plot of measured large signal conjugate input impedance. Correlation is good enough to develop first-cut test fixture circuits.

The collector matching used on microwave transistors consists of a shunt inductor (L_{shunt}) and associated dc blocking capacitor. At low frequencies, the blocking capacitor is in parallel with the transistor parasitic $C_{b'c}$ making it impossible to measure the output capacitance.

(continued on p. 43)

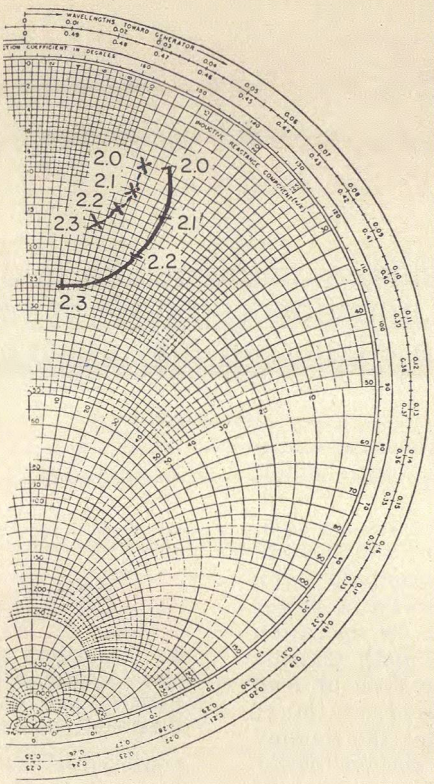
However, if a data sheet specifies typical C_{ob}, and some do, the inductance value may be determined as follows. The transistor's output loss, S_{22}, is observed using a directional coupler and a swept oscillator. At the parallel resonant frequency of C_{ob} and the internal shunt inductor, an absorption "pip" will be observed. This determines the resonant frequency of C_{ob} and L_{shunt} so that L_{shunt} may be calculated. The calculated shunt inductance is then added across the output capacitance in the model of Fig. 3. ••

References

1. Linvill, "Models Of Transistors And Diodes," McGraw Hill Book Company, (1963).
2. Kamnitsis and Minton, "Thin Film Rf Integrated Amplifiers For Uhf Broadband Communications Systems," *Microwave Journal*, Vol. 13, No. 12, pp. 37-40 (December, 1970).
3. Pitzalis and Gilson, "Broadband Microwave Class C Transistor Amplifiers," *IEEE Transactions on MTT*, (November, 1973).

Test Your Retention

1. How are power transistor models used?
2. Is the input impedance of an unmatched power transistor inductive or capacitive at microwave frequencies? Why?
3. How are impedance parameters of microwave transistors measured? Are they subjective or objective?
4. What is the purpose of internal transistor matching networks and how are they realized?



9. Smith Chart plot of S_{11} and large signal input impedance of a PH2310 shows close correlation.

Appendix—Derivation of the unilateral equivalent circuit

The circuit of Fig. 2 can be modified by changing the current generator and parallel capacitor to a voltage generator and series capacitor. This reduces circuit complexity resulting in Fig. A-1. The input current is set to one amp so that the input impedance is given by:

$$Z_{in} = E_s/I_{in} = E_s$$

Writing the loop equations:

$$E_s = [j\omega(L_e + L_b) + r_{b'b}] \times 1 - [j\omega L_b + r_{b'b}]\, i_2 \qquad (A\text{-}1)$$

$$\frac{-j\alpha}{\omega C_{ob}} = [j\omega [(L_b + L_e + L_L] - \frac{1}{j\omega C_{ob}} + r_{b'b} + R_L]\, i_2 - [j\omega L_b + r_{b'b}] \times 1 \qquad (A\text{-}2)$$

For conjugate collector load match,

$$j\omega [L_b + L_e + L_L] - \frac{1}{j\omega C_{cb}} = 0 \qquad (A\text{-}3)$$

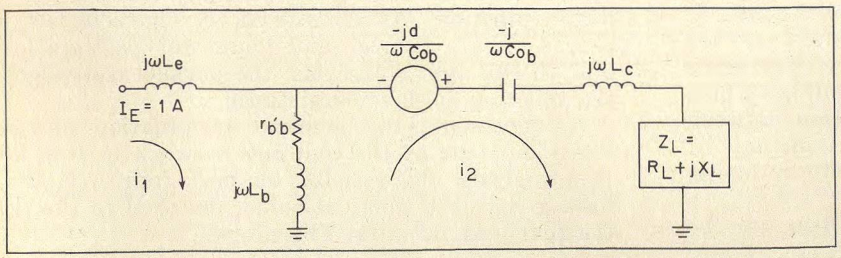
Therefore, solving for i_2 in Eqn. (A-2), and substituting in Eqn. (A-1),

$$Z_{in} = E_s = [j\omega (L_e + L_b) + r_{b'b}] - [j\omega L_b + r_{b'b}] \times \left[\frac{\frac{-j\alpha}{\omega C_{ob}} + j\omega L_b + r_{b'b}}{r_{b'b} + R_L}\right]$$

For typical microwave power transistors, $R_L >> r_{b'b}$ and the last term in the equation is small compared to the first. Therefore, it's possible to ignore the last term and simplify

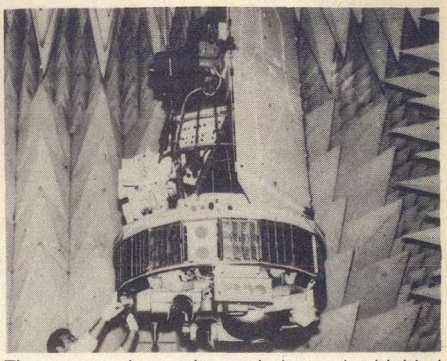
$$Z_{in} = j\omega (L_e + L_b) + r_{b'b}$$

giving the input model of Fig. 3. The output circuit is developed in the same way.



A-1. This simplified "T" equivalent model of Fig. 2 shows the current generator redrawn as an equivalent voltage generator.

ECCOSORB® ANECHOIC CHAMBERS



The most advanced anechoic and shielded chambers . . . used worldwide for antenna pattern, radar cross-section, VSWR and RF compatibility measurements. Send for data.

READER SERVICE NUMBER 43

GUIDE TO DIELECTRIC MATERIALS



Short form catalog is a useful illustrated guide to product lines and literature. Eighteen different product lines are described. Useful applications and outstanding properties are listed. The catalog contains a reader service card for requesting more detailed information on specific product lines.

READER SERVICE NUMBER 46

NEW DATA APPLICATION GUIDE EMI/RFI GASKETS



ECCOSHIELD® folder describes the broadest line of conductive plastic gaskets, including forms and applications. All materials feature high insertion loss, hermetic seal, low closing pressures, low compression set, low maintenance. Send for FREE copy.

READER SERVICE NUMBER 48

Emerson & Cuming, Inc.

CANTON, MASS.
GARDENA, CALIF.
NORTHBROOK, ILL.
Sales Offices in Principal Cities
EMERSON & CUMING EUROPE N.V., Oevel, Belgium

Hybrid-Coupled Amps: Can They Weather A Mismatch?

Two power transistors, combined by quadrature couplers, can 'see' different output impedances under mismatch conditions. One transistor is endangered since it may absorb rf power from the other.

A common building block for multistage amplifiers is the modular, balanced transistor amplifier (Fig. 1). But a nonlinear large signal analysis of two transistors combined by quadrature couplers reveals that a mismatched load can cause one transistor to dissipate more than its dc input power because it absorbs rf power from the second device. As a result, if cw operation into a mismatched load is a possibility, both transistors must be severely derated or some type of load mismatch sensing must be used to shut down the rf drive. The analysis goes on to show that the dummy load of the output combiner does not receive power under mismatch conditions, and therefore cannot be used as a sensor.

This analysis considers the change in transistor power dissipation due to common malfunctions of the load circuit; a disconnected antenna or intermittent contact in a connector, for example. While it's true that a circulator can protect the amplifier from mismatch at the output jack, today's design trends often call for an amplifier "system" with modules that plug into the output combiner network. A poor contact in one of these connectors or an arc in an interdigital coupler can easily cause a reflection large enough to endanger one group of transistors.

A simple observation shows why such an analysis is important. The two transistors in Fig. 1 are excited in phase quadrature. Therefore, the electrical path from one of them to the load must be 90° longer than the other path. Since the round trip distance from one amplifier to the load is 180° longer, the amplifiers can be expected to "see" reflection coefficients of opposite signs. That is, in the event that the load is disconnected, one transistor might be operating into a low impedance, while the other is operating into high impedance.

Linear analysis predicts impedance difference

The first step in predicting mismatch behavior is to consider the linear Class A amplifier. This relatively simple analysis yields a scattering matrix description which can be modified to predict Class B behavior.

High power microwave transistor amplifiers are operated Class C for maximum efficiency. But since the emitter junction breaks down at a small back bias (compared to the rf swing), the distinction between Class C, where current flows duing less than half of the rf cycle, and Class B, where current flows during a full half cycle, is negligible.

For a linear analysis, the two amplifiers can be represented as a pair of current generators whose internal conductance (G) characterizes parasitic loss mechanisms like the external matching network. The remaining components of the amplifier's output circuit—the collector capacitance, internal tuning and parasitic reactances, and the external tuning circuit—are lumped with the description of the quadrature coupler. It may not be physically possible to separate resistances and reactances in this manner, so the equivalent circuit must be regarded as a single frequency model, or an approximation for a specific band. The lossless portion of the equivalent circuit is combined with the quadrature coupler to form a four-port network whose properties are given by the scattering matrix:

$$\begin{bmatrix} b_1 \\ b_2 \\ b_3 \\ b_4 \end{bmatrix} = \begin{bmatrix} 0 & 0 & t & -jt \\ 0 & 0 & -jt & t \\ t & -jt & 0 & 0 \\ -jt & t & 0 & 0 \end{bmatrix} \times \begin{bmatrix} a_1 \\ a_2 \\ a_3 \\ a_4 \end{bmatrix} \quad (1)$$

where a_n signifies an incoming traveling wave voltage and b_n represents an outgoing traveling wave voltage.

The voltage (V_n) at any port is:

$$V_n = a_n + b_n, \quad (2)$$

and the current entering any port is:

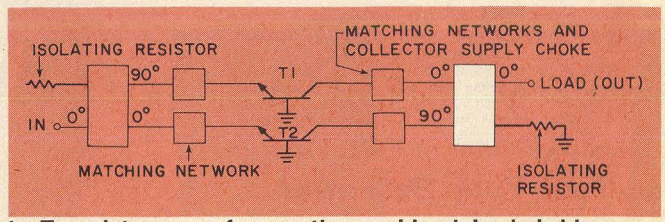
$$I_n = G_o (a_n - b_n). \quad (3)$$

The characteristic admittance of the four-port network under consideration (G_o) is not the same as the amplifier's nominal output load. The sum, (G_o + G) represents the conductance normally loading the collector junction. As mentioned, G characterizes the output circuit, coupler and transistor package losses and, in this linear analysis, the parallel equivalent of the collector epi-layer resistance.

G_o represents the nominal termination on ports three and four of the coupling network in Fig. 2. In this analysis, the resistor on port four will always have a constant, nominal value, matched to the G_o of the four-port network. Therefore:

$$a_4 = 0 \quad (4)$$

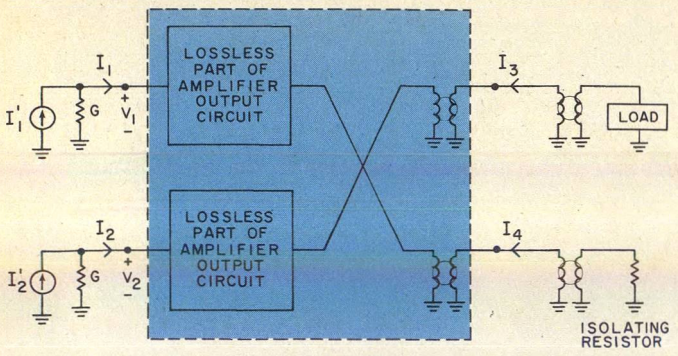
The load on port three will depart from its nominal value as described by its load reflection coefficient:



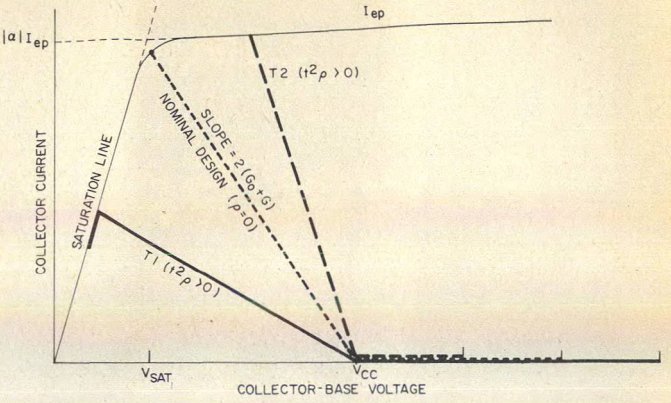
1. Transistors are frequently combined by hybrid couplers to form a balanced amplifier module. A load mismatch could endanger one transistor by causing it to dissipate an excessive amount of power.

(continued on p. 46)

Dr. Richard LaRosa, Electrophysics Lab Head, Hazeltine Corporation, Greenlawn, NY 11740.



2. This equivalent circuit represents two generators feeding a load through a quadrature coupler. The scattering matrix described by Eqn. (1) is based on the four-port network enclosed by the dashed line.



3. The actual operating point loci for the two transistors are compared to the nominal design locus. The voltage swings are symmetrical about V_{cc} if harmonics are short circuited.

$$\rho = \frac{a_3}{b_3} \qquad (5)$$

The transmission coefficient (t) in the scattering matrix has a magnitude of $1/\sqrt{2}$ for a lossless coupler. The phase angle of t includes the total phase shift of the transistor package, the exterior circuit, the coupler and the line out to the point where ρ is measured.

To calculate the impedance into which each current generator operates, Eqns. (4) and (5) are substituted into Eqn. (1):

$$b_3 = t(a_1 - ja_2) \qquad (6)$$

$$b_1 = t^2 \rho\,(a_1 - ja_2) \qquad (7)$$

$$b_2 = -jt^2 \rho\,(a_1 - ja_2) = -jb_1 \qquad (8)$$

The boundary conditions at ports 1 and 2 give:

$$I'_1 = GV_1 + G_0\,(a_1 - b_1) \qquad (9)$$

$$I'_2 = GV_2 + G_0\,(a_2 - b_2) \qquad (10)$$

$$I'_2 = jI'_1 \qquad (11)$$

Equations (2), (7), (8), (9), (10) and (11) are sufficient to yield:

$$\frac{V_1}{I'_1} = \frac{1}{G_0 + G}\left(1 + \frac{4\,G_0 t^2 \rho}{G_0 + G}\right) \qquad (12)$$

and

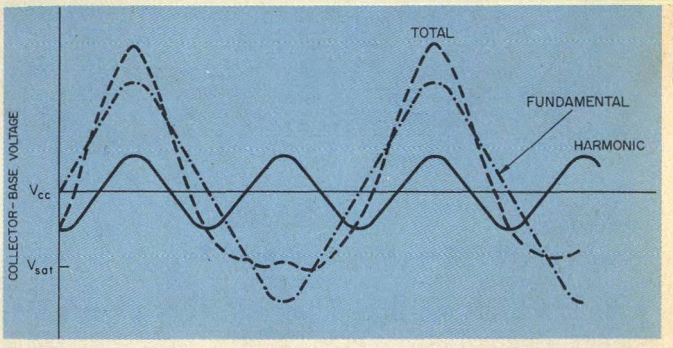
$$\frac{V_2}{I'_2} = \frac{1}{G_0 + G}\left(1 - \frac{4\,G_0 t^2 \rho}{G_0 + G}\right) \qquad (13)$$

which can be regarded as the "impedance" into which the two current generators operate.

For the case of a low power, Class A amplifier, it is possible to match the transistor to the load ($G = G_0$). In this case, a unity reflection coefficient of a certain phase will allow one current generator to be short circuited while the other operates into a resistance twice as high as the nominal value (that obtained when $\rho = 0$).

The linear analysis also predicts that for $G = 0$, and for a completely reflecting load of phase such that $t^2\rho$ is real, one generator operates into a load resistance three times nominal while the other current generator operates into a negative resistance. To visualize this in other terms, picture two transistors each capable of a 30 watt output, combined, so that when a matched load receives 60 watts, the isolating resistor receives zero power. If the load is short circuited at a certain distance, one transistor can be generating 90 watts of rf, of which 60 watts goes to the isolating resistor while 30 watts is dissipated in the other transistor.

Thus, there is no need to consider all phases of load mismatch—only the case of $t^2\rho$ real. It is also obvious that the voltage swing of one transistor will increase over its nominal value, while the voltage swing of the other transistor will decrease.



4. The flat (I_c = 0) region above V_{cc} in Figure 3 indicates the presence of a second harmonic. Plotted against time, the sum of this harmonic plus the fundamental forms a distorted sinusoid with a flat, negative peak at V_{sat}.

Modifications needed for Class B

In the Class B amplifier, the collector voltage cannot swing past the saturation line. Therefore, when $t^2\rho$ is real (the worst case), the transistors operate as shown in Fig. 3. The lower extreme of the voltage waveform of transistor number one (for $t^2\rho > 0$) is flattened, which implies a second harmonic content (Fig. 4).

Since transistor number one swings into V_{sat}, the generator current is no longer controlled solely by the drive, but also by the collector voltage. The current waveform is notched (Fig. 5a) with a consequent decrease in fundamental and second harmonic components.

Although it would be desirable to work the problem through for the actual case of the second harmonic of the collector voltage terminated in the collector junction capacitance, the problem is simplified by assuming that all harmonics are short circuited. Then, the peak rf voltage swing of transistor number one is approximately $(V_{cc} - V_{sat})$, and the collector current notch disappears.

Under these conditions, the peak fundamental current of transistor number two is $(G_0 + G)\,(V_{cc} - V_{sat})$, the same as it would be for the correct loading. (Remember that only half of the peak current

(continued on p. 48)

is fundamental. The other half is harmonics as indicated in Fig. 5b.) The collector current and voltage of transistor number two are in phase with the emitter current for $t^2\rho$ real and positive.

In general, it is not proper to assume that the fundamental collector current of transistor number one is in phase with αI_e, but for the case of $t^2\rho$ real, the linear results of Eqns. (12) and (13) indicate that collector voltage and current are in phase with the emitter drive.

A few simple modifications to the linear analysis can adapt it to the problem of a Class B amplifier. The objective is to find values for V_2 and I'_1. The scattering matrix developed in the linear analysis is still valid; the only difference being that I'_1 and I'_2 are specified in the linear case. What follows is a mathematical manipulation to find V_2 and I'_1 for the Class B case, starting from the known quantities:

$$|V_1| = V_{cc} - V_{sat} \quad (14)$$

$$|I'_2| = (V_{cc} - V_{sat})\,G \quad (15)$$

For $t^2\rho$ real, the phase of the number one collector current is not changed due to the voltage clamping (i.e., I'_1 still lags I'_2):

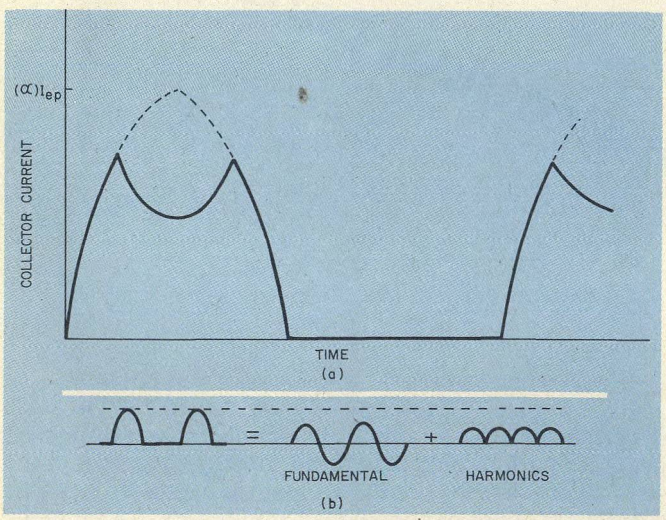
$$\frac{I'_1}{|I'_1|} = -j\,\frac{I'_2}{|I'_2|} \quad (16)$$

Since most of the collector loss is accounted for by the parameter V_{sat}, we can make the approximation:

$$G = 0 \quad (17)$$

Substituting Eqn. (2) and (7) in Eqn. (14):

$$(1 + t^2\rho)^2\,|a_1|^2 + t^4\rho^2\,|a_2|^2 + jt^2\rho\,(1 + t^2\rho)\,(a_1a^*_2 - a_1{}^*a_2) = (V_{cc} - V_{sat})^2 \quad (18)$$



5. The collector current of the saturating transistor (T1 in this example) is notched in an actual amplifier (a). The analysis is simplified, however, by considering the normal collector current (a half-wave rectified sine) which can be represented by a sine wave plus a full-wave rectified waveform (b).

Substituting Eqns. (8) and (10) in Eqn. (17) gives:

$$t^4\rho^2\,|a_1|^2 + (1 + t^2\rho)^2\,|a_2|^2 + jt^2\rho\,(1 + t^2\rho)\,(a_1a^*_2 - a^*_1a_2) = (V_{cc} - V_{sat})^2 \quad (19)$$

Subtracting (19) from (18) yields the information:

$$|a_1| = |a_2| \quad (20)$$

Substituting Eqn. (7) in (9) gives:

$$\frac{I'_1}{a_1G_0} = (1 - t^2\rho) + j\,t^2\rho\,\frac{a_2}{a_1} \quad (21)$$

Substituting Eqn. (8) in (10) gives:

$$\frac{-j\,I'_2}{a_1G_0} = t^2\rho - j\,(1 + t^2\rho)\,\frac{a_2}{a_1} \quad (22)$$

Equation (15) requires that the right-hand sides of Eqns (21) and (22) have the same phase angle. The ratio a_2/a_1 has unit magnitude, according to Eqn. (20). The second term in Eqns. (21) and (22) must be real in order to satisfy Eqn. (15). This requires that: $\frac{a_2}{a_1} = \pm j$.

For $\frac{a_2}{a_1} = j$, we have:

$$\frac{I'_1}{a_1G_0} = 1 - 2\,t^2\rho \quad (23)$$

$$\frac{-jI'_2}{a_1G_0} = 1 + 2\,t^2\rho \quad (24)$$

Equations (23) and (24) agree with the observation that I'_2 remains at the full driven value because transistor number two does not swing into the V_{sat} line, while I'_1 is reduced, as shown in Fig. 3. This says that

$$\frac{a_2}{a_1} = +j \quad (25)$$

is the correct choice.

Substituting Eqn. (25) in (18) or (19) gives:

$$|a_1| = \frac{V_{cc} - V_{sat}}{1 + 2\,t^2\rho} \quad (26)$$

No phase reference has been established for any of the voltages or currents. Since quantities are most easily given in terms of a_1, assume that:

$$a_1 = \frac{V_{cc} - V_{sat}}{1 + 2\,t^2\rho} \quad (27)$$

Using Eqn. (27) in (23) and (24) yields the current phasers:

$$I'_1 = \left(\frac{1 - 2\,t^2\rho}{1 + 2\,t^2\rho}\right) G_0\,(V_{cc} - V_{sat}) \quad (28)$$

$$I'_2 = j\,G_0\,(V_{cc} - V_{sat}) \quad (29)$$

Using Eqn. (27) in (2), (7), (8) and (25) gives the voltage phasers:

$$V_1 = V_{cc} - V_{sat} \quad (30)$$

$$V_2 = j\left(\frac{1 - 2\,t^2\rho}{1 + 2\,t^2\rho}\right)(V_{cc} - V_{sat}) \quad (31)$$

Each transistor delivers an rf output power of:

$$P = 1/2\left[\frac{1 - 2\,t^2\rho}{1 + 2\,t^2\rho}\right](V_{cc} - V_{sat})^2\,G_0 \quad (32)$$

The factor of 1/2 in Eqn. (32) comes from the fact that the phasers (28) to (31) are peak values. Remembering that for a lossless quadrature coupler $|t|^2 = 1/2$, Eqn. (32) reduces to:

$$P = \frac{1 - |\rho|}{1 + |\rho|}\,\frac{G_0}{2}\,(V_{cc} - V_{sat})^2 \quad (33)$$

which can be shown to be equal to half of the power reaching the load:

$$P_{LOAD} = \frac{|b_3|^2}{2}\,G_0\,(1 - |\rho|^2) \quad (34)$$

Comparing generated and load powers

Equations (33) and (34) can be used to illustrate what happens when a Class B balanced amplifier is subjected to an output mismatch. The mismatch is specified by a reflection coefficient, ρ, which can have any complex value inside a unit circle. The particular phase angle chosen for ρ, that which makes $t^2\rho$ real, is indeed the worst case, as shown in the linear analysis.

From these equations, it can be seen that as the load changes from the nominal value to a complete reflection, the rf output of both transistors falls off at the same rate, decreasing to zero for $|\rho| = 1$.

The power input to the transistor with the smaller voltage swing is not affected by load mismatch, be-

cause the current waveform is not altered.

If we have a pair of 30-watt transistors operating at 50% collector efficiency, the collector input to each one with a matched load is 60 watts. A completely reflecting load will cause one transistor to dissipate the entire 60 watts, which will very quickly burn it out—while the current supplied to the other transistor drops to zero, so its power dissipation is zero.

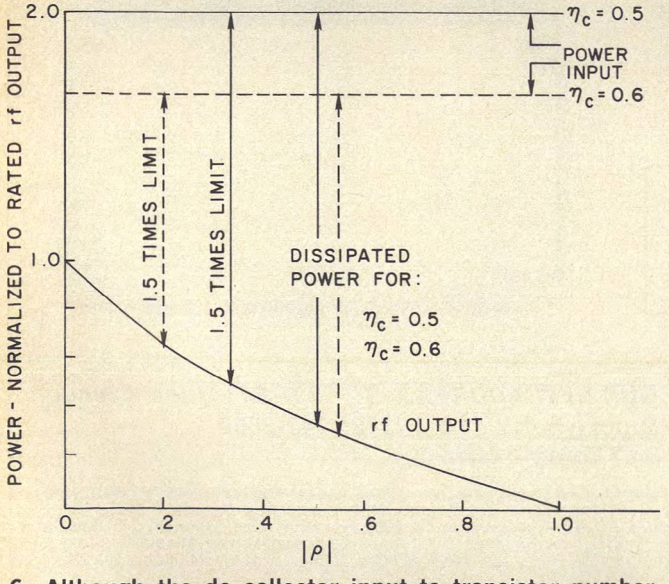
Figure 6 is a plot of Eqn. (33) and illustrates how the rf output of number two transistor drops off as $|\rho|$ is increased The collector input of transistor number two is drawn for the cases of 50% and 60% collector efficiency. Assume that in either case the transistor dissipation can be increased by a factor of 1.5 due to load mismatch before burning out. In the 50% case, the dissipation is increased 1.5 times for $|\rho| = 0.333$. For 60% efficiency, the same dissipation ratio corresponds to $|\rho| = 0.2$. These reflection coefficients translate to VSWRs of 2.0 and 1.5 respectively.

Obviously, a design based on a highly efficient transistor operating near its dissipation limit is prone to burnout under frequently encountered mismatch conditions. The importance of adequate safety margins is clear.

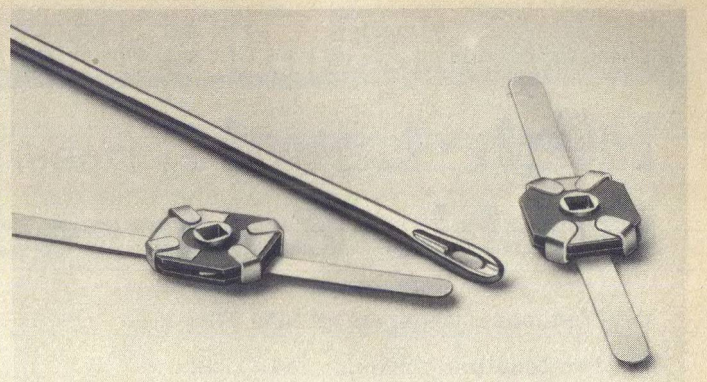
But, the situation is actually worse than depicted in Fig. 6 because one of the approximations made in the Class B analysis assumes that the voltage on the saturating transistor is sinusoidal and clamped to an amplitude of $(V_{cc} - V_{sat})$. In reality, however, the fundamental amplitude is actually greater since the bottom of the waveform is merely flattened as shown in Fig. 4. Therefore, the true solution tends toward the linear case of $G = 0$, where one transistor actually dissipates some of the rf generated by the other transistor.

Sensing a mismatch

Using Eqn. (6), it can be shown that P_{LOAD} is equal to the sum of the two transistor outputs. This leaves no power available for the isolating resistor. Referring back to the matrix equation (1), we see that the incident voltage wave to the isolating resistor:



6. Although the dc collector input to transistor number two remains constant, this hybrid-combined transistor's rf output drops with increasing values of $|\rho|$. The increasingly-large difference between the input power and output power must be dissipated within the device.



THIN-TRIM CAPACITORS FOR HYBRIDS AND MIC'S

Series 9401 Thin-Trims are sub-miniature variable capacitors for applications where size and performance are critical. Featured are high Q's for low circuit losses, high capacity values for broadband applications and low profile for "gap trimming" in tiny MIC's. Body size .140" x .110" x .030" T. Available in 4 capacitance ranges from 0.2-.6 pf to 3.0-12.0 pf.

Johanson®

MANUFACTURING CORPORATION
Rockaway Valley Road
Boonton, N.J. 07005
(201) 334-2676 TWX 710-987-8367

READER SERVICE NUMBER 49

$$b_4 = -j\,ta_1 + ta_2 \qquad (35)$$

is indeed zero when Eqn. (25) is substituted in (35).

Although it is commonly expected that a detector could be added to the isolating port of a quadrature coupler to sense load mismatch, analyzing Eqn. (35) proves that the isolating port cannot be used to sense load reflection because it receives no power.

Load mismatch sensing at the output of each module with suitable rf switching to cut off drive to the module is necessary to protect the transistors. A straightforward means of sensing load mismatch is to incorporate a directional coupler at the output port and detect the reflected power. Thus, in a modularized amplifier, each module should incorporate a directional coupler to sense reflections in its output connector or defects further down the line. ••

Test your retention

1. What type of load mismatch sensing is most effective for hybrid-coupled amps?
2. What are some common, physical causes of an output mismatch?
3. How serious must an output mismatch be before it endangers a hybrid-coupled transistor?

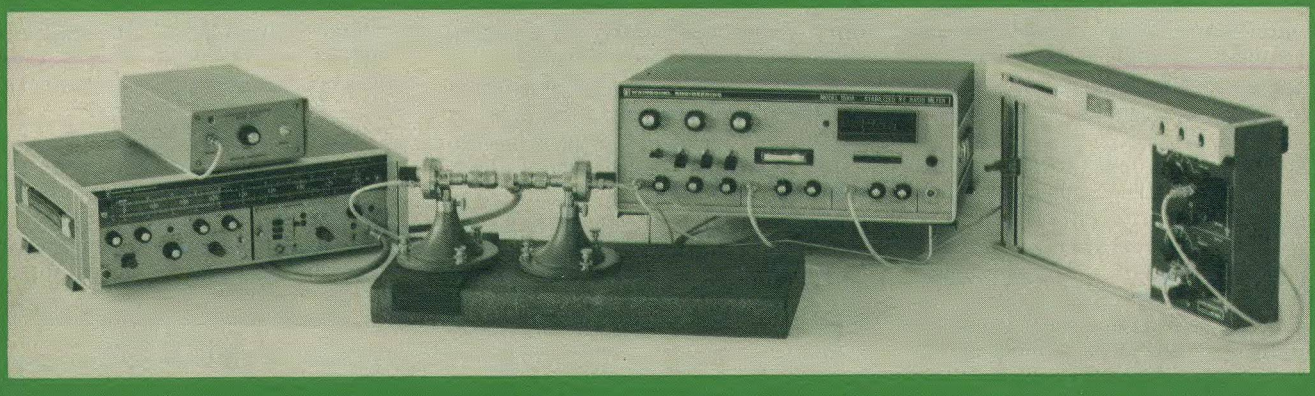
MICROWAVES

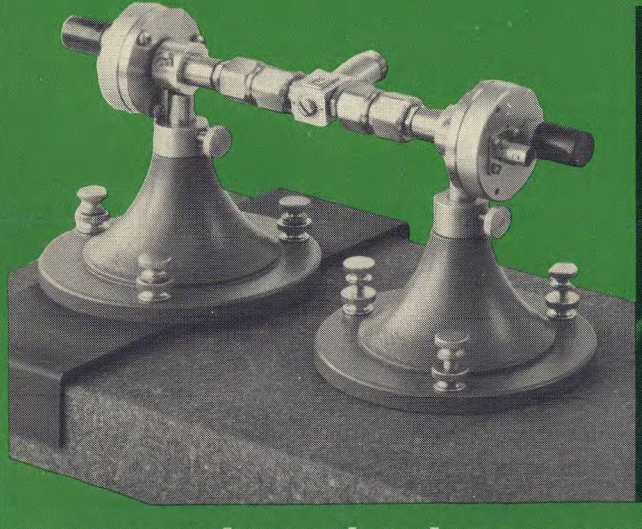
HIGHLIGHTS OF THIS SECTION:

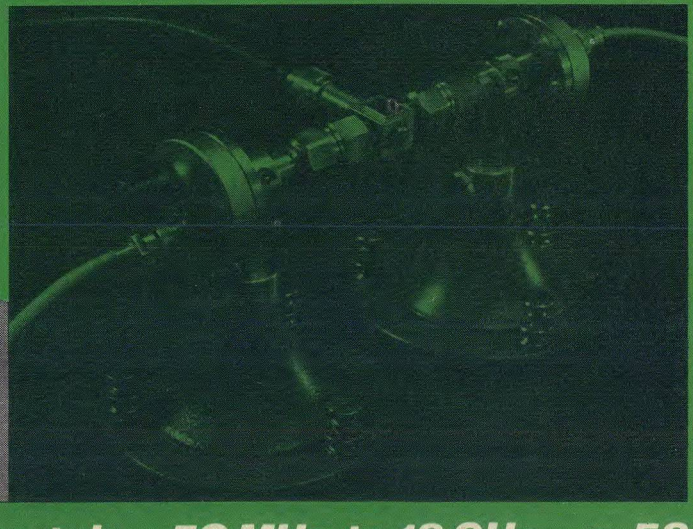
What's new in microwave frequency counters?...p.52
Synthesized signal generator offers keyboard convenience...p.60

FEBRUARY 1975

TEST & INSTRUMENTATION SECTION







Measure insertion loss accurately— 50 MHz to 18 GHz...p.58

What's New In Microwave Frequency Counters?

Fully automatic operation and the ability to make measurements within pulses are new. Transfer oscillator, heterodyne converter and reciprocal frequency counters are described.

WITH today's automatic counters, rapid measurements can be performed without operator intervention or the myriad of dials and level indicators. Of course, manually-operated instruments are still available at lower costs capable of equivalent measurement accuracy. The means by which automatic operation has now become more economical is the introduction of "state machine" design concepts to the counters; in this technique, the counter is led step-by-step through its measurement algorithm by a semiconductor memory in the logic section of the instrument. All of the instruments discussed in this article are fully automatic. Furthermore, various counter design approaches have been developed to optimize measurements under high-noise conditions, wide fm deviation and pulsed rf service.

The performance specifications of microwave frequency counters have been steadily tightening in recent years due to a variety of technical improvements. Input sensitivity is now specified as low as −35 dBm and frequency range is available to 23 GHz (even to 40 GHz in manually-operated instruments). Microwave frequencies can now be measured to a resolution of 1 Hz with accuracies of a few parts in 10^{10}. The direct count bandwidth in microwave counters (maximum frequency range without down-conversion techniques) has now been extended to 500 MHz and tolerance to frequency modulation is now available at a very impressive 250 MHz peak-to-peak.

Some of the recent technical improvements in microwave counters have led to capabilities that did not exist before. One such new capability is the automatic measurement of carrier frequencies of pulsed rf signals. A second important new capability of microwave counters is aimed at systems users and their demanding requirements for speed and digital input/output. Today's microwave counters have the ability to program most front-panel controls by the same control processor which is sampling the digital output. Codes used for this programming range from simple one-line-per-function inputs through more flexible BCD commands to sophisticated, byte-serial ASCII-coded communication. Input circuitry of these counters has also been optimized for systems use; their sophisticated designs allow measurement of a wide range of input frequencies during the course of a data-acquisition routine.

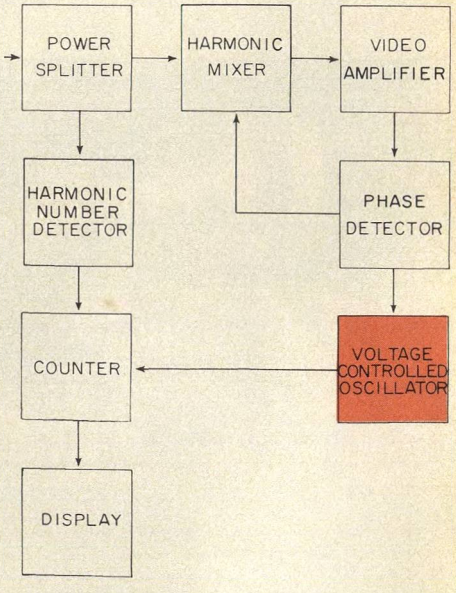
For a more thorough discussion of the features now available in microwave counters, we will consider separately three classes of instruments: counters using the transfer oscillator technique for frequency down-conversion, those using a heterodyne technique for down-conversion, and counters having pulsed rf measurement capability.

For higher sensitivity, the transfer-oscillator

This counter performs automatic frequency measurements by locking the harmonic output of a VCO to the unknown signal in a phase-lock loop, Fig. 1. A portion of the unknown input frequency is directed to a harmonic mixer where it enters into phase lock with the output of the VCO. Once lock is achieved, the output frequency of the VCO is an integral subdivision of the unknown. This VCO output frequency can be counted directly to yield the correct answer if the time base of the counter section is altered using the correct hamonic number. Determining this number is the function of the harmonic number detector block. Since the harmonic multiplication is achieved by altering the time base of the counter section, no computation is required within the instrument.

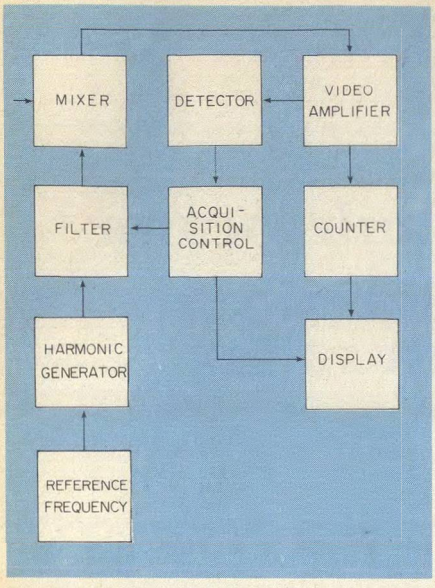
The automatic transfer oscillator has inherent advantages over other techniques. Since the limited bandwidth of the phase-lock loop suppresses most of the noise spectrum, sensitivities as fine as −35 dBm can be reasonably achieved. Thus, the user of the transfer-oscillator counter can measure extremely low-level signals or signals with a significant degree of am or otherwise induced amplitude fluctuations. This technique has the potential to achieve exceptionally wide frequency ranges; for example, the range of the HP 5340A is 23 GHz.

The principle of the transfer-oscillator technique allows instantaneous automatic amplitude discrimination to be built into these counters so that the counter will measure only the predominant signal in a complicated spectrum. A counter employing this feature becomes quite tolerant of noise and spurious signals on the input and



1. With the transfer-oscillator technique, the unknown signal is locked with the harmonic output of a VCO.

Duncan Mac Vicar, Product Manager, and **David Martin,** Product Marketing Manager, Hewlett-Packard Company, 5301 Stevens Creek Blvd., Santa Clara, CA 95050.



2. The heterodyne converter counter mixes the known and unknown signals, counts the difference and adds this count to the known frequency on the display.

becomes immune to false measurements of harmonic signals. The signal-to-noise ratio tolerance of a transfer-oscillator counter operating in a wideband noise environment is 20 dB and up.

A final significant feature of the automatic transfer-oscillator is the ability to track rapidly sweeping signals in S-band and above. This ability arises from the fact that the input is mixed with a relatively high multiple of the output frequency of a VCO. Since the VCO can sweep through an entire octave range without losing lock, input signals which vary over an octave range can be easily tracked.

For wide FM tolerance, the heterodyne converter

The heterodyne converter counter mixes the unknown frequency with a known microwave frequency, counts the resulting video difference signal and adds this count to the known frequency in the display, see Fig. 2. The known signal is generated by filtering one element of a comb line from a harmonic generator in a filter tuned by the acquisition control circuit. This circuit is designed such that the counter will measure and display the lowest frequency in the input which is within its sensitivity.

Two types of filters are used in automatic-heterodyne converter counters. Most common is a YIG sphere, whose harmonic oscillations are dependent upon the strength of a magnetic field. The second technique uses a "switchable filter"—a set of narrowband thin-film filters with switching circuitry which directs the comb line to the appropriate filter. The switchable filter technique has the potential for being a lower-cost technique since the thin-film components are considerably less expensive than the YIG. This cost advantage is only realized at low-frequency ranges since the range of switchable filter technique is directly proportional to the number of filters in the instrument.

A significant advantage to the heterodyne counter using the switchable filter technique is fast acquisition time. The HP 5341A can acquire an arbitrary signal within its bandwidth in 600 microseconds; under some conditions, this time is reduced to 100 microseconds.

The fm tolerance of heterodyne counters is extensive, since the bandwidth limitation of a measurement is determined solely by the direct-count ability of the counter section. Thus peak-to-peak deviations as great as 250 MHz may be tolerated by these counters. Such a tolerance allows measurements of fully-loaded communications carriers as well as carriers with the wide deviations found in some military applications.

A further advantage of the heterodyne technique is that the counter may be preset to search only a limited frequency band by merely setting the filter to the appropriate band center. Thus, several signals of a complicated spectrum can be detected and measured by the counter provided the difference is greater than the counter's i-f bandwidth. (The automatic transfer-oscillator may also be preset in similar fashion; but in that case, the "bands" become octave ranges).

Finally, the heterodyne approach also includes the advantage that 1 Hz resolution may be achieved in a one second measurement time since the time base of the direct counter need not be altered for automatic measurements.

For pulsed rf, the reciprocal frequency counter

Automatic measurement of pulsed rf signals requires an especially sophisticated counter design. Potentially at least, the heterodyne converter lends itself to these measurements. Since phase information is retained in the mixing process, the i-f output from the heterodyne converter is identical to the pulsed input signal except

(continued on p. 55)



Get cleaner mm waves with Hughes GUNN effect oscillators.

Our low-noise, solid-state oscillators come in two basic types in frequency ranges above 18 GHz. The voltage-controlled oscillators provide broad tuning bandwidths and minimum power outputs to 35 mW. The mechanically-tuned models offer higher power outputs of up to 150 mW adjustable over 100 MHz.

All feature standardized solid state design, small size, ruggedness, low cost and high stability.

Find out more about less noise. Write or call: Hughes Electron Dynamics Division, 3100 W. Lomita Boulevard, Torrance, Calif. 90509. (213) 534-2121, ext. 215.

HUGHES
HUGHES AIRCRAFT COMPANY
ELECTRON DYNAMICS DIVISION

Making waves in millimeter-wave technology.

READER SERVICE NUMBER 53

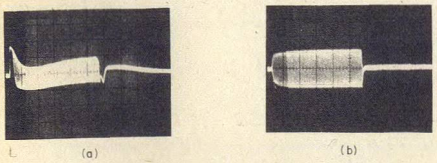
for the carrier frequency. In particular, any frequency variations of the microwave input are also present on the i-f output.

Converters designed for cw measurements can be used with pulsed inputs. Most converters, however, employ a mixer which is single-ended to the input signal. Application of a pulsed input to such a converter will produce distortion and make measurement impossible on the leading edge of the i-f. This distortion can exist for several microseconds or longer; however, it may be minimized by reducing the input signal level. Figure 3 illustrates how this problem is avoided using a balanced mixer in the input of a counter designed for pulsed measurement. Even a balanced input is never perfect so it becomes good practice to employ the lowest possible signal level for the pulsed microwave input.

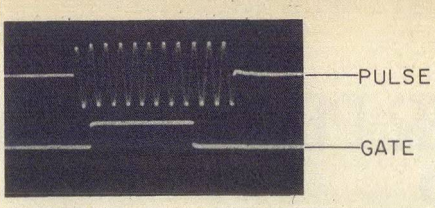
Assuming the conversion has been accomplished successfully, there still remains the problem of measuring the pulsed rf signal at the i-f frequency. By its very nature, the reciprocal frequency counter (desribed later) automatically measured pulsed rf inputs, since the measurement does not start until the first input signal zero crossing. The conventional frequency counter can also be designed to perform essentially the same thing, and in fact, many versions of both types of counters are marketed today. In both cases, the measurement is performed provided the counter's "gate time" switch is set to a time less than that of the pulse width, see Fig. 4.

One serious limitation of this technique lies in the fact that the measurement is constrained to start at the leading edge of the input pulse. In practice, many of the pulsed microwave signals have substantial leading edge noise, distortion, etc., and for these type of signals the measurement becomes impossible to perform.

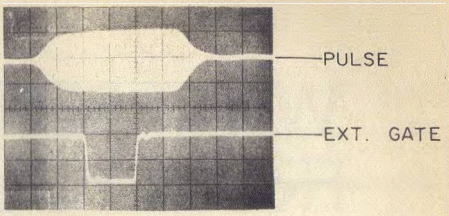
To overcome this limitation, the HP 5345A 500 MHz reciprocal counter features an externally-gated mode of operation. As Fig. 5 indicates, the operator applies the external gate control signal at the desired point with respect to the pulsed input where the frequency measurement is required. This then allows the commonly encountered leading edge distortion to be eliminated from the measurement.



3. Comparing the i-f response from a single-ended (a) and balanced (b) mixer, note the distortion at the leading edge.



4. With the reciprocal frequency counter, the measurement starts at the leading edge of the pulse and measurement time is set by the "gate-time" switch.



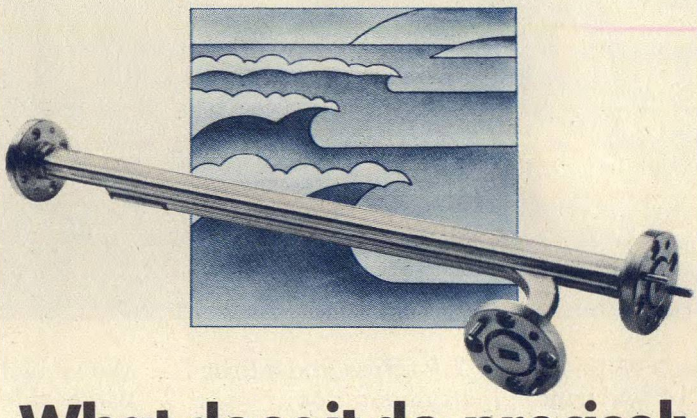
5. External gating allows the pulsed frequency measurement to be made inside the pulse.

In the external gated mode, the HP 5345A can accept external gate pulse widths ranging from 50 nsecs to 1000 seconds. Thus, pulsed frequencies can be measured for pulse widths as small as 50 nsecs. In addition, this plug-in counter's 500 MHz frequency range can be extended to 4 GHz via the 5345A heterodyne converter plug-in.

The measurement or gate time in the externally-gated mode is determined by the gate pulse width. During the time this pulse is present, 500 MHz clock pulses are accumulated in one register resulting in a total of T counts; and the input signal zero crossings are accumulated in a second register, resulting in N counts. The frequency is computed as N/T and then displayed. If the measurement is made through the plug-in, the necessary additional information is sent from the plug-in so that the mainframe displays the total microwave frequency.

One advantage of external gating is that it allows non-standard gate times to be employed. Thus, the user can obtain maximum accuracy if he positions the leading edge of

(continued on p. 57)



What does it do, precisely? It samples mm waves precisely.

Hughes millimeter-wave directional couplers provide high directivity (greater than 40 dB) and predictable accuracy for precise control of mm waves.

You get flat frequency response (±1 dB) with an accurate coupling curve over the full waveguide bandwidth. And reduced coupling variation from unit to unit, thanks to a computer-optimized, precision-machined coupling plate.

Our directional couplers are ideally suited for broadband measurements and instrumentation. What's more, they are competitively priced and available for off-the-shelf delivery.

If we're on the same wave length, write or call: Hughes Electron Dynamics Division, 3100 W. Lomita Boulevard, Torrance, Calif. 90509. (213) 534-2121, ext. 215.

HUGHES
HUGHES AIRCRAFT COMPANY
ELECTRON DYNAMICS DIVISION

Making waves in millimeter-wave technology.

READER SERVICE NUMBER 55

the gating pulse inside the rf pulse and away from leading edge distortion and then sets the width of the pulse so that the trailing edge is coincident with the end of the pulsed signal. The measurement is now made over as much of the pulse as possible, and it follows that measurement accuracy and resolution are maximized.

A second advantage is that external gate allows the user to determine the point in real time at which a measurement will be made. This allows frequency profiles to be determined, Fig. 6.

In summary, external gating offers the following distinct advantages in pulsed-microwave frequency measurements:

- Measurements inside the leading edge of the pulse burst can be made, thereby avoiding the frequently encountered frequency, phase and amplitude noise at the leading edge of the pulse burst.
- Non-standard gate times are possible thereby allowing maximum measurement accuracy to be achieved.
- The technique offers the ability to make frequency profile measurements.

Measurement resolution and frequency averaging

The reciprocal-measurement technique provides an important advantage over the conventional frequency counter in that it provides improved measurement resolution (and accuracy). The importance of this lies behind the fact that the measurement times are typically quite small (e.g., 1 μsec or less) because pulse widths are narrow.

The resolving power of the reciprocal frequency counter is compared with a conventional counter of like frequency range in Fig. 7. Note the high and constant resolution of the reciprocal counter. Thus, for example, an i-f frequency of 50 MHz can be resolved to 2×10^{-9} with the 5345A reciprocal counter compared to 2×10^{-8} with the conventional counter—an order of magnitude improvement.

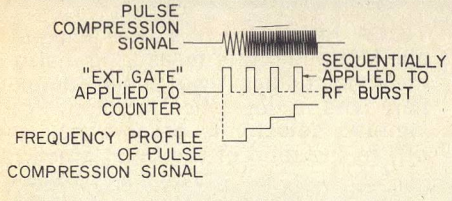
Assume now that the input signal consists of a 2.9 GHz pulsed signal with pulse widths of 100 nsecs. The maximum measurement time is 100 nsecs and the i-f frequency being measured is 400 MHz (= 2.9 GHz − 2.5 GHz); thus, the measured resolution is $(2 \times 10^{-9}/1 \times 10^{-7}) \times 4 \times 10^{8} = 8 \times 10^{6} = 8$ MHz. Relative resolution thus becomes 8/2900 or 2.8×10^{-3} approximately, just a little better than 0.3%.

If the input signal is repetitive, the resolution can be improved by averaging. The concept of frequency averaging is similar to time interval averaging in that N measures are taken and averaged, the average measurement has a resolution that is $\sqrt{N}$ times better than the individual measurements.

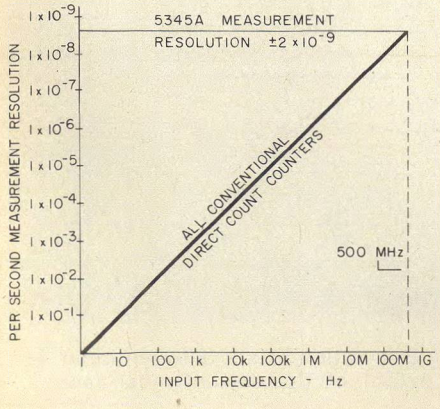
Continuing with the example above, if we assume 10^6 measurements in the average, the measurement resolution now becomes 2.8×10^{-6}. Finite noise within the instrument limits the resolution improvement to 10^3 over the single-shot measurement case. Nevertheless, it is impressive to be able to resolve the frequency of a signal to parts in a million when the measurement window is only one ten-millionth of a second. ••

Test your retention

1. Which counter approach is best when considerable noise accompanies the signal to be measured?
2. Which counter approach is best suited for pulse rf?
3. Which counter approach offers fastest acquisition time?
4. Which counter approach is best suited where wide frequency deviations will be encountered?

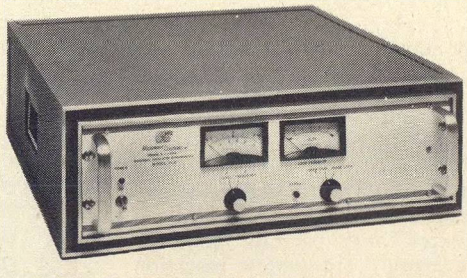


6. Frequency profiles can be developed with external gating and are useful for doppler, frequency agile and pulse compression radar systems.

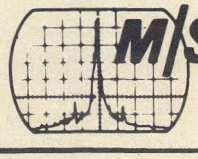


7. Comparison of measurement resolution using a reciprocal frequency counter vs a direct-count counter.

CONSTANT
O-F-F-S-E-T
FREQUENCY
FOR
:TRANSMITTER-RECEIVERS
:ATTENUATION MEASUREMENTS
:MICROWAVE SPECTROSCOPY
:PHASE LOCKING MILLIMETER
RF SOURCES TO 200 GHz



IF (Offset) Frequencies From
20 MHz to 500 MHz



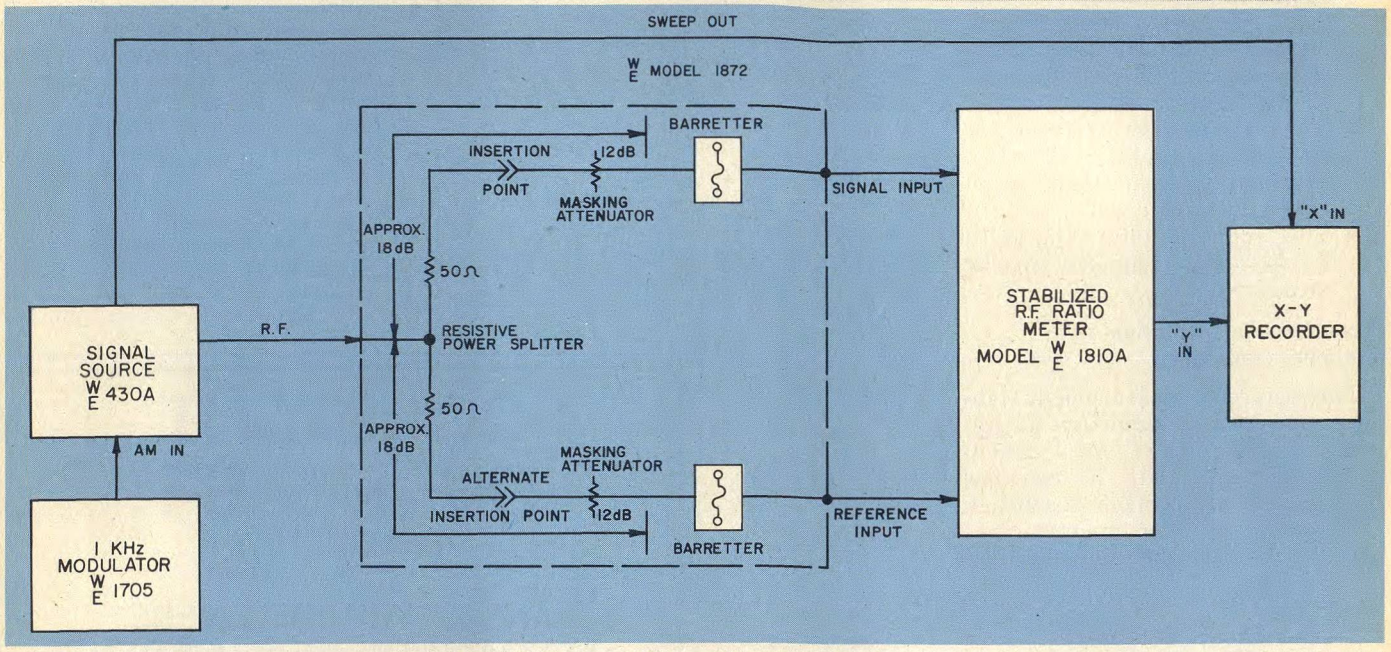
M/S MICROWAVE/SYSTEMS, INC
1 Adler Dr., East Syracuse, New York 13057
Tel. (315) 437-9951

READER SERVICE NUMBER 57

Measure insertion loss accurately, 50 MHz-18 GHz

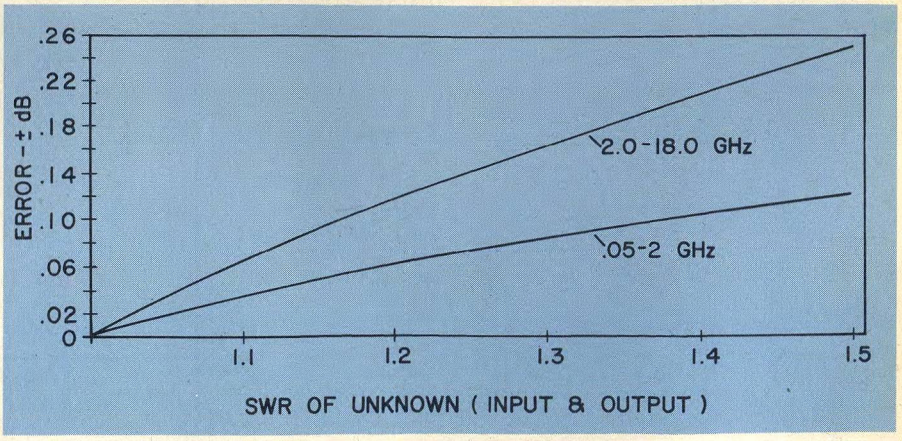


1. **Weinschel's model 1872 test unit is used here in a 0 to 30 dB insertion loss test setup.** The other instruments shown are (l to r): model 430A solid-state sweeper with model 1705 square-wave oscillator on top, model 1810A dual-channel stabilized rf ratiometer and an HP (model 1035B) X-Y recorder. Note the granite slab which is recommended to obtain a flat work surface and the leveling screws on the 1872 which provide precise connector alignment.



2. **Insertion loss test unit consists of a resistive power divider (A unit) and two matched detectors (B units).** The power divider is in the form of a "T" with a series 50-ohm resistor in each of the two output ports. The 1810A ratiometer is a dual channel one kHz audio rate measuring instrument containing two tuned amplifiers and a log-ratio detector. The log-ratio detector is proportional (in dB) to the ratio of the input signals.

A highly-accurate insertion loss test unit, which incorporates two matched square-law detectors and a precision 50-ohm resistive splitter, has been developed by Weinschel Engineering. The test unit, model 1872, is offered principally as an accessory to Weinschel's model 1801A stabilized rf ratiometer and permits accurate fixed and swept frequency insertion loss measurements from 50 MHz to 18 GHz, Fig. 1. Its insertion point VSWR is less than 1.07 to 2 GHz and less than 1.15 to 18 GHz (source and load). As such, accuracy and bandwidth far exceed what is obtainable with conventional components such as directional couplers and crystal detectors. Another key feature of the model 1872 is its low input power



3. **First order approximation** of mismatch error assumes that at least 20 dB isolation exists between input and output of the device under test.

requirements (+10 dBm peak) which makes it compatible with today's solid-state sweepers. Dynamic range is 30 dB when used with a 10 mW output source.

The detectors each consist of two broadband barretter mounts and a masking attenuator. Barretters are ideal for accurate insertion loss measurements because of their true square-law properties.

The barrier mount itself is a new and improved design which has an operating range of 0.050 to 18.0 GHz with a VSWR of under 1.75. A low VSWR masking attenuator of 12 dB is incorporated in the detector unit to reduce the input VSWR of the barretter mount to less than 1.15 as seen at the detector unit input.

As shown in Figs. 1 and 2, rf energy modulated at a 1 kHz rate is applied to the rf input of the 1872 and divided equally by a power divider into two channels. The power divider is in the form of a "T" with a series 50 ohm resistor in each of the two output ports. (Conventional symmetrical resistive power dividers have a series 16 2/3 ohm resistor in each of the three ports).

The reference channel of the 1810A provides constant level at midpoint of the power divider as seen by the measuring channel. This causes the midpoint of the power divider to look like a generator with a zero source impedance. The 50-ohm series resistor then provides a source impedance of 50 ohms to the device under test.

The overall accuracy of the system depends on four factors:

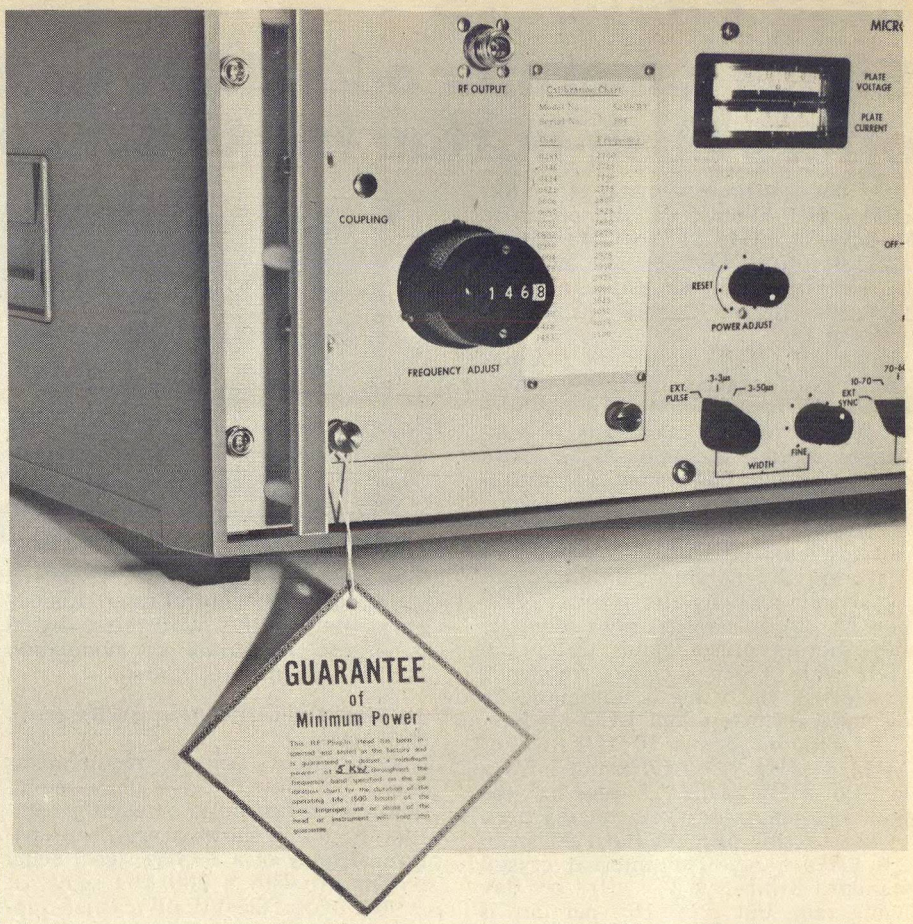
- Instrumentation error of the 1810A. In direct mode it is 0.02 dB/10 dB; in full substitution mode it is 0.02 dB/30 dB.
- Non square law response of barretter: +0.000 dB, −0.01 dB.
- Connector repeatability (±3 σ limit): ±0.012 dB (three connector pairs using Weinschel 7 mm connectors).
- Mismatch errors at zero reference:

from 0.05 to 2 GHz = +0.000 dB, −0.029 dB
from 2 to 18 GHz = +0.000 dB, −0.078 dB

For mismatch error when device under test is inserted, see Fig. 3.

P&A: model 1870 is $2,495; stock to 30 days. **Weinschel Engineering, One Weinschel Lane, Gaithersburg, MD 20760 (301) 948-3434.**

CIRCLE NO. 205



Sometimes more, never less

That's what you get with our signal sources and oscillators - the rated power as an *absolute minimum* throughout the frequency band of the plug-in head in use. In fact, we're so confident we can deliver that power, we've hung a guarantee tag on each and every oscillator we sell.

In a model to suit your needs up to 100 watts CW or 40 kilowatts pulsed. Guaranteed. You can depend on it.

For more information call or write

Epsco INCORPORATED

APPLIED MICROWAVE DIVISION
411 Providence Highway, Westwood, MA 02090
Tel. (617) 329-1500 TWX (710) 348-0484

READER SERVICE NUMBER 59

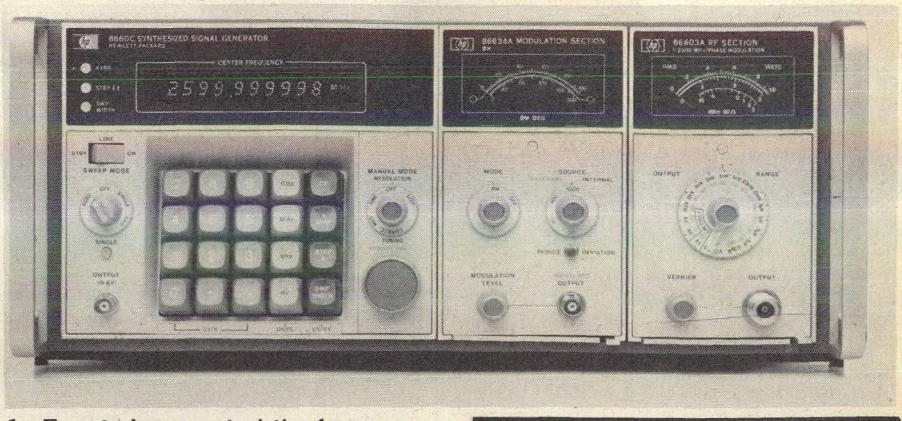
Signal generator adds 1300 to 2600 MHz band, offers push-button frequency control

A new synthesized signal generator, model HP 8660C, can be equipped to cover 1 MHz to 2.6 GHz with 2 Hz resolution. Options are available to achieve calibrated phase modulation rates up to 10 MHz, as well as am and fm.

The HP 8660C mainframe is a new design built to accommodate a variety of plug-in rf and modulator modules (Fig. 1). The new mainframe is engineered around a 20-button keyboard which provides convenient digital control of center frequencies, frequency steps and sweeps. Direct frequency settings, entered with a resolution of 2 Hz, may be incremented up or down by simply pressing the proper STEP key. A useful sweep mode digitally steps across preset bands up to 2.6 GHz wide. Once a center frequency is selected, the value is automatically dispayed on a ten-digit LED readout.

Rf plug-ins cover 10 kHz to 110 MHz, 1 MHz to 1.3 GHz and 1 MHz to 2.6 GHz. One rf plug-in, the 86603A, generates levels ranging from −136 to +7 dBm in the 1 MHz to 2.6 GHz band. The internal crystal standard exhibits a 3×10^{-8} per day aging rate, but 3×10^{-9} per day is optional. An indirect synthesis technique provides typical switching times of 6 ms (to settle within 100 Hz).

Modulator plug-ins provide am, pm and fm, and feature front panel meters. Phase modulator plug-in, model 86634A, should prove especially useful for satellite telemetry and communications applications. An internal source provides either 400 Hz or 1 kHz modulation with peak deviations ranging from 0 to 100° (0 to 200° for output frequencies above 1.3 GHz). External phase modulation is possible at rates ranging from dc to 10 MHz for carrier frequencies above 100 MHz

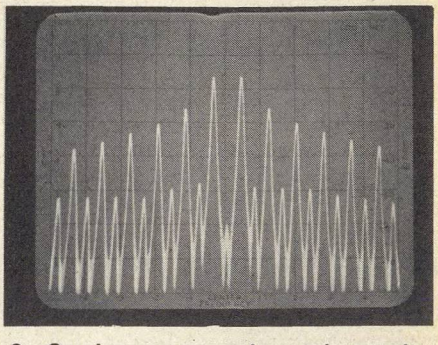


1. Twenty keys control the frequency parameters of this synthesized signal generator. A variety of modulation and rf plug-ins are offered.

Low input voltage requirements ($\approx$ 1 V) allow direct bi-phase modulation with fast pulse or word generators. Figure 2 shows a spectrum analyzer display of a 1 GHz signal being modulated with a 200 kbit signal at ±90°. Note the 40 dB carrier suppression and low-modulation distortion, shown with intermediate sidebands 30 dB down.

Another modulator plug-in, the 86635A, provides either phase or frequency modulation. External modulation rates range from dc to 1 MHz with fm deviations up to 200 kHz peak (400 kHz above 1.3 GHz).

Kits are also available to extend the frequency range and add phase modulation capability to the older 8660A and 8660B mainframes. P&A: Model 8660C mainframe: $7900; 86603A rf plug-in: $6000; Rf plug-in phase modulation option (002): $1500; 86634A phase modulation plug-in: $1400; 86635A fm and phase modulation plug-in: $2,200; 12 to 16 wks. **Hewlett-Packard Company, 1501 Page Mill Road, Palo Alto, CA 94304 (415) 493-1501.** CIRCLE NO. 114



2. Carrier suppression of greater than 40 dB is shown in this spectrum analyzer photo of a 1 GHz carrier with 200 kbit bi-phase modulation.

Gaussmeter accurate to ±0.2%

Digital gaussmeter, model 811, provides accuracy of better than ±0.2% of full scale reading. The stability figures are 100 ppm from −20°C to +70°C, ±0.01% of full scale from 90 V ac input to 140 V ac and a max drift of ±0.1% over any time period. The 811 measures magnetic flux density over five full scale ranges; 0-10 gauss (0-0.001 tesla), 0-100 gauss (0-0.01 tesla), 0-1,000 gauss (0.0.1 tesla), 0-10 kgauss (0-1 tesla), 0-100 kgauss (0-10 tesla). Probes are available to meet the requirements of virtually any application. Frquency response is from dc to 400 Hz. **Bell, Inc., 4949 Freeway Drive, East, Columbus, OH 43229 (614) 888-7501. (614) 888-7501.** CIRCLE NO. 140

Analyzer measures sidebands 60 dB down

Spectrum analyzer, model SSB-50-1, operates from 10 Hz to 40 MHz (usable to over 200 MHz) with 10 Hz resolution over the entire tuning range. Sensitivity is better than 0.5 mV, while steep skirt selectivity (using three crystal filters), plus freedom from internal hum and residual fm permits measurement of 60 Hz sidebands 60 dB down. All in-band intermodulation products are at least 70 dB down. Preset scan widths are 150 Hz, 500 Hz, 3.5 kHz, 7 kHz and 14 kHz, all with automatic optimum resolution. P&A: $7,000; 4 wks. **Singer Instrumentation, 3176 Porter Drive, Palo Alto, CA 94304 (415) 493-3231.** CIRCLE NO. 139

Scope weighs only 18.5 lbs.

50 MHz dual-trace oscilloscope, PM3240, is the lightest oscilloscope in its class. 5 mV/div. is sensitivity at full bandwidth and 10 ns/div max sweep rate. The 50 MHz bandwidth and 7 nanosecond risetime can be displayed in separate, alternate, chopped and X-Y modes. 1 MHz chopping rate helps to eliminate interference. Voltage, current and time calibration signals are provided at 3 V_{p-p} (1%, 6 mA_{p-p} (1%) and 2 kHz (2%), respectively. A 1 megohm, 15 pF input impedance and delay lines, providing 20 ns of visible delay, enable accurate viewing. P&A: $1,470 without probes, $1,560 with probes. **Philips Test & Measurement Instruments, Inc., 400 Crossways Park Drive, Woodbury, NY 11797 (516) 921-8880.** CIRCLE NO. 138

APPLICATION NOTES

Mixer circuit extends generator's range

With the do-it-yourself circuit described in application note 171-2, the lower frequency limit of Hewlett-Packard's model 8640A (B) signal generator may be extended downwards from 450 kHz to dc.

The four-page note shows how to build a simple external heterodyne circuit with common off-the-shelf parts. The circuit simply mixes the rear panel, fixed 5 MHz crystal output against the front panel tuned output signal. Frequency of the heterodyned signal can be read directly from the instrument's readout; frequency, fm and am remain calibrated. By simply considering the insertion loss of the external circuitry, output levels can be predicted over the extended dc to 450 kHz band. **Hewlett-Packard Company, 1501 Page Mill Road, Palo Alto, CA 94304 (415) 493-1501.** CIRCLE NO. 207

Sh! White noise spoken here

"The White Noise Book" is aptly titled. Literature claiming to be "THE" book is often suspect, but there's no credibility gap here. This 104-page text from Marconi should prove to be a valuable reference for the practicing communications engineer, as well as a comprehensive primer for students.

Author Michael J. Tant approaches the subject of multichannel communications system white noise testing from both historical and technical viewpoints.

Historically, the text is intriguing. The Marconi engineer traces the growth and sophistication of telephony from the single wire circuit of 1876 to the 2,700 channel satellite systems of the 1970's.

Technically, the text is useful. Profusely illustrated, most charts, graphs and tables are drawn to a large scale and are intended as working references.

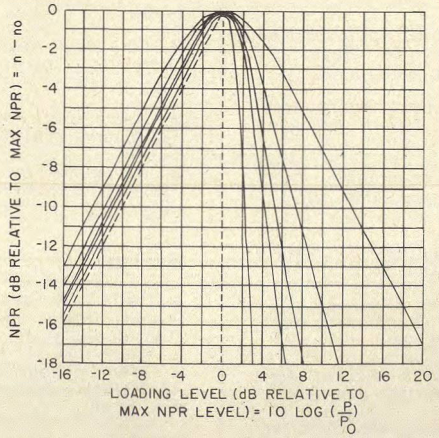
Tant begins the technical discussion by examining a series of concepts and definitions germane to telephony. Using CCITT symbology, the multi-channel group system is developed in detail. An entire chapter is devoted to defining power units and psophometric weighting. Special emphasis is placed on explaining conversions between European and American units of measurement.

After laying a strong foundation of definition, the author summarizes the noise objectives of telephone systems. Hypothetical reference circuits are suggested and compared to real links.

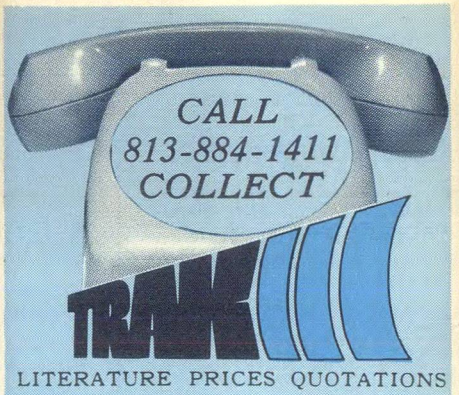
Baseband noise loading techniques are outlined with special attention to measurement accuracy. Normalized noise power ratio (npr) curves are presented and analyzed by considering three regions (see fig.): the linear region, where thermal noise is the only contributor; the region around maximum npr, where both intermodulation and thermal noise contribute; and the nonlinear region where intermodulation distortion predominates.

Finally, the noise loading recommendations of regulatory bodies—CCIR, CCITT, DCA, DOD and INTELSAT—are evaluated.

The hardcover publication measures 275 x 210 mm and costs £ 2 (approximately $4.75). **Publicity Department, Marconi Instruments, Ltd., St. Albans, Herts AL40JN, England.**



This normalized noise power ratio curve shows the effect of loading level.

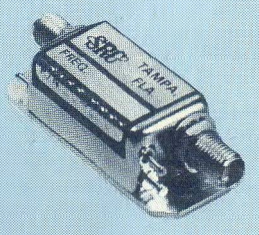


LITERATURE PRICES QUOTATIONS

Miniature size, high gain, wide dynamic range, low noise IF amplifiers in a completely shielded package. Uses thin-film hybrid technology, for proven reliability with no sacrifice in performance.

FREQUENCY: Customer specified from 20 to 150 MHz.
3 DB BANDWIDTH: 10 MHz typical.
GAIN: 70 ±3 db.
1 DB COMPRESSION POINT: 0 dbm.
NOISE FIGURE: 3 db max.
AGC RANGE: 60 db min.
AGC VOLTAGE RANGE: 0 to +5 volts.
INPUT DYNAMIC RANGE (WITH AGC): 80 db min.
POWER SUPPLY: +12 VDC at 35 ma nominal.
TEMPERATURE: −55°C to +85°C.
INPUT IMPEDANCE: 50 ohm nominal.
OUTPUT IMPEDANCE: 50 ohms nominal (detected output optional).
INPUT AND OUTPUT CONNECTORS: SMA female.
SIZE: 1.16" x .66" x .49" nominal excluding projections (smaller version available).
For further information contact Trak Microwave Corporation, 4726 Eisenhower Boulevard, Tampa, Florida 33614. Telephone (813) 884-1411, Telex 52-827.

MINIATURE LINEAR LOW NOISE IF AMPLIFIER



READER SERVICE NUMBER 63

1974 ANNUAL INDEX

Abbreviations: (TA) - Technical Article, (N) - News, (FP) - Feature Product, (SR) - Staff Report.

Acoustic Wave Devices

■ *1 GHz Acoustic Wave Filters Offer 500 MHz Bandwidths,* (N), Feb, p. 14.

■ *Rocky Road Seen For SAW Applications,* (N), Aug, p. 10.

■ *Surface Acoustic Wave Oscillators Operate Into Mircowave Range,* (N), Feb, p. 28.

Amplifiers

■ *Build A 12 Octave Hybrid Amplifier,* (TA), June, p. 54.

■ *Clean Up Your Design With A Systems Approach,* (TA), Jan, p. 48.

■ *Designing Amplifiers For Optimum Noise Figure,* (TA), Apr, p. 36.

■ *Designing Compact Log Amps,* (TA), Apr, p. 58.

■ *Drop-In I-f Preamps Exhibit Linear AGC Response,* (PF), Aug, p. 64.

■ *Dual-Gate FET Amp Offers Variable Gain,* (N), Aug, p. 26.

■ *80 GHz Impatt Amplifier Designed For mm Repeater,* (N), Apr, p. 30.

■ *Gunn Amplifiers Come Of Age,* (TA), Apr, p. 52.

■ *Hybrid Combined Transistor Amplifier Delivers 500 W cw,* (N), June, p. 9.

■ *Linearizing Amplifiers For Multi-Signal Use,* (TA), Apr, p. 46.

■ *Microwave Power On The Rise . . . Through Improved Devices And Combining Techniques,* (N), Apr, p. 9.

■ *Miniature 5-500 MHz Unit Amplifiers Deliver Up To 20 mW With 13 dB Gain,* (PF), Jan, p. 60.

■ *150 W L-Band Amplifier Has 15 Ns Rise/Fall Time,* (PF), Apr, p. 66.

■ *Optimizing Multi-Stage Amplifiers For Linearty, Part II,* (TA), May, p. 60.

■ *Optimizing Multi-Stage Amplifiers For Low Noise, Part I,* (TA), Apr, p. 62.

■ *Predicting Linear Power Amplifier Performance,* (TA), Feb, p. 56.

■ *Wideband Log Amplifiers Handle 10 ns Pulses Over 60 dB Dynamic Range,* (PF), Jan, p. 60.

Antennas and Phased Arrays

■ *Array Designers Fight To Shave Component Costs,* (N), Sept, p. 10.

■ *Attractive Antenna Offers Performance Bonus,* (N), Sept, p. 9.

■ *Conformal Arrays Pose Analytical Problems,* (TA), Sept, p. 42.

■ *Conical Beam Antenna Developed For Maritime Satellite,* (N), Aug, p. 26.

■ *Equi-Area Projection Improves Antenna Analysis,* (TA), Mar, p. 64.

■ *Graph Aids Phased-Array Design,* (TA), May, p. 59.

■ *Inexpensive Phasers Slash Array Costs,* (TA), Sept, p. 36.

■ *Knitted Antenna Solving Knotty Problems,* (N), Mar, p. 14.

■ *Limited Scan Antenna Cut Costs For Sat Terminals,* (N), May, p. 10.

■ *Measure Axial Ratio Error Accurately,* (TA), May, p. 58, 59.

■ *New Antenna Calibration Measurement Developed,* (N), June, p. 10.

■ *Nomograph Saves Time In Converting Antenna Gain,* (TA), Mar, p. 54.

■ *The Crux Of Flux In Free Space Loss,* (TA), Sept, p. 48.

■ *Weather Watchdog To Use Electronically Despun S-Band Array,* (N), May, p. 9.

■ *World's Largest Radio Telescope Being Developed,* (N), July, p. 9.

Commercial Products

■ *Automobile Pulse Radar Reduces False Alarms,* (N), Feb, p. 12.

■ *Fool-Proof Auto Radar Developed In Japan,* (N), Apr, p. 30.

■ *Vatican Museums Protected With Microwave Sensors,* (N), Feb, p. 28.

Communications

■ *AT&T Loses Ground To FCC Court,* (N), Nov, p. 19.

■ *AT&T Private-Line Conflict Heats,* (N), Feb, p. 24.

■ *Balloons Raise Repeaters For Greater Range With Less Power,* (N), Jan, p. 9.

■ *British P. O. Approves New MW Tower To Beam To France,* (N), Jan, p. 26.

■ *Cable Outlook Bright, Forecasts OTP Report,* (N), Mar, p. 23.

■ *Digital Modulation Techniques Okayed,* (N), Nov, p. 19.

■ *FCC Clarifies Microwave Rules,* (N), Oct, p. 19.

■ *FCC Gives Green Light To Specialized Common Carriers,* (N), June, p. 24.

■ *FCC Gives Packet New Carrier Role,* (N), Jan, p. 21.

■ *FCC Reallocates Spectrum For Common Carriers,* (N), Aug, p. 21.

■ *FCC Vacancies Finally Filled,* (N), July, p. 21.

■ *FCC Vacancies Still Abound,* (N), Apr, p. 24.

■ *FCC Will Peak At Bell System Tariffs,* (N), Sept, p. 20.

■ *FCC Will Peek At Unrouted Message Traffic,* (N), Jan, p. 22.

■ *First European Digital Line System Under Test,* (N), May, p. 26.

■ *ITT Will Join Private Line Field,* (N), Nov, p. 20.

■ *Interconnection Disputes Surface Again,* (N), Mar, p. 23.

■ *MCI Wants Fairness Doctrine Expanded,* (N), Mar, p. 24.

■ *New Faces At OTP, FCC,* (N), Feb, p. 23.

■ *New OTP Head "Eger" To Please,* (N), Dec, p. 20.

■ *OTP Proposes Cable Legislation,* (N), June, p. 23.

■ *Reduced Fee Schedule Offered By FCC,* (N), Oct, p. 22.

■ *Senate Bill Would Abolish OTP,* (N), Jan, p. 21.

■ *Specialized Carriers—A Boom For Telecom Equipment Manufacturers,* (N), Jan, p. 10.

■ *Supreme Court Gives Big Win To Cable,* (N), Apr, p. 24.

■ *Swiss Buying High-Capacity Data System,* (N), Sept, p. 26.

■ *The Year Of Giant Growth Arrives For Land-Mobile Communications* (SR), Jan, p. 38.

■ *World's Highest Communications Tower Planned For Toronto,* (N), May, p. 26.

Components

■ *Coax Connector Checks Multi-Moding Up To 43 GHz, (N), May, p. 14.*

■ *Looking For A 3 To 8 dB Microstrip Coupler?,* (TA), Mar, p. 58.

■ *Polyester Package Leads To $60 Hybrid Coupler,* (PF), Aug, p. 64.

■ *Take The Hassle Out Of Microstrip Coupling,* (TA), July, p. 48.

■ *Watch Out For Spurious Reflections,* (TA), May, p. 44.

■ *Waveguide In Waveguide Expands Bandwidth,* (TA), Nov, p. 74.

Design

■ *CAD With Graphics Make Circuit Design A Science,* (TA), June, p. 42.

■ *Clean Up Your Design With A Systems Approach,* (TA), Jan, p. 48.

Diodes

■ *Take The Trouble Out Of Diode Mounting,* (TA), Nov, p. 78.

Economic Outlook

■ *Army Study Boost Contracts,* (N), Apr, p. 23.

■ *Bell's Monopoly Sacked By OTP,* (N), Sept, p. 20.

■ *Bill Would Cut Contract Headaches,* (N), July, p. 21.

■ *China Rebuffs U. S. Trade Mission,* (N), Oct, p. 26.

■ *Commerce Department Boosts Industry,* (N), Feb, p. 23.

■ *Congress Clears Defense Appropriations,* (N), Nov, p. 19.

■ *Defense Dept. Supplemental Clears Both Houses,* (N), June, p. 23.

■ *Experts Give Trade Bill 50-50 Chance,* (N), May, p. 24.

■ *Higher Defense Spending Likely,* (N), Dc, p. 20.

■ *IRS Opens Door For Pension Reform,* (N), June, p. 12.

■ *Industry Is Bullish On Ford Administration,* (N), Sept, p. 22.

■ *Industrial Outlook Bright, Commerce Dept. Reports,* (N), Dec, p. 19.

■ *MARV Contract Goes To Lockheed,* (N), Oct, p. 19.

■ *Metric Bill On Its Way,* (N), Apr, p. 23.

■ *Missile Contracts To Soar In New Defense Largesse,* (N), Mar, p. 24.

■ *Monopoly Subcommittee Focuses On AT&T,* (N), Aug, p. 22.

■ *OTP Budget Chopped In Senate,* (N), Sept, p. 22.

■ *Portable Pensions Are Cleared By President,* (N), Oct, p. 22.

■ *Portable Pensions At Last?, (N), Nov, p. 10.*

■ *Slow Growth Projected For Mw Industry?,* (N), Dec, p. 14.

■ *Soviets Eager To Buy . . . But Doing Business Is Tough,* (N), June, p. 36.

■ *Trade Policies: Subject Of Review Here And Abroad,* (N), Nov, p. 24.

ECM

■ *Britain Investigates Smart Bombs, (N), June, p. 36.*

■ *Chirping RPM Data Links For ECM Protection,* (TA), Dec, p. 54.

■ *Mini-RPV's For Cheap And No Risk Air Power,* (SR), Oct, p. 40.

■ *Transplexing SAW Filters For ECM, Part I,* (TA), Dec, p. 43.

Filters

■ *Determine Filter Loss Quickly And Accurately,* (TA), Aug, p. 52.

Front Ends

■ *Calculate The Effects Of Noise On ECM Receivers,* (TA), Oct, p. 65.

■ *Integrating Components For New Front-End Design,* (TA), Aug, p. 35.

■ *What To Look For In Mixer Specs,* (TA), Nov, p. 48.

■ *World's Largest Radio Telescope Being Developed,* (N), July, p. 9.

Instrumentation and Measurement

■ *Add Power To Your Network Analyzer,* (TA), Oct, p. 51.

■ *Calculate Temperature Rise Quickly Under High-Power Testing,* (TA), Jan, p. 59.

■ *Coaxial Resonator Simplifies Permittivity Measurements,* (N), Oct, p. 26.

■ *18 GHz Automatc Counter Sells For Under $4000,* (CF), Nov, p. 59.

■ *Extend Transmission Distortion Testing To Microwave Bands, (PF), Sept, p. 76.*

■ *How Sharp Are Your Skills At Trace Photography?,* (N), Sept, p. 66.

■ *Improved TDR Techniques And Equipment Emerging,* (N), Nov, p. 35.

■ *Measuring Hard-To-Get-At Impedance By Translation,* (TA), June, p. 68.

■ *NBS 56-65 GHz Metrology Capability Ready For Customers,* (N), Sept, p. 60.

■ *Noise Transmitter Cuts Expense Of Noise Load Testing,* (CF), Oct, p. 58.

■ *Power Meters: New Designs Add Accuracy And Convenience,* (SR), Nov, p. 38.

■ *Probe Extends Handheld DMM To 500 MHz,* (PF), Aug, p. 68.

■ *Simple DC Tests Predict Transistor Performance,* (TA), Feb, p. 48.

■ *$16,000 Frequency Synthesizer Covers 100 MHz To 18 GHz,* (PF), May, p. 67.

■ *Radio Astronomy May Help Forecast Earthquakes,* (N), Nov, p. 9.

■ *Spectrum Analyzer Covers 10 MHz To 40 GHz With 70 dB Dynamic Range,* (PF), June, p. 69.

■ *Sweeper Modules Deliver Over 16 dBm,* (PF), Jan, p. 61.

■ *Understand Resolution For Better Spectrum Analysis,* (TA), Dec, p. 32.

■ *Y Factor Curves Simplify Noise Evaluations,* (TA), Aug, p. 48.

Lasers and Holography

■ *Diffraction Grating Extends BW Of CO Waveguide Laser,* (N), Jan, p. 12.

■ *GaAs Laser Uses Ion Implantation,* (N), Apr, p. 14.

■ *Laser Fusion: An Alternative Energy Source?,* (N), Feb, p. 10.

■ *Point Sources Laser Has Filamentory Active Region,* (N), Nov, p. 24.

■ *Simple Circuit Triggers Lasers,* (TA), Jan, p. 54.

■ *Transfer Chemical Laser Delivers 13% Efficiency,* (N), Jan, p. 14.

■ *0.3 MM X-Ray Waveguide Developed,* (N), June, p. 10.

Microwave Sources

■ *Design A High Power S-Band Doubler,* (TA), June, p. 58.

■ *Getting The Drift Of VCO Instability,* (TA), Mar, p. 42.

■ *Gunn Oscillator Array Belts Out 45 W Peak At 16 GHz,* (N), Sept, p. 26.

■ *Invar Disc Improves TEM Cavity Stability,* (TA), Aug, p. 58.

■ *Low-Noise Japanese Impatt Source Developed At 80 GHz,* (N), Aug, p. 26.

■ *Microstrip M-M Wave Source Achieves 1/4 W Output At 30 And 60 GHz,* (N), Aug, p. 9.

■ *MW Sources Improving In Tuning And Stability,* (SR), Mar, p. 36.

■ *Modular Source Boasts VCO Bandwidths And Crystal Stability* (PF), Dec, p. 62.

Millimeter Waves

■ *Bell's Millimeter System Hits The Dirt,* (N), Oct, p. 12.

■ *French Evaluate M-M Wave Communications System,* (N), Sept, p. 26.

■ *Microstrip M-M Wave Source Achieves 1/4 W Output At 30 and 60 GHz,* (N), Aug, p. 9.

■ *MICs Invade Millimeter Wavelengths* (N), Aug, p. 14.

■ *M-M Radar Tracks Low-Flying Targets,* (N), Dec, p. 12.

■ *M-M Transceiver Provides Covert Communications,* (N), Oct, p. 9.

■ *Multiplexers Tested For Britain's Developing M-M Communications,* (N), Oct, p. 26.

■ *New Transmission Media Emerging For Millimeter Wavelengths,* (N), Sept, p. 12.

■ *Simple Mode Filters Developed For M-M Communications,* (N), May, p. 26.

■ *Sweden To Get 66 Ft. M-M Radio Telescope,* (N), Mar, p. 26.

■ *30 GHz Digital Data Link Folds Flat For Easy Handling,* (N), July, p. 24.

Miscellaneous

■ *Microwaves: Hazardous To Your Health?,* (N), July, p. 21.

■ *Patent Policy Attacked By Nader Group,* (N), Mar, p. 24.

Radar

■ *Aegis Gets Set For Sea Trials,* (N), Apr, p. 12.

■ *Air Force Okays Traffic Radar System,* (N), Mar, p. 23.

■ *Are We Really Ready For S-Band Solid-State Arrays?,* (TA), Mar, p. 46.

■ *Computer-Scanned Radar Eyes Ice,* (N), Dec, p. 9.

■ *Doppler Radar Boasts Design Innovations,* (TA), Oct, p. 72.

■ *European Air-Traffic Control Market To Grow 2.5% Annually,* (N), Nov, p. 24.

■ *Fire-Control Radars Take A Modular Look,* (N), Mar, p. 9.

■ *For High-Power Protection . . . Try Multipacting,* (TA), July, p. 52.

■ *Phased Arrays To Update Mobile Radar Instrumentation,* (N), Apr, p. 18.

■ *Radar Marries The Minicomputer For Low-Cost Versatility,* (N), Nov, p. 12.

■ *Weather Radars Get Federal Largesse,* (N), Apr, p. 23.

Research and Development

■ *Do You Hear What I Hear?,* (N), Feb, p. 9.

■ *New Theory Proposed For Hearing Microwaves,* (N), Oct, p. 10.

Satellite Communications

■ *AT&T To Lease More Satellite Circuits,* (N), Aug, p. 21.

■ *Another Green Light For AEROSAT Launch,* (N), July, p. 22.

■ *Brazil To Get Second Satellite Ground Terminal,* (N), Jan, p. 26.

■ *COMSAT Hot Over ITT Worldcom Hotline Contract,* (N), Jan, p. 21.

■ *DOD's Space Shift Prompts Budget Boost,* (N), May, p. 24.

■ *FCC Intervenes Over Satellite Consortium Rift,* (N), June, p. 23.

■ *FCC, Justice, Could Clash On IBM Satellite Bid,* (N), Sept, p. 22.

■ *FCC's Navy/Marisat Order Draws Heavy Flack,* (N), Aug, p. 21.

■ *FTC Justice, Would Scuttle IBM's Satellite Plans,* (N), Nov, p. 20.

■ *Inexpensive Receiver Developed For Satellite Broadcasting,* (N), July, p. 24.

■ *Italy To Get ERTS Ground Station,* (N), July, p. 24.

■ *Launch Failure Sets Back Britain's Skynet II,* (N), Mar, p. 26.

■ *Maritime Administration Teams With COMSAT,* (N), Feb, p. 23.

■ *Meteosat To Provide Improved Satellite Weather Pictures,* (N), June, p. 36.

■ *Muzac Eyes Domsats For Nationwide Distribution,* (N), Oct, p. 12.

■ *NASA Gets Budget, Moves Toward More Satellites,* (N), May, p. 24.

■ *OTP Updates Satellite Broadcasting,* (N), Oct, p. 22.

■ *OTP's Updating Communications Satellite Act,* (N), Jan, p. 22.

■ *RCA Inaugurates Domestic Satellite Service—Others To Follow,* (N), Apr, p. 14.

■ *U.S. Earth Station To Track Russian Birds,* (N), Apr, p. 12.

Semiconductors and MICs

■ *Automatic Load Contour Mapping Devised For Power Transistors,* (N), Sept, p. 64.

■ *Biasing FETs For Optimum Performance,* (TA), Feb, p. 38.

■ *Improved Stability Offered With Dual-Gate FET,* (N), Jan, p. 26.

■ *Match Impedances With A Variable Transformer,* (TA), Nov, p. 69.

■ *New Transistor Plant Opens In France,* (N), Jan, p. 26.

■ *Simple DC Tests Predict Transistor Performance,* (TA), Feb, p. 48.

■ *2 GHz Transistor Belts Out 20 W cw With Infinite VSWR,* (PF), Apr, p. 66.

Systems

■ *Canada Certifies MLS For STOL Operations,* (N), June, p. 14.

■ *Hawk Missile Systems In Europe Updated,* (N), Mar, p. 26.

■ *Interim MLS System Chosen By FAA,* (N), Oct, p. 19.

■ *MLS Symposium Notes Released By FAA,* (N), Aug, p. 22.

■ *Mariner Peers At Planets With X- and S-band Eyes,* (N), July, p. 12.

■ *MW Data Bus: An Avionic Information Artery,* (N), July, p. 34.

■ *Radio Astronomy May Help Forecast Earthquakes,* (N), Nov, p. 9.

Tubes

■ *Collector Keeps Its Cool By Riding Outside Of Spacecraft,* (N), May, p. 12.

■ *Dual-Mode TWTs: The Nitty Gritty,* (TA), May, p. 38.

■ *Multi-Beam TWTs, Tomorrow's Tubes Today!,* (TA), Sept, p. 50.

■ *To Grid, Or Not To Grid?,* (TA), May, p. 52.

■ *200 kW S-Band Klystron Has TWT BW Capability,* (N), Jan, p. 26.

■ *Want More Power From Your TWTs? . . . Parallel'em,* (TA), p. 38, July.

new products

TRANSISTORS

Tuned Q transistors operate at 900 MHz

Rf power transistors cover 900 MHz with available ratings of 1, 5, 15, 25 and 40 W. The 1, 5 or 15 W types come in either common emitter or common base configurations; the 25 to 40 W ratings are common base only. All five values can be supplied in the standard 0.380 flange or 0.380 SOE package. **Solid State Scientific, Commerce Drive, Montgomeryville, PA 18936 (215) 855-8400.**

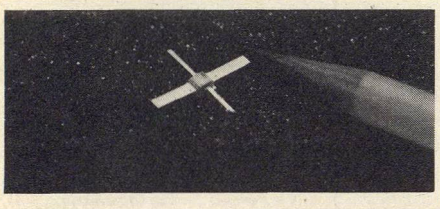
CIRCLE NO. 108

$35 transistors operate to 1500 MHz

One-half watt Class A transistors for use in low power driver applications ranging in frequency from 100 MHz through 1500 MHz, Models E1E and F1E, are 2 and 3 GHz transistor chips. Both devices have been fully characterized for Class A with full "s" parameters covering 100 MHz through 3 GHz as well as the dc safe operating area. P&A: E1E: $22, F1E: $35; stock. **Communications Transistor Corporation, 301 Industrial Way, San Carlos, CA 94070 (415) 591-8921.**

CIRCLE NO. 102

Quiet GaAs FETs boast 4 dB X-band NF

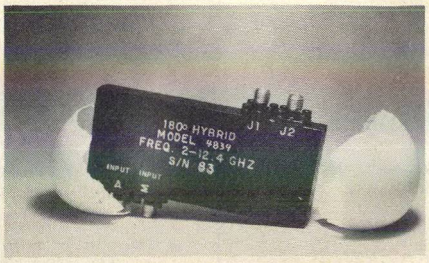


Model V244 is a developmental GaAs FET designed for low-noise amplifier and oscillator applications up to X-band. Features include an f_{MAX} of 40 GHz (for packaged devices), 11 dB MAG at 8 GHz and a noise figure of 4 dB at 8 GHz. Maximum drain current is 100 mA and max total power dissipation is 500 mW at an ambient temperature of 25°C. Chips or packaged devices are available and can be screened to high-rel specs for spacecraft. P&A: packaged device: $310 (qtys 1-9); chip only: $150 (min qty 10). **California Eastern Laboratories, Inc., One Edwards Court, Burlingame, CA 94010 (415) 342-7744.**

CIRCLE NO. 200

PASSIVE COMPONENTS

180° hybrid covers 2-12.4 GHz



Three dB hybrid coupler, model 4834, covers 2-12.4 GHz with a VSWR of 1.40 and isolation of 17 dB. Ampltiude unbalance is ±0.5 dB while phase unbalance is ±7°. Insertion loss is 1.7 dB and input power is 20 W average, 2 kW peak. Size is 3 1/2 x 1 1/2 x 1/2 in. and weight is 4.0 oz. P&A: $450. **Norsal Industries, Inc., 34 Grand Boulevard, Brentwood, NY 11717 (516) 231-4040.**

CIRCLE NO. 132

Miniature acoustic line provides 10 μs delay

Model CR02, an acoustic delay line, offers a delay of 1.5 to 10 μs with a delay tolerance of ±5 ns. Measuring only 1.5 × 0.5 × 0.5 in., the new line incorporates OTC glass to minimize delay drift. Center frequency is 60 MHz; bandwidth, 15 MHz min; max insertion loss, 23 dB and max spurious signal content is −26 dB. Both input and output impedances are 50 ohms. OSM connectors are standard. **Walther M. A. Andersen & Associates, Inc., 4 Main Street Extension, Tariffville, CT 06081 (203) 658-7666.**

CIRCLE NO. 112

Coax phase shifter handles 1 kW peak

Variable, coaxial phase shifters, LPS series, cover 1.0 GHz to 18 GHz and have a phase linearity of 2%. Minimum phase shift at 12 GHz is from 90 to 360 GHz and max VSWR is from 1.25 to 1.50 depending on models. Maximum insertion loss is from 0.5 dB at 1.3 dB with max power 1 kW peak, 10 W average. **Frequency Engineering Laboratories, P. O. Box 527, Farmingdale, NJ 07727 (201) 938-9221.**

CIRCLE NO. 107

MIXERS

Harmonic mixer covers 5.9-6.5 GHz

Harmonic mixer, model HMN-2065, features signal frequency range from 5.9-6.5 GHz while LO frequency range is 2.95 to 3.25 GHz. For a LO input power of O, +3, +7 and +10 dBm the conversion loss is 11, 10, 9 and 8 dB, respectively. LO/rf-rf/LO isolation is 15 dB while emperature range is −60 to +85°C. Size is 2 × 1.5 × 0.81 in. and weight is 2.5 oz. P&A: $450; 45 days. **Aercom Industries, Inc., P. O. Box 1946, Sunnyvale, CA 94088 (408) 734-1160.**

CIRCLE NO. 134

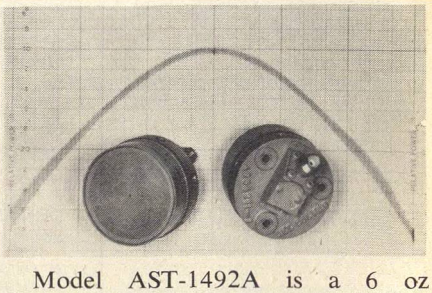
Mixer overlaps i-f and input freqs

The MX8171 mixer/converter is unique in that its i-f band overlaps its rf band. An rf input of 4.5-7.5 GHz is mixed with a 10.0 GHz LO signal for i-fs ranging from 2.5-5.5 GHz. Conversion loss is 10 dB; isolation is 20 dB and the third order intercept is set at +15 dBm. **Aertech Industries, 825 Stewart Drive, Sunnyvale, CA 94086 (408) 732-0880.**

CIRCLE NO. 117

ANTENNAS

Airborne spiral antenna blankets a 10:1 BW



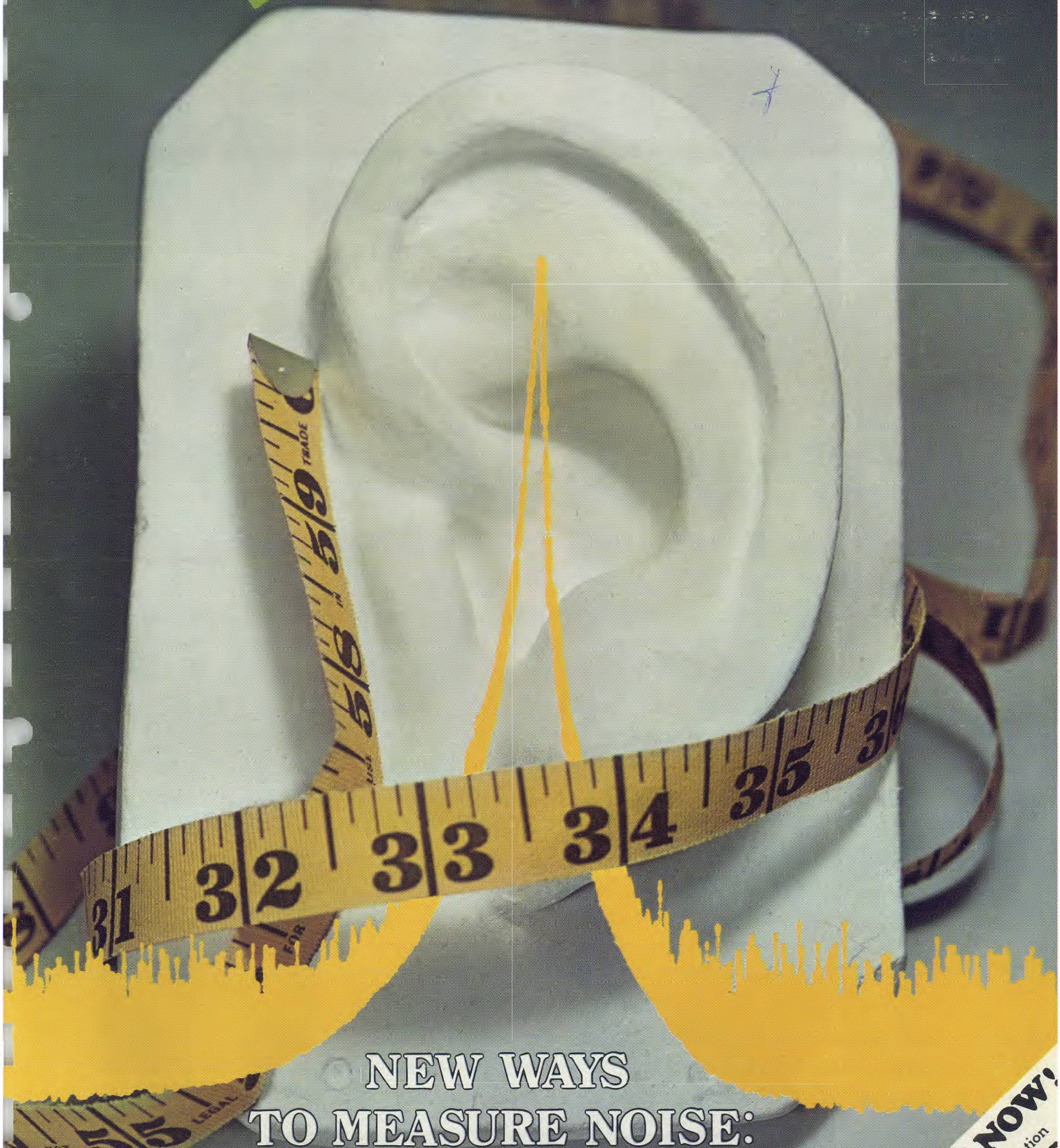
Model AST-1492A is a 6 oz cavity-backed spiral antenna that covers 2.0 through 20 GHz. Qualified for airborne use (MIL-E-5400), the antenna features a 10 dB beamwidth of 125° nominal, a half-power beamwidth of 75° nominal and axial ratios that vary from 2.0 dB on axis to 6.0 dB within ±80° of boresight. VSWR is 2.5:1. LHCP is standard; RHCP optional. Either a TNC or SMA connector may be specified. P&A: $190; stock. **American Electronics Laboratories, Inc., P. O. Box 552, Lansdale, PA 19446 (215) 822-2929.**

CIRCLE NO. 113

MARCH
1975

MICROWAVES

laser technology



NEW WAYS TO MEASURE NOISE:

Single Y-factor eliminates mismatches ● Simplify mixer excess noise measurement

ALSO: Automate transistor efficiency measurements
Pinpoint errors in mismatch measurements

RENEW NOW!
Before Your Subscription
EXPIRES
See card on p.1

MICROWAVES

March 1975
Vol. 14, No. 3

news

9 Arrayed Antennas Improve S/N Of Signals From Mariner
10 Microwave Altimeter Shows Ocean Surface Has Bumps
12 Chemically-Etched Antennas Look Promising, X-Band Impatt Source Pulses Out 100 Watts
16 Meetings
18 Industry
21 Washington
24 International
26 R & D
30 For Your Personal Interest . . .

editorial

28 A Question Of Ethics

technical section

Test & Instrumentation

32 **A New Way To Measure Noise.** Algie Lance, Wendell Seal and Paul Fujimoto of TRW present a new single Y-factor measurement approach that eliminates many mismatch uncertainties. Only one noise-temperature reference source is required.

42 **Measure Mixer Noise With Your Power Meter.** Daniel Cheadle of Watkins-Johnson outlines a simple method of determining a mixer's noise figure without resorting to precision, calibrated components. The Problem of excess noise is treated in depth.

50 **Pinpoint Errors In Mismatch Measurements.** Duane Dunwoodie of Wiltron Co. points out that many of the errors associated with directional devices can be minimized by using a reflection bridge. Several practical error curves are included.

62 **Calculate Transistor Efficiency Automatically.** Ray Gutierrez formerly of Microwave Semiconductor and now with Optimax shows how you can save time and improve accuracy in measuring transistor efficiency with an automatic efficiency calculator. The readout is digital.

82 Application Notes

68 **Intercon Product Features:** 2 Hz to 18 GHz Counter Handles Noisy Signals, Compact Plug-in Sweeps From 10 MHz TO 18.5 GHz

70 **Intercon Product Features:** Plug-In Synthesizer Series Offers Spectral Purity For $8995, Versatile 1-520 MHz Signal Generator Costs Under $2,000

71 New Products
84 New Literature

products and departments

79 New Products
83 Application Notes
86 New Literature
87 Advertiser's Index
88 Product Index

About the cover: Noise measurements, the bane of many microwave engineers, are evolving with new techniques for improved accuracy and more efficient methods for mass production. Cover composition and photo by Robert Meehan.

coming next month—Systems

"Reducing Radar Clutter in Radar Systems" . . .Peter Dax of Westinghouse provides an overview of the various techniques used to see targets in clutter. The basics of MTI and pulsed doppler are presented along with the advantages of digital processing.

"Integrated Optics: Microscopic Microwaves for Tomorrow"—(Part 1) . . . Fred Blum of Texas Instruments introduces this growing new technology of optical communication, explaining how microscopic optical components being developed are functionally and conceptionally similar to microwave components.

"Economic Forecast of Commercial Communications" . . . Jeff Montgomery of Gnostic Concepts, Market Researchers in Menlo Park, Ca, gives a preview of what is ahead for microwave communications in the next 5 years. Details on market growth, market share and what companies will be up or down in the microwave market will be presented, based on computer derived models.

"SAW Devices: Tips on Specifying Acoustic Wave Devices" . . . Surface acoustic wave devices are finding their way into a variety of microwave systems. Chuck Grasse, of Teledyne MEC explains how to spec these versatile signal processors and how to apply them in microwave systems.

DON'T LET YOUR SUBSCRIPTION EXPIRE!

If you haven't renewed in 75, turn to page 16A. Fill out your renewal card NOW and MAIL IT TODAY.

Publisher/Editor
Howard Bierman

Managing Editor
Richard T. Davis

Associate Editor
Stacy V. Bearse

Contributing Editor
Harvey J. Hindin

Washington Editor
Paul Harris
Snyder Associates
1050 Potomac St., NW
Washington, DC 20007
(202) 965-3700

Editorial Assistant
Gail Murphy

Production Editor
Sherry Lynne Bogen

Art
Robert Meehan, Dir.

Production
Dollie S. Viebig, Mgr.
Dan Coakley

Circulation
Trish Edelmann, Mgr.
Peggy Long, Reader Service

Promotion Manager
Walter Salm
Albert B. Stempel (Reprints)

Editorial Office
50 Essex St.,
Rochelle Park, N.J. 07662
Phone (201) 843-0550
TWX 710-990-5071

A Hayden Publication
James S. Mulholland, Jr., President

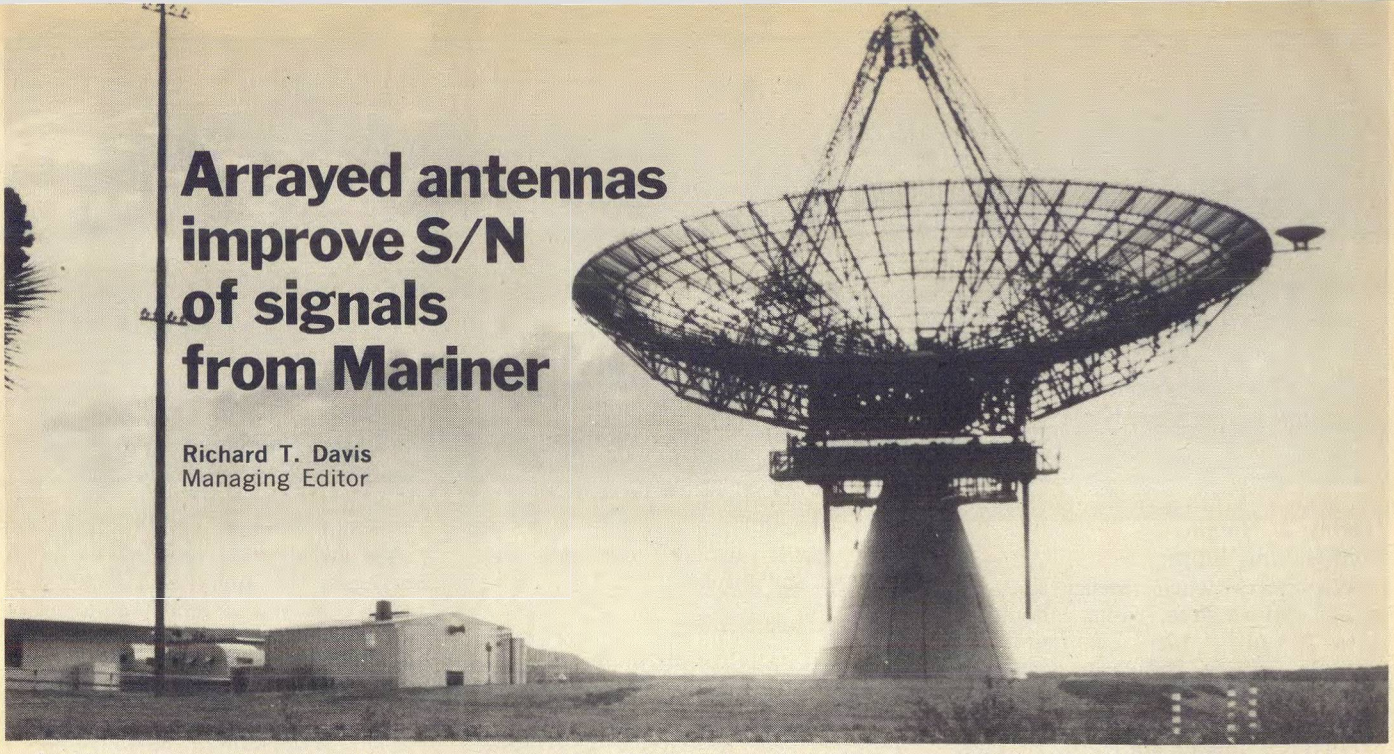
MICROWAVES is sent free to individuals actively engaged in microwave work at companies located in the U.S., Canada and Western Europe. Subscription price for non-qualified copies is $10.00 for U.S., $15.00 a year elsewhere. Additional single copies $1.50 ea. (U.S.); $2.00 ea. (foreign); except additional Product Data Directory reference issue, $10.00 ea. (U.S.); $18.00 (foreign).

Hayden Publishing Co. Inc., James S. Mulholland, President, printed at Brown Printing Co., Inc., Waseca, MN.

Copyright © 1974 Hayden Publishing Co., Inc., all rights reserved.

Arrayed antennas improve S/N of signals from Mariner

Richard T. Davis
Managing Editor



Getting an improvement of only 0.82 dB in signal-to-noise ratio for a receiver may hardly seem worth the effort. But for scientists at the Jet Propulsion Laboratory in Pasadena, CA, it meant receiving considerably clearer pictures from Mariner 10 in its September 21, 1974, encounter with Mercury. What makes this slight yet significant S/N improvement possible is a newly developed signal combiner that coherently phases and sums the real time telemetry data received simultaneously by three tracking stations. Using the combiner the bit error rate is reduced from 4.7 errors/100 bits to 3.3 errors/100 bits, a small but significant difference.

Basically, it's a matter of closely phasing signals buried in noise—the S/N of the data being added is as far down as −8.6 dB. In Mariner's first encounter with Mercury in March, 1974, the well-known 64-meter dish at Goldstone tracking station, was used to receive the very weak signals from Mariner 10 over a distance of about 148,500,000 km. In its second encounter, however, the distance from the spacecraft to earth was about 17% greater (169,500,000 km). "We realized we couldn't obtain the same picture quality as in the first encounter with just the single dish," says Helmut C. Wilck, a research engineer at JPL's communications system research station. "We therefore decided to use two additional smaller (26 meter) antennas available at the Goldstone facility to enhance the received signals."

The 64-meter dish was then used as a reference channel, although it only provides a 1.6 dB signal-to-noise ratio. The trick was to come up with a variable (50 to 100 μs) delay line that could automatically track the changing signal delays from the three antennas and keep the signals correctly phased to within a few nanoseconds throughout the spacecraft's pass.

"By arraying the two 26-meter antenna stations with the one 64-meter station at Goldstone, we were able to produce an improvement in signal-to-noise ratio of 0.8 dB when compared to the 64-meter station operating by itself," says Wilck.

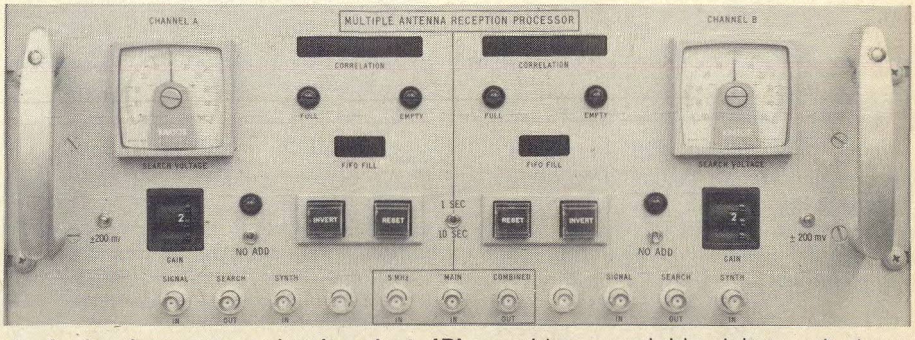
Phasing signals buried in noise

The two major questions that had to be addressed in designing the combiner (Fig. 1), were where in the receiver to combine the signals and how to accomplish the time phasing. "Signal combination at the rf (S-band) or the i-f level would be most desirable," explains Robin Winkelstein, group supervisor of the Digital Projects Group, "but it wasn't possible to the degree required." Combining the signals at the subcarrier level where synchronization requirements are less severe was, therefore, the next alternative. "We decided to process the baseband signals from the three antennas just before the subcarrier demodulation assembly (SDA)," Fig. 2.

Baseband signals, consisting of a 177.1 kHz square-wave subcarrier modulated by the 117.6 kbps telemetry data, are fed via short haul microwave links to the input of a signal combiner. The combiner delays the signals from the two smaller dishes by the proper amount in order to synchronize them with the signal from the 64-meter dish. (To insure that the reference signals from the 64-meter dish always arrive later at the combiner input, a fixed delay of 100 μ is maintained).

"The delay mechanism is basically a first-in, first-out (FIFO) memory," says Winkelstein. The signal to be delayed is sampled at a 2.5 MHz rate. Samples are then converted from analog-to-digital form and stored in a FIFO buffer

(continued on p. 14)



1. A signal processor developed at JPL provides a variable delay and phase correlation of baseband data to within 1% of a bit (bit time = 8.5 μs). A first-in/first-out (FIFO) buffer provides the variable delay for the input data stream.

Microwave altimeter shows ocean surface has bumps

S.V.B.

Harvey J. Hindin
Contributing Editor

Who says water seeks its own level? Microwave radar altimeter data recently received from the Skylab vehicle indicates that the ocean's surface has peaks and valleys—instead of being flat as your experience might indicate. In fact, a strong correlation exists between the shape of the ocean's surface and the ocean floor topology. And as strange as it may seem, when the ocean floor changes shape in some unknown way, there is a corresponding effect on the surface. The displacement might be as large as 70 miles over a surface radius of 1,000 meters—an interesting deviation if, for example, you are concerned with Polaris submarine systems guidance.

These anamolies caused by the local warping of the earth's gravitational field were detected at 13.9 GHz by the Earth Resources Experimental Package aboard the first Skylab. The data was analyzed by J. T. McGoogan, director of Applied Sciences at the NASA Wallops Flight Center in Virginia and his associates. The General Electric manufactured altimeter showed the ocean's surface variations and by extension made possible of the mapping of major features of the ocean bottom.

Getting the data

The altimeter can operate in any one of three selectable pulse widths (10, 20 or 100 nsecs) at a prf of 250 pulses/second. It has five operating modes, three of which are suitable for altimeter readings. During the space flight, eight altitude measurements were made in approximately one second with a transmitted power of 2 kW from a TWT. The receiver has a tunnel-diode front-end with bandwidth variable from 10 to 100 MHz. The i-f is set at 350 MHz. A 44-inch paraboloid is used as the antenna. An unusual feature of the altimeter is that certain rf circuits are also shared with other systems (the radiometer, for example) aboard the Skylab.

System functioning

For a satellite altimeter to work properly, a highly stable moving reference system is needed. Skylab, precisely positioned by ground-tracking instruments, provides this. Thus, the altimeter can precisely measure the distance from the reference orbit to the sea.

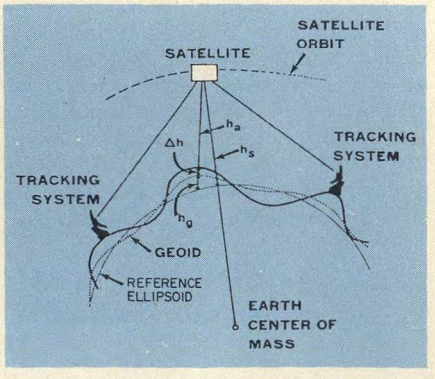
The altimeter is basically a conventional range-tracking-only-radar. The time taken for transit, as measured to the half-power point of the leading edge of the return pulse, is proportional to the altitude of interest. A system bandwidth of only a few Hz enables the determination of fine details of the ocean surface.

Real system error include inaccuracies with antenna pointing, pulse or bandwidth changes, system calibration, reference altitude error and atmospheric effects. Estimates of typical systematic instrument errors are thought to cause an altitude reading error of less than two meters. Atmospheric refraction is a much smaller problem with effects causing less than 10 cm error if temperature, pressure and humidity are known. As far as the overall system is concerned, independent measurements at C and S-band have confirmed an absolute accuracy of at least 10 meters, with a precision slightly under 1 meter rms.

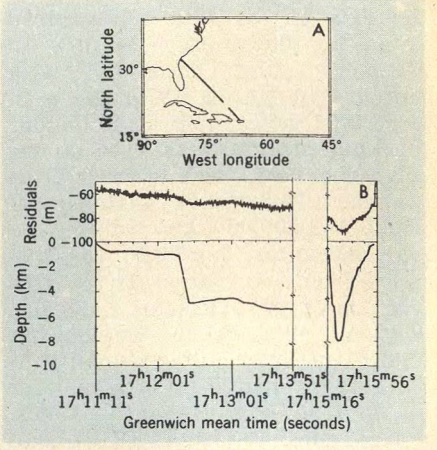
Mapping mechanics

In order to understand why the ocean surface is not flat, it is important to realize that except for effects like tides and currents, it is an equipotential surface. The equipotential surface of the earth's gravity field which corresponds to mean sea level is called the geoid. However, the geoid is an irregular shape due to local variations in gravity force. To simplify matters, an elipsoid is chosen which best fits the geoid and the separation

(continued on p. 14)



1. **The relationship between the geoid height** h_g, the satellite height above the reference ellipsoid determined from tracking data h_s, the satellite altitude measured by the altimeter h_a and the dynamic ocean effects due to tides, currents, etc. Δh enables the determination of geoid height from altimeter data. Since the water surface of the ocean seeks an equilibrium with gravity forces the altimeter provides a direct measurement of the shape of the surface.



2. A satellite pass from South Carolina to Puerto Rico (a) shows the surface irregularities of the Blake Escarpment and the Puerto Rico Trench (b). The slight shifts in the position of the minima are due to local gravity conditions. Analysis of all data obtained proved that altimeter error is not a consequential factor in profile determination.

Chemically-etched antennas look promising



1. Clearance between plates is only 0.005, so the antennas must be assembled under a microscope. Applications include reconnaissance, interception or rough direction-finding from 1 to 12 GHz.

Designers at GTE Sylvania believe that an adaptation of printed circuit chemical etching techniques can produce antennas faster, cheaper and more accurately than the conventional procedure of outlining elements and cutting them by hand. Using the new method, a log-periodic receiving antenna has been developed that can respond to vertical, horizontal and circular polarizations over a 1 to 12 GHz band.

"The antenna elements are essentially printed circuits without dielectric backing," notes Klaus Elfving, an engineering specialist at GTE Sylvania in Mountain View, CA. "The fabrication method is extremely accurate. With a different technique, you couldn't maintain the accuracy necessary for good performance at 12 GHz."

The antenna begins its life on a drawing board, where a draftsman lays out the exact element pattern many times life-size. A negative is then made of the drawing and the pattern is reduced to actual size. The negative is placed on a sheet of 0.001-inch thick brass, which has been coated with a light-sensitive compound. After exposure to intense light, the negative is removed and the brass sheet is placed in a chemical etching bath. Areas that were not covered by the negative are accurately etched away.

Four identical plates are etched in this manner, then glued on a tapered (0.50 to 0.125 inch) eight-inch long Rexolite support to form the crossed log-periodic (Fig. 1). Two lengths of 0.047 inch coax feed the antenna. The outside conductors are soldered along the lengths of two adjacent plates while the center conductors are crossed over and attached to the two opposite plates.

"The two inputs can be fed through a 90° hybrid to obtain circular polarization," Elfving says, "or you can feed either one alone or both simultaneously to get vertical, horizontal or slant 45° polarization."

The gain of the receiving antennas with respect to matched polarization is reported to vary between seven and eight dB. Half-power beamwidths are 60° in one plane and 100° in the other.

Two antennas have thus far been built using the chemical etching technique. These have been sold to the University of Kansas for $1,500 apiece, including "some non-recurring engineering work." Mounted on a dielectric backplate and encased in a conical dielectric radome, each unit weighs less than three pounds. •• *SVB*

X-band Impatt source pulses out 100 watts

Scientists at Hughes Research Laboratories in Malibu, CA, have successfully combined the outputs from eight double-drift silicon Impatt diodes to form a 100 W X-band pulsed power source. The record power level was measured at 10.3 GHz, when the source was operating with a 1 μs pulse width and a 25% duty factor.

The tiny (approx. one cubic inch) aluminum power combiner utilizes a high Q, TM_{010} mode resonant cylindrical cavity to coherently consolidate the outputs of commercially available Hewlett-Packard diodes. Individually, the diodes furnish 12.8 to 16 W peak power in X-band.

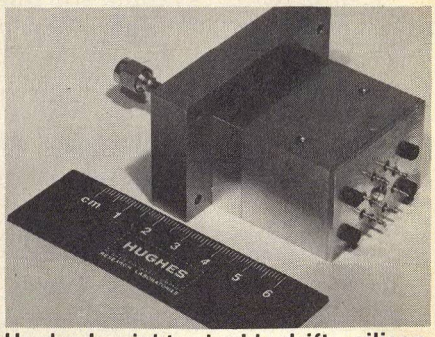
"The combiner was derived from a version designed for operation with cw Impatts," notes Dr. Robert Harp, a member of the technical staff at Hughes. Last year, Dr. Harp and colleagues from Hughes reported a 34 W cw combiner that operated at 10.5 GHz. Eight specially-made Raytheon GaAs Impatts (doped with a modified Read profile) were combined with an overall efficiency of 24.5%.

"Modifications include changes in the coaxial modules in which the diodes are located for more efficient operation with the pulsed diodes and in the matching circuits. It took us about three months to find the magic combination of transformers and reactive elements for matching," Dr. Harp relates.

A more effective heat sink was also designed to handle the increased power dissipation.

A transistor bias supply, built on a 4 × 5 inch circuit card, hits the combiner with 1 A current pulses with up to a 50% duty cycle and usable pulse widths up to 800 μs. The rise and fall times of the current pulses are on the order of 30 ns.

According to Dr. Harp, the major application for this type of device is in missile radar systems: "Its major impact is in terms of cost and weight." He indicates that minus diodes, the combiners could be made for "a couple of hundred dollars apiece." •• *SVB*



Hughes' eight double-drift silicon Impatt combiner delivers 100 W at X-band.

news/Microwave altimeter shows ocean surface has bumps

(continued from p. 10)

of the geoid above and below the ellipsoid (called geoidal undulation), can be measured—in this case by the microwave altimeter. Such estimates can, of course, be compared with data from other sources. Figure 1 indicates the pertinent relationships.

Not only did the satellite measurements show agreement with a variety of geoid models developed from geological theory, but a clear correlation exists between ocean floor topology and surface features. As such, mapping may be done of major features of the ocean bottom.

The difference between the altitude calculated to the reference ellipsoid and the altitude measured by the altimeter to the ocean surface (called the residual), is shown in Fig. 2 along with the actual ocean bottom topography. There is a four meter drop in the ocean's surface profile over the so-called Blake Escarpment (a slope between two different levels) and a 15 meter depression over the Puerto Rico Trench, two well-known ocean floor features. Data taken in similar situations shows much the same results. There is no doubt that the bottom features can be mapped more easily and quickly than by the use of surface ships.

Possible applications

According to McGoogan, "There are many possible practical applications of microwave satellite altimetry. These include geoid determination, correlation with known or determination of new ocean floor topography and land mapping. In addition, since the Gulf Stream has a rise of one meter over distances of 50 to 100 kilometers, it may be possible to track this important determinant of the weather."

Other potential uses of the system are under study. Further refinements as well as increases in accuracy are on the way. The services are interested because of potential military applications. In any case, it's an interesting civilian application of microwave radar technology. ••

Array antennas improve S/N of signals from Mariner

(continued from p. 9)

for a controlled length of time. The control for the buffer delay is derived from the correlation of the buffer output with the reference signal from the large dish. After leaving the FIFO buffer, the synchronized signals are reconverted to analog form and fed to a summing amplifier.

"Correlators are used to tell when the signals are lined up," explains Winkelstein. "The data streams are multiplied together and a statistical average taken. When they line up, the processing is at a maximum and when uncorrelated, they'll average zero. A second S-curve correlator is also used to correct for delay deviations —a zero when correlated, a plus signal when advanced and a negative signal when the data is delayed with respect to the reference."

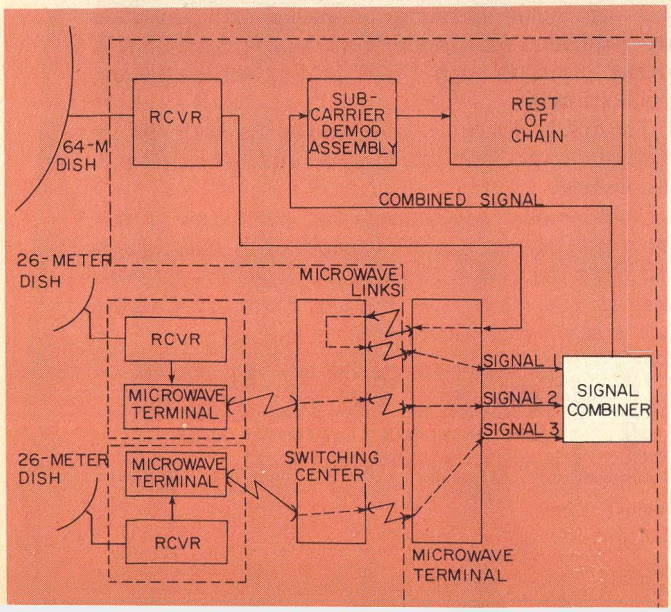
"In tests conducted, we found that 68% of the time the standard deviation of the alignment error is less than 5 ns and it's within 10 ns alignment 95% of the time."

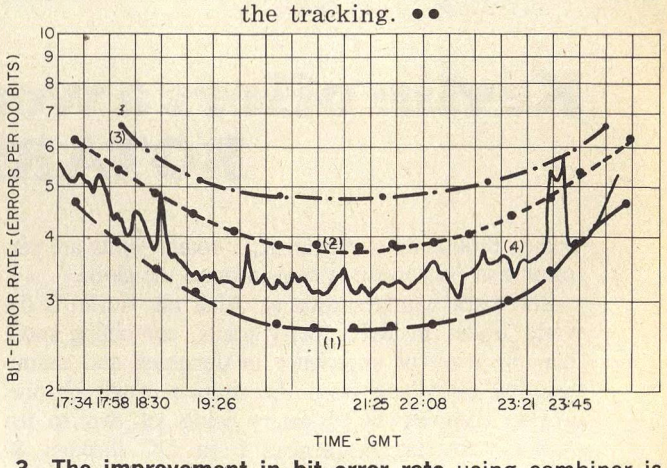
During the five to six hour encounter of Mariner 10 with Mercury during which four hours are suitable for taking pictures, the maximum rate of signal delay between antennas due to the earth's rotation was found to be 10 μs/hour. The signal combiner had to provide delays ranging from 22 to 85 μ and 46 to 98 μs for each of the 26 meter dishes, respectively.

The Mariner 10 TV enhancement experiment clearly demonstrated that antenna arraying is practical. A combination of two 64 meter antennas, if available in the same complex could produce a 3 dB improvement in signal-to-base ratio," claims Winkelstein.

The next encounter of Mariner with the planet Mercury is March 16, 1975. During this third encounter however, the combiner won't be used because a 64 m antenna in Australia will be doing the tracking. ••

2. To enhance pictures from Mariner 10, the received baseband output from the three arrayed antennas are transmitted to the 64 meter receiving station where they're fed to a signal combiner and synchronized with the reference baseband signal from the 64 meter dish. Once properly phased, the signals are weighted depending on their SNRs and then combined in a summing amplifier. They then go to the SDA and are processed in the normal manner by the rest of the telemetry chain.





3. The improvement in bit error rate using combiner is shown in this six hour pass of Mariner with Mercury in September, 1974. (1) Predict for combined operation and (2) normal operation; (3) extrapolation for normal operation and (4) measured data for combined operation. Signals degrade at ends of the plot because the antenna is looking closer to the horizon. Note that at 23:45, when the combiner is briefly shut off, the signal degrades immediately to its normal operating level; from about four bits of error/100 bits to about 5.5 bits of error/100 bits.

A New Way To Measure Noise

Here's a technique which permits you to choose the magnitude of Y-factor and devise a measurement system that eliminates many mismatch uncertainties. Theory is presented along with error curves.

THE common Y-factor method used for measuring noise figure depends upon having a known cold reference and a known hot reference temperature. To insure maximum accuracy, special attention must be placed on:

- the choice of hot and cold noise standards and
- the associated mismatch problems.

This article describes a unique noise figure test procedure that requires only a known cold or known hot-reference temperature as a standard. The analysis is performed in terms of an unknown hot-reference temperature.

This new method originated as a three Y-Factor technique which was then reduced to a two Y-Factor and finally a single Y-Factor technique. The original calculations of noise figure involved solving four different equations to determine the same effective temperature at the system input. Corresponding noise figures were then obtained from these calculated effective temperatures. The four equations are in precise agreement only when the correct value of Y-Factor/s and ENR (Excess Noise Ratio corresponding to the hot temperature at the measurement plane) are inserted in the equations. It was thus only necessary to increment the ENR until all noise figures were equal. The four equations and the incrementing technique are not covered in the paper since direct calculations are more convenient.

As a point of interest, the original equation for direct calculation of the effective temperature, using the two Y-factor technique, was not pursued after an initial cross check with the four basic equations indicated an apparent error of a few thousandths of a dB in calculated noise figure. However, this equation was later verified as being valid after Mr. T. Y. Otoshi of the Jet Propulsion Laboratory, Pasadena, CA, studied the original manuscript and derived equations for direct calculation of effective temperature and noise figure. His equations are included in the Appendix.

The error curves associated with this measurement technique indicate that in addition to knowing the cold-reference temperature very accurately, there is a stringent requirement for accurate Y-factor measurement and obtaining a very precise rf attenuator value. As will be shown, the errors become progressively greater as the cold-reference temperature approaches the ambient temperature (T_a) of the attenuator and the technique does not hold when the temperature T_a and the cold temperature T_c are equal.

Even though this technique is proven in terms of an unknown hot-reference temperature, the equations can be rearranged to satisfy the case of a known-hot reference temperature and an unknown cold reference temperature.

By using this new technique, it is possible to extend noise figure and excess noise ratio measurement capability to labs which do not have the necessary hot or cold reference loads; or calibrated noise sources with the required accuracy. Also, a choice of Y-factor magnitude (with Y-factor in dB) can now be chosen for best measurement accuracy. This eliminates errors associated with small Y-factors and is the principal advantage of this measurement procedure.

Reviewing the Y-factor method

To best understand how the new technique works, a review of the basic Y-factor method is helpful. Consider Fig. 1(a), where the indicated temperatures T_1 and T_2 serve as the hot temperatures.

Effective temperature, T_{e1}, is then

$$T_{e1} = \frac{T_1 - y_1 T_c}{y_1 - 1} \qquad (1)$$

where $y_1 = 10^{Y_1/10}$

and Y_1 is the Y-factor (in dB) obtained by switching between T_1 and the cold-reference temperature T_c ($T_e = 300°K$), Fig. 1(b).

If a 3 dB attenuator is placed in front of the noise source as shown, the hot temperature (T_2) is calculated as:

$$T_2 = (10^{(ENR_1 - A)/10} + 1)\ 290 \qquad (2)$$

where ENR_1 is the excess noise ratio corresponding to the temperature (T_1) and 290 is the IEEE standard temperature used in defining noise figure.

Then

$$ENR_1 = 10 \log \left[\frac{T_1}{290} - 1 \right] \qquad (3)$$

The temperature T_2 can also be obtained by

$$T_2 = T_1 \tau + T_a (1 - \tau) \qquad (4)$$

where T_a = the temperature of the attenuator in °K

and τ = the transmission coefficient corresponding to the attenuation value.

In this case,

$$\tau = 10^{-A/10} = 10^{-0.3}$$

Substituting $ENR_1 = 10$ dB and A = 3 dB in Eqn. 2,

$$T_2 = (10^{(10-3)} + 1)\ 290 = 1743.4429°K \qquad (5)$$

Using Eqn. (4)

$$T_2 = T_1 \tau + 290\ (1 - \tau) = 1743.4429°K \qquad (6)$$

The above agreement indicates that Eqn. (2) is valid only when the attenuator is at an ambient temperature of ($T_a = 290K$). As an example, if the attenuator ambient temperature is ($T_a = 300K$), then

(continued on p. 36)

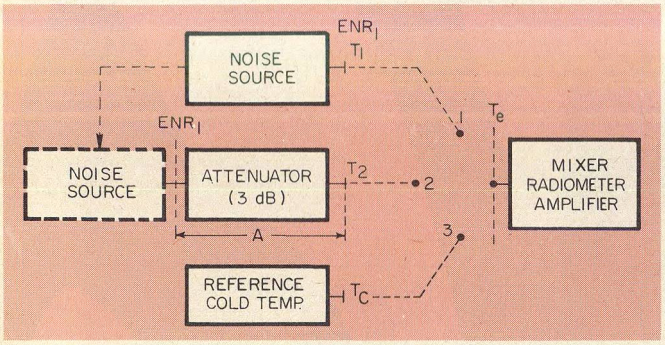
Algie Lance, Section Head, Electrical Standards, **Wendell D Seal,** Metrology Engineer, Rf and Microwave Standards and **Paul M. Fujimoto,** Supervisor, Rf and Microwave Standards, TRW Systems Group, Equipment Management Center, Metrology, One Space Park, Redondo Beach, CA 90278.

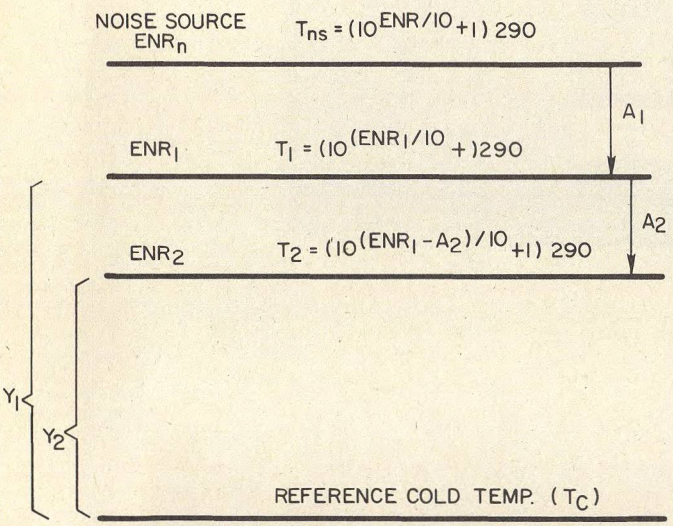
$$T_2 = T_1 \tau + 300\,(1-\tau) = 1748.431105°K \qquad (7)$$

This significant difference is very important and must be taken into account in the present proposed measurement technique. This can be illustrated by the following example. Assume a noise figure of 5.0 dB, A = 3 dB and a cold temperature reference of 300K for the system under test in Fig. 1(a). The resulting system parameters for the two attenuation temperatures are

	T_1	T_2	y_1	y_2
$T_a = 290$	3190	1743.443	4.11738008	2.55701051
$T_a = 300$	3190	1748.431	4.11738008	2.56239110

Note the differences in T_2 and the y_2 ratios.





1. (a) The basic test setup for measuring noise figure uses two separate hot temperature references obtained from a single noise source. (b) The magnitude of the Y-factors, Y_1 and Y_2, can be set to optimum values in the two-Y factor method.

Now define an excess noise ratio (EN_1) (corresponding to the temperature T_1) by replacing the IEEE standard temperature of 290 with the ambient temperature of the attenuator, T_A.

If the ambient temperature of the attenuator is 300K, then

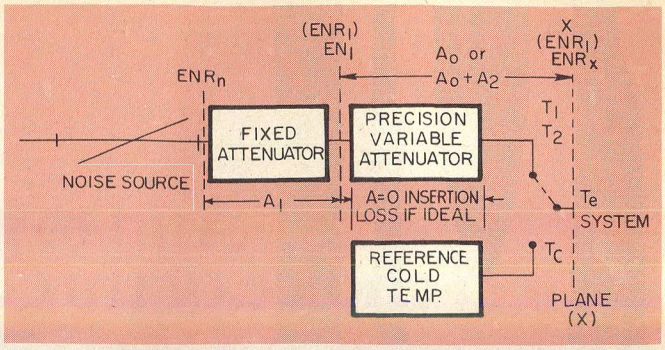
$$EN_1 = 10 \log \left(\frac{3190}{300} - 1 \right) = 9.837765 \qquad (8)$$

$$T_2 = (10^{(EN_1 - A)/10} + 1)\, 300 = 1748.431 \qquad (9)$$

Note that this value of T_2 is the same as previously obtained for T_a = 300K in the basic Eqn. (7). The preceding analysis thus shows that the correct ENR is arrived at once similar results are achieved in Eqns. (2) and (4).

The two Y-factor measurement

Now let's consider the two Y-factor measurement technique using one temperature as a known reference. The required test setup of the two Y-factor measurement technique is shown in Fig. 2. There are many refinements that can be made when precision measurements are involved. Often in some measurement systems, the effective noise temperature (T_e), the excess noise ratios (ENR_1 and ENR_2) as well as the corresponding hot temperatures, T_1 and T_2, are the values seen at the system input (mixer, radiometer, amplifier, etc.). In other words, there is no attenuation between the reference plane and what the system sees.



2. In a practical two Y-factor measurement system, either a cold-reference temperature or a hot-reference temperature is required as shown. An ideal system would use a variable attenuator with zero insertion loss. The excess noise values shown in parenthesis apply under ideal conditions.

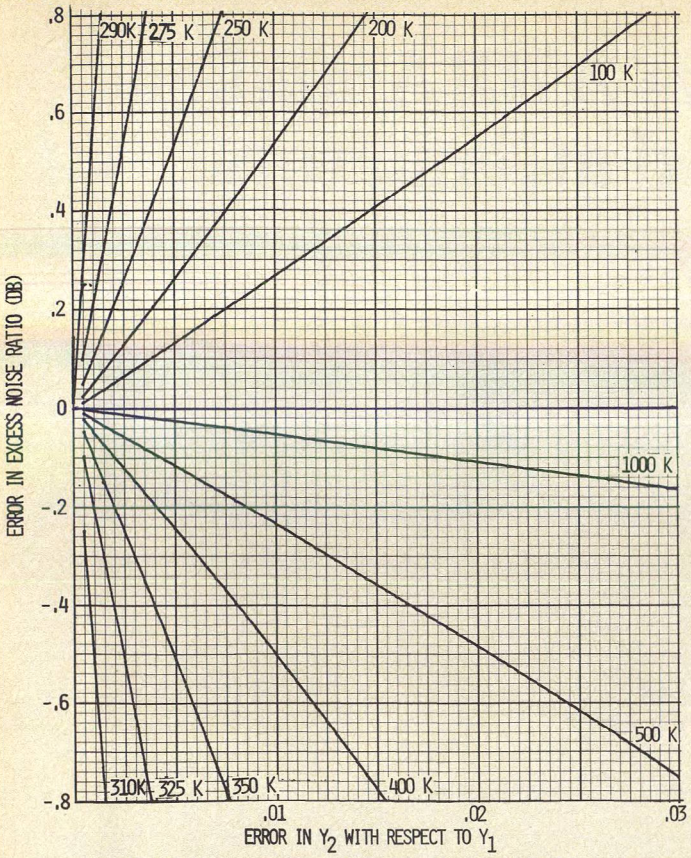
In this analysis, assume that the attenuator insertion loss is zero when the attenuator is on the zero dB dial reading. Then, the following additional conditions apply:

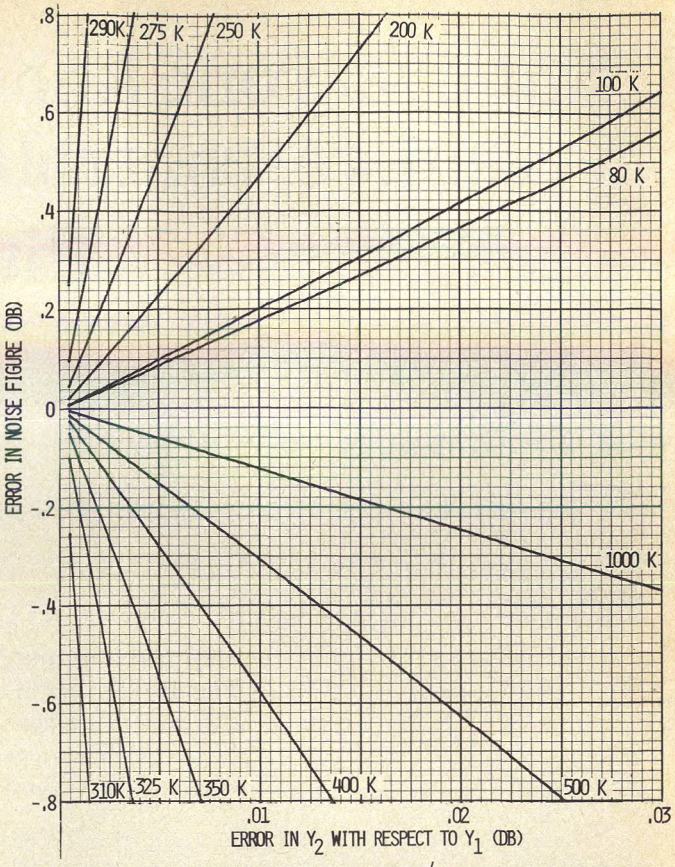
- A_1 = a chosen value of system attenuation determined by the ENR of the noise source; and the approximate value of ENR_1 at the measurement plane, which will provide the desired magnitude of Y-factor. (This is an important objective since a large Y-factor is desired to insure accuracy.)
- A_2 = a chosen value of attenuation which is obtained by a precision variable attenuator as shown in Fig. 2. (Fortunately you have a choice of this value now.)
- ENR_n = excess noise ratio of the noise source in dB.
- T_n = noise temperature of the noise source in °K.
- ENR_1 = the initial excess noise ratio that is seen at the system input reference plane (mixer, etc.) with the precision attenuator set at zero.
- T_a = the absolute temperature of the attenuator (A_2) in °K.
- T_1 = noise temperature in °K corresponding to ENR_1.

ENR_2 and T_2 are the excess noise ratio and noise temperature at the reference plane. In some systems, these values are seen by the mixer, radiometer, etc., when the precision attenuator is set to obtain the chosen value A_2. Note: ENR_1 and ENR_2 in Fig. 1a are defined in terms of the attenuator temperature (T_a) and not the defined standard IEEE temperature of 290°K. The indicated Y-factors, Y_1 and Y_2, are measured using standard measurement techniques.

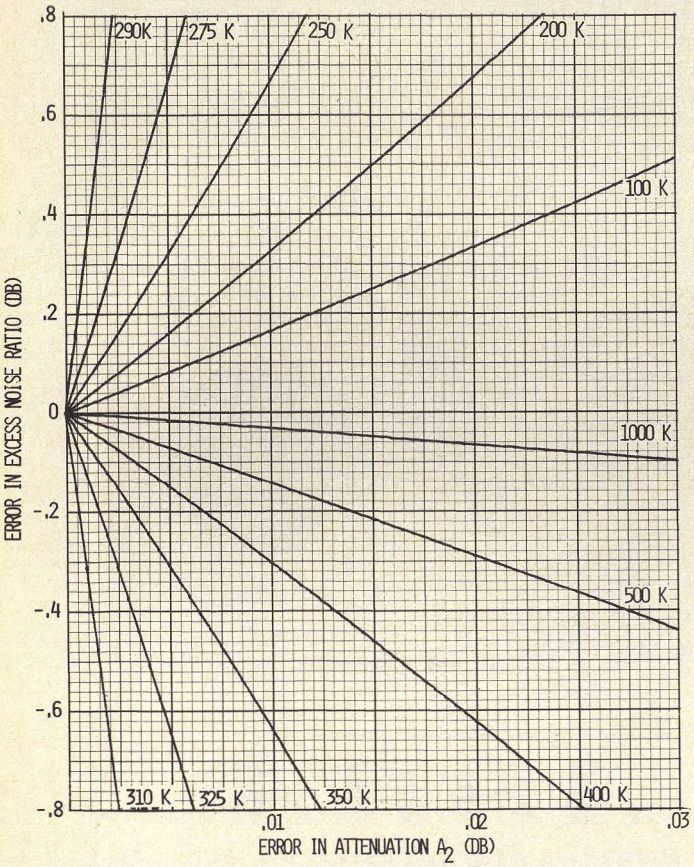
Figure 2 shows a practical measurement system. In this system, A_0 is the insertion loss of the variable

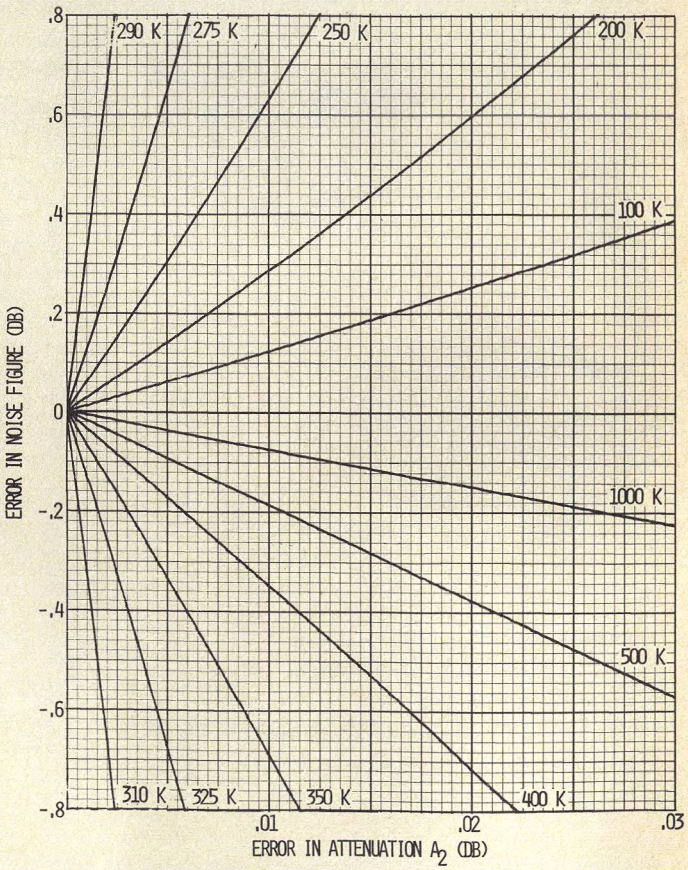
(continued on p. 38)





3. Noise errors are minimized by maximizing the amplitude of the Y-factor and the difference between the cold-reference temperature and ambient. Nominal values are A_2 = 3 dB, noise figure = 5 dB and ENR_x = 10 dB.





4. Error in measuring noise is also a function of attenuation accuracy. A large value of A_2 is best; about 50 to 70 dB in practice.

(continued on p. 40)

precision rf attenuator at zero dial setting. This value of attenuation must be included with the attenuation designated A_1 when calculating the excess noise ratio of the noise source from the ENR_x value at the measurement reference plane.

The Y-factor (Y_1) is obtained by switching from the hot to cold ports with the variable attenuator set to zero dB. Y_2 is obtained by switching between the hot and cold ports when the attenuator is set to a value of attenuation (A_2). The noise figure and excess noise ratio ENR_x are calculated using Eqns. (14), (12), (15) and (16) which are derived as follows:

The first Y-factor as defined in the original analysis:

$$y_1 = \frac{T_1 + T_e}{T_c + T_e} \qquad (10)$$

The second Y-factor is defined by inserting the value of T_2 of Eqn. (4) in the basic equation to obtain:

$$y_2 = \frac{T_1 \tau_2 + T_a (1 - \tau_2) + T_e}{(T_c + T_e)} \qquad (11)$$

where τ_2 is the transmission coefficient corresponding to A_2.

$$\tau_2 = 10^{-A_2/10}$$

and T_a is the ambient temperature of the attenuation A_2. The effective temperature (T_e) of Eqn. (10) is the basic equation

$$T_e = \frac{T_1 - y_1 T_c}{(y_1 - 1)} \qquad (12)$$

The effective temperature as calculated using Eqn. (11) is

$$T_e = \frac{T_1 \tau_2 + T_a (1 - \tau_2) - y_2 T_c}{(Y_2 - 1)} \qquad (13)$$

Equating Eqns. (12) and (13) and solving for T_1 results in

$$T_1 = \frac{y_1 T_c (y_2 - 1) + T_a (1 - \tau_2)(y_1 - 1) - y_2 T_c (y_1 - 1)}{(y_2 - 1) - \tau_2 (y_1 - 1)} \qquad (14)$$

The effective temperature is calculated using Eqn. (12) and the noise figure is then calculated as

$$\text{Noise Figure} = 10 \log \left[\frac{T_e}{290} + 1 \right] \qquad (15)$$

The excess noise ratio at the measurement plane is then,

$$ENR_x = 10 \log \left[\frac{T_1}{290} - 1 \right] \qquad (16)$$

The excess noise ratio (ENR_x) of the noise source is higher than ENR_x by the value of A_1. The noise source temperature and ENR can also be obtained by the following equations if you are calculating in terms of temperature.

$$T_n = \frac{(T_e + T_c)(y_1 - 1) + T_a (\tau_1 - 1) + T_c}{\tau_1} \qquad (17)$$

$$ENR_n = 10 \log \left(\frac{T_n}{290} - 1 \right) \qquad (18)$$

where τ_1 is the transmission coefficient corresponding to the dissipative part of the attenuation $A_1 \cdot [\tau_1 = 10^{(-A_1)/10}]$ T_a is the ambient temperature of the attenuation A_1.

One Y-factor technique

The one Y-factor measurement technique requires a measurement of y_1 and adjustment of the rf attenuator to obtain 3.0103 dB change in the system output power. (A precise 2:1 ratio of y_1 to y_2). This, of course, requires a very accurate attenuator. Assuming that an i-f attenuator with the required characteristics is available in the system, the measurement can be performed as follows:

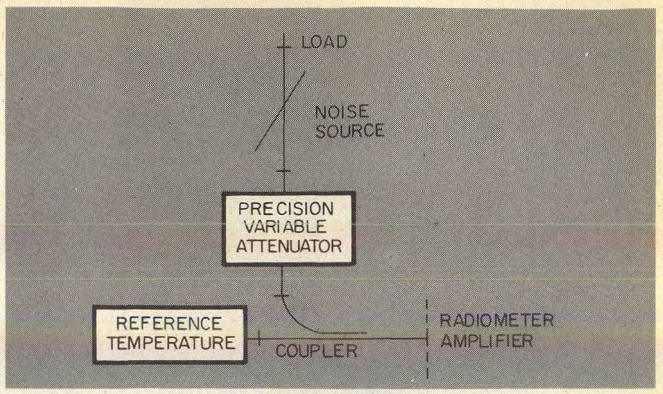
- Set the rf attenuator to its 0 dB reference and obtain a convenient output level reference.
- Measure the Y-factor Y_1 using the techniques previously outlined.
- Re-establish the 0 dB reference level of Step 1.
- Decrease the i-f attenuator value by precisely 3.0102 dB.
- Adjust the rf attenuator to a setting (A_2) which produces the original output reference level.
- Calculate the hot reference temperature as follows:

$$T_1 = \frac{y_1 T_c (y_1 - 2) + 2T_a (1 - \tau_2)(y_1 - 1) - y_1 T_c (y_1 - 1)}{(y_1 - 2) - 2\tau_2 (y_1 - 1)} \qquad (19)$$

Equation (19) is obtained by substituting $y_1/2$ for y_2 in Eqn. (14) as follows:

- Use the above T_1 in Eqn. 12 to obtain T_e.
- Use the value of T_e to obtain noise figure using Eqn. (15).
- Use the value of T_1 to obtain ENR_x using Eqn. (16).

Note: T_1 and T_e can also be calculated using Eqns. (7) and (8) of Otoshi's derivations described in the appendix.



5. This practical measurement technique uses a directional coupler to provide the needed results for either the two Y-factors or one Y-factor method. It allows maintaining constant mismatches during the measurement.

Error curves show how far off

As mentioned earlier, the new method is subject to error depending on the value of the reference-cold temperature, the accuracy in measurements of Y-factors (Y_1 and Y_2) and the rf attenuation value A_2. Figures 3 and 4 show just how much error is involved in the measurement of noise figure and ENR_x. Note that the errors become progressively greater as the cold-reference temperature approaches the ambient temperature (T_a) of the attenuator. The value of T_a is 300°K for the calculations. The curves also indicate that the technique does not hold when the temperature T_a and the cold temperature T_c are equal. A larger value of A_2 also results in better accuracy. The limiting case would be infinite attenuation (maximum of 50 to 70 dB in practical systems) and the T_2 temperature would then be T_a. The error analysis data shown in Figs. 3 and 4 was obtained using Eqns. (13) through (16) and the equations derived by Otoshi (see appendix).

The measurement system in Fig. 5 is an example of the type of system that can be devised to perform accurate noise measurements. The cold reference

temperature that the system sees can be calculated by taking into account all of the noise contributions. This type of system makes it possible to maintain constant mismatches during the measurements. Variations of this system and standard measurement systems using switching techniques can also be used.

Even though this technique was proven in terms of an unknown hot-reference temperature, you can rearrange the equations to satisfy the case of a known hot reference temperature and an unknown cold-reference temperature. ••

Bibliography

1. C. K. S. Miller, W. C. Daywitt, M. G. Arthur, "Noise Standards, Measurements and Rec. Noise Def., *Proc. IEEE,* Vol. 55, pp. 865-877, (June, 1967).
2. "IRS Std. On Electron Tubes, Definitions of Terms," 57-IRE 7.S2, *Proceedings IRE,* Vol. 45, (July, 1957).
3. A. L. Lance, W. D. Seal and F. J. Bayuk, "Noise Measurement Uncertainty," *Journal of Applied Measurements,* (February, 1974).
4. D. F. Wait, "Measurement of Amplifier Noise" Technical Feature, National Bureau of Standards.
5. M. G. Arthur, The Measurement of Noise Performance Factors: A Metrology Guide, NBS Monograph 142, (June, 1974).
6. A. L. Lance, "Reviewing Noise Figure and Excess Noise Ratio Measurements," *Journal of Applied Measurements,* 2, 12-21, (1974).

Acknowledgement

The authors thank Marlyn L. Hed, Manager of TRW Metrology, and Drs. J. S. Honda and J. E. Raue for their interest and suggestions during the development of the technique.

Test your retention

1. What is the advantage of this technique over conventional Y-factor noise measurements?
2. What would be the advantage of using 1000°K reference temperature instead of cold (liquid nitrogen) reference temperature?
3. Why can't T_a be substituted for T_e?

Appendix

Equations derived by T. Y. Otoshi of the Jet Propulsion Laboratory, California Institute of Technology Pasadena, CA. are as follows:

$$y_1 = \frac{T_1 + T_e}{T_c + T_e} \quad (1)$$

$$y_2 = \frac{T_1 \tau_2 + T_a (1 - \tau_2) + T_e}{(T_c + T_e)} \quad (2)$$

From manipulations of Eqns (1) and (2) one obtains

$$T_1 - T_e (y_1 - 1) = y_1 T_c \quad (3)$$

$$T_1 \tau_2 - T_e (y_2 - 1) = y_2 T_c - T_a (1 - \tau_2) \quad (4)$$

Applying Cramer's Rule to Eqns (3) and (4) and performing the determinant expansion, the values of T_1 and T_e for the two Y-factor technique are;

$$T_1 = \frac{T_c (y_1 - y_2) - T_a (1 - \tau_2)(y_1 - 1)}{\tau_2 (y_1 - 1) - (y_2 - 1)} \quad (5)$$

$$T_e = \frac{T_c (y_2 - y_1 \tau_2) - T_a (1 - \tau_2)}{\tau_2 (y_1 - 1) - (y_2 - 1)} \quad (6)$$

The equations for T_1 and T_e using the one Y-Factor technique are;

$$T_1 = \frac{T_c y_1 - 2 T_a (1 - \tau_2)(y_1 - 1)}{2 \tau_2 (y_1 - 1) - (y_1 - 2)} \quad (7)$$

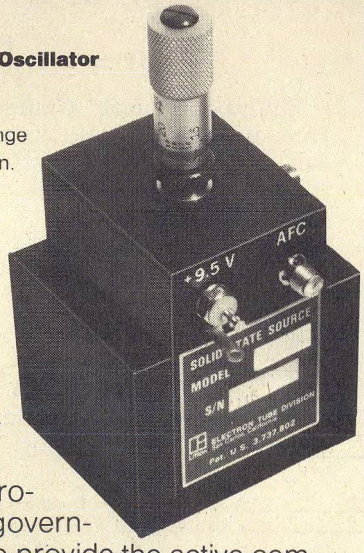
$$T_e = \frac{T_c y_1 (1 - 2 \tau_2) - 2 T_a (1 - \tau_2)}{2 \tau_2 (y_1 - 1) - (y_1 - 2)} \quad (8)$$

These equations make it easier to perform a complete error analysis. For example, the functional form expressed in terms of three standard deviations can be applied as follows

$$\Delta T_1 = \left\{ \left[\frac{\partial T_1}{\partial y_1} \Delta y_1 \right]^2 + \left[\frac{\partial T_1}{\partial y_2} \Delta y_2 \right]^2 + \left[\frac{\partial T_1}{\partial T_a} \Delta T_a \right]^2 + \left[\frac{\partial T_1}{\partial \tau_2} \Delta \tau_2 \right]^2 + \left[\frac{\partial T_1}{\partial T_c} \Delta T_c \right]^2 \right\}^{1/2} \quad (9)$$

New 8.0-8.4 GHz Litton solid state sources for telecommunications transmitter chains.

M-1014 Voltage Controlled Oscillator
Power Output—150 mW, Min.
Frequency—8.0 to 8.4 GHz
400 MHz mechanical tuning range
Mod Sensitivity—1.6 MHz/V, min.
FM Noise—−78dBm0, (200 kHz ref. 0 dB)
Waveguide output—WR-112





M-1002 Injection Locked Amplifier
Power Output—1000 mW, min.(+31 dBm typ)
Frequency—8.0 to 8.4 GHz
400 MHz mechanical tuning range
Locking bandwidth—50 MHz min. (70 MHz typ)
Locking gain—>15 dB (17dB typ)
Temperature coefficient—<125 kHz/°C
Waveguide output—WR-112

We have sources that will fit into your plans for point-to-point microwave radios used in government applications. We provide the active components—a Gunn Voltage Controlled Oscillator driving an Injection Locked Amplifier—you supply your own interstage coupling. Sources are also available for CARS (including CATV), ETV and STL bands.

Look to Litton—the performance and reliability leader—as *the* source for your solid state source requirements. Send today for complete catalog. Electron Tube Division, 960 Industrial Road, San Carlos, CA 94070. (415) 591-8411.

Litton ELECTRON TUBE DIVISION

READER SERVICE NUMBER 41

Measure Mixer Noise With Your Power Meter

A simple method of determining a mixer's noise figure without precision, calibrated components is presented. Use caution, however, don't neglect the effects of excess noise.

MEASURING excess mixer noise in a rapid, accurate way poses a problem. Most excess mixer noise occurs at i-f frequencies below 10 MHz, precluding the use of commercially-available noise monitors which are usually limited to i-fs greater than 10 MHz.

In addition, these instruments generally employ a solid-state noise source, which causes the accuracy of the measurement to be highly dependent on the accuracy of the source calibration. A ±0.5 dB overall uncertainty is usually the best that can be hoped for.

In contrast, the well-known Y-factor method using hot and cold noise generators can yield accuracies as high as ±0.1 dB. This technique, however, requires a precision attenuator that must be accurately calibrated at each i-f frequency and doesn't lend itself to fast, production testing.

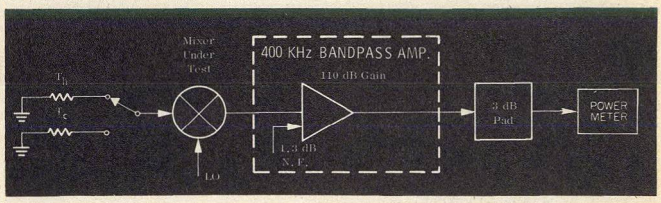
The noise measurement method described in this article can yield accuracies of ±0.2 dB or better and relies on a standard microwave power meter in place of any specially calibrated device (Fig. 1). It is similar to the Y-factor method, except that a power meter is used as the detector, giving a power ratio instead of an attenuation ratio.

Using this method, the hot resistor is placed in the circuit first, and the power meter is set for a full scale reading. The cold resistor is then placed in the circuit and the power is read as a percentage of full scale. This power ratio is referred to as the P-factor and may be converted directly to a corresponding noise figure.

An expression for the equivalent noise temperature (T_e) as a function of the P-factor is derived as follows. T_e is defined as the equivalent noise temperature of the input termination of the device under test at which the available output noise power is twice that which would be available if the input termination was at absolute zero[1].

The total noise power from the hot resistor is defined as kT_hB and the total noise power from the cold resistor as kT_cB. Then, the equivalent noise power available at the input of the device when the hot resistor is connected, to the total noise power when the cold resistor is connected is:

$$\frac{P_{HOT}}{P_{COLD}} = \frac{kT_hB + kT_eB}{kT_cB + kT_eB} = \frac{T_h + T_e}{T_c + T_e}$$



1. A conventional power meter takes the place of calibrated components in the P-factor method.

The P-factor is defined as the ratio of P_{COLD} to P_{HOT}, when $P_{HOT} = 1$. Then:

$$\text{P-factor} = \frac{P_{COLD}}{1} = P = \frac{T_c + T_e}{T_h + T_e}$$

Solving for T_e yields:

$$T_e = \frac{PT_h - T_c}{1 - P} \quad (1)$$

Applying this to the standard definition of noise figure in terms of temperature[2]:

$$NF = 1 + \frac{T_e}{T_o} \quad (2)$$

$$NF = 1 + \frac{PT_h - T_c}{(1 - P)\,T_c} \quad (3)$$

Equivalent noise figures for P-factors ranging from 0.35 to 0.88 are listed in Table 2, which was derived using the following standard temperatures adopted by the IEEE: $T_h = 373°K$, $T_c = 80°K$ and $T_o = 290°K$.

In a normal mixer noise figure measurement, both sidebands are present in the output because the noise source is broadband and contains the image frequency.

Seven[3] has shown that $F_{SSB} = F_{DSB}\left(1 + \frac{G_{sig}}{G_{im}}\right)$.

The signal (G_{sig}) and image (G_{im}) gain are assumed to be equal (true for most lower frequency i-f measurements). Therefore:

$$F_{SSB} = 2F_{DSB}$$

Thus, the image response has the effect of reducing the conversion loss to the input noise signal by a factor of two (3.01 dB), assuming that both sidebands are of equal magnitude. Thus, 3.01 dB must be added to the measured noise figure to determine the single sideband noise figure.

Subtract noise figure of i-f amp

Excess noise is defined as that noise which causes a mixer's noise figure to exceed its conversion loss. In

(continued on p. 44)

Daniel L. Cheadle, Member of the Technical Staff; Watkins-Johnson Company, 3333 Hillview Avenue, Palo Alto, CA 94304.

general, a mixer manufactured with a Schottky-barrier diode operating at normal low-level conditions and at frequencies above the 1/f region (above 400 kHz) will not produce excess noise. The following derivation will show that under these conditions (no excess noise), the noise figure of a mixer may be measured by evaluating it in series with an i-f amplifier, then simply subtracting the amplifier's noise figure from the overall reading.

The classical definition of noise for cascaded stages is:

$$F = F_1 + \frac{F_2 - 1}{G_1} + \cdots\cdots + \frac{F_n - 1}{G_1 G_2 \cdots G_n - 1} \quad (4)$$

When G_2 is greater than 30 dB—which is always the case when the HOT-COLD system is used—all but the first two terms of Eqn. (4) can be dropped. Doing this and using the notation in Table 1 yields:

$$NF = F_m + \frac{F_a - 1}{G_m} \quad (5)$$

The standard definition of noise figure in terms of signal to noise powers is given by

$$NF = \frac{\text{available output noise power}}{\text{available input noise power}} \times \frac{\text{available input signal power}}{\text{available output signal power}} \quad (6)$$

(continued on p. 46)

Table 1: Definitions used in derivations

NF:	Overall noise figure
F_{SSB}:	Single sideband noise figure
F_{DSB}:	Double sideband noise figure
F_a:	I-F amplifier noise figure
G_M:	Gain of mixer (conversion loss)
kTB:	Thermal noise power (k is Boltzman's constant, T is temperature in degrees Kelvin, and B is the 3 dB bandwidth of the system)
Nom:	Excess noise power from mixer
G_2:	Gain of I-F amplifier
T_h:	Temperatures of HOT resistor source
T_c:	Temperatures of COLD resistor source
T_o:	Temperature of input of device under test (Ambient temperature)
T_e:	Equivalent temperature at input of device under test

Screening diodes for excessive noise

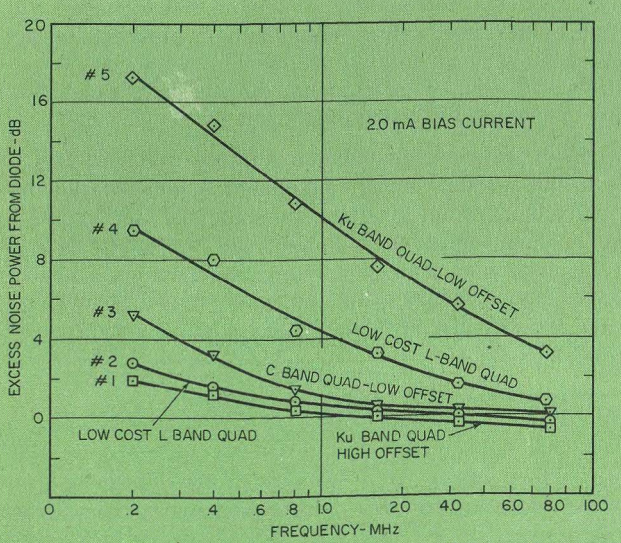
Excess, or 1/f, noise occurs at relatively low frequencies. The curves in Fig. A1 show measured excess noise characteristics of several types of diode quads that are used in commercially-available mixers.

During the measurements, the diodes were ac coupled to an i-f amplifier and a low-noise metal film series resistor so that the sum of the dynamic impedance of the diode and the series resistance equalled approximately 50 ohms. Thus during the measurement, the i-f amp always sees the same source impedance and therefore, has a constant noise figure.

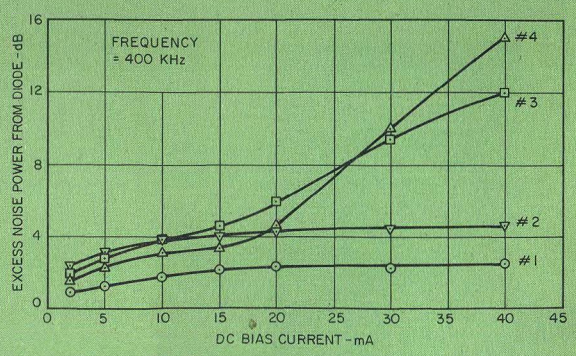
The power output of the diodes was measured relative to a 50-ohm termination over the range of 200 kHz to 6 MHz. Note the wide variation in excess noise for different types of diodes. For example, a Ku-band quad can display a very low excess noise curve (curve No. 1) or a very high curve (curve No. 5).

Lower frequency discrete diodes tend to have no excess noise above 400 kHz. Diodes that do not perform well at this i-f frequency can be expected to have a high-noise figure spec when used in a mixer.

The effect of dc current on excess noise measured at 400 kHz is shown in Fig. A2. This characteristic is important in high-level mixers where diode peak currents can reach as high as 40 mA. Curves No. 3 and 4 represent reject diodes for high-level applications.



A1. Mixer diodes should be screened for excess noise at an i-f of 400 kHz. Note the variation between similar types of diode quads.



A2. Excess diode noise increases with bias current. If this effect is severe (curves 3 and 4), the diodes should be rejected.

which reduces for equal input and output impedances to:

$$NF = \frac{\text{output noise power}}{\text{input noise power}} \times \frac{1}{\text{Gain}} \qquad (7)$$

Using this definition, the mixer noise figure (F_m) becomes (Fig. 2):

$$F_m = \frac{kTB + Nom}{kTB} \times \frac{1}{G_m} = \left(1 + \frac{Nom}{kTB}\right) \times \frac{1}{G_m} \qquad (8)$$

Substituting in Eqn. (5), the overall noise figure is:

$$NF = \left(1 + \frac{Nom}{kTB}\right) \times \frac{1}{G_m} + \frac{F_a - 1}{G_m} \qquad (9)$$

If the excess noise (Nom) from the mixer is zero, then:

$$NF = \frac{1}{G_m} + \frac{F_a - 1}{G_m} \text{ or } F_m = \frac{1}{G_m}$$

which states that the mixer noise figure is equal to its conversion loss.

$$\text{Replacing } G_m \text{ by } \frac{1}{F_m} \text{ gives: } F = F_m F_a$$

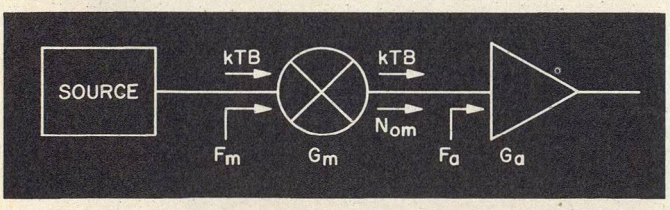
Taking the log of both sides we obtain:

$F_{m\,dB} = F_{dB} - F_{a\,dB}$

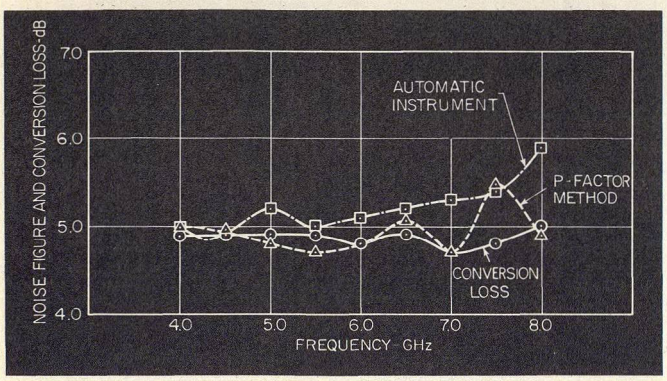
This result shows that the mixer noise is equal to the overall measured noise figure minus the i-f amplifier noise figure when the excess mixer noise is assumed to be zero.

Once a P-factor is determined for the measurement scheme shown in Fig. 1, find the equivalent overall double side-band noise figure from Table 2. To determine the single side-band noise figure of the mixer under test, simply add 3.01 dB to this value, then subtract the noise figure of the i-f amplifier used in the measurement.

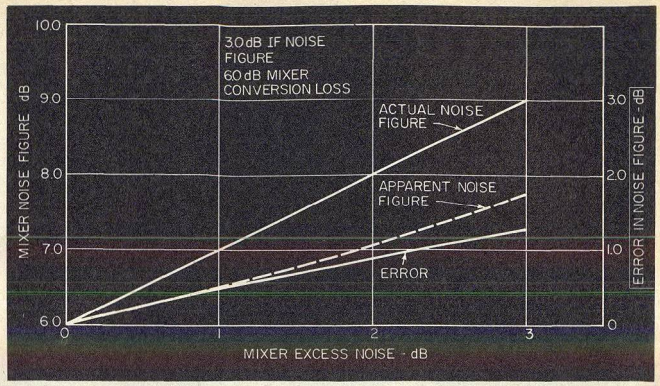
(continued on p. 48)



2. This notation is used in the derivation. For definitions, refer to Table 1.



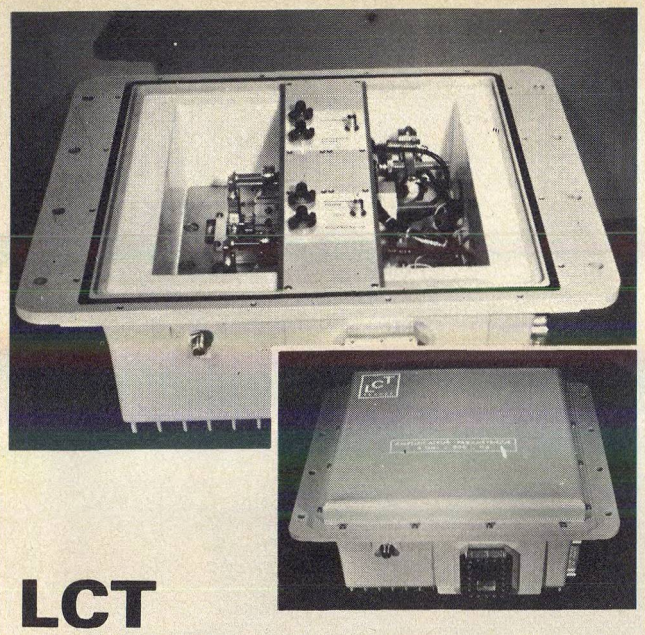
3. Compared to an automatic instrument (AILtech type 75), the P-factor method tracks conversion loss more closely. This measurement was on a WJ-M14 mixer using a 30 MHz i-f.



4. If excess noise is present, subtracting the i-f noise figure from the system noise figure could lead to a considerable error.

Table 2: P-Factor to noise figure conversion

P-FACTOR	OVERALL NOISE FIGURE (DSB)
0.35	1.03
0.36	1.11
0.37	1.20
0.38	1.28
0.39	1.37
0.40	1.45
0.41	1.54
0.42	1.63
0.43	1.72
0.44	1.81
0.45	1.91
0.46	2.00
0.47	2.10
0.48	2.19
0.49	2.29
0.50	2.39
0.51	2.49
0.52	2.60
0.53	2.70
0.54	2.81
0.55	2.92
0.56	3.03
0.57	3.15
0.58	3.26
0.59	3.38
0.60	3.50
0.61	3.63
0.62	3.75
0.63	3.88
0.64	4.01
0.65	4.15
0.66	4.29
0.67	4.43
0.68	4.58
0.69	4.73
0.70	4.89
0.71	5.05
0.72	5.21
0.73	5.39
0.74	5.56
0.75	5.75
0.76	5.94
0.77	6.13
0.78	6.34
0.79	6.56
0.80	6.78
0.81	7.02
0.82	7.26
0.83	7.53
0.84	7.80
0.85	8.10
0.86	8.41
0.87	8.74
0.88	9.10



LCT paramps

LCT manufactures a complete family of all solid-state uncooled parametric amplifiers featuring wide band, high gain and low noise temperatures for centre frequencies of 1.7, 2.3, 4, 5.5, 7.5, 11.5 GHz.

In the **HSTC** (Hermetically Sealed Thermostatically Controlled) series the 4-500 model, for example, features a 500 MHz bandwidth at 4 GHz, a noise temperature of 80,60 or 50°K * and :

- All RF components housed in a thermostat-controlled, air-tight oven
- Gain-stability of ± 0,1 dB/day and ± 0,3 dB/month
- Stabilization time at start-up less than 10 minutes
- Built-in test and alarm facility
- Fundamental Gunn diodes as pump sources

LCT produces also a series of **Compact** paramps. Among these, the 4-501 model operates at 4 GHz with a 500 MHz bandwidth and a 95°K noise temperature.

All these amplifiers are in current production with short delivery terms. Several European ground stations are now equipped with LCT paramps, including two stations using the model 4-500.

Laboratoire Central de Télécommunications
18-20, rue Grange-Dame-Rose
78140 VELIZY - France
Phone : (1) 946.96.15 - Telex 69 892

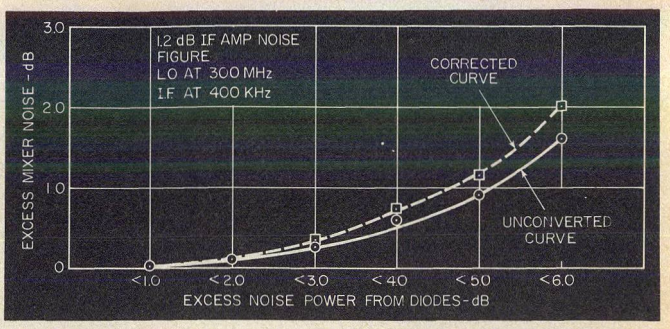
* Typical value

Laboratoire Central de Télécommunications **LCT**

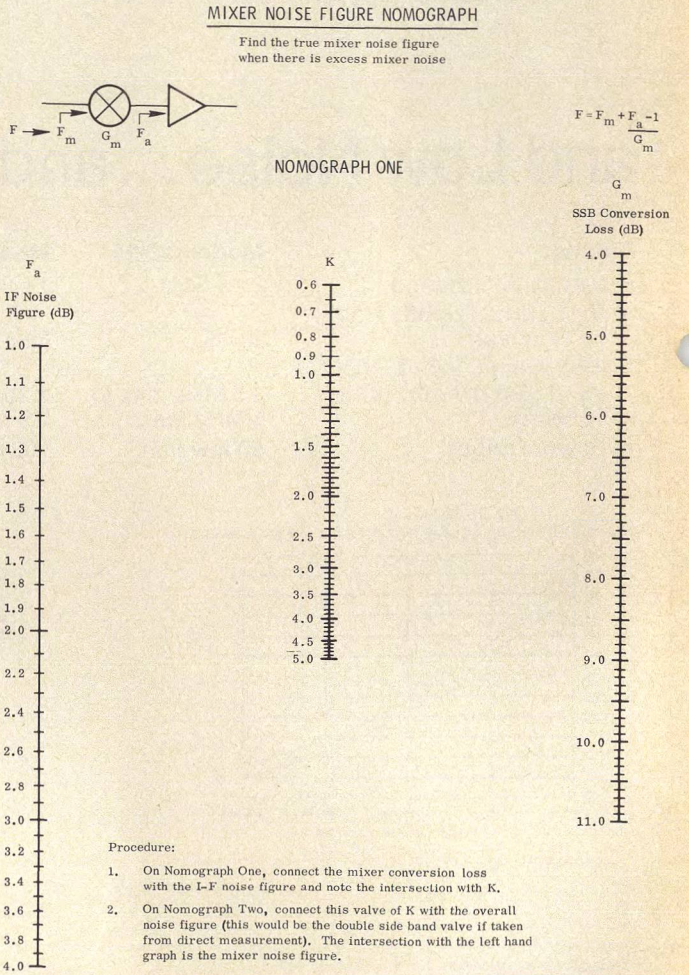
READER SERVICE NUMBER 48

MIXER MEASUREMENTS

Using this concept in conjunction with the P-factor method outlined above, the noise figure of a C-band mixer with a 30 MHz i-f was measured and plotted in Fig. 3. There was no excess mixer noise. Note that in general, the P-factor method tracked the conversion loss of the mixer much better than a commercial diode source noise figure meter. The one exception is at 7.5 GHz, which shows the effect of VSWR on the measurement.



5. The relationship between excess diode noise and excess mixer noise can be clearly seen. Avoid diodes with excess noise above 400 kHz.



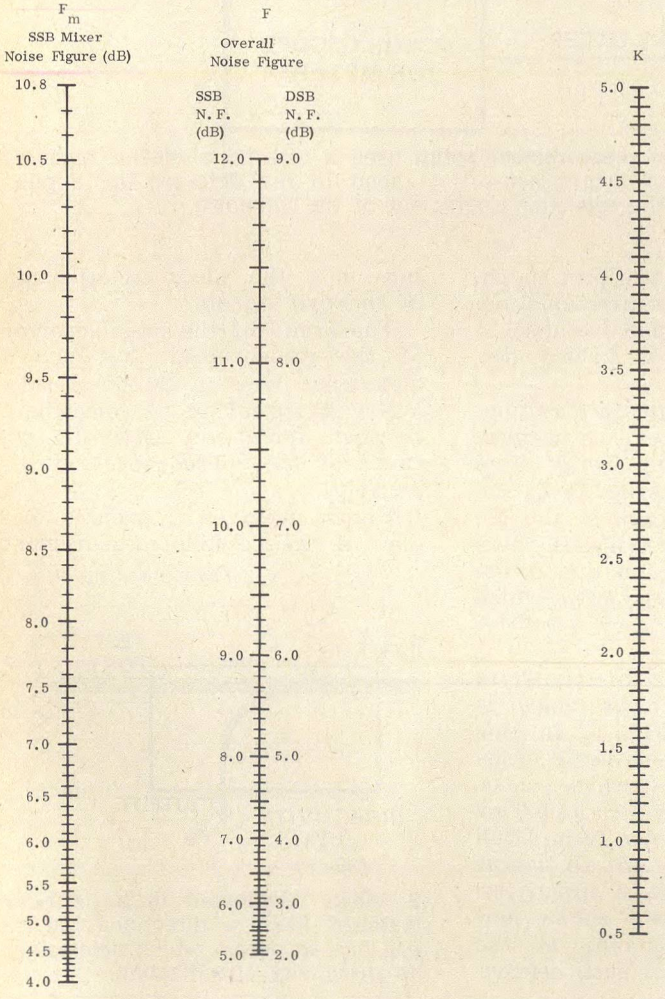
6. These nomographs can be used to calculate the noise figure of a mixer when excess noise is present.

Watch out for excess noise

If excess noise is present in the mixer, subtracting the i-f amplifier from the overall noise figure will give a false mixer noise figure. The error as a function of excess noise is shown in Fig. 4 for the case of an i-f amplifier with a 3.0 dB noise figure. If the mixer has 2 dB excess noise and the i-f noise figure is subtracted from the overall noise figure, the result would give an apparent mixer noise figure of 7.1 dB. The actual noise figure using Eqn. (5) is 8.0 dB. The error in this case is 0.9 dB, which is quite substantial.

Figure 5 further shows the effect of excess diode noise on the measured noise figure of a mixer. In this case, the diodes were each measured with 2.0 mA bias at 400 kHz and then installed in a mixer. The rf noise frequency is 300 MHz. The curve shows that 6 dB of excess diode noise (relative to 50-ohm resistor noise at room temperature), results in a mixer noise figure of 2 dB greater than its conversion loss. The important point here is that the excess noise will show up if either the input or output frequency is in the excess noise region. The problem will still crop up, for example, even if the rf input frequency is 8 GHz, if one is downconverting to a lower frequency where excess noise is a problem.

NOMOGRAPH TWO

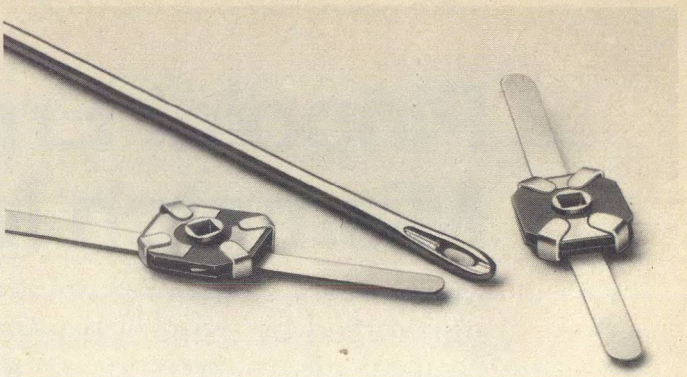


To obtain the true noise figure when excess noise may be a problem, use the nomographs shown in Fig. 6. The nomographs accommodate i-f amplifiers with noise figures ranging from 1.0 to 4.0 dB and can be used to calculate single sideband mixer noise figures ranging from 4.0 to 10.8 dB.

Measurements have shown that the single-tone intermodulation products will also affect noise figure measurements. The largest contributor is the $3f_L \pm f_R$ product which is typically only 13 dB (5%) below the desired output. Other single tone intermodulation signals on a typical double-balanced mixer will contribute an additional output of about 1.5%. Thus, the noise figure measurement will be approximately 6.5% or 0.3 dB lower than it should be. To correct, 0.3 dB must be added to the noise figure for $f_L < 1/3f$ maximum of the mixer. Above this frequency, the contribution of $3f_L \pm f_R$ falls off as the response of the mixer rolls off. ••

References

1. W. R. Bennett, "Methods of Solving Noise Problems," Proc. IRE. Vol. 44, pp. 609-638, (May 1956).
2. W. W. Mumford and E. H. Scheibe, "Noise Performance Factors in Communication Systems," Horizon House, Dedham, Mass., p. 65, (1968).
3. R. L. Sleven, "A Guide to Accurate Noise Measurements," Microwaves, p. 14, (July 1964).
4. W. P. Hooper, "Noise Temperature Summary," Frequency Technology, pp. 22-25, (March 1970).



THIN-TRIM CAPACITORS FOR HYBRIDS AND MIC'S

Series 9401 Thin-Trims are sub-miniature variable capacitors for applications where size and performance are critical. Featured are high Q's for low circuit losses, high capacity values for broadband applications and low profile for "gap trimming" in tiny MIC's. Body size .140" x .110" x .030" T. Available in 4 capacitance ranges from 0.2-.6 pf to 3.0-12.0 pf.

Johanson MANUFACTURING CORPORATION
Rockaway Valley Road
Boonton, N.J. 07005
(201) 334-2676 TWX 710-987-8367

READER SERVICE NUMBER 49

Pinpoint Errors In Mismatch Measurements

Many of the errors associated with directional devices can be minimized by using a bridge. Here's a discussion of bridge and coupler characteristics complete with usable error curves.

MODERN rf systems involve the interconnection of many individual units by transmission lines. The performance of these systems is often limited by the ability to control and accurately measure the mismatches that occur at every interconnection.

Measurements are at the heart of analytical system design and controlled production. To insure top performance from today's complex systems, measurements are called for that can be performed both fast and accurately. Recent developments in rf sweep generators meet these two challenges by providing swept data with accuracies exceeding the best point-by-point slotted line data of yesteryear.

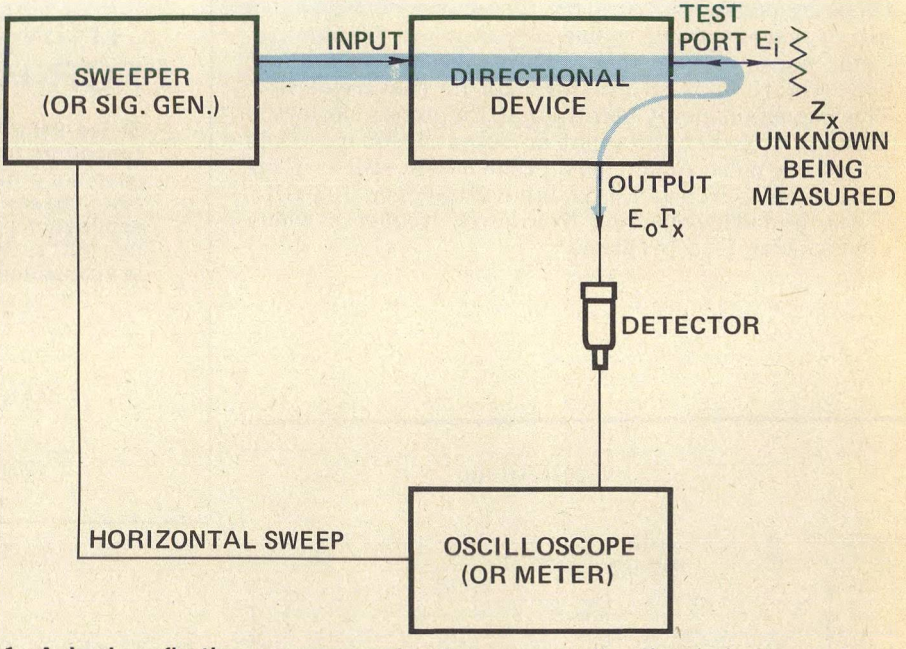
Major error reductions are also readily available by going to a simpler measurement configuration than the dual coupler system in common use: the reflection bridge. Bridges offer double-barreled accuracy gain, providing better directivity and at the same time, inherently padding down system errors.

Recent developments have carried bridge performance to higher frequencies and multibands giving improved coaxial measurements to 18 GHz.

To measure reflected signals, a directional device—bridge, coupler or hybrid network—must separate the reflected signal from the incident or test signal (Fig. 1). Thus, the accuracy of reflection measurements is limited by both the directional device and the system in which it is applied.

Directivity can cause an error

Two characteristics of the directional device influence its contribution to measurement accuracy: directivity and test port match. This is true of any directional device, be it a directional coupler, a reflection bridge or hybrid network.



1. A basic reflection measurement setup uses a directional device such as a bridge, coupler or hybrid network to send to the detector the applied signal modified by the reflection coefficient of the unknown.

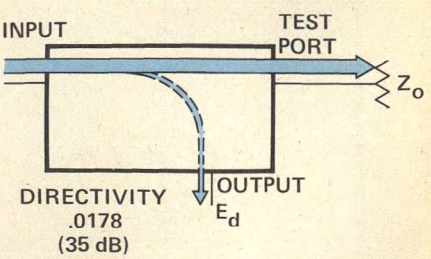
Figure 2 illustrates a directional device terminated in an ideal Z_o. Assume that all energy from the test port is absorbed in Z_o and none is reflected back to the device. Under these conditions, there is a small output and this is defined as the directivity (E_d), which is measured in dB below a full reflection.

The way that the directivity influences an actual measurement is demonstrated in Fig. 3. In this example, the unknown being measured is a 1.22 SWR, which can be stated as a 20 dB return loss. This reflection, 20 dB down from a full reflection, is only 15 dB larger than the signal due to directivity. The phaser diagram shows how directivity can combine at the measurement output port, depending upon the phase relationship of the two signals.

The limits of the possible error of the measurement are shown alongside. Thus, a 20 dB return loss will appear to be somewhere between 18.58 and 21.70 dB because of the consequences of directivity.

Figure 6 gives a graphic display of the possible measurement

(continued on p. 52)



2. When terminated in a perfectly matched load, a directional device still has an output which determines its directivity specification.

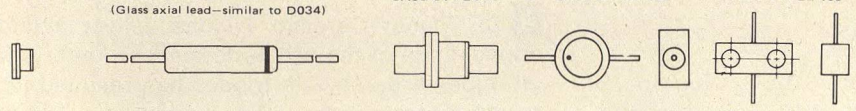
Duane E. Dunwoodie, Vice President and Technical Director; Wiltron Company, 930 East Meadow Drive, Palo Alto, CA 94303.

PIN & Limiting Diodes

☐ Delivery: Stock to 30 days
☐ RF Series Resistance = <1.0 Ohms
☐ 100 MHz to 18.0 GHz
☐ Applications Include: RF Switches, Current Controlled RF Resistors, Leveling, AGC Circuits, RF Duplexers, Phase Shifters, Attenuators, Limiters, and Modulators.

Diode Series	Available Total Capacitance Range (pF)	Series Resistance Range (Ohms)	Reverse Recovery Time (Range)	Lifetime (Range)	Voltage Breakdown (Range)
A5S100 and A5S120	.28 to .35	1.2 to 1.5	150 nSec.	100-200 nSec.	100-300
A5S110	.38 to .45	1.0 to 1.5	5-15 nSec.	5-20 nSec.	70-100
A5S300	.25 to .40	1.2 to 3.5	5 nSec. to 9.0 μSec.	100 nSec. to 2.0 μSec.	70-400
A5S150 Series	.12 to .15	1.0 to 2.3	30 to 150 nSec.	15 to 100 nSec.	60-70
A5S160 Series	Isolation: 20 to 22 dB Insertion Loss: 0.5 to 0.7 dB		Frequency: 100 MHz to 12.4 GHz Switching Speed: 10 to 100 nSec.		

CASE STYLE "G" CASE STYLE "H" (Glass axial lead—similar to D034) CASE STYLE "J" CASE STYLE 108 CASE STYLE 109



Aertech is a volume manufacturer of Step Recovery Diodes, PIN Diodes, Schottky Barrier Diodes (Hot Carrier), Tuning Varactors, Tunnel Diodes, Backward Diodes, and MOS Capacitors.

Aertech INDUSTRIES

825 STEWART DR. • SUNNYVALE • CALIF. 94086
(408) 732-0880 • TWX 910-339-9207

READER SERVICE NUMBER 52

errors due to a range of directivity specifications. From the above discussion, it is easy to see why this error approaches zero for large reflections and increases dramatically as smaller reflections are measured. Notice that attempting to measure a return loss equal to the directivity specification can result in a -6 dB to $+\infty$ dB error.

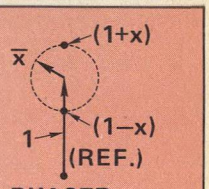
To minimize directivity errors, adopt this rule of thumb: Always use a coupler or bridge with 10 to 15 dB greater directivity than the return loss to be measured.

A convenient means of easily determining the dB interaction of one signal upon another is provided by Table 1. The first three columns provide easy conversion between inputs of SWR, reflection coefficient and return loss. The next four columns show the limit effect of a smaller, coherent signal upon a larger signal, which is taken as the reference.

The directivity error of Fig. 3 can be conveniently used to demonstrate the use of the chart. Given that the directivity of the coupler in use is 35 dB minimum and the observed measurement is near 20 dB, one can note that the directivity error may be only 15 dB below the measurement level. Relating this to the chart, x is 15

TABLE 1. RF MEASUREMENT CHART

Conversion tables for Return Loss, Reflection Coefficient, and SWR with tabular values for interactions of a small phaser x with a large phaser (unity reference) expressed in dB related to reference



PHASER INTERACTION

			RELATIVE TO UNITY REFERENCE			
SWR	REFLECTION COEFFICIENT	RETURN LOSS dB	x dB BELOW REFERENCE	1 + x dB	1 − x dB	1 ± x PEAK TO PEAK RIPPLE dB
17.3910	.8913	1	1	5.5350	−19.2715	24.8065
8.7242	.7943	2	2	5.0780	−13.7365	18.8145
5.8480	.7079	3	3	4.6495	−10.6907	15.3402
4.4194	.6310	4	4	4.2489	− 8.6585	12.9073
3.5698	.5623	5	5	3.8755	− 7.1773	11.0528
3.0095	.5012	6	6	3.5287	− 6.0412	9.5699
2.6146	.4467	7	7	3.2075	− 5.1405	8.3480
2.3229	.3981	8	8	2.9108	− 4.4096	7.3204
2.0999	.3548	9	9	2.6376	− 3.8063	6.4439
1.9250	.3162	10	10	2.3866	− 3.3018	5.6884
1.7849	.2818	11	11	2.1567	− 2.8756	5.0322
1.6709	.2512	12	12	1.9465	− 2.5126	4.4590
1.5769	.2239	13	13	1.7547	− 2.2013	3.9561
1.4985	.1995	14	14	1.5802	− 1.9331	3.5133
1.4326	.1778	15	15	1.4216	− 1.7007	3.1224
1.3767	.1585	16	16	1.2778	− 1.4988	2.7766
1.3290	.1413	17	17	1.1476	− 1.3227	2.4703
1.2880	.1259	18	18	1.0299	− 1.1687	2.1986
1.2528	.1122	19	19	.9237	− 1.0337	1.9574
1.2222	.1000	20	20	.8279	− .9151	1.7430
1.1957	.0891	21	21	.7416	− .8108	1.5524
1.1726	.0794	22	22	.6639	− .7189	1.3828
1.1524	.0708	23	23	.5941	− .6378	1.2319
1.1347	.0631	24	24	.5314	− .5661	1.0975
1.1192	.0562	25	25	.4752	− .5027	.9779
1.1055	.0501	26	26	.4248	− .4466	.8714
1.0935	.0447	27	27	.3796	− .3969	.7765
1.0829	.0398	28	28	.3391	− .3529	.6919
1.0736	.0355	29	29	.3028	− .3138	.6166
1.0653	.0316	30	30	.2704	− .2791	.5495

			RELATIVE TO UNITY REFERENCE			
SWR	REFLECTION COEFFICIENT	RETURN LOSS dB	x dB BELOW REFERENCE	1 + x dB	1 − x dB	1 ± x PEAK TO PEAK RIPPLE dB
1.0580	.0282	31	31	.2414	− .2483	.4897
1.0515	.0251	32	32	.2155	− .2210	.4365
1.0458	.0224	33	33	.1923	− .1967	.3890
1.0407	.0200	34	34	.1716	− .1751	.3467
1.0362	.0178	35	35	.1531	− .1558	.3090
1.0322	.0158	36	36	.1366	− .1388	.2753
1.0287	.0141	37	37	.1218	− .1236	.2454
1.0255	.0126	38	38	.1087	− .1100	.2187
1.0227	.0112	39	39	.0969	− .0980	.1949
1.0202	.0100	40	40	.0864	− .0873	.1737
1.0180	.0089	41	41	.0771	− .0778	.1548
1.0160	.0079	42	42	.0687	− .0693	.1380
1.0143	.0071	43	43	.0613	− .0617	.1230
1.0127	.0063	44	44	.0546	− .0550	.1096
1.0113	.0056	45	45	.0487	− .0490	.0977
1.0101	.0050	46	46	.0434	− .0436	.0871
1.0090	.0045	47	47	.0387	− .0389	.0776
1.0080	.0040	48	48	.0345	− .0346	.0692
1.0071	.0035	49	49	.0308	− .0309	.0616
1.0063	.0032	50	50	.0274	− .0275	.0549
1.0057	.0028	51	51	.0244	− .0245	.0490
1.0050	.0025	52	52	.0218	− .0218	.0436
1.0045	.0022	53	53	.0194	− .0195	.0389
1.0040	.0020	54	54	.0173	− .0173	.0347
1.0036	.0018	55	55	.0154	− .0155	.0309
1.0032	.0016	56	56	.0138	− .0138	.0275
1.0028	.0014	57	57	.0123	− .0123	.0245
1.0025	.0013	58	58	.0109	− .0109	.0219
1.0022	.0011	59	59	.0097	− .0098	.0195
1.0020	.0010	60	60	.0087	− .0087	.0174

dB below the reference phaser (the measurement in this case), and entering at 15 dB, one can read the resultant effect of 1 + x = 1.42 dB and 1 − x = −1.70 dB, or a 3.12 dB ripple.

Since return loss is being measured, the reference is negative and the loss deviation becomes −1.42 and +1.70 giving a possible range of 18.38 to 21.70 dB. The first three columns may be used to convert the dB limits into reflection coefficient or SWR by simple interpolation.

Be aware of test port match

The second source of measurement error in directional devices arises from their match at the measuring port (Fig. 4). Coupler specifications usually refer to this as main line SWR.

A full reflection returns all of an incident signal and gives a reference output. Some of this return signal will be re-reflected due to the test port mismatch. For the example shown in Fig. 4 (1.25 SWR at the test port), 11.2% of the test signal will be re-reflected, resulting in a signal 19 dB below complete reflection. This reflected signal, arriving again at the short, is fully reflected so that it arrives at the output differing by only 19 dB from the reference signal. The phaser diagram illustrates the effect for different phasing, showing that a variation from −0.92 dB to +1.03 dB is possible.

In a sweeping application, the phasing may indeed vary between the fully reflected and the re-reflected signal, causing a ripple pattern to be displayed. This ripple is dependent upon the width of the frequency sweep and the electrical distance from the short to the mismatch.

The error due to the test port match becomes much smaller as the unknown is better matched. This is demonstrated in Fig. 5, using the same test port match as in the prior example. In this case, measuring a 1.22 SWR unknown, the error contribution of the test port match is ±0.098 dB. Note that this is significantly smaller than the error due to directivity shown in Fig. 3.

Test port mismatch error has just the opposite effect from the expectations of many engineers. Note that in the preceding exam-

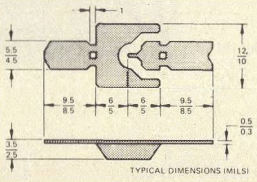
(continued on p. 55)

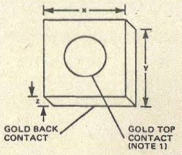
MOS Capacitors

- ☐ For Use Through 18 GHz
- ☐ Low Temperature Coefficient
- ☐ Less than 0.1 dB Loss at 10 GHz
- ☐ Silicon Dioxide Dielectric
- ☐ Standard Tolerance: ±20%
- ☐ Delivery: Stock to 30 days

Package Style	Available Capacitance Range (pF)	Voltage Breakdown (Volts)
Chip	1 to 5	100
Chip	1 to 10	100
Chip	10 to 40	100
Chip	40 to 200	100
Chip	200 to 900	50
Beam Lead	1 to 10	50

Chip Size		
X	Y	Z
.015	.015	.005
.020	.020	.005
.030	.030	.005
.060	.060	.005
.080	.080	.005
Beam Lead		



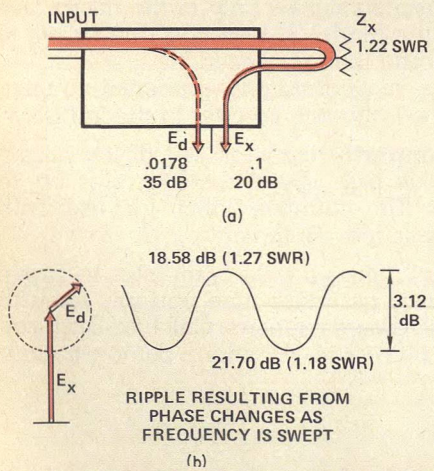


Aertech is a volume manufacturer of Step Recovery Diodes, PIN Diodes, Schottky Barrier Diodes (Hot Carrier), Tuning Varactors, Tunnel Diodes, Backward Diodes, and MOS Capacitors.

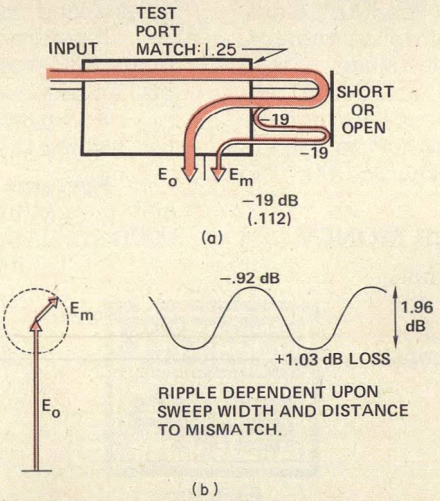
Aertech INDUSTRIES

825 STEWART DR. • SUNNYVALE • CALIF. 94086
(408) 732-0880 • TWX 910-339-9207

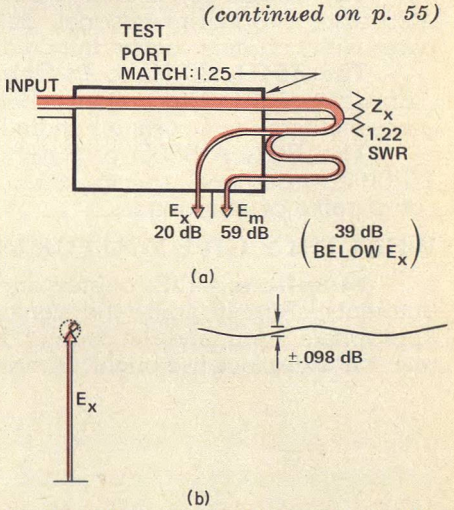
READER SERVICE NUMBER 53



3. A substantial error could result if a component's directivity approaches the return loss of the device under test. Here, a unit with 35 dB directivity measures a return loss of 20 dB with 3.1 dB uncertainty.



4. Test port mismatch can result in false reference outputs since they are taken with open or short circuits. As shown, for a test port match of 1.25:1, the error signal could be only 19 dB below the desired reference.



5. As the load becomes better matched, the error caused by test port mismatch becomes less serious. Here, the same coupler used in Fig. 5 measures a 1.22 SWR with a return loss uncertainty of ±0.098 dB as a result of test port mismatch.

ple a 1.22 SWR was measured accurately through a 1.25 SWR test port. This is possible because any internal reflection from the test port is included in the directivity specification.

Error limits for test port mismatch are graphically shown in Fig. 6 for different values of measured return loss. Note that the contribution is maximum at full reflection and diminishes rapidly for higher return losses. Since this error is maximum at full reflection, a calibration error will be introduced unless preventative steps are taken. These will be discussed in a later section.

In practice, one is typically concerned only with the total possible error at the poorest indicated return loss or at the specification limit. The general error limit curves presented in Fig. 6 enable one to draw in the error related to a specific coupler or bridge, or compare two devices for measurement performance. A very good approximation to the total possible error can be constructed by simply summing the two limits on the curve.

It should be noted that in the previous examples the measured reflection and error signals are assumed to be uniform with changing frequency. Although this would seldom be the case in an actual measurement, it presents the clearest picture of the effect of the error. The same technique for determining error limits can also be applied in the more typical case.

Bridges feature high directivity

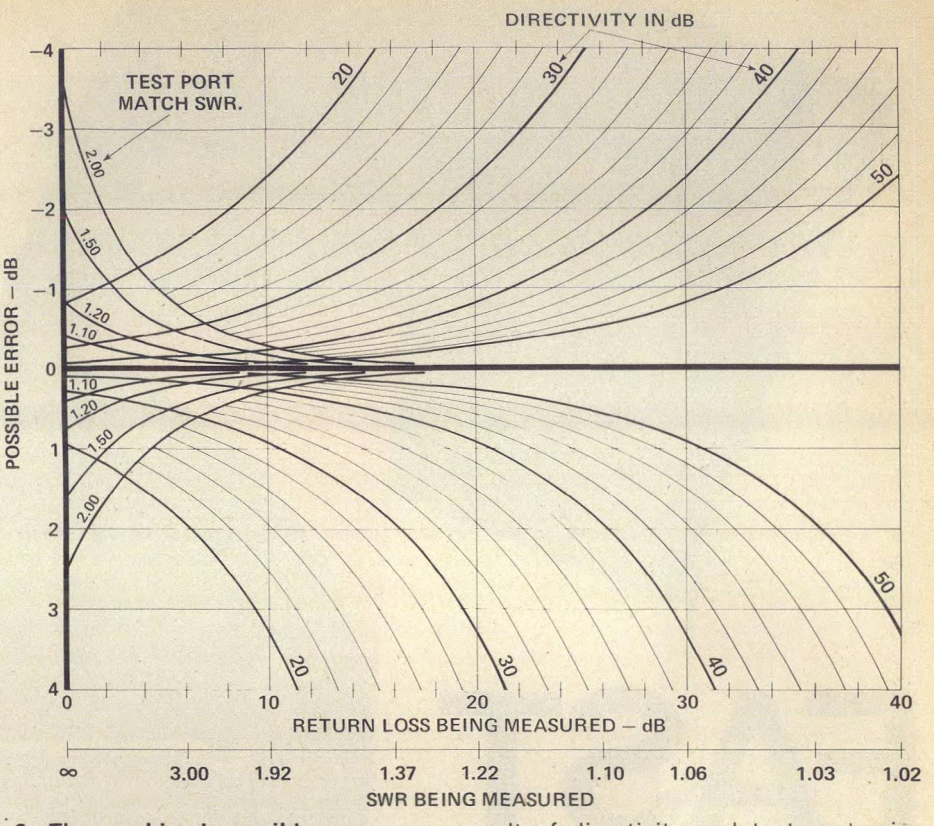
The reflection bridge is an important device that warrants better understanding by microwave and communications engineers. Bridges are available as catalog components with directivities exceeding coaxial couplers over the entire frequency range to 18 GHz.

A typical modern bridge is shown in Fig. 7. Covering a frequency range of 7 to 12.4 GHz, this example has a directivity of 40 dB and a test port match of 1.25. The high directivity of a bridge can give it an advantage in accuracy over couplers designed for measurement applications, as shown by the X-band comparison in Fig. 8.

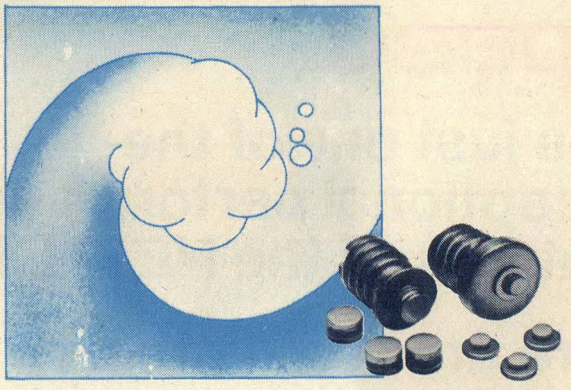
Older bridges were four-element circuits that were limited in frequency response and required calibrated mismatches to determine a limit value for Z_x.

The modern bridge is a six-element circuit with an internal reference termination (Fig. 7). A

(continued on p. 57)



6. The combined possible error as a result of directivity and test port mismatch can be predicted from this chart. Simply sum the limits from both sets of curves.



Introducing four new IMPATT diodes. With higher power, higher frequencies and lower prices.

Hughes now has a complete line of low-cost millimeter-wave IMPATT diodes providing up to 50 mW at 100 GHz or 300 mW at 40 GHz. And they all feature the longest life and greatest reliability available in any commercial diodes.

For operation below 40 GHz, our diodes are packaged with a 50-mil diameter ceramic ring. For applications above 40 GHz, they are packaged with a 30-mil diameter quartz ring—both developed by Hughes. And you have a choice of either unmounted or stud-mounted models.

For more information, call or write the IMPATT diode capital of the world: Hughes Electron Dynamics Division, 3100 West Lomita Boulevard, Torrance, CA 90509. (213) 534-2121, extension 215.

HUGHES
HUGHES AIRCRAFT COMPANY
ELECTRON DYNAMICS DIVISION

Making waves in millimeter-wave technology.

READER SERVICE NUMBER 55

special property of this bridge circuit is that the output voltage can be expressed as:

$$E_{det} = \frac{E}{4}\left(\frac{Z_x - R_o}{Z_x + R_o}\right) \qquad (1)$$

which is exactly proportional to the reflection coefficient of the unknown impedance[1]. This output signal is balanced off ground and is converted to a single-ended output by a balanced to unbalanced internal transforming network.

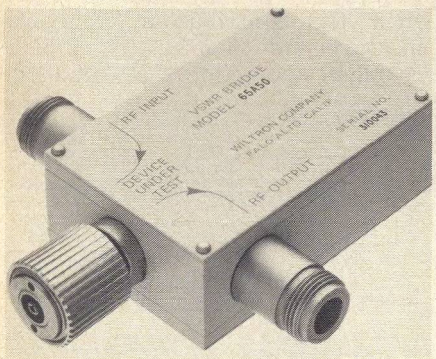
Equation 1 shows that when Z_x equals zero and infinity, the output is $-E/4$ and $+E/4$, giving the expected phase reversal for short and open reflections. The equal magnitudes show that the bridge is properly matched with respect to R_o (the transmission line impedance) so that an open or short termination causes the same output. Since this output is one-fourth the maximum available, the ideal insertion loss is 12 dB: 6 dB from the source to the test port and another 6 dB from the test port to the detector port. Practical realizations of the bridge circuit will have losses slightly higher than 6 dB when operated at high frequencies.

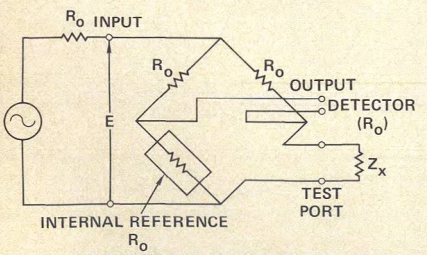
The 12 dB insertion loss of the bridge is analogous to the coupling factor of a coupler. A 10 dB coupler would appear to have a 2 dB sensitivity advantage over the bridge, but it will be shown that the additional bridge loss can be beneficial.

When Z_x is terminated in R_o the input signal is split into two arms, each equal to 2 R_o. Thus, the impedance presented to the generator is R_o, and the drop across the test port and the reference are equal, so that no output results. The input and the output are isolated, giving the bridge directional characteristics.

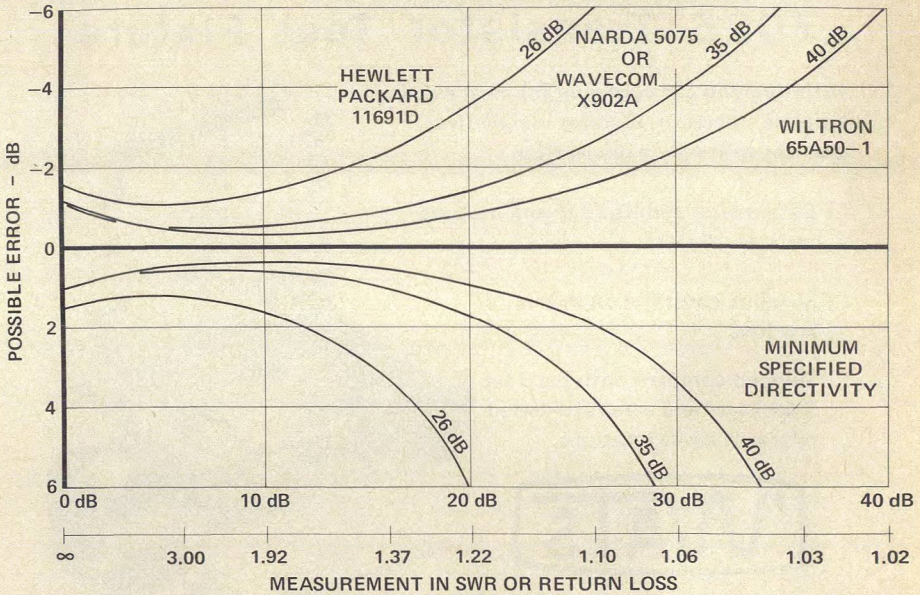
Similarly, one can see that the impedance looking in any port is R_o when the other ports are terminated, and that the port is iso-

(continued on next page)

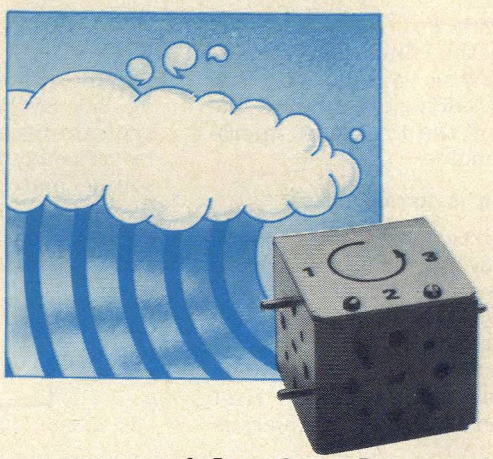




7. Reflection bridges are three-port devices incorporating a six-element circuit. This particular bridge requires an external detector, but others are available with an internal detector and increased directivity.



8. The reflection bridge's high directivity can reduce one source of potential measurement error. Comparisons are with popular directional couplers on the basis of minimum specified directivity.



This waveguide circulator will fit your mm-waves to a "T"

Our three-port, T-junction circulators are designed for mm-wave frequencies from 26.5 to 110 GHz in six waveguide bands. They feature high isolation, low insertion loss and low VSWR over a broad bandwidth. That makes them ideal for use in negative resistance amplifiers and phase modulators.

Our unique T-junction accommodates typical waveguide routing patterns better than commonly used Y-junction devices and eliminates the sprawl effect they can cause.

Find out more about the world's only practical T-junction mm-waveguide circulators. Call or write: Hughes Electron Dynamics Division, 3100 West Lomita Boulevard, Torrance, California 90509. (213) 534-2121, extension 215.

HUGHES
HUGHES AIRCRAFT COMPANY
ELECTRON DYNAMICS DIVISION

Making waves in millimeter-wave technology.

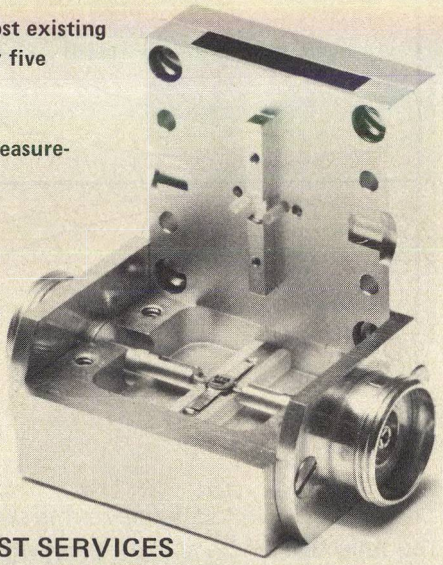
READER SERVICE NUMBER 57

Quick Change Artist

7025 Transistor Test Fixture

A fixture you can configure for most existing stripline transistor packages in only five minutes with only a screwdriver.

- ☐ **S-Parameter and Noise Figure measurement to 10 GHz.**
- ☐ **Slab-line construction means low loss.**
- ☐ **Shipped complete with parts for 5 packages and computer-tested reference plane locations.**



WATS

WESTERN AUTOMATIC TEST SERVICES
470 Persian Drive Sunnyvale, CA. 94086 ☐ (408) 734-0941

READER SERVICE NUMBER 58

(continued from p. 57)

lated from the diametric bridge element. Having a characteristic R_o match at each port enables the application of the bridge at microwave frequencies.

Source match is important

When a directional device is applied in a measurement system, a third source of error arises from the interaction between reflections from the source match (typically the sweep generator output match) and the unknown Z_x. Consider first the situation when a coupler is used (Fig. 9A).

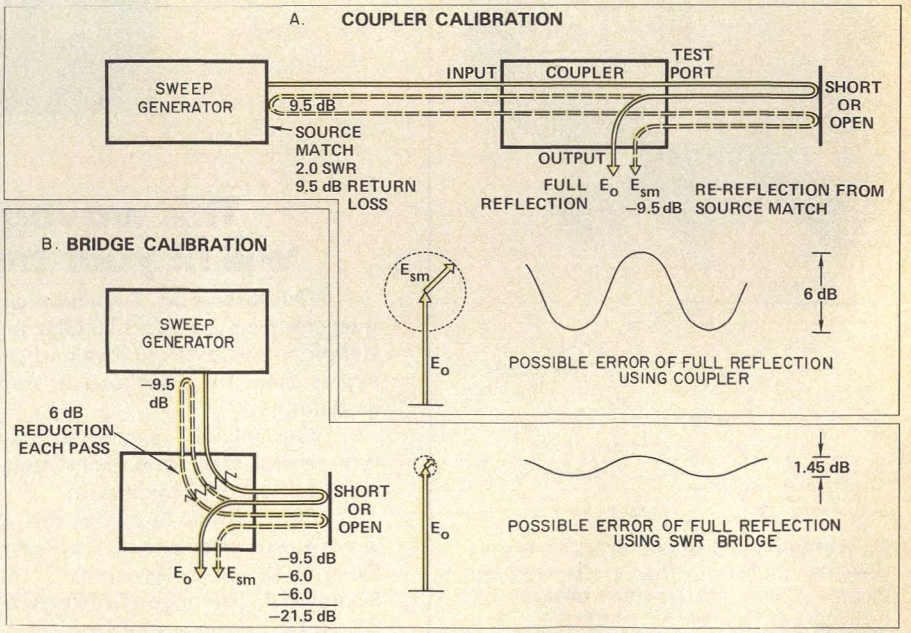
The coupler has a main arm loss that is low (0.045 dB loss for 20 dB coupling), which makes it capable of handling very high power levels. However, for measurement applications, this low-loss path has a distinct disadvantage. When a full reflection is applied to establish the reference output, it travels unattenuated back to the signal source and becomes re-reflected against the source match. Unattenuated, the reflection passes through the coupler a second time, and is re-reflected from the calibrating short or open and summed with the full reflection in the detector.

This path is shown in Fig. 9A for the example of a source match of 2.0 SWR, which represents a typical sweeper in X-band. This re-reflected error signal from the source match is down only 9.5 dB when using a coupler. There is, of course, a series of these reflections each delivering an output 9.5 dB reduced from the previous reflection output. For simplicity, only the first and largest error is shown in Fig. 9A which alone can cause a 6 dB variation in the readout.

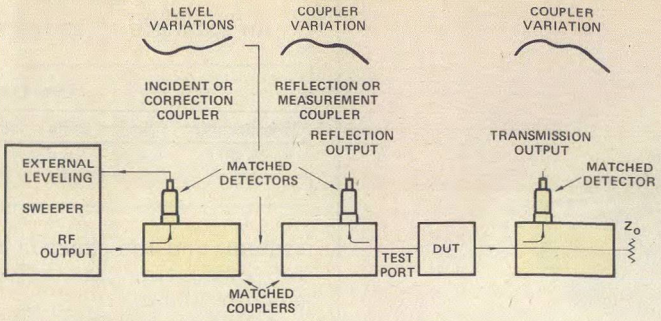
In comparison, the reflection bridge used in the same system has only a 1.45 dB error possibility. The bridge has a 6 dB insertion loss between the input and the test port, which means that the re-reflected signal would be attenuated by an additional 12 dB (6 dB twice). The typical bridge always has this 12 dB advantage over the coupler.

Coupler performance can be improved by adding a 6 dB pad on its input connector, but not without introducing the connector mismatch of the added pad. Also, note that the coupler loss, which was 10 dB before, has now effectively grown to 16 dB. An isolator could be used instead of a pad to gain further improved performance; however, this is an expensive and frequency-limiting solution.

If added cost is permitted, then by adding a second coupler and detector, the effective source match can be improved and relocated closer to the measurement coupler (Fig. 10). This essentially creates an external leveling loop. The effective source match is then determined by the correction coupler. The frequency sensitivity of the correction coupler (and the leveling detector) affects the measurement calibration in an opposite sense than the contribution from the measurement coupler. If similar couplers are used, the frequency



9. Used alone, a coupler passes reflections unattenuated, which can result in a large error during calibration. Bridges pad these reflections by 12 dB.



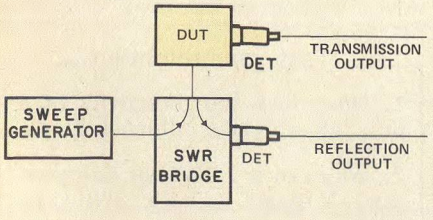
10. By adding a second coupler and detector, the effective source match can be improved. A third coupler permits simultaneous transmission measurements. All three couplers and detectors must be matched.

sensitivity variation will be significantly reduced. However, a second detector characteristic now must be considered making it necessary to use a matched pair of detectors.

To take full advantage of this correction scheme, a dual coupler is generally used. Since one coupler largely cancels the frequency variation of the other, it's not surprising that the manufacturer usually optimizes the product for best directivity and tolerates a greater variation with frequency. A ±1.2 dB or 2.4 dB permitted variation over an octave band is common.

A logarithmic display may be used with a reference input connected to the detector of the first coupler instead of being returned to the sweeper for external leveling. Such a system functions in the same manner as the leveling system described and has the same problems and solutions.

The level variation with frequency imposed on the device under test is largely canceled for reflection measurements, but creates a large variation for simultaneous transmission measurements. A third coupler and a third matched detector are required to similarly cancel this variation from the transmission output, as shown in Fig. 10. Not only is this an extra expense for hardware and matching service, but the coupling factor of the third coupler reduces the measurement range on transmission.



11. With a bridge, simultaneous transmission and reflection measurements can be made by adding a second detector.

Compare the complexity of the coupler measurement of reflection and transmission with the simple configuration using the bridge as shown in Fig. 11. The bridge needs only one detector for transmission and one for reflection. Since no corrective loops are required, the detectors do not have to be matched.

Steer clear of adapters

When an adapter is used on the test port to adapt to a different sex or connector type, the measurement accuracy is reduced in two ways. The effective directivity of

(continued on next page)

No need to look further for a reliable R-F power source. MCL has one.



And here's what we built into it:

- solid state circuitry
- short and open circuit protection
- frequency stability ± .001%
- external pulse or AM modulation
- internal square wave modulation
- low tube cost/operating hour
- qualified to MIL-STD-461 and 810

It has six different plug-in heads

Model	Freq. (MHz)	Pwr. (MIN)
6047	10-50	65
6048	50-200	65
6049	200-500	65
6050	500-1000	65
6051	1000-2000	40
6052	2000-2500	25

You have now ended your search for a stable, reliable 65 watt oscillator. Just call or write for detailed engineering data. Or ask for a demonstration

MCL, INC.,
10 North Beach Avenue,
LaGrange, Illinois, 60525.
(312) 354-4350

MCL INC

Now on GSA contract GSOOS-27086 See us in EEM—Vol. 1 pp. 284-291

READER SERVICE NUMBER 59



READER SERVICE NUMBER 60

the measuring device is reduced due to reflection from the adapter, and the test port match is degraded as well.

Table 2 shows the measurement limits for a 20 dB return loss when measured with and without the adapter. Note that a 2.8 dB error limit has grown to 8 dB as a result of adding a 1.05 SWR adapter! When an adapter is added to the device under test, the uncertainty that the adapter alone contributes to the DUT is shown in Fig. 12. This uncertainty must be added to that of the measuring system, and the chart is convenient for evaluating the effect of the adapter alone.

Table 2.
An example of adapter error

Measurement	Error Limits: Bridge Only	Error Limits: Adapter Only
20 dB	+1.3/−1.5 dB Δ = 2.8 dB	+3.1/−4.9 dB Δ = 8.0 dB

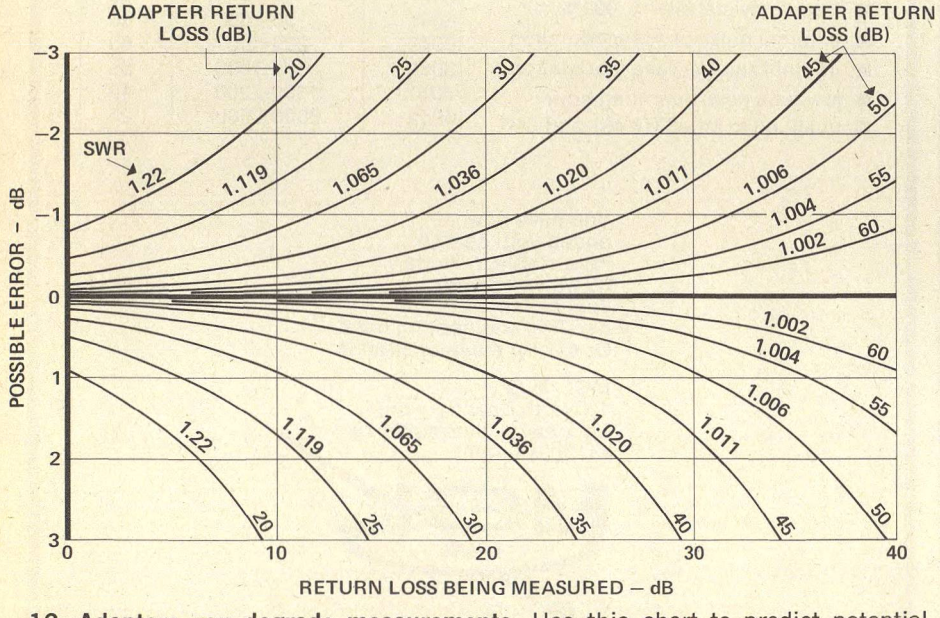
Adapters added elsewhere in the measurement setup have less error contribution and generally make the system residuals larger and more complex.

In conclusion, specific ways to reduce measurement errors are suggested by the source of the errors. Many coupler-related errors can be minimized by using a reflection bridge. In addition to reducing directivity errors, bridges reduce the signal source match error and simplify the measurement setup.

The use of adapters should be minimized, especially on the test port. Never apply a pad on the test port of a bridge unless you want to measure the match of the pad as well.

Calibration uncertainty in a coaxial system can be reduced by establishing a full reflection reference with both an open and a short. The average between the two responses is the best reference.

The sweeper exerts an important influence to measurement accuracy. This discussion has assumed a pure test signal, but be aware that harmonics can introduce severe errors. Be sure to use a sweeper with the best harmonic specifications and a specified output match[2]. ••



12. Adapters can degrade measurements. Use this chart to predict potential error limits based on the specified SWR of the connector adapter.

References

1. W. W. Oldfield, "Present-Day Simplicity in Broadband SWR Measurements," Wiltron Technical Review, Vol. 1, No. 1, (revised 1973).
2. D. E. Dunwoodie and Dr. P. D. Lacy, "Why Tolerate Unnecessary Measurement Errors." Wiltron Technical Review, Vol. 3, No. 1, (1975).

Acknowledgement

Many contributions that helped establish the character of this presentation were made by Dr. Peter Lacy and William Oldfield of the Wiltron Development Laboratory.

Test your retention

1. How does the directivity of a directional device influence its accuracy?
2. Why can a 1.22 SWR be measured through a 1.25 SWR test port?
3. How can the effective source match be improved in a measuring system using a coupler?

Calculate Transistor Efficiency Automatically

Save time and insure accuracy in measuring efficiency of discrete matched transistors or multi-stage amplifiers with an efficiency calculator. A digital voltmeter is used for the display.

THE three parameters which are of the utmost importance when testing any single-stage power amplifier are power output (P_{out}), power reflected (P_{ref}) and collector efficiency (η_c). P_{out} and P_{ref} are easily read from power meters, but the collector efficiency must be obtained from a calculation of the values of P_{out} collector dc supply voltage, V_{cc} and collector current, I_c, using the expression:

$$\eta_c = \frac{P_{out}}{(V_{cc})(I_c)} \times (100)\% \qquad (1)$$

This efficiency measurement can be automated by building an inexpensive efficiency calculator. It consists of a few linear integrated circuits, variable resistors, switches, a digital panel voltmeter and a low-cost current dc power supply. The total cost of parts is approximately $200. It's real value, however, lies in the time saved in performing efficiency measurements particularly for a production line setup, where a large number of units have to be tested in rapid succession. The minutes saved in each calculation amounts to hours at the end of a week.

The efficiency calculator also is very useful for testing new designed circuits, which must be trimmed for optimization of power reflection, power output flatness and efficiency. These three parameters can be observed instantaneously while frequency sweeping the device. Figure 1(a) shows the efficiency calculator in a typical rf test setup.

The efficiency calculator, Fig. 1(b), uses dc inputs to make the evaluation of efficiency and therefore can be adapted to any discrete transistor, internally-matched device or multi-stage amplifier test-setup. The only differences may be a few additional dc hook-up leads.

In the case of a MIC power amplifier which uses a chain of series and paralled devices, the main concern is overall efficiency instead of collector efficiency. In this case, the power input and power reflected must be included in the efficiency equation using:

$$\frac{\text{Overall}}{\text{Efficiency}} = \frac{\text{Power Output}}{V_{cc}\, I_c + P_{in} - P_{ref}} \qquad (2)$$

Since the power input and power reflected in a MIC amplifier having greater than 20 dB gain is 100 times less than the output power, the error in using Eqn. (1) instead of Eqn. (2) is less than 1%.

Ray Gutierrez, formerly Project Leader, Applications Engineering, Microwave Semiconductor Corporation, Somerset, NJ. Now Engineering Manager, Optimax/Subsidiary of Alpha Industries, Colmar, PA 18915.

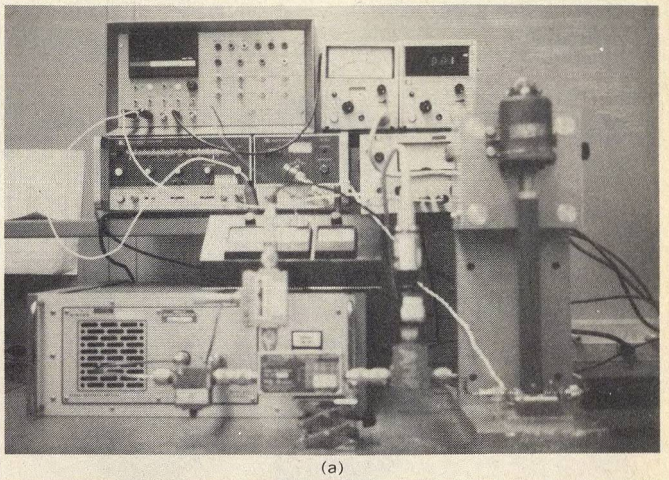
How the efficiency calculator works

The efficiency calculator, as shown in Fig. 2, consists of five main parts:

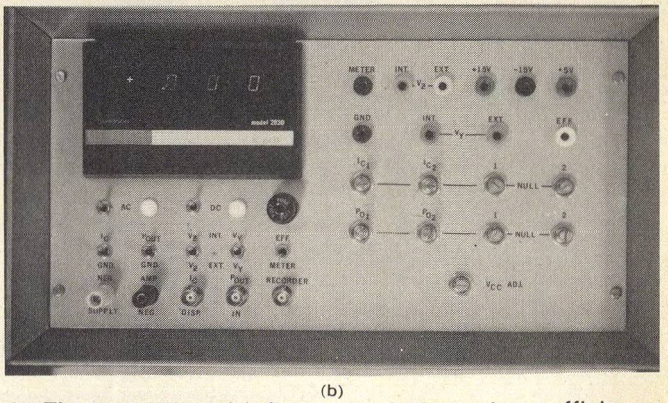
- a current sampling and scaling section
- a power sampling and scaling section
- a divider section
- an efficiency display section
- a power supply section

The current is sampled by a current sensing resistor in series with the dc negative supply terminal and the test amplifier ground. The resistor value must be such that the voltage drop V_I across it is around

(continued on pg. 65)



(a)



(b)

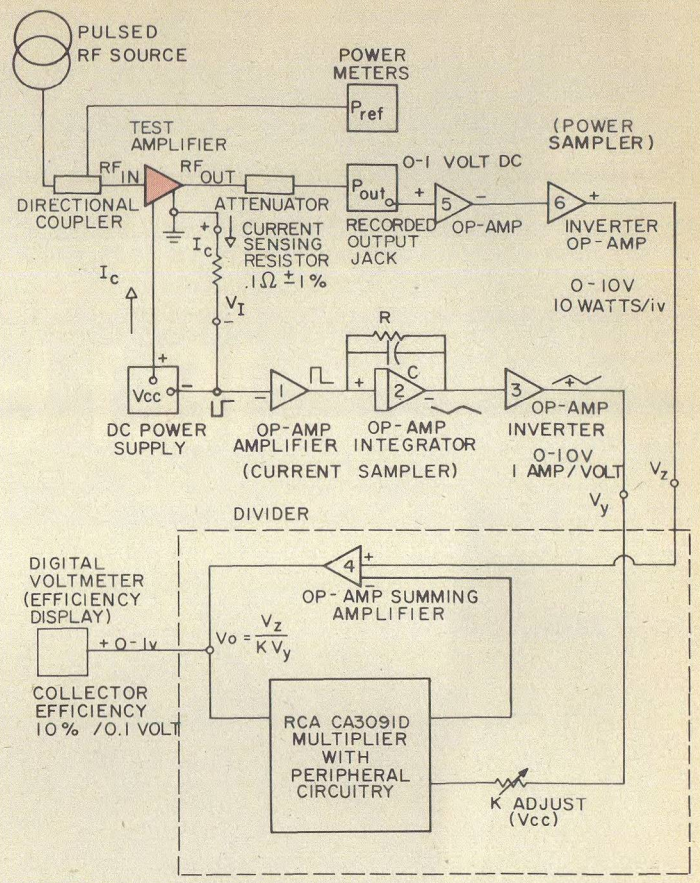
1. **The test set up** (a) for measuring transistor efficiency can be automated by introducing the automatic efficiency calculator (b). Efficiency is read out directly on a digital voltmeter.

CALCULATE TRANSISTOR EFFICIENCY AUTOMATICALLY

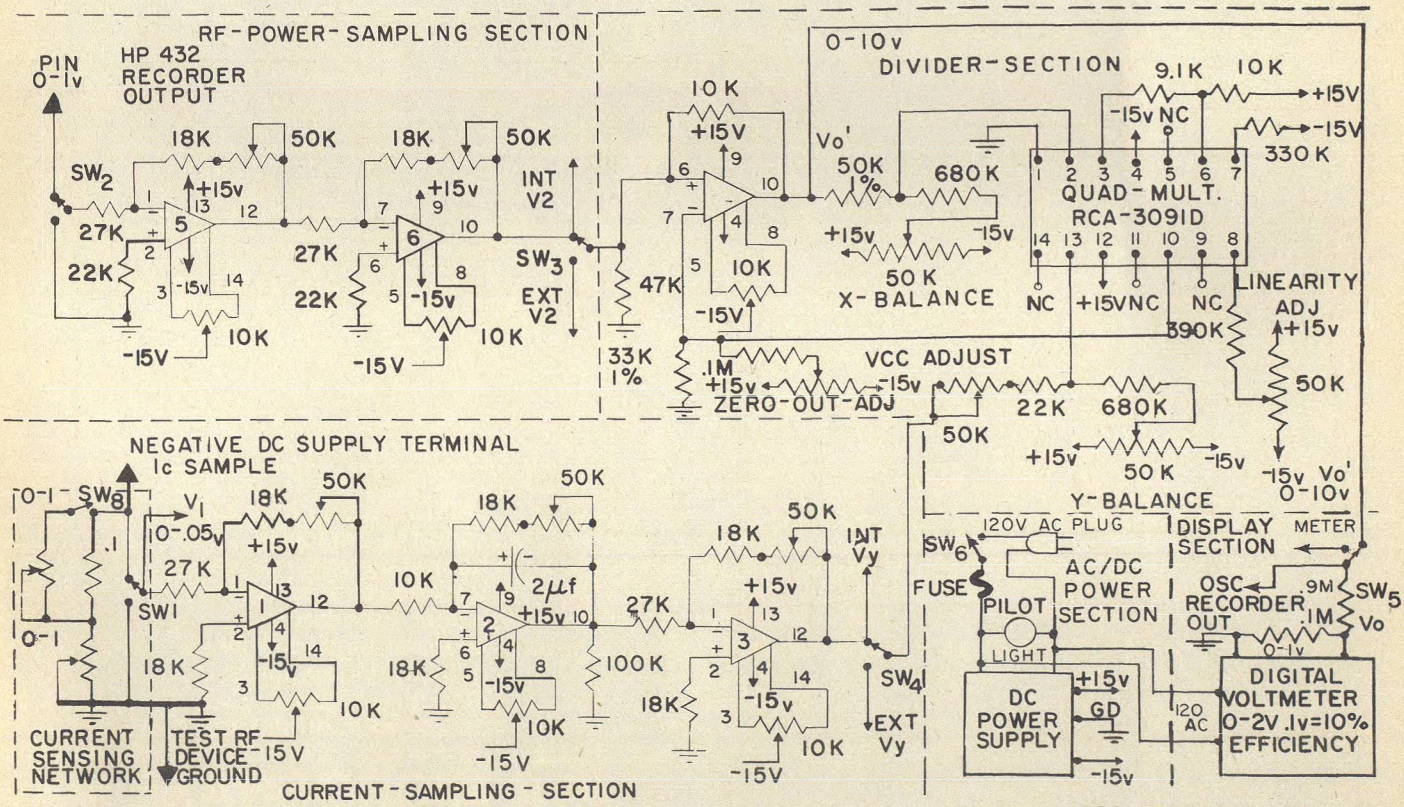
50 millivolts so as not to alter the supply voltage to the transistor or amplifier under test when the current varies. The voltage V_I is then amplified by an operational amplifier (1). An integrator (2) then integrates the pulse signals of up to 10 μsec, 10% duty and sets them to some negative dc levels. Or it may just amplify the signal in case of long pulse or cw operation. An operational amplifier (3) finally amplifies and inverts the signals to a value between 0 to 10 volts. The scaling operation is accomplished by control of the gain of amplifiers 1 and 3 so that the current can be scaled to a voltage at the output of amplifier (3). This signal is then used for the V_y input to the divider; i.e., 1 amp/volt, 0.1 amp/volt; etc. In the power sampling and scaling section, the power is sampled from the rear jack in the Hewlett-Packard, model 432 power meter (recorder output), shown in Fig. 2. The sample is a dc signal proportional to the output power from 0-1 volt. It is then fed into operational amplifiers (5) and (6) which sets the dc voltage signal to a level between 0-10 volts according to the desired scaling factor, such as 10 watts/volt; 1 watt/volt; etc. This signal can then be used as the V_z input to the divider.

In case the power meter used is other than the model mentioned, the power can be sampled by using a directional coupler with a crystal detector positioned between the output of the transistor or amplifier under test and the power meter. This method is also useful if it is desired to sweep the frequency at a fast rate since the recorder output of the HP model 432 does not respond instantaneously.

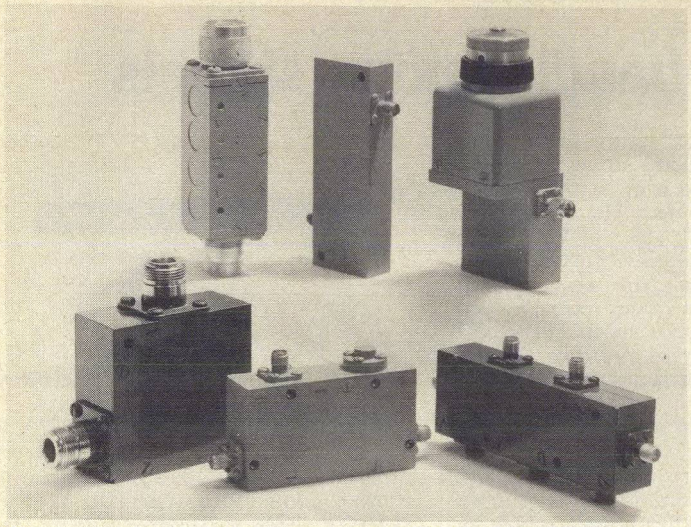
(continued on p. 67)



2. **Digital efficiency calculator** consists of a current sampling and scaling section, power sampling and scaling section, a divider section, a power supply section and the digital display.



3. **Schematic diagram** shows polarities, circuit element values and types of operational amplifiers required. Amplifiers (1) through (6) are RCA CA3747E's. V'_o is the divider output voltage (0-10 V) and V_o is the display put (0-1 V)



OTHER TYPES AVAILABLE WITH EITHER WAVEGUIDE OR COAX INTERFACES.



- ☐ Cavity type bandpass filters
- ☐ Band-rejection filters
- ☐ Tunable filters (single knob or individually tuned sections)
- ☐ Coaxial resonator devices
- ☐ Integral filter - circulator assemblies
- ☐ Diplexers and multiplexers
- ☐ Phase shifters

UTE MICROWAVE, INC.

3500 Sunset Ave., Asbury Park, N.J. 07712
(201) 922-1009 • Telex 132-461

One of a kind...or many of a kind

UTE Microwave

sets high standards in CIRCULATORS · ISOLATORS AND FILTERS

Octave Band — Circulator and Isolator configurations both have 20dB isolation, 0.4dB loss and 1.25 max VSWR. Size for 4-8 GHz is 1¼ sq x 11/16. SMA connectors.

4 Port Circulator — Isolation 20dB per junction, Insertion loss 0.3dB max per junction pass VSWR 1.25 max. H and Pi configurations.

Hi Ratio Isolators — Feature multiples of 20dB isolation. Popular units have 40 or 60dB. Typical X-band unit is 2¼ x ⅞ x ⅝ with SMA connectors. Loss is less than 0.9dB for 3 junctions.

Isolator-Adaptors — Transition from most common waveguide sizes from S thru Ku bands with 20dB isolation, 0.5dB loss and 1.25 max VSWR. SMA coax ports standard.

Interdigital Filters — Standard bandwidths of 7½, 15 & 25% available in S thru X bands with 2 standard selectivity options. VSWR is typically less than 1.25 and loss as low as 0.3dB. C band units 1½" x 2¾" x ¾", SMA connectors.

READER SERVICE NUMBER 67

CALCULATE TRANSISTOR EFFICIENCY AUTOMATICALLY

The divider section uses an RCA CA3091D quad-multiplier with a summing operational amplifier. It performs the following function with inputs V_z and V_y.

$$V_o' = \frac{V_z}{K V_y} \qquad (3)$$

where V'_o is the divider output signal from 0-10 volt.

Figure 3 is a detailed wiring diagram of the efficiency calculator. Note the distinction and locations of V_o and V_o'. Refer to RCA Solid-State Databook series SSD-201A for operation, alignment and theory of the quad-multiplier.

Since the efficiency equation (Eqn. 1) has the same form:

$$\frac{\text{Collector}}{\text{Efficiency}} = \frac{P_{out}}{V_{cc}\, I_c}$$

The following relationships can then be established in the units indicated.

$P_{out} = V_z$ # watts/1 volt
$I_c = V_y$ # amps/1 volt
$V_{cc} = K$ # volts/# ohms
efficiency $= V_o$ 10%/0.1 volt (after the 10:1 voltage divider)

V_{cc} is a constant (K) which controls the divider gain. It is introduced by a variable resistor in series with the V_y input. In measuring an "Ampac" matched transistor, for example, the variable resistor is adjusted since the bias for a gain of 0.28 voltage, since the bias voltage V_{cc} is 28 V.

The calculator is quite useful in an rf production test setup and calibrated within five minutes to read true at some value within the frequency band. Accuracy is within ±2% of the value calculated from the meter readings.

The use of the calculator in the setup shown in Fig. 2 increased the production testing time by 25% and provided the operator with another important parameter for judging device performance at any given time. ••

Test your retention

1. How is the scaling operation accomplished so that the current is scaled to voltage at output of op-amp No. 3?
2. If the power meter used for sampling doesn't have a rear jack or needs to be swept rapidly, what can be done?
3. What does the quad-multiplier do in conjunction with a summing operational amplifier?

If there is a renewal card on page 16A, it means

YOU MUST RENEW NOW

or your subscription will

EXPIRE.

2 Hz to 18 GHz counter handles noisy signals

By means of a frequency-locked automatic computing transfer oscillator (FLACTO), additional flexibility has been added to today's modern frequency counters. Systron-Donner's model 6054A- an 11-digit readout microwave counter, is capable of accepting a wide variety of complex signals—from pure cw to those having large amounts of noise. This is accomplished by selecting either a narrowband, high resolution mode or a wideband mode which measures signals with high fm deviations.

This high speed, highly sensitive counter spans the entire 0.02 to 18 GHz frequency range without any need for range selection. Only two connectors are used—the BNC input accepts signals from 20 Hz to 20 MHz while the type N input connector handles signals from 20 MHz to 18 GHz. Input sensitivity covers a dynamic range of up to 45 dB from −15 dBm (up to 12 GHz) and −7 dBm (above 12 GHz) to +30 dBm maximum input level.

A visual alarm advises the operator of pending overloads which may damage the counter. As long as the input remains below +20 dBm, a green annunciator light indicates a normal lock condition. Should the input level exceed +20 dBm, the green light will flash alternately with a red warning light and the least significant digit of the readout will also start flashing. Measurements can still be made and displayed by the counter right up to its maximum input level of 1 W.

The FLACTO feature makes possible two very useful modes of operation—narrow and wide, both of which are push-button selectable. The narrow mode is suitable for making high speed, high resolution measurements (1 Hz resolution in one second) such as emitted from phase-locked sources, microwave synthesizers and multiplied crystal source. The fm tolerance of the narrow mode is 10 MHz p-p, regardless of modulation rate.

The wide mode of operation allows tracking and measuring signals with high fm deviation limits. Thus, signals with considerable power supply noise or that drift rapidly are able to be measured accurately. The peak-to-peak deviation this wide mode can tolerate depends on the fm modulation rate. For example, in a typical voice communication signal with f_o = 18 GHz, deviations in the order of 500 MHz p-p can be handled. At power line rates, the maximum deviation that can be tolerated is about 3.5 GHz p-p.

The use of a sequencing circuit, automatic amplitude discriminator and an internal rfi-shielder design insure a correct readout. If the input locking-circuit is not activated, the counter will yield no display.

The standard crystal oscillator reference used in the 6054A provides ±1 part in 10^6/year stability. Three higher stability oscillators are optionally available (at extra cost), one with an aging rate of ±5 parts in 10^{10}/24 hours.



Systron-Donner's 18 GHz microwave counter provides an 11-digit LED display. Size is 3.5 in. × 16.75 in. × 17.5 in. (8.9 × 42.5 × 44.4 cm) and weight is 30 lbs (13.6 kg). Power consumption is 106 W from 115 or 230 V service (48-62 Hz) and the unit operates over a 0 to 50°C temperature range.

Another option that's available is a frequency offset such that any of four specified offset frequencies can be added or subtracted from the display. This is useful in receiver applications which require directly reading a received frequency.

Although designed for bench use, the front-panel controls of the 6054A may be programmed remotely in single-line format. The 11-digit readout, decimal point, annunciator and lock lamp are available on the rear panel in parallel 1-2-4-8 format. P&A: $5,900; 90 days. **Systron-Donner Corp., 10 Systron Drive, Concord, CA 94518 (415) 676-5000 (IEEE Booth No. 2426-31).** CIRCLE NO. 162

Compact plug-in sweeps from 10 MHz to 18.5 GHz

Since the introduction of microwave solid-state sweep generators in the late 1960's, the move has been toward providing wider sweep coverage. A new sweeper plug-in from Wiltron leads this trend by providing the broadest sweep available in a solid-state plug-in—a full 10 MHz to 18.5 GHz.

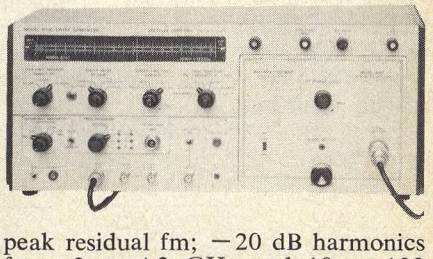
Plug-in model 6247 (Fig. 1), covers this ultra-wide bandwidth by sweeping through four rf bands: 0.01 to 2 GHz, 2 to 8 GHz, 8 to 12.4 GHz and 12.4 to 18.5 GHz. The complete frequency range is multiplexed using a PIN diode switch to a single precision type N output connector and can be swept in less than 30 ms to produce a flicker-free display.

Coverage above 2 GHz is provided by three fundamental YIG-tuned oscillators: an Avantek 2 to 8 GHz source and two Watkins-Johnson Gunn diode sources, one covering 8 to 12.4 GHz and the other, 12.4 to 18.5 GHz. The 10 MHz to 2 GHz range is swept by a heterodyne converter consisting of a 4.1 GHz cavity-tuned oscillator, balanced mixer and 10 MHz to 2 GHz amplifier. The 2 to 8 GHz oscillator is used as the variable low-level signal into the mixer and is swept from 4.1 to 2.1 GHz during the 10 MHz to 2 GHz output. Harmonics and spurious signals from the heterodyne module are 30 dB down.

Drive circuitry for the oscillators and related control circuitry is modularly constructed on three main printed circuit cards which are easily removable.

Internal leveling is standard and is accomplished by automatically multiplexing the signal from a 10 MHz to 2 GHz and a 2 GHz to 18.5 GHz directional detector into the level control loop. Power output is +7 dBm leveled to ±1 dB (Fig. 2). A front-panel slope adjustment compensates for frequency-dependent losses of the test set-up.

Other specifications include 32 kHz peak residual fm; −20 dB harmonics from 2 to 4.2 GHz and 10 to 100 MHz, −30 dB harmonics over the rest of the frequency range; −55 dB spurious, except from 10 MHz to 2 GHz where spurious is −30 dB; weight is 14 lbs, size is 7 x 18 x 14 in.



The new plug-in is designed for Wiltron's model 610B or 610C mainframes. Rack-mount models are also available at no extra cost. The solid-state oscillators are covered under a two-year warranty. P&A: 6247 plug-in: $19,000; model 610C mainframe: $1,325. **Wiltron Company, 930 E. Meadow Drive, Palo Alto, CA 94303 (415) 321-7428.** CIRCLE NO. 123

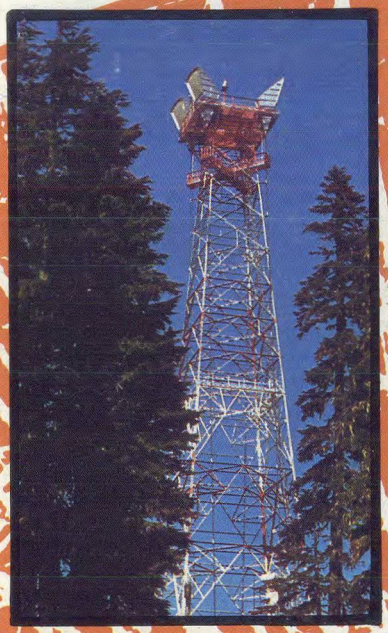
APRIL
1975

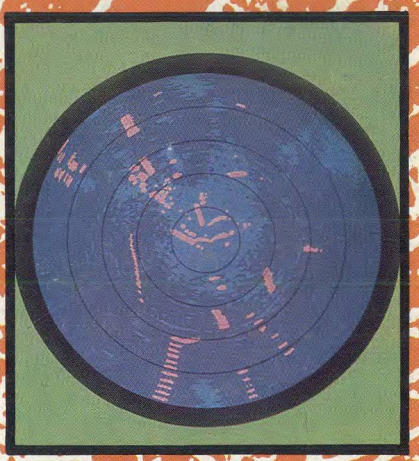
MICROWAVES

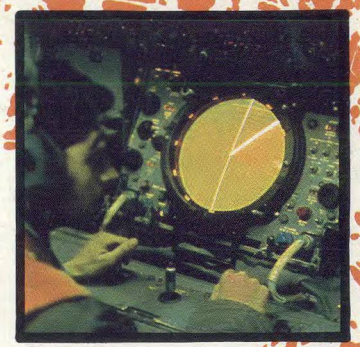
laser technology

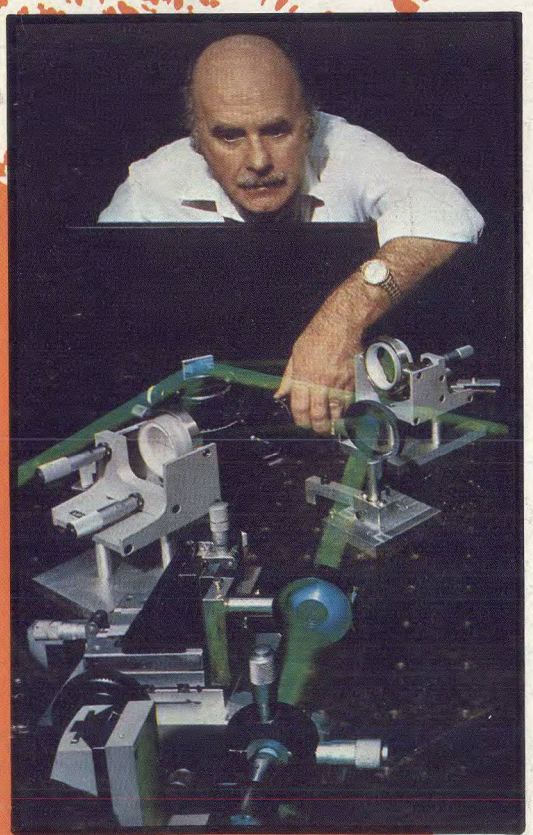
Systems:

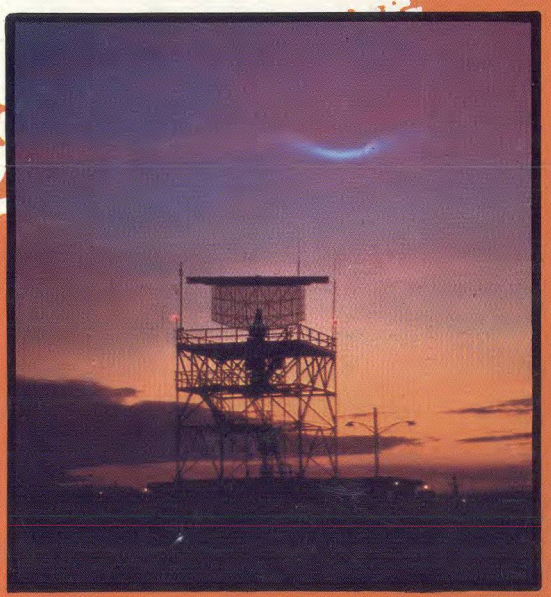
- Communications: Satellite systems pace growth
- Integrated optics mirror microwave concepts
- Eliminating clutter in radar system design











MICROWAVES

April 1975
Vol. 14, No. 4

news

11 GaAs Fets Pose Serious Challenges To Traditional Solid-State Devices
14 Airborne Steerable Beam Antenna Automatically Tracks Target Drones
16 Indonesia To Get Satellite System
19 Industry
21 Washington
24 Meetings
26 International
28 R & D
30 For Your Personal Interest . . .

editorial

32 Microscopic Microwaves for Tomorrow

technical section

Systems

34 **Eliminating Clutter In Radar Systems.** Peter Dax of Westinghouse presents a comparative review of the merits of analog and digital MTI and pulse-doppler systems.

44 **What's The Future For MW Communications? (Part I).** Jeff Montgomery of Gnostic Concepts takes a look at tomorrow's commercial communications market place. Satellite communications will be the major catalyst as the overall market grows at a strong rate.

54 **Integrated Optics Mirrors Microwaves Concepts (Part 1).** Fred Blum of Texas Instruments describes some of the hybrid optical communications systems that have been developed using optical fibers. Coupling and pulse spreading problems are described.

products and departments

60 New Products
71 New Literature
69 Application Notes
70 Advertisers' Index
72 Product Index

About the cover: The radar and communications systems depicted on this month's cover illustrate three major areas where microwave and laser technology are playing a significant role. The laser photo, provided by Texas Instruments, shows a split-beam argon ion laser test set-up. Integrated optics could eventually put all this on a single chip.

coming next month: Solid-State Sources

S-PARAMETERS SIMPLIFY ACCURATE VCO DESIGN. Gene Strid of RCA Alaska Communications, describes how oscillator design technique need not be a hit or miss procedure. He presents a simple, computerized approach that requires resonating the active port's reactive component and cancelling out the tank circuit losses with negative resistance.

SIMPLIFY HIGH-POWER GUNN OSCILLATOR DESIGN. W. Wagner of Sanders Associates and Fred Manasse of Drexel University present a practical design guide for building Gunn oscillators.

ECONOMIC FORECAST: PART 2: WHAT'S THE FUTURE FOR MILITARY SYSTEMS? In his continuing series, Jeff Montgomery of Gnostic Concepts, Menlo Park, CA, breaks out the various segments of the government microwave market and projects their growth patterns on the basis of computer modeling. The military demand for microwave components still dominates 85% of the market. Important programs are described.

INTEGRATED OPTICS MIRROR MICROWAVE CONCEPTS: Part 2. Fred Blum of Texas Instruments continues his discussion on optical communications getting into the analogies between integrated optics and microwave components.

Publisher/Editor
Howard Bierman

Managing Editor
Richard T. Davis

Associate Editor
Stacy V. Bearse

Contributing Editor
Harvey J. Hindin

Washington Editor
Paul Harris
Snyder Associates
1050 Potomac St., NW
Washington, DC 20007
(202) 965-3700

Editorial Assistant
Gail Murphy

Production Editor
Sherry Lynne Bogen

Art
Robert Meehan, Dir.

Production
Dollie S. Viebig, Mgr.
Dan Coakley

Circulation
Trish Edelmann, Mgr.
Peggy Long, Reader Service

Promotion Manager
Walter Salm
Albert B. Stempel (Reprints)

Editorial Office
50 Essex St.,
Rochelle Park, N.J. 07662
Phone (201) 843-0550
TWX 710-990-5071

A Hayden Publication
James S. Mulholland, Jr., President

MICROWAVES is sent free to individuals actively engaged in microwave work at companies located in the U.S., Canada and Western Europe. Subscription price for non-qualified copies is $10.00 for U.S., $15.00 a year elsewhere. Additional single copies $1.50 ea. (U.S.); $2.00 ea. (foreign); except additional Product Data Directory reference issue, $10.00 ea. (U.S.); $18.00 (foreign).

Hayden Publishing Co. Inc., James S. Mulholland, President, printed at Brown Printing Co., Inc., Waseca, MN.

Copyright © 1974 Hayden Publishing Co., Inc., all rights reserved.

GaAs FETs pose serious challenges to traditional solid-state devices

Stacy V. Bearse
Associate Editor

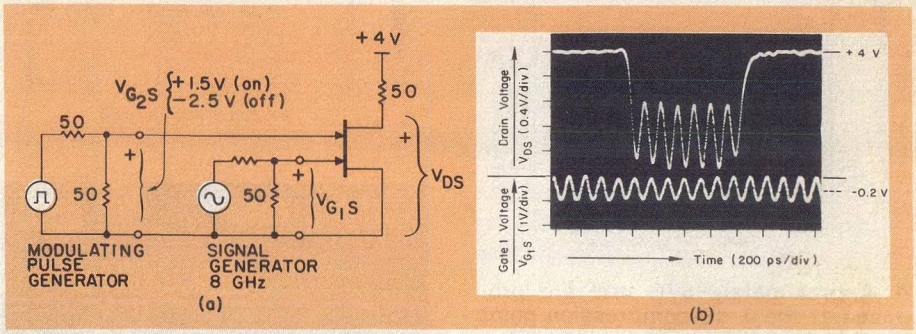
Advances in gallium arsenide field effect transistor technology indicate that the versatile devices are continuing to elbow their way into frequency ranges and applications long dominated by more established solid-state devices.

Cellular FETs have been combined to form powerful—and extremely efficient—linear power amplifiers, rivaling the best bipolar transistors at frequencies as low as 4 GHz. FETs are believed by some to combine the best virtues of Schottky and tunnel diodes without the isolation problems inherent in a two-terminal device. As gate lengths shrink, experts envision FETs operable to 30 GHz, encroaching on the frequency domain of transferred electron devices. And a relatively new structure—the dual-gate GaAs MESFET—could greatly simplify many now complex components.

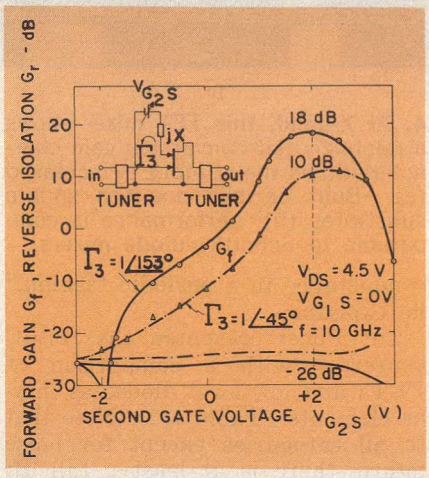
Although chronologically still in its infancy, the dual-gate GaAs MESFET is rapidly maturing into a promising, practical device. As reported at the 1974 S-MTT International Microwave Symposium, researchers from Hitachi exploited the dual-gate FET's variable gain capability in the design of an amplifier that has a dynamic gain range of 35 dB. At the 1975 International Solid-State Circuits Conference, Hewlett-Packard's Dr. Charles A. Liechti demonstrated that the dual-gate device's gain could be changed fast enough to use the MESFET as an X-band modulator.

To illustrate the dual-gate MESFET's modulation capability, Dr. Liechti, section head of design and development at H-P's Solid-State Lab in Palo Alto, CA, points to the design of the pulsed amplitude modulator circuit shown in Figure 1. The circuit employs a developmental dual-gate GaAs MESFET which exhibits an available gain of 18 dB at 10 GHz and a minimum noise figure of 4.0 dB with an associated gain of 12 dB.

In operation, an 8 GHz cw signal is fed to the first gate, while a synchronized modulating pulse



1. **Both gates are driven** in this dual-gate MESFET pulsed amplitude modulator. Waveforms at the drain and first gate are shown in (b) .



2. A 44 dB change in forward gain occurs when the voltage on the second gate (V_{G2S}) is varied from +2.0 to −2.0 volts. Note that the reverse isolation (G_r) never rises above −25 dB over the entire bias range.

drives the second gate. By varying the second gate potential, gain modulation can be realized over a 44 dB dynamic range (see Fig. 2). With the rf drive turned off, a drain voltage fall time of 65 ps and a risetime of 100 ps are reported.

"This result demonstrates the dual-gate MESFET's capability to switch between gain and high insertion loss within less than one rf cycle at X-band frequencies," Dr. Liechti observes. "This ultrafast switching speed makes the device very useful for subnanosecond PSK carrier modulation," he concludes.

In a session entitled, "Microwave FETs," Dr. Liechti explained that the dual-gate devices offered several advantages over their single-gate counterparts: "Dual-gate MESFETs have a low-noise figure—but not the lowest noise figure. If one wants to build an amp with the lowest noise figure, one would use a single-gate MESFET in the first stage. However, for all the intermediate stages, with the exception of the power stage, the dual-gate MESFET has distinct adavntages.

"First, it has higher gain, therefore reducing the number of required amplifier stages and, thus reducing the cost of an amplifier. Second, it has a large gain modulation range, and is, therefore, very suitable for AGC in an amplifier. And third, it allows gain slope compensation with a simple circuit between the second gate and source."

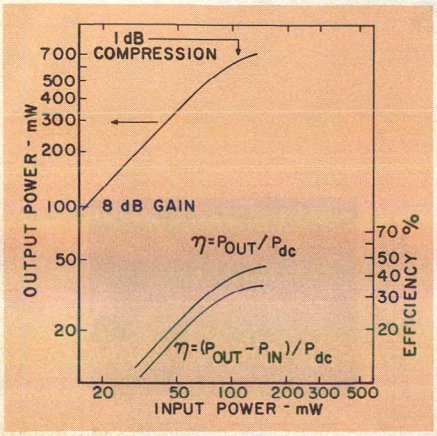
Class A applications eyed

Although the dual-gate MESFET certainly looks promising, the majority of ongoing FET R&D programs are dedicated to realizing the full potential of single-gate designs. For example, researchers at RCA's Microwave Technology Center in Princeton, NJ, are studying the potential of the single-gate GaAs MESFET as a linear power amplifier. "Even at the relatively low frequency of 4 GHz, the performance of GaAs MESFETs is superior to that of silicon-bipolar transistors for high efficiency linear amplifier applications," contends Dr. Raymond L. Camisa, a member of the technical staff at RCA.

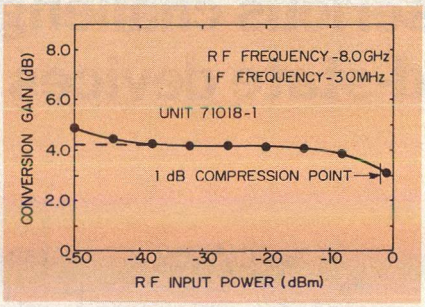
At the 1975 ISSCC, Dr. Camisa discussed the performance of several developmental MESFET linear

(continued on p. 12)

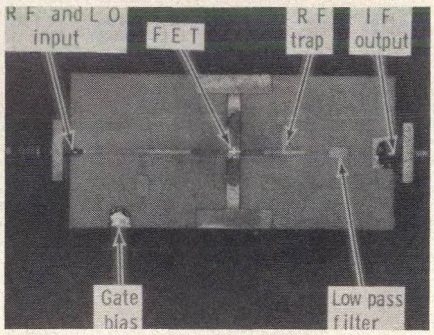
GaAs FETs pose serious challenges to traditional solid-state devices



3. Approximately 670 mW are produced at the 1 dB compression point for this MESFET linear amplifier. The characteristic represents a single-tone input.

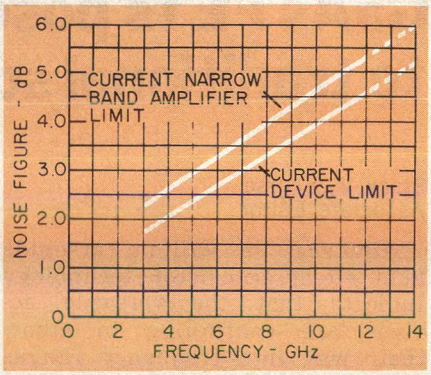


(a)



(b)

4. At X-band, this FET mixer shows a relatively flat conversion gain characteristic as the rf input is increased (a). Built on two one-inch square substrates (b), performance is comparable to Schottky diode mixers.



5. Here's about the best that you can expect from commercially-available GaAs MESFET devices and amplifiers. Generalized data was derived from product specifications.

(continued from p. 9)

amplifiers to reinforce his point. One, a three-cell device (each cell consisting of four 2.5 x 150 μm gates in parallel), produces an output power of 670 mW at the 1 dB gain compression point with a power added efficiency ($\eta_{PA} = (P_{out} - P_{in})/P_{dc}$) of 35% (see Fig. 3). A second amplifier, tailored for the 7.25 to 7.75 GHz satellite communications band, was designed to produce a linear gain of 7.45 ±0.15 dB over the complete 500 MHz bandwidth. At 7.5 GHz, this single-cell device produces 140 mW at the 1 dB compression point with a power added efficiency of 16%.

"In comparison, present bipolar transistors when operated as Class A linear amplifiers, can achieve 8 dB linear gain at 4 GHz with 100 mW output power (1 dB compression) and a power added efficiency of 15%. With developmental bipolars, 500 mW with a power added efficiency of 16% has been achieved at 4 GHz," Dr. Camisa comments.

FET mixers offer gain

GaAs FET oscillators and mixers for integrated front-end assemblies are other areas being intensely investigated. "As a microwave mixing element, the FET can exhibit a large dynamic range with conversion gain thus combining the best features of Schottky and tunnel diode mixers," concludes Dr. Robert A. Pucel, a consulting scientist in the microwave transistor program at Raytheon in Waltham, MA. "Mixing in an FET is produced by the local oscillator signal, by modulating the device's transconductance in a periodic fashion," he explains.

Dr. Pucel presented the ISSCC conferees with a comparison of FETs and low-level diodes as mixer elements (Table 1). "Note that in all categories except for noise figure, there is at least a full dB advantage for the FET mixer. The slight differential in noise figures should change sides in the very near future," Dr. Pucel summarized.

As an example of an FET mixer application, the Raytheon scientist discussed the X-band mixer shown in Fig. 4, and stressed the high rf input level corresponding to the 1 dB gain compression point. Noise figure for the mixer is 7.8 dB which, according to Dr. Pucel, is the lowest noise figure reported for an 8 GHz FET mixer. The FET used in the circuit has a transconductance of 30 mmho, a pinch-off voltage of 4.3 volts and a 2.5 μm gate length.

Gazing in the crystal ball

Although the devices described at the 1975 ISSCC promise a variety of interesting applications for GaAs MESFETs, only a handful of companies currently offer the devices as off-the-shelf components. In an informal discussion session at the ISSCC, HP's Charles Liechti summarized the performance of the best devices sold by each company and attempted to define the "generalized state-of-the-art" noise figure limits for commercially available devices and amplifiers. Oddly, although there are many scattered data points, the limiting values seem to form the linear characteristics shown in Fig. 5. "There is approximately a constant 0.8 dB difference between MESFET amplifier and device limits," Dr. Liechti notes.

There are some ways to improve these limits and cooled environments are showing great potential. Work done by Dr. Paul Bura, of RCA, Ltd., Government and Commercial Systems Division in Quebec, Canada, shows that the 4.9 dB noise figure of an 8 GHz MESFET amplifier operating at room temperature (+20°C) can be improved to 3.0 dB when the amplifier is cooled to −80°C. "Eventually," Charles Liechti predicts, "cooled FET amplifiers will be capable of 1 to 2 dB noise figures in the 8 to 11 GHz range."

This year, circuit designers can look forward to the market debut of some very interesting, practical MESFET designs. "We be-

(continued on p. 16)

Table 1: Comparison Of FETs and Diodes In Mixers

	Maximum gain	Minimum noise figure	Third order IM intercept	1 dB gain compression level
GaAs FET	+6 dB	7.8 dB	+18 dBm	+5.5 dBm
Low-Level Diode	+5 dB	5-7 dB	+5 dBm	−6 to-1 dBm

Airborne steerable beam antenna automatically tracks target drones

Richard T. Davis
Managing Editor

A steerable beam antenna with 360 degrees of azimuthal scan and a −45 to +45 degree range of elevation angles has been developed and is now undergoing laboratory tests at Motorola's Government Electronics Division, Scottsdale, AZ. The 4.6 GHz antenna developed for the Naval Air Systems Command is designed to be placed atop a C-130 aircraft in a way resembling a scaled-down AWACS aircraft (Fig. 1). It will serve as a control/relay station for up to four target drones.

The drones flying in widely scattered directions could thus be monitored and communicated with from a single ground terminal instead of having an individual terminal for each drone. Airborne relays are desirable for target drone use because they extend the drone's range beyond line-of-sight as required with ground terminals. Range with the relay will be a total of 400 nautical miles (250 n. mi. from ground station to relay and 150 n. mi. from relay to drone).

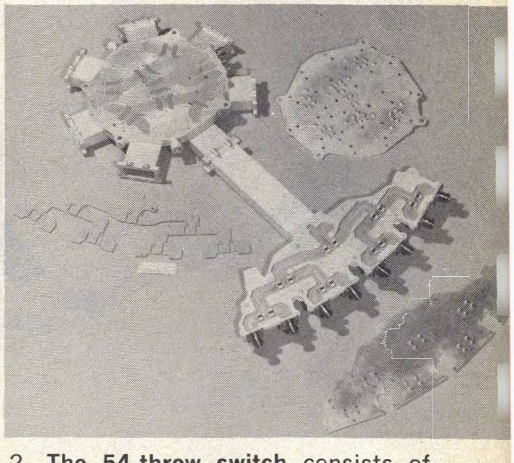
The cylindrical antenna is unique in that it can handle up to 600 W cw transmit power by means of specially designed single-pole, two-throw PIN diode switches. The antenna includes a lens which accepts the transmitter signal and, by means of an array of switches, applies the signal to a group of radiators on the periphery of the antenna. Coarse beam steering is achieved by selecting the appropriate lens terminal. Fine steering is also provided by the setting of a power divider which controls relative power levels applied to the switch matrices. The result is a shaped (2° wide) beam that can communicate with each vehicle sequentially over a −45 degree to +45 degree elevation angle. According to Dr. Peter Kennedy, senior engineer in the Drone Electronics Section, the output from the divider is used to feed two adjacent terminals on the antenna.

"When a signal is applied to these terminals, energy spreads across the lens as a TEM wave and excites a group of probes on the opposite side of the lens. There are 108 ports on the lens, two-thirds of which or 72, are excited at any one time. Cables then conduct these signals to the appropriate group of 72 radiating elements among the 216 radiating elements making up the cylindrical array," says Kennedy. "In the present system the input lens terminals are used to obtain the proper element excitation." Intermediate beam positions are generated by varying the relative excitations of the adjacent terminals. To connect the transmitter to the desired lens terminals, the system uses two identical 54-throw switch matrices, one connected to 54 odd-numbered terminals, the other to 54 even.

The biggest design challenge presented was in designing and building the two 600 W 54-throw



1. **The AN/ASW-35 airborne control station** is used as a relay to control up to four drones sequentially using a 50 kb/sec data rate. A C-130 aircraft which is presently used to carry target drones aloft, will carry the 3500 lb. cylindrical array antenna atop its fuselage just aft of the wings.

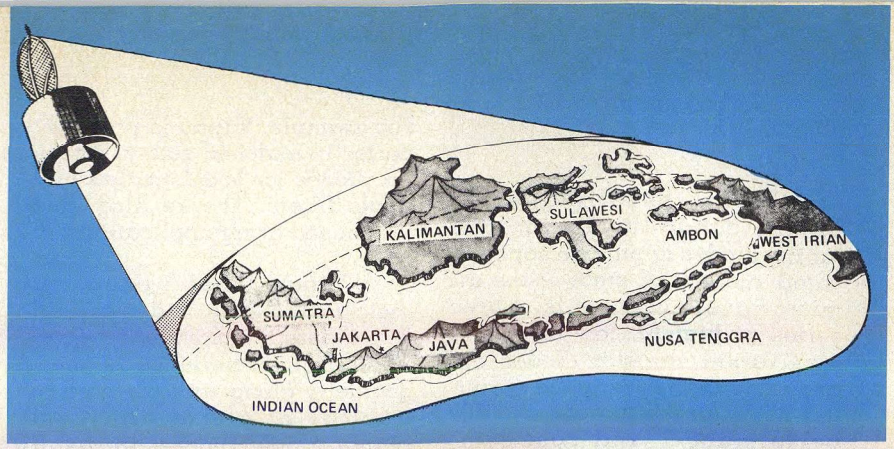


2. **The 54-throw switch** consists of a central module with seven outputs surrounded by seven modules having eight outputs each. The input to the switch takes the 600 W cw and routes it to the proper lens terminals.

(continued on p. 16)

news

Indonesia to get satellite system



The Republic of Indonesia has announced plans to become the third nation in the world to develop and operate a domestic communications satellite system. When the system becomes operational, which is expected in mid-1976, it will provide telephone, telegraph, television and teletype links between 120 million Indonesians living on the country's 5,000 scattered islands.

According to Moenadir Mangoendiprodjo, first director of Permutel, the government-owned telecommunications company, two subsidiaries of the Hughes Aircraft company were selected to provide the spacecraft, ground control facilities and certain earth stations. Hughes Communications International, Inc., an El Segundo, CA based firm, will build the two satellites under a $23.6-million contract. Nearly twice this amount, $47-million, has been committed to Hughes Aircraft Services International for a master control station and nine earth stations.

The remaining 30 earth stations initially planned will be purchased from two other sources: Federal Electric International, a subsidiary of ITT Federal Electric in Paramus, NJ, and Philco-Ford's WDL division in Palo Alto, CA. Under a $30-million contract, the ITT company will build 15 earth stations. Financial details of the Philco-Ford agreement are not available.

The first of the two 543-kilogram satellites is scheduled to be launched into geosynchronous orbit early in 1976 by the U. S. National Aeronautics and Space Administration from Cape Canaveral, FL. The second satellite is expected to be launched within two years. Both will be identical to the Anik and Westar satellites, now operational over Canada and the United States.

Indonesia will become the first nation in Asia to have its own domestic satellite system. Although the U. S. S. R. maintains a communications satellite system, the spacecraft does not operate in a synchronous orbit. ••

S.V.B.

Airborne antenna tracks drones

(continued from p. 14)

switch matrices. It was found that two-throw switches were best suited to make up the 54-throw switch matrix. Each matrix is constructed as a central module with seven outputs which in turn is surrounded by seven modules having eight outputs each, Fig. 2. (This gives 56 outputs, but two aren't used). Since the maximum power the antenna can handle is limited by the PIN diodes in the matrix, diode selection and packaging were critical.

"We found commercially packaged PIN diodes with their 10 mils wide x 1 mil thick gold leads simply couldn't handle the high RF currents involved," (approximately 4.5 amperes for 600 watts), says Hugh Malone, senior engineer, in the Microwave Section. "We, therefore, developed our own packages using 50 mil gold leads. Two, 0.25 pF, 1 ohm diode chips paralleled in a low parasitic diode package were decided upon." The net thermal resistance is under 3°C/W at 25°C.

The high power SP2T switches use two diode packages spaced $\lambda/4$ from the pole of the switch. "The maximum insertion loss measured at 1 mW for a SP2T switch is 0.4 dB over a 20% band," says Malone. Maximum VSWR is 1.3:1 and minimum isolation is 25 dB." When three levels of switches are combined to form a SP7T switch (one of the possible 8 ports is unused), max VSWR is 1.6:1 and max insertion loss is 2.4 dB over a 4 to 5.2 GHz band. In biasing the high power 1P2T diode switch, it was found necessary to float the diode case at the bias potential, (100 V reverse; 1 V, 100 mA forward).

The lens used in the antenna was designed by Bill Sasser, senior engineer in the Antenna Section. It is built in the form of two flat parallel metal disks, joined around their edges by a metal ring to form a closed waveguide region. Sidelobes are only 15 dB down from the main beam but this is considered adequate for target drone vehicles. ••

GaAs FETs pose serious challenges to solid-state devices

(continued from p. 12)

lieve that HP will be on the market with a one micron device by the end of the year," claims Dr. Leichti. "You will also see a new package coming on the market soon that you will really like!," he adds. Indications are that the new package will incorporate some type of internal impedance matching.

"In two years, the MESFET will move into Ku-band (16 GHz) with noise figures on the order of 4.5 dB and associated gains of 6 to 8 dB," the researcher forecasts.

Dr. Gailon E. Brehm of Aertech/TRW in Sunnyvale, CA, also believes that tomorrow's GaAs MESFET has a high-frequency future: "Based on today's 1 μm gate length technology, we have an f_{max} in the region of 60 GHz. This leads me to believe that someday we may have millimeter-wave FETs. In the near future, I see FETs operable at 15 GHz and beyond that, perhaps further improvements to reach 25 or 30 GHz."

"I think that in the very near future, two technologies will invade MESFET fabrication," Dr. Liechti continues. "Electron-beam lithography will shrink gate lengths to tenths of microns. If you shrink gate length, you must also keep the channel length to thickness ratio constant. To do this, doping density must be increased. Ion-implantation techniques will do the job nicely. These two technologies will revolutionize the MESFET." ••

Eliminating Clutter In Radar Systems

Clutter, the bane of radar designers, can be dealt with by using the doppler frequency shift of radially-moving targets. Here's a review of the merits of analog and digital MTI and pulse-doppler systems.

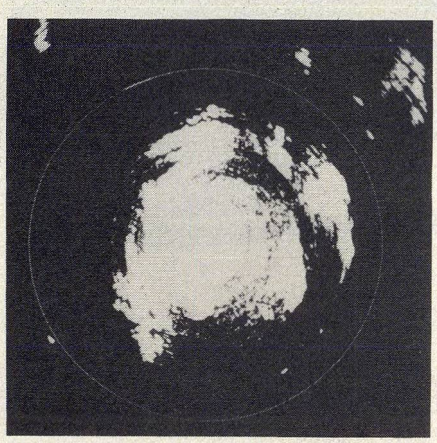
WITH the exception of certain specialized radars such as meteorological or navigational radars that are required to detect clouds or mountains and coastlines, most radars are required to detect man-made objects, such as aircraft, ships or tanks to the exclusion of ground, sea or weather returns. These unwanted echoes are usually lumped together under the classification of clutter.

Clutter basically consists of a large number of small scatterers. When it is spread over a large area, it is known as "extended" clutter. These scatterers may be rain, chaff, surface of the sea, forests, etc. In other cases, clutter originates from specific point sources such as tall buildings or water towers. In practice, of course, for any particular radar location, the clutter will be a combination of these types.

Figure 1 shows a PPI display of a conventional S-band search radar without MTI. Clutter can be seen to extend to beyond 40 miles with some mountains appearing at still greater ranges. Depending on the meteorological situation, the display could be further cluttered up with returns from weather, such as rain and snow. This latter effect is particularly noticeable at the higher radar frequencies.

Clutter is one of the major problems in radar design. As a result, considerable effort and ingenuity has gone into the design of clutter elimination circuits.

If the desired target is moving relative to the clutter (e.g., an aircraft in flight near the ground), it is possible to use the doppler frequency shift produced by the target's motion to filter out the undesired stationary returns not shifted in frequency. This is the basic principle behind moving target indicator and pulse doppler radars.



1. Plan-position indicator (PPI) display of an S-band radar without MTI shows considerable clutter inside the 50 nmi range ring. Mountains show up at still greater range.

Up to a few years ago, there were two basic techniques widely used for combatting clutter: analog MTI (Moving Target Indicator) systems with ultrasonic delay lines, and pulse doppler systems with banks of analog filters. These two schemes have usually been treated separately in the literature. It seemed natural to give a time-domain explanation of the MTI and a frequency domain explanation of the pulse doppler.

Delay-line MTI systems were normally reserved for relatively low prf (say, 300 pulses per second) search radars that derive relatively few hits (say 10) from each look at the target. The pulse doppler systems are used by relatively high prf (say 5000 pulses per second) track radars, continuously illuminating the target.

With the advent of hybrid radar systems such as gated MTI and especially with the advent of sophisticated digital signal processing allowing more complex systems, the distinction between MTI and pulse doppler became unclear. In fact some systems are labeled as MTI by some and pulse doppler by others.

This article provides an overview of the whole subject of clutter rejection and places the various existing schemes in proper perspective. This is accomplished by describing the various clutter reduction circuits with the same frequency-domain approach and by identifying the different radar types with which they are associated.

Five different clutter reduction schemes based on doppler difference are examined:

- analog delay line MTI
- pulsed doppler systems with banks of contigous filters
- gated MTI
- digital MTI
- digital pulse doppler.

All five systems are faced with the same problem of separating the clutter energy from the energy of the wanted moving target. The main problems are:

- The radar system must be very stable.
- In the usual case of a pulsed radar, the spectra overlap.
- The lines of the spectra are broadened and often overlap.
- When the doppler shift equals a multiple of the prf, a blind speed occurs and the target cannot be resolved from the clutter.

Ideally, the solutions to these problems require a high prf, low frequency radar with long dwell time on target, a small radar cell

(continued on p. 36)

Peter R. Dax, Advisory Engineer, Westinghouse Electric Corporation, P. O. Box 1897, Baltimore, MD 21203.

size and, of course, a very stable system to start with. Most of these requirements are in conflict with other requirements of the radar such as narrow beamwidths, high scan rate (for a search radar) and unambiguous range.

Non-doppler methods

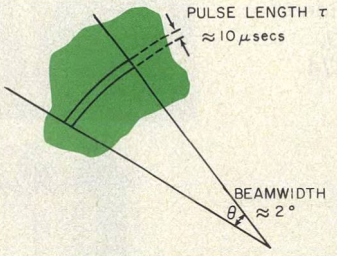
The basic objective of employing clutter reduction circuitry is to see the target in the clutter and not merely to eliminate the clutter. Under certain conditions, such as when a radar feeds an automatic digital target extractor and when all else fails, the video is blanked in a clutter mapper. Because it is important to avoid overloading the subsequent processing circuits with false alarms (caused by clutter peaks crossing the threshold), a mapper is usually controlled by an operator at a PPI display. All target information is, of course, lost in the blanked areas and as such, this clutter reduction method is a brute force approach.

A less drastic step is to automatically adjust the system gain so that the level of the clutter is reduced to that of the normal background noise. Any target larger than the clutter will then be detectable. Several circuits coming under the heading of constant-false-alarm-rate (CFAR) circuits can do the job. Historically, logarithmic amplifier detectors followed by a fast time constant RC circuit were first used for this purpose in World War II radars. However, targets smaller than the this scheme, i.e., no sub-clutter-visibility will be provided.

STC (sensitivity-time-control) circuitry is commonly used to vary the system gain automatically as a function of range. This is desirable in any case to reduce the number of false alarms caused by small targets such as birds. If ground clutter is random and uniform, controlling the system gain inversely as the cube of the range, will maintain a constant clutter background. This enables targets larger than the clutter to be detected.

Another rather crude scheme for clutter reduction is the area-MTI technique where target returns that do not change their plan positions from scan to scan are eliminated. Threshold velocity is that target speed at which the return moves from one resolution cell to another in one scan. Some form of storage tube is usually used where the previous scan is stored and subtracted from the current scan. The only good feature of area-MTI is stability demands are not made on the radar itself.

Before submitting the radar signal to any further processing, it is desirable to reduce, to the maximum extent possible, the clutter energy competing with the target. Clutter energy is proporional to the size of the radar cell, Fig. 2. The first step to improve target visibility in extended clutter is to reduce the radar cell size. This is done by reducing the beamwidth and/or the pulse length. The possibility of reducing the beamwidth is limited by maximum antenna dimensions, among other considerations. The requirement for very short pulse length is normally incompatible with the requirement for high pulse energy for long range. Pulse compression can, however, be used to reduce the effective cell size while maintaining high energy level in the pulse.

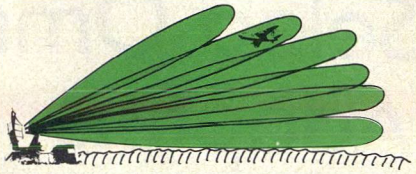


2. **A radar cell,** is determined by the beamwidth and the pulse length and should be minimized to reduce the effects of clutter competing with the targets. σ_o is the clutter cross section in m^2 per m^2 of clutter cell area.

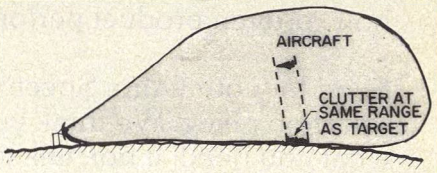
Unwanted clutter energy from point sources or from extended areas can be further reduced by discriminating in the vertical plane. Using stacked beams, Fig. 3, with separate processing for each beam (as opposed to a single fan beam, Fig. 4), reduces the ground or sea clutter energy competing with targets in the upper beams by the sidelobe levels of these beams. It also reduces the total radar cell dimensions which help in the presence of clutter, such as rain or chaff, which are distributed vertically as well as horizontally.

Doppler difference cuts clutter

Having reached an irreduceable level of clutter at this point, the next step is to see targets smaller than the clutter. The only known way to do this is to discriminate between target and clutter on the basis of doppler frequency. To achieve this, it is necessary to have a coherent radar system, where



3. **Separate receiver channels in a stacked beam search radar** limit the effect of clutter principally to targets in the lower beam. Other targets are in the clear and are only affected by clutter to the extent of the vertical sidelobes of the upper beam.



4. **In a fan beam search radar,** all targets are affected by clutter because clutter-returns from the same range cell compete against target energy in the single receiver channel.

the phase of the transmitted pulse is remembered and compared with the received pulse.

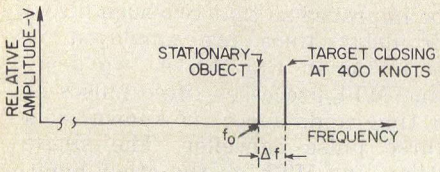
Consider a stationary radar transmitting an unmodulated rf signal of wavelength λ, such that the signal is reflected back to the radar from a moving target. The return from the target will be shifted in frequency by an amount given by: $\Delta f = 2\ v/\lambda$

where v = radial velocity

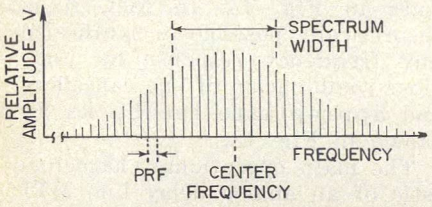
λ = wavelength

The polarity of the doppler shift is such that are received frequency increases (Δf is positive) for a target closing on the radar.

A radar which makes use of this basic doppler principle without any modulation is a cw radar. Maximum discriminaton of targets is possible with a cw radar because of the simple form of its spectrum, Fig. 5. But it does not permit range measurement without some kind of modulation on the transmission. This modulation may be fm but is more usually pulsed, resulting in the spectrum shown in Fig. 6. As can be seen, a pulse modulated radar has a spectrum with lines separated by the prf. Its overall width corresponds to the reciprocal of the pulse length. If the modulating pulse is square, the envelope will be the familiar sin x/x shape. (Usually, the pulse is shaped to reduce the spread of



5. **Spectrum for a cw radar continuously illuminating the target** shows stationary target at the same frequency as the transmitted signal, but the moving target shifted as shown. Discrimination between the target and stationary target is thus clear and unambiguous. Typically, $\Delta f = 1.5$ kHz for 450 knot target at L-band.



6. **Line spectrum of pulsed modulated radar** has a spectrum width equal to reciprocal of pulse length—typically, 100 kHz for a 10 μsec pulse. For a medium range, 3 GHz (S-band) radar, the prf is typically 1 kHz.

the sidelobes, thereby minimizing possible interference with other radars). If two targets are illuminated with a pulsed radar, such as a stationary target and another moving radially, there spectra will normally overlap, Fig. 7, making discrimination difficult. Only very high velocity differences will result in complete separation of the spectra, Fig. 8.

Clearly, what is needed is to pass those frequencies that fall between the clutter lines and reject the clutter lines themselves. This can be done by filtering. The classical analog delay line MTI is, in fact, a filter with rejection bands located about the clutter lines as shown in Fig. 9. A conventional pulse doppler system on the other hand achieves a similar result with banks of analog filters that accept the frequencies of moving targets (Fig. 10).

This filtering operation takes place at some convenient intermediate frequency (e.g., 30 MHz) using a mixer and LO. The received spectrum is then translated to the i-f and the principle of the filtering operation is unchanged. Frequently, everything is translated right down to zero frequency. The mixer is then called a synchronous-detector. It preserves both phase and amplitude as opposed to a phase-detector only that follows a limiter.

Since the doppler change in fre-

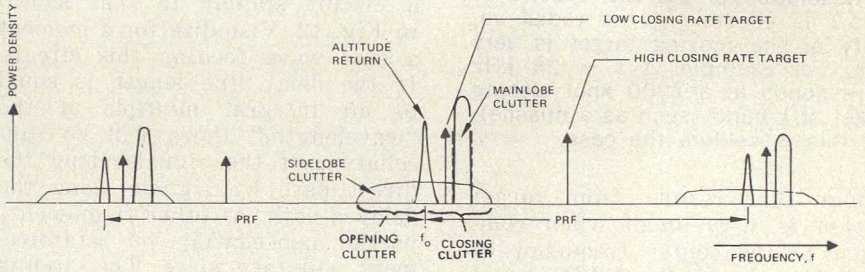
(continued on next page)

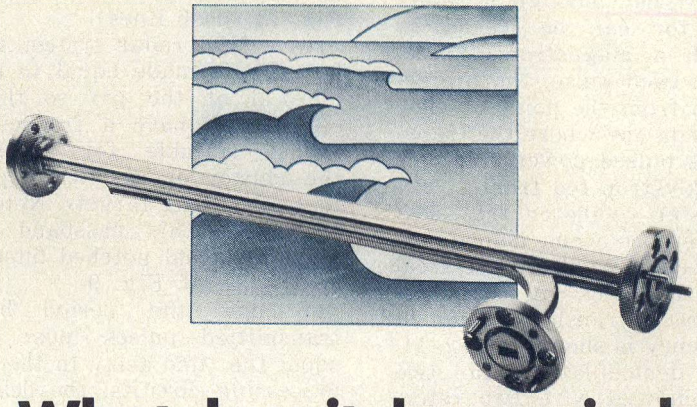
Wide range of clutter doppler with airborne radars

The clutter reduction techniques described assume that clutter doppler is zero. The clutter does not move with respect to the radar, apart from internal movement such as the swaying of trees. At sea, the motion of the ship will cause the clutter to move in apparently the opposite direction. This can be compensated for by suitably adjusting the coherent reference oscillator (COHO) knowing the velocity of the ship and the direction in which the radar is pointing alternatively, the COHO can be locked to the clutter itself.

With airborne radars, the problem is more complicated because clutter is received over a whole range of relative velocities. If the main beam of the airborne radar dips below the horizon, strong main beam clutter will be received moving relatively fast. The sidelobes will also intersect the ground at various angles giving rise in each one to its own doppler. In particular, a sidelobe looking straight down will generate a fairly large signal (because the earth will be at a right angle to the beam) at zero doppler. Fig. A shows how the doppler is typically distributed in frequency. To appear in the clear doppler-wise, a target must have a closing doppler greater than the closing clutter. On the other hand, its closing doppler cannot be too great or it will run into the opening clutter of the next clutter line.

A. **An airborne radar's spectrum** must have a high prf, such as 5,000 so that there is a large enough gap for accommodating moving target spectral lines.





What does it do, precisely? It samples mm waves precisely.

Hughes millimeter-wave directional couplers provide high directivity (greater than 40 dB) and predictable accuracy for precise control of mm waves.

You get flat frequency response ($\pm$1 dB) with an accurate coupling curve over the full waveguide bandwidth. And reduced coupling variation from unit to unit, thanks to a computer-optimized, precision-machined coupling plate.

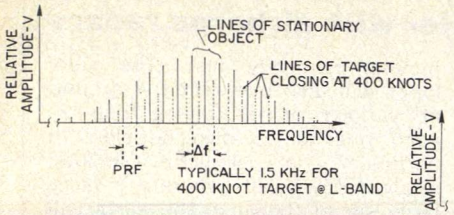
Our directional couplers are ideally suited for broadband measurements and instrumentation. What's more, they are competitively priced and available for off-the-shelf delivery.

If we're on the same wave length, write or call: Hughes Electron Dynamics Division, 3100 W. Lomita Boulevard, Torrance, Calif. 90509. (213) 534-2121, ext. 215.

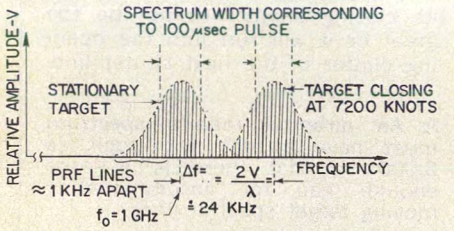
HUGHES
HUGHES AIRCRAFT COMPANY
ELECTRON DYNAMICS DIVISION

Making waves in millimeter-wave technology.

READER SERVICE NUMBER 37

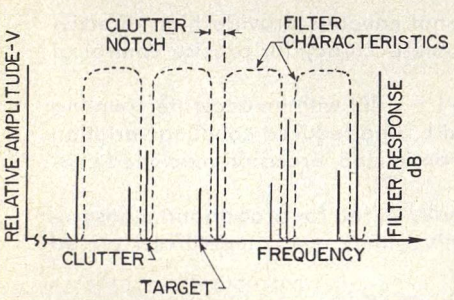


7. **A pulsed modulated radar,** illuminating stationary and moving targets, produces overlapping spectra, making discrimination difficult. Δ f is typically 1.5 kHz for 450 knot target at S-band.

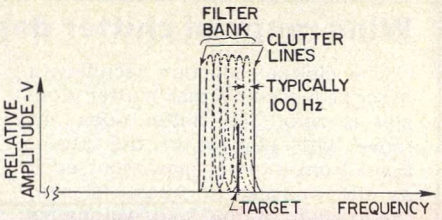


8. **Resolution of the two spectra** of Fig. 7 is possible if the radial velocity of the moving target is very high. For example, Δ f = 24 kHz corresponds to a 7200 knot closing target at L-band (such as a missile), but this is seldom the case.

quency that results from target motion is very small when compared to the center frequency of the radar (typically 1 kHz vs. 1 GHz), it is essential to have a coherent system. Though a reference collector can be locked in phase with a magnetron's transmission on each pulse, the preferred system from the point of view of stability is one where the transmitter is a pulsed power amplifier such as a klystron fed from a very stable master oscillator that acts as the reference when demodulating the received pulse. A typical form of processing where the received pulse is translated down to zero frequency is shown in Fig. 11. Coherent demodulation in two steps is achieved with two reference oscillators, the STALO and the COHO that, together, generate the transmit frequency.



9. **A classical delay line MTI** has a frequency response with notches that reject the spectral lines of the clutter. Spectral lines of the target are shown.



10. **Pulse doppler radar** makes use of a set of continuous narrow band filters (about 100 Hz wide) which accept spectral lines of moving targets. A measurement of radial velocity is provided by noting which filter gives an output.

Classical analog delay line MTI[1,2,3]

In a classical analog delay line MTI, the output of the synchronous detector, Fig. 11, is fed to a circuit similar to that shown in Fig. 12. Visualize for a moment a sine wave feeding this circuit. If the delay line length is equal to an integral multiple of the "wavelength," there will be cancellation of the signals along the direct path by signals along the delayed path. At other frequencies, partial cancellation or reinforcement will take place. The circuits act, therefore, as a filter the overall response of which is shown in Fig. 13 (dash lines).

In a MTI radar system, the delay (T) is made equal to the reciprocal of the prf so that the circuit will have a frequency response suitable for attenuating the clutter energy while passing that of moving targets. Note, however, that this passband is far from the ideal notched filter characteristics of Fig. 9.

Because the period between transmitted pulses must exactly equal the time delay in the signal-processing circuits, the delay line itself is made to control the transmitter trigger, or the radar prf.

The basic system in Fig. 12 may be improved so that two such filters or delay lines are employed in series as in Fig. 14. A two delay line MTI processes three pulses at a time and, hence, is known as a three pulse canceller. The single delay line MTI, on the other hand, processes two pulses at a time and is known as a two pulse canceller. The improved response of the three pulse canceller is that of a squared sine wave (bold lines in Fig. 13).

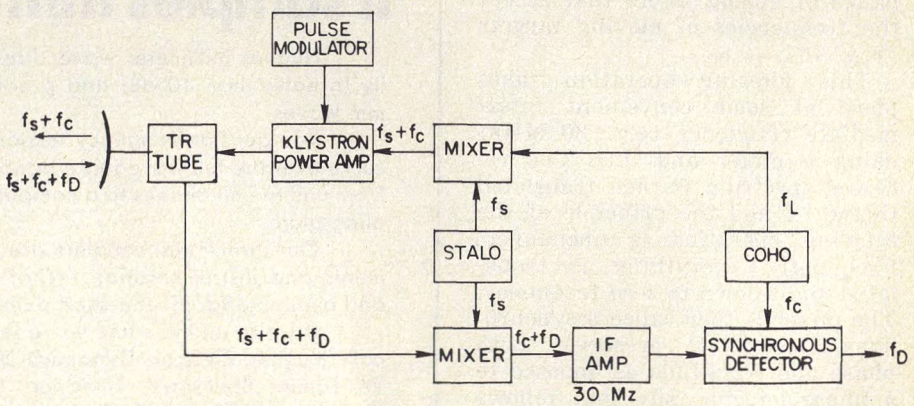
This frequency response can be further modified or shaped to approach that of Fig. 9 by internal feedbacks, as shown by the solid lines in Fig. 14. In fact, it is theoretically possible to synthesize any frequency response by judicious combination of (n) cancellers and appropriate feedbacks as shown in Fig. 13.

The main operational characteristic of an analog delay line MTI is that it works fine in the laboratory but degrades rapidly in the field. The problems of matching gain and bandpass characteristics of the delayed and undelayed channels and of controlling the absolute time delay, severely limit use in an operational environment. The additional complexity required to remove blind speeds only exacerbates the situation.

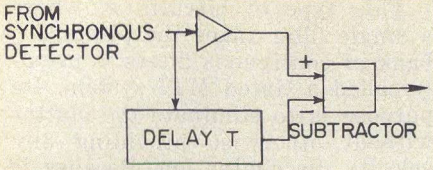
Pulse doppler uses filter banks[1,3,4]

Instead of generating rejection notches as in the case of a delay line MTI, a pulse doppler system has a bank of filters (as shown in Fig. 10) that will accept the spectral lines of moving targets and exclude those of the clutter. Velocity of the target can be determined by noting which filter gives an output.

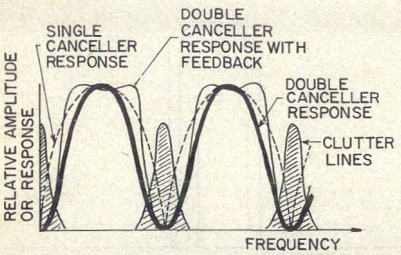
Each filter must be appreciably narrower than the prf in order to fit inbetween the clutter lines spaced one prf apart. They're usually only 100 Hz wide. Thus, the response time of each one will



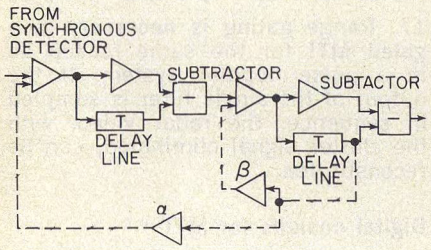
11. **Coherent demodulation** is achieved by using the same reference oscillators as those that generate the transient waveform.



12. **In a basic MTI canceller,** the delay line is exactly one interpulse period long. The radar prf is in fact controlled by the delay line instead of the other way around.



13. **Comparisons of the frequency responses of MTI cancellers** show improvement over a simple single canceller (dotted) by going to a double canceller (bold) and finally a double canceller with feedback (solid line). The objective is to reject as much clutter as possible while maximizing the response to the moving target spectral lines. The single canceller exhibits rejection notches 1/T apart and hence one prf apart (T = time delay of delay line).



14. **Double canceller consists of two single cancellers in series** and improves upon the response of Fig. 13. However, the matching of the two analog delay lines to the prf presents problems. Usually the first delay line controls the prf and the second is matched to the first.

be several times the interpulse period. All range information at the outputs of the filters will be lost unless range gating is carried out as shown in Fig. 15 and a complete bank of filters is provided for each range increment. The number of filters required equals the number of velocity resolution cells.

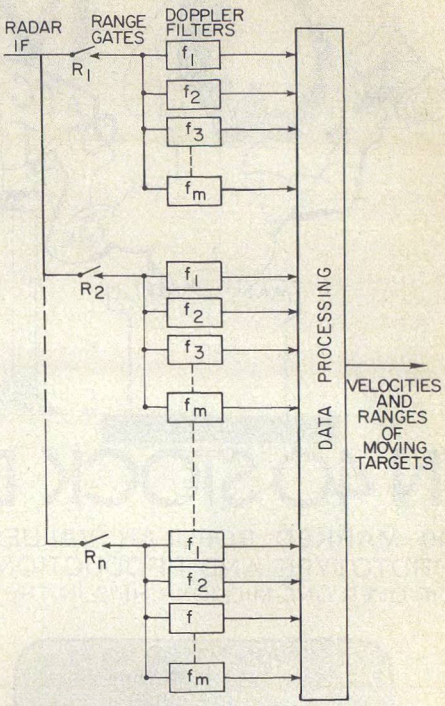
Range gating is also required to avoid a "collapsing loss." This results from the noise energy occurring outside the pulse width of the target return, adding to that coinciding with the target.

The width of each filter can be matched to the width of the target line for optimum detection. Furthermore, coherent integration of a train of pulses will occur in the filter, signifiantly improving the performance when there is a large number of hits on target.

The main disadvantage of the analog-pulse-doppler system is the large number of filters that are required. Otherwise, since all the radar data is processed in parallel, there is no real limit to the capacity of the system. Doppler hardware doesn't suffer from the stability and matching problems of MTI.

If velocity information is not required, the conventional pulse doppler system described above can be simplified by combining the contiguous filter band into a single filter, each providing range increment with the passband shown in Fig. 16. Range gating is required as in the pulse doppler scheme. When the synchronized sampling switches are used at the output, Fig. 17, the radar information will appear in the proper sequence on a single output line with most of the clutter filtered out.

(continued on next page)



15. **In a pulse-doppler system,** range resolution can only be maintained by gating the signal in each range increment to its own bank of filters by means of a series of switches.



Now you can switch your mm-wave direction without distorting your mm wave.

Our 4-port rotary waveguide switches let you switch mm waves in four different directions. Just turn the convenient selector knob. It's that easy.

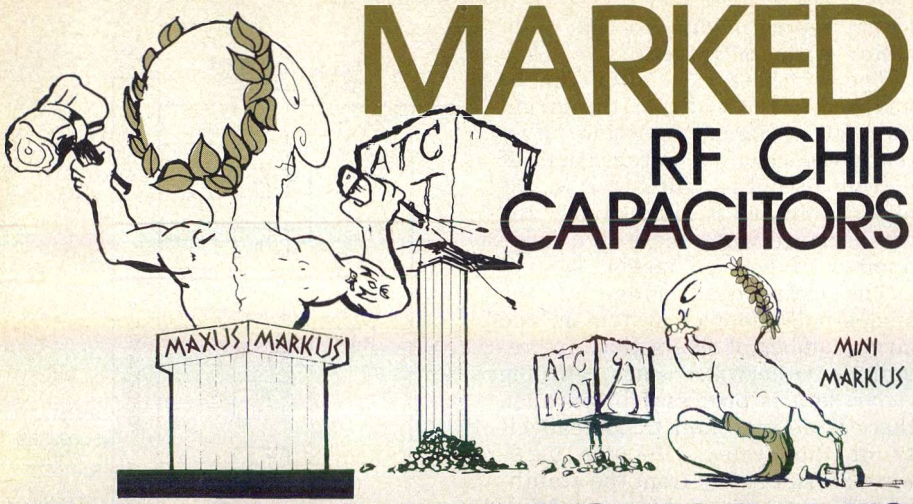
Six waveguide bands are available covering 26.5 to 110 GHz—and each operates over the entire waveguide bandwidth. They give you low insertion loss and high isolation between waveguide ports. And they're available for quick delivery at a low cost.

If you need waveguide switches, write or call: Hughes Electron Dynamics Division, 3100 W. Lomita Blvd., Torrance, CA 90509. (213) 534-2121, Ext. 215.

HUGHES
HUGHES AIRCRAFT COMPANY
ELECTRON DYNAMICS DIVISION

Making waves in millimeter-wave technology.

READER SERVICE NUMBER 39



MARKED RF CHIP CAPACITORS

IN 40 STOCK DESIGN VALUES

40 MARKED POPULAR VALUES IMMEDIATELY AVAILABLE IN PROTOTYPE AND PRODUCTION QUANTITIES (BACKED BY A STOCK OF OVER ONE MILLION CHIPS IN THE DESIGN VALUES SHOWN BELOW):

DESIGN VALUE KIT A1
mini-cube® A trim kit
(55 mil cube)

QTY.	CASE	CAP. (pF)	TOL.
10	A	0.1	B
10	A	0.5	B
10	A	0.8	B
10	A	1.8	B
10	A	3.3	B
10	A	4.7	C
10	A	6.2	C
10	A	8.2	C
10	A	9.1	C
10	A	10.0	J

DESIGN VALUE KIT A2
mini-cube® A Tune Kit
(55 mil cube)

QTY.	CASE	CAP. (pF)	TOL.
10	A	12.0	J
10	A	15.0	J
10	A	18.0	J
10	A	22.0	J
10	A	27.0	J
10	A	33.0	J
10	A	47.0	J
10	A	62.0	J
10	A	82.0	J
10	A	100.0	M

mini-cube® is a registered trademark and MAXI-"Q"UBE T.M. is a proprietary trademark of ATC.

DESIGN VALUE KIT A3
MAXI-"Q"UBE™ B trim kit
(110 mil cube)

QTY.	CASE	CAP. (pF)	TOL.
10	B	1.6	C
10	B	1.8	C
10	B	2.4	C
10	B	4.7	C
10	B	5.6	C
10	B	6.2	C
10	B	7.5	C
10	B	8.2	K
10	B	10.0	K
10	B	12.0	K

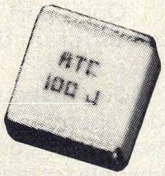
DESIGN VALUE KIT A4
MAXI-"Q"UBE™ B Tune Kit
(110 mil cube)

QTY.	CASE	CAP. (pF)	TOL.
10	B	18.0	K
10	B	24.0	J
10	B	27.0	K
10	B	30.0	J
10	B	43.0	J
10	B	68.0	J
10	B	110.0	J
10	B	120.0	J
10	B	180.0	J
10	B	220.0	J

BUY ANY DESIGN VALUE KIT OF 100 ATC 100 LOW LOSS PORCELAIN CHIP CAPACITORS FOR $77.00.

If you need further information on these Design Value Kits, just circle the number below.

To place your order, or for samples of other ATC Capacitors, call Ralph Wood at (516) 271-9600.



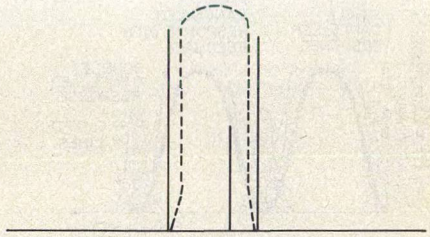
ACTUAL SIZE:
55 MIL CUBE

american technical ceramics
ONE NORDEN LANE, HUNTINGTON STATION, N.Y. 11746
(516) 271-9600 • TWX 510-226-6993

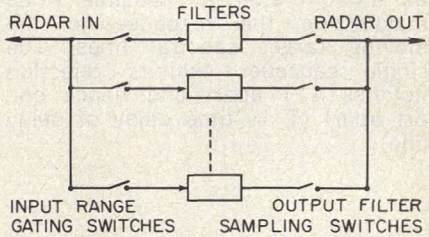
READER SERVICE NUMBER 40

RADAR CLUTTER

This type of circuit i.e. where a single filter takes the place of a bank of contiguous filters is usually called a Gated MTI system. Its purpose is to eliminate the clutter without otherwise providing any velocity discrimination. Because it usually uses lumped constant circuit element filters, it can be considered as a pulse doppler system as opposed to an MTI system using delay lines.



16. **A hybrid "gated MTI"** has a single filter that replaces the pulse doppler filter bank. Only moving target spectral lines are accepted, but there is no velocity resolution.



17. **Range gating is necessary in a gated MTI** for the same reason as in a pulse doppler system. If the output of the single filter is sampled in sequence, the radar video, with the clutter signal eliminated, can be reconstituted.

Digital designs for MTI[1,6,7]

The capability of present day, high-speed, digital processing hardware has made it possible to build digital equivalents to both the analog MTI and pulse doppler. Signal amplitude samples to be processed are converted to digital numbers. These numbers are stored and retrieved, weighted, combined and so on, just as digital entries might be handled in a general-purpose computer. Once completed, the processing system has the reliability, precision, repeatability and flexibility that are characteristic of the digital computer. The processing system comprises, in fact, an analog-to-digital (A-D) converter and usually a high-speed special-purpose digital computer which operates in real time. Ordinarily, the input to the A-D converter is the bipolar video from

the synchronous detector of Fig. 11. In a digital MTI (DMTI), Fig. 18, the output of the synchronous detector is sampled at least once during each effective pulse length. The sampled voltage is converted to a digital word in a high speed A/D converter, stored in a conventional digital store and subtracted from the sampled synchronous detector output one prf interval later.

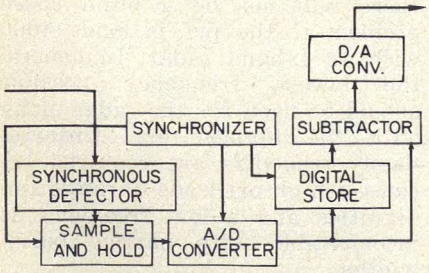
If the target has not moved, the digital number does not change and the output of the subtractor is zero. If it has moved, the second digital number is different from the previous one, the output from the subtractor is non-zero and a pulse appears on the display after being converted back to analog. A D/A converter restores the analog form of the signal for feeding a conventional display.

Figure 18 is the exact digital equivalent of an analog two-pulse MTI canceller. This circuit can also be considered as a filter with the frequency response of Fig. 13. The notches remove the clutter signals that appear about the prf lines in the received spectrum.

This operation requires delaying the signal just as the analog delay lines of the classical MTI do. However, because it's now digital processing, the samples can now be delayed for long and precisely controlled periods of time. The A/D converter is the heart of the circuit. It must convert each analog sample to a 10-bit-word (or of that order) at a rate set by the pulse length, i.e., at a 1 to 10 MHz rate. The timing between the transmitter pulse and the sampling pulse is critical but after the information has been digitized, the problems are relatively easy.

The number of bits in the A/D conversion determine the faithfulness with which the output of the

(continued on next page)



18. **Digital equivalent of a delay line MTI** performs the same functions: the output of the synchronous detector is sampled at a particular time corresponding to a particular range. The analog sample is converted to a digital number and stored to be compared one prf later with the next sample.



the source of many faces...

Our versatile Model PH40K Pulsed Signal Source wears many simulator faces: Transmitter, Radar, TACAN, IFF, DME. And you don't really have to change front panels. Just plug in an RF oscillator head for the frequency range you need. Standard heads available covering various ranges from 150 to nearly 25,000 MHz. With guaranteed minimum peak powers as high as 40 kilowatts. Internal pulse generator. Continuous metering. A dependable, self-contained source of pulsed RF power for your simulator application. For detailed specifications or information on special instruments/heads customized for your requirements, call or write

Epsco INCORPORATED

APPLIED MICROWAVE DIVISION
411 PROVIDENCE HIGHWAY, WESTWOOD MA 02090
(617) 329-1500 TWX (710) 348-0484

READER SERVICE NUMBER 41

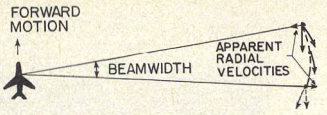
synchronous detector is reproduced and, hence, eventually the cancellation. The only critical item is the timing relationship between the transmitter pulse and the sampling control of the A/D converter. Once past this point, all processes are carried out with the precision of a digital computer.

By extension, any (n) pulse MTI canceller with or without feedback can be synthesized. In fact, since the individual samples can be stored and recovered at precise times (and weighted if necessary), very complex processing can be carried out without any of the stability problems encountered in analog systems. A staggered prf can be destaggered with ease so that the most complex prf programming called for to smooth out the velocity response can be accommodated.

Pulse doppler uses algorithms[1]

The digital equivalent of a bank of relatively narrow band filters is used in a digital pulse doppler system, with digital processing resolving the targets in velocity. The main advantage of digital pulse doppler over the analog equivalent is that the very large number of required filters is eliminated and replaced by specialized processing. The digital implementation is, however, faced with a time problem in this processing. It's the equivalent problem of the sheer numbr of filters in the analog version. (The tradeoff depends on range resolution and range. A long range, 10 μsec pulse radar is better served by digital processing. On the other hand, a 10 mile, 0.1 μsec radar demands too high a speed for the processor and should look to an analog solution).

All the received radar pulses, after A/D conversion, must be grouped into range bins for further processing. Each bin is then submitted to a Fast Fourier Transform (FFT) algorithim. Special algorithims and special processors for implementation of the FFT, have been developed to provide a manageable solution. The Cooley-Tukey algorithm for implementation of the FFT defines a set of recurring or "recursive" operations to obtain the Fourier Transform of discrete samples. The number of recursive equations depends on the number of samples, i.e., pulses to be processed. If there are N pulses and if $N = 2^m$ where m is an integer, then m recursive operations must be carried out. Cascaded processors have been developed specifically to carry out this FFT and take advantage of certain computational simplicities of the Cooley-Tukey algorithm.



19. **If a radar platform is moving,** the apparent motion of the clutter will result in apparent closing or opening radial velocities. The amount is dependent on the clutter position within the radar beam. For a motion of say, 400 knots and a beamwidth of four degrees, apparent radial velocities of ±14 knots will result when the beam is at a right angle to the direction of motion.

Practical performance limitations

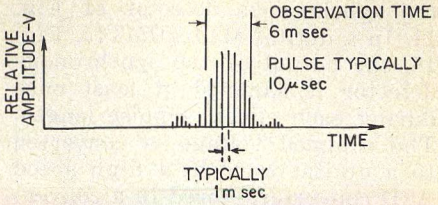
If a target has some random motion associated with it (for instance, rain turbulence), its spectrum lines will be broadened to a finite bandwidth. Typically ±15 knots at L-band, will spread a line ±50Hz. The same effect also results from the observation of stationary clutter broadside from an aircraft, Fig. 19, where there is a spread of radial velocities of the clutter over the radar cell.

Similarly in a scanning search radar, target returns will be modulated by the antenna pattern, Fig. 20. The target lines are broadened by the reciprocal of the observation time—during which the target is illuminated by the radar.

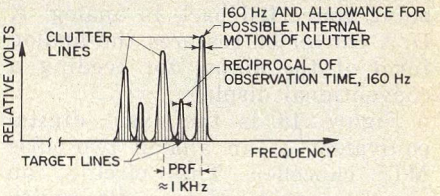
Broadening of the clutter spectral lines means that the clutter notches will have to be relatively wide, and this will attenuate some of the wanted target energy particularly if this target has a low radial velocity or is near a blind speed. The MTI's response will have to be a compromise between accepting too much clutter energy or having a minimum velocity cutoff that is too high.

Instabilities in the radar itself also cause the individual lines to spread. The overall resultant effect, detailed in Fig. 21, shows that a certain amount of overlap of the spectral components of the clutter and the wanted target occur. It is not always possible therefore to separate them completely.

Another problem associated with the simple radar designs discussed so far is that of velocity blind zones. As the closing velocity of a target increases, its spectral lines, such as shown earlier in Fig. 7, will shift over to



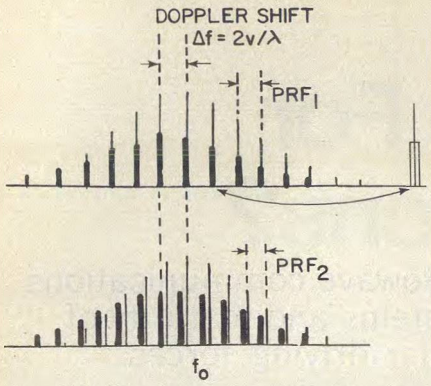
20. **With a stationary-scanning search radar,** target returns are modulated by the antenna pattern. Spectrum lines are broadened proportionally to the reciprocal of the observation time in the same way that the width of the overall spectrum corresponds to the reciprocal of the pulse length. In this case a 1 degree beamwidth radar is rotating at 30 rpm.



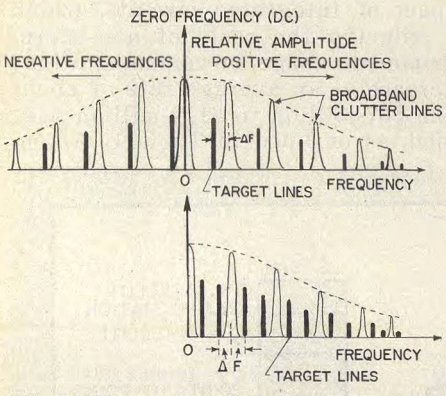
21. **Portion of complete spectra** shows how target and clutter lines are broadened by various instabilities of the radar system.

the right. When the doppler shift corresponds to the prf, the target lines will coincide with the clutter lines. When this occurs, the target is inseparable from the clutter. Since $\Delta f = 2v/\lambda$, the first blind speed, occurs when $v = 1/2$ (prf) λ; the second blind speed will then occur when $v =$ (prf) λ and so on. At L-band and with a prf of 1 kHz, blind speeds will occur at n · 300 knots where (n) is an integer. To get around this, the product (prf) · λ must be chosen so that the first blind speed is greater than the highest radial velocity likely to be encountered in practice. For instance, if the highest target speed is 1200 knots, there will not be a blind speed problem if the prf is made 4000 with an L-band radar. In general the lowest frequency possible should be used for the radar along with the highest prf. Unfortunately tradeoffs are required because a high prf leads to range ambiguities and a low frequency is incompatible with narrow beamwidths.

The problem can be alleviated by varying the interpulse period so that the target can be seen on at least some of the pulses, Fig. 22. This is, unfortunately, not easy to implement with a simple analog MTI system since it requires switching delay lines.



22. **Blind speeds,** result when the doppler shift corresponds to the multiples of the prf, with target lines coinciding with clutter lines. By varying the prf, line spacing can be changed so that a blind speed condition at prf_1 doesn't occur at prf_2.



23. **Folding over the spectrum at zero i-f,** allows two target spectral lines (in color) to exist in each interval between clutter lines. Unambiguous velocity measurement is only possible for a doppler range corresponding to half the prf.

As mentioned earlier, most MTI systems use a synchronous-detector to translate the received spectra to zero frequency. In this case, the lines of the spectra fall on either side of zero with the negative-frequencies being indistinguishable from the positive frequencies. The resulting spectra are, therefore in effect, folded over, as shown in Fig. 23 with each moving target having two lines, symmetrically disposed, in each prf interval. Target radial velocity can, therefore, only be determined without ambiguity over half the previous range since there is no way of distinguishing between the two lines. At the same time, the noise density is also doubled and the signal-to-noise ratio at the output of each filter is 3 dB worse. System implementation at this frequency may, however, be easier.

(continued on p. 67)

THE SMALLEST OCTAVE BANDWIDTH CIRCULATORS EVER BUILT

(In stock now)

TRAK octave bandwidth circulators represent the state-of-the-art in miniaturization of broadband ferrite components. Each unit is magnetically shielded and features stable performance and exceptional reliability since the number of component parts has been minimized.



TRAK unit shown actual size as compared with competitive units.

	2-4GHz	4-8GHz
	Model No. 1450-1300-1	Model No. 1450-1600-1
ISOLATION:	18 db minimum.	18 db minimum.
INSERTION LOSS:	0.5 db maximum.	.5 db maximum.
VSWR:	1.30 maximum.	1.30 maximum.
OPERATING TEMPERATURE:	−10° to +70° C.	−45° to +95° C.
SIZE:	1″ x 1″ x .625″ (nominal).	.75″ x .75″ x .5″ (nominal).
WEIGHT:	2.000 ounces (nominal).	1.1 ounces (nominal).
CONNECTORS:	SMA female.	SMA female.

For further information contact TRAK Microwave Corporation, 4726 Eisenhower Boulevard, Tampa, Florida 33614. Telephone (813) 884-1411. Telex 52-827.



LITERATURE PRICES QUOTATIONS

READER SERVICE NUMBER 43

Economic Forecast: Part 1

What's The Future For MW Communications?

Recovering from the current slowdown, microwave communications will resume a strong growth rate. Satellite systems and maturity of today's state-of-the-art devices will be the major driving forces.

This article is the first of a three part series forecasting the economic future of important segments of the microwave industry. Parts two and three will concentrate on government electronics and ECM.

FOLLOWING the output pattern of many other industries, the United State's production of microwave equipment for commercial communication applications declined in the turbulent economic conditions of late 1974. On the basis of computer-modeling techniques (see box), it is safe to conclude that this shrinkage will continue through the first half of 1975. But projecting these economic models further into the future reveals that production should slowly recover during the second half of this year, pick up momentum, and resume strong growth in 1976. This momentum should carry the level of equipment production to a record of $381-million in 1978, rising from the 1974 level of $285-million at an average annual growth rate of 7.2%.

The overall growth in demand for microwave communications equipment will be driven primarily by the 15% annual growth of the data communications market. Data transmission channel requirements will exceed voice telephone demand by 1979, although voice channels also will continue to expand.

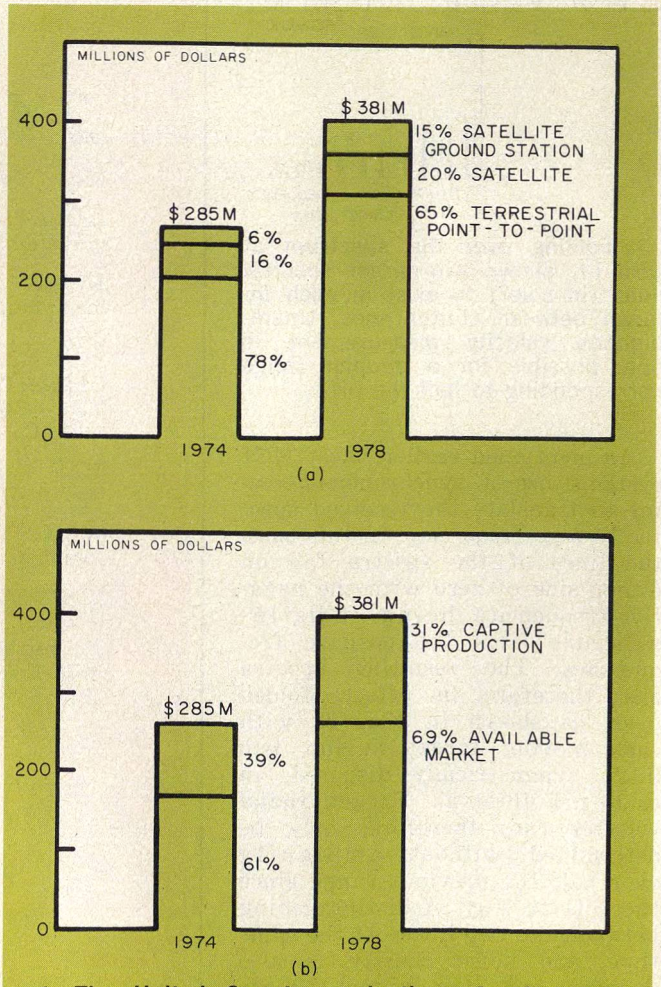
Captive production of microwave communications equipment, predominantly by Western Electric with $103-million or 39% of the 1974 production total, will be a declining factor in overall demand, as outlined in Fig. 1(b). Thus, the available market will grow faster than the overall industry average at a rate of 11.2% per year. This available market expansion will be fueled by the burgeoning demand for satellite communications and for private and specialized common carriers.

Although terrestrial point-to-point systems will continue to lead the communications industry in microwave equipment users, most of the equipment production growth over the 1974-1978 period will be due to increased satellite communications demand, as shown in Fig. 1(a). Commercial microwave communications satellite production will increase from $45-million to $77-million over the 1974-1978 interval, for an average growth rate of over 12% per year. Satellite ground station production will grow at 32% per year, from $19-million to $57-million over the same period. Interestingly, over half of the satellite-related production will be for export.

Jeff D. Montgomery, Vice President, Gnostic Concepts, Inc., 2710 Sand Hill Road, Menlo Park, CA 94025.

Amplifiers will pace component growth

In the next three year period, microwave component usage will grow faster than the production of the communications equipment. This is due primarily to the impact of integrated circuits, which are substantially reducing the costs of non-microwave circuits. Component usage in communications equipment will increase at an average rate of about 14% per year, from $67-million to $114-million over the 1974-1978 period, as outlined in Table 1. Anten-



1. The United State's production of microwave communication equipment will grow by about 22% from 1974 to 1978 (a). The available market (b) will grow faster, fueled by a growing number of Bell system competitors.

Mapping the future

This economic forecast is derived by computer modeling techniques which take into account overall economic (macroeconomic) forecasts, historical data, technical trends and backlog. The macroeconomic forecasts are provided by Chase Econometric Associates, Inc., a subsidiary of Chase Manhattan Bank

Component forecasts are based upon extensive interviews with equipment designers, component buyers and producers. These interviews help establish the relationship between each class of equipment surveyed, and the individual components used in the production of the equipment. The total component demand is then defined and forecasted by input-output methodology, whereby all component production is accounted for by considering the sum of OEM use in marketable equipment, plus all components manufactured for non-production uses such as replacement parts, R&D and inventory level change. The demand forecasts for devices and materials used in the production of components are similarly derived from the component forecasts.

Each quarter, Gnostic Concepts forecasts the production of over 400 categories of electronic and electrical equipment. A comprehensive, 1,400 page **Microwave Component Forecast** is one of the most recent publications. ••

na system demand, driven by satellite ground stations and specialized common carrier requirements, added $37-million to the 1974 overall communication systems market, but will expand its segment to $63-million in 1980.

These figures do not include components manufactured for non-production uses such as replacement parts, R&D projects and inventory level change. Inventory build-up was a substantial contributor to the market growth in 1973, and inventory trimming is a major factor in the 1974-1975 slackening of demand.

Discrete circuit solid-state amplifier use in communications equipment will triple, from $17-million to $51-million over the 1974-1978 period, reflecting an average annual growth rate of 32%. The demand for solid-state oscillators will grow less dramatically, increasing at 4.6% per year to a 1978 figure of $18-million.

One of the major forces behind the projected 32% annual growth in amplifier usage will be the exploitation of new amplifier designs including gallium arsenide field-effect transistors, low-noise amplifiers, low-cost solid-state paramps and C-band bipolar transistor power amplifiers. The usage of GaAs FET amplifiers alone will grow at over 70% per year, reaching $2.4-million in 1978. While Avantek and Watkins-Johnson are the early competition, several other companies will offer GaAs FET amplifiers by 1978. A side benefit from the growing use of low-noise front ends will be the ability to use smaller antennas.

Solid-state power amplifiers offer an even more exciting potential with communications demand more than tripling from $12-million to $39-million, a growth rate of about 35% in the 1974-1978 period. Solid-state power amplifiers will impact TWT use in newly designed equipment operating in L through C bands. According to the computer forecasts, the leading suppliers of communications TWTs will continue to be the current leading medium power tube manufacturers, Hughes and Varian. Substantial retrofit of Impatt amplifiers by Western Electric will hasten the demise of communications TWTs.

Microwave-integrated circuit use in communications equipment, led by Collins and Raytheon, will expand rapidly from $3.9-million in 1974 to $10.3-million in 1978. MICs increasingly will bite into the discrete circuit amplifier and oscillator markets in the late 1970s. Over 70% of this production will be captive either at the OEM or at the device (semiconductor) producer. This will bring increasing pressure on current component producers who buy devices, fabricate components and sell to OEMs.

Common carriers lead demand

The majority of microwave components produced for communications applications will continue to find their way into terrestrial point-to-point relay systems. Although this market will remain the leader in component demand, terrestrial usage will increase at the snail's pace of 2.5% per year, reaching a level of $247-million in 1978. Keep in mind that this growth is in terms of current dollars and is less than the forecasted inflation rate which will average 6.4% over the three-year period.

The slackening in terrestrial point-to-point equipment demand will be due to several factors:

- Much of the basic microwave plant is already installed, and future channel growth often can be achieved by expanding existing plant at a lower incremental cost per channel.
- "Brick and mortar" (buildings and real estate) requirements will gain a growing share of the available telephone company investment dollar due to their more rapidly rising costs.
- Available expansion funds will be stringently limited due to high interest rates, although rates may drop some over the 1974-1978 span.
- A large share of telephone company electronics spending over the next several years will be for improved signal processing and handling, including major expansion into electronic switching systems and improved interconnection subsystems.

Currently, Collins is the leading independent producer of terrestrial point-to-point microwave equipment with about 35% of the available market. Farinon is a strong contender, with GE, Motorola, RCA, Raytheon and Microwave Associates also participating.

Specialized common-carrier expansion encouraged by FCC rulings which opened to competition both

(continued on p. 48)

Table 1: Component use in microwave communication equipment production

Microwave component	Usage ($ Million) 1974	1978	Average annual growth (%)
Tubes	9.4	2.5	−40
Antenna systems	37.4	62.5	13.8
Discrete circuit amplifiers	17.4	50.5	31
Discrete circuit oscillators	12.8	18.3	9.8
MICs	3.9	10.3	27.5
Passive components & modules	23.4	32.2	8.7
Total	**104.3**	**176.3**	**13.8**
Components, less antennas	66.9	113.8	14.0

interconnection and point-to-point transmission services, was a significant factor in 1973 communications equipment production. Although common-carrier applications constituted 77% of terrestrial point-to-point equipment produced in 1974 (Fig. 2), equipment shipments plummeted last year. Recovery will be modest in 1975, but strong growth is expected to resume in 1976. Specialized common-carrier demand has created a substantial upward shift in the available microwave market since over 55% of point-to-point equipment produced through 1972 was captive at Western Electric and GTE/Lenkurt.

Changes seen at Bell

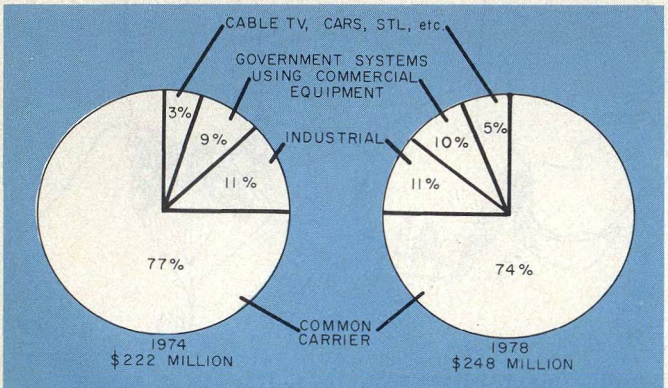
The Bell System, including the Bell operating companies plus AT&T Long Lines, dominates common-carrier mircowave and therefore deserves special attention. While specialized common carrier, independent telephone companies and expanding private systems will continue to chip away at Bell's control, Ma Bell's dominant position looks secure through the 1970s. But competition has awakened Bell, and the ponderous giant is now battling on many fronts.

As a result, major changes in the Bell System's operating philosophy are now underway and will continue to evolve. Stepped-up public relations campaigns and revised pricing schedules are two obvious responses to increased competition, but more subtle changes are being precipitated by onrushing, accelerating technology, the growing difficulty of acquiring capital and new transmission demands such as facsimile, data communications and the long-tauted Picture-phone.

Historically, Bell Labs typically devoted a decade or more to the development of any significant new piece of equipment. After this development stage, it generally took Western Electric several years to phase the design into volume production, which continues over the equipment life span of 20 to 50 years. This cautious design process typically resulted in equipment that reliably met the needs of most subscribers, but that lagged substantially behind the latest available technology and was expensive to produce.

In contrast, the typical design cycle of leading competitors in the data communications field is three to five years, and typically the product is in service for about ten years before it is rendered hopelessly obsolescent by newer technology.

Technological obsolescence is a meaningless term in a monopoly. Competition, however, has pushed Bell into a new way of life. To blunt the penetration of



2. Common carriers will continue to dominate the demand for terrestrial point-to-point microwave communications equipment.



3. State-of-the-art amplifier designs and MICs will nudge out older components in many applications. The demand for communication TWTs will drop some 40%.

specialized common carriers and interconnect equipment producers, the Bell system has substantially shortened their design and production starting cycles. To accomplish this without a major expansion of the technical staff and production facilities, Western Electric increasingly is depending on outside suppliers for components, especially specialty and small quantity requirements. Nearly all of Western Electric's state-of-the-art microwave semiconductor device, oscillator, amplifier and MIC production, however, will remain captive with older devices and components bought outside.

Indications are that the current efforts by the Federal government to break Western Electric away from the Bell system are likely to succeed, pushing this huge captive producer into the competitive marketplace by 1980. Over the shorter term, Western will try to become more cost competitive through more realistic make or buy decisions on components and subsystems.

The Bell system has monopolized major metropolitan areas and long haul transmission between these areas leaving the rural countryside to about 1,800 independent telephone companies led by General Telephone and Electronics. As residential, commercial and industrial communication demands continue to accelerate in the suburbs, while major urban areas become relatively saturated, the independent companies will achieve more rapid growth, especially in microwave transmission capabilities. These companies have traditionally depended heavily on GT&E subsidiaries for equipment, but increasingly will turn to the newly competitive outside market.

MCI and Datran have been the leading contenders in the specialized common carrier market. MCI has been offering relatively conventional voice and data communication service, using off-the-shelf equipment. Conversely, Datran proposed digital data transmission only, using new-generation time division multiplex units. MCI plunged ahead with network installation, producing a rapid build-up in the 1972-1973 available market for microwave transceivers

and related components. The capital crunch, however, forced a major stretchout in MCI plans, with the result that much of the equipment delivered in 1973 is not being installed until 1975.

A major part of MCI microwave procurement over the 1976-1980 period will be for expansion of capacity of present links, with less emphasis than originally planned on extending new routes. Datran, meanwhile, reportedly has been crippled by both the capital shortage and unanticipated difficulties in development of their new generation equipment. When Datran requirements finally surface in 1976-77, they will be met mainly by Japanese imports.

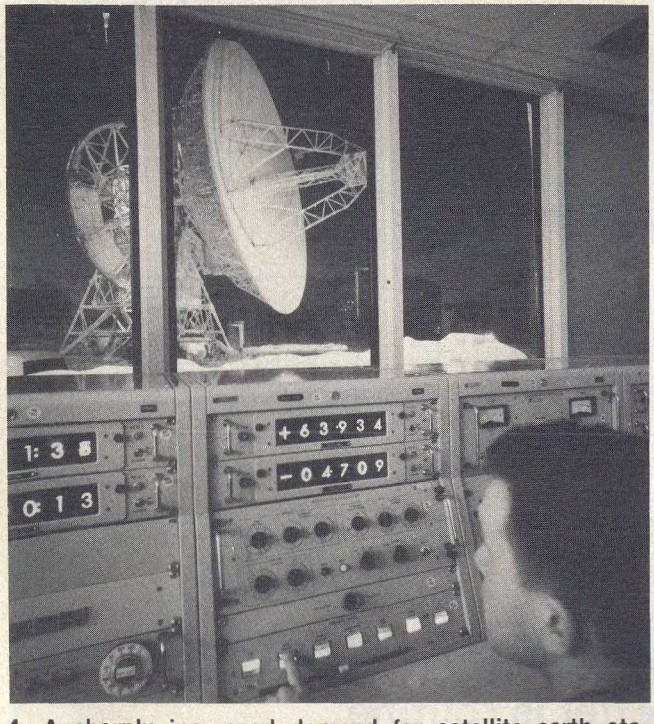
By the early 1980s, competitive pressure will force specialized common carriers to consolidate into two or three national networks, each consisting of interconnected subsidiaries or affiliates. MCI and Western Union will be among the survivors. Private system operators, such as Union Pacific, can profitably pursue the regional markets, however, they will not find it economical to pursue, independently, the national connections desired by many of their customers.

Satellite communications market mostly export

Ground terminal export was the main constituent of 1974 U. S. production demand and will remain so as the total market accelerates from $19-million in 1974 to $57-million in 1978 as noted in Fig. 5. Philco-Ford, Hughes and ITT are the giants contending for this market, challenged by the small but rapidly growing Comtech. While U. S. leading edge technology has given domestic producers a commanding early position in this marketplace, Japanese and European competition will become increasingly severe over the next half decade.

International or domestic, earth terminals will represent the main U. S. demand over the next five years. Only a few, but very large and expensive, stations will be installed in 1975-1976, but numerous small installations for cable television and similar applications will become significant in 1977-1980.

(continued on p. 53)



4. A sharply increased demand for satellite earth stations will be a major factor in the 1974-1978 production picture.

Precision Radar Calibration
with

TARGET SPHERES

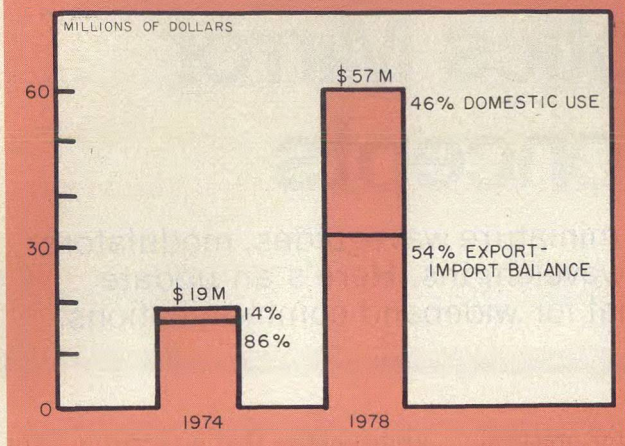
from

UMSCO

a pioneering
leader in the field



READER SERVICE NUMBER 49



5. The number of satellite earth stations exported will continue to be a large fraction of the number produced, but much future growth will be due to domestic applications.

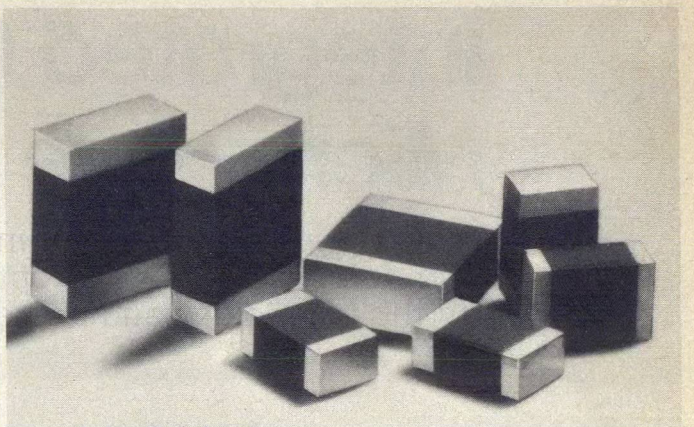
United States commercial communication satellite production, although down by about 15% in 1974 compared to 1973, will rebound strongly in 1975 with continued steady growth through 1978. The average growth rate over the 1974-1978 span will be 14%, from $45-million in 1974 and $65-million in 1975 to $77-million in 1978. But it's important to note that this overall modest growth rate masks two significant opposing trends, and therefore provides a poor indication of the magnitude of production growth.

Communication satellites are rapidly growing more complex, tending to push prices upward. The number of transponders will be multiplied, antenna size increased and multiplexing will become much more complicated. On the other hand, component and subsystem prices are dropping rapidly as the technology matures, tending to push prices down. Much of the early satellite component costs, often on the order of 90%, consisted of qualification testing, documentation, establishment of adequate production facilities and other software and starting costs. As production proceeds, these costs are dropping dramatically.

The net result of these two trends is a significant downward trend in the average unit price of communication satellites. This will partially offset the strong growth in quantity produced.

The leadership of U. S. companies in satellite design and in launch vehicles has resulted in a virtual monopoly—a situation that will continue over the next half decade. Interestingly, the leading producers of communications satellites are Philco-Ford and Hughes, rather than leading terrestrial microwave equipment producers such as Collins and Western Electric or military satellite leaders such as RCA and TRW.

The International Satellite System (INTELSAT) has accounted for most satellite and associated ground station production to date. Most of this communications demand, after the initial flurry, has centered in countries with little or no national communications network. Many of these countries, leapfrogging over a century of transmission evolution through wire, coaxial cable and terrestrial microwave are going directly to national satellite communication. The tapping of this vast market has just begun and will continue through the next five years and beyond. ••

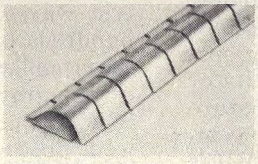


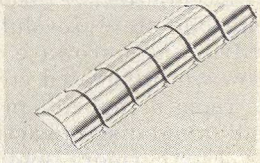
HIGH Q
CHIP CAPACITORS

High Q multilayer capacitors feature very high quality factors at microwave frequencies. Superior dielectric properties and structure permit operation at high voltage and high current at microwave frequencies through the full temperature range with minimum dielectric loss. Offered in 4 standard sizes from .040" x .030" to .125" x .095". Applications include UHF-microwave hybrids and MIC's.

Johanson
Monolithic Dielectrics
Box 6456 / Burbank, California 91505
(213) 848-4465 / TWX 910-498-2735
READER SERVICE NUMBER 53

When RFI problems get sticky,
try stickyfingers®
Attaches faster, shields better than anything else!


SERIES 97-500 The original Sticky Fingers with superior shielding effectiveness.


SERIES 97-520 A smaller size strip; highly effective in less space.


SERIES 97-555 New Single-Twist Series for use when space is at a premium. Measures a scant 3/8" wide.


SERIES 97-560 New 1/2" wide Double-Twist Series, ideal for panel divider bar cabinets.

Now you can specify the exact type beryllium copper gasket that solves just about every RFI/EMI problem. Perfect for quick, simple installation; ideal for retro-fitting. Self-adhesive eliminates need for special tools or fasteners. Write for free samples and catalog.



INSTRUMENT SPECIALTIES COMPANY, Dept. MW-57
Little Falls, N.J. 07424
Phone—201-256-3500 • TWX—710-988-5732
READER SERVICE NUMBER 54

Part I:

Integrated Optics Mirror Microwave Concepts

A new revolution is beginning in miniature waveguides, modulators and detectors . . . but at optical wavelengths. Here's an update on the technology and its potential for wideband communications.

This is the first of a two-part article on optical communications. This installment describes some of the hybrid systems that have been developed. Next month, advancement in integrated optical circuits will be covered.

OVER the past quarter century, the transistor and its descendant, the integrated electronic circuit, have revolutionized low frequency electronics and communications. This was accomplished, first, by replacement of the bulky vacuum tube with miniature semiconductor devices and then by integration of the transistor and other electronic devices into a single miniature circuit on a semiconductor chip. While solid-state microwave devices such as Gunn oscillators, Impatt diodes and varactors have made possible invaluable advances in microwave technology, no such solid-state revolution has occurred in the micowave region.

Microwave integrated circuits or MIC's[1] remain hybrid in nature with individual discrete active components. Furthermore, while MIC's are miniature, microscopic circuits can only be achieved at millimeter wave frequencies where the technology is awkward and signal transmission becomes difficult, particularly over long distances. However, because optical wavelengths are short ($< 1\ \mu m$), all optical systems components can, in principle, be made in microscopic form and integrated in a fashion similar to IC's. In addition, recently developed optical fibers with extremely low loss (1-2 dB/km), show promise as candidates for practical transmission lines. These IOC's and fiber optic cables may, in fact, replace microwave components in some communications systems of the future. The enormous bandwidth capability of IOC's, in the multi-GHz range, is the main impetus behind the development of integrated optical circuits. Many of the microscopic optical components being developed are functionally and conceptionally similar to microwave components. Indeed, integrated optics and fiber optics may furnish a microscopic microwave technology for tomorrow.

Fred A. Blum, Member Technical Staff, Adv. Components Laboratory, Texas Instruments, Inc., 13500 N. Central Expressway, Dallas, TX 75222.

More optics than integration

The field of integated optics was born in 1969, when a visionary article by Miller[2] of Bell Telephone Laboratories suggested using photolithographic techniques for the fabrication of complex optical circuits. It was proposed that coherent light could be trapped and circulated through channel dielectric waveguides. Since that time, hundreds of technical articles have been published carrying the banner of integrated optics. However, the bulk of the work has, in fact, dealt with discrete but microscopic optical components generally in the form of dielectric waveguides. For this reason, integrated optics may be characterized as has the older field of optical communications over the past decade: *much optics with little integration.* Nevertheless, many novel active and passive devices have evolved in an endeavor to fabricate actual IOC's. These include surface laser sources, waveguide electro-optic modulators, waveguide photodetectors, directional couplers and grating couplers. The real problem that lies ahead is that of fabricating a number of these devices in compatible material systems and integrating them onto a single circuit.

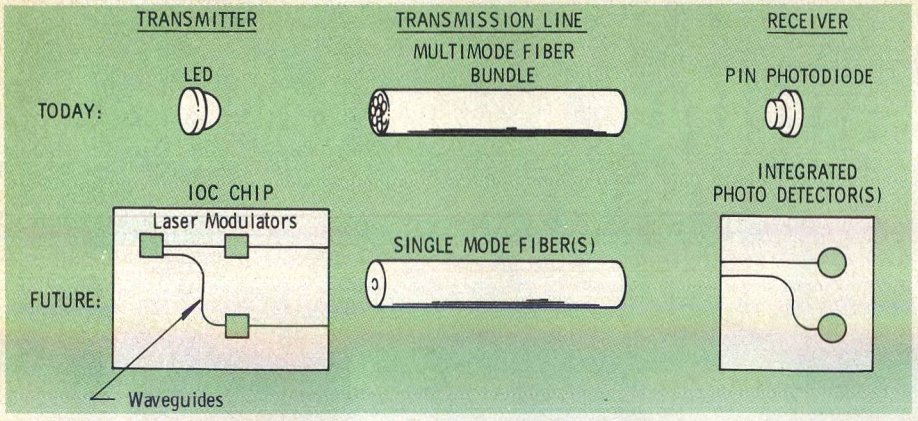
One big breakthrough for integrated optics that occurred in 1970 at the Corning Glass Works, Elmira, NY, was the development of low-loss fiber optical transmission lines[3] with losses as low as < 20 dB/km. Since 1970, Corning[4] has obtained losses of approximately 2 dB/km at 0.83 μm and 1.05 μm. More recently, researchers at Bell Telephone Laboratories[5] have reported a loss of 1.1 dB/km at 1.02 μm. Such a low loss is phenomenal for a transmission line at any freqency.

Table 1 gives for comparison the nominal attenuation in decibels per 100 ft of several coaxial and rigid waveguide transmission lines. The frequency range covered is 1 MHz to 10 GHz, where it's expected to be easiest to modulate optical sources in the foreseeable future. For the optical fiber, the carrier frequency (approximately 10^{14} Hz) is essentially infinite and the relevant limiting bandwidth is the modulation rate. The fiber loss is, of course, independent of the modulation rate as shown in Table 1.

(continued on p. 56)

Table 1. Transmission Line Attenuation In Decibels Per 100 Ft.

Transmission line	Frequency (GHz) 0.001	0.1	1	10
Optical fiber	0.06	0.06	0.06	0.06
Rigid copper coax (6-1/8 inch diameter)	—	—	0.2	0.5
Coax RG-19/U (1.1 inch diameter)	—	0.7	4.0	18
Coax RG-58/U (0.2 inch diameter)	0.4	2.0	5.0	100
X-band waveguide	—	—	—	4.0



1. **Expected design of a fiber-optic communications link** would evolve from the discrete components to the integrated system of future.

The advantage of fibers over other transmission lines is particularly noticeable at high frequencies.

IOC-fiber optic systems limitations

The fundamental components of an optical communications system are functionally the same as those of a microwave system[6]. Transmitters, receivers, repeaters and a transmission medium are needed. The difference lies in the components themselves. These components must generate, modulate, transmit and detect optical waves —in which optical photons replace moving electrons in the system. In the near term, practical engineering limitations are the discrete incoherent LED's for sources, Si photodiodes for detectors and multimode optical fibers for the line, as shown in Fig. 1. These are the only miniature components commercially available in reasonable quantities. In the future, lasers and/or IOC's will be used with single-mode fibers. The evolution from incoherent to coherent optics is a natural one dictated largely by the current state of diode emitter technology. LED's have the disadvantage of being slow (response time 5 ns), having a power output of just a few milliwatts and with a large spectral width (0.03-0.04 μm) and beam divergence. The slow response time limits the useful data rate to under 100 MHz. The large spectral width leads to increased pulse dispersion which in turn limits the data rate. And finally, the large beam divergence makes it more difficult to efficiently couple their outputs into fibers. Input coupling losses for low-loss fiber bundles can be as high as 20-25 dB.

On the other hand, semiconductor lasers have been modulated at rates in the gigahertz range. Their emission is limited to a narrower cone and their spectral bandwidth can be one to two orders of magnitude smaller. Also, as much as 30% of the output of a GaAs diode laser has been coupled into single mode glass fibers. However, room temperature cw diode lasers are not readily available. In fact, only recently have researchers obtained laboratory lifetimes of a few thousand hours for selected lasers. No equivalent evolution is anticipated for optical detectors since incoherent detection appears adequate and state-of-the-art PIN and avalanche photodiodes have sufficient speed and sensitivity for most applications now envisioned.

The expected bandwidth evolution for optical communications systems is given in Table II. In progressing from LED's to integrated lasers, data transmission rates in the 1 to 10 GHz microwave range should become possible.

IOC's: Advantages are many

Ultimately the optical pulse generation, detection and processing will be accomplished by IOC's performing complex multiplexing and switching operations with optical waves. These IOC's will be manufactured using a fabrication technology very similar to that now used for digital IC's. They will be rugged, cheap and efficient. Additional technical advantages include:

- Small size, lightweight components
- No crosstalk, pickup—EMI/EMP free
- Noncritical materials—no copper needed
- Immense bandwidth (in the multi-GHz range)
- No grounding or short circuit problems
- Secure, covert, difficult to monitor
- Low-loss transmission
- Low power requirements using IC/IOC technology

The small size advantage is apparent and stems from the short wavelength ($\sim$ 1 μm) the radiation. (Note: Green light has a 1/2 μm wavelength and GaAs diodes emit in the near infrared at 0.9 μm). Typical multimode optical fibers have outer diameters of a few mils. Single-mode fibers have inner diameters of a few microns and their size is limited by convenience in manufacture and handling. The active devices themselves are small with dimensions measured in mils. The freedom from interference and pickup also stems from the shortness of the wavelength. Being made from a material other than copper will become an increasingly important advantage as the world's copper supply is depleted. Since the carrier frequency is so high, the available bandwidth is essentially infinite relative to present communications systems.

Table 2. Bandwidth Evolution of Optical Fiber Communications Systems

Source	Fiber type	Bandwidth
LED	Multimode	$<$100 MHz
Discrete laser	Multimode, single mode	$<$1 GHz
Integrated laser	Single mode	$<$10 GHz

The real limitation is the ability to modulate the carrier and to transmit that modulation without loss of information. Also, since the nonconducting fibers provide excellent electrical isolation, they're not suitable for transmitting power on the line. As a result, many applications will probably involve hybrid cables containing both fibers and twisted pairs.

Optical fibers

The concept of fiber optics is an old one stemming from the notion of a "light pipe."[7] However, it is only in the last 25 years that the development and application of optical fibers have received much attention. And only in the last five years, marked by the achievement of low-loss transmission, have fibers become widely recognized as transmission lines. The trapping of light in a fiber results from the phenomenon of total internal reflection, Fig. 2. When a light ray is traveling from the more dense core (optically) to a less dense cladding, it is transmitted into the cladding only if the angle the ray makes with respect to the interface normal is sufficiently small. Other wise, the ray is totally reflected by the core-cladding boundary. The critical angle is given by Snell's

law of refraction, which yields

$$\theta = \sin^{-1}(n_1/n_2) \quad (1)$$

where n_1 and n_2 are the indices of refraction and $n_1 < n_2$.

Note that the larger the difference between n_1 and n_2, the smaller θ is, and transmitted rays are restricted to a narrower cone of incidence. Multimode fibers have large core diameters, about ten times larger than those of single mode fibers. For this reason, multimode fibers are easier to couple light into when dealing with a real source of finite area.

Note in Fig. 2, that of the light emitted by a point source, only that within a certain cone will be transmitted by the fiber. Light emitted outside this cone will escape. The sin of the half angle of θ_c of this cone is

$$\sin\theta_c = \sqrt{n_2^2 - n_1^2} \quad (2)$$

This quantity is called the numerical aperture (N. A.) of a fiber and is a measure of its ability to trap light emitted in an uncollimated beam. For small differences in the core and cladding indices

$$\text{N.A.} \approx \theta_c \approx \sqrt{2n\Delta n} \quad (3)$$

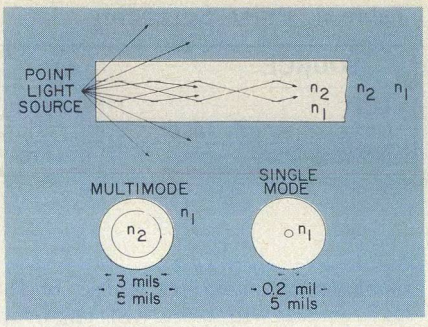
where $\Delta n = n_2 - n_1$. For an isotropic point source, the fraction of light trapped by the fiber is given by

$$\text{Fraction trapped} \approx \frac{(\text{N. A.})^2}{4} \quad (4)$$

Thus, the larger the N. A., the greater is the light-gathering capability of the fiber. Typical N. A.'s of three types of fibers are given in Table 3. The numerical aperture concept is particularly useful for LED, multimode fiber systems. Note from Table 3 that the lowest loss fibers, which make the best transmission lines are the hardest to couple into. For a fiber with a $(\text{N.A.})^2 = 0.01$ which yields a coutrapped from an idea Lambertian (emission :: cos θ) LED is $\approx$ $(\text{N.A.})^2 = 0.01$ which yields a coupling loss of 20 dB. (This loss was calculated ignoring the Fresnel reflection at the fiber end). Also, for fiber bundles, there is a coupling loss due to the geometrical packing fraction of the round fibers in a bundled array.

Coupling source to fiber a problem

The problem of efficiently coupling LED's to low-loss fibers is a serious one which has plagued current optical communications technology. Indeed, the general source —fiber coupling problem (for both incoherent and coherent sources)



2. **Fiber optics consist of a core** with refractive index n_2 and an outer cladding of lower refractive index, n_2. Together they collominate the light. Multimode fibers have larger core-diameters.

remains a significant difficulty seeking a clever solution. Two approaches which have reduced this coupling loss are: (1) the use of miniature spheres to act as a thick lens to reduce the effective emission cone size; and (2) custom shaping of LED's to make the material above the junction act as integral lens.

Optical fibers have been made from a variety of materials in various geometrical forms and are usually drawn from a macroscopic preform. Glasses which have been used include high-silica glasses. soda-lime glasses, lead silicates and borosilicates. For low-loss fibers, the index difference between the core and the cladding is achieved by doping the core with impurities. Liquid core fibers with losses < 10 dB/km have also been fabricated. These fibers consist of hollow cylindrical silica fibers which are filled with organic liquids such as tetracholorethylene and hexachlorobuta-1, 3-diene. Unclad, single material fibers (lowest loss $\approx$ 2.5 dB/km) have also been fabricated from high purity fused silica.[8] These fibers consist of a large annular cylinder which supports a thin diametrical slab which, in turn, supports a small cylindrical (or a rectangular) fiber at its center. The light is trapped in the small, central fiber which is protected from the outside world by the outer hollow cylinder. Finally, two glass clad fibers do not necessarily have the abrupt index boundaries shown in Fig. 2. The Japanese have developed a fiber in which the refractive index is continuously graded from the fiber center to its periphery[9]. The index gradient produces a lensing effect and these fibers have been named "Selfoc." Such index gradients reduce modal dispersion in multimode fibers and will prove extremely important in the development of long-distance fiber-optic transmission lines.

Table 3. Numerical Aperatures

Fiber Type	Loss (dB/km)	Δn	N.A.
Low-loss glass	<10	0.003-0.01	0.1-0.2
High-loss glass	>200	0.1	0.5-0.7
Liquid core	<10	0.07	0.5

The electromagnetic modes of an optical fiber are those of a circular dielectric transmission line and are similar to those of a circular metallic waveguide. However, the modes of the metallic guide can be separated into TE and TM sets, while those of the dielectric guide are hybrid modes. For multimode fibers, the number of modes supported increases with both N. A. and the core radius by

$$N = 2\pi^2 (r/\lambda)^2 (\text{N.A})^2 \quad (5)$$

where r is the core radius. For a fiber with $r = 40$ μm and N. A. $=$ 0.1 at $\lambda = 1$ μm approximately 300 propagating modes will exist. Each of these modes travels at a different group velocity. As a result, an input light pulse is distorted as it travels along the fiber. Ultimately, this pulse distortion due to modal dispersion limits the modulation rate at which one can transmit information down the fiber. The variation in the group velocities of the modes has two sources: (1) bulk material dispersion, i.e., change in the core refractive index with wavelength and (2) geometrical waveguide dispersion which depends on both Δ n and r. The material dispersion can be derived directly from the wavelength dependence of the index of refraction; and the pulse spreading Δ t is proportional to the fiber length L. For a source with a wavelength spread $\Delta\lambda$, it has the form

$$\Delta t \approx \frac{\Delta\lambda}{\lambda}\,\frac{L}{V_g} \quad (6)$$

where V_g is the group velocity. For low-loss, single mode guides, this material dispersion is dominant over the mode dispersion (Table 4). The geometrical modal dispersion

(continued on next page)

of a uniform core fiber is also proportional to the fiber length

$$\Delta t \approx \frac{\Delta\lambda}{\lambda}\frac{\Delta n L}{c} \qquad (7)$$

For graded index fibers (e.g., Selfoc), the ray focusing reduces the spreading with

$$\Delta t \approx \frac{\Delta\lambda}{\lambda}\frac{(\Delta n)^2 L}{c} \qquad (8)$$

The ideal parabolic index variation produces the smallest pulse spreading and, therefore, the highest bandwidth fiber. Equations (7) and (8) apply for uncoupled modes. For randomly coupled modes, the pulse spreading varies as the square root of the fiber length

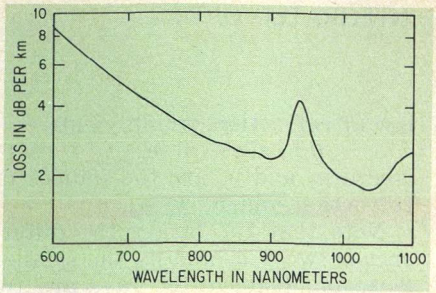
$$\Delta t \approx \frac{\Delta\lambda}{\lambda}\frac{\Delta n}{c}\sqrt{L} \qquad (9)$$

Mode coupling effects become very important for very long fibers. Thus, the higher the bandwidth needed, the shorter the transmission line and the narrower the spectral emission of the source must be.

The major mechanisms for losses of fibers are (1) material absorption and (2) scattering due to material imperfections and waveguide boundary roughness. Ionic impurities are the major source of intrinsic material absorption. The most troublesome of these is the OH^- radial which has a strong overtone peak near 0.95 μm. All low-loss fibers exhibit this peak in one form or another. Reduction of the size of this peak has received much attention since it occurs near the peak emission wavelength of GaAs lasers and LED's. Material scattering is predominantly Rayleigh scattering which are small compared to the wavelength. It varies as $1/\lambda^4$ and is slightly less than 1 dB/km at $\lambda = 1.0$ μm. The characteristics of a very low-loss graded index fiber are shown in Fig. 3.[5] Note that over the whole wavelength range covered, the loss is under 10 dB/km and the OH^- content of this particular fiber results in only a small peak. The background loss follows the Rayleigh curve. A uniform core fiber with a loss of 1.1 dB/km at 1.02 μm was also made which is surprisingly close to the Rayleigh scattering limit[5]. These fibers have been made in 1 km lengths in the lab and the chemical vapor deposition technique used is a simple one. ••

Table 4. Pulse Spreading

SOURCE	Δt
LED	1-5 ns/km
GaAs injection laser	100 ps/km
Nd:yag laser	20 ps/km



3. Loss of a very low graded index fiber is less than 10 dB/km over wavelength range. The small peak is caused by the OH content of the fiber.

References

1. Two special issues of IEEE Microwave Theory and Techniques devoted to MIC's have been published: Vol. MTT-16, No. 7, 1968, and Vol. MTT-19, No. 7, 1971.
2. S. E. Miller, "Integrated Optics: An Introduction," *Bell Sys. Tech. Journal*, Vol. 48, pp. 2059-2069 (September 1969).
3. F. P. Kapron, D. B. Keck, and R. D. Maurer, "Radiation Losses in Glass Optical Waveguides," *Appl. Phys. Lett.*, Vol. 17, pp. 423-25 (November 1970).
4. For a recent review, see F. L. Thiel and W. B. Bielawski, "Optical Waveguides Look Brighter than Ever," *Electronics*, pp. 89-96 (March 21, 1974).
5. W. G. French, J. B. MacChesney, P. B. O'Connor, and G. W. Tasker, "Optical Waveguides with Very Low Losses," *Bell Sys. Tech. Journal*, Vol. 53, pp. 951-954 (May-June 1974).
6. A recent and thorough review of optical communications systems research is given by S. E. Miller, E. A. J. Marcatili, and T. Lee, "Research Toward Optical Fiber Transmission Systems, Parts I and II." *Proc. IEEE*, Vol. 61, pp. 1703-1751 (December 1973).
7. W. B. Allan, *Fibre Optics*, London, Plenum Press, (1973); N. S. Kapany, *Fiber Optics*, New York, Academic Press (1967).
8. P. Kaiser, E. A. J. Marcatili, and S. E. Miller, "A New Optical Fiber," *Bell Sys. Tech. Journal*, Vol. 52, pp. 265-269 (February 1973).
9. T. Uchida, M. Furukawa, I. Kitano, K. Koizumi, and H. Matsumura, "Optical Characteristics of a Light-Focusing Fiber Guide and Its Applications," *IEEE J. Quantum Electronics*, Vol. QE-6, pp. 606-12 (October 1970).

Test Your Retention

1. What are three major advantages of optical fibers for communications applications.
2. Why is a laser better than an LED for coupling light to optical fibers?
3. What type of optical fiber has the smallest pulse spreading?

For next month, part 2:

4. How can you make a monolithic diode laser?
5. What is the most promising optical modulation technique?
6. Is coherent or incoherent detection required for most applications?



"If we take it in a bit here, it will be perfect"

DON'T SETTLE FOR A SHABBY DEAL

Amplifier Research can't sell you a suit of clothes. That's not our business. But if you need a reliable broadband amplifier, we probably have one that fits your needs -- with few if any alterations. We offer the world's largest selection of high quality RF power amplifiers -- from DC to 700 MH_Z and up to 5000 watts.

Send today for free short form catalog or call 215-723-8181.

AMPLIFIER RESEARCH

Amplifier Research
160 School House Road
Souderton, Pa. 18964

Your Best Source for RF Power Amplifiers

READER SERVICE NUMBER 58

RADAR CLUTTER

(continued from p. 43)

Another practical problem, encountered in a synchronous detector design is blind phase. A typical doppler frequency is usually about 10 to a few hundred Hz. However, a radar pulse is only a few microseconds long. The output of a synchronous-detector represents, therefore, only a very short sample of the doppler frequency and it is possible for the sampling to take place at the instant of zero phase of the doppler, thereby giving no output. This can be overcome by having in-phase and quadrature processing channels and recombining the outputs in a $\sqrt{x^2 + y^2}$ circuit.

In practice, internal system instabilities will also cause problems, that if not treated, will exceed the combined effects of all the factors listed above. Time jitter, amplitude jitter (some caused by such simple things as vibration from fans), stray pick up and hum can nullify the sophistication of the clutter reduction circuitry. ••

References

1. Merrill I. Skolnik, *Radar Handbook,* McGraw-Hill Book Company, New York, (1970).
2. D. Barton, *Radar System Analysis,* Prentice-Hall, Inc., Englewood Cliffs, NJ, (1964).
3. Fred Nathanson, *Radar Design Principles,* McGraw-Hill Book Company, New York, (1969).
4. L. Goetz, "Fundamentals of Pulse Doppler Radar," *Westinghouse Engineer,* (March, 1969).
5. Merrill L. Skolnik, *Introduction To Radar Systems,* (Section 4.4), McGraw-Hill Book Company, (1962).
6. Linden and Kutz, "Digital Moving Target Indicators," *Suppl. to IEEE Trans. Aero Space and Electronic Systems,* Vol. EAS-3, No. 6, (November, 1967).
7. *Linden and Taylor,* "Digital Technique Advance Tactical Radar," *Westinghouse Engineer,* (September, 1971).

Figures of merit for clutter reduction

Clutter-cancellation ratio indicates the amount by which the clutter is attenuated in an MTI system. Typical numbers are 30 dB for a two pulse canceller MTI and 40 dB for a three pulse canceller MTI. The figure can be much higher for a pulse doppler system—in excess of 60 dB.

The sub-clutter visibility factor is defined as the ratio at the input to the system of the clutter energy to the signal energy of a target when it is just detectable at the output in the clutter residue. The target is assumed to be moving at optimum speed, i.e., its doppler frequency places its lines half way between the clutter lines. Because it is difficult to define "just detectable" and due to the fact that the SCV ratio does not take into account the overall performance at all target speeds, a preferred figure of merit is the target-improvement factor. This is defined as the improvement in target-to-clutter ratio through the receiver processing, averaged over all target speeds.

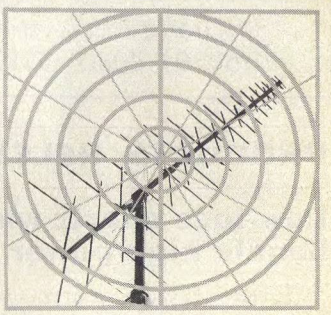
Typically, for a scanning radar with ten hits per beamwidth, this ratio is 18 dB for a two pulse canceller and 30 dB for a three pulse canceller.

When SCV claims for different equipments are compared, the methods of making the measurements as well as the conditions under which they were made must be closely examined. In fact, it is difficult to make a completely realistic measurement. Usually, this is carried out with a synthetic target moving at optimum speed over a block of real clutter with the antenna stopped so that the effect of antenna modulation is disregarded. □

Test your retention

1. Other than on the basis of doppler frequency difference, what techniques can be employed for reducing clutter?
2. What are the main problems associated with an analog-delay-line MTI?
3. What is the cause of a collapsing loss?
4. What condition would prompt implementing an analog pulse doppler over a digital design?
5. How do blind-speeds occur and how are they eliminated?





Turn on... Tecom Rotators

Now, Tecom Industries manufactures its own family of rotators and controllers to offer you a complete subsystem capability from one reliable source. Light, medium and heavy rotators bear up to 12,000 lbs. limited or continuous rotation, with speed variable from 0 to 2 RPM. Essentially backlash-free with readout accuracy better than 1 degree. All units are thermostatically heated for instant service in bad weather.

Several controllers are available, with storage scope and synchro dial indicators, displaying azimuth bearing within ±0.03 degrees and designed to MIL-E-16400.

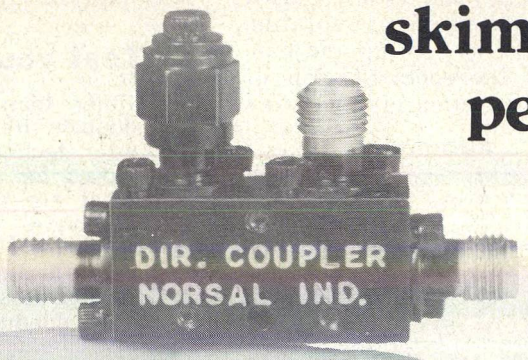
For complete rotatable antenna subsystems, call your Tecom technical representative.

TECOM INDUSTRIES INC.

9000 Owensmouth Ave.
Canoga Park, Ca. 91304
(213) 341-4010

READER SERVICE NUMBER 67

Norsals' Miniature Directional Couplers skimp on price, not on performance...$120.



Model	Frequency (GHz)	Directivity (dB min)	VSWR (max)	†Insertion Loss (dB max)	Price
4401	.5-1	25	1.10	0.2	$120
4501	1-2	25	1.10	0.2	$120
4601	2-4	22	1.15	0.2	$120
4808	2.6-5.2	20	1.25	0.2	$130
4701	4-8	20	1.25	0.2	$120
4801	7-12.4	17	1.30	0.3	$135
4881	7-16	15	1.35	0.3	$145
4861	7-18	15	1.35	0.3	$175
4901	12-18	15	1.35	0.3	$160

COUPLING VALUES; 6, 10, 20, 30 dB
†Excluding coupled power

NORSAL INDUSTRIES INC
34 Grand Boulevard Brentwood, N.Y.
516-231-4040 TWX 510-227-9865

READER SERVICE NUMBER 68

PRODUCTS RELEASED AT PRESSTIME

Low-loss quartz windows handle high power levels

These fused quartz waveguide pressure windows are designed to operate at extremely high temperatures. Model MA-14137Q fits WR-137 over 5.9-6.4 GHz and handles 6 kW cw. Model MA-14159Q fits WR-159 over 5.9-6.4 GHz and withstands 10 kW cw. Model MA-14284Q is for WR-284, and is rated at 15 kW cw over 2.45-2.65 GHz. Model MA-14112Q covers a 10% bandwidth in WR-112 at levels up to 5 kW cw. **Microwave Associates, South Avenue, Burlington, MA 01803 (617) 272-3000.**

CIRCLE NO. 226

$10 terminations handle 1 kW peak

Coaxial feedthrough terminations, models FT-50, FT-75 and FT-90, are available in 50, 75 and 90 ohm impedances, BNC or TNC connectors. Model FT-50 covers dc to 1 GHz, FT-75 covers from dc to 500 MHz and FT-90 covers dc to 150 MHz. These units handle 1 W cw or 1 kW peak power. P&A: $10 in small qtys; stock to 30 days. **Elcom Systems, Inc., 127F Brook Avenue, Deer Park, NY 11729 (516) 667-5800.**

CIRCLE NO. 227

Odd power division cuts insertion loss

These power dividers split an input into an uneven (3, 5 or 7) number of outputs. A typical model, D348S, a three-way splitter, covers 4-8 GHz and offers 15 dB min isolation and an insertion loss of only 0.7 dB above the 4.8 dB theoretical loss. Other specs include a 1.5 max VSWR, ±0.3 dB amplitude balance, ±5 degree phase balance and −55 to +85°C temperature range. P&A: $185. **Englemann Microwave Co., Skyline Drive, Montville, NJ 07045 (201) 334-5700.**

CIRCLE NO. 228

Phase shifter offers low insertion loss

Phase shifter, model PQ-28, covers 1-2 GHz with a 0.6 dB max insertion loss. Phase shifts of 0-50° can be achieved with power levels up to 1 W. Amplitude variation with phase shift is ±0.1 dB max, VSWR measures less than 1.3 and control time is 25 nsec. Dc requirements range 2-25 Vdc, size is 1.5 × 2.5 × 0.375 in. and weight is 3 oz. P&A: $575; 6 wks. **Lorch Devices, Inc., 105 Cedar Lane, Englewood, NJ 07631 (201) 569-8282.**

CIRCLE NO. 229

50-ohm loads are less than one inch long

BNC termination model 2048 covers dc to 2.5 GHz. Max VSWR is 1.15, and power capacity is 2 W avg. The load is rated over a temperature range of −54 to +125°C. Also, model 2050, a 50-ohm feedthrough shunt termination, handles 2 W avg. and 1 kW peak. BNC male/female connectors are standard. P&A: model 2048: $14.50; model 2050: $17.50; stock to 20 days. **Midwest Microwave, 3800 Packard Road, Ann Arbor, MI 48104 (313) 971-1992.**

CIRCLE NO. 231

PPM focused TWT covers 18-26 GHz

TWT instrumentation amplifier, model 1077H11, covers 18-26 GHz and provides a min power output of 1 W cw. It features min gain at saturation of 30 dB and operates from a 115 V, 60 Hz input voltage. Size is 15.5 × 16.75 × 3.5 in. and weight is 20 lbs. P&A: $9,620; 90-120 days. **Hughes Electron Dynamics Division, 3100 West Lomita Blvd., Torrance, CA 90509 (213) 534-2121.**

CIRCLE NO. 232

Turn to page 59 to make an
ADDRESS CORRECTION
or to request a
NEW FREE SUBSCRIPTION

MAY
1975

MICROWAVES

laser technology

Sources:

S-Parameters Insure Accurate VCO Design
Simplify The Design Of High-Power Gunn Oscillators

Also: What's The Future For Military Systems?



PRODUCT FEATURES: Tunable mm Sources ... Ultra-miniature VCOs... Low Noise Tunable Cavity Oscillator

MICROWAVES

May 1975
Vol. 14, No. 5

news

9 Inexpensive 12 GHz Mixers Developed For Satellite Broadcasting
10 Laser Triggers 10 ps rf Switch
12 Westinghouse Leads EW Contractors
14 International Showdown On MLS Expected
Silicon Transistor Hits 1 W In X-Band
MM Flange MIL-Specs Are In Sight
16 Meetings
18 R & D
20 Industry
23 Washington
26 International
28 For Your Personal Interest . . .

editorial

30 The Great Race

technical section

Sources
34 **S-Parameters Simplify Accurate VCO Design.** Gene Strid of RCA Alaska Communications introduces a computerized approach to VCO design which relies on a simple s-parameter characterization.
43 **Simplify High-Power Gunn Oscillator Design.** W. Wagner of Sanders Associates and Fred Manasse of Drexel University discuss ways to cope with the practical problems of Gunn oscillator design.
46 **What's The Future For Military Systems?** Jeff Montgomery of Gnostic Concepts examines the technological and economic trends that are shaping the major market for microwave components.
56 **Integrated Optics Mirror Microwave Concepts (Part 2).** Fred Blum of Texas Instruments describes how the transistion from fiber to integrated optics influences such components as transmission lines, couplers, sources and detectors.

products and departments

66 **Cover Feature:** MM-Wave Sources Tune 10 GHz Bandwidth, 26-110 GHz
69 **Cover Feature:** Low-Noise Cavity Sources Tune Over a 10% Bandwidth
70 **Cover Feature:** Ultra-Miniature VTO's Tune Over 1 GHz Bandwidths
72 Solid-State Source Survey
73 Source New Products
79 New Products
84 New Literature
86 Application Notes
87 Advertisers' Index
88 Product Index

About the cover: Three new state-of-the art microwave sources debut this month. The millimeter Impatt diode sources from Hughes now make swept measurements from 26-100 GHz practical. The low-noise cavity sources by SST provide very low residual fm noise but over a 10% tuned bandwidth, ideal for frequency agile LO applications. And Avantek has now combined a buffer amplifier into their ultra-miniature VCO series. They cover 2-6 GHz in 1 GHz bandwidth, and it's all in a dual in-line package. These cover features are described on pp. 66 through 70.

coming next month: ECM

WHAT'S THE FUTURE FOR ELECTRONIC WARFARE/? Jeff Montgomery of Gnostic Concepts presents short term economic and technical forecast of the electronic warfare market. Microwave needs are expected to nearly double, rising from $0.83-billion in 1974 to $1.47-billion in 1978. The forecast incorporates predictions for individual components, as well as a review of the influential technical trends and Government projects shaping this growing market.

TIPS ON SPECIFYING ACOUSTIC WAVE DEVICES. Chuck Grasse of Teledyne/MEC examines the significance of each specification used to describe surface wave devices. Included is a summary of major application classes for SAW devices, and an outline of their current capabilities and limitations.

A GUIDE TO SOLID-STATE SOURCE TERMS. Consultant Bernard Siegal offers a clear, concise set of basic definitions of source parameters.

Publisher/Editor
Howard Bierman

Managing Editor
Richard T. Davis

Associate Editor
Stacy V. Bearse

Contributing Editor
Harvey J. Hindin

Washington Editor
Paul Harris
Snyder Associates
1050 Potomac St., NW
Washington, DC 20007
(202) 965-3700

Editorial Assistant
Gail Murphy

Production Editor
Sherry Lynne Bogen

Art
Robert Meehan, Dir.

Production
Dollie S. Viebig, Mgr.
Dan Coakley

Circulation
Trish Edelmann, Mgr.
Peggy Long, Reader Service

Promotion Manager
Walter Salm
Albert B. Stempel (Rerpints)

Editorial Office
50 Essex St.,
Rochelle Park, N.J. 07662
Phone (201) 843-0550
TWX 710-990-5071

A Hayden Publication
James S. Mulholland, Jr., President

MICROWAVES is sent free to individuals actively engaged in microwave work at companies located in the U.S., Canada and Western Europe. Subscription price for non-qualified copies is $10.00 for U.S., $15.00 a year elsewhere. Additional single copies $1.50 ea. (U.S.); $2.00 ea. (foreign); except additional Product Data Directory reference issue, $10.00 ea. (U.S.); $18.00 (foreign). POSTMASTER, please send Form 3579 to Fulfillment Manager, MICROWAVES, P.O. Box 13801, Philadelphia, PA 19101.

Back Issues of MicroWaves are available on microfilm, microfiche, 16mm or 35mm roll film. They can be ordered from Xerox University Microfilms, 300 North Zeeb Road, Ann Arbor, MI 48106. For immediate information, call (313) 761-4700.

Hayden Publishing Co., Inc., James S. Mulholland, President, printed at Brown Printing Co., Inc., Waseca, MN.

Copyright © 1974 Hayden Publishing Co., Inc., all rights reserved.

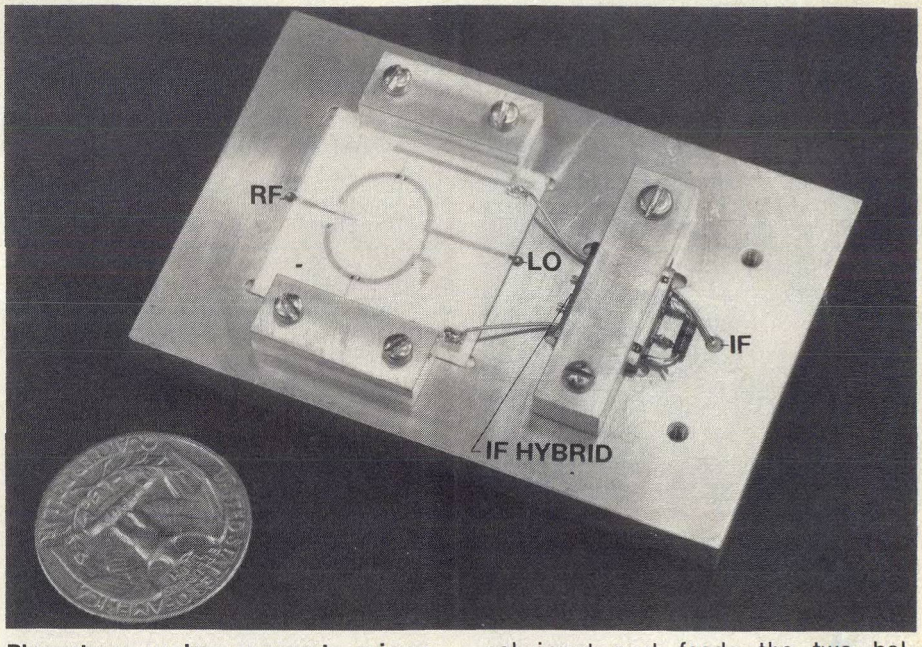
Inexpensive 12 GHz mixers developed for satellite broadcasting

Richard T. Davis
Managing Editor

Recent developments of ultra-high cutoff frequency GaAs Schottky diodes and improved image enhance mixer designs at X-band, have made possible significant reductions in the noise figures attainable with mixer front ends. "It is now possible to build an integrated image enhanced mixer/i-f preamplifier combination having a noise figure of less than 4 dB at 12 GHz or within a couple dB of that usually achieved with far more complex parametric amplifiers," says Marvin Cohn, Manager in the Systems Development Division of Westinghouse, Baltimore, MD. These mixers are now possible because the GaAs mixer diodes have a cut-off frequency of about 800 GHz at zero bias.

The significance of this development lies largely in the cost savings that can be achieved without greatly sacrificing the performance of a series of planned inexpensive ground stations. These mixers are being considered for use in terminals for receiving satellite broadcasts at 12 GHz from the new Communications Technology Satellite, (CTS), planned for launch in December, 1975. (See "Canadians See Costs Up For Their Technical Satellite," p. 26, April, MicroWaves). Approximately 17 experiments are to be performed over the North American Continent with CTS, such as teleconference broadcasting, propagation studies and educational and medical instruction.

These latter two programs have already been proven successful by HEW in tests with the ATS-6 satellite during the past year. To be specific, NASA's Application Technology Satellite, ATS-6, launched in May, 1974 has enabled medical doctors to prescribe treatment for patients in remote Alaskan villages by observations via satellite. Instructional programming has also been beamed directly at 2.6 GHz to remote community schools in Alaska and throughout several rocky mountain states. Approximately 110 low cost satellite television terminals have been built for the U.S. Department of Health, Education and Welfare at an approximate cost of about $4000 each. These terminals are currently deployed in three main areas: the Rocky Mountain region, the Appalachian States and in Washington State and Alaska.



Phase-type enhancement mixer uses 2 balanced mixers each of which contains 2 diode chips. The mixer is designed to short circuit the image, open circuit the second idlers and short circuit all higher idlers. The "T" junction at the signal input port feeds the two balanced mixers. The LO power supplied to them has a constant phase difference of 90 degrees. The i-f outputs are combined in an i-f quadrature hybrid mounted in a low profile flatpack package.

The ATS program, however, is coming to an end in the U. S., at least temporarily, because the satellite is being shifted this month to a new geosynchronous orbit. By July, it will be visible to the subcontinent of India where another uhf instructional television experiment will be conducted for broadcasting to remote Indian villages.

CTS continues broadcasting

The Communications Technology Satellite Experiment, which eventually will take up where ATS-6 leaves off, is a joint Canadian/U. S. venture. The Canadians are building the satellite itself and the U. S. is providing the launch facilities and the 200 W TWT on the satellite used for the 12 GHz down-link. (See "Collector Keeps Its Cool By Riding Outside Of Spacecraft, p. 12, May, 1974.)

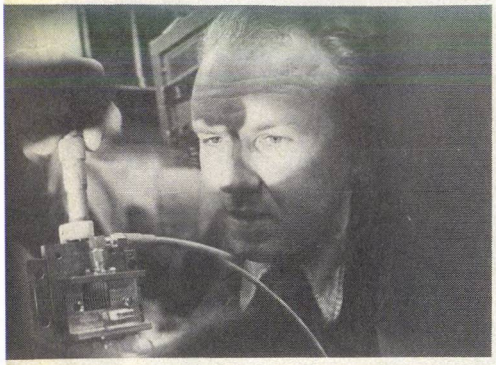
Because the downlink frequency of the CTS is considerably higher than the 2.6 GHz broadcasting frequencies of ATS-6, a greater challenge exists in designing low cost ground stations. Mixer front-ends seem to be the answer—using image-enhanced mixing techniques to minimize conversion losses. To meet this need Westinghouse is currently building 12 GHz image enhanced mixers with i-fs covering 70 MHz to 2.6 GHz. The units with a 2.6 GHz i-f are specifically intended for retrofitting the approximately 110 earth terminals used by HEW under the ATS-6 experiment.

"Once the development of these mixers is completed," says Cohn, "it will be possible to build them in large quantities for just a few hundred dollars."

(continued on p. 10)

Laser triggers 10 ps rf switch

By using a laser to trigger a photo-conductive substrate, a researcher at Bell Laboratories in Murray Hill, NJ, has developed a switch that operates at 10 ps. Electrical signals as large as 100 V can be switched by a few microjoules of optical energy.



According to David H. Auston, developer of the new switch, "further developments should make it possible to extend the time resolution to 1 ps or less and reduce the optical energy requirements to a few nanojoules."

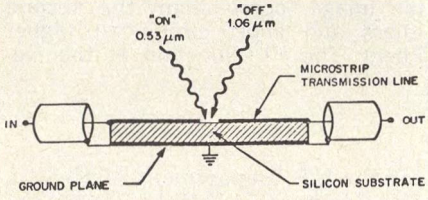
In describing how the new switch works, Auston explains that beams of laser light are focused on a piece of light-sensitive semiconductor. The semiconductor exhibits both surface and bulk photoconductivity.

One side of the semiconductor chip contains a microstrip transmission line that has a gap of high resistance, which prevents the signal from being propagated (Fig. 1). The other side of the chip contains a ground plane.

"The microstrip transmission line is particularly suitable for these devices since it can support a TEM-like electro-magnetic mode of low dispersion over bandwidths of a few hundred GHz for substrate thicknesses equal to a fraction of a millimeter," Auston explains.

Optical pulses of different wavelengths are used to turn the switch on and off. Two pulses are generated by taking a single pulse, extracted from a neodymium glass laser, and doubling it in a KDP crystal to get a second pulse at half the wavelength.

The two pulses are then separated by a beam splitter, delayed and focused onto the gap in the silicon microstrip structure. The shorter, 0.53-μm pulse brings the surface photoconductivity mechanism into play and causes a thin layer of high conductivity near the surface of the silicon, turning the switch on. The longer, 1.06-μm pulse is delayed and then used to turn the switch off. The longer absorption depth of this pulse penetrates to the ground plane, shorting the transmission line and preventing propagation.



1. **Unilluminated, the gap prevents rf transmission.** Gap capacitance is typically 10^{-14} F, which corresponds to a charging time of less than 1 ps.

"The conductivities (induced by the laser) are sufficiently large that the dielectric relaxation time is much less than 1 ps, and consequently, the intrinsic switching speed is primarily limited by the optical pulse durations," the Bell researcher notes.

According to Auston, peak transmission through the gate is better than 95% when the switch is on and less than 5% when it is off.

Until now, the fastest switch available has been the Josephson junction device. But it is capable of switching only a few volts and must be operated at cryrogenic temperatures. In addition, it needs fast electronic control pulses which are difficult to generate.

The opto-electronic switch has some disadvantages, however, the biggest being that it requires rather bulky optics and lasers. But Auston is hopeful that eventually less bulky optics and solid-state lasers will be used.

Initial applications will be limited to scientific uses such as the study of electrical properties of semiconductor materials and the evaluation of high-speed electronic devices. Longer range uses, though, may include applications such as high-speed electronic measuring instruments and short-pulse microwave radar and transmission systems. •• *SVB*

Inexpensive 12 GHz mixers developed for satellite broadcasting

(continued from p. 9)

Filter and Phase types developed

"Image enhancement mixers are capable of providing lower noise figures than conventional wideband mixers because they recover internally-generated image frequency energy and reject external signals at the image frequency," explains Cohn.

"There are two types of image-enhancement mixers, he continues. "Filter types incorporate a filter in the signal input line and as such, require a tradeoff between signal band insertion loss and image band rejection. A relatively high i-f (about 10% of the rf) must be used with the filter type since the separation frequency between the signal and image is twice the i-f. As a result, a slight increase in noise figure occurs due to the higher noise figure associated with the higher i-f frequency and also due to the insertion loss of the filter itself.

A phase type image enhanced mixer gets around this high i-f requirement by providing the needed isolation between signal and image frequencies through integral hybrid junctions on the MIC substrate. A pair of balanced mixers are used, each one providing a reactive termination for the image frequency generated by the other.

This type of mixer was recently described at the Microwave Theory and Techniques Conference in Palo Alto, CA, May 12-14. According to Lawrence Dickens of Westinghouse, a development phase-type image mixer demonstrated a conversion loss of 2.2 dB in converting a 12 GHz input signal to an i-f of 70 MHz. The mixer shown in the Fig. consists of a single rf signal port and a pair of i-f outputs. The magnitude of the image rejection is a function of the balance achieved between the two balanced mixers. For under 10%

(continued on p. 12)

Westinghouse leads EW contractors

Many notable shifts in the rankings of government electronic warfare contractors have occurred since FY 1972, according to "Electronic Warfare," a study published recently by Frost and Sullivan, a New York City based market research firm. Westinghouse heads the F&S list, with identified DOD contracts totaling more than $200-million. Sanders, which has been recognized as the leading EW contractor for the past six years, slips to second position in the 522-page report.

Other companies whose rankings are significantly changed in the annual list include Textron/Dalmo Victor, rising from twenty-fifth position in FY 1972 to ninth in FY 1973-74, Litton Industries, ascending from twenty-sixth to twelfth and Northrup/Hallicrafters, improving its ranking from twenty-third to eleventh.

The Frost and Sullivan list is based on all identified EW contracts, and differs from a ranking published in the January 24, 1975 issue of Aviation Week and Space Technology, which is based on "estimated sales of electronic countermeasures and signal intelligence systems, equipment, analysis, studies and related activities." Sanders heads the AW&ST list with assessed sales of $77-million, followed closely by Westinghouse at approximately $75-million. The sales ranking, compiled for calendar year 1974, includes:

1. Sanders
2. Westinghouse
3. E-Systems
4. AIL/Cutler-Hammer
5. Raytheon
6. ITT Avionics
7. Itek/ATI
8. Textron/Dalmo Victor
9. GTE Sylvania
10. Watkins-Johnson
11. AEL
12. Northrup Hallicrafters
13. Amecom
14. Loral
15. Cincinnati Electronics
16. Bunker-Ramo
17. Motorola
18. MBAssociates
19. Tracor
20. ESL

Westinghouse is the leading Air Force EW contractor, and its rise to the number one position in Frost and Sullivan's rankings is partially due to dramatic increases in Air Force expenditures. Air Force funds for RDT&E and procurement have risen from $187-million in 1971 to more than $398-million in 1974, according to the report. Naval needs, of which Sanders is a prime supplier, rose less dramatically, from $184-million in 1971 to about $282-million in 1974. The Air Force alone has dedicated $75-million in FY 1975 for new jammer pods and modification of existing pods to improve the capability of tactical aircraft to cope with Soviet tactical air defense threats, says the study.

Microwave components are cited in the F&S study as one area slated to receive increased attention. "One of the biggest complaints from (the microwave component) industry has been the lack of sufficient DOD RDT&E funding in this important technology area," the report states. "In response to this, the DOD has directed the military services to increase their funding in this area by 20% for FY 1976." Funds for microwave device technology in FY 1975 are listed in the study at about $26-million, with $8-million for microwave tubes and $18-million for solid-state development programs. Procurement of microwave equipment for electronic warfare is estimated by the report to be about $60-million. Areas called out to receive most of the near future RDT&E funds are dual-mode TWT's, CFAs, solid-state modules for phased arrays, solid-state low-noise amplifiers and low-cost phase shifters.

"Electronic Warfare" forecasts ECM budgets and trends through 1980 and provides a comprehensive review of DOD EW programs and details of ongoing contracts. •• *SVB*

FY 73 through third quarter FY 74	Rank for FY 72	Contractor	Millions of Dollars
1	2	Westinghouse	204.4
2	1	Sanders	89.2
3	6	ITT Avionics	84.2
4	5	Raytheon	82.8
5	3	GTE Sylvania	45.0
6	7	Hughes Aircraft	32.0
7	8	AIL/Cutler-Hammer	30.0
8	4	Itek/ATI	29.0
9	25	Textron/Dalmo Victor	28.0
10	9	General Dynamics	24.9
11	23	Northrup/Hallicrafters	24.0
12	26	Litton Industries	22.0
13	21	Tracor	19.0
14	20	AEL	16.0
15	29	Philco-Ford	15.8
16	16	Loral	12.7
17	17	General Electric	12.5
18	18	Watkins-Johnson	12.2
19	11	Sperry	12.0
20	22	MBAssociates	11.8

Inexpensive 12 GHz mixers developed for satellite broadcasting

(continued from p. 10)

rf bandwidth, about 25 dB of image rejection can be predicted.

In his paper, "A New Phased Type Image Enhanced Mixer," Dickens explains how loss in converting an rf signal to an i-f signal depends not only on properly matched rf and i-f impedances, but also upon properly terminated sum and image frequencies as well as other idler frequencies.

"In practical circuits, we are limited by the parasitics of the diode. Also, in a broadband circuit, the open-/short- circuited idler requirements cannot be readily attained. While the control of the idlers is important in obtaining the lower conversion loss, the dominant frequency to be controlled is the image. If the image cannot be well shorted or opened across the full band then control of the other idlers will do no good."

By using balanced mixers, the rf inputs can be directly connected together and the LO inputs and i-f outputs coupled by 90-degree quadrature hybrids. "This configuration causes the image signals appearing at the rf input line and generated by each of the balanced mixers to be out of phase with each other, resulting in maximum image current or equivalently the short-circuited image condition. This short-circuit condition is not bandwidth limited because the electrical length between the diodes of the two balanced mixers is essentially zero," explains Dickens.

The microstrip mixer shown will eventually be connected to a pair of matched lower noise i-f amplifiers and then the i-f combined by a hybrid. The ultimate noise figure of the mixer for a 70 MHz i-f using a 1 dB noise figure preamp is expected to be less than 3.0 dB over a 250 MHz bandwidth. The instantaneous bandwidth is 40 MHz and is limited by the i-f hybrid used.

Another important feature of filter and phase type image-enhancement mixers is their linearity and low intermodulation products. "The signal level can be within 3 dB of the LO power level before 1 dB compression is observed," says Cohn.

Gunn LO sources are being developed for both types of mixers and will be an integral part of the aluminum casting used to house the circuits. Westinghouse is planning to use these image-enhanced mixer front-ends in their teleconferencing experiment between Baltimore and Lima, OH.

S-Parameters Simplify Accurate VCO Design

Oscillator design need not be a hit-or-miss procedure. Here's a simple computerized approach that resonates the active ports reactive component and cancels out tank circuit losses.

UNTIL now, most oscillator design has been attempted through much laborious equation shuffling involving y-parameters, hybrid Π's or other models and analysis techniques that seem to be more aesthetically pleasing than practical. When the mind has been sufficiently boggled, the usual technique is to sit down at the bench with some device that looks potentially unstable and "tweak" it into a source that may or may not deliver some desired power at some predetermined frequency.

Microwave oscillator design, however, can be a relatively simple and fast procedure if a designer applies some simple facts about s-parameters.

A typical oscillator design should take no more than a day's work from spec sheet to a working prototype with oscillator power at a predetermined frequency successfully approximated.

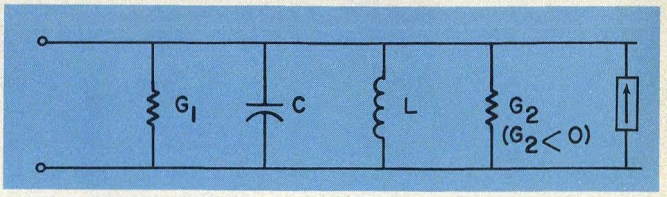
This article describes a design technique that satisfies the fundamental conditions for oscillation, i.e., the task of creating oscillation and coupling energy out from a reasonably matched port. As an example, a 2-15 GHz voltage-tuned oscillator is developed. Other design considerations such as stability, biasing schemes and fm noise are not covered.

Developing a model

The basic negative resistance oscillator, Fig. 1, has its resonant frequency determined by inductive and capacitive components. Component losses are lumped into conductance G_1 with initial energy input to the circuit indicated by the current generator. Oscillation starts when a negative conductance source, G_2 ($G_2<0$), is added to the circuit to cancel the losses represented by G_1.

This negative resistance source can be considered a one-port network whose reflection coefficient has a magnitude greater than one representing an impedance point outside the unit circle Smith Chart. Although this indicates potential instability, it can provide gain in the sense that the reflected wave is larger than the incident wave. This concept can be used to explain the oscillation build up.

Certain active devices, such as Gunn diodes, provide this negative resistance component. Oscillation is created when the one-port's reactive component is tuned out and the associated external losses are smaller than the active port's negative resistance



1. **Negative resistance oscillator model** requires losses of G_1 to be less than the negative conductance source, or $G_1 + G_2 < 0$. Oscillation frequency, $f_o = \frac{1}{2}\pi\sqrt{LC}$.

component. Mathematically this is:

$$|S_{11}| > |1/\Gamma_T| \qquad (G_1 + G_2 < 0) \qquad (1)$$

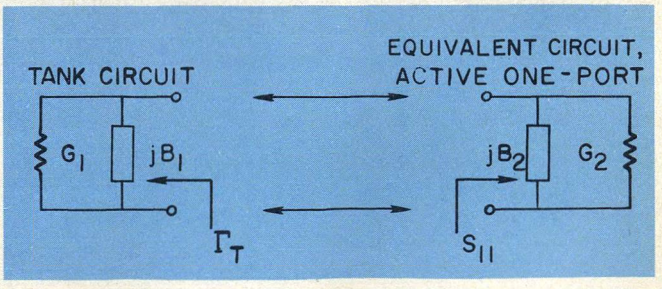
$$-B_1 = B_2 \qquad (2)$$

Γ_T = reflection coefficient of the tank circuit
S_{11} = s-parameter for the active port
G_1 = tank circuit conductance component
G_2 = active port conductance component
B_1 = tank circuit susceptance component
B_2 = active port susceptance component

Note that when oscillation occurs the phase angle of S_{11} is not necessarily the negative of the phase angle of the tank circuit reflection coefficient. If for instance, the magnitude of each is unity, then they would be equal. However, in general the magnitude of S_{11} is greater than one; and for Γ_T less than one. By plotting on a Smith chart, Fig. 3, oscillations can be shown to occur where the reactances are opposite and not where the phase angles sum to zero.

It may be quite difficult to couple out any significant portion of the energy from the circuit of Fig 2, without disturbing the frequency of oscillation or by adding more losses. If instead of the diode, a

(continued on p. 36)

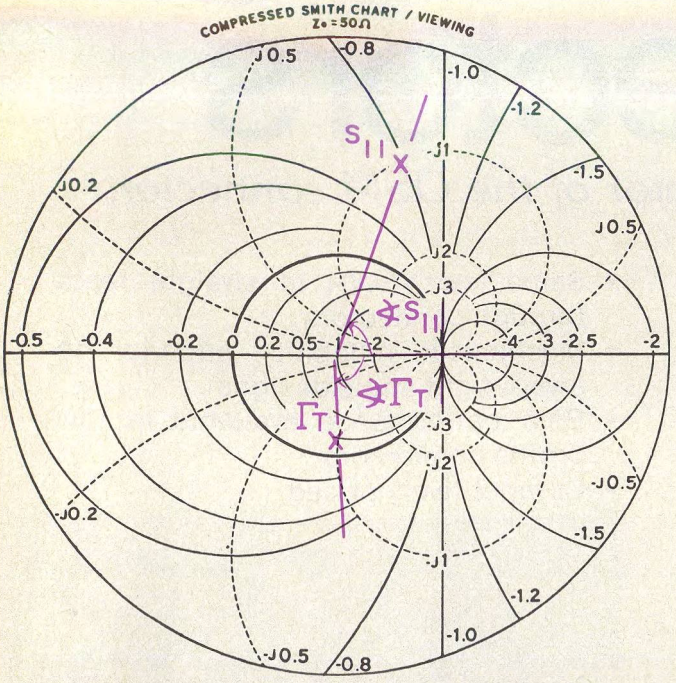


2. **Active one-port oscillator** shows pertinent parameters described in Eqs. 1 and 2.

Gene Strid, Radio Engineer RCA Alaska Communications, Inc. Anchorage, AK, (formerly with Farninon Electric, San Carlos, CA).

two-port device is used, such as a transistor, at least one of its ports can then have a reflection coefficient with magnitude greater than one. With some reverse isolation between ports the oscillation could be sustained at the first port, while power is coupled out from the second port.

By using transistors with certain series or shunt feedback elements[1], one port's reflection coefficient

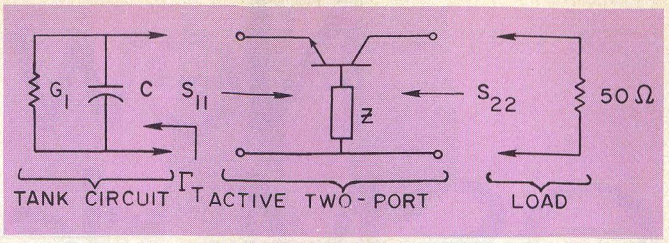


3. **Compressed Smith Chart** shows that in general $\sphericalangle S_{11} \neq \sphericalangle \Gamma_T$. For oscillations to occur the reactive components are opposite (+j1 and −j1).

can be maximized[2] and the second port can be matched[3]. Simultaneously, some isolation from tank circuit to output network can be provided to minimize frequency pulling, Fig. 4.

Up to now, the model described implies a linear situation, where the conditions for oscillation are (and must be) described with small-signal parameters. With the use of Classical Laplace transform techniques[4] to analyze the tank circuit, oscillation is started by positioning the poles in the right half s-plane, where $S = \theta + j\omega$. However, when oscillations build up, non-linearities of the overall circuit change the active port's impedance, limiting the signal swing, in which cases the poles are positioned on the $j\omega$ axis, Fig. 5. The active device bias conditions determine the limits of signal swing (cutoff and/or saturation) and proper analysis should then be performed using large signal conditions[5].

These large signal parameters would be considered some average of the conditions existing in the circuit for each cycle of oscillation. For example, one active model might be a combination of small signal parameters and the parameters describing the conditions of saturation or cutoff (the clipped condition). The important aspect is that small signal parameters (that characterize the circuit to create oscillation) and large signal parameters are not, in general, equal. For practical purposes, however, the design can be based on the small-signal parameters.



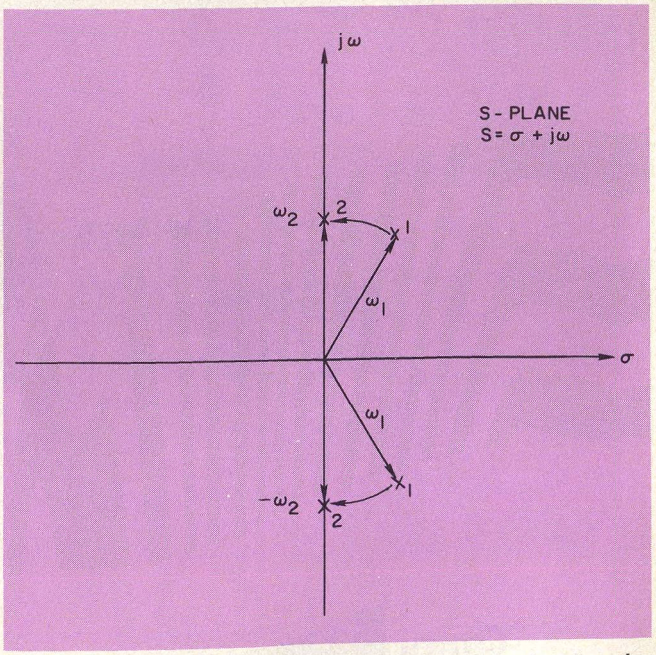
4. **Simplified example of a two-port negative resistance oscillator** uses a series feedback element.

Design procedure requires computer

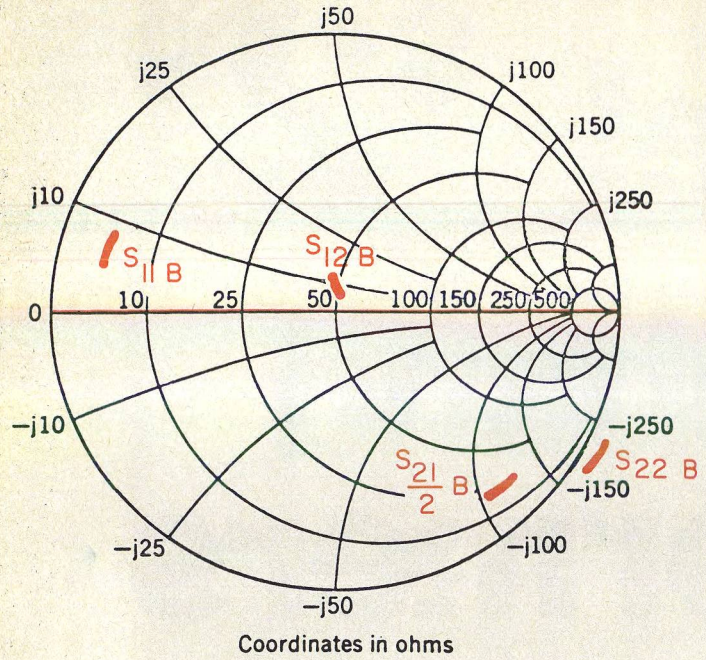
The first step in designing an oscillator is to select and subsequently characterize to an active device that shows some potential as a negative-resistance source. This is easily implemented with a network analyzer. In choosing the device; two initial criteria are that: $f_{max} > f_{osc}$; and the stability factor, K, be less than one (50-ohm system) at f_{osc}. The optimum configuration (CB, CE, CC) may not be obvious from the measured parameters; but in general, it should be the one that provides one port with a large reflection coefficient and some isolation from the second port.

A computer program should then be used in analyzing the effects on reflection coefficient for various impedances in series and shunt feedback configurations. Particularly useful for this task is the mapping capability of "COMPACT"[6] but other computer programs with mapping capabilities may be used as well, such as "Bamp." Simultaneous maximizing the phase angle spread of the resonated port impedance[3] with frequency (for wide-sweep capabilities in VCO's for instance) is an easy optimization routine. Moreover, interaction between the two ports is now accounted for. Computer-aided analysis of the tank circuit and output network is, of course, also possible. Remember the characterization is based on small signal parameters.

(continued on p. 38)



5. **S-plane shows the positioning of the tank circuit poles** when oscillation begins to build up (1) and when oscillation signal swing is limited (2). Initial frequency may not be the same as final oscillation frequency.



6. **Smith Chart of transistor s-parameters** shows negative resistance potential of the device.

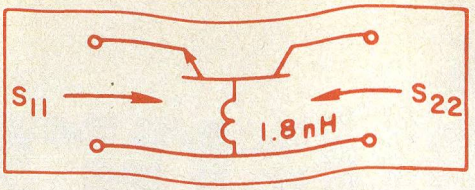
As an example, consider the transistor in common-base configuration with s-parameters shown in Fig. 6. Already S_{22} has magnitude greater than one and S_{11} is approaching the negative resistance region. However, S_{12} is much smaller than S_{21}, indicating a preference to tune the emitter port and match the collector port. Another consideration is the phase of S_{11} and S_{22}. For example, the inductive reactance of S_{11} shows potential to be easily tuned with the capacitance of a varactor diode.

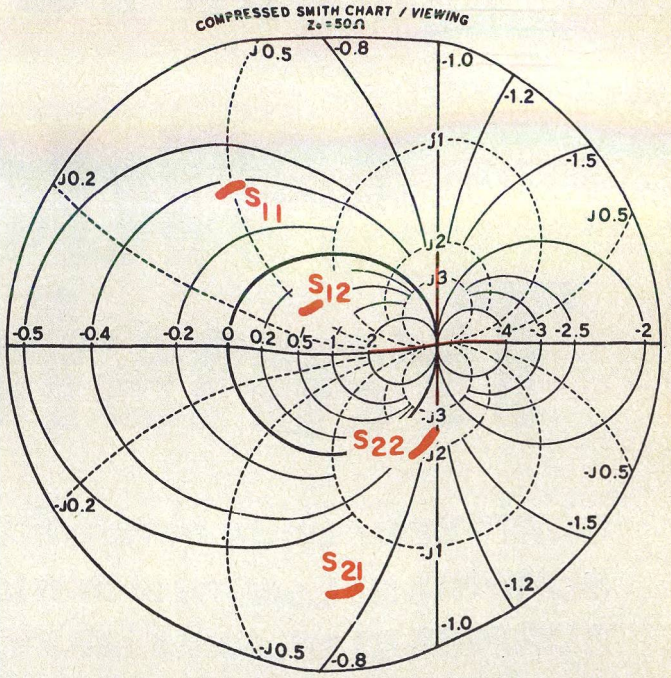
Next, this transistor's measured s-parameters are loaded into a computer data file of the network illustrated in Fig. 7. Using both the mapping and optimization capabilities of "COMPACT," it is found that 1.8 nH of series feedback in the base lead gives the best set of overall two-port parameters. Note that S_{11} has a magnitude much greater than one, the ratio of S_{21} to S_{12} still indicates isolation from output port to tuned port and although S_{22} has a magnitude greater than one, only slight resistive loading will be necessary to pull S_{22} inside the unit circle.

Figure 8 shows a possible technique for matching the output of the two port. Other possible solutions include: Series resistance and series inductance; shunt inductance and shunt resistance; series resistance; series inductance and shunt capacitance; and so forth. The computer again is the place to try these different schemes. Broadband matching and the interaction with the tuned port are better handled in this step of the design than later on the bench.

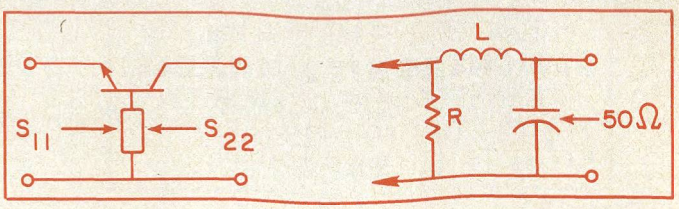
Finally, any analysis of the network used to tune out the reactive component of S_{11} is performed by the computer. For instance, the varactor characteristics about a certain operating point may need to be transformed with lossless elements. Objectives could be to obtain the conjugate reactive component that would cancel the reactance of S_{11} of the active circuit over a frequency band or to obtain a certain tuning rate or tuning linearity. With an rf circuit now determined, the circuit can now be implemented using the usual rf common sense, such as accounting for or minimizing circuit parasitics and properly supplying

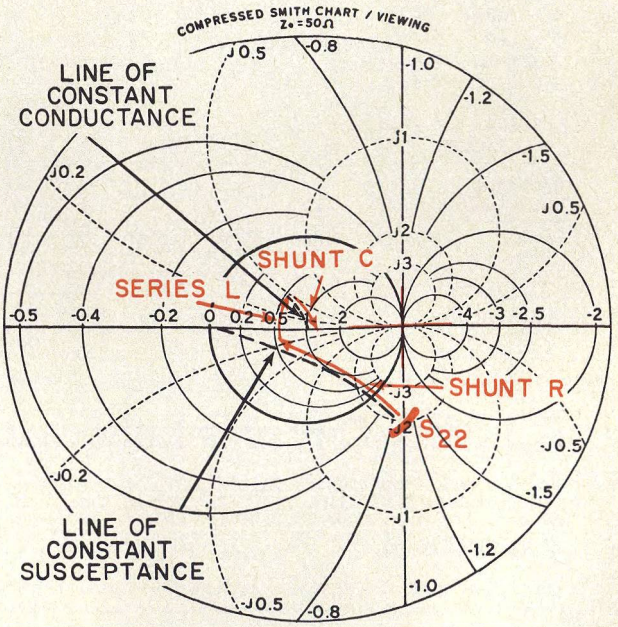
(continued on p. 40)





7. **Compressed Smith Chart reflects** the resultant s-parameters of the two port formed by adding 1.8 nH of series feedback.





8. **Compressed Smith Chart illustrates an output matching scheme,** neglecting the interactive effects with the tuned port.

dc bias to the device. Some means to control device current to adjust oscillation output power should be provided. It might also be wise in this prototype layout stage to incorporate a 50-ohm monitor transmission line for observing with a network analyzer the device's negative resistance port.

After the prototype is built, check to observe the reflection coefficients of the active port (to verify the presence of negative resistance) and of the tuning circuit. Connecting the tank circuit to the active circuit should then yield oscillaton at a frequency quite well predicted by the tuning port and tank circuit reactances. Output port VSWR can be approximated with a triple stub tuner and a power meter is $|S_{22}| < 1$. (See box for an alternative source impedance measurement technique that also holds for negative resistance components).

Consider an s-parameter oscillator design, Fig. 9, centered around the following specifications:

- Center frequency: 2.15 GHz
- Varactor tuned, tuning voltage range: −5 V ± 2 V
- Tuning rate: 20 MHz/V
- Output power: +13 dBm
- Output VSWR: 2:1

How to determine the output impedance of an oscillator

By using the concept of constant gain circles, a method of measuring an oscillator's output impedance is possible that can reduce the interactive effects of the matching network or measurement system on the oscillator and its output impedance.

Using the circuit below, a line stretcher presents a constant VSWR load of varying phase to the source. Maximum and minimum power readings are noted. The ratio of these powers in conjunction with the known mismatch provides enough information to calculate the magnitude of the source reflection coefficient. The solutions of the equations are quickly executed on a computer and tables can be easily generated that tabulate magnitude of output reflection coefficient versus known mismatch and the difference in (dB) of maximum and minimum power readings.

The equations to be solved are:

1. $K = P_1/P_2$
2. $|\Gamma_s| = (1 - K^{1/2})/[(1 + K^{1/2})\,|\Gamma_k|]$

where

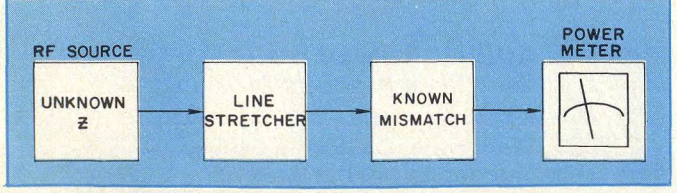
P_1 is the minimum power noted

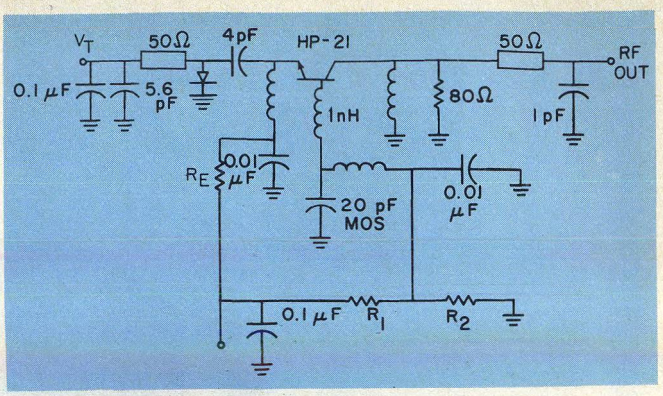
P_2 is the maximum power noted

$|\Gamma_k|$ is the magnitude of the known mismatch reflection coefficient

$|\Gamma_s|$ is the unknown source reflection coefficient

For example, suppose a known mismatch reflection coefficient of 0.2 is used and by stretching the line at least $\lambda/2$ wavelengths, a 1.8 dB difference in power readings is noted. This would then correspond to a source reflection coefficient whose magnitude is 0.52.





9. 2.15 GHz voltage-tuned oscillator delivers +16 dBm output. It can be built on a 1 in. x ½ in. thick alumina substrate.

The transistor is an HP-21 in common base configuration with approximately 1 nH of series feedback inductance to maximize $|S_{11}|$ at 2150 MHz. The 20 pF MOS chip capacitor is self-resonant at this frequency, yet allows base biasing through voltage divider R_1 and R_2. All dc currents are supplied to the device through self-resonated inductances.

The two port network's S_{11} (looking into the emitter lead of the transistor and ground) is resonated with the varactor diode, an Alpha Industries type DVH 6633 D. Tuning sensitivity is achieved with the shunt inductance of the 50-ohm transmission line across the diode (the 5.6 pF NPO chip capacitor is nearly self-resonant and the series 4 pf MOS capacitor). Output matching is accomplished with the help of an 80-ohm resistor, which pulls S_{22} inside the Smith Chart, a 50-ohm series transmission line and a shunt 1 pF capacitor. The transistor is attached to the Al_2O_3 substrate in chip form but the varactor diode is packaged in a 0.30 x 0.080 in. channel pack, (the chip component was not readily available at time of design). For the initial turn-on, a 2pF fixed capacitor is substituted for the varactor diode. A clean oscillation occurs at 1.9 GHz with $P_{out} = +18$ dBm (before the 80 ohms were added in the output network).

After installing the varactor, adjusting the center frequency and matching the output to 50 ohms, the following results were achieved:

- Center frequency = 2.15 GHz @ −5 V
- Tuning rate: 22 MHz/V @ −3 V
  15 MHz/V @ −7 V
- Output power: +16 dBm ± 0.2 dB
- Magnitude of output reflection coefficient: 0.25.

••

References

1. P. M. Ollivier, "Microwave Yig-Tuned Transistor Oscillator Amplifier Design," *IEEE SSC Journal*, pg. 54, (February, 1972).
2. Les Besser, F. Ghoul and C. Hsieh, "Computerized Optimization of Transistor Amplifiers and Oscillators Using COMPACT," 1973 European Microwave Conference, A-12-3.
3. Les Besser, "Computerized Optimization of Microwave Oscillators," 1973 Wescon Technical Program, Session 15-4.
4. R. Spence, *"Linear Active Networks,"* Wiley-Interscience, New York, (1970).
5. J. Gonda, "Large Signal Transistor Oscillator Design," 1972 IEEE G-MTT International Symposium.
6. F. H. Ghoul, Les Besser and Chi Hsieh, "Design A High Power S-Band Doubler," *MicroWaves*, Vol. 13, No. 6, pp. 58-65, June, 1974).

Test Your Retention

1. What conditions are necessary for oscillations to occur?
2. What two criteria should be considered in selecting and characterizing an active device to use as a negative resistance source?
3. How can the interactive effects of the matching network or the measurement system be minimized when measuring an oscillator's output impedance?

Simplify High-Power Gunn Oscillator Design

Note a departure from merely a theoretical discussion of Gunn oscillators. Here's a practical design guide with an example using device characterization with experimental results.

MANY articles have apepared in the last few years which deal with the theoretical design of Gunn oscillators or report on experimental measurements but which do not give generally useful techniques. A procedure is described for accurately characterizing a Gunn diode as a negative resistance one port and designing an optimum load for maximizing power output. An example of device characterization and oscillator design is given with experimental results comparing favorably with predictions.

In order to accurately design an oscillator using a negative-resistance device (such as a Gunn diode), it is not sufficient merely to determine the device's small-signal impedance and provide a conjugately-matched load. The oscillation process requires the device to operate in the large-signal region where its impedance is signal-amplitude dependent and a systematic design procedure requires that the device be characterized in this overdrive region[1,2].

Finding the device's negative resistance specs

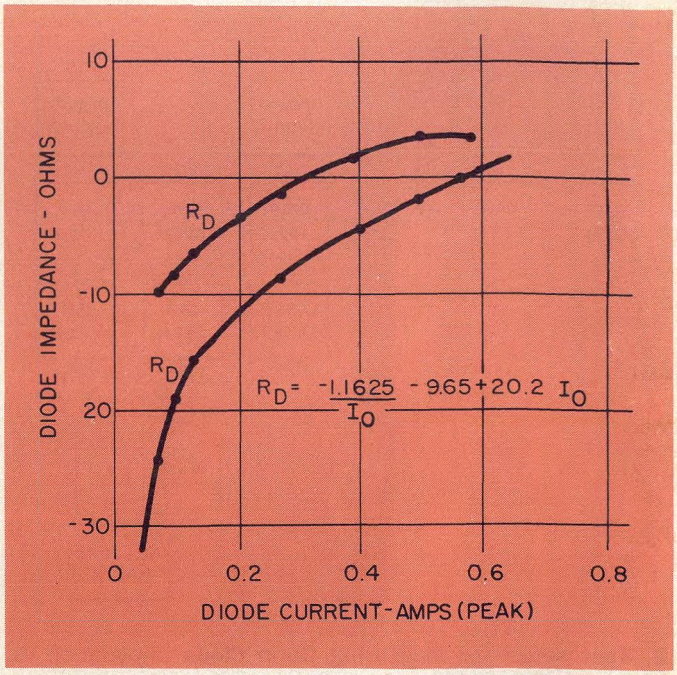
A simple model of a negative-resistance one port with small-signal driving point impedance $Z_1 = R_1 + jX_1$ connected to a load $Z_L = R_L + X_L$ is shown in Fig. 1. In the small-signal region, Z_1 is a function of frequency, ω, only and over some frequency range $R_1(\omega) < 0$. Oscillations will initiate at a frequency ω_0 for which $X_1(\omega_0) = -X_L(\omega_0)$ provided the real part condition, $|R_1| > R_L$ is satisfied. More generally, Z_1 is a function of both frequency and signal amplitude,

$$Z_1(\omega,A) = R_1(\omega,A) + jX_1(\omega,A)$$

The signal amplitude in the oscillating circuit will continue to grow until a steady-state amplitude, A_0, is reached when $|R_1(\omega_0, A)| = R_L$. Qualitatively then, the oscillation process requires the device negative resistance to compress from its small-signal value, which must be greater than the load impedance level, to a value equal to the load impedance level. The functional relationship of negative resistance with signal amplitude will now be shown to predict the load impedance level for maximizing power out. Consider the

(continued on next page)

W. Wagner, Member Technical Staff, Sanders Associates, Inc., Microwave Division, Manchester, NH and **Fred K. Manasse,** Professor Electrical Engineering and Assistant Dean of Continuing Education, Drexel University, Philadelphia, PA 19104.



1. Simple equivalent circuit of a negative-resistance one-port connected to a load.

circuit of Fig. 1 oscillating at a frequency ω_0, sustaining a peak steady state current I. Power consideration require[3]

$$\frac{I^2}{2}(R_1 + R_L) = 0 \qquad (1)$$

A generalized relationship between R_1 and I can be given by

$$R_1 = a_{-1} I^{-1} + a_0 + a_1 I + a_2 + \cdots \qquad (2)$$

Substitution of (2) into (1) yields an equation for I in terms of R_L. The output power can then be expressed in terms of, and optimized with respect to, R_L. For example, to simplify (2), let

$$R_1 = -R_0 + a_1 I \qquad (3)$$

$$\text{then } I = \frac{R_0 - R_L}{a_1}. \qquad (4)$$

$$\text{The output power is } P = \frac{1}{2} R_L \left(\frac{R_0 - R_L}{a_1}\right)^2 \qquad (5)$$

The value of R_L which optimizes the output power is

$$R_L \text{ opt} = \frac{R_0}{3} \qquad (6)$$

and the maximum output power is

$$P_{max} = \frac{2R_0^3}{27\,a_1^2} \qquad (7)$$

The above has demonstrated that the specification of negative resistance with current amplitude for a given device completely defines the oscillation behavior of that device. It allows a load to be chosen which maximizes the output power of an oscillator using that device and specifies the maximum power available from the device.

Testing device impedance vs. signal amplitude

The experimental determination of a device's impedance versus signal amplitude can be made in several ways. Fig. 2 shows a setup using a microwave network analyzer. In this system, the device is mounted in a 50-ohm holder and its voltage reflection coefficient is monitored as a function of input power at a fixed frequency. In the case of a negative-resistance device, it is necessary to determine the peak value of rf current for each data point. By measuring the incident power, P_{av}, and the voltage reflection coefficient, ρ, the current is given by

$$I = (1 - \rho)\sqrt{P_{av}\ 125}$$

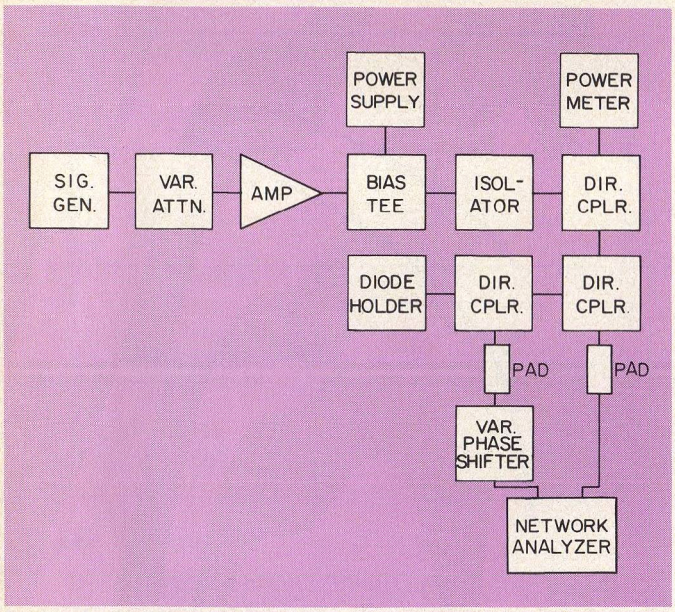
in a 50-ohm system. Fig. 3 shows a typical impedance vs. current characteristic obtained with a GHz 5630B Gunn diode, biased at 10 V and 1.1A at 7.0 GHz. Incident power was varied between 100 mW and 2 W to obtain this data. A good fit to the experimental data is given by

$$R_1 = \frac{-1.1625}{I} - 9.65 + 20.2I$$

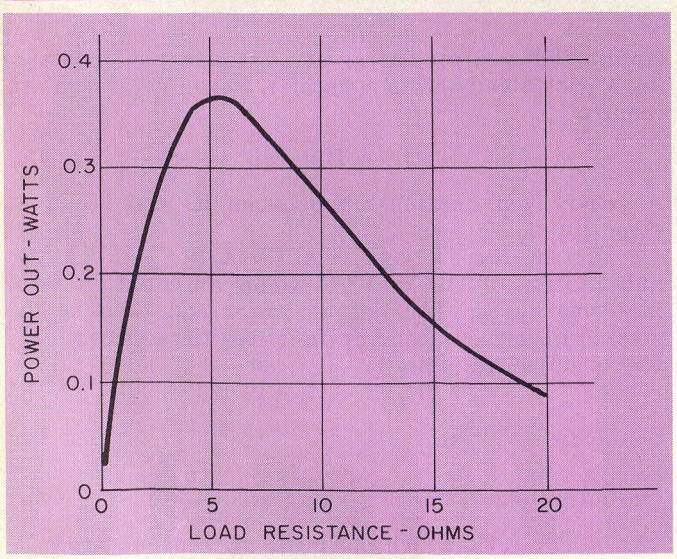
Using this expression, the power out vs. load impedance level shown in Fig. 4 was obtained which maximizes at 365 mW corresponding to an optimum load impedance of

$$R_L\ opt = 5.0 - j2.0\ ohms$$

In order to test the validity of this data, an experimental oscillator was built. The oscillator equivalent circuit is shown in Fig. 5(a) as a simple two-pole ladder network with element values normalized to 7.0 GHz and impedance level normalized to 50 ohms. The Q of the circuit is approximately 10.

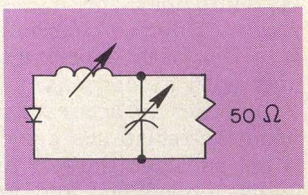


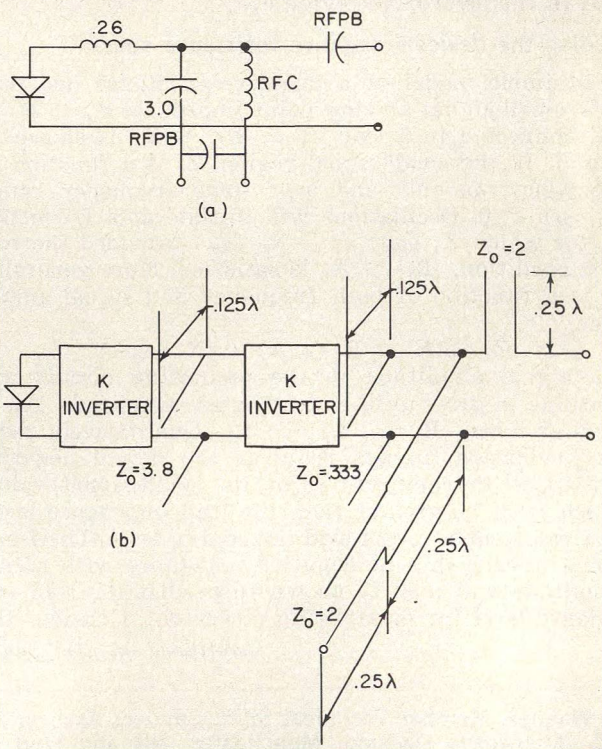
2. Test setup for measuring Gunn diode impedance vs. signal amplitude characteristic.



3. Typical impedance vs. current characteristic of a GHz 5630B Gunn diode biased at 10 V and 1.1 A at 7 GHz.

4. Power out vs load impedance level maximizes at 365 mW.





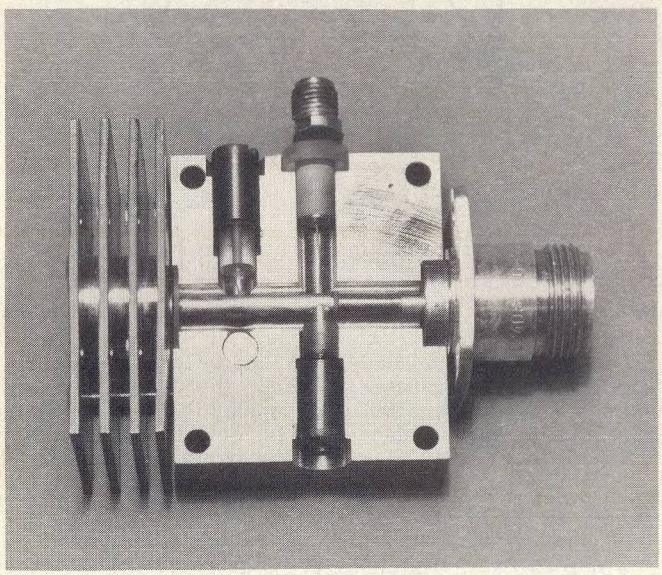
5. Gunn diode oscillator equivalent circuit (a) with element values normalized to 7.0 GHz and 50 ohm impedance, (b) two wire realization of 5(a).

GUNN OSCILLATOR DESIGN

Building the Gunn oscillator

The oscillator circuit was realized as shown in Fig. 5(b) using two shunt open-circuited transmission lines and impedance inverters. The oscillator was constructed in a coaxial medium using quarter-wavelength transmission lines as narrowband impedance inverters. Adjustment of the tuning elements was provided by dielectric slugs. Bias was applied through a two-pole band stop filter using a "bucket choke" construction. The test oscillator is shown in Fig. 6.

When tuned, the test oscillator delivered 385 mW at 7.05 GHz which compares favorably to the predicted level of 365 mW, the error being within measurement tolerance. As a further check, the impedance seen by the diode was measured directly by replacing the diode heat sink assembly with a coaxial connector and measuring the load impedance directly. The experimental optimum load impedance was 7.0 + j3.0 ohms which again compares favorably with the predicted optimum impedance of 5.0 — j.2 ohms. The discrepancy in the real part can be attributed to the broad maximum power vs impedance level which varies only by 0.2 dB between 4 and 7 ohms. The discrepancy in the imaginary part can be attributed to reference plane inaccuracy.

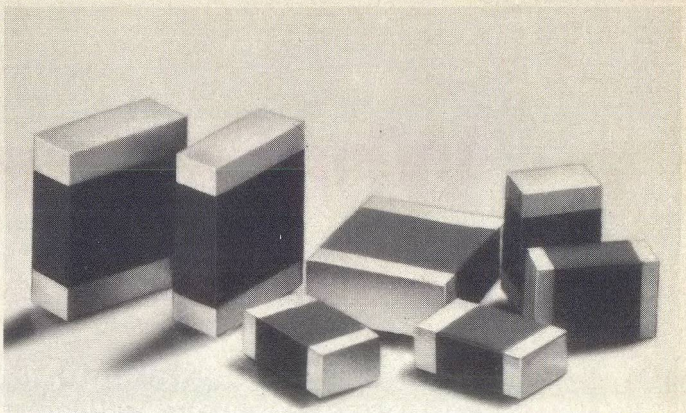


6. This 7.05 GHz test oscillator delivered 385 mW output, close to the 365 mW predicted level.

Negative resistance devices which are active over a broad range of frequencies are susceptable to spurious oscillations. Microwave oscillators of this type very often generate low-frequency oscillations through the bias network and power supply. The test oscillator produced severe fm modulation which was traced to a bias circuit oscillation at approximately 10 MHz. When driven from a voltage source, the net resistance through the diode-bias circuit power supply loop was negative. In order to raise the resistance to a positive value, a parallel RL network was series connected between the oscillator and power supply as shown in Fig. 7.

Initially a 1 μh choke was used and spurious oscillations were suppressed at the 12 V operating point. However, it was not found completely effective over the full range of voltages between the diode threshold, 4 V, and the operating point due to the limited effective frequency range of the choke. Use of an L-section broadband EMI filter was found to effectively suppress bias circuit oscillations for all voltages between threshold and 12 V.

Although the device characterization technique has been given for Gunn diodes, it is generally valid for any active device such as Impatt diodes, tunnel diodes and transistors. In the case of transistors, however, a preliminary step is required to reduce the three-port device to a one-port network. This reduction can be performed optimally to maximize the negative real part of the network immittance. The large-signal characterization can then be applied to design an optimum load. ••



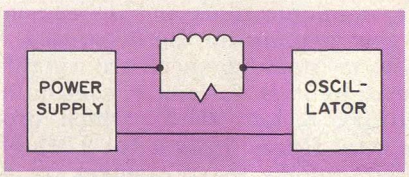
HIGH Q
CHIP CAPACITORS

High Q multilayer capacitors feature very high quality factors at microwave frequencies. Superior dielectric properties and structure permit operation at high voltage and high current at microwave frequencies through the full temperature range with minimum dielectric loss. Offered in 4 standard sizes from .040" x .030" to .125" x .095". Applications include UHF-microwave hybrids and MIC's.

Johanson
Monolithic Dielectrics

Box 6456 / Burbank, California 91505
(213) 848-4465 / TWX 910-498-2735

READER SERVICE NUMBER 45



7. **A parallel RL network is included** between the oscillator and power supply to suppress bias circuit oscillations.

References

1. K. Kurokawa, "Some Basic Characteristics of Broadband Negative Resistance Oscillator Circuits," BSTJ 48, 1937, (July, 1969).
2. N. D. Kenyon, "A Lumped Circuit Study of Basic Oscillation Behavior," BSTJ, (February, 1970).
3. S. Furukawa and T. Nakagami, "Design Theory of a Self-Excited Frequency-Multiplying Oscillator," *IEEE Journal Solid State Circuits*, SC-5, No. 3, 87, (June, 1970).

What's The Future For Military Systems?

Emphasis on digital interfacing, off-the-shelf components, and phased arrays will continue. Component usage in military microwave systems will be at about 10% per year from now till 1978.

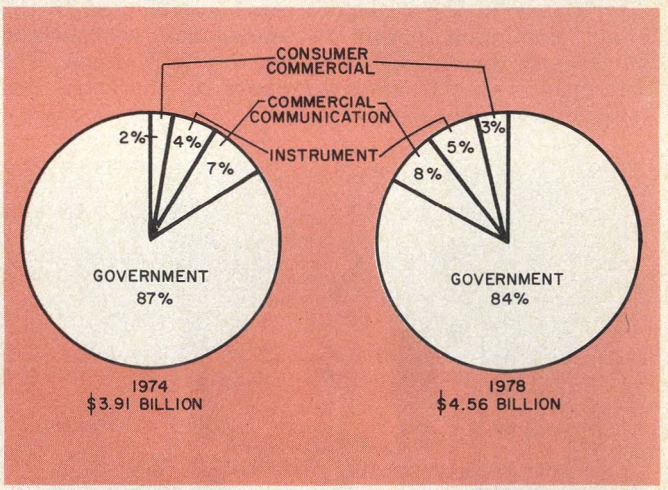
This is the second of a three-part series forecasting the economic future of important segments of the microwave industry. Part 1 on commercial communications appeared last month. Next month's concluding installment will project growth patterns for the ECM industry.

MILITARY procurement of microwave systems and equipment, the traditional bulwark of the microwave industry will continue to dominate the market place over the next five years. However, on the basis of computer-modeling techniques (see box), the U.S. Government's market share will decline by about 3% with commercial communications and instrumentation production largely making up the difference, Fig. 1.

In a sense, military planners are caught in a bind. National sentiment is forcing a continuing decrease in the military budget share, which dropped from 42% of the total federal budget (or 9.3% of the GNP) in 1968 to 27% of the federal budget (or 5.9% of the GNP) in 1974. On the other hand, the switch to an all-volunteer armed force and continuing inflation will cause payroll-related costs, which were 58% of the military budget in 1974, to take an increasing share of the available funds.

The production of microwave systems and instrumentation for both military and civilian agencies of the U. S. government will grow at 5% per year through 1976. This growth largely represented by increased defense spending is however, a short-term recession-fighting measure. On a long-term basis, i.e., through 1980, annual growth will average only about 3%, which is insufficient to keep pace with current inflation rates.

Another major area of importance to the government microwave market is the export market. During FY 1974, the U. S. Department of Defense sold about $8-billion worth of military equipment abroad with over 50% going to Iran. The microwave content of this equipment averages about 10%. Contrary to recent reports, however, this amount can be expected to drop to $4-billion in FY 1975, largely because the Iranian government has reached a level they consider sufficient to meet their needs.



1. **Although the total budget for microwave systems and equipment** will increase in 1978, the federal government's market share will decline slightly. The commercial and industrial sector will still only represent about 15% of the total U. S. microwave equipment market.

Another factor influencing the export market is the growing concern of Congress over advanced weapons system getting into the hands of foreign countries before U. S. forces receive them. (See "Senate Bill Would Check Overseas Arm Sales," *MicroWaves*, p. 21, April, 1975).

Component demands exceed system production

A systems breakdown of the microwave equipment sold to the U. S. government, Fig. 2, reveals that sales will increase from $3.39-billion in 1974 to $3.77-billion in 1978 with radar and electronic countermeasure systems maintaining their dominant market share.

What does this all mean to the microwave component manufacturer? The systems applications described in Fig. 2 accounted for $287-million or 54% of the total 1974 production of microwave components. Looking ahead, it can be expected that the relatively strong 1975-1976 production of military microwave equipment will support continued microwave component production while the recession slows requirements in many other areas.

(continued on p. 48)

Jeff D. Montgomery, Vice President, Gnostic Concepts, Inc., 2710 Sand Hill Road, Menlo Park, CA 94025.

Voltage Tunable Filters



2900 Series

10 Microsecond Tuning

Linear Frequency Response

3 dB bandwidth from 2 to 10%

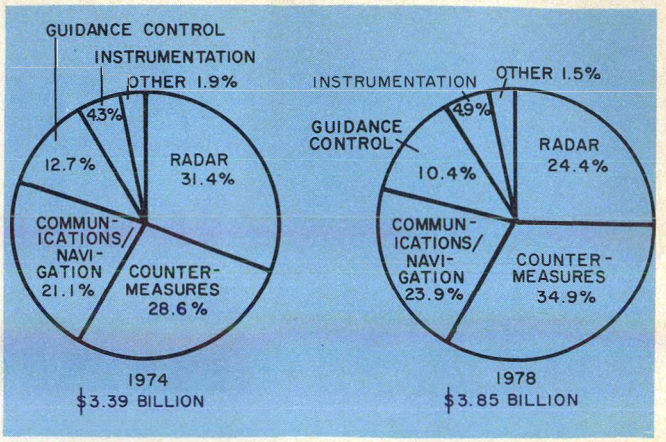
The 2900 series of voltage tunable filters are operable in the 10 to 2000 MHz region in 2 to multiple pole filter designs.

Update your system with highly reliable miniature voltage tuned filters. Units available operable over the −54 to +95°C temperature range.

Send for Zeta's literature package describing its voltage tuned filters.

ZETA LABORATORIES, INC.
616 National Ave., Mt. View, CA 94043
415/961-9050

READER SERVICE NUMBER 48



2. **The U. S. government's share** of microwave systems and equipment market consists of five major areas. Note that the radar sector will decline by about 7% but the ECM area will increase by over 6%. Overall demand will increase at an annual rate of about 3% between 1974 through 1978. This is considered inadequate to keep pace with current inflation projections.

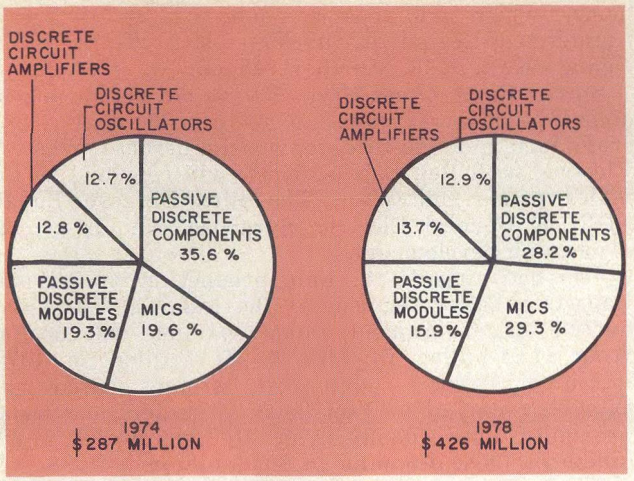
However, over the longer terms and as suggested in Fig. 1, growth will be slower in military microwave applications than in the commercial markets. Component usage in military microwave, on the other hand, will grow at an average annual rate of over 10% over the 1974-1978 span, as broken out in Fig. 3. This is substantially faster growth than overall government microwave equipment production due primarily to solid-state displacement of tubes.

Off-the-shelf components stressed

Several trends are noticeable that will have a bearing on the marketing strategies of microwave component manufacturers. While military equipment producers have had an historical bias toward captive component production, they are shifting toward greater reliance on noncaptive sources. Three factors mitigate these changes:

- The wide swings in military contract funding make it economically unfeasible for the equipment producer to maintain a qualified component design staff.
- The growing complexity of military electronic systems is forcing the system houses to devote a greater share of management and design attention to higher level system integration problems, such as digital control.
- The strong new emphasis on design-to-price favors use of standard, off-the-shelf components readily available from the marketplace, rather than expensive captive custom designs.

This increased use of off-the-shelf components and the subsequent retreat from state-of-the-art components is the result of extreme cost pressures caused by inflation and increasing system complexity. Military planners are also specifying designs for longer operational-life-cycles with lower maintenance in accordance with the concept of "total cost of ownership." For example, the growing difficulty of maintaining qualified technicians will lead to emphasis on designing for simpler operations and maintenance. For non-battlefield environment, there will be a trend away from full military specification hardware to high-quality industrial grade equipment, which generally is more reliable and less expensive.



3. **Microwave components used in government systems and equipments** represent about 54% of total consumption in 1974. This will grow to $426-million by 1978, an annual growth rate of over 10% over the 1974-1978 span. Much of this will be due to retrofitting older tube-type systems with solid-state devices.

Demand for strategic weapons returns

With the retreat from Vietnam, planning emphasis has reverted to strategic weapon systems comprising the Triad force of land ICBM's, fleet ballistic missiles and bombers. The new tactical systems development will proceed, but fewer systems will be selected for large volume production. Southeast Asia operations drained funds from modernization and R&D efforts. As a result, the Soviet weapons have gained substantially in technology compared to United States weaponry, as demonstrated in the 1973 Arab-Israeli war. U. S. R&D programs will gain a much greater share of military funds over the next five years. These efforts will be directed mainly to moving earlier research and development on to a stage of dependable and cost-effective production.

Weapon systems, which will be developed to advance strategic capability include:

- The B1 bomber, now in advanced development, with a projected 25 year service life, to replace the B-52 bomber
- The Trident fleet ballistic missile submarine to augment the Poseidon system
- The CVN-70 nuclear powered aircraft carrier
- The F-15, F-4J, F-5E, A-10A, F-16, A-4AM and other fighter aircraft.

Each of these major weapon systems uses, to varying degrees, the microwave systems described in Fig. 2. These major market areas will now be analyzed in more detail with the exception of the ECM market, which will be covered separately next month.

Radar production drops by detente

The arms limitations negotiated between the United States and Russia in the SALT talks effectively removed anti-ICBM search and track radar from future production. Research and development, however, is not restricted by the treaty and will continue at a high level, over $100-million per year, with a substantial portion classified and concealed. Much of this funding will be allocated to radar and penetration aids, both of which are substantial users of microwave components. Radar development emphasis will be on multiple-beam phased array radar. Laser-radar development also will be pursued, as an interceptor/

(continued on p. 50)

New 8.0-8.4 GHz Litton solid state sources for telecommunications transmitter chains.

M-1014 Voltage Controlled Oscillator
Power Output—150 mW, Min.
Frequency—8.0 to 8.4 GHz
400 MHz mechanical tuning range
Mod Sensitivity—1.6 MHz/V, min.
FM Noise—−78dBm0,
(200 kHz ref. 0 dB)
Waveguide output—WR-112





M-1002 Injection Locked Amplifier
Power Output—1000 mW, min.(+31 dBm typ)
Frequency—8.0 to 8.4 GHz
400 MHz mechanical tuning range
Locking bandwidth—50 MHz min.
(70 MHz typ)
Locking gain—>15 dB (17dB typ)
Temperature coefficient—
<125 kHz/°C
Waveguide output—WR-112

We have sources that will fit into your plans for point-to-point microwave radios used in government applications. We provide the active components—a Gunn Voltage Controlled Oscillator driving an Injection Locked Amplifier—you supply your own interstage coupling. Sources are also available for CARS (including CATV), ETV and STL bands.

Look to Litton—the performance and reliability leader—as *the* source for your solid state source requirements. Send today for complete catalog. Electron Tube Division, 960 Industrial Road, San Carlos, CA 94070. (415) 591-8411.

Litton ELECTRON TUBE DIVISION

READER SERVICE NUMBER 49



LCT paramps

LCT manufactures a complete family of all solid-state uncooled parametric amplifiers featuring wide band, high gain and low noise temperatures for centre frequencies of 1.7, 2.3, 4, 5.5, 7.5, 11.5 GHz.

In the **HSTC** (Hermetically Sealed Temperature Controlled) line the 4-500 model, for example, features a 500 MHz bandwidth at 4 GHz, a noise temperature of 80,60 or 50°K * and :

- All RF components housed in a thermostat-controlled, air-tight oven
- Gain-stability of ± 0,1 dB/day and ± 0,3 dB/month
- Stabilization time at start-up less than 10 minutes
- Built-in test and alarm facility
- Fundamental Gunn diodes as pump sources

LCT produces also a line of **Compact** paramps. Among these, the 4-501 model operates at 4 GHz with a 500 MHz bandwidth and a 9,5°K noise temperature.

All these amplifiers are in current production with short delivery terms. Together with the new low-noise, wideband microwave transistor-amplifiers, they will be presented by LCT at the **Paris Air Show** and **Telecom 75**, Geneva.

Laboratoire Central de Télécommunications
18-20, rue Grange-Dame-Rose
78140 VELIZY - France
Phone : (1) 946.96.15 - Telex 69 892

* Typical value

Laboratoire Central de Télécommunications **LCT**

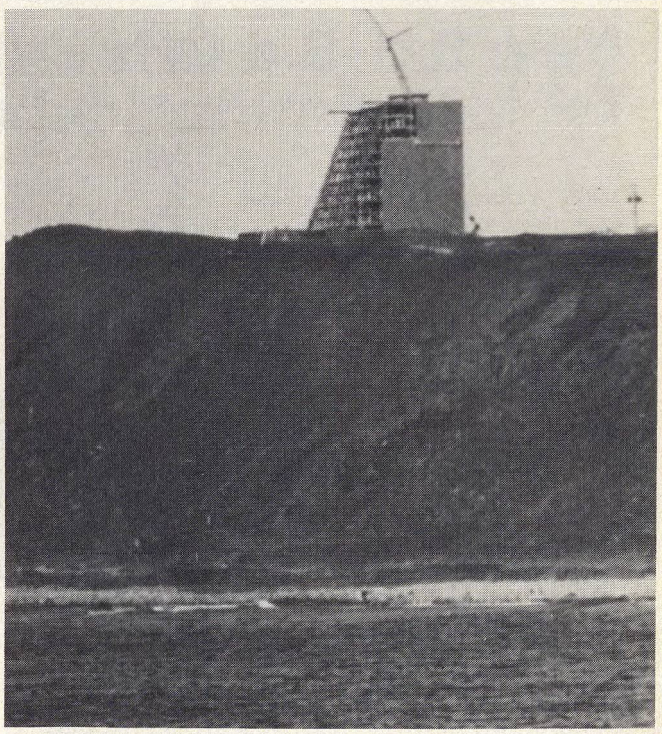
READER SERVICE NUMBER 50

homer which will not be deterred by electronic countermeasures or by nuclear blast effects. Laser fuzing also will be further refined.

Sperry Rand, Great Neck, NY, is developing a new dome phased array radar, providing 360-degree coverage from a single face, for missile defense. Western Electric, with Bell Labs support, will continue as the major prime contractor. The Site Defense Radar, SDR, by General Electric, Syracuse, NY, is typical of ongoing development.

The declining U. S. unit production of aircraft impacts a major segment of the radar market. Production of government radar systems will decline from $1.31-billion in 1974 to $1.3-billion in 1978, including airborne, shipboard, ground based and satellite radar, as well as radar altimeters and radar proximity fuzes. Radar is mostly microwave, $1.04-billion in 1974, dropping to $0.92-billion in 1978.

To be more specific, surface-radar production, ground plus shipboard, will continue its slow decline over the 1974-1978 period, from $966-million to $853-million. While production quantities will shrink substantially, this will be partially offset by increasing prices. The reason for this is the new surface radars will make heavy use of data processing equipment. Also, phased array antennas have become an established production concept. The Aegis phased array radar, developed by RCA, Moorestown, NJ, for use on DG fleet escort vessels, is now undergoing sea tests and will be a substantial factor in radar production over the next decade. The computer-controlled phased array radar of the SAM-D ground-to-air missile system will also be significant. Raytheon in Bedford, MA, also is developing a new digitized version of their TARTAR area defense missile system, including radar, for use on guided missile ships.



4. **Cobra Dane, a new phased-array-radar system** is being constructed by Raytheon at Shemya Air Force Station on the Aleutian Island Chain. It will be used for tracking Soviet ballistic missile flights. The 94-ft diameter antenna array consists of 15,000 elements providing a 120-degree sector of airspace into the northwest.

Development and production of the Cobra Dane L-band large, precision phased array radar, Fig. 4, is also underway at Raytheon, Waltham. This radar uses power tubes and a microwave distribution network rather than active elements. A total of 35,000 antenna elements will be used, of which about 15,000 will be active during transmission. Cobra Dane will be installed in Alaska to monitor Russian missile tests. Subcontractors include System Development Corporation, Santa Monica, CA; Microwave Associates, Burlington, MA; AIL, Deer Park, NY and Control Data, Minneapolis, MN.

Modern military aircraft often require three or four radar system functions, but there is room for only one radar. This will encourage continued development of multifunction radars, following the lead established in the F-111. Multiple-target capabilities are urgently needed and will drive continued development of airborne phased array such as RASSR at Texas Instruments in Dallas.

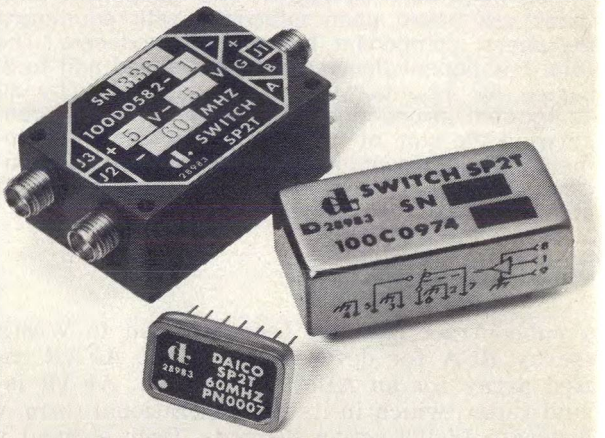
Westinghouse, Baltimore, MD, in mid 1974 received a $22-million Air Force contract for development of the EAR (Electronically Agile Radar), Fig. 5, for strategic applications. This is an X-band phased array radar using a coupled-cavity TWT for power output. EAR will use synthetic-aperture techniques for high resolution ground mapping, terrain following and ground speed determination. Two units will be built under the present contract with options for two more flight tests planned for 1978. This will potentially lead to major production in the late 1970's. Possible platforms for the EAR will be the B-1, the B-52 and the FB-111.

(continued on p. 52)



5. **Electronically Agile Radar (EAR) is a 700 lb., X-band, multimode phased array radar** being developed by Westinghouse for the Air Force Avionics Lab. It is being designed under the total cost of ownership concept. As such, performance specs can be changed in order to be more cost effective. It will be modulatar in design (use LRU's) and implement many off-the-shelf component designs. The radar beam shape and position is rapidly changed via digital processing to provide essentially simultaneous fine resolution terrain mapping, all weather terrain following and precision position and velocity information.

A Switch in Time....



Daico high speed SP2T switches utilize thin-film circuitry. Balanced diode design allows nanosecond switching speeds with millivolt level video transients. Integral drivers provide complete T²L compatibility. Packaging is available with conventional connectors, plug-in mount, or DIP thin-film hybrid. What are your unique switching problems? Call DAICO, we have probably already solved them.

Typical Specifications	High Speed	Low Transient	Minimum Loss
Type			
Frequency (specify fo) (MHz)	20-400	10-400	10-1500
Bandwidth (Octaves)	2	3	5
R.F. Power cw max. (dBm)	+13	+15	+10
Thru VSWR (1.02/1 Termination)	1.2/1	1.15/1	1.13/1
Termination of Unused port (ohms)	Open	50	50
Insertion Loss (dB) at fo	1.0	1.5	0.3
I.L. Flatness over B.W. (dB)	±0.05	±0.10	±0.10
Insertion Phase Match at (fo) (deg.)	±1	±1	±1
Isolation (dB) to 100 MHz	55	60	65
to 200 MHz	50	55	60
to 400 MHz	40	45	50
Control T²L Load Factor	6	2	2
Sw. Speed 50% control to 90% RF nanosec.	15	125	500
R. F. Transition 10% to 90% RF nanosec.	5	50	300
In-band transients dBm	−40	−60	−25
Video transients (millivolts)	250	40	1000
3rd order intercept point (dBm)	+30	+35	+30

Also — Solid State Voltage Controlled Attenuators and Phase Shifters

DAICO INDUSTRIES, INC.

2351 East Del Amo Blvd., Compton, Calif. 90220
Telephone: (213) 631-1143 · TWX 910-346-6741
©1975 Daico Industries, Inc. mp75403

READER SERVICE NUMBER 51

Mapping the future with computer models

This economic forecast is derived by computer modeling techniques which take into account overall economic (macroeconomic) forecasts, historical data, technical trends and backlog. The microeconomic forecasts are provided by Chase Econometric Associates, Inc., a subsidiary of Chase Manhattan Bank.

The microwave equipment and component forecasts are based upon interviews with equipment designers, component buyers and producers. The total component demand is then defined and forecasted by input-output methodology, whereby all component production is accounted for by considering the sum of OEM use in marketable equipment, plus all components manufactured for non-production uses such as replacement parts, R&D and inventory level change. □

A subcontract has also been awarded to Westinghouse by RCA for development of the AFAR radar phased array for an ABMDA program. AFAR is an L-band radar, which in its final operational form, will incorporate 16,800 active elements. Each element will provide 50 watts peak output with a high duty factor and consists of nine thick-film captive MICs in a single multifunction enclosure.

Laser radars have also been under development at the AF Avionics Laboratory for several years and more recently by the Air Force Cambridge Research Laboratories, Bedford, MA. This R&D effort will increase with a few production prototypes operational by 1978. Fuze radar applications will undergo growing penetration by optical fuzes, which basically consist of a LED transmitter and a phototransistor receiver. Optical countermeasures will also obtain an expanding share of the available countermeasures budget. (This is discussed more fully in next month's installment).

In non-military government radar, the major production system over the next decade will be an ARSR-V Air Route Surveillance Radar, now being developed by Westinghouse, Baltimore, for the FAA. The FAA will spend about one billion dollars for air-traffic control improvement over the next four years, most of it radar related.

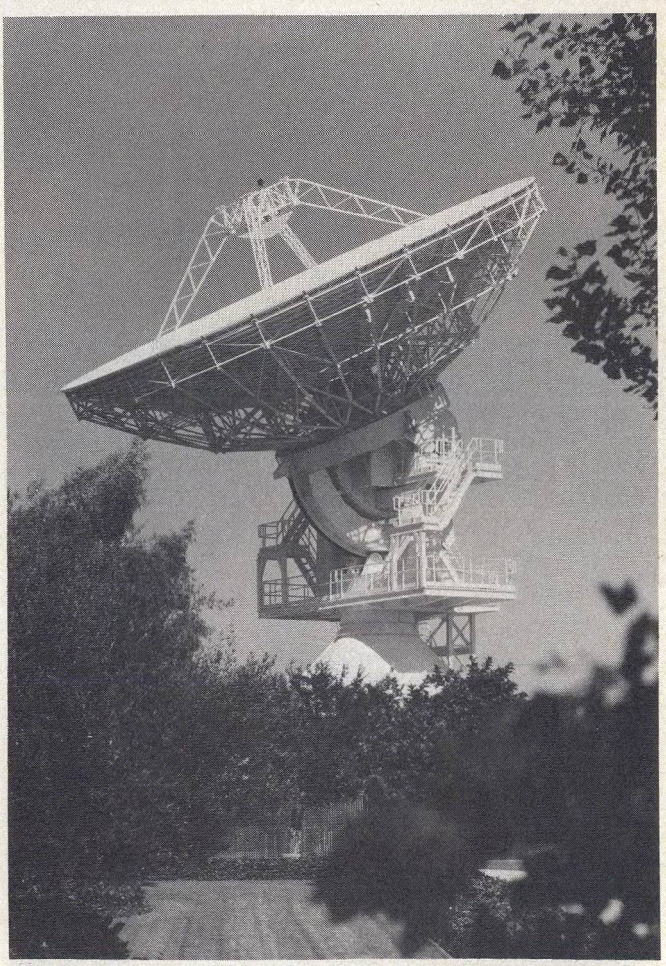
Communications requirements will expand

The growing U. S. global commitment and the concomitant necessity for instantaneous worldwide multichannel communications spurs continued growth in production of military communications equipment. Both voice and data links will proliferate with satellites accommodating most long haul transmission. The communications and navigation equipment markets will grow from $1.7-billion to $2.14-billion over the 1974-1978 period. The microwave equipment portion of this market will expand from $715-million to $899-million over the same interval.

Spread-spectrum communications techniques will be used increasingly over the next decade. This technique will be used, for instance, in the Space Shuttle S-band communications to avoid interference with terrestrial systems. Advanced RPV (Remotely Piloted Vehicle) command and guidance communication is using spread-spectrum to elude jamming. (See "The Search For Smarter and Scrappier Drones," *Micro-Waves*, October, 1973, pp. 42-52, and "Mini-RPV's: For Cheap and No Risk Air Power," *MicroWaves* pp. 40-48, October, 1974).

There is a strong trend to use of digital transmission techniques. Use of speech processors such as the E-Systems, (Garland, TX) 2000 bps VADAC, will be required for converting voice to digital signals to permit simultaneous transmission of voice and data. Satellite-related military microwave communications equipment production will expand from over $200-million in 1974 to over $300-million in 1978. Major programs of interest are:

- The AN/MSC-60, ground terminals of which 21 will be built by Philco-Ford, Palo Alto, CA, over the 1974-77 period, under a $96-million Army Electronics Command Contract. These ground stations will be linked to the DSCS-2 (Defense Satellite Communications System) satellite. Comtech, Smithtown, NY, will provide paramps, downconverters, upconverters and other components to Philco under an $11-million subcontract. Earlier ground terminals were the AN/MSC-46 and AN/TSC-54.
- The AN/WSC-2 advanced shipboard satellite communications terminal is being developed by ITT Defense Communications Div., Nutley, NJ, under a $10-million NESC contract.

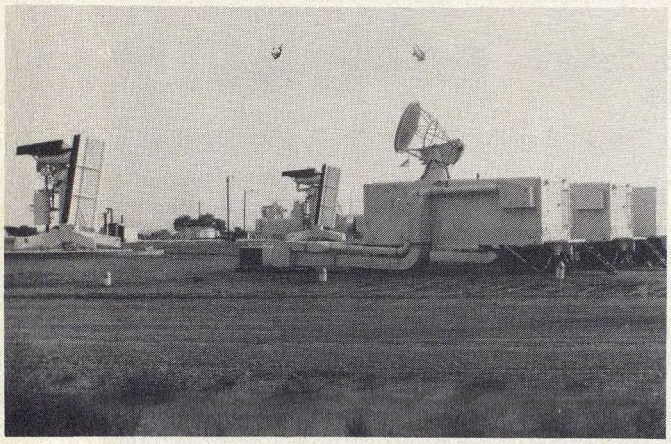


6. **The AN/MSC-60 earth terminal with its 60 ft diameter dish** is one of 21 stations to be built by Philco-Ford for the second generation Defense Satellite Communications System (DSCS-2). It operates over a 7.25-7.75 (downlink) and 7.9 to 8.4 GHz (uplink).

(continued on p. 54)

- The Satellite Data System, SDS, a multi-purpose communications satellite, will be developed and produced by Hughes, El Segundo, CA, for the Air Force at a cost of over $150-million.
- The Air Force Avionics Laboratory, Electronic Technology Division, Wright Patterson AFB, is developing a laser space communications system, program 405-B, for communication between spacecraft at a one gigabit rate.

In that regard, optical communications techniques including fiber optics, will receive heavy military R&D funding over the next five years. Secure operation is a major advantage of optical systems. Optical communication via fiber optics or on-the-air laser beams, now in limited prototype production will become significant by 1978.



7. **The AN/MPQ-T2 training set,** built by Tasker Systems, simulates Soviet radar characteristics at Eglin Air Force Base, FL.

Guidance and control production declines

Guidance and control systems are used primarily in missiles. Missile production is expected to decline over the 1975-1982 period, after the 1972-1973 replenishment of Southeast Asia losses. Production of guidance and control electronics was $1.23-billion in 1974 and will decline to $1.11-billion in 1978. The microwave equipment content of guidance and control electronics was $430-million in 1974 and will decrease to $390-million in 1978.

The SAM-D Program has been stretched out and is under congressional attack. The projected tactical environment now appears different from that assumed when SAM-D development was initiated several years ago. The October, 1973 war, in particular, indicates that some revision of configuration may be in order. Development of high altitude air defense technology will continue at a high level, but commitment to large volume production is still to be decided. SAM-D guidance is a combination of mid-course command correction plus semi-active teminal homing. The Army is considering several alternatives, including the Hughes guidance of the Navy Phoenix Missile and the Raytheon Hawk guidance.

There is a strong trend to use electro-optical homing guidance of various types, but mostly by laser guidance. The new Hellfire missile will be laser guided. The Goodyear AIMPOINT and RADAG navigation/guidance systems use optical correlation techniques for missile guidance. Radar guidance for weapons delivery has already been impacted in a major way by the laser and other optically-guided weapons. The laser and optics portion of the weapons guidance budget will grow over the next five years.

NASA-generated microwave demand constant

The NASA microwave equipment demand will continue to be heavily oriented toward spacecraft and ground-terminal communications, radar, instrumentation and control. The space shuttle will be the major program over the next half decade. Microwave equipment procurement will continue at a constant level of about $300-million per year with a heavy content of "software" (qualification testing and documentation).

AIL, Deer Park, NY, will develop the airborne microwave scanning beam landing system for the space shuttle. The system will include Ku-band DME. Each shuttle orbiter will have three redundant systems, which are modified versions of the AIL AN/ARQ-31. The system is similar to the AN/SPN-41, built by AIL for navy carrier aircraft approach control. The airborn system includes a DME transponder and an all solid-state receiver/decoder. The ground-based DME interrogator will also be solid-state with the exception of the magnetron power tube.

The space shuttle orbitor vehicle will incorporate six S-band phased arrays developed by Texas Instruments, controlled by an on-board computer for communication with ground stations and data-relay satellites.

Technician shortage boosts instrumentation demand

The growing shortage of skilled technicians in the armed forces creates a growth market for automated test systems such as the VAST (Versatile Avionic Shop Test) developed by PRD/Harris, Westbury, NY. This is an extensive automated maintenance system which can be used for several aircraft. PRD has delivered 46 VAST systems to the Navy. Typical of newer systems is the Hewlett-Packard HP9500 Series automatic test system for fault isolation and performance verification of avionics. Production of such systems plus conventional instrumentation, telemetry, classroom equipment and trainers/simulators will total $1.84-billion in 1978. The microwave participation in this instrumentation will total $186-million or 10% in 1978.

Typical of conventional, government-specified microwave instruments is the spectrum analyzer being supplied by Systron-Donner, Concord, CA, to the FAA for their ASR-8 radar maintenance program. One hundred eleven units are to be delivered at $5,400 each. Systron-Donner has sold over 350 of these instruments to government agencies.

AEL, Lansdale, PA, will build a $1-million test transmitter for the missile electronic warfare technical area. The AN/ALQ-5 simulator for EW training was produced by AAI Corporation, Baltimore, MD, in 1973 under a $5.8-million Air Force contract. Simulation of Soviet radars and other microwave equipment is a major market for microwave simulators. The Air Force simulation range at Eglin AFB in Florida is the main market for these simulators and Tasker Systems, Chatsworth, CA, has been a leading supplier. General Dynamics, San Diego, CA, also is a leading producer of Soviet surface radar simulators, including shipments to Iran under the Air Force "coronet ruby program." ••

Part 2:

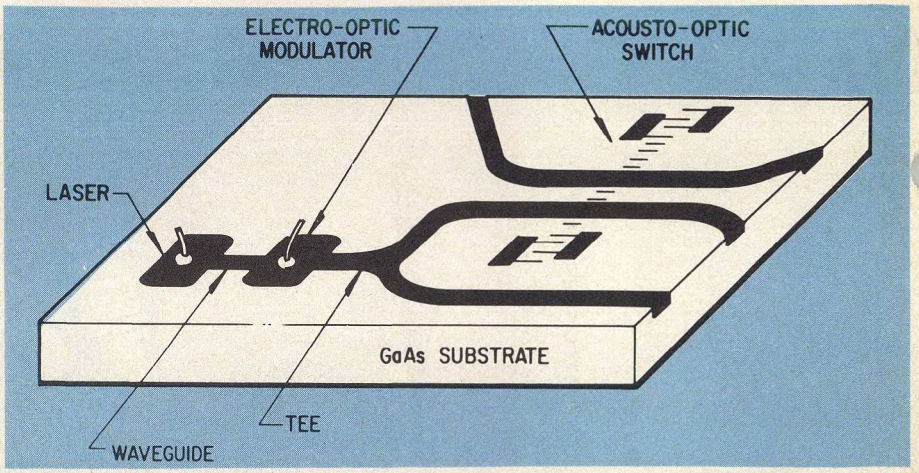
Integrated Optics Mirror Microwave Concepts

A new revolution is beginning in miniature waveguides, modulators and detectors . . . but at optical wavelengths. Here's an update on the technology and its potential for wideband communications.

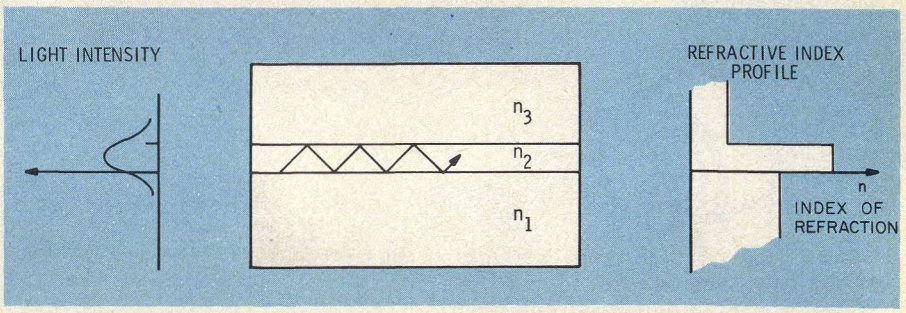
This is the conclusion of a two-part series on optical communications. Part 1 appeared last month and described fiber optics and some hybrid systems. This installment covers recent advancements in integrated optics.

Classically, the term optics bring to mind large, bulky components (much larger than a wavelength) which are often placed on a large, specially designed optical table. The goal of integrated optics is to miniaturize many of these components to the point that they can be constructed simultaneously on a single substrate. These miniature components must transmit, receive, modulate and otherwise, manipulate optical waves for signal transmission. The optical component miniaturization, as with electronic miniaturization, will lead to more reliable, more efficient devices which are rugged and stable. Integration will also minimize interconnections which, ultimately, are the main limiting factors of all solid-state electronics. The types of devices suitable for integration include thin-film prisms and lenses, channel waveguides, surface lasers, grating reflectors and couplers, directional couplers, waveguide detectors, modulators and beam deflectors.

What would an IOC look like? Figure 4 is a local surface laser feeding a channel optical waveguide circuit. Ideally, such IOC's should not be hybrid, but monolithic, constructed using a single material. The most promising materials system for monolithic IOC's is the semiconductor GaAs and its ternary alloys with In and Al.[10] In principle, all of the requisite functions for complex IOC's can be performed in GaAs: (1) waveguiding, (2) light generation, (3) light detection, (4) electro-optic modulation/switching and (5) acousto-optic reflection/modulation. Also, the emission wavelengths of the alloys can be adjusted to match bands of low-fiber loss by changing their composition. Furthermore, GaAs is amenable to standard semiconductor processing which has made IC's possible. The other candidates for monolithic IOC's are (1) the garnets,[11] and (2) the lead-salt semiconductor [(Pb. Sn) Te, etc.]. Perhaps the most serious drawback of the garnets is the lack of a convenient thin-film laser source. Lead-salts on the other hand, limited to the middle infrared region ($\lambda \approx 10\ \mu m$) and their material technology is rather undeveloped.



1. **Prototype IOC transmitter** shows various active and passive elements on a single GaAs substrate.



2. **Thin-film waveguide** traps an optical wave by total internal reflection. Indices of refraction, $n_1 < n_2$. For asymmetric waveguides $n_1 >> n_3$ and $\Delta n = n_2 - n_1$ is small.

Waveguides losses only 0.1 dB/cm

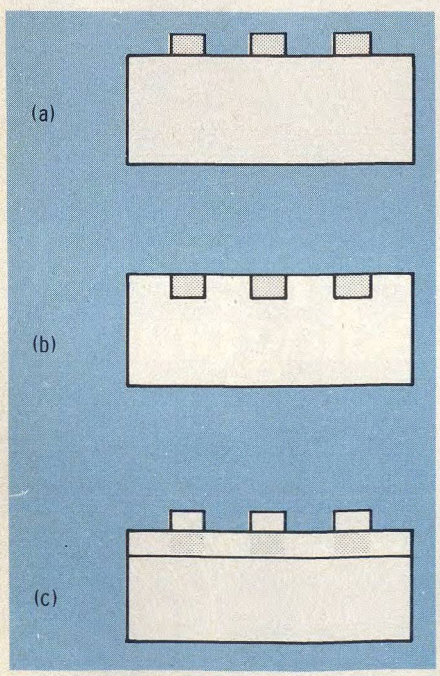
Most of the ideas for IOC's are closely related to the notion of a thin-film waveguide, Fig. 2. A thin

Fred A. Blum, Member Technical Staff, Adv. Components Laboratory, Texas Instruments, Inc., 13500 N. Central Expressway, Dallas, TX 75222.

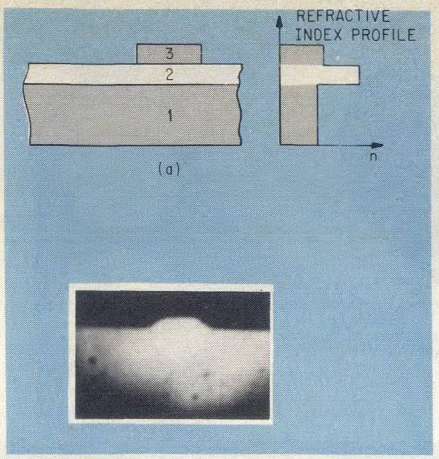
film of slightly higher refractive index than its supporting substrate traps an optical wave by total internal reflection, just as the fibers discussed earlier. Waveguides have been made in a variety of materials including glasses, semiconductors, garnets, liquid, crystals, epoxies, lithium niobate and lithium tantalate. Most waveguide studies have been carrier out in the near infrared or visible, although some measurements have been made at 10 μm with modulation and detection of CO_2-laser radiation in mind. The losses of these waveguides range from 0.1 to more than 10 dB/cm. Since IOC's are envisioned to have dimensions measured in millimeters, any waveguide with a loss under 10 dB/cm will be adequate for most applications. In general, the choice of a waveguide material depends on its compatibility with active devices. The propagation characteristics of a thin-film guide depend on its dimensions and index step. For an asymmetric waveguide ($n_1 >> n_3$) with Δn small there are propagating modes only if

$$B \equiv \frac{2\pi t}{\lambda} \sqrt{2n_1 \Delta n} > \frac{\pi}{2} \quad (10)$$

where t is the film thickness and $\Delta n = n_2 - n_1$. A new mode appears as B becomes greater than each odd multiple of $\pi/2$. For GaAs at $\lambda = 1$ μm with $(\Delta n/n) = 10^{-3}$, the first mode propagates for $t > 2.9$ μm. For glass at $\lambda = 1$ μm with $(\Delta n/n) = 10^{-2}$, the first mode propagates for $t > 1.7$ μm. In general, single node thin-film waveguides have thicknesses ranging from 1000 Å to 10 μm.



3. **Channel waveguide cross sections** may be (a) raised ridge, (b) imbedded channel or (c) optical stripline—the analog of dielectric microstripline. The shaded region shows where the light beam is trapped.

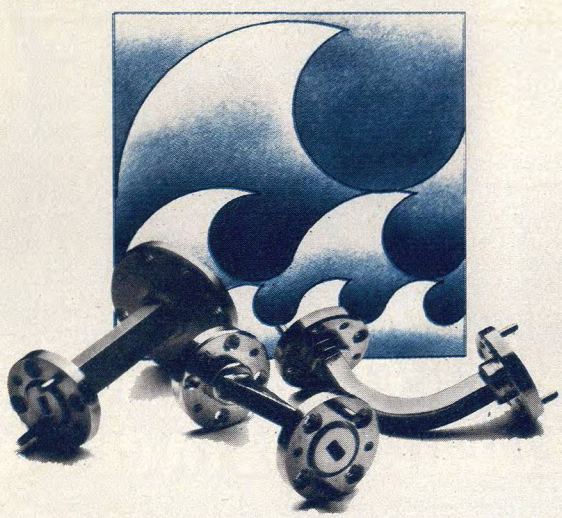


4. **Optical stripline waveguide** has less light scattering due to ridge wall roughness. (b) **Photomicrograph shows near field intensity pattern** at end of a stripline which has trapped a 1.15 μm laser beam. Blum, et al., Ref. 12.

While two dimensional thin films may be useful for some IOC's, channel waveguides which function like a microwave rectangular guide are clearly needed. Three schemes for the fabrication of such channel guides are possible. The raised ridge. Fig. 3a, can be made by photomasking and etching a thin-film guide, and imbedded channel waveguides. Fig. 3b, by diffusion and implantation, again using a mask to define the channel. The third channel guide, Fig. 3c, is an analog of a metal-dielectric microstrip line. The light is trapped beneath rather than within the defined channel; provided the refractive index of the ridge is less than the index of the underlying film. Because the beam is excluded from the ridge, it suffers less scattering loss due to ridge wall roughness than the other types of channel guides. Figure 4 shows the near-field intensity pattern of the end of a Texas Instruments' GaAs stripline guide which has trapped a 1.15 μm laser beam.[12] This guide supports only the lowest order $TE_{1,1}$ mode.

Because optical waveguides have dielectric rather than metallic boundaries common to microwave guides, they can easily become antennas, radiating away energy. Wall imperfections and waveguide bends generate losses due to this radiation process. Optical photolithography is generally limited to a resolution on the order of 1 μm and the scattering losses due to such wall variations can be serious. Finer resolution requires the use

(continued on p. 59)



Hughes mm waveguides cut insertion loss to a trickle.

Hughes announces three new series of millimeter waveguide components. E and H-plane bends, tapered transitions, and 45 and 90° twists are precision manufactured to assure minimum insertion loss and VSWR for lab and system applications. All three are available in six standard waveguide sizes in the 26.5 to 110 GHz range.

Call or write: Hughes Electron Dynamics Division, 3100 W. Lomita Blvd., Torrance, CA 90509. (213) 534-2121, Extension 215.

HUGHES
HUGHES AIRCRAFT COMPANY
ELECTRON DYNAMICS DIVISION

Making waves in millimeter-wave technology.

READER SERVICE NUMBER 57

of electron beam and/or X-ray lithography, both new and sophisticated techniques.

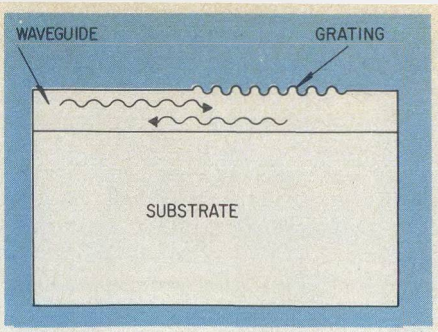
Channel waveguides have been made in a variety of glasses and semiconductors by etching, implantation and diffusion. In semiconductors, a thin-film guide can be made by growing an epitaxial film of low-carrier concentration ($< 10^{16}$ cm^{-3}) on a substrate of higher carrier concentration (10^{17} to 10^{18} cm^{-3}). In fact, an $n^+ - n - n^+$ GaAs sandwich made for fabricating Gunn oscillators makes a good optical waveguide if the n-region is sufficiently thick. The lightly doped n-region has the highest refractive index and guides the wave. Proton bombardment (of GaAs) and ion diffusion (into ZnS and ZnSe) have both been used to change the refractive index, creating channel waveguides.

Potential for DFB and mesa diode/lasers

The simplest miniature light source for communications applications is the semiconductor light emitting diode (LED). It is small, lightweight, efficient and can easily be incorporated in a more complex semiconductor chip. However, as pointed out earlier, GaAs LED's are incoherent devices with emission bandwidth of several hundred angstroms and switching times slow compared to lasers. Furthermore, full use of the potential of optical waveguides (both fiber and dielectric film) requires a coherent source. Therefore, most research on sources for IOC's centers on lasers.

The key to the incorporation of a laser in an IOC lies in the fabrication of a local, nondiscrete surface laser which can be placed at will in a monolithic optical circuit. Solid-state lasers require mirrors to furnish optical feedback and form a cavity. Standard external mirrors are obviously inappropriate for an IOC. Semiconductor diode lasers use the reflection from cleaved facets for feedback. This makes the "mirror" integral with the device, but it also makes the diode laser inherently a discrete device which is not readily incorporated in a larger optical circuit. Thus, IOC technology demands a radical departure from conventional laser technology for making laser cavities.

One of the first concepts introduced for a surface laser compatible with thin-film waveguides is the distributed feedback (DFB) laser,[13] Fig. 5. A corrugation



5. **Distributed feedback laser** has a grating on the surface of a thin-film waveguide to coherently scatter a guided wave using Bragg's reflection technique.

(grating) on the surface of a thin-film waveguide coherently scatters a guided wave provided the period is chosen correctly. In fact, if the period is chosen to be one-half the wavelength of the guided wave, the first-order grating will act as a mirror, reflecting the wave backwards. For the m^{th} order reflection from the grating, The Bragg DFB condition is

$$d = \frac{m\lambda_g}{2} \qquad (11)$$

where λ_g is the wavelength in the guide. If this Bragg reflector is in the active gain region of the laser, then the reflection or feedback is distributed along that region, hence the name distributed feedback. The first DFB laser[13] was an organic dye laser. A group at the California Institute of Technology under A. Yariv has pioneered the application of the DFB concept to semiconductors.[14] They made several GaAs devices which were optically pumped with a conventional dye laser. More recently, researchers at Xerox Research Laboratories[15], Aerospace Corporation, Hitachi and Coltech have fabricated GaAs electrical injection (diode) DFB lasers. These devices are made by ion milling a grating in a GaAs surface and incorporating this grating in a layered p-n junction structure so that the corrugation is nearby and reflects the wave. The emission spectrum of one of the Xerox devices is shown in Fig. 6. Note that the emission occurs in a very narrow band of under 41 Å width when optically pumped at 35 Amperes. This is considerably narrower than a standard discrete laser which usually runs on many longitudinal and transverse modes over a band of tens of angstroms. For a GaAs laser emitting near 0.9 μm (in air), $\lambda_g = (0.9/3.6)$ μm and $d \approx 0.125$ μm. This is a very short period indeed and requires special fabrication tech-

(continued on p. 60)



This waveguide circulator will fit your mm-waves to a "T"

Our three-port, T-junction circulators are designed for mm-wave frequencies from 26.5 to 110 GHz in six waveguide bands. They feature high isolation, low insertion loss and low VSWR over a broad bandwidth. That makes them ideal for use in negative resistance amplifiers and phase modulators.

Our unique T-junction accommodates typical waveguide routing patterns better than commonly used Y-junction devices and eliminates the sprawl effect they can cause.

Find out more about the world's only practical T-junction mm-waveguide circulators. Call or write: Hughes Electron Dynamics Division, 3100 West Lomita Boulevard, Torrance, California 90509. (213) 534-2121, extension 215.

HUGHES
HUGHES AIRCRAFT COMPANY
ELECTRON DYNAMICS DIVISION

Making waves in millimeter-wave technology.

READER SERVICE NUMBER 59

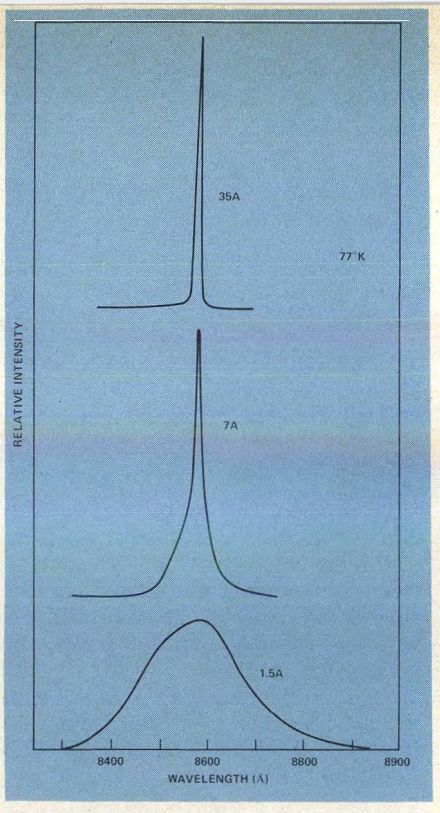
niques. In fact, most GaAs DFB lasers have third-order gratings with d $\approx$ 0.375 μm. Even these gratings require electron beam lithography or holographic grating exposure using a visible laser (typically an argon laser emitting near 0.5 μm). In the latter, photoresist is exposed to two coherent laser beams (split from the same source) which generate an interference fringe pattern with a spacing

$$D = \frac{\lambda}{2 \sin (\theta/2)} \qquad (12)$$

where θ is the angle between the two beams. Clearly, fabrication of first order DFB gratings requires a UV laser. Developing the photoresist leaves a corrugation mask on the GaAs which is usually ion sputtered to form a grating in the GaAs itself. Other techniques for making the grating might be ion implantation or diffusion. Note that a physical corrugation of the waveguide surface itself may not be necessary. What is needed is any periodic perturbation of the optical or gain properties of the waveguide.

A second concept for the fabrication of a monolithic, nondiscrete GaAs diode laser has been demonstrated at Texas Instruments[16]. Selective vapor phase epitaxy is used to grow n-type island-like layers which have the shape of a vertical mesa with parallel opposite sides. The mesas grow only in diamond-shaped holes which have been opened in a SiO_2 coating using a photomask. Because each mesa is a single crystal, its surfaces are extremely smooth and the opposite sides form an optical cavity. A p-n junction is formed in the mesas by diffusion of Zn into the mesa tops converting the top portion of mesas to p-type. The injection mesa lasers have the advantage of being placed at will on a substrate using conventional photomasking techniques. In fact, several hundred have been grown at a time on a single slice and then batch processed to make injection lasers. Figure 7 shows the first monolithic semiconductor diode laser fabricated in a batch-type process. All the processing steps involve standard techniques already employed by the semiconductor electronics industry.

Another solid-state laser often mentioned as a candidate for optical communications is the Nd: Yag laser which emits at 1.06 μm. However, this laser must be optically pumped, a distinct disadvantage for IOC's since it inherently leads to hybrid, non-monolithic devices. The GaAs laser has the advantage of directly converting electrical current to optical photons.



6. **Emission spectra** of a distributed **feedback (DFB) laser** (after Seifres, et. al, Ref. 15) shows optical intensity for three levels of optical pumping. It is made in a GaAs (Ga,Al) single heterostructure. Note how bandwidth increases as pump power drops from 35 Amperes to 1.5 Amperes. Laser must be cooled to 77°K using liquid nitrogen to operate.

The development of GaAs lasers for optical communications is now limited by two factors: (1) no surface-injection laser has yet been coupled to a waveguide circuit and (2) long-lived discrete devices are not routinely fabricated. Long lived room-temperature cw diode lasers are complex, multilayered heterostructure devices involving alternate layers of GaAs and the alloy Ga_{1-x} Al_x As. Several laboratories in the U. S. and Japan have only recently succeeded in making selected lasers with lifetimes approaching 10,000 hours.

Couplers

As with microwave guides, special techniques are needed for efficient coupling to and between optical waveguides. Three techniques have been used for coupling sources in air to thin films: (1) end-fire coupling with a tightly focused beam, (2) a surface grating which Bragg deflects the incoming radiation and (3) a prism pressed against the guide surface. The grating and the prism couplers are illustrated in Fig. 8. The surface grating effectively shifts the phase of the incoming wave by an amount ($2m\pi$ x/d) where m is the Bragg order, necessary to match the phase of the wave in the guide. The full phase matching condition is

$$\frac{2\pi}{\lambda_0} \sin\theta \pm m\frac{2\pi}{d} = \frac{2\pi}{\lambda_g} \qquad (13)$$

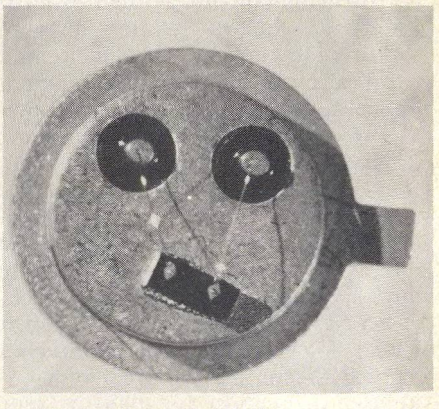
where λ_0 is the wavelength in air, λ_g is the wavelength in the guide and θ is the angle the incoming wave makes with respect to the surface normal. Grating coupling efficiencies of 40-50% have been obtained. The DFB condition described earlier is a special case of this grating coupler equation. The basic effects are the same, i.e., coherent Bragg scattering. The prism coupler depends on the evanescent field of the incoming wave at the prism-field interface. That is, the leaky wave which decays below the prism bottom surface excites a wave in the guide. The phase match condition is

$$\frac{2\pi}{\lambda_p} \sin\theta_p = \frac{2\pi}{\lambda_g} \qquad (14)$$

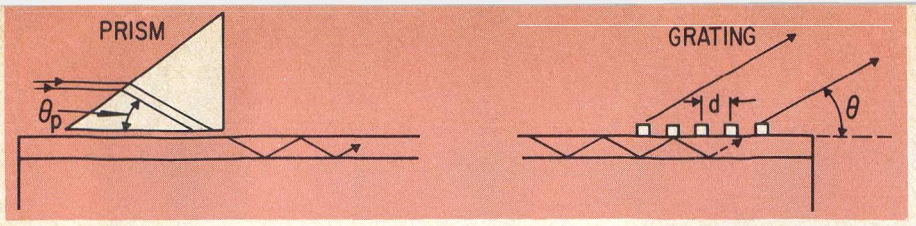
where λ_p is the wavelength in the prism. Prism coupling efficiencies as high as 80% have been obtained. Note that both the grating and prism couplers allow coupling to different waveguide modes (which have different λ_g's) by varying the incoming beam angle. The prism has the disadvantage of being a bulky component making the prism film coupler a large hybrid device.

The evanescent field character of the prism coupler is actually a more general technique for coupling between dielectric waveguides. Since the fields of an optical guide reach

(continued on p. 62)



7. **These two monolithic mesa diode lasers** are mounted on a TO-46 header. They're cut from a batch-processed slice using standard processing steps common to the semiconductor industry. (After Blum, et al, Ref. 16).



8. **Two techniques for coupling laser sources** from air to thin-film waveguides are the prism and surface grating which deflects incoming radiation. These techniques allow coupling to different waveguide modes by varying incoming beam angle.

beyond its boundaries, one guide can become coupled to another if they are placed close enough to each other. The data taken by a Caltech-Hughes Aircraft[17] group show the exchange of intensity between the parallel channel guides which were formed by proton bombardment in GaAs. The evanescent field coupling, Fig. 9, is a coherent phenomena which increases with increasing propagation length. The amount of energy coupled from one channel to another can be controlled by their separation and the length over which they run parallel to each other (See Fig. 1).

Another technique used for coupling between and from optical waveguides is to taper the film thickness. Varying the film thickness changes the phase velocity of the guided wave. At some point, the phase velocity becomes equal to that of light in the surrounding medium (either a substrate or another waveguide) and efficient coupling occurs. The tapered-waveguide coupler has the advantage over the evanescent-field technique of not requiring phase coherence over long distances.

Modulator/switches

While injection lasers and LED's can be directly modulated by varying their electrical drive current, it is desirable to have more general modulation capabilities. Optical multiplexing will require techniques for the modulation and switching in waveguide circuits which are independent of the source. Three basic effects which involve changes in the optical properties of crystals through the influence of applied fields are the electrooptic, acoustooptic and magnetooptic effects. All three have been used in thin-film waveguide devices to demonstrate their utility.

If a dc electric field is applied to the electrooptic (EO) material, the index of refraction is changed by an amount proportional to the strength of that field. By forming a Schottky Barrier on top of a high resistivity GaAs waveguide, the Caltech group[18] showed in 1970 that they could control the cutoff of the guide. In the absence of an applied voltage, the waveguide was below cutoff and would not propagate light. The high electric field E in the depletion region of the reverse biased Schottky Barrier increased the index by an amount

$$\Delta n = \frac{n^3}{2} r_{41} E, \qquad (15)$$

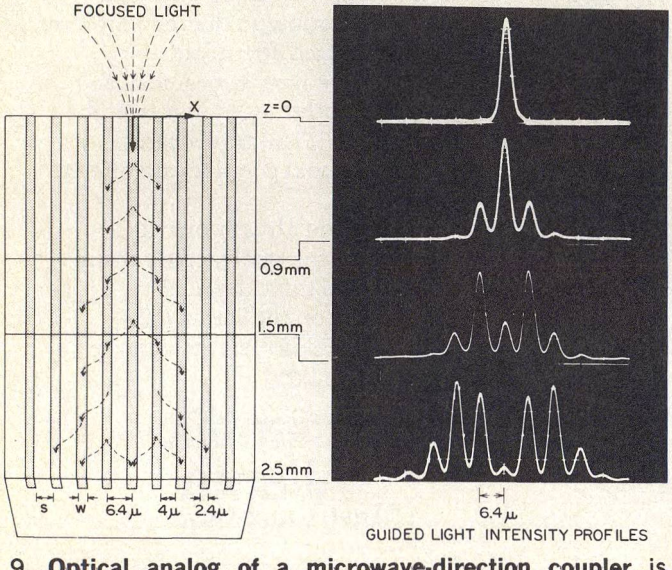
where r_{41} is the electrooptic coefficient for the particular polarization and propagation direction chosen. This index change Δn is large enough to make the waveguide above cutoff and allow propagation. EO modulation has also been observed in II-VI channel waveguides, lithium niobate ridge waveguides, ZnO films, p-n junction waveguides and ferroelectric waveguides. Power requirements as low as 20 μW per MHz of bandwidth have been observed. The Japanese have recently achieved 70% modulation depth at 900 MHz using interdigital electrodes to form a Bragg-type phase gating for beam deflection in $LiNbo_3$.

A surface-acoustic wave in an acoustooptic (A) material generates a traveling wave of refractive index variation. This spatially periodic index variation can act as a phase grating to Bragg deflect a light beam propagating in a waveguide. The Bragg angle is given by

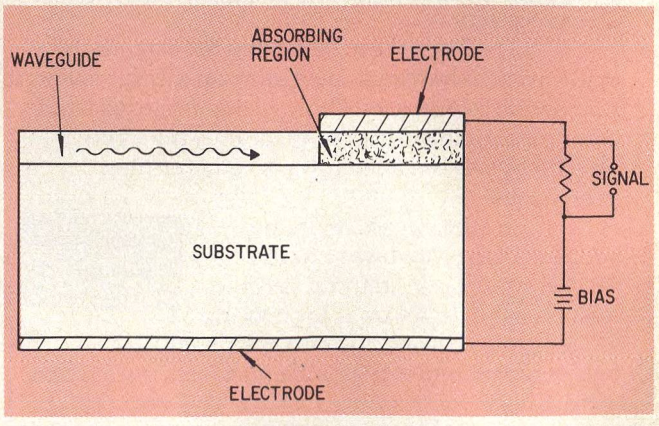
$$\theta_B = \sin^{-1}(\lambda_3/2\Lambda) \qquad (16)$$

where Λ is the acoustic wavelength. This acoustic deflection can serve either to switch or modulate the light beam depending on the waveguide configuration. Acoustooptic deflection of guided waves have been observed in thin films made of lithium niobate, As_2S_3, Ta_20_5 and glass. Typical deflection angles are $\theta_B = 1$ to 2 degrees. While these are small angles, they can be magnified by refracting the deflected beam through a lower index region (diverging lens).

The AO switch shown in Fig. 1 uses interdigital fingers on a piezoelectric pad to launch a surface acoustic wave. This wave partially deflects the guided wave beneath



9. **Optical analog of a microwave-direction coupler** is the evanescent field coupling in GaAs imbedded channel waveguides (after Somekh, Ref. 17). Coupling is a function of separation and length of the channels.



10. **Waveguide photodetector** has a p-n or Schottky-Barrier junction and an optical absorption edge at longer wavelengths than that of the guided wave.

one waveguide, thus inducing coupling to the second waveguide. Channel waveguides of the optical stripline type would be best suited for this application since they permit propagation in the region between the parallel channels. AO induced mode conversion has also been observed using colinear propagation of the guided light and the acoustic surface wave. Finally, bulk-acoustic waves have also been used to modulate guided light waves.

In general, active devices based on the AO effect do not have the high data rate potential of EO modulators. The AO deflection experiments performed to date have involved sound wave frequencies in the 200 to 300 MHz range. Also, the fabrication of AO devices requires the special technology of acoustic transducer fabrication, while EO devices basically require a simple patterned metallization. Furthermore, AO devices require conversion from electrical to acoustic energy via the transducer, a rather inefficient process. Transducer coupling losses for surface waves can be quite high. As a result, the use of AO devices in IOC's will probably be limited.

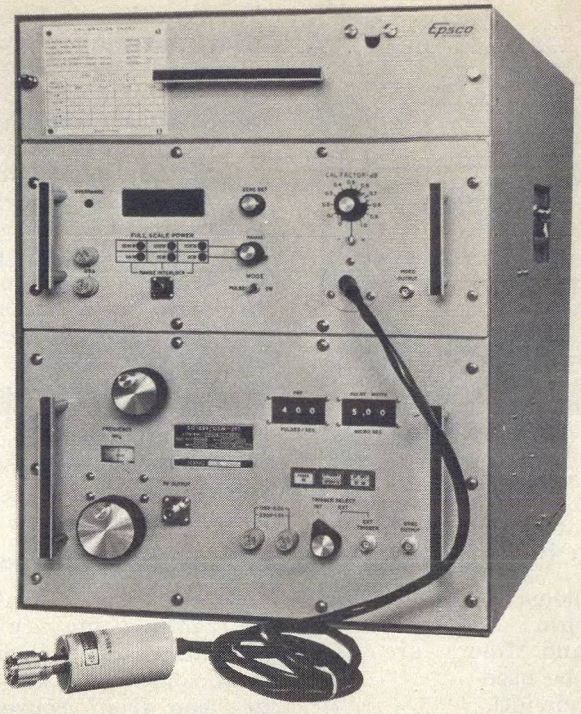
Magnetooptic (MO) modulators have been made using prism-coupled iron-garnet films.[11] A surface electric current induces a change in the direction of the film magnetization. This, in turn, changes the polarization of the guided wave. If such a device is followed by a polarizer, amplitude modulation is achieved. Modulation rates as high as 300 MHz have been predicted for the MO modulator. However, the application of the MO effect in integrated optics is likely to be limited since it requires a magnetic film material.

Detectors

The problem of photodetection in IOC's is technologically not as critical as the signal generation problem. For most application, coherent defection will not be required, while a coherent source is needed. This is the crux of the difference. Incoherent detectors can be fabricated in waveguide structures without radical departures from current detector technology. For this reason, very little of the research effort in integrated optics has dealt with detectors.

The characteristics needed for a good detector for optical communications and IOC's are apparent:

(continued on p. 64)



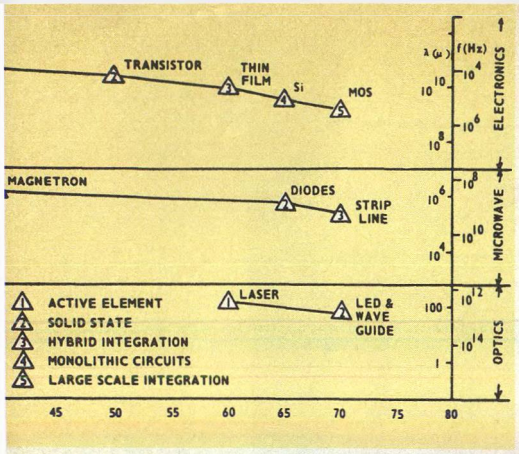
takes the worry out of being close

We can get you just as close as you need to be. Within 0.3 dB when calibrating peak powers from milliwatts to 5 kilowatts. And our accuracy is directly traceable to the National Bureau of Standards. A significant advantage when you're calibrating TACAN, DME, DABS, ATC, IFF and other accuracy-demanding systems in the 925 to 1225 MHz frequency range. Direct readout of pulse power, pulse width, PRF, and operating frequency. Pulse duration from 0.35 to 5 microseconds. Automatic sequencing. Sync output. Accepts internal/external trigger. The Peak Power Calibration System from Epsco. So stop worrying. We can get you close enough and help keep you there. We're sure.

Test our confidence. Call or write for complete data.

Epsco INCORPORATED
APPLIED MICROWAVE DIVISION
411 PROVIDENCE HIGHWAY, WESTWOOD MA 02090
(617) 329-1500 TWX (710) 348-0484

READER SERVICE NUMBER 63



11. Are integrated optics on the threshold of launching from an infant technology into a mature field? If integrated optics follow the pattern established by electronics and microwave systems, the lasers during the next 20 to 30 years will play a very important part in our society and technology. Hudson, Ref. 23.

- High responsivity in the 0.8 to 1.1 μm region where sources and fibers are expected to be used
- Large bandwidth
- Low noise and cost
- Compatibility with waveguide demodulation circuitry

As might be surmised, the semiconductor photodiode is the small, low-cost reliable device which meets these requirements. Incoming photons generate electron-hole pairs in the high field depletion region of the diode. These carriers are swept out generating an external electric current. The characteristics of discrete photodiodes relevant to optical communications systems design have been extensively discussed previously.[4,6] Standard commercial silicon p-n and p-i-n structures are adequate for many near-term applications.

Photodiodes have been directly fabricated in GaAs planar waveguides by two techniques: (1) proton bombardment of a local region in an epitaxial layer, creating defect levels which shift the optical absorption edge[19] and (2) selective eptiaxial growth of $Ga_{1-x}In_xAs$ in holes etched in an epitaxial layer[20]. The $Ga_{1-x}In_xAs$ Schottky Barrier avalanche photodetector has the advantage of having its peak response wavelength tunable by changing the In content. Stillman, et al.,[20] obtained a 275 MHz bandwidth with their waveguide photodiodes and expect to be able to improve on this result. The basic configuration for both techniques, Fig. 10, requires the local detector region to have (1) a p-n junction (or Schottky Barrier) and (2) an optical absorption edge at longer wavelengths than that of the guided wave. A hybrid integrated photodetector has been made at Thomson-CSF (France)[21] using glass waveguides sputtered on a silicon substrate which incorporated a p-n photodiode. A waveguide taper is used to couple the signal to the silicon photodiode.

Corherent detection is important for one area; namely, the laser radar field. Integrated-optical techniques are being considered for the fabrication of heterodyne receivers for CO_2 laser radars at 10.6 μm. Such a receiver would incorporate a waveguide detector and a diode laser local oscillator. $Pb_{1-x}Sn_xTe$ is the material most likely to be used. Such a device would necessarily operate at low temperature and its fabrication will be formidable.

Potential for GHz bandwidths

Optical communications via fiber cables using IOC components presents a new communications technology which has the potential to "leap frog" conventional technology and lead us, technologically, into a new era. The potential of low-loss transmission at data rates in the gigabit range is tremendous. In view of how communications bandwidths are becoming overcrowded, telephone companies are very interested in the possibility of replacing some of their intracity trunk lines with optical fiber cables. Indeed, if the development of the optical techniques proceed rapidly enough, they may actually supplant planned millimeter wave links which require precision and very expensive metal waveguides. The picture telephone, if and when it is revived, may send and receive signals on optical fibers. Other applications include:

- Internal communications for avionic, shipboard and factory systems
- On site and intracity interactive computer data links
- New community interactive television
- Facsimile transmission

In the near term, special military systems will probably yield the first significant applications of optical communications techniques. In fact, estimates of the cost savings which optical communications may yield the Department of Defense are in the $50-million/year category[22]. High performance military aircraft and ships have become increasingly crowded electronically. Interference problems are becoming more severe due to interconnect problems associated with LSI technology and increasing data rates. The Navy currently has a program to retrofit an A-7D aircraft with an optical data bus. Other military and industrial uses will also be applicable particularly those involved with hazardous, harsh and/or noisy electromagnetic environments.

Needless to say, many technological breakthroughs are needed before the components and techniques outlined in this article become practical. However none of the technological barriers are insurmountable. The materials (glass, semiconductors, etc.) to manufacture these communication systems should be plentiful and cheap. A perspective of the recent progress in electronics and the promise of optical communications is given in Fig. 14[23, 24]. It depicts the major advancements in the electronic, microwave and optical portions of the electromagnetic spectrum. Each region spans three to five orders of magnitude in frequency spread, yet barely a generation in time. If the progress in the development of optical communications in the next 20 to 30 years is as rapid as the past electron and microwave development, new achievements in optical communications will be phenomenal. ••

References

10. A. Yariv, "Components for Integrated Optics," *Laser Focus,* pp. 40-42 (December, 1972).
11. P. K. Tien, "Integrated Optics," *Scientific American,* Vol. 230, pp. 28-35 (1974).
12. F. A. Blum, D. W. Shaw, and W. C. Holton, "Optical Striplines for Integrated Optical Circuits in Epitaxial GaAs," *Appl. Phys. Letters,* Vo. 25, pp. 116-8 (1974).
13. H. Kogelnik and C. V. Shank "stimulated Emission in a Periodic Structure," *Appl. Phys. Lett.* Vol. 18, pp. 152-4 (1971); "Coupled Wave Theory of Distributed Feedback Lasers."
14. See, M. Nakamura, H. W. Yen, E. Garmire, E. Somekh, and H. L. Garvin, "Laser Oscillation in Epitaxial GaAs Waveguides with Corrugation Feedback," *Appl. Phys. Lett.,* Vol. 23, pp. 224-5 (1973), and references therein.
15. D. R. Scifres, R. D. Burnham, and W. Streifer, "Distributed Feedback Single Heterojunction GaAs Diode Laser," *Appl. Phy. Lett.* Vol. 25, pp. 203-6 (1974).
16. F. A. Blum, K. L. Lawley, F. H. Doerbeck and W. C. Holton, "Monolithic GaAs Injection Mesa Laser with Grown Optical Facets," *Appl. Phys. Lett.* 25,620-21 (1974).
17. S. Somekh, E. Garmire, A. Yariv, H. L. Garvin, R. G. Hunsperger, "Channel Optical Waveguide Directional Couplers," *Appl. Phy. Lett.,* Vol. 22, pp. 46-48 (1973).
18. D. Hall, A. Yariv, and E. Garmire, "Observation of Propagation Cutoff and Its Control in Thin Optical Waveguides," *Appl. Phys. Lett.,* Vol. 17, pp. 127-9 (1970).
19. H. Stoll, A. Yariv, R. G. Hunsperger, and G. L. Tangonan, "Proton-Implanted Optical Waveguide Detectors in GaAs," *Appl. Phys. Lett.,* Vol. 23, pp. 664-665 (1973).
20. G. E. Stillman, C. M. Wolfe, and I Melngailis, "Monolithic Integrated In_xGa_{1-x} As Schottky-Barrier Waveguide Photodetector,"*Appl. Phys. Lett.,* Vol. 25, pp. 36-38 (1974).
21. D. B. Ostrowski, R. Poiner, L. M. Reiber, and C. Deverdun, "Integrated Optical Photodetector," *Appl. Phys. Lett.,* Vol. 22, pp. 463-464 (1973).
22. C. M. Stickley, D. Albares, H. F. Taylor, and T. G. Giallorenzi, "Anticipated Uses of Fiber and Integrated Optics in the Defense Department," (unpublished).
23. R. Hudson, "The Future of Integrated Optical Technology," *Naval Research Reviews,* Vol. 26, No. 1, pp. 43-48 (1973).
24. IEEE Transactions on Microwave Theory and Techniques: Vol. MTT-23, No. 1, Jan. 1975 "Special Issue on Integrated Optics and Optical Waveguides."

JUNE
1975

MICROWAVES

laser technology

ECM:

EW Market Headed Toward $2.17 Billion
SAW Devices: What Should You Look For?

Also: Try CAD For Accurate MESFET Models



MICROWAVES

June 1975
Vol. 14, No. 6

news

11 Large Scale Production Techniques Eyed For Millimeter Component
14 N-way Combiner Design Can Consolidate 5 kW At S-Band
16 Microwaves Help Make Moon Model
18 Meetings
20 Industry
23 Washington
26 R & D
28 For Your Personal Interest . . .
30 International

editorial

32 To Trade Or Not To Trade . . . With East Bloc Customers

technical section

ECMI

34 **What's The Future For Electronic Warfare?** Jeff D. Montgomery of Gnostic Concepts completes a three-part forecast series with a look at the forces shaping tomorrow's EW market. Microwave needs are expected to soar to nearly $1.5-billion in 1978.

42 **A Specifier's Guide To Solid-State Source Terms.** Consultant Bernard S. Siegal offers a clear, concise set of basic definitions for solid-state source parameters. This compendium was written to foster better government-industry agreement on frequently misunderstood specs.

48 **Tips On Specifying Acoustic Wave Devices.** Chuck Grasse of Teledyne/MEC takes the mystery out of specifying all types of SAW devices. Included is a summary of the practical capabilities and limitations of these versatile signal processors.

58 **Try CAD For Accurate GaAs MESFET Models.** George D. Vendelin and Dr. Masahiro Omori of Varian Associates introduce an improved high-frequency GaAs FET model. S-parameters are fitted to experimental data using CAD routines, and projected to 24 GHz.

products and departments

72 **Product Feature:** Close-Tracking i-f Amp Offers a 75 dB Dynamic Range.

75 **Product Feature:** TWT Amplifier Designed For New 14 GHz Satellite Band.

75 New Products
89 Application Notes
90 New Literature
91 Advertisers' Index
92 Product Index

About the cover: Two F-5E Tiger IIs take off into the desert dawn. Photo by Robert T. Thornton, courtesy of Northrop.

coming next month: Antennas and Phased Arrays

News: **The Dome Array Antenna Cuts Phased Array Costs.** A new type of phased-array radar, offering hemispheric coverage from a single planar array, has been developed at Sperry. The novel proto-type system uses a passive dome with 3,636 fixed phase-shift modules, which cause the beam from the planar array to be deflected by fixed angles as it passes through the dome. This means it even can look backwards through an angle of up to 30 degrees from broadside (e.g., for side-looking radar applications). The system has important cost-saving implications!

Articles: **Graphs Simplify Corner Reflector Antenna Design.** David Proctor of NELC presents a series of computer derived design charts for maximizing the radiated field from a corner reflector. Optimum feed positions for various corner reflector angles are shown.

Determine Polarization Loss The Easy Way. E. Kramer of ESL, Inc., shows graphically how to determine polarization loss with a 0.1 dB resolution. Loss equations are also described that may be solved with a pocket calculator.

Measure That Field With Any Antenna. H. Carnagan of White Sands Missile Range, presents a method for determining antenna factor of most antennas. This parameter is useful in measuring electric-field intensities and once known, allows any antenna to be calibrated, and used in field-intensity measurements.

Publisher/Editor
Howard Bierman

Managing Editor
Richard T. Davis

Associate Editor
Stacy V. Bearse

Contributing Editor
Harvey J. Hindin

Washington Editor
Paul Harris
Snyder Associates
1050 Potomac St., NW
Washington, DC 20007
(202) 965-3700

Editorial Assistant
Gail Murphy

Production Editor
Sherry Lynne Bogen

Art
Robert Meehan, Dir.

Production
Dollie S. Viebig, Mgr.
Dan Coakley

Circulation
Trish Edelmann, Mgr.
Peggy Long, Reader Service

Promotion Manager
Walter Salm
Albert B. Stempel (Reprints)

Editorial Office
50 Essex St.,
Rochelle Park, N.J. 07662
Phone (201) 843-0550
TWX 710-990-5071

A Hayden Publication
James S. Mulholland, Jr., President

MICROWAVES is sent free to individuals actively engaged in microwave work at companies located in the U.S., Canada and Western Europe. Subscription price for non-qualified copies is $10.00 for U.S., $15.00 a year elsewhere. Additional single copies $1.50 ea. (U.S.); $2.00 ea. (foreign); except additional Product Data Directory reference issue, $10.00 ea. (U.S.); $18.00 (foreign). POSTMASTER, please send Form 3579 to Fulfillment Manager, MICROWAVES, P.O. Box 13801, Philadelphia, PA 19101.

Back Issues of MicroWaves are available on microfilm, microfiche, 16mm or 35mm roll film. They can be ordered from Xerox University Microfilms, 300 North Zeeb Road, Ann Arbor, MI 48106. For immediate information, call (313) 761-4700.

Hayden Publishing Co., Inc., James S. Mulholland, President, printed at Brown Printing Co., Inc., Waseca, MN.

Copyright © 1974 Hayden Publishing Co., Inc., all rights reserved.

Large scale production techniques eyed for millimeter component

Richard T. Davis
Managing Editor

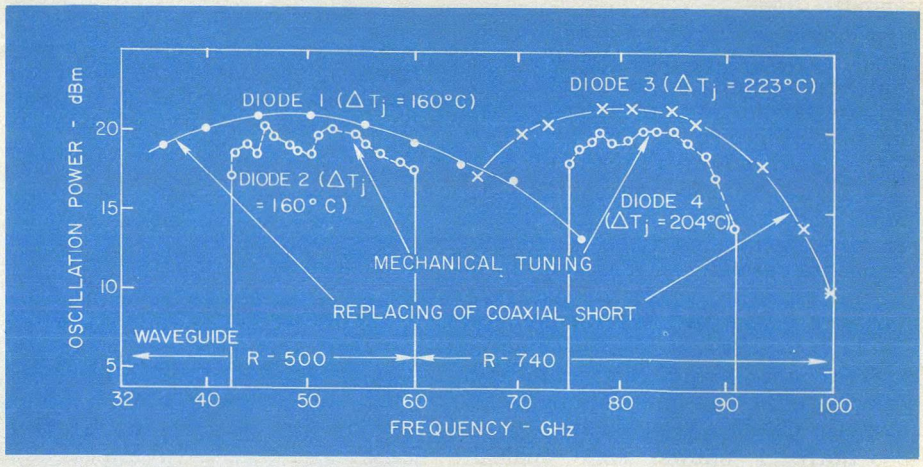
The need for reliable, low-cost and wideband millimeter-wave components, from 30 to 100 GHz, is bringing about improved wideband designs, particularly for tunable solid-state oscillators and some innovative manufacturing methods for many passive components. This trend was clearly evident at last month's Microwave Theory and Techniques Conference, May 12 through 14, in Palo Alto, where several sessions were devoted exclusively to millimeter-wave technology.

Much of the progress in the passive component area is taking place in Japan, and seems to be centered on satisfying the requirements of a recently developed millimeter-wave transmission system. This underground waveguide system operates from 43 to 86 GHz and was developed by Nippon Telegraph and Telephone. A portion of this 300,000 telephone channel (W-40G) system, consisting of two terminals and a repeater, recently completed field trials over a 22.7 km length of waveguide run.

Many of the newer Japanese passive millimeter components are being fabricated using techniques that lend themselves to low cost and mass production. In many cases, parts are fabricated and inspected prior to final assembly which allows closer control of surface tolerances. Indeed, many of the surface finishes exceed those obtained using conventional, "custom tailored machine shop" methods, common in building millimeter components. One Japanese firm, in fact, is using cold hobbing and honing to make precision cavity parts.

In the solid-state source area, the Impatt diode has clearly taken the lead as the most practical means of generating significant amounts of power at millimeter wavelengths. Two reasons for this are its wideband tuning capacity and frequency stability over temperature.

Hughes Aircraft Company is very active in the millimeter source area, and at the conference discussed a convenient way to tune



1. **Mechanical tuning characteristics** of Fujitsu's Impatt oscilaltors show output powers "peaked up" at each frequency increment.

Impatt diodes by varying their dc bias current. Two units were described which bias tuned from 26.5 to 35 GHz and 31 to 40 GHz with output powers increasing from 1 mW to 40 mW with frequency. (These electrically-tuned millimeter sources are now commercially available from Hughes and were just introduced last month in MicroWaves. See "M-M Sources Tune 10 GHz Bandwidths, 26-110 GHz," May 1975, pp. 66 and 69).

In his paper, "Wideband Electronically-Tuned M-M Wave Impatt Oscillators," Chente Chao of Hughes, Electron Dynamics Division, Torrance, CA, claims "This bias-tuned method exhibits a broad swept range which is not yet achievable with either varactor or YIG-tuned oscillators using Impatt, Gunn or Barrett devices."

Chao claims the output power is sufficient for typical m-m mixer applications and the noise characteristics of the sources make them particularly suitable as scanning LOs.

"A double sideband am noise-to-carrier ratio ranging from −113 to −125 has been measured in a 100 Hz bandwidth, 50 kHz from the carrier," says Chao. "Noise figure of a receiver using these scanning local oscillators and a balanced mixer was also measured from 30 to 38 GHz resulting in a DSB noise figure of 7 to 14 dB.

The Impatt diodes used for this work are single drift, p^+nn^+ silicon diffused junction diodes sealed in a quartz package with very low parasitics. To achieve the broadband tuning, the waveguide circuits include a multiple-step quarter-wavelength impedance transformer to reduce the waveguide impedance near the diode. "The low-noise characteristics are maintained by eliminating loops in the circuit impedance and suppressing of second harmonic and bias circuit oscillations," explains Chao.

RCA has developed wideband Impatt diode oscillators at Ka-band but they are using varactors to tune from 26 to 32 GHz and 32 to 39.2 GHz. Both sources are in microstrip form and use similar chip-mounted Impatt diodes for both oscillation and varactor tuning.

According to Edgar J. Denlinger, MTS at RCA Labs, Princeton, NJ, one advantage of the varactor tuning is less am noise because the bias on the Impatt is held constant. Denlinger bases this claim on previous noise testing of the type of diodes used, although he admits no am noise tests have been made on these microstrip oscillators to date.

The two Ka-band sources use complementary n^+pp^+ Impatt diodes (for both the oscillation and the varactor tuning function). Each diode has a highly doped n^+ and p^+ layer with an integral copper heat sink.

The circuit is series tuned with the load impedance in shunt with the diode. It includes two wideband

(continued on next page)

Chebyshev band reject filters for the bias circuits of the Impatt and varactor diodes, a broadband tapered-ridge waveguide microstrip transition and a two-section $\lambda/4$ impedance transformer in the output circuit designed to present a 300 ohm load impedance to the Impatt diode.

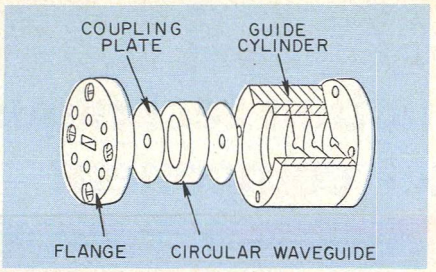
Fujitsu Laboratories of Kawasaki, Japan, has also developed a number of Impatt diode oscillators whose frequency can be adjusted and stabilized over the 43 to 87 GHz band (where the W-40G system operates). According to Takakiyo Nakagami of the Transmission Systems Lab, the oscillator series is intended for use as both signal generators for characterizing and measuring circuit components as well as local oscillator applications where the frequency can be adjusted and stabilized at specific channel frequencies.

Figure 1 shows some typical results that have been achieved covering the 35 to 60 GHz and the 60 to 100 GHz frequency bands. The dotted lines are the continuous tuning characteristics of two waveguide oscillators using mechanically-tunable coaxial shorts. One tunes approximately from 42 to 60 GHz with an output of about 18 dBm. The higher frequency oscillator mechanically tunes from about 75 to 92 GHz. Each oscillator is tuned up for peak output power at each frequency increment," explains Nakagami.

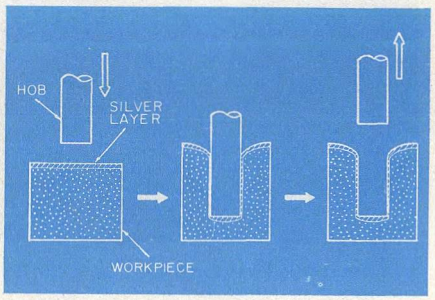
The solid-line curves shown in Fig. 1, covering the overlapping bands 33 to 76 GHz and 65 to 100 GHz, are the result of replacing fixed lengths of coaxial shorts at the intervals shown. The same basic oscillator circuit as the tunable oscillator is used. A high-stabilized oscillator was also developed with high-Q invar cavity (TE_{012} mode) replacing the coaxial short. The stabilization factor is on the order of $2 \times 10^{-6}/°C$. Two units operating at 42.1 GHz and 81 GHz were developed providing outputs of 20 dBm and 15 dBm, respectively. Frequency deviations over a 0 to 50°C temperature change were under ±2.5 MHz and ±4 MHz. The diodes used for all these oscillators are silicon $p^+ nn^+$ Impatts fabricated with beam-leads and quartz standoffs.

New manufacturing methods evolving

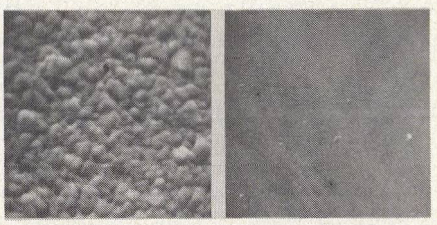
Millimeter waveguide data transmission systems, once in operation, can be expected to use large numbers of filters, circulators and other passive components for eliminating spurious signals and modes, as well as reducing the interference between receivers and transmitters. As a result, some rethinking in terms of manufacturing these devices has occurred, resulting in some innovative production and fabrication techniques. This is particularly true in Japan where, according to Nakagami of Fujitsu, emphasis is being placed on high productibility, low insertion loss and high precision of dimension for many passive components. "In order to satisfy this requirement, parts are being precisely fabricated and inspected separately and assembled together afterwards," he explains. An example of this type of manufacturing is the four-section cylindrical TE_{111}-mode bandpass filter, Fig. 2, designed for 80 GHz operation. It consists of thin-coupling plates and circular waveguides piled up alternately and screwed together with rectangular waveguide input and output flanges. "All ports are plated with pure silver to reduce the loss in the metal wall of the structure and are accurately aligned along the central axis with the aid of an external guide cylinder. Tolerances as small as 10 to 20 microns are achieved with this method.



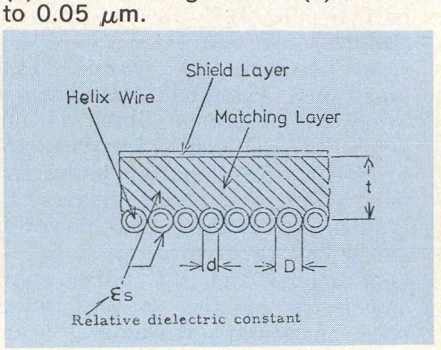
2. **Four-section cylindrical TE_{111} mode filter** has parts assembled and microscopically inspected prior to assembly. Tolerances are as small as 10-20 μ.



3. **Cold hobbing using silver-clad metal** allows making low-loss TE_{111} resonant cavities in the 75 to 110 GHz range.



4. **Surface finish obtained by cold hobbing** (b) is considerably better than that obtained by electroforming (a). Surface roughness in (b) is 0.02 to 0.05 μm.



5. **Wall structure of a 42-80 GHz TE_{on} mode filter** consists of helix wire, encased in dielectric.

The coupling plate is prepared by etching the coupling aperture as a 20 μ thick brass plate using photolithographic techniques. "As the size of each element is very small proportionally to the millimeter wavelength, the wall thickness of the coupling aperture has a substantial influence on the overall performance. Accordingly, the dimensions of coupling aperture and the cavity lengths are determined by considering the thickness of the coupling plate," says Nakagami.

The four-section filter provides over 35 dB out-of-band rejection. It has an unloaded Q of about 50% that is theoretically obtainable.

Another four-section filter operating at 50 GHz with a $Q_L = 28.5$ was also developed which provided good spurious mode rejection. The responses of the TM_{010} and TE_{011} modes adjacent to the TE_{111} modes were not observed because they're weakly coupled to the structure. Many other bandpass filters from 40 to 100 GHz have been constructed statisfactorily using this fabrication method.

Hitachi Electronics Co., Ltd., in Tokyo, has developed a cold hobbing and honing method for making precision millimeter cavity resonators. According to Kunio Ohi, senior engineer, "Tolerances of ±2 to ±5 μm and a surface roughness of 0.02 to 0.05 μm is obtainable using cold hobbing under proper conditions." The basic process shown in Fig. 3, results in a mirror-finished silver surface

(continued on p. 14)

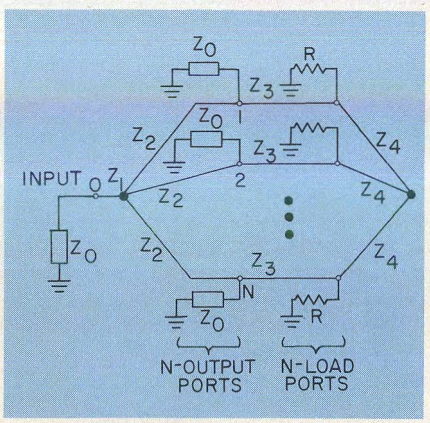
N-way combiner design can consolidate 5 kW at S-band

A new type of n-port power divider/combiner that handles higher power levels than the popular Wilkinson design and provides a means of monitoring unmatched input or output connections has been developed at Stanford Research Institute in Menlo Park, CA.

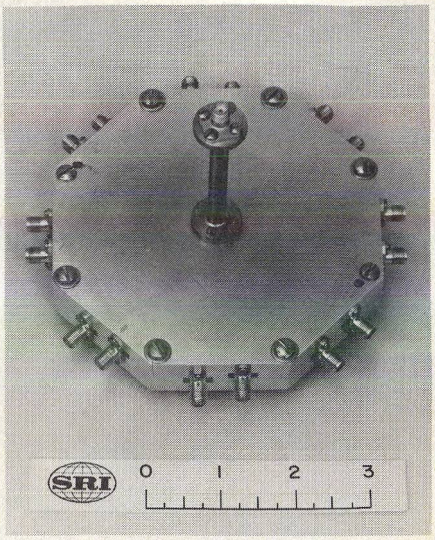
"The main disadvantage of the Wilkinson combiner is that the resistive star required is difficult to realize in practice, particularly for a large number of output ports," states the developer, Ulrich H. Gysel, a research engineer at SRI. "The chip resistors usually employed for the resistive star limit the power-handling capability of the Wilkinson combiner to less than 100 watts cw because adequate heat sinking is not possible."

Gysel's design replaces the resistive star with a combination of transmission lines and shunt-connected resistors (Fig. 1). These loads are not an integral part of the design, but are fitted to exterior ports allowing high-power elements to be used. "Construction of the divider/combiner is relatively easy either in stripline, slabline or microstrip," the researcher notes. "The power-handling capability is restricted only by the breakdown voltage of the transmission lines, or the heat dissipation capacity of the lines."

According to Gysel, designs capable of handling combined cw output powers of 10 kW at L-band and 5 kW at S-band are realizable.



1. All transmission lines in this n-way divider/combiner design are a quarter-wavelength long at the center frequency.



2. This eight-way power combiner has 17 ports: eight inputs, one output and eight ports for external shunt-loads.

Measured performance of an experimental eight-way divider (Fig. 2), designed with a center frequency (f_o) of 1.15 GHz and a 20% bandwidth, includes 36 dB isolation and 9.2 dB insertion loss (input to output 1) at f_o. Input VSWR is below 1.25:1 while a typical output VSWR doesn't rise about 1.15:1 in the specified bandwidth.

The SRI researcher feels that for a typical 20% bandwidth design, the new approach is "clearly superior" to the original Wilkinson combiner, and "compares favorably" with modified versions. "The somewhat higher VSWRs in the passband of the new design compared with the other two are insignificant," he explains, "because junction effects and connector VSWRs are likely to be the dominant factors, particularly at higher frequencies."

The design, which was revealed last month at the 1975 MTT in Palo Alto, CA, also exhibits a limited amount of directivity, which Gysel notes, can be taken advantage of to monitor imbalances in the power delivered to output ports when used as a combiner, or to monitor unequal load VSWRs in the case of a divider. •• *SVB*

Large scale production techniques eyed for millimeter components (cont.)

obtained by cladding the surface of the work piece with a silver layer. A comparison of surface finishes using cold hobbing and that achieved by electroforming or ordinary machining is shown in Fig. 4.

"Honing and polishing are also promising methods for finishing the insides of millimeter waveguides," explains Ohi. "In one case, an extrusive honing using a clay-like soft elastomer mixed with abrasives was forced into and extruded from m-m waveguide. The surface finish of the rectangular guide was improved to 0.8 μm. The process is also considered effective for plated waveguides. For a piece of WR-12 waveguide, it was found that at 90 GHz the insertion loss could be improved to 1.23 of that theoretical obtainable.

A frequency cavity meter was demonstrated which incorporated a TE_{111} mode resonant cavity made using these cold hobbing and honing procedures. It operated from 75 to 110 GHz and provided an unloaded Q twice that obtainable from a conventional frequency meter using an electroformed cavity. "This means that frequency resolution will be twice as good," explains Ohi.

Nippon Electric is also developing simplified manufacturing techniques for m-m waveguide components such as waffle-iron filters, bandpass and bandstop filters and flexible waveguides. They're using electroforming and photoetching techniques to build individual parts and then assembling them.

According to Susumn Kitazume, engineering manager in the millimeter wave development lab, "A waffle-iron bandstop filter consisting of three kinds of sections, capacitive, inductive and two-end sections was developed using the image parameter method and scaling from a well proven 7 GHz design. The thickness of each section formed by photoetching is typically less than 0.4 mm. Each part is then assembled to form a five stage filter. The transforming section to standard waveguide is constructed from two section, quarter-wave transformers which are made by electroforming. Stop-band attenuation for three filters exceeds 40 dB over bands of 43-53 GHz, 55-65 GHz and 76-86 GHz and insertion loss is less than 0.25 dB. 0.3 dB

(continued on p. 16)

news

Microwaves help make moon model

Harvey J. Hindin
Contributing Editor

That the moon isn't made of green cheese we already know—but what is it made of? We know what's on the top surface from samples taken on manned lunar missions. Now, we're starting to get a picture of the crust below. With the help of earth-based radiometer measurements of lunar microwave brightness temperature (a measure of the natural electromagnetic emission at these wavelengths), a model has been made that simulates the upper 50 meters of lunar crust.

Emission data was analyzed over the frequency range of about 1 to 6 GHz from sources which included both Russian and American observatory measurements. Since the material in the pulverized lunar top layer (regolith) becomes increasingly transparent as wavelength increases, the determination of the brightness temperature at different wavelengths can be correlated with sub-surface physical properties such as kinds of material present, layer thickness and density.

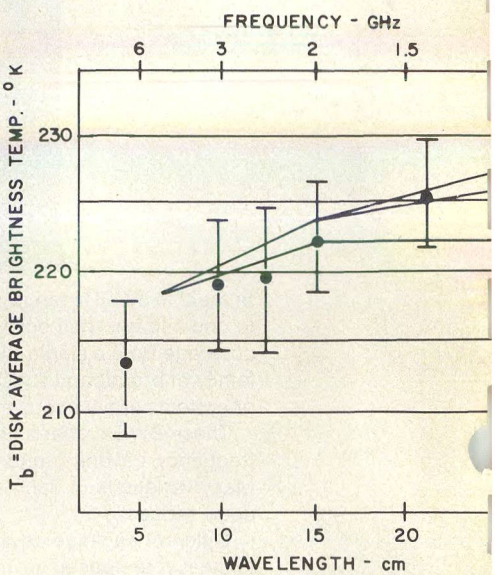
The model was developed by Stephen J. Keihm, research scientist and Marcus G. Langseth, senior research associate of Lamont-Doherty Geological Observatory of Columbia University in Palisades, NY, under a NASA contract. It was used to simulate the effects of scattering on the microwave emission spectrum and consists of a compact powdered regolith over alternating layers of rock and soil.

The interrelationships between these layers are very complex and several different designs were proposed in an attempt to correlate with different parts of the spectrum, some of which do not totally agree. Typically, insofar as thermal conductivity and density of the layers is concerned, four distinct regions may be defined. Region one is on the surface, region two goes from about 1 to 3 meters, region three from 3 to 10 meters and region four goes from 30 meters on down to about 50 meters.

Exact numerical values are a function of compaction, particle size, distribution and compressive load and only certain conditional numbers may be given at this time. For example, the thermal conductivity is about 0.2 watts x 10^4/cm/°K in the top cm, climbs to 1.0 at 15 cm and extends smoothly to 2.2 at 30 cm. It's about 2.2 in regions two and three and greater than 2.2 in region four.

The layer density is about 1.25 gm/cm^3 in the top 2 cm and varies from 1.3 to 2.0 linearly in the 2 to 30 cm region.

The change in brightness temperature with wavelength, a measure of the disc average lunar heat flow and an apparent emission peak at about 50 cm wavelength (a measure of the regolith thickness), are particularly critical to the models. A regolith thickness between 10 and 30 meters is necessary to fit the available microwave data, some of which is shown in the figure for the 1.5 to 6.0 GHz (5 to 20 cm) band. Slope matching is a difficut problem in this particular spectral region, and three different models are proposed as shown.



The steady state, disk average lunar brightness temperature is shown as a function of microwave wavelength. Data points were obtained from earth-based measurements. The theoretical curves are based on the multi-layer model of the moon's crust which is discussed in the text. Models A, B and C have regolith thicknesses of 10, 20 and 30 meters, respectively.

More work is needed

Keihm and Langseth point out that more accurate data has to be obtained before their models can be refined sufficiently to account for all observed phenomena. Errors in the available microwave emission data, especially in the spectral gradient, strongly affect the conclusions drawn. In particular, high accuracy and resolution data at discrete wavelengths in the 1.5 to 6.0 GHz region, perhaps obtained from a lunar orbiter, would permit more sophisticated analysis.

While the hardware used to obtain the data is relatively standard, it's nice to know that microwave technology has again been used to probe the basic structure of a part of our universe. ••

Large scale production techniques eyed for millimeter components (cont.)

and 0.4 dB, respectively.

Other filters built using these methods include harmonic rejection bandpass and band-stop filters.

Because unwanted modes can easily be generated at the corners and bends of a millimeter waveguide line, the Fujikura Cable Works in Tokyo has developed a simple polygonal type TE_{0n} mode filter using a deformed circular waveguide. According to K. Inada, the design is particulary effective in eliminating troublesome TE_{02} and TE_{03} modes with only a minimal loss for the desired TE_{01} mode (0.1 dB over the entire frequency range of 42 to 80 GHz). This is done by converting TE_{02} mode to a TE_{51} mode and the TE_{03} to a TE_{81} mode which are then easily absorbed by an ordinary helix waveguide connected to the mode filter.

The wall structure to achieve this conversion consists of helix wire, encased in a dielectric, a matching dielectric layer and finally an outer shield layer, as shown in Fig. 5. This structure is quite similar to that of conventional helix waveguide on dielectric lined waveguide. "By increasing the length of the mode filter and decreasing the deformation factor, it is possible to reduce the TE_{01} mode loss without changing the TE_{0n} mode attenuation," says Inada. ••

Economic Forecast: Part III

What's The Future For Electronic Warfare?

The electronic warfare market will nearly double by 1978. Responding to weaknesses uncovered in the 1973 October War, EW programs are expanding, with a growing role for microwaves.

This concludes the current series of economic forecasts. Parts one and two examined commercial communications and government electronics.

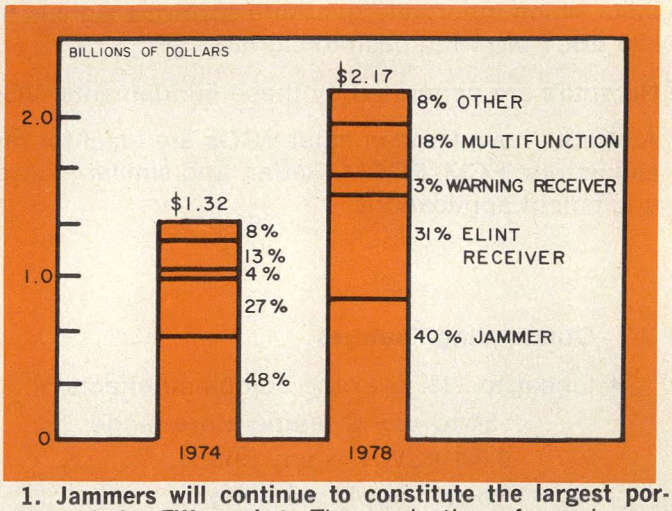
IN the 35 years since the advent of World War II, electronics has evolved from a minor supporting role to the key element in modern warfare. The accuracy and efficiency of weapons delivery, the scope of situation analysis, speed of command decisions and reach of control communications have been dramatically increased by electronic systems, and more recently, by electro-optics. These technologies have become so interwoven into modern warfare that any combatant whose electronic systems are suddenly rendered inoperative would be virtually helpless.

This is the purpose of electronic countermeasures, and the reason that ECM will continue to hold a large share of microwave equipment production and R&D spending. The total U.S. electronic warfare market was $1.32-billion in calendar year 1974, and will expand to $2.17-billion by 1978, as shown in Fig. 1. This is an average annual compound growth rate of 13.3%, including an inflation factor of 6.4%, and incorporates all related research, development, test and evaluation (RDT&E) costs, as well as the electronic content of emitter-suppression systems. Also included in these figures is U.S.-produced equipment for foreign governments, most of which is not reflected in Department of Defense budgets. Finally, the considerable EW expenditures of non-military agencies, such as the CIA, NSA and FBI, are lumped in these totals.

The microwave portion of the total EW market will expand at 15.3% per year from $0.83-billion to $1.47-billion over the 1974 to 1978 span (Fig. 2).

Countermeasures—a volatile market

The absolute necessity for operational ECM/EW equipment to counter the most current threat was made very clear in Vietnam and in the recent Mid-East conflicts. After being caught unprepared in Vietnam by Soviet SA-3 medium level and SA-2 high level ground-to-air missiles, the United States developed adequate countermeasures, only to be caught unprepared again in the Arab-Israeli October War by the Soviet SA-6 low-level missile. Unanticipated cw guidance systems and the use of multiple frequencies for acquisition and guidance made jamming and detection warning of the SA-6 unusually difficult.



1. Jammers will continue to constitute the largest portion of the EW market. The production of warning receivers will decline as their duties are integrated into multifunction systems.

The Israeli aircraft losses to the SA-6 led to a rapid evaluation of U. S. countermeasure systems, and industry sources indicate that the Air Force and Navy are currently modifying existing hardware to correct the cw vulnerability exposed in the 1973 war. This serves to illustrate that although the ECM market will continue to grow at a healthy rate over the long term, the unpredictable volatility of world political tensions will inevitably cause cyclical short-term behavior.

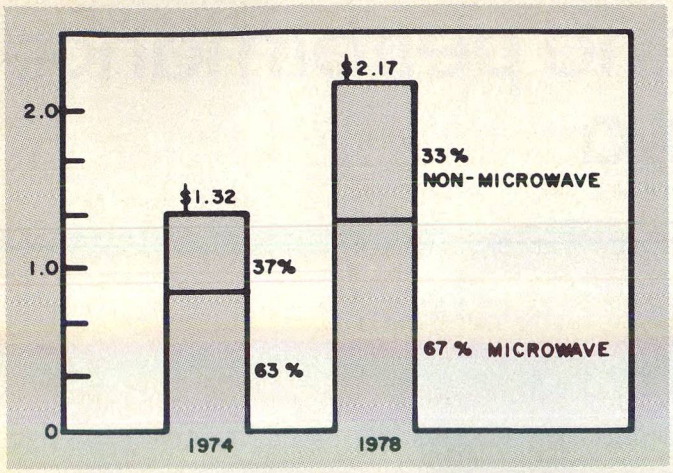
(continued on p. 36)

Mapping the future

This economic forecast is derived by computer modeling techniques which take into account overall economic (macroeconomic) forecasts, historical data, technical trends and backlog. The macroeconomic forecasts are provided by Chase Econometric Associates, Inc., a subsidiary of Chase Manhattan Bank.

Component forecasts are based upon extensive interviews with equipment designers, component buyers and producers. The total component demand is then defined and forecasted by input-output methodology, whereby all component production is accounted for by considering the sum of OEM use in marketable equipment, plus all components manufactured for non-production uses such as replacement parts, R&D and inventory level change. ••

Jeff D. Montgomery, Vice President, Gnostic Concepts, Inc., 2710 Sand Hill Road, Menlo Park, CA 94025.



2. The demand for microwave equipment will grow faster than the total EW market.

Electronic warfare development and production requirements will continue to be driven by the rapid development and deployment of new weapons by the U.S.S.R. R&D funding, increased by 18% in the calendar year 1974 to a total of $212-million, will accelerate by 38% to $295 within calendar 1975. This includes Army, Navy and Air Force funding, plus financial support from non-military agencies such as CIA and NSA.

The emphasis over the next five years will shift from airborne attack warning receivers to countermeasures directed at the early warning and ground-controlled interception electronics of surface-to-air missile systems. Most component development funding over the next five years will be directed toward cost reduction or major advances in capability, rather than to minor performance improvements. The design-to-cost concept will increasingly be applied to equipment procurement.

Major potential in microwave components

The usage of selected microwave components will outrace the growth in EW equipment value, increasing at 22.5% per year from $66.1-million in 1974 to $148.5-million in 1978, as shown in Table 1. This faster growth rate will be due partially to the retrofit of earlier design components such as low-noise traveling wave tubes and their associated power supplies.

Microwave-integrated circuits hold a strong position in EW equipment and will provide the fastest growth rate: 27.5% per year. MIC diode switches are a significant factor in this market representing $5.2-million in 1974. Low-noise MIC amplifiers, as supplied by Avantek and Watkins-Johnson, represent a strong growth market, which should expand from $4.9-million to $13.8-million in the 1974 to 1978 period. GaAs FET amplifiers will find a worthwhile niche in this market.

Discrete circuit oscillators are a significant factor in EW equipment, with usage expected to double from $16.2-million in 1974 to $37.8-million in 1978. This market is strongly dominated by broadband voltage-tunable units, which represented a $14.9-million segment in 1974. While YIG-tuned units were dominant in 1974, the demand for varactor-tuned oscillators will grow more rapidly at 29% per year as the faster tuning rate of varactors becomes increasingly important.

The growing displacement of TWT amplifiers by solid-state circuits will be slowed by new generation TWTs now phasing into production. The largest component R&D area now being government funded is TWT miniaturization with an emphasis on cost reduction. A Department of Defense analysis indicates that miniaturized TWTs offer substantial savings in size and cost, compared to a solid-state system of comparable bandwidth and power output. Litton, Varian, ITT and the RCA tube division recently assumed by Raytheon have made major strides in the development of miniaturized TWTs, using samarium-cobalt magnets for the 2.5-18 GHz range. Potential applications include phased arrays and the lens-fed multiple beam arrays now under development at Raytheon.

Jammers pace Air Force EW

Jammers constitute the largest category of electronic warfare equipment, accounting for U. S. production of $630-million or 48% of all EW spending in 1974. This market will expand slowly at 8% per year to $864-million in 1978. This includes both deception jammers, such as the ALQ-101 and ALQ-119 built for the Air Force by Westinghouse, and barrage jammers such as the ALQ-135 now in preproduction status at Northrop's Hallicrafters Division. Much of the jammer demand acceleration over the past five years has been for retrofit of operational aircraft, particularly in Vietnam operations. The outfitting of new aircraft, modifications to counter new threats and expansion of ground jammers will maintain the modest growth rate.

The major ongoing Air Force jammer program has been the series of pods developed and produced by Westinghouse, the leading Air Force EW contractor. This program began in early 1967 with the ALQ-101, which represented one of the first production applications of the TWT for noise jamming. With an eye on dual-mode capability, the Air Force commissioned Westinghouse to design the ALQ-119 as a successor to the ALQ-101 (Fig. 3). The ALQ-119 has been produced at a peak rate of over 300 units per year with total production of over 700 units to date. It is being produced at a rate of about 30 pods per month, and as the ALQ-101 phases out of production, production will increase to 45 systems per month.

Superseding the ALQ-119 will be a more flexible, modular pod: the ALQ-131. This unit provides a choice of eight different types of jammer modules and covers five bands fitting the Pentagon philosophy of evolution to multi-function EW systems. Under development for the past two years, the ALQ-131 was flight tested and entered production in late 1974. Forecasted production of the jammer pod will expand to 250 systems in 1976.

(continued on p. 38)

Table 1. Microwave equipment production for electronic warfare

Component Type	Production ($ Million) 1974	1978	Growth (Percent)
Discrete Circuit Oscillators	16.2	37.8	23.6
Discrete Circuit Amplifiers	6.1	14.4	24.2
Microwave Integrated Circuits	17.1	45.2	27.5
Passive Components	15.4	28.6	16.7
Passive Modules	11.3	22.5	19.1
TOTAL	61.1	148.5	22.5

The leading Air Force development program will be the EW system for the F-111A with ultimate development costs exceeding $60-million. Production requirements are for 40 sets at $10-million each (including the required aircraft modification). Other substantial Air Force EW production systems will be the Tactical Electronic Warfare Systems (TEWS) for the F-15 and the B-1 EW system now under development at the AIL division of Cutler-Hammer.

Other significant future projects include a tactical expendable drone system (TEDS) outfitted with jammers or radar enhancement devices to saturate enemy air defenses. High explosive payload delivery is another likely mission for these drones. Also, in 1975, the Air Force will proceed with the development of a precision emitter location strike system (PLESS) for rapidly locating enemy radars.

Army and Navy step-up EW activity

The Army is moving into a phase of strongly increased funding of development and production of a wide range of electronic-warfare equipment. During the Vietnam conflict, the electronic threat to ground forces was minimal, hence, nearly all EW emphasis was related to airborne requirements. This has placed Army EW in a potentially obsolescent position in the event of future conflicts.

To head off this situation, greater emphasis will be placed on the protection of light aircraft and helicopters against low altitude air defense systems and on systems for communications interception and disruption. Although most of the activity will be in the hf through uhf ranges, several new systems have substantial potential for microwave components. These include:

- Multiple Target Electronic Warfare System (MULTEWS), for radar detection and jamming in I and J bands (Hallicrafters).
- Automatic Ground Transportable Emitter Location and Identification System (AGTELIS), to determine the bearing of enemy radar (Bunker-Ramo).
- Quick Look-2, computer-controlled ELINT system, proposed for the A-10, for detection and location of emitters from uhf through 18 GHz (United Technology Labs).

The Navy will fund development of a new radar warning and threat analysis receiver for the EA-6B, to displace the Itek ALR-45 and the Magnavox ALR-50. The present receivers, developed under the Charger Blue program along with the Sanders ALQ-126 deception jammer, use analog signal processing. To handle the ten-fold increase in radar signal densities expected in future conflicts and as indicated in the 1973 October War, the new system will incorporate a digital signal processor such as the ALR-46 produced by Dalmo-Victor and others.

Updating of existing jammers, such as the Grumman ALQ-99 barrage jammer for the EA6B and the Sanders Associates ALQ-137 deception jammers for the F-111, will continue. Typical of such modifications is the expansion of capacity of the IBM computer which manages the ALQ-99.

Interest grows in multi-function systems

The reaction time available in many future tactical situations will be too short to afford a human in the loop. The threat must be analyzed and the appropriate jammer, weapons launch or other action effected automatically and instantaneously. On-board missile and maneuverable warhead counter-



3. Nestled under the belly of an F-104, this ALQ-119 jamming pod provides limited dual-mode capability.

measures are leading-edge examples of these multifunction systems, along with the MULTEWS automatic multifunction jammers now being developed by Hallicrafters. Multifunction system production plus RDT&E spending will expand rapidly, at 2.8% per year, reaching $388-million or 18% of the total EW market by 1978.

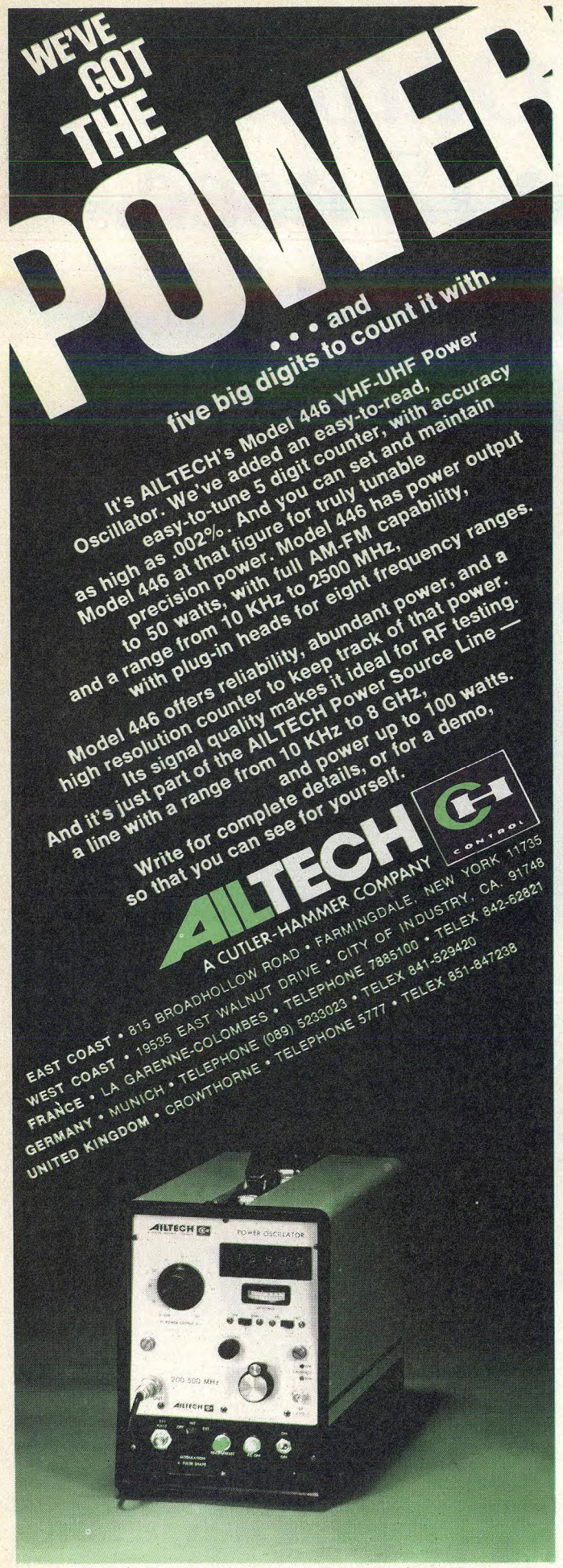
The growth of the ECM market will incorporate increasing sophisticated equipment, including greater use of computer controls and continued development of phased arrays. Computers will be used to control the search pattern of surveillance receivers, for threat analysis and for ordering the appropriate counter-jamming. The newer ECM jammer systems are computer-controlled, with the ability to quickly shift frequencies and to modulate in order to meet new threats.

There will be strong growth over the next five years in the demand for computer-controlled receivers for detection, identification and avoidance functions as well as power-managed transmitter systems and expendable ECM devices. Micro-Tel, for example, is now producing a computer-controlled surveillance receiver system covering the 0.03-40 GHz range incorporating a frequency synthesizer local oscillator source and a PDP-11 minicomputer.

Also typical of the evolution complexity of military microwave equipment is a radar warning receiver system recently developed by General Instrument Corporation. While earlier production systems, primarily by ATI/Itek, simply gave an indication that the aircraft was being illuminated by a radar, the new General Instrument system stores in its 8,000-word digital computer memory, the signal characteristics of more than 100 radars. Emitters are identified automatically by type and operating mode. The location of up to 15 different illuminating radars may be displayed in the cockpit.

Warning-receiver expenditures, however, will remain almost constant, expanding only from $58-million in 1974 to $60-million in 1978 in current dollars. This significant decline in real terms will be due to the shift in emphasis from aircraft protec-

(continued on p. 40)



READER SERVICE NUMBER 40



4. The locations of up to 15 hostile radars can be "displayed" by General Instrument's Pointer warning receiver, selected for the Navy's LAMPS MKI ESM system.

tion to surface and space warfare. The warning function also will become an integral part of multifunction systems in some future applications.

Expendable ECM system development has proceeded across a broad front over the past five years, providing a wide variety of prototype units from HF through X band. Over a dozen development programs are now under way, with not significant production yet contracted. Sub-microwave communication jammers can be built with over 100 watts cw output, all solid-state, for a few hundred dollars. The high cost of effective microwave jammers, however, has discouraged their deployment. Development efforts over the next four years will be focused on cost reduction of a few selected systems, primarily for deployment by remote piloted vehicles. RCA, Van Nuys, California, has developed several microwave expendables over the past five years. Others active in this field include Tasker Industries, AIL Division of Cutler Hammer, Sanders Associates, Motorola and GTE Sylvania.

The relatively low power output and low efficiency of microwave transistors has inhibited interest in solid state microwave transmitters except schemes for delivering the payload within a few hundred yards of the target. Several microwave expendables based on magnetrons and traveling wave tubes, have been proposed, but while providing higher power and higher efficiency, are too heavy and too expensive for widespread deployment. The continued upward thrust of transistor arrays to higher power and frequency, however, will lead to production of several thousand solid state jammers per year, L band through C band, by 1978.

Electronic Intelligence, ELINT, the interception, decoding and analysis of electronic information transmission, will continue to account for a substantial share of total U. S. electronic warfare costs, expanding from 27% of total EW to 31% over the 1974-1978 period. This equipment ranges from the extremely complex, broadband, high-speed systems produced by Watkins-Johnson, Litton and GTE/Sylvania to the miniaturized "attache case" receivers of Rockwell Autonetics.

Electro-optical countermeasures (EOCM), electronic counter-countermeasures and other miscellaneous EW accounted for 7%, or $97-million of the EW market in 1974. This market will expand at 17.5% per year over the next four years with EOCM a major driving force in this growth. ••

A Specifier's Guide To Solid-State Source Terms

Specifiers often misinterpret many of the terms used by oscillator manufacturers. This compendium gets back to basics in an attempt to improve specifier-manufacturer communications.

Rapid growth in the number of applications for solid-state oscillators in ECM and communications systems has created a need for a clear, concise set of basic definitions of source parameters. Here, in alphabetical order, is a general review of what makes an oscillator tick, and how to describe how well it's ticking.

Acquisition Time: Time required for the output of a phase-locked oscillator or synthesizer to become locked to a reference signal.

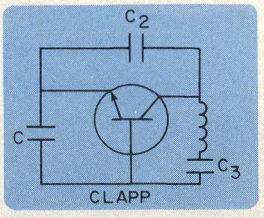
Am Noise: Random and/or systematic variations in output power amplitude. Usually expressed in terms of dBc for a specified video bandwidth away from the carrier.

Capture Bandwidth: The frequency range over which an unlocked, free-running oscillator can be brought into lock by either phase or injection-locking techniques.

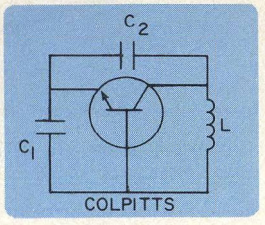
Carrier: The desired portion of an unmodulated oscillator's output frequency spectrum.

Cavity Oscillator (CO): An oscillator in which the primary frequency determining element is either a waveguide or coaxial cavity. Oscillator frequency can be mechanically tuned and voltage tuned (via a tuning varactor) over a relatively narrow band.

Clapp Oscillator: A high-stability version of the Colpitts circuit utilizing a series-tuned circuit in the output network.



Colpitts Oscillator: A regenerative feedback amplifier utilizing a tapped capacitor in the resonant network to provide the correct level and phase of the feedback signal to the input circuit.



Comb Generator: Usually a step-recovery diode circuit which converts a single frequency rf input into an rf output signal that contains a large number of spectral lines, each of which are harmonically related to the input frequency.

Bernard S. Siegal, Microwave Consultant, 1780 Holly Avenue, Menlo Park, CA 94025.

Material for this article was compiled in conjunction with Addington Laboratories, Inc.

Common-Base Configuration: Normally the most effective bipolar transistor circuit for oscillator or amplifier applications at microwave frequencies, providing higher gain, efficiency and stability than other possible configurations. Transistor base connection is grounded and common to both input and output circuit ports.

Common-Base Feedback Oscillator: A common-base bipolar transistor amplifier with a feedback network between the collector (output) and the emitter (input) to produce oscillations at a desired frequency.

Component Aging: The slight shift in component characteristics as a function of time. Usually 80 to 90% of the total characteristic shift occurs within the first several hundred hours of operation.

Crystal-Stabilized Oscillator (XSO): A microwave rf source that uses a crystal oscillator operating at some low frequency (usually below 150 MHz) to drive a multiplier or sampler to obtain a microwave output frequency. A crystal oscillator can also be used for injection-locked stabilization of a free-running microwave oscillator.

C-Swing Varactor: A p-n junction diode with its non-linear capacitance—reverse bias voltage relationship optimized for use in frequency multiplier and/or tuning circuits.

dBc: A unit that is logarithmically referenced to the carrier, noting decibels below the carrier.

Digitally-Programmable Oscillator (DPO): A VCO designed to accept a digital tuning word instead of the usual analog signal. Internal digital-to-analog (D/A) converter circuits transform the digital input to an analog voltage. Tuning-curve linearization is usually accomplished through a digital memory. The frequency speed is primarily limited by the D/A circuits.

Direct Synthesizer: A synthesizer producing an output frequency which is related to the reference frequency by the ratio of two intergers. The primary advantage of this type synthesizer lies in its ability to change output frequencies at a moderately fast rate (typically in the microsecond range) and in a random way. Principal applications include frequency-agile radars, secure communication links and electronic countermeasures.

Distributed Constant Oscillator: A power generation circuit that is realized by using sections of transmission lines to obtain the required inductances and capacitances.

Fine-Grain Variations: Either incremental changes in power output for incremental changes in output frequency or incremental changes in tuning signal. The former is usually expressed as power differential over a specified frequency "window" (i.e., 0.5 dB or 10 mW in a 10 MHz segment), while the latter is expressed as frequency change per unit tuning signal (i.e., MHz/volt or MHz/mA).

Fm Noise: Short-term frequency variations in the output frequency which appear as energy at frequencies other than the carrier. Usually expressed as an rms frequency deviation into a specified video bandwidth away from the carrier.

(continued on p. 44)

Frequency Deviation: A measure of the output frequency excursion around the carrier, caused by modulating the oscillator's tuning input which produces a frequency modulated output signal.

Frequency Range: The tunable bandwidth over which the oscillator meets all specifications.

Frequency Synthesizer: An rf source that can provide, by external command, any discrete and precise frequency within its range and resolution. The output signal is stabilized to a fixed-frequency reference, which may be internal or external to the synthesizer. Primary applications include automatic test equipment, electronic warfare and communications systems.

Fundamental Oscillator: A circuit in which output freqquency is the same as that determined by the primary frequency tuning network. For comparison, a harmonic oscillator is one in which the output frequency is harmonically related to the primary frequency.

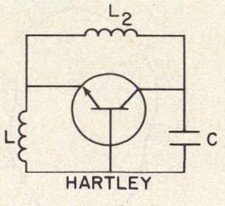
Gunn Diode: A two-terminal device that exhibits a negative resistance characteristic under proper operating conditions: low voltage (less than 20 V) and high current (usually greater than 200 mA). Commercially-available devices are made from gallium arsenide. Not truly a diode in the classical sense as the device has only one kind (usually N-type) of impurity doping.

Gunn Oscillator: An oscillator in which the active element is a Gunn diode operating in the negative resistance mode. This type of oscillator is one of the simplest means of generating microwave signals as only a microwave-tuned circuit, Gunn diode, bias network and low voltage power supply are required. Presently available units are restricted to operation above 4 GHz, and have dc to rf conversion efficiencies of less than 10%.

Harmonic Oscillator: A circuit in which the active device's oscillating frequency and the output frequency are not the same. For example, in a push-push configuration, each transistor oscillates at f_o but the output is combined to provide 2 f_o.

Harmonic Signals: Signals harmonically related (by a ratio of two integers) to the rf output signal. The most prevalent harmonic signal for fundamental transistor oscillators is 2 f_o; for push-push configurations, 1/2 f_o and 3/2 f_o. Signal level is usually expressed in -dBc.

Hartley Oscillator: A regenerative feedback amplifier utilizing a tapped inductor in the output-tuned network to provide the correct level and phase of the feedback signal to the input circuit.



Hysteresis: An effect in oscillators in which tuning from different directions will result in different frequencies even though the final value of the tuning signal is the same. For example, let T_1, T_2 and T_3 correspond to three different tuning positions (on a mechanically-tuned oscillator), voltages (for a VCO) or currents (for YTO). Hysteresis would be observed if the frequency obtained by going from T_1 to T_2 was different than that obtained by going from T_3 to T_2. In mechanically-tuned cavity oscillators, hysteresis could be due to mechanical backlash. Thermal effects would contribute to hysteresis in VCOs. The magnetic-tuning structure in YTOs is the primary cause of hysteresis.

I-F Noise: Am and/or fm noise present in the local oscillator signal that falls within the intermediate frequency (i-f) bandwidth of a superheterodyne receiver.

Impatt Diode: IMPact Ionization Avalanche Transit Time diodes are a special form of p-n junction device which operate at a reverse bias sufficient to cause avalanche breakdown (typically 65 to 100 V at 100 to 150 mA). The combination of avalanche generation and drift of carriers across the diode's active region produces negative resistance at microwave frequencies. Devices are commonly made with silicon or gallium-arsenide.

Impatt Oscillator: An oscillator in which the active element is an Impatt diode operating in a negative resistance mode. Dc to rf conversion efficiencies are normally less than 20%. Present devices operate above 5 GHz.

Impulse Generator: A circuit, typically using a step-recovery diode, used to convert a sinusoidal input to a voltage impulse output. The basic circuit block in both SRD multiples and comb generators.

Incidental Fm: Peak-to-peak variations of the carrier frequency due to external variations with the tuning line held constant.

Indirect Synthesizer: A synthesizer employing phase-locked loops, digital dividers and high Q-varactor tuned oscillators. The discrete output frequencies are not limited to interger ratios of the reference frequency. Frequency step size or increments, are primarily determined by the digital dividers. Switching speed between discrete output frequencies is usually limited by the phase-lock circuits. Applications include automatic test and satellite communications systems.

Injection-Locked Oscillator (ILO): A free-running microwave oscillator that is stabilized by injecting a reference signal into the oscillator's resonant circuitry. The required injected signal level is determined by the output signal characteristic requirements (i.e., noise, stability, etc.) and is typically in the range of 70 to 30 dB below the output level of the ILO.

Invar: A metal alloy material often used in building microwave cavities that must operate in temperature varying environments. The material has a low coefficient of thermal expansion (1.1×10^{-6} in/in/°C).

Linearity: The maximum output frequency deviation from a best fix straight line under specified load and constant temperature conditions.

Linearizer: A low-frequency circuit which acts on the input tuning signal to produce a linear tuning curve.

Linearizer Bandwidth: The circuitry used to obtain a linear relationship between the frequency output and the tuning signal input will have limited bandwidth due to intracircuit impedances, amplifying devices, required accuracy, etc. Generally, circuits providing the largest output voltage swing are of the lowest bandwidth.

Load: Specified as the maximum VSWR seen by the oscillator at the output port.

Local Oscillator (LO): The oscillator mixed with the incoming signal in superheterodyne receivers to produce an intermediate frequency for signal processing (i.e., filtering, amplifying, detecting, etc.).

Locking Bandwidth: The frequency range over which the feedback network in a PLO or the injection signal in an ILO can maintain the free-running oscillator in a locked condition.

Long-Term Stability: Maximum frequency and/or power output variations that occur in time intervals greater than 24 hours after an oscillator has stabilized with a given set of environmental (supply voltage/current, tuning signal, temperature, etc.) conditions. Frequency variations are usually expressed in percent of output frequency in MHz; power variations in mW or dB around a reference level.

Lumped-Constant Oscillator: A microwave power generation circuit that is realized by using discrete circuit elements such as inductors and capacitors.

Mechanically-Tuned Oscillator (MTO): Any oscillator that is specifically designed for frequency tuning by mechanical means. Typically a cavity or discrete element (i.e., a mechanically-tunable capacitor) type oscillator.

Modulation Bandwidth: The maximum modulating signal frequency minus the minimum modulating signal frequency. Since the modulation signal port typically provides response to dc, the bandwidth is usually specified as some maximum acceptable frequency down by 1 or 3 dB from the mid-band response.

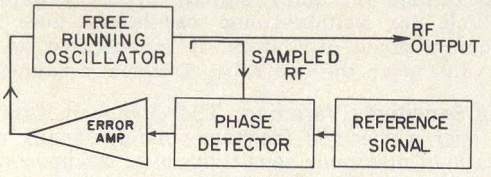
Modulation Sensitivity: The slope or first derivative of the tuning curve (Δ MHz/Δ V).

Monotomicity: In a VCO, continuously increasing output frequency for a continuously increasing tuning voltage.

Multiplier: A microwave circuit used to convert input rf power at one frequency to power output at a higher, harmonic frequency. Low-order multipliers, in which the output frequency is four or less times the input frequency, are usually built with C-swing varactors. High-order multipliers, typically use step-recovery diodes and depending on power output requirements, can provide frequency multiplication as high as 100 times.

Oven-Controlled Oscillator: An oscillator that has part or all of its circuitry enclosed within a carefully regulated oven in order to improve its stability with regard to temperature.

Phase-Locked Oscillator (PLO): A microwave source in which the rf output of a free-running oscillator is sampled for phase comparison with a reference signal. Detected phase differences are fed to an error amplifier which drives the free-running oscillator to the correct operating point.

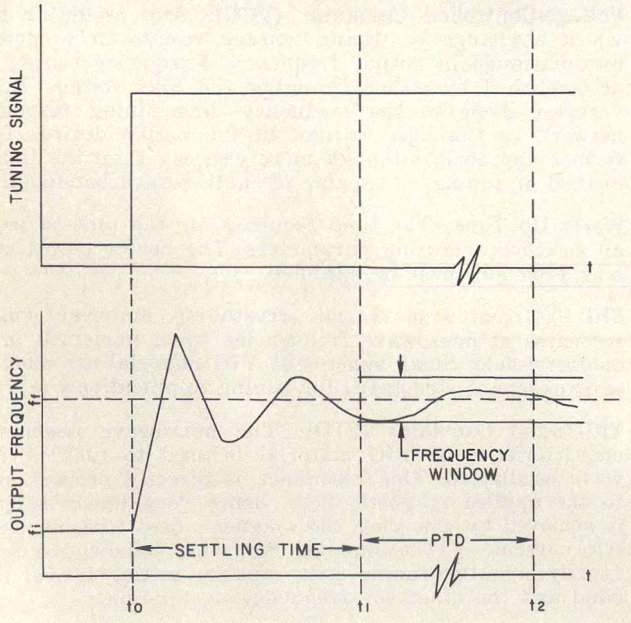


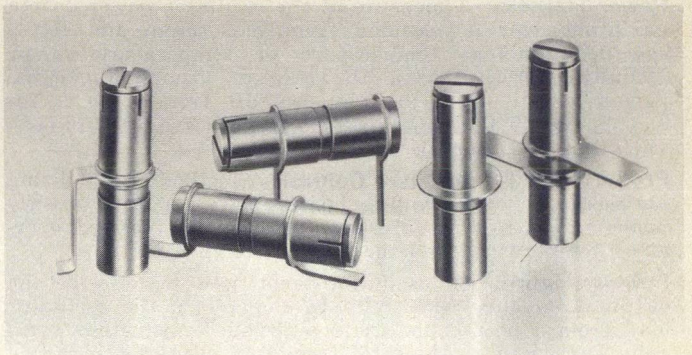
PHASE-LOCKED OSCILLATOR

Phase Noise: Short-term phase variations in the output signal, usually expressed as an rms phase deviation. Closely related to fm noise.

Post-Tuning Drift (PTD): The maximum output frequency drift that occurs over specified time range after the oscillator frequency has settled within the specified frequency window (expressed as a percent of the final frequency in MHz) around the final output frequency at t_2. The PTD time interval, t_2-t, typically lies in the range of minutes up to one hour.

(continued on p. 46)





GIGA-TRIM CAPACITORS FOR MICROWAVE DESIGNERS

GIGA-TRIM (gigahertz-trimmers) are tiny variable capacitors which provide a beautifully straightforward technique to fine tune RF hybrid circuits and MIC's into proper behavior.

APPLICATIONS

- Impedance matching of GHz transistor circuits
- Series or shunt "gap trimming" of microstrips
- External tweaking of cavities

Available in 5 sizes and 5 mounting styles with capacitance ranges from .3 - 1.2 pf to 7 - 30 pf.

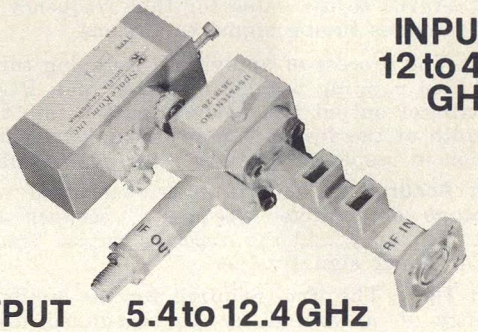
Johanson®

MANUFACTURING CORPORATION
Rockaway Valley Road
Boonton, N.J. 07005
(201) 334-2676 TWX 710-987-8367

READER SERVICE NUMBER 44

DOWNCONVERTERS

INPUT 12 to 40 GHz



OUTPUT 5.4 to 12.4 GHz

Typical of Spacekom's line of downconverters and low-noise mixers is Model CA-1 downconverter assembly. It consists of 5 balanced downconverters with integrated LO sources. Downconverters may be ordered separately or as an assembly complete with power supply. Key performance parameters are: Image Rejection, 50 db min.; LO Radiation, -60 dbm max.; LO Stability, 1 x 10^7 short term.

BAND	1	2	3	4	5
RF Input (GHz)	12.0 - 18.3	18.0 - 22.3	22.0 - 26.9	26.5 - 33.5	33.0 - 40.0
IF Output (GHz)	5.4 - 11.7	5.4 - 9.7	5.4 - 10.3	5.4 - 12.4	5.4 - 12.4
LO Frequency (GHz)	23.7	27.7	32.3	38.9	45.4
Conversion Loss max.	7 db	6 db	6 db	8 db	7 db

SPACEKOM, INC.
212 E. Gutierrez St., Santa Barbara, CA 93101
Telephone (805) 965-1013

READER SERVICE NUMBER 45

Power Flatness: A measure of the oscillator power output variation over a specified frequency range and for a specified ambient temperature or temperature range. Usually expressed as a dB variation around a nominal power output. For example: ±2 dB from f_1 to f_2 for $T_{ambient}$ = 85°C. Sometimes expressed as a peak-to-peak variation in either dB or watts.

Proportional Temperature Control: A method of stabilizing an oscillator by providing heater power that is directly proportional to the difference between the desired operating temperature and the ambient temperature.

Pulling Figure: An oscillator term used to describe the output frequency sensitivity to changes in the oscillator load from a perfect match to a specified mismatch. Typically expressed as the total frequency excursion observed as a load of specified VSWR varies over 360 electrical degrees.

Punch Through Varactor (PTV): A special form of C-swing varactor that has a rapid change in capacitance for small values of reverse bias voltage and an almost constant value for all large values of reverse bias voltage. Used in high-efficiency multipliers.

Pushing Figure: A term used to describe the output frequency sensitivity to changes in the power supply voltage. Typically expressed in terms of actual or percentage output frequency change per actual supply voltage variation (i.e., MHz/V or %/V).

Push-Pull Configuration: A fundamental oscillator design in which each half of the circuit operates during a portion of the rf cycle. Primary advantages are increased power output over a single or parallel pair of transistors and reduction of second harmonic content in the output.

Push-Push Configuration: An harmonic oscillator design in which the signals from each output transistor operating at f_o are combined to produce an output signal at 2 f_o. The main advantage of this configuration is the extension of a transistor's operating frequency limits without the use of an extra frequency doubler circuit.

Reference Oscillator: The high stability, usually crystal and temperature controlled, rf signal source used as a phase reference in phase-locked oscillators.

Resetability. Defined as the ability to repeatedly obtain the same output frequency whenever the tuning input signal returns to the value for that frequency, independent of previous tuning signal excursions.

Search: The process of applying a sweeping tuning signal to the free running oscillator portion of a PLO, causing the oscillator output frequency to pass within the capture bandwidth of the feedback network and insuring a locked condition in response to a new reference frequency.

Set-On Accuracy: The difference, expressed in MHz or percentage of expected frequency, between the actual output frequency and the expected output frequency for a given tuning signal value.

Set-On Time: The time required for the oscillator output frequency of a voltage or current-tuned oscillator to change from the initial value to within the set-on accuracy in response to a tuning signal command.

Settling Time: The time required for the output frequency of a voltage or current-tuned oscillator to change from the initial value to within a specified window around the final value in response to a voltage or current step on the tuning input port.

Short-Term Stability: Maximum frequency and/or power output variations that occur in the time interval from one hour to 24 hours after an oscillator has stabilized with a given set of environmental (supply voltage/current, tuning signal, temperature, etc.) conditions. Frequency variations are usually expressed in percent of output frequency or in MHz; power variations in mW or dB around a reference level.

Slew Rate: The rate which the voltage or current-tuned oscillator frequency can change in response to a step input on the tuning port. The step input waveform must be carefully defined.

Snap Varactor (SV): See step-recovery diode.

Spurious Signals: Harmonic or non-harmonic undesired output signals that are caused by oscillator circuit instabilities. Usually specified for both in-band and out-of-band conditions and expressed in units of dBc.

Stabilized Master Oscillator (STAMO): The master oscillator in complex microwave systems that acts as the frequency reference for all rf signals within the system. Usually crystal and temperature controlled for maximum frequency stability.

Step-Recovery Diode (SRD): A special form of p-n junction in which the charge storage and switching characteristics are optimized for use in microwave frequency multipliers and comb generators. The device stores charge while in forward conduction and a large reverse bias current can be obtained until all the charge is removed. The device impedance then goes from a low value to a very high one in transition times as low as 50 picoseconds. Sometimes referred to as a Snap Varactor.

Tuning Curve: The graphical presentation of the output frequency-tuning signal relationship.

Tuning Linearity: The difference between the actual tuning signal-to-output frequency relationship and the desired straight line (linear) relationship. Usually expressed as a worst case and/or typical percentage over the whole tuning image.

Tuning Sensitivity: A numerical value relating the incremental change in output frequency due to an incremental change in tuning signal. Typically expressed as MHz/Volt for voltage-tuned oscillators and MHz/mA for current-tuned oscillators, it is specified as a maximum value over the operating frequency range.

Tuning Sensitivity Variation: The change in tuning sensitivity over a specified frequency band, usually expressed as a ratio of maximum sensitivity over the operating band.

Varactor-Tuned Oscillator (VTO): An oscillator in which a varactor diode is used in the frequency determining network that encompass the circuit's active device(s).

Voltage-Tuned Cavity Oscillator (VTCO): Primarily a cavity oscillator with the addition of a varactor diode to slightly modify the cavity's resonant frequency. VTCOs are capable of fm and/or phase-locking.

Voltage-Tuned Crystal Oscillator (VTXO): A crystal-controlled oscillator with a varactor diode in the frequency determining network that is used to slightly vary the crystal frequency. Output frequency bandwidth is typically less than 0.1%.

Voltage-Controlled Oscillator (VCO): Any oscillator for which a change in tuning voltage results in predetermined change in output frequency. Frequency tuning is accomplished by either changing the bias voltage on a varactor diode in the frequency determining resonant network or the bias voltage to the active device. The former approach, although more complex than the latter method of tuning, is capable of multi-octave bandwidth.

Warm Up Time: The time required for the unit to meet all specified operating parameters. The heater power and bias program must be specified.

YIG: Yttrium Iron Garnet crystalline material which resonates at microwave frequencies when immersed in a magnetic field. Small spheres of YIG material are mounted in resonant structures for tuning appliications.

YIG-Tuned Oscillator (YTO): The microwave resonance characteristics of YIG material is used to tune microwave oscillators. This resonance is directly proportional to the applied magnetic field, hence very linear tuning is achieved by changing the magnetic field with an electric current. YTOs intended for wide bandwidths will usually have two tuning coils—one for setting f_o over the band and the other for frequency modulation.

Tips On Specifying Acoustic Wave Devices

New applications for surface acoustic wave devices are finding their way into a variety of microwave systems. Here's a guide to the specification of these versatile signal processors.

THERE is currently a dramatic surge of interest in surface acoustic wave (SAW) devices. The technology has matured to the point where designers can seriously consider their application in many types of advanced systems. But, being a relatively young science, SAW devices are still unfamiliar to many. This article will help answer such fundamental questons as: What can SAW devices do? What are their limitations and how are they specified?

Signal processing applications for SAW devices can essentially be grouped into four categories:

- **Delay lines** are finding use in rf memories, as multiple-target-indicator cancelers, replacements for certain bulk delay lines and to obtain video delays for synchronization purposes in digital processors.
- **Bandpass filters** appear to have the highest volume potential of any SAW device and are finding their way into electronic warfare systems (contiguous arrays), communications receivers and, of course, TV i-f circuits.
- **Dispersive delay devices** show potential in linear fm pulse compression radars, high-resolution frequency discriminators and compressive receivers. They are also used in wideband, bandpass filter applications.
- **Tapped delay lines** are principally used as analog matched filters to shape PSK waveforms in spread spectrum (secure) communications and navigation systems. Other applications include pulse compression doppler radars and preample correlators. Noncoded, tapped delay devices have found applications in switchable microwave memories as well as in transversal filters and equalizers.

These applications represent a mere sampling of the potential of acoustic technology in signal processing. Of course, the advantage of using a SAW device depends on the application, but the designer can generally look forward to a reduction in size and weight, increased reliability and in many cases lower cost. This is not to mention that the SAW device may allow him to perform certain functions that would otherwise be extremely difficult or costly, or even impractical.

But, as one might expect, there are some constraints. Most limitations arise from the photomask and piezoelectric substrate. For example, conventional photolithographic and mask techniques limit the upper frequency of operation to about 1 GHz. Bandwidths are generally restricted to less than one octave and the designer is often faced with a rather large insertion loss. Notwithstanding, there may be a use for a SAW device in your system.

Substrate specs are important

Since SAW devices have become a popular area of investigation, a number of different substrate materials have been studied. The final selection of a substrate depends on the type of device being designed, frequency of operation, bandwidth and the time delay, along with any particular requirements imposed by the system in which the component will be used. Table I shows how well several substrate materials meet these needs.

The surface-wave propagation velocity of the substrate defines the acoustic wavelength and transducer geometry, and therefore, directly influences the degree of fabrication difficulty. For example, a

(continued on p. 50)

Chuck Grasse, Engineering Group Leader; Teledyne/MEC, 3165 Porter Drive, Palo Alto, CA 94304.

Table 1. Material Properties For Surface-Wave Substrates

Piezoelectric Substrate Material	Orientation	Surface Wave Velocity (m/sec)	Time Delay (msec cm)	2 k (%)	Estimated Optimum Bandwidth (%)	Delay For Total Beam Steeping Loss (msec)	Delay for 3 dB Diffraction Loss (msec)	Temperature Coefficient of Delay (ppm)
Lithium niobate	ROTY-Z	4000	2.50	5.7	27	—	—	−57
Lithium niobate	Y-Z	3488	2.88	4.5	24	152	1820	91
Quartz	Y-X	3159	3.16	0.23	5.4	278	106	−22
Quartz	ST-X	3158	3.16	0.16	4.5	480	131	0
Bismuth Germanium Oxide	(100)-(011)	1681	5.95	1.5	14	1210	256	130
Bismuth Germanium Oxide	(111)-(110)	1708	5.86	1.7	15	917	131	128
Lithium Tanalate	Y-Z	3230	3.09	0.74	10	841	225	37

large velocity material such as lithium niobate is attractive because the correspondingly large acoustic wavelength for a given frequency calls for a larger, simpler-to-manufacture transducer. Long acoustic wavelengths also improve the accuracy to which each electrode can be located. A placement error of a given magnitude will be more serious on bismuth germanium oxide than on lithium niobate, for instance, since it constitutes a larger fraction of a wavelength.

Propagation velocity also determines the overall length of the device. A delay line on lithium niobate requires almost twice as much crystal length as a similar device on bismuth germanium oxide (BGO).

The acoustic-surface wave propagation loss must also be considered when selecting a substrate, particularly for long time delays at high frequencies. Losses are small below 100 MHz for most materials (**Fig. 1**).

When choosing a substrate that may be subjected to unfavorable environmental conditions, it is desirable to select a material whch will minimize any thermal effects. For most devices, the two most important temperature dependent parameters are the surface-wave velocity and the linear dimensions of the material. The combination of their effects can alter a device's delay versus frequency (temperature coefficient of time delay) or after its frequency response (via the temperature coefficient of velocity). The combined effect of the coefficient of expansion and the coefficient of velocity make up the temperature coefficient of time delay (approximately 100 ppm/°C for lithium niobate and 0 ppm/°C for ST-quartz). A 10 μsec delay line on lithium niobate, for example, could vary as much as 100 nsec when operated over a 100°C temperature range. The performance of a similar device on BGO would degrade more severely (by about 25%).

Materials such as lithium niobate and BGO are also quite susceptible to temperature-caused shifts in center frequency (again caused by the combined effects of the coefficients of material expansion and velocity). This effect is particularly critical for narrowband filters and tap-coded devices where a frequency shift of a few hundred kHz can render it virtually useless. The temperature coefficient of time delay (Table 1) is representative of the magnitude of these effects and, therefore, may be used to estimate the performance of a surface-wave device with temperature. If performance requirements are such that a closer tolerance is desired over a given temperature range, the lithium niobate and BGO devices will require a temperature-control oven. If an inrcease in insertion loss can be tolerated, ST-quartz can serve as a substitute.

The beamwidth of acoustic energy radiated by a transducer of finite electrode length (overlap) will tend to increase due to diffraction, causing additional loss. The amount of diffraction loss can be decreased by increasing the electrode overlap. As seen in the table, lithium niobate is the best material for minimum diffraction loss.

Beam steering refers to the angular misalignment of the propagating acoustic energy due to the transducer axis being slightly misoriented with respect to the desired propagation direction of the crystal. Proper substrate orientation (see box) and careful attention to the alignment of the photo mask and crystal generally eliminate this problem, even for very long time delay devices. Lithium niobate requires more careful orientation accuracy than any of the other crystals.

The electromechanical coupling coefficient (k^2) is a figure of merit expressing the efficiency with which electromagnetic energy is converted into acoustic energy by a surface-wave material. Better known as conversion loss, this factor is usually the prime contributor to a device's insertion loss. Lithium niobate has the highest coupling coefficient (lowest loss) of known surface-wave materials.

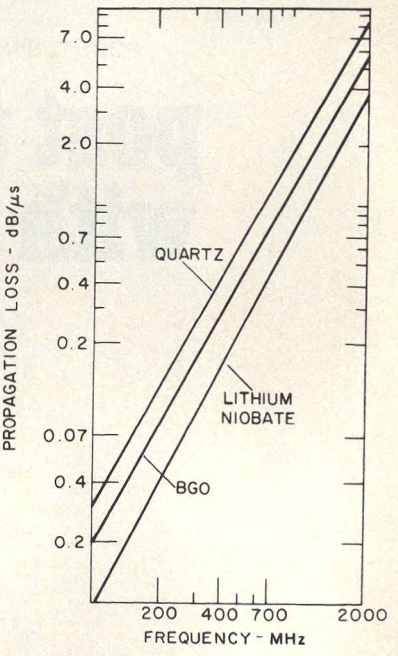
Watch out for spurious

Acoustic materials with high coupling coefficients are especially susceptible to multiple-transit spurious signals, and therefore, should be carefully considered before being specified for components whose amplitude/phase response or sidelobe levels (filters, correlators, pulse compressors) are of primary concern. Multiple-transit spurious signals are surface-wave signals which reflect back and forth between the input and output transducers. This undesirable energy adds ripple to amplitude and phase characteristics but may be minimized by designing transducers with "split" fingers. Investigators have been particularly successful

How Important Is Orientation?

The orientation of a surface-wave substrate material is a very complex process as each material has its own crystalline structure (and notation)—for example, <001> cut, <110> propagating BGO and Y cut, Z propagating lithium niobate. However, there are a few pertinent comments which may be of some help in identifying the proper substrate for a given application. The specified orientation of a material is such that it will provide a particular characteristic or set of characteristics which are beneficial to the designer. As an example, one substrate orientation may provide lower loss and less generation of spurious signals while another would provide for a minimum of diffraction loss. These preliminary judgements can be made from Table 1.

Once a particular orientation has been selected, it remains to determine the accuracy to which the substrate orientation must be specified. This is not an insignificant consideration as it will impact on the cost of the substrate. Most substrates are oriented routinely to within 0.5 degrees; and for most applications, this is probably sufficient. Care should be taken, however, when specifying the orientation of the propagation axis on certain materials for certain applications like long time delays. Table 1 indicates data for 0.1 degree orientation of this axis. Relaxation of the orientation tolerance of a given crystalline axis can be specified (up to about 1.0 degrees maximum) as a tradeoff between performance and cost for those high-quantity applications where the ultimate cost is most important.



1. Lithium niobate has the lowest propagation loss of known surface-wave materials. Losses for all materials are small below 100 MHz.

FREQUENCY RANGE (MHz)	10-250	250-500	500-750	750-1000
BANDWIDTH (3 dB)	← 1 MHz to 40% →			
LOSS (dB) VERSUS TIME DELAY:[1][2][3]				
<1 μsec	8-11 dB	12-13 dB	13-15 dB	15-18 dB
1-10 μsec	10-17 dB	12-22 dB	16-25 dB	21-30 dB
10-20 μsec	12-18 dB	17-28 dB	23-27 dB	27-35 dB
20-35 μsec	15-25 dB	20-35 dB	25-50 dB	28-55 dB
MAXIMUM VSWR	← 2:1 →			
SPURIOUS SIGNAL SUPPRESSION	Spurious signal suppression can range from 15 dB to greater than 50 dB, depending on other electrical parameter requirements.			
INPUT POWER	← +15 dBm →			

(1) Lithium niobate material is assumed; if ST-quartz is desired the insertion loss will be about 15 dB higher.
(2) The insertion loss figures are predicated on nominal 10-20% bandwidths. Figure 3 can be used to estimate the effect of changes in bandwidth on insertion loss. The insertion loss values given represent the "best-to-worst" loss for each set of parameters. For example, a 10 MHz, 1 μsec. delay line would have approximately 10 dB of insertion loss, where a 250 MHz, 10 μsec. delay line would have about 17 dB.
(3) A temperature stability of 90 ppm/°C is assumed. For improved temperature stability (~0 ppm/°C) ST-quartz material may be specified.

(a) DELAY LINE

CENTER FREQUENCY	10 MHz to 1 GHz
BANDWIDTH (3 dB)	100 kHz to 40%
INSERTION LOSS (MIN.)(1)	7-8 dB
SHAPE FACTOR (3 dB to 30 dB)	2.1 (1.5:1 POSSIBLE)
SIDELOBE REJECTION (NEAR IN)	35 dB (>40 dB POSSIBLE)
SIDELOBE REJECTION (FAR OUT)	60 dB
PHASE DEVIATION (FROM LINEAR)(2)	±1.5°
AMPLITUDE RIPPLE	±0.25 dB

(1.) FIGURE 3 CAN BE USED TO ESTIMATE THE EFFECT OF BANDWIDTH ON INSERTION LOSS.

(2.) OVER THE CENTER 80% OF THE OPERATING BANDWIDTH. AT THE BAND EDGES, ±5-10° IS MORE TYPICAL FOR LOW SHAPE FACTORS.

(b) BANDPASS FILTER

CENTER FREQUENCY (MHz)	TYPICAL BANDWIDTHS[1] (MHz)	TYPICAL TAP SPACING[2] (nsec)	MINIMUM INSERTION LOSS[3] (dB)	PEAK-TO-SIDELOBE ACCURACY
20-1000	2-20 MHz	>100	35	Note 4

(1) The required RF bandwidth is dictated by the "information" bandwidth (i.e., the tap spacing), and should be broad enough to allow impulse testing.
(2) The minimum tap spacing should be at least 100 nanoseconds in order to keep multiple transit signals from degrading the peak-to-sidelobe ratio.
(3) CW insertion loss for a typical 32 bit sequence on ST-quartz is assumed. This loss must be adjusted for the longer sequences. If lithium niobate substrates are used an improvement of between 10 and 15 dB in insertion loss can be realized.
(4) The peak-to-sidelobe ratio, of course, depends on the code sequence and its "goodness" . . . however, a given sequence (32 to 64 bits typically) can be correlated to within ± .5 dB of its theoretical peak-to-sidelobe ratio on quartz. On lithium niobate this figure is reduced to about ± 1.0 dB.

(d) TAPPED DELAY LINE

FREQUENCY RANGE (MHz)	20-100	100-350	350-500	500-700	700-1000
BANDWIDTH (MHz)	← bandwidths from 10% to 50% are typical →				
DISPERSIVE TIME-DELAY (μSEC)	← from a few nanoseconds up to about 20 microseconds →				
MINIMUM INSERTION LOSS[1]	15 dB	20 dB	30 dB	40 dB	50 dB
TIME-BANDWIDTH PRODUCT[2]	← lithium niobate: less than 1500:1 ST-quartz: less than 2500:1 →				

(1) Insertion loss is a function of many inter-related parameters, therefore, the values indicated are intended to serve only as gauges of typical performance within each category.
(2) A "figure-of-merit" which may be used to gauge the relative difficulty of a given design approach. Generally, the smaller time-bandwidth products indicate the less difficult tasks.

(c) DISPERSIVE DELAY LINE

2. These design guidelines summarize what SAW devices are capable of in each application category. The range of specifications is purposely broad since they depend on the substrate material (Table 1) and the specific application.

in removing this effect from quartz material.

A second type of spurious energy is generated by the interdigital transducer and radiated directly into the volume of the substrate. These bulk-mode signals either propagate at a very shallow angle immediately beneath the surface, or take a steeper path and reflect off the bottom of the crystal where they interfere with the desired signal. The result is also added ripple in the phase and amplitude responses, as well as uncharacteristically high sidelobes in bandpass filters and pulse-compression devices. Techniques for suppressing these signals are being investigated, and for most applications, 45 dB rejection can be obtained.

Electrical feedthrough also interferes with the performance of a surface-wave device. Feedthrough is a portion of the input signal that radiates directly from the input to the output transducer, thus appearing as a zero-delay signal.

(continued on p. 53)


Actual Size

Get cleaner mm waves with Hughes GUNN effect oscillators.

Our low-noise, solid-state oscillators come in two basic types in frequency ranges above 18 GHz. The voltage-controlled oscillators provide broad tuning bandwidths and minimum power outputs to 35 mW. The mechanically-tuned models offer higher power outputs of up to 150 mW adjustable over 100 MHz.

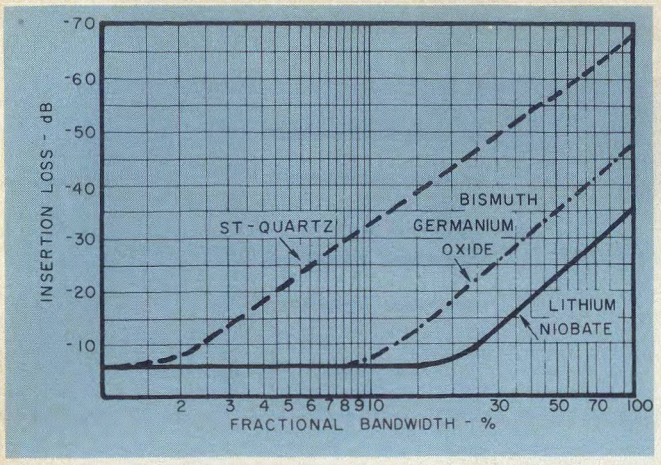
All feature standardized solid state design, small size, ruggedness, low cost and high stability.

Find out more about less noise. Write or call: Hughes Electron Dynamics Division, 3100 W. Lomita Boulevard, Torrance, Calif. 90509. (213) 534-2121, ext. 215.

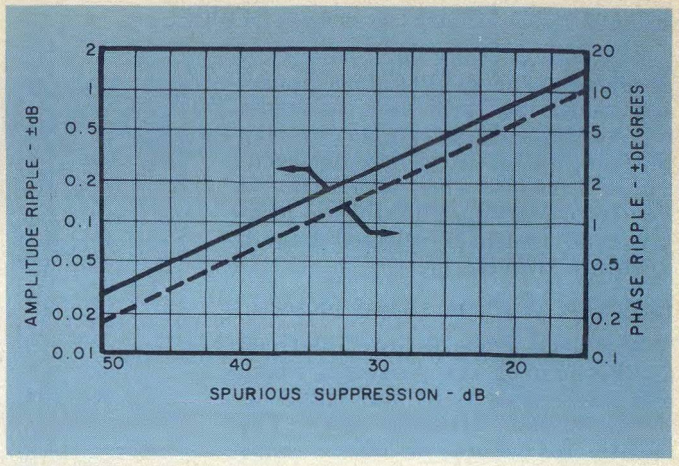
HUGHES
HUGHES AIRCRAFT COMPANY
ELECTRON DYNAMICS DIVISION

Making waves in millimeter-wave technology.

READER SERVICE NUMBER 51



3. ST-quartz has a high insertion loss, but finds many applications due to its superior thermal properties. These losses are given for fractional (percent) bandwidths.



4. Amplitude and phase ripple are directly proportionate to the level of spurious signal suppression. This graph applies to all substrate materials.

Minimizing the electrical feedthrough is largely a packaging consideration, although the larger the separation between input and output transducers, the less severe the problem becomes.

Individual consideration needed

Up to now, this discussion has described how each parameter influences SAW action in general. However, due to the specialty of each class of acoustic device, it's necessary to consider how each parameter relates to specific types of signal processing. Design guidelines for the four classes of SAW devices are summarized in Fig. 2. Data for insertion loss and amplitude and phase response appear in Figs. 3 and 4, respectively.

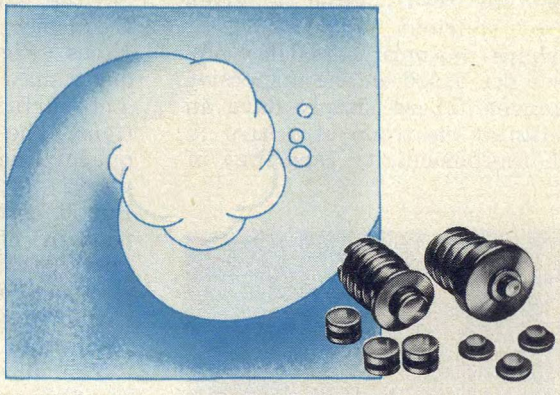
Delay lines are the most fundamental of all SAW devices. They simply consist of input and output transducers deposited on a piezoelectric substrate. Bismuth germanium oxide is a good material for long delays ($>$ 70 μs on a single substrate) at frequencies less than 300 MHz. Lithium niobate is preferred for long delays up to 1.0 GHz, and ST-quartz is best for shorter time delays where more stringent temperature performance is required. For extremely short delays (less than 500 ns), transducers are very closely spaced and a penalty is paid in the amount of spurious signal suppression achievable. This, of course, will adversely affect the amplitude and phase performance (Fig. 3).

The accuracy of a given time delay depends on the resolution of the photomask and the accuracy to which the material velocity is known. It is possible to resolve a given time delay (on lithium niobate and quartz) to an accuracy of approximately ± 2 nsec (although to within 10 nsec is more typical). Don't forget, a small degradation in time-delay resolution may have to be accepted when a slower velocity material such as BGO is specified.

In many respects, the SAW bandpass filter is similar to the delay line. In its simplest form, it consists of two interdigital transducers, one or both of which may be weighted in order to improve the frequency response.

The term "weighting," as used in surface-wave technology, is often misunderstood. Weighting is a technique for obtaining improved performance (low out-of-band signals and reduced sidelobes are examples) by altering the transducer

(continued on next page)



Introducing four new IMPATT diodes. With higher power, higher frequencies and lower prices.

Hughes now has a complete line of low-cost millimeter-wave IMPATT diodes providing up to 50 mW at 100 GHz or 300 mW at 40 GHz. And they all feature the longest life and greatest reliability available in any commercial diodes.

For operation below 40 GHz, our diodes are packaged with a 50-mil diameter ceramic ring. For applications above 40 GHz, they are packaged with a 30-mil diameter quartz ring—both developed by Hughes. And you have a choice of either unmounted or stud-mounted models.

For more information, call or write the IMPATT diode capital of the world: Hughes Electron Dynamics Division, 3100 West Lomita Boulevard, Torrance, CA 90509. (213) 534-2121, extension 215.

HUGHES
HUGHES AIRCRAFT COMPANY
ELECTRON DYNAMICS DIVISION

Making waves in millimeter-wave technology.

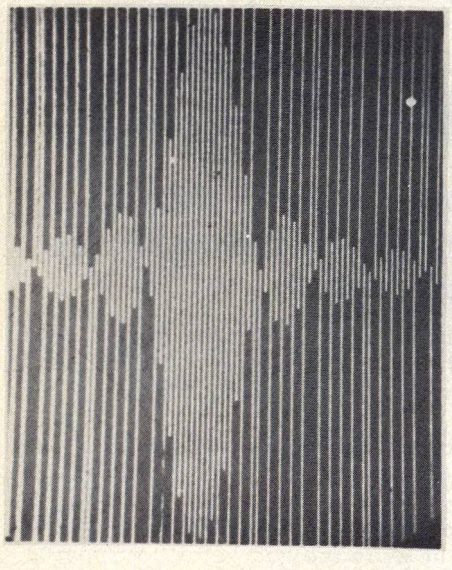
READER SERVICE NUMBER 53

geometry. The modification generally takes the form of a variation in the interdigital finger overlap pattern, (Fig. 5). A second technique involves phase-weighting a device by varying slightly the location and width of selected fingers within a transducer.

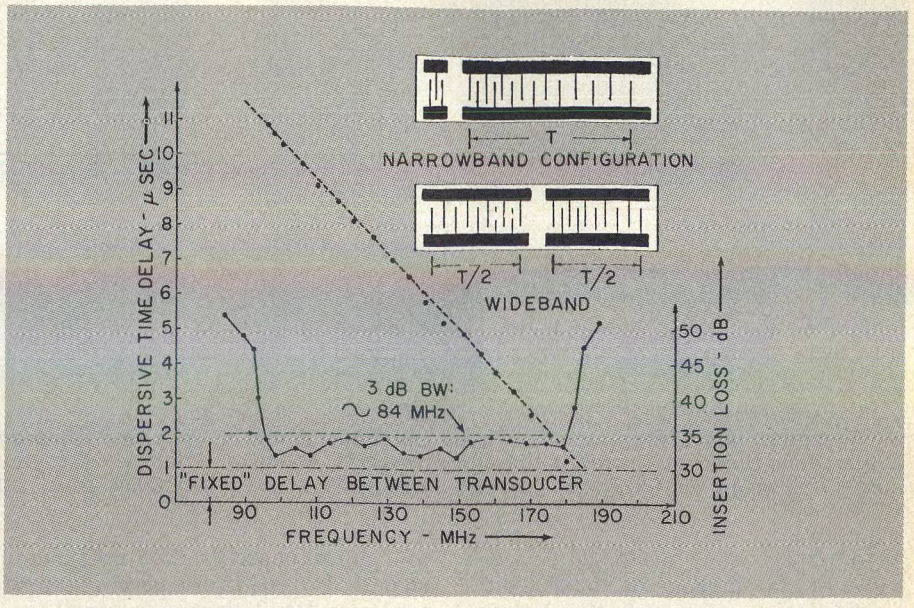
Spurious governs shape factor

A filter's shape factor is defined as the sum of the passband width and the transistion bandwidth divided by the passband width. The ability to achieve a given shape factor depends on the level of spurious bulk and surface signals, since this determines the accuracy to which the filter weighting function may be implemented. There are several fundamental influences on sidelobe response in a SAW filter, but spurious signals and non-optimum implementation of the weighting function are the most critical. Distortion effects have all but been eliminated for quartz substrates, making it a top-notch material for applications where precise out-of-band rejection and amplitude-phase performance is desired. Again, Fig. 3 may be used to estimate the amount of amplitude and phase distortion which will result from a given level of spurious signals.

Perhaps the most versatile SAW devices are based on the dispersive transducer. These simply have an interdigital electrode structure in which the periodicity (spacing) of the fingers is varied in such a manner that different regions of the transducer are sensitive to different frequencies.



5. Weighting is modification of a transducer geometry by varying the interdigital finger overlap to achieve certain performance benefits. This shows (sin x)/x weighting.



6 A dispersive transducer is used to "down chirp" the time delay/frequency characteristic.

If possible, the slope of the transducers dispersive characteristic must be down-chirped. That is, the signal must decrease in frequency with increasing delay times (Fig. 6). An up-chirp transducer may lead to aggravated bulk and surface-mode induced distortions. The time delay versus frequency linearity of a dispersive device is typically better than 1%. But since this characteristic is dependent on the accuracy of the computerized placement of each electrode, a lower frequency device should provide better linearity and resolution.

The insertion loss response of the dispersive device may be specified to within ±1 dB (min) while the phase deviation from quadrature will be typically ±5 degrees.

In the pulse-compression application, sidelobe reduction is accomplished by weighting the receiver-transducer. The penalty paid is approximately 2 dB of additional insertion loss and a 50% widening of the compressed pulse. Sidelobes can be reduced to greater than 30 dB from the peak of the auto-correlation signal. For sidelobe reduction greater than 35 dB, an external weighting filter may have to be used in conjunction with the surface-wave matched-filter receiver. In the frequency discriminator, it may be desireable to shape the input signal pulse as a means of reducing close-in sidelobes.

For each design application, a different characteristic may need to be optimized. For example, phase characteristics are very important to radar application in order to achieve low-time sidelobes, whereas linear-time delay versus frequency and output pulse shape are critical to the discriminator. A designer may have to choose between a large time bandwidth product and insertion loss while the frequency of operation will impact on the time delay versus frequency ("chirp") linearity. In general, the amount of difficulty and cost attendant with producing a device is proportional to the size of the time bandwidth products. It is not required that each dispersive device operate alone. For example, devices may be used in series to increase the time-bandwidth product (the time delay is extended, while the bandwidth remains the same). Dispersive-delay lines may also be designed contiguously in order to increase the amount of bandwidth covered.

The basic bi-phase coded signal processor consists of two devices: a sequence generator and a matched-filter correlator. Each device consists of an input transducer and a tapped transducer into which the code sequence is designed. The code of each tap is determined by the "polarity" of each electrode.

(continued on p. 56)

When specifying a substrate for tap-coded lines, it is most important to accurately know the velocity of the material. This is particularly true if the coded sequence is being produced actively (not with an acoustic device) and controlled to within a few kHz of the design-center frequency. Any appreciable deviation of the acoustic-correlator frequency from that of the sequence generator will seriously degrade the auto-correlation performance. For example, deviation of approximately ±50 kHz is probably tolerable, but a shift of 200 kHz or greater could render the device useless.

If possible, the tap separation should be at least 100 ns (a 10 MHz data rate) to insure a minimum of intertap reflections which tend to degrade the correlation peak to sidelobe performance.

Spurious signals in a SAW correlator are a result of interactions between taps. The result is a triple-travel sequence which can interact with the correlator transducer to produce a bogus correlation signal. This signal is considerably below the sidelobe level of the compressed output signal, particularly when ST-quartz material is used.

The amount of degradation due to variations in temperature will depend on the type of code, the number of cycles per bit and the code length. Thermal stability points to ST-quartz as the preferred material, but in many applications (or when insertion loss requirements dictate lithium niobate), thermal regulation may be required.

A more thorough discussion of individual SAW designs appears in "Surface Acoustic Wave Devices," which may be obtained by circling RSN 210. ••

Test your retention

1. How does a material's characteristic propagation velocity affect the design and construction of a SAW device?
2. What SAW substrate material has the lowest propagation loss?
3. How does spurious energy modify the performance of a surface wave device? What are some ways to reduce these effects?
4. How are transducers "weighted"? Why?
5. What is the most critical substrate specification for a tap-coded line?



Sometimes more... never less.

That's what you get with our signal sources and oscillators — the rated power as an absolute minimum throughout the frequency band of the plug-in head in use. In fact, we're so confident we can deliver that power, we've hung a guarantee tag on each and every oscillator we sell.
In a model to suit your needs up to 100 watts CW or 40 kilowatts pulsed. Guaranteed. You can depend on it.
For more information call or write

Epsco INCORPORATED
APPLIED MICROWAVE DIVISION
411 PROVIDENCE HIGHWAY, WESTWOOD MA 02090
(617) 329-1500 TWX (710) 348-0484

READER SERVICE NUMBER 57

Try CAD For Accurate GaAs MESFET Models

Working with a new equivalent circuit, it's possible to fit s-parameters to experimental data using CAD routines. The model is valid to 12 GHz, but projections to 24 GHz can be made.

A good circuit model is essential to understand improvements in the electrical performance of GaAs MESFETs. This article presents a new circuit model which is valid to at least 12 GHz. Beyond this frequency, s-parameter measurements are subject to errors due to fixture losses and are difficult to calibrate accurately. Although, difficult to confirm experimentally, the new model can be extended to predict MESFET performance to 24 GHz.

Six recently reported GaAs FETs[1,2,3,4] are analyzed with this new model and a table of equivalent circuit elements is presented. The similarity among these devices is striking. To fit the measured s-parameter data to the model, a microwave computer-aided design[5] program proves to be very useful, especially for s_{12}, which is very difficult to fit over the 1 to 12 GHz range.

There are two basic differences in this new model (Fig. 1). First, the lumped element representing the output drain-source capacitance (C_o) is connected to the source pad instead of to the substrate, since the capacitance between the drain contact and the substrate ground connection is typically 0.002 pF and can be neglected.

Secondly, a resistor (R_s) is included in series with the gate-drain capacitor. This modification is necessary to adequately model the frequency behavior of s_{12}, which is wholly determined by R_f C_f, R_s and L_s. C_f is the predominant feedback element at low frequencies, but L_s becomes dominant as the frequency is increased.[6]

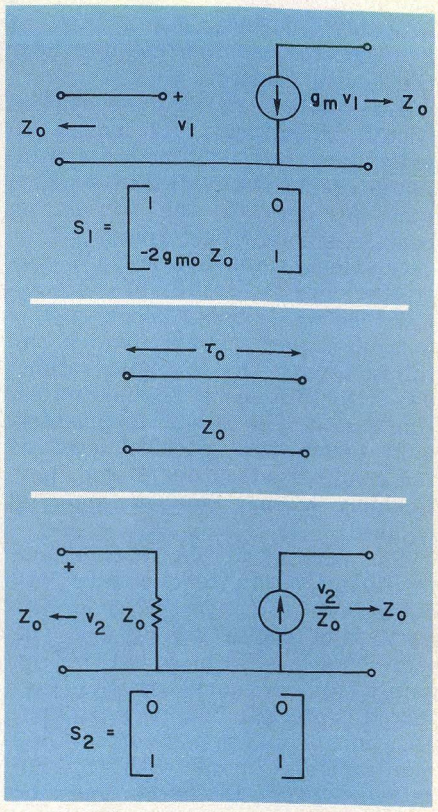
The only package parasitics represented in the new model are the inductances of the bonding wires: L_i, L_o and L_s.

Four loss elements are included: R_i, the sum of the gate and channel resistances; R_o, the output conductance and drain resistance; R_f, the resistance of the gate-drain fringing capacitance; and R_s, the source-channel parasitic resistance. Additional resistance elements may be required to create a more accurate model for some FETs, but they are not necessary for the MESFETs reported here. Conversely, for high-frequency MOSFETs, the source-channel resistance (R_s) can usually be omitted.

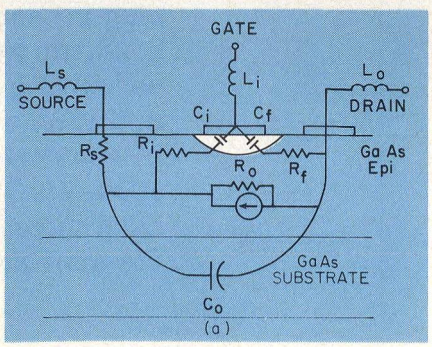
The input reflection parameter, s_{11}, is easily modeled by a series RLC network. The amount of resistance and inductance needed for the common-source load can be determined by fitting the s_{12} data as described below.

The output reflection parameter, s_{22}, was modeled by a parallel RC network in series with an output inductor. An additional resistor with a value of R_s should probably appear in series with L_o, but this extra component is not necessary to adequately fit s_{22}. The transfer parameter, s_{21}, is determined by estimating the transistor transcon-

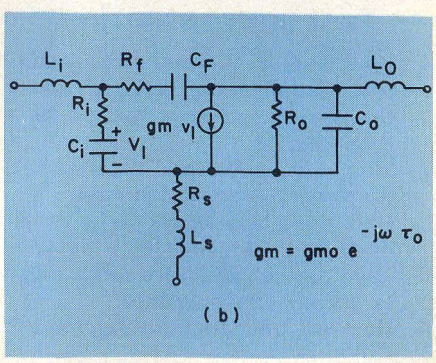
(continued on p. 60)



2. S-parameters are derived for the basic current generator (S_1) and for an output isolation generator (S_2). A lossless transmission line provides the necessary phase delay (τ_o).

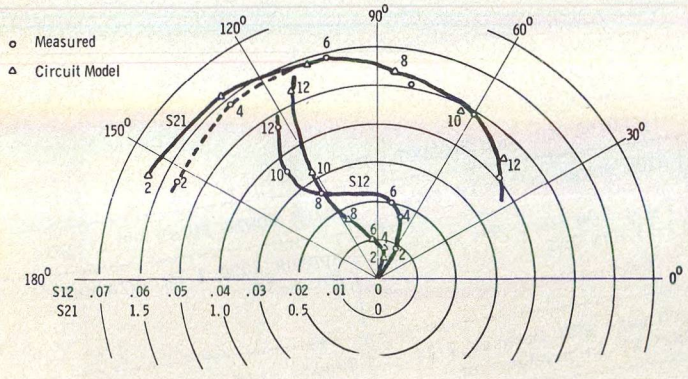


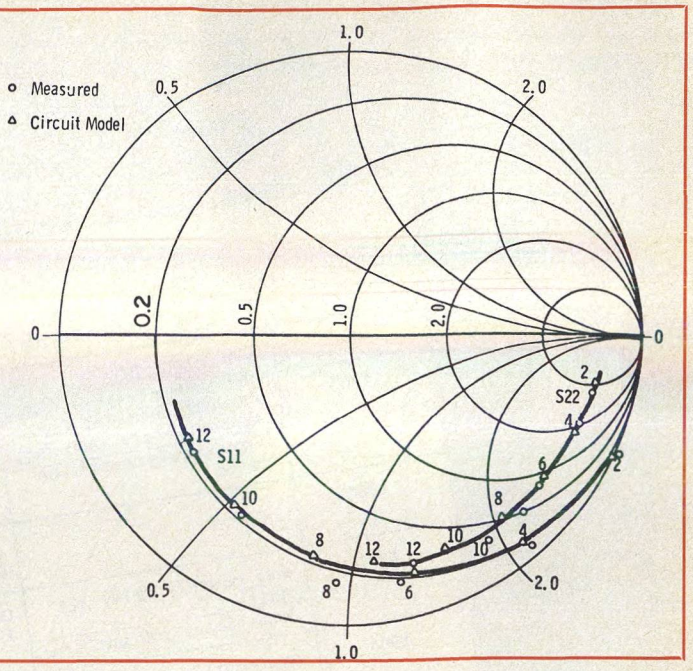
1. This GaAs equivalent circuit differs from earlier models. The source-drain capacitance connects to the source pad, not the substrate, and a resistor is introduced in series with the gate-drain capacitor.



George D. Vendelin and **Dr. Masahiro Omori**, Members of the Technical Staff; Varian Associates, 611 Hansen Way, Palo Alto, CA 94303.

3. **Although s_{11}, s_{21}, and s_{22} are easily fitted, s_{12} poses some problems.** Note the close correlation between predicted and measured values in these plots for the NEC device described in Table 1.





ductance (g_m) and using:

$$s_{21} = -2g_m Z_o = -100\ g_m$$

For a transconductance of 20 mmho: $s_{21} = -2.0$.

Fitting s_{12} proves troublesome

Although the model will quickly converge for s_{11}, s_{21} and s_{22}, modeling s_{12}, the feedback parameter, is not as simple since its frequency dependence is not easily predicted (Fig. 3). Computer analysis is called for. Les Besser's design program, "Compact," is capable of fitting any set of measured s-parameters to a second set of calculated s-parameters and is ideally suited for modeling the troublesome feedback s-parameter.

The equivalent circuit can be conveniently modeled with a microwave analysis program by deriving the s-parameters of the current generator, S_1, shown in Fig. 2. A less critical generator, S_2, is also necessary to prevent the transmission line from loading the output circuit. The basic current generator has an s_{21} of $-2g_{mo}\ Z_o$. Phase delay is introduced by adding a lossless transmission line with an electrical length of:

$$\ell = c\,\tau_o$$

where c is the velocity of light and τ_o is the phase delay of the current generator.

It's important to consider the physical meaning of τ_o. This delay corresponds to the time required for electrons to traverse a portion of the gate length at the scattering-limited velocity. For a 1μm gate GaAs FET,

$$\tau_o \approx \frac{L_g}{V_s} \approx \frac{10^{-4}\ \text{cm}}{2 \times 10^7\ \text{cm/sec}}$$

$$\approx 5\ \text{psec.}$$

Using the s-parameter matrices of Fig. 2, the equivalent circuit model introduced in Fig. 1 can easily be written into a computer file. Since the current generator can be described as a frequency-independent s-parameter matrix, the computer file is very brief, even though the analysis may be required over many frequencies.

The s-parameters of the model are described by a two-port called "JJ." A second two-port, entered in the computer file as "KK," contains the measured s-parameters. When the command "SET JJ KK" is issued, the program compares the s-parameters and varies selected elements in an effort to minimize the error function described by

$$EF = \frac{1}{N}\sum_{FI}^{FF}\{W_1|S_{11_{JJ}} - S_{11_{KK}}|^2 + W_2|S_{22_{JJ}} - S_{22_{KK}}|^2 + W_3|S_{21_{JJ}} - S_{21_{KK}}|^2 + W_4|S_{12_{JJ}} - S_{12_{KK}}|^2\}$$

Since s_{11}, s_{21} and s_{22} are already accurately modeled, the weighting functions $W_1 = W_2 = W_3 = 0$. A weight for s_{12} must be selected to achieve a prescribed value of the criterian function which will terminate the optimization. For a criterian function of 0.001:

$$EF = \frac{1}{N}\sum_{FI}^{FF}\{W_4|S_{12_{JJ}} - S_{12_{KK}}|^2\} = 0.001$$

$$W_4(0.003)^2 = 0.001$$

$$W_4 = 100$$

This weighting function requires an average error of 0.003 for s_{12} before the optimization will terminate. An example will further illustrate the procedure.

Consider the modeling of data presented by Liechti and Tillman.[2] They have shown that the MESFET's input can be modeled

(continued on p. 62)

Table I: Circuit Parameters For GaAs MESFETs

Manufacturer	Z μm	L_g μm	V_D V	I_D mA	R_i Ω	C_i pF	R_o Ω	C_o pF	R_f Ω	C_f pF	R_s Ω	L_s nH	L_c=L_o nH	g_{mo} mmho	τ_o psec
Varian	200	1.6	4	40	6	.4	1000	.18	205	.007	0.5	.029	.3	17	10
Fairchild	285	1	3	25	11	.25	400	0.4	237	.007	7.28	.059	.3	20	5
Nippon Electric Co.	300	1	4	80	9	.35	600	.16	2027	.004	1.33	.043	.3	18	4.2
Avantek	500	1	3	30	11	.4	500	.06	166	.014	6.18	.133	.3	32	2.5
Hewlett Packard	500	1	4	30	6.5	.50	192	.16	658	.014	3.74	0.26	0	43	2.5
Varian	600	1.6	4	110	5	1.0	450	.2	357	.009	2.61	0.27	.4	42	8.3

by a seven-ohm resistor in series with 0.58 pF and that its output can be approximated by 192-ohm resistor in parallel with 0.16 pF. An adequate fit for s_{21} occurs when $S_{21} = -4.3$, which is a transconductance of 43 mmho. The initial values of feedback elements were estimated as:

$R_s = 0.5$ ohm
$L_s = 0.05$ nH
$R_f = 1200$ ohms, and
$C_f = 0.008$ pF.

But these initial values of feedback give a large error in the phase angle of s_{12} at 12 GHz, predicting $s_{12} = 0.42 \angle 137°$, compared to the measured value of $s_{12} = 0.05 \angle 62°$.

A computer file titled "HPFET" was written to optimize the feedback parameters to the measured values of s_{12}, S_{11}, s_{21} and s_{22} were each set to equal one for simplicity. The initial s-parameters and the final values following optimization are given in Fig. 4. Note the change in the equivalent circuit elements. The total cost of this computer run was about $14, including the terminal connect line of $3.75.

The solution obtained in Fig. 4 is slightly different from the values reported in Table 1, which was derived by selecting different starting values for the four variables. The feedback solution is not unique, since the solution contains an average error of 0.003 for s_{12}, but fitting the parameters over a frequency band will always converge to a solution that is nearly equal to the measured values of s_{12}.

```
CIRCUIT OPTIMIZATION WITH  4 VARIABLES

INITIAL CIRCUIT ANALYSIS:

                    POLAR S-PARAMETERS IN   50.0 OHM SYSTEM

  F          S11              S21              S12              S22          S21      K
 MHZ     (MAGN)ANGL)      ( MAGN)ANGL)     ( MAGN)ANGL)     (MAGN)ANGL)     DB     FACT.

2000.0 ( .96) -35) ( 3.12) 152) ( .008)  75) ( .59) -12)    9.87     .95
4000.0 ( .88) -65) ( 2.63) 128) ( .012)  70) ( .59) -24)    8.39    2.22
6000.0 ( .82) -87) ( 2.16) 110) ( .012)  66) ( .59) -35)    6.67    3.90
8000.0 ( .77)-104) ( 1.78)  97) ( .016) 116) ( .60) -45)    5.01    4.15
10000.0 ( .74)-116) ( 1.49)  85) ( .027) 133) ( .61) -55)   3.47    3.10
12000.0 ( .73)-126) ( 1.27)  76) ( .042) 137) ( .63) -64)   2.06    2.32

OPTIMIZATION BEGINS WITH FOLLOWING VARIABLES AND GRADIENTS

     VARIABLES:                GRADIENTS:

  ( 1): 1200.000            ( 1):    .042
  ( 2):    .008             ( 2):   -.052
  ( 3):    .500             ( 3):   -.033
  ( 4):    .050             ( 4):    .135
 ERR. F.=   .169   CUM. CPU TIME (INCL. PREMIUM)= 1.43 SECONDS
    ----********----
  ( 1): 353.705             ( 1):    .000
  ( 2):    .016             ( 2):   -.003
  ( 3):   2.877             ( 3):   -.002
  ( 4):    .030             ( 4):    .001
 ERR. F.=   .000   CUM. CPU TIME (INCL. PREMIUM)= 5.07 SECONDS
    ----********----
FUNCTION TERMINATION WITH ABOVE VALUES. FINAL ANALYSIS FOLLOWS

2000.0 ( .96) -34) ( 2.87) 152) ( .021)  73) ( .62) -14)    9.17     .34
4000.0 ( .89) -63) ( 2.45) 129) ( .035)  61) ( .61) -27)    7.78     .69
6000.0 ( .82) -85) ( 2.02) 110) ( .043)  56) ( .60) -38)    6.12    1.04
8000.0 ( .78)-102) ( 1.67)  96) ( .046)  55) ( .61) -49)    4.48    1.39
10000.0 ( .75)-114) ( 1.41)  84) ( .049)  57) ( .62) -58)   2.96    1.70
12000.0 ( .73)-124) ( 1.20)  74) ( .052)  63) ( .63) -67)   1.57    1.93
```

4. The results of optimization are vividly illustrated in this printout. S_{12} was measured to be 0.05 $\angle 62°$. Before optimization, the model predicted 0.042 $\angle 137°$; after optimization: 0.052 $\angle 63°$. Equivalent circuit elements (variables) optimized are: (1) R_f, (2) C_f, (3) R_s and (4) L_s.

24 GHz gain and stability forecasted

The preceding example illustrates the utility of the GaAs FET model in design problems up to 12 GHz. But what about designs above that frequency? The engineer working with amplifiers above 12 GHz must decide to base his design on s-parameters measured at that higher frequency or on s-parameters derived from the lower frequency model. Basically, the decision comes down to a question of the accuracy of the higher frequency measurements.

Generally, s-parameter measurements become progressively more inaccurate at higher frequencies. Random measurement errors increase, causing calculated gains and stability factors (K) to become increasingly less reliable. Feedback may also influence the measments and cause peaks and valleys in gain and stability.

S-parameter curves based on the model will generally be much smoother than measured data because of the absence of random measurement errors. The s-parameters of three FETs of comparable gate widths have been calculated for frequencies up to 24 GHz. Plotted in Fig. 5, the smoothness of these curves compared to measured data points illustrate the validity—and usefulness—of the model in design problems above 12 GHz.

Calculated gain and stability factor curves for four of the other circuit models reported in Table 1 are presented in Fig. 6. In Fig. 6(a), the dashed curves refer to the maximum stable gain (G_{ms})

(continued on p. 66)

Model bipolars, as well

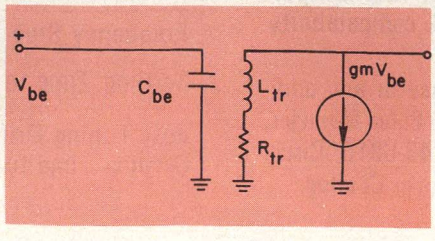
A similar computer-aided modeling technique can be used for bipolar transistors[7,8]. The current generator model can be approximated by a shunt RL network which does not load the output. For this equivalent circuit, the current generator s-parameter matrix is given by

$$S = \begin{bmatrix} 1 & 0 \\ s_{21} & 1 \end{bmatrix}$$

S_{21} is frequency dependent and given by:

$$s_{21} = \frac{-2Z_o}{R_{tr} + jwL_{tr}}$$

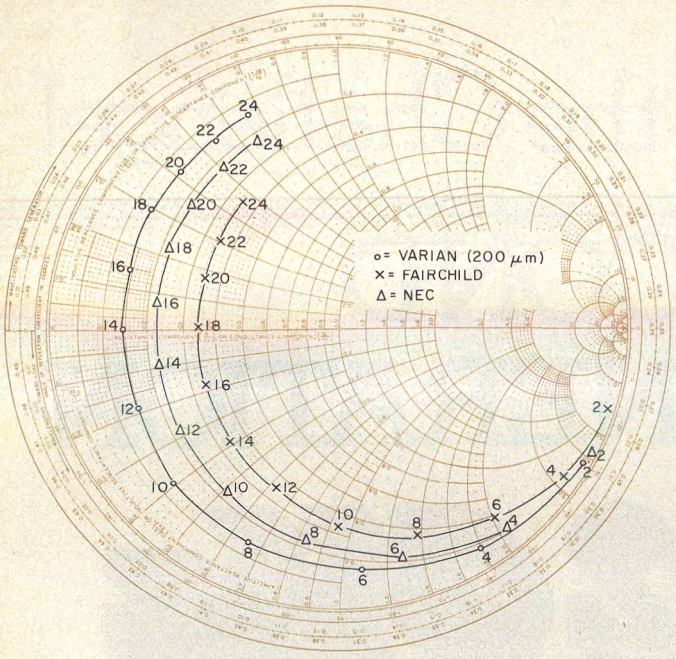
A computer analysis of the packaged bipolar transistor reported by Hartman and Strutt[8] (the Avantek AT-561) predicts a MAG of 3.5 dB at 6 GHz. Fairchild's "Speedy" program was used and provided the s-parameters and gain presented in the table below.



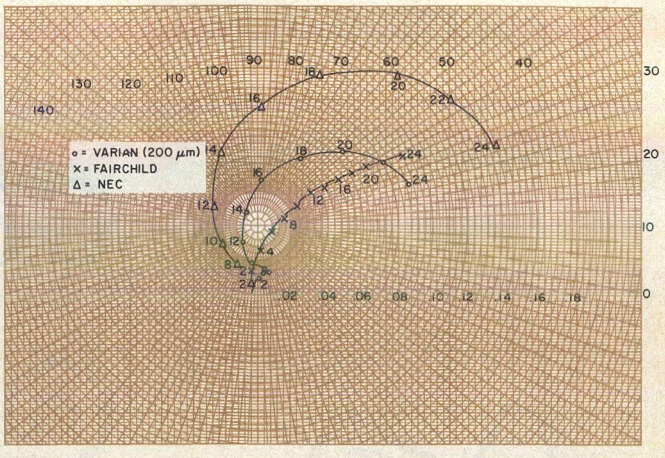
* * * OVERALL S PARAMETERS * * *

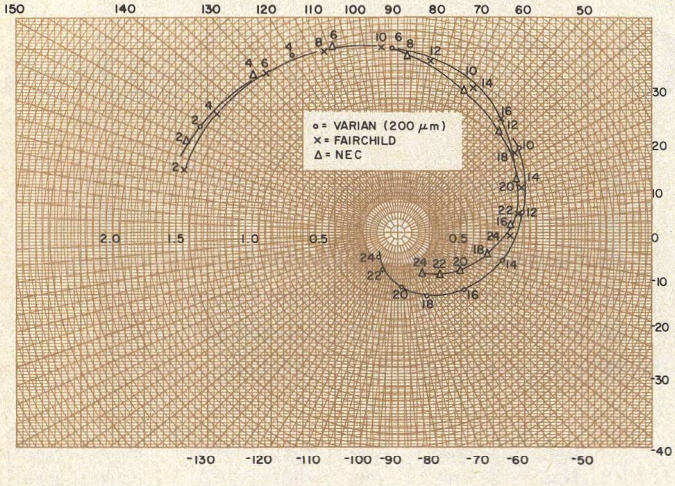
FREQ (MHZ)	S21 (DB)	S11 MAG	S11 ANGLE	S21 MAG	S21 ANGLE	S12 MAG	S12 ANGLE	S22 MAG	S22 ANGLE	K FACTR
6000.0	0.99	0.37/	153.7	1.12/	4.6	0.121/	8.7	0.56/	-60.8	2.20
8000.0	-1.77	0.36/	128.7	0.82/	-23.7	0.129/	2.9	0.66/	-85.6	2.27
10000.0	-4.61	0.35/	101.5	0.59/	-48.6	0.143/	1.4	0.76/	-113.1	2.06
12000.0	-7.77	0.33/	70.5	0.41/	-65.6	0.178/	-1.2	0.82/	-141.0	1.75

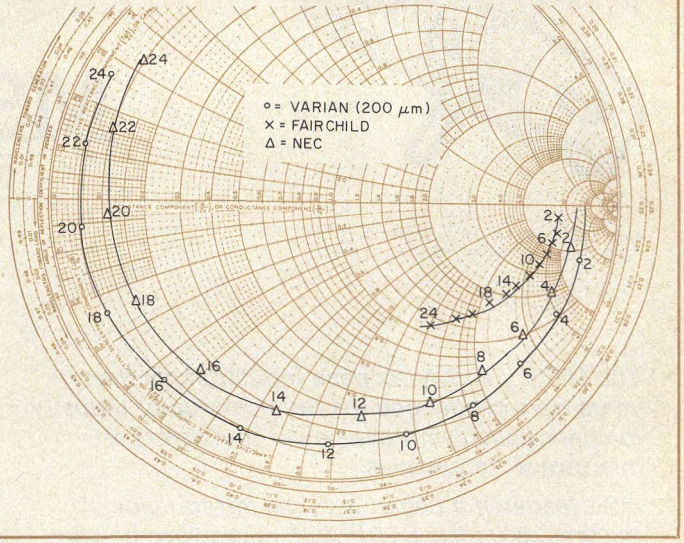
FREQ	FT(MHZ)	S21(DB)	FS(MHZ)	MSG(DB)	K	MAG(DB)	FM(MHZ)	U(DB)
6000.0	6956.	0.99	6728.	9.67	2.20	3.47	10492.	4.85
8000.0	7888.	-1.77	6525.	8.00	2.27	1.66	10439.	2.31
10000.0	9874.	-4.61	5880.	6.13	2.06	0.26	10383.	0.33
12000.0	14708.	-7.77	4908.	3.60	1.75	-1.42	10108.	-1.49



5. High frequency (above 12 GHz) projections can be made with the circuit model. Here, the s-parameters of three comparable MESFETs are predicted for frequencies ranging from 2 to 24 GHz. Note the smoothness of the curves.







where the device's stability factor is less than unity. Note that the GaAs FET has a maximum predicted gain of 10 dB at 16 GHz and about 3 dB at 24 GHz.

Experimentally obtaining the s-parameters at 24 GHz is very difficult due to measurement errors. The measurement system can be accurately calibrated up to the test-jig connectors, but the measured s-parameters of a GaAs MESFET should be corrected for test fixture losses, especially above 8 GHz.

Let's consider the NEC FET listed in Table 1 and see how test-fixture losses can influence measurements at 12 GHz. S-parameters derived from the model values listed in Table 1 appear in the first column of Table 2. These values already include loss correction. Column two (Table 2) tabulates calculated s-parameters that are based on the corresponding parameters in column one, but assume an additional 1 dB through-loss in the test fixture. Note that merely 1 dB of additional test-fixture loss would result in a false gain figure that is nearly one-third the magnitude of the actual gain. Conversely, the predicted stability factor would seem to be more than three times its actual value. Clearly, considerable error could be the result of test fixture losses.

By reversing the corrections for loss and assuming 1 dB gain at 12 GHz, the NEC device would appear to have a maximum stable gain of 13.1 dB and a stability factor of −0.6. This would approximate the predicted gain and stability factor if no corrections for fixture loss are made in the calibration, and the test fixture has only a 1 dB through loss.

Table 2: Effect of Fixture Loss on Measurements at 12 GHz

	True s-parameters including loss correction	S-parameters assumning an additional 1 dB fixture loss
s_{11}	0.660 /−147°	0.524 /−147°
s_{21}	1.090 /44°	0.971 /44°
s_{12}	0.053 /114°	0.047 /114°
s_{22}	0.780 /−84°	0.620 /−84°
G_{ma}	9.0 dB	3.5 dB
k	1.5	4.6

Pre-test calibration required

Compensating for fixture losses requires the use of a low-loss, 50-ohm through-line which approximates the loss of the chip test fixture (Fig. 7). An acceptable through-section would exhibit 0.2 to 0.5 dB loss at 12 GHz (including connector losses). With special care, it is possible to build a through-section with less than 1 dB loss at 18 GHz.

(continued on p. 68)

The through-line fixture, which has the length of the test jig minus the length of chip or chip carrier, is substituted in the test line during calibration and the measured loss is stored in the computer for later corrections to the measured transistor s-parameters. Since this correction is approximate, a low-loss test fixture is essential. The location of the device is determined by another fixture (Fig. 7) which is identical but has a good rf short at the device reference plane. This test fixture also provides phase dispersion from TEM propagation at higher frequencies.

Practically the same test and reference jig can be used when measuring a packaged device. But securing the packaged device without causing additional mismatches is still another challenge. Many problems can be overcome by simply pressing down the source leads from only the top.

Additional sources of measurement errors include connector reflections, microstripline dispersion (which changes the transistor reference plane) and possible waveguide modes due to the width of the test fixture.

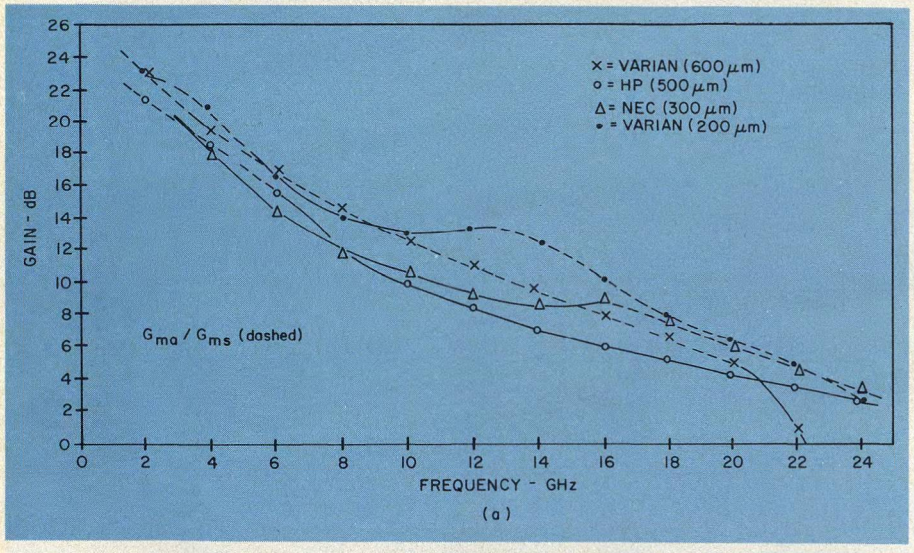
However, a well-made test jig with well-matched, low-loss connectors (such as APC 7 mm) and the shortest possible microstrip line on a low dielectric constant substrate should eliminate most of the problems. Care should also be taken to enclose the transmission line in a narrow channel to suppress any potential higher mode excitation.

Design example: A K-u band amplifier

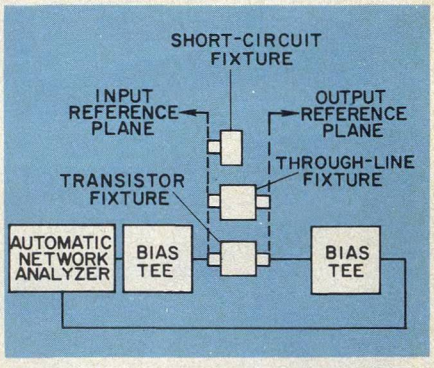
An example of a 14.25 GHz amplifier design using the Fairchild GaAs MESFET described in Table 1 further illustrates the value of the circuit model. This design used the Fairchild's program, "Speedy," and was built with both open-and short-circuited stubs (Fig. 8). The predicted gain for both versions is 6.7 + 0.1 dB.

The short-circuit stub design proceeds as follows. The input is approximated by 18 ohms in series with an LC network of 0 25 pF and

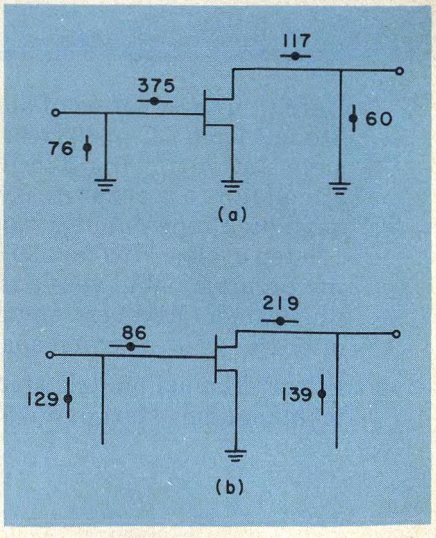
(continued on p. 70)



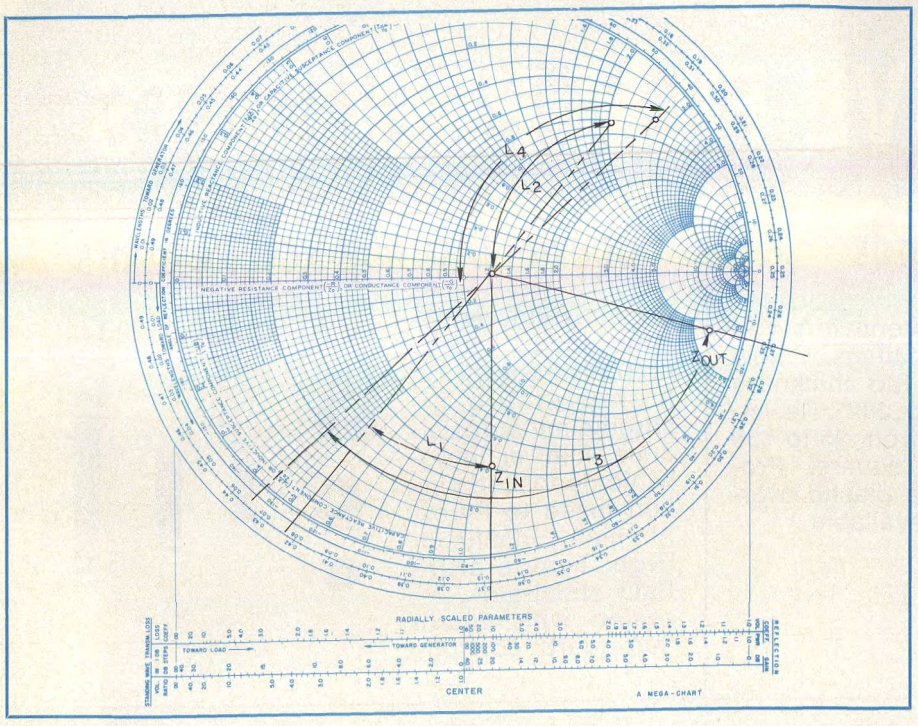
6. Calculated gain and stability factor curves are based on the circuit models presented in Table 1. Note the similarity of the gain curves.



7. The s-parameter measurement system must be corrected for fixture losses. The through-line section approximates the test fixture loss, while the short-circuit determines the location of the device under test.



8. Both short-circuit (a) and open-circuit (b) 14.25 GHz amplifier designs were built with the aid of the model. The electrical lengths given above are in mils. All microstrip lines have a characteristic impedance of 50 ohms.



9. Rough line lengths are first calculated on a Smith chart, then optimized with the computer.

0.3 nH. Thus, the input impedance is 18-j42, shown as Z_{in} in Fig. 9. This impedance is matched to 50 ohms by a series transmission line of length L_1 and a short-circuited stub of length L_2. At 14.25 GHz, the electrical length is:

$$\ell_o = \frac{30}{14.25}\ 2.11\ \text{cm} = 832\ \text{mils.}$$

Thus,

$$L_1 = 0.05\ \ell_o = 42\ \text{mils.}$$

For the calculation of L_2:

$$\frac{B_2}{Y_o} = -j\ 1.85$$

$$L_2 = 0.079\ \ell_o = 66\ \text{mils.}$$

These values were later optimized to 375 mils (or −41 mils) and 76 mils using Speedy and the complete circuit model.

The output is approximated by a parallel RC network of 400 ohms in parallel with 0.04 pF. This is an output impedance of 130-j190 ohms shown as Z_{out} in Fig. 9. This impedance is matched to 50 ohms by a series transmission line of length L_3 and an open-circuited stub of length L_4. Thus, $L_3 = 0.168\ l_o = 140$ mils.

For the calculation of L_4,

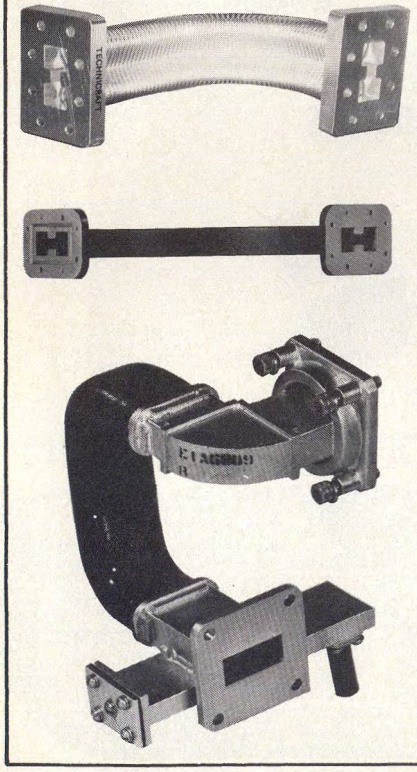
$$\frac{B_4}{Y_o} = -j2.5$$

$$L_4 = 0.061\ \ell_o = 51\ \text{mils.}$$

These values were later optimized to 117 mils and 60 mils. For both the input and output design, the initial starting values gave excellent gain, indicating the value of a circuit model that emphasizes design simplicity.

The open-circuit stub amplifier was evaluated by simply laying indium stubs on the 50-ohm s-parameter test fixture. A gain of 5.6 dB was achieved in an early test amplifier, which is an indication of the accuracy of the model. ••

Best by Test!



We've earned this reputation by producing top quality waveguide and related components for nearly 30 years.

In an average month, we'll ship five miles of rigid and flexible waveguide to some of the most demanding customers in the world. And our hardware will exactly match their stringent specifications.

Need complex bends? We bend rigid waveguide in all sizes from WR 430 down to millimeter. Twists? We produce them in rigid and certain types of flex from WR 650 to millimeter.

For interlocked or seamless flexible waveguide, for rigid waveguide —rectangular or circular — it pays to . . . . . .

Let Technicraft be your guide!

TECHNICRAFT
a division of Tech Systems Corp.
401 Watertown Road, Thomaston, Connecticut 06787
(203) 283-5801 TWX 710-475-0537

READER SERVICE NUMBER 70

References

1. J. A. Archer, G. E. Brehm and G. D. Vendelin, "Exploratory Development of Small-Signal Low-Noise X-Band Transistors," Final Report, Contract DAAB07-73C-0091, (July, 1974).

2. C. A. Liechti and R. L. Tillman, "Design And Performance Of Microwave Amplifiers With GaAs Schottky-Gate Field Effect Transistors," *IEEE Trans. MTT*, pps. 510-517, (May, 1974).

3. D. R. Chen and A. N. Woo, "A Low Noise C-Band GaAs FET Amplifier," MTT Symposium, Late News Paper, (1974).

4. G. D. Vendelin and M. Omori, "A Circuit Model For The GaAs MESFET Valid To 12 GHz," *Electronic Letters*, to be published.

5. R. T. Davis, "Microwave Circuit Design is Now as Close as Your Telephone," *Microwaves*, p. 9, (August, 1973).

6. G. E. Brehm and G. D. Vendelin "Biasing FETs For Optimum Performance," *Microwaves*, pps. 38-44, (February, 1974).

7. K. Hartman, W. Kotyczka and M. J. O. Strutt. "Computer-Aided Determination of the Small Signal Equivalent Network of Bipolar Microwave Transistor," *IEEE Trans. MTT*, pp. 120-126, (February, 1972).

8. K. Hartman and M. J. O. Strutt, 'Computer Simultation of Small-Signal and Noise Behavior of Microwave Bipolar Transistors Up To 12 GHz," *IEEE Trans. MTT*, pp. 178-183, (March, 1974).

new products

Close-tracking i-f limiting amp offers a 75 dB dynamic range

The WJ-5030-37 is a 300 to 500 MHz phase tracking amplifier-limiter that offers exceptionally close phase tracking over a wide dynamic range. Sets of these limiting amplifiers are phased matched to better than ±3 degrees (typical) over a 75 dB input dynamic range and an instantaneous bandwidth of 200 MHz (400 MHz optional). The wide bandwidth allows construction of phase matched i-f subsystems capable of processing very short pulses; amplifier rise and fall times are less than 10 nanoseconds.

Typical applications include passive interferometry, DF systems, radar receivers and other systems where multiple channels of phase tracking i-f circuitry is required. Power-limited characteristics of these units are extremely flat—less than a 0.5 dB output power variation for a −70 to +5 dBm input range—allowing ±0.5 dB amplitude tracking.

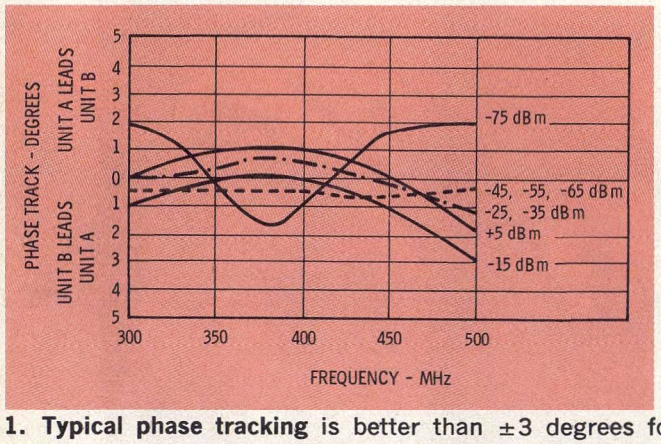
All amplifiers and limiters in the WJ-5030-37 are realized with low parasitic chip devices attached to thin-film circuits with integral gold metalization and tantalum nitride resistors. Thus the gain and phase match specifications apply over an operating temperature range of −40 to +52°C, without the need for temperature compensation circuitry. P&A: $3,150 each in qtys. of 2; 90 days. **Watkins-Johnson Company, 3333 Hillview Avenue, Palo Alto, CA 94304 (415) 493-4141.**

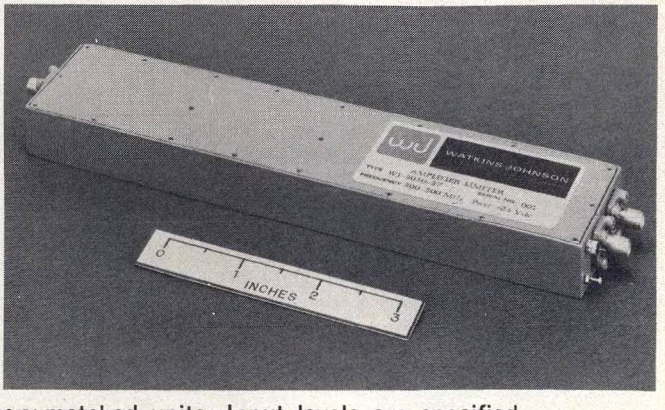
CIRCLE NO. 124

Specifications for Model WJ-5030-37

PARAMETER	MIN.	TYP	MAX.	UNIT
Input Dynamic Range for Constant Output	-70	N/A	+5	dBm
Frequency	300	N/A	500	MHz
Pout	-5.3	-4.7	-3.7	dBm
Gain Flatness (Constant Input)		±0.2	±0.5	dB
Input VSWR		1.5:1	2.0:1	N/A
Output VSWR		1.5:1	1.7:1	N/A
Phase Tracking (Equal Input Levels) a) +25°C		±3.0	±6.0	Degrees
b) -40°C to +52°C		±5.0	±8.0	Degrees
Output Power Tracking (Equal Inputs, -70 dBm to +5 dBm)		±0.3	±0.5	dB
Phase Tracking (Input Level Inequality of 10 dB or Less)		±10.0	±13.0	Degrees
Harmonically Related Outputs (Relative to Desired)		-20	-17	dB
Size	7.5" × 1.75" × .75"			
Weight	12 ounces			
DC Power	+24V @ 325 mA			
Isolation Between Outputs	15 dB, minimum			

*Measured in 50 Ω system With VSWR ≤ 1.5:1





1. Typical phase tracking is better than ±3 degrees for factory-matched units. Input levels are specified.

Noise loader offers test flexibility with plug-in filters

The AT-9003, noise load source, uses plug-in band stop and band limit filter modules for noise load testing any telecommunications system with a baseband up to 12.5 MHz. It is designed to work with a general purpose selective level meter such as W&G Instruments, models AT-463, or the AT-611 as shown. The unit accommodates two band-limiting filters at 316 kHz-5.6 MHz and 316 kHz −11.404 MHz and three band stop (slot) filters with center frequencies at 1.248 MHz, 5.340 MHz and 9.624 MHz. These filters allow testing all standard 1,200, 1,500, 2,100 and 2,400 channel systems. The noise load source generates a maximum output of 0 dBm adjustable in 1 dB steps to −39 dBm using a precision attenuator. There is an automatic correction for any loss in power output caused by the bandstop filters.

Standard output impedance is 75 ohms; a 124 ohm output and pre-emphasis network is available as an option. Power consumption is about 50 W using 120/220 Vac, 45-65 Hz. Operating temperature is 5°C to 40°C. Size: 19 in. (478 mm) x 7 in. (176 mm) x 16 in. (407 mm). Weight is 29 lbs. The AT-9003 is a simplified version of the Wandel & Goltermann, model RS-50 white noise source.

P&A: $2,290; a preselector, W&G model AT-9004 is also available at $350 for short haul measurements where precision NPR measurements of greater than 50 dB are desired. **W&G Instruments, Inc., 119 Naylon Avenue, Livingston, NJ 07039 (201) 994-0854.**

CIRCLE NO. 126

